U.S. Department
of Commerce

Volume 102
Number 4
October 2004

Fishery Bulletin

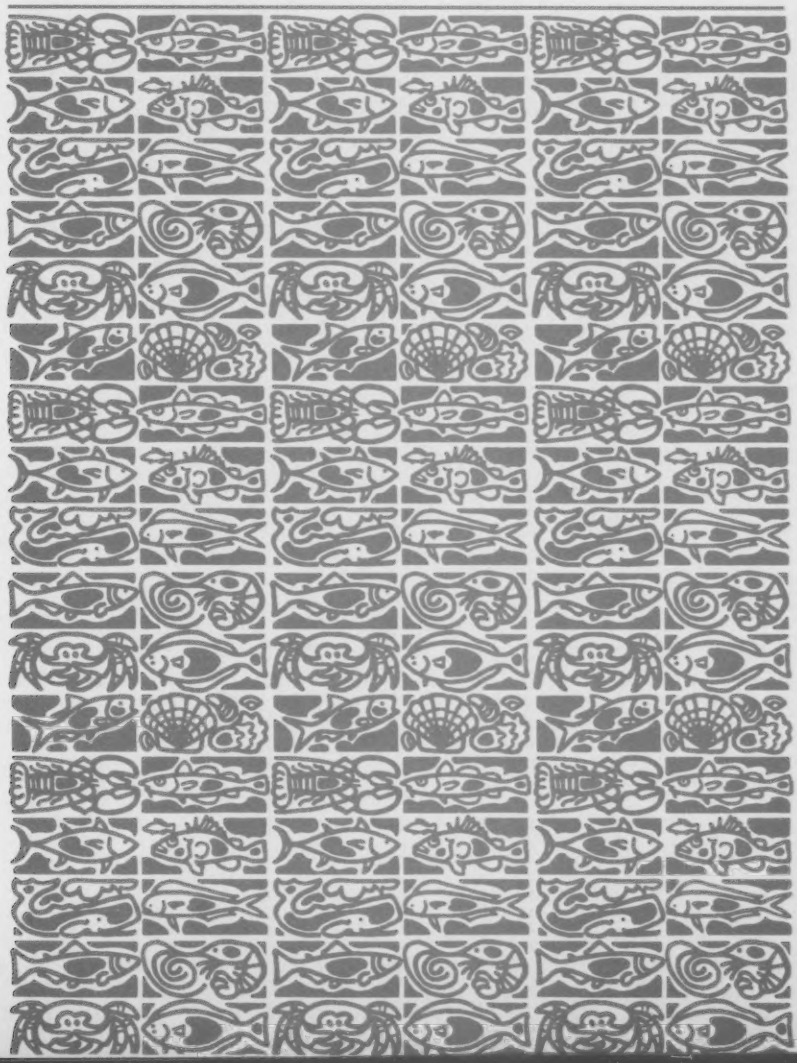

U.S. Department of Commerce
Donald L. Evans
Secretary

National Oceanic and Atmospheric Administration
Vice Admiral
Conrad C. Lautenbacher Jr., USN (ret.)
Under Secretary for Oceans and Atmosphere

National Marine Fisheries Service
William T. Hogarth
Assistant Administrator for Fisheries

The *Fishery Bulletin* (ISSN 0090-0656) is published quarterly by the Scientific Publications Office, National Marine Fisheries Service, NOAA, 7600 Sand Point Way NE, BIN C15700, Seattle, WA 98115-0070. Periodicals postage is paid at Seattle, WA, and at additional mailing offices. POSTMASTER: Send address changes for subscriptions to Fishery Bulletin, Superintendent of Documents, Attn.: Chief, Mail List Branch, Mail Stop SSOM, Washington, DC 20402-9373.

Although the contents of this publication have not been copyrighted and may be reprinted entirely, reference to source is appreciated.

The Secretary of Commerce has determined that the publication of this periodical is necessary according to law for the transaction of public business of this Department. Use of funds for printing of this periodical has been approved by the Director of the Office of Management and Budget.

For sale by the Superintendent of Documents, U.S. Government Printing Office, Washington, DC 20402. Subscription price per year: $55.00 domestic and $68.75 foreign. Cost per single issue: $28.00 domestic and $35.00 foreign. **See back for order form.**

Fishery Bulletin

Scientific Editor
Norman Bartoo, PhD

Associate Editor
Sarah Shoffler

National Marine Fisheries Service, NOAA
8604 La Jolla Shores Drive
La Jolla, California 92037

Managing Editor
Sharyn Matriotti

National Marine Fisheries Service
Scientific Publications Office
7600 Sand Point Way NE, BIN C15700
Seattle, Washington 98115-0070

Editorial Committee

Harlyn O. Halvorson, PhD	University of Massachusetts, Boston
Ronald W. Hardy, PhD	University of Idaho, Hagerman
Richard D. Methot, PhD	National Marine Fisheries Service
Theodore W. Pietsch, PhD	University of Washington, Seattle
Joseph E. Powers, PhD	National Marine Fisheries Service
Harald Rosenthal, PhD	Universität Kiel, Germany
Fredric M. Serchuk, PhD	National Marine Fisheries Service
George Watters, PhD	National Marine Fisheries Service

***Fishery Bulletin* web site: www.fishbull.noaa.gov**

The *Fishery Bulletin* carries original research reports and technical notes on investigations in fishery science, engineering, and economics. It began as the Bulletin of the United States Fish Commission in 1881; it became the Bulletin of the Bureau of Fisheries in 1904 and the *Fishery Bulletin* of the Fish and Wildlife Service in 1941. Separates were issued as documents through volume 46; the last document was No. 1103. Beginning with volume 47 in 1931 and continuing through volume 62 in 1963, each separate appeared as a numbered bulletin. A new system began in 1963 with volume 63 in which papers are bound together in a single issue of the bulletin. Beginning with volume 70, number 1, January 1972, the *Fishery Bulletin* became a periodical, issued quarterly. In this form, it is available by subscription from the Superintendent of Documents, U.S. Government Printing Office, Washington, DC 20402. It is also available free in limited numbers to libraries, research institutions, State and Federal agencies, and in exchange for other scientific publications.

U.S. Department of Commerce
Seattle, Washington

Volume 102
Number 4
October 2004

Fishery Bulletin

Contents

Articles

563–580 **Calambokidis, John, Gretchen H. Steiger, David K. Ellifrit, Barry L. Troutman, and C. Edward Bowlby**
Distribution and abundance of humpback whales (*Megaptera novaeangliae*) and other marine mammals off the northern Washington coast

581–592 **Danilewicz, Daniel, Juan A. Claver, Alejo L. Pérez Carrera, Eduardo R. Secchi, and Nelson F. Fontoura**
Reproductive biology of male franciscanas (*Pontoporia blainvillei*) (Mammalia: Cetacea) from Rio Grande do Sul, southern Brazil

593–603 **Fischer, Andrew J., M. Scott Baker Jr., and Charles A. Wilson**
Red snapper (*Lutjanus campechanus*) demographic structure in the northern Gulf of Mexico based on spatial patterns in growth rates and morphometrics

604–616 **FitzGerald, Jennifer L., Simon R. Thorrold, Kevin M. Bailey, Annette L. Brown, and Kenneth P. Severin**
Elemental signatures in otoliths of larval walleye pollock (*Theragra chalcogramma*) from the northeast Pacific Ocean

617–633 **Gaughan, Daniel J., Timothy I. Leary, Ronald W. Mitchell, and Ian W. Wright**
A sudden collapse in distribution of Pacific sardine (*Sardinops sagax*) off southwestern Australia enables an objective re-assessment of biomass estimates

634–647 **Griffiths, Shane P., Ron J. West, Andy R. Davis, and Ken G. Russell**
Fish recolonization in temperate Australian rockpools: a quantitative experimental approach

The conclusions and opinions expressed in *Fishery Bulletin* are solely those of the authors and do not represent the official position of the National Marine Fisheries Service (NOAA) or any other agency or institution.

The National Marine Fisheries Service (NMFS) does not approve, recommend, or endorse any proprietary product or proprietary material mentioned in this publication. No reference shall be made to NMFS, or to this publication furnished by NMFS, in any advertising or sales promotion which would indicate or imply that NMFS approves, recommends, or endorses any proprietary product or proprietary material mentioned herein, or which has as its purpose an intent to cause directly or indirectly the advertised product to be used or purchased because of this NMFS publication.

648–660 **Hesp, S. Alexander, Ian C. Potter, and Sonja R. M. Schubert**
Factors influencing the timing and frequency of spawning and fecundity of the goldlined seabream (*Rhabdosargus sarba*) (Sparidae) in the lower reaches of an estuary

661–670 **Maxwell, Michael R., Annette Henry, Christopher D. Elvidge, Jeffrey Safran, Vinita R. Hobson, Ingrid Nelson, Benjamin T. Tuttle, John B. Dietz, and John R. Hunter**
Fishery dynamics of the California market squid (*Loligo opalescens*), as measured by satellite remote sensing

671–681 **Murray, Kimberly T.**
Magnitude and distribution of sea turtle bycatch in the sea scallop (*Placopecten magellanicus*) dredge fishery in two areas of the northwestern Atlantic Ocean, 2001–2002

682–692 **Snover, Melissa L., and Aleta A. Hohn**
Validation and interpretation of annual skeletal marks in loggerhead (*Caretta caretta*) and Kemp's ridley (*Lepidochelys kempii*) sea turtles

693–710 **Stehlik, Linda L., Robert A. Pikanowski, and Donald G. McMillan**
The Hudson-Raritan Estuary as a crossroads for distribution of blue (*Callinectes sapidus*), lady (*Ovalipes ocellatus*), and Atlantic rock (*Cancer irroratus*) crabs

711–722 **Stevens, Melissa M., Allen H. Andrews, Gregor M. Cailliet, Kenneth H. Coale, and Craig C. Lundstrom**
Radiometric validation of age, growth, and longevity for the blackgill rockfish (*Sebastes melanostomus*)

723–732 **Tolan, James M., and David A. Newstead**
Descriptions of larval, prejuvenile, and juvenile finescale menhaden (*Brevoortia gunteri*) (family Clupeidae), and comparisons to gulf menhaden (*B. patronus*)

733–739 **Uchikawa, Kazuhisa, John R. Bower, Yasuko Sato, and Yasunori Sakurai**
Diet of the minimal armhook squid (*Berryteuthis anonychus*) (Cephalopoda: Gonatidae) in the northeast Pacific during spring

740–749 **Weinberg, Kenneth L., Robert S. Otto, and David A. Somerton**
Capture probability of a survey trawl for red king crab (*Paralithodes camtschaticus*)

Notes

750–756 **Kerstetter, David W., Jeffery J. Polovina, and John E. Graves**
Evidence of shark predation and scavenging on fishes equipped with pop-up satellite archival tags

757–759 **Vladimir V. Laptikhovsky**
Survival rates of rays discarded by the bottom trawl squid fishery off the Falkland Islands

760 **Acknowledgment of 2004 reviewers**

761 **2004 indexes**

770 **Subscription form**

Distribution and abundance of humpback whales (*Megaptera novaeangliae*) and other marine mammals off the northern Washington coast

John Calambokidis
Gretchen H. Steiger
David K. Ellifrit
Cascadia Research Collective
Waterstreet Building
218½ West Fourth Ave.
Olympia, Washington 98501
E-mail address (for J. Calambokidis): calambokidis@cascadiaresearch.org

Barry L. Troutman
Washington Dept. of Fish and Wildlife
600 Capitol Way
Olympia, Washington 98501

C. Edward Bowlby
Olympic Coast National Marine Sanctuary, NOAA
115 Railroad Ave E, Suite 301
Port Angeles, Washington 98362

Abstract—We examined the summer distribution of marine mammals off the northern Washington coast based on six ship transect surveys conducted between 1995 and 2002, primarily from the NOAA ship *McArthur*. Additionally, small boat surveys were conducted in the same region between 1989 and 2002 to gather photographic identification data on humpback whales (*Megaptera novaeangliae*) and killer whales (*Orcinus orca*) to examine movements and population structure. In the six years of ship survey effort, 706 sightings of 15 marine mammal species were made. Humpback whales were the most common large cetacean species and were seen every year and a total of 232 sightings of 402 animals were recorded during ship surveys. Highest numbers were observed in 2002, when there were 79 sightings of 139 whales. Line-transect estimates for humpback whales indicated that about 100 humpback whales inhabited these waters each year between 1995 and 2000; in 2002, however, the estimate was 562 (CV=0.21) whales. A total of 191 unique individuals were identified photographically and mark-recapture estimates also indicated that the number of animals increased from under 100 to over 200 from 1995 to 2002. There was only limited interchange of humpback whales between this area and feeding areas off Oregon and California. Killer whales were also seen on every ship survey and represented all known ecotypes of the Pacific Northwest, including southern and northern residents, transients, and offshore-type killer whales. Dall's porpoise (*Phocoenoides dalli*) were the most frequently sighted small cetacean; abundance was estimated at 181–291 individuals, except for 2002 when we observed dramatically higher numbers (876, CV=0.30). Northern fur seals (*Callorhinus ursinus*) and elephant seals (*Mirounga angustirostris*) were the most common pinnipeds observed. There were clear habitat differences related to distance offshore and water depth for different species.

Manuscript submitted 25 September 2003 to the Scientific Editor's Office.
Manuscript approved for publication 4 June 2004 by the Scientific Editor.
Fish. Bull. 102:563–580 (2004).

Marine mammals have had an important role in the history of the Olympic Peninsula for centuries. Many species, including sea otters (*Enhydra lutris*), harbor seals (*Phoca vitulina*), humpback whales (*Megaptera novaeangliae*), and gray whales (*Eschrichtius robustus*) were hunted by the Makah tribe (Swan, 1868; Huelsbeck, 1988). Much later, modern whalers targeted humpback whales in this region from stations at Bay City, Washington (1911–25, Scheffer and Slipp, 1948), and southern Vancouver Island, British Columbia (1905–43, Gregr et al., 2000). A small aboriginal hunt for gray whales resumed in these waters in 1998, and the Makah killed one gray whale in May 1999. Since the end of commercial whaling, marine mammals have been afforded protection under the Marine Mammal Protection Act of 1972. In addition, the waters off the northern Washington coast were designated as the Olympic Coast National Marine Sanctuary in 1994.

A number of studies have documented marine mammals in this region. Some surveys of broader areas have included the waters off northern Washington (Von Saunder and Barlow, 1999; Brueggeman[1]; Green et al.[2]). Species-specific studies also

[1] Brueggeman, J. J. 1992. Oregon and Washington marine mammal and seabird surveys. Final report of OCS Study MMS 91-0093 by Ebasco Environmental, Bellevue, Washington, and Ecological Consulting, Inc., Portland, Oregon, for the Minerals Management Service (MMS), 445 p. MMS, Pacific OCS Region, U.S. Dept. of Interior, 770 Paseo Camarillo, Camarillo, CA 93010.

[2] Green, G. A., M. A. Smultea, C. E. Bowlby, and R. A. Rowlett. 1993. Delphinid aerial surveys in Oregon and Washington offshore waters. Final report for contract 50ABNF200058 to the National Marine Mammal Laboratory, National Marine Fisheries Service, 100 p. Nat. Mar. Mamm. Lab., NMFS, 7600 Sand Point Way NE F/AKC3, Seattle, WA 98115.]

have been conducted on harbor porpoise (*Phocoena phocoena;* Barlow et al., 1988; Osmek et al., 1996; Calambokidis et al.[3]) and, to a limited degree, on humpback whales (Calambokidis et al., 1996, 2000) and gray whales (Darling, 1984; Green et al., 1995; Shelden et al., 2000; Calambokidis et al., 2002). Studies on pinnipeds and sea otters have also been conducted in this region (Jeffries et al., 2003; Jameson et al., 1982, 1986; Kvitek et al., 1992, 1998; Bowlby et al.[4]).

Information on humpback whales is of particular interest because they were the primary species hunted by whalers off Washington in the early 1900s. Since then, little has been known about their movements and distribution in this region. Photo-identification research has helped define the movements and stock structure of the humpback whales feeding off California (Calambokidis et al., 1990, 1996, 2000). Calambokidis et al. (1996) suggested that a demographic boundary exists between humpback whales that feed off the coasts of California, Oregon, and Washington and humpback whales feeding farther north off British Columbia and Alaska. The identity and degree of interchange of the whales that feed in this boundary area have been unclear.

Similarly for killer whales, photo-identification studies have revealed much about whale groups that frequent the inland waters of Washington and British Columbia (Bigg et al., 1990; Ford et al., 1994). Very little is known about their occurrence off the coast, in particular, about the "offshore" groups that are believed to be a distinct race (Ford et al., 1994) that are seen primarily offshore but occasionally also enter inland waterways.

We report here on the summer distribution of marine mammals off the northern Washington coast based on six ship line-transect surveys conducted between 1995 and 2002. These surveys were initiated to understand marine mammal distribution and abundance in the newly designated Olympic Coast National Marine Sanctuary, as well as to collect information on seabirds, oceanographic conditions, and juvenile fish. Each ship survey was conducted between mid-June and late July. Density estimates were made for the two most common species: humpback whales and Dall's porpoise. In addition, photo-identification data gathered during these ship surveys and from supplemental small boat surveys within the same area between 1989 and 2002 provided information on humpback and killer whale movements and stock structure.

Materials and methods

Ship surveys

Generally, ship surveys covered the area between the 20-m isobath and the landward margin of the continental shelf (200-m isobath) from the entrance to Strait of Juan de Fuca to the mouth of the Copalis River to include the boundaries of the Olympic Coast National Marine Sanctuary (Fig. 1). Although the northern extent of these waters is off southern British Columbia (Vancouver Island), the entire overlapping region will be referred to as northern Washington.

Fourteen east-west tracklines were selected, following permanent tracklines established by the NOAA ship *Miller Freeman* in 1989. Tracklines were spaced at 5-nmi intervals and were surveyed each year except in 2002, when only ten lines were surveyed (four southernmost lines were not included). Extra ship time allowed for replicate surveys of the northern survey legs in 1995, a short offshore extension of two lines in 1996 and 2000 (up to 17 nmi in 1986), the addition of three short east-west lines off southern Vancouver Island around La Perouse Bank in 1997, and one additional line that was surveyed south of the study area in 2000 (Fig. 1).

Ship surveys were conducted over a two-week period in late-June and July 1995, 1996, 1997, 1998, and 2000 (Table 1). In 2002, a shorter, one-week survey was done in mid-June. The marine mammal ship surveys were conducted by a single primary observer from the vessel's flying bridge (the sighting platform) with a viewing height of 10 m above the water level. All surveys were conducted from the NOAA ship *McArthur* (55 m) except during 2000, when the naval ship *Agate Passage* (33 m) was used. From these platforms, the primary observer scanned a 180-degree arc encompassing the area ahead of the ship and abeam to either side. Observers used reticle binoculars when possible and obtained measurements of distance to a sighting derived from the angle below the horizon (measured with graded reticles in the binoculars) and the known platform height. For sightings where the species could not be determined by the observer, animals were identified to a general taxonomic level (e.g., unidentified pinniped).

Photo-identification surveys

In addition, photo-identification data were examined that had been gathered within the survey area. Researchers took photographs directly from the survey ship, or from a *Zodiac* rigid-hulled inflatable that was launched when animals were sighted. In 1996, the last two days of vessel time on the *McArthur* were used to photograph whales for identification.

[3] Calambokidis, J., J. C. Cubbage, J. R. Evenson, S. D. Osmek, J. L. Laake, P. J. Gearin, B. J. Turnock, S. J. Jeffries, and R. F. Brown. 1993. Abundance estimates of harbor porpoise in Washington and Oregon waters. Report to the National Marine Mammal Laboratory, National Marine Fisheries Service, 55 p. Nat. Mar. Mamm. Lab., NMFS, 7600 Sand Point Way NE F/AKC3, Seattle, WA 98115.

[4] Bowlby, C. E., B. L. Troutman, and S. J. Jeffries. 1988. Sea otters in Washington: distribution, abundance, and activity patterns. Final report to National Coastal Resources Research and Development Institute, Hatfield Marine Science Center, 2030 S. Marine Dr., Newport, Oregon 97365, 131 p. Cascadia Research Collective, Wash. State Dept. of Wildlife, Olympia, WA.

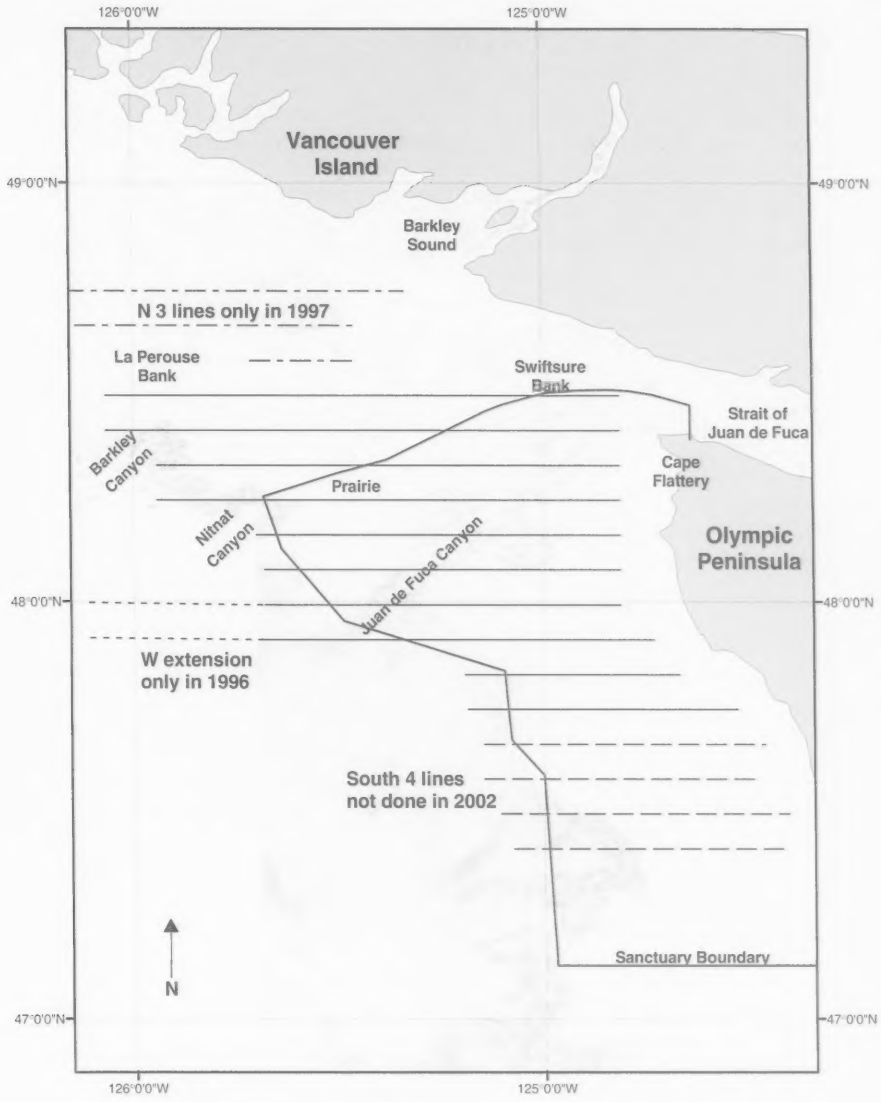

Figure 1

On-effort ship survey tracklines (horizontal lines) off the northern coast of Washington between 1995 and 2002. The Olympic Coast National Marine Sanctuary boundary is delineated and labeled. Dashed and dotted lines show three northern lines surveyed only in 1997, the western extension of two lines surveyed only in 1996, and the southern four lines missed in 2002.

In addition, dedicated photo-identification surveys were conducted by Cascadia Research scientists using a 5.3-m *Novurania* rigid-hulled inflatable that was launched from nearby ports and operated in areas where whales were concentrated. Photo-identification data in the present study includes data collected off the northern Washington coast between 1989 and 2002 (Table 2). It also includes photographs contributed by other researchers and boat operators taken in the area during this time (Table 2).

Generally, photographs were taken with Nikon 8008 35-mm cameras equipped with 300-mm Nikkor telephoto lenses. High-speed black-and-white film (Ilford HP 5+) was pushed 1½ stops so that exposure times were generally 1/1000 or 1/2000 of a second. Identification photographs were taken with standard procedures used

Table 1

Summary of ship survey effort off northern Washington (does not include small boat surveys).

Year	Dates of effort		No. of legs	Effort (h)	nmi on effort	Ship	Observers
	Start	End					
1995	21 Jul	27 Jul	10	46	546	*McArthur*	Troutman, Ellifrit
1996	28 Jun	5 Jul	14	46	540	*McArthur*	Troutman, Ellifrit
1997	9 Jul	18 Jul	17	52	513	*McArthur*	Troutman, Ellifrit
1998	25 Jun	4 Jul	14	55	572	*McArthur*	Troutman, Quan
2000	16 Jun	24 Jun	14	60	589	*Agate Passage*	Rowlett, Nelson
2002	12 Jun	18 Jun	10	32	315	*McArthur*	Troutman, Douglas
All years				291	3075		

Table 2

Photo-identification effort off the coast of northern Washington between 1989 and 2002. These data include whales identified from the ship or small boats launched from the ship, dedicated small boat surveys, and opportunistic photographs taken by others. Unique = number of different animals.

Year	Days IDs obtained			Humpback whales identified				Other sources of photographs
	No.	First	Last	No.	Unique	No. of mothers	No. of calves	
1989	1	1 Oct	1 Oct	1	1	0	0	
1990	3	25 Aug	6 Sep	10	10	1	1	Balcomb/Bloedel[1]
1991	4	23 Aug	4 Sep	14	13	0	0	Balcomb/Bloedel[1]
1993	1	15 Jul	15 Jul	3	3	0	0	
1994	3	25 Jun	15 Jul	20	16	0	0	G. Ellis,[2] R. Baird
1995	7	14 Jul	25 Jul	50	35	4	2	S. Mizroch[3]
1996	9	29 Jun	6 Oct	55	34	1	0	
1997	9	13 Jul	18 Oct	25	23	2	0	
1998	19	28 May	16 Oct	71	48	1	1	V. Deeke, B. Gisborne
1999	28	20 May	20 Oct	103	60	2	0	B. Gisborne
2000	12	2 Jun	4 Oct	56	40	2	1	B. Gisborne
2001	15	8 Jun	5 Oct	59	41	2	1	SWFSC,[4] B. Gisborne
2002	9	13 Jun	5 Sep	41	32	0	0	
Total	120			508	356	15	6	
Unique					191			

[1] Center for Whale Research, P.O. Box 1577, Friday Harbor, WA 98250.
[2] Dept. of Fisheries and Oceans, Pacific Biological Station, Nanaimo, BC, V9T 6N7, Canada.
[3] National Marine Mammal Laboratory, NMFS, 7600 Sand Point Way NE, Seattle, WA 98115.
[4] Southwest Fisheries Science Center, 8604 La Jolla Shores Dr., La Jolla, CA 92037.

in past research (Calambokidis et al., 1990). For humpback whales, photographs were taken of the ventral side of the tail flukes. For killer whales, the dorsal fin and surrounding saddle-patch area were photographed from both sides.

Photographs of individuals were first compared to those identified in the same region. To analyze interchange with other regions, we compared these individuals with existing catalogs to obtain sighting histories. For humpback whales, a catalog was used of over 1000 humpback whales identified since 1986 along the West Coast. The regions used for comparison were Oregon, northern California (Oregon-California border to Pt. Arena), northern central California (Pt. Arena to north of Monterey Bay), southern central California (north of Monterey Bay to Pt. Conception) and southern California (southern California Bight). For killer whales, whales were matched to existing catalogs (Bigg et al., 1987; Ford et al., 1994; Black et al., 1997). All identifications and group determinations were confirmed by one of the authors (DKE) or Graeme Ellis (Dept. of Fisheries and Oceans, Nanaimo, British Columbia).

Data analysis

For ship surveys between 1995 and 2000, position and oceanographic data (including depth, sea surface temperature) logged by the ship's computer were later reconciled with the sighting and effort data recorded by the observers. Sighting positions were analyzed for each species for water depth, distance from shore, distance from shelf edge (200-m depth contour) and sea surface temperature. Data analysis and mapping were conducted by using a geographic information system (GIS) with ArcInfo software (ESRI, Redlands, CA). Data from the shorter 2002 ship survey were included in the summary of sightings but were not available for the analyses of sightings related to oceanographic features.

Line-transect analysis to determine density and abundance was conducted for the two species with more than 30 sightings (humpback whales and Dall's porpoise). We used the program (Distance, version 3.5, Research Unit for Wildlife Population Assessment, University of St. Andrews, St. Andrews, UK) to conduct analyses. For these analyses, we used only effort and sightings from the regular east-west transect lines and did not include on-effort data from opportunistic lines or cross-tracks. We included sightings made by secondary as well as the primary observer. Although whales were reportedly seen out to 6 nmi, we truncated the sightings at 3 nmi for humpback whales and 2.5 nmi for Dall's porpoise. For humpback whales we included 16 sightings of unidentified whales (unidentified mainly because of distance). These were probably humpback whales because the only other large whales that were seen in the surveys were a few gray whales seen close to shore. Distance position data were incomplete for 13 of the 188 whale sightings and 14 of 82 Dall's porpoise sightings; for these the missing value was randomly selected from the observed measurements.

The Distance program was used to select the best model for sighting probability in relation to distance off the transect. We allowed the program to select among models (half-normal, uniform, hazard-rate, and negative exponential) and varying numbers of adjustment terms (cosine and simple polynomials) based on lowest Akaike's information criterion (AIC) score. All years were pooled for the model of sighting probability, but encounter rate and group size were calculated by year. An adjustment to group size was calculated if there was a significant group size bias with distance from the track line, which was not the case for humpback whales but was present in some years (1996 and 1997) for Dall's porpoise.

Area was calculated for abundance estimation based on the zone covered by the regularly scheduled transect lines covered in most years (study area was considered to encompass waters 2.5 nmi north of the northernmost line and 2.5 nmi south of the southernmost line). The only annual adjustment for area was for humpback whales in 2002. Surveys in that year did not cover the southern end of the study area (because of limited ship time), an area with a typically lower abundance of whales. To avoid extrapolating the higher density of whales from the northern portion of the study area to this region, we excluded this missed area from the abundance estimates.

Estimates of abundance for humpback whales were also calculated by using capture-recapture models (Seber, 1982; Hammond, 1986). We used identifications obtained in pairs of adjacent years taken from 1994 to 2002 to generate Petersen capture-recapture estimates. The Chapman modification of the Petersen estimate (Seber, 1982) was used because it was appropriate for sampling without replacement (Hammond, 1986).

Results

In total, there were 706 sightings of 2467 animals over the six ship surveys combined (Table 3). Fifteen different marine mammal species were seen: nine cetacean species, five pinniped species, and the sea otter were identified. Each year, 9 to 12 different species were seen, except in 2002 when only six species were observed. This 2002 survey, although shorter than those of the other years, showed a dramatic change in the species diversity and numbers of animals. We saw many more humpback and Dall's porpoise than in previous years. We also noted the absence of six regularly observed species: harbor porpoise, gray whales, Pacific white-sided dolphins (*Lagenorhynchus obliquidens*), Risso's dolphin (*Grampus griseus*), harbor seals, and California sea lions (*Zalophus californianus*).

Humpback whales

Of the large cetaceans, humpback whales were the most common species seen; there were 232 sightings of 402 animals during ship surveys (Table 3). Largest numbers of humpback whales were seen in 2002, when there were 79 sightings of 139 individuals during the one-week survey. Group sizes ranged from 1 to 8 animals (mean=1.7, SD=1.1). Only six calves were recorded from the ship surveys—probably because it was difficult to identify calves at the distance at which most sightings were made. Of these six sightings of mothers with calves, four sightings were outside the primary areas where other humpback whale groups were seen.

Sightings were concentrated in the northern part of the study area between Juan de Fuca Canyon and the outer edge of the continental shelf, an area known as "the Prairie" (Fig. 2). A small area east of the mouth of Barkley Canyon and north of the Nitnat Canyon where the water depth was 125–145 m had a high density of sightings in all years. A smaller number of humpback whales were also seen on Swiftsure Bank. Sightings in 2002 were not only more numerous but more broadly distributed; sightings were recorded in the areas described above and also farther south and closer to shore than those seen in previous years.

Line-transect estimates for humpback whales were very consistent in the first five surveys (1995 to

Table 3

Summary of marine mammal sightings by year during ship surveys off northern Washington. Opportunistic sightings (non-transect) are included.

	1995		1996		1997		1998		2000		2002		All years	
Species	No. of sightings	No. of animals	No. of sightings	No. of animals	No. of sightings	No. of animals	No. of sightings	No. of animals	No. of sightings	No. of animals	No. of sightings	No. of animals	No. of sightings	No. of animals
Baleen whales														
Humpback whale	25	40	54	86	23	44	27	36	24	57	79	139	232	402
Gray whale	1	1	2	3	2	3					5	7		
Minke whale	3	3	1	1	4	4								
Unidentified whale	4	8	3	3	11	12	1	1	3	3	4	6	26	33
Odontocetes														
Dall's porpoise	27	72	20	64	16	43	13	46	14	48	25	133	115	406
Harbor porpoise	4	10	11	20	2	5	14	43	7	11		38	89	
Pacific white-sided dolphin	4	596	16	149					4	369	4	19	28	1133
Northern right-whale dolphin					1	6		1	6					
Risso's dolphin	5	57	1	5	2	11	1	6		9	79			
Killer whale	3	16	2	38	2	21	2	5	3	36	2	8	14	124
Unidentified delphinid	6	9	8	56	2	4	3	5			4	18	23	92
Pinnipeds and otters														
Harbor seal	2	2	3	3	2	3	7	7	1	1			15	16
Elephant seal	6	6	10	10	2	2	2	2			20	20		
California sea lion	1	1	3	3			4	4						
Steller sea lion	3	5	1	1			4	6						
Northern fur seal	6	6	5	5	1	2	9	9	1	1	6	6	28	29
Sea otter	3	3	3	3										
Unidentified pinniped	4	4	3	3	1	2	4	4	1	1			13	14
Total sightings	94	772	141	495	65	146	91	179	66	545	125	330	706	2467

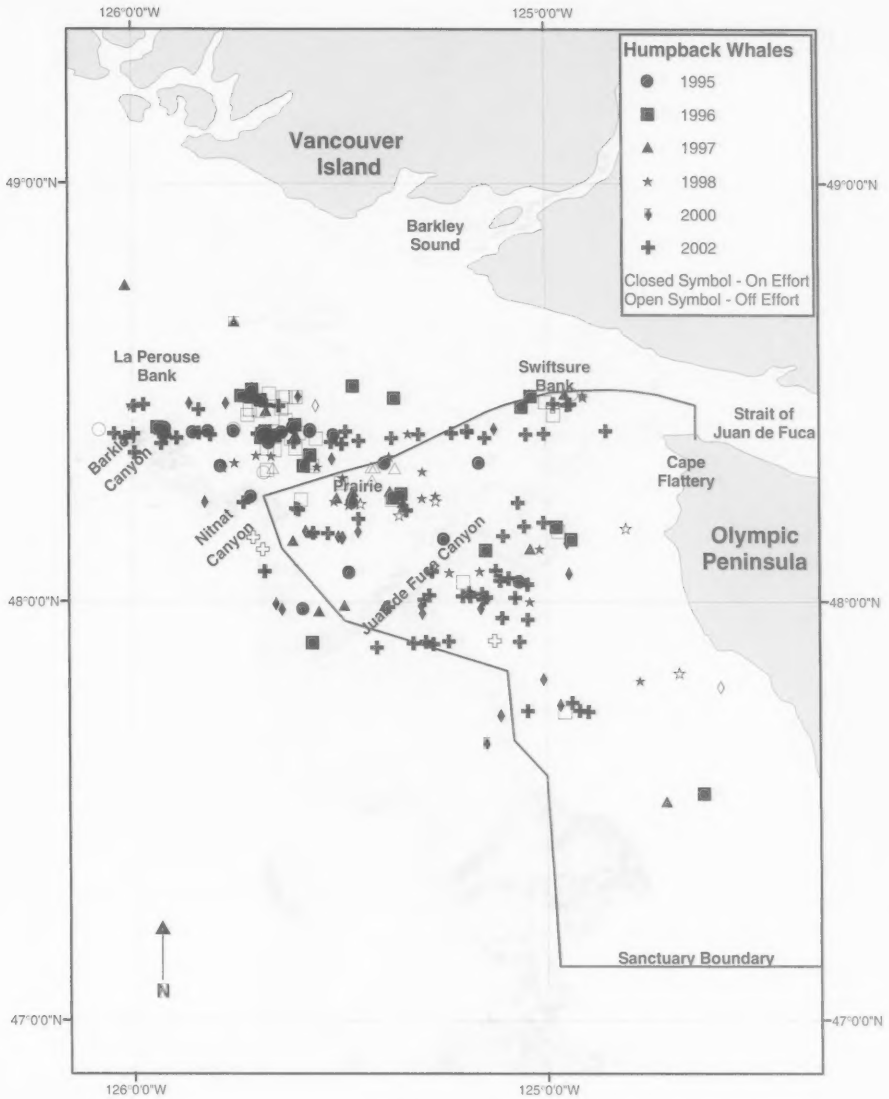

Figure 2

Locations (by year) for humpback whales (*Megaptera novaeangliae*) seen during ship surveys off the northern Washington coast between 1995 and 2002.

2000, Table 4, Fig. 3). The encounter rate of groups (0.046–0.053 sightings per nmi), density (0.034–0.050 whales per nmi^2), and abundance (85–125 individuals) were similar among these years. These data indicate that about 100 humpback whales used the study area during this period.

The sighting rate of humpback whales was dramatically higher in 2002 than in all previous years and was reflected in the line-transect estimates (Fig. 3). Estimated density (0.23 whales per nmi^2) was more than four times higher than any previous year. Applying this density to only the reduced area surveyed in 2002 (1953 instead of 2505 nmi^2) still yielded much higher estimates of abundance (562, CV=0.21) than in any previous year. These higher abundance estimates could not have been an artifact of random variation; the lower bound of the 95% confidence interval for the 2002 estimates was well above the upper confidence interval of any of the previous years (Table 4).

Of the humpback whales photographed during small boat surveys off the northern Washington-BC border between 1989 and 2002, 508 individuals were success-

Table 4

Results of line-transect analysis for humpback whales off northern Washington. On-effort sightings of humpback and unidentified large whales made during regular transects (not including deadheads [areas between transect lines] and opportunistic sightings) within 3 nmi of ship were used. Best detection model fit (AIC scores) was a negative exponential with 1 cosine adjustment yielding $f(0)=1.05$. Effective strip width was 0.95 nmi with CV=0.09.

Year	Sightings n	Survey effort lines	Survey effort nmi	Encounter rate	Group size	Density (per nmi^2)	Area (nmi^2)	Estimated abundance	CV	95% Conf. int. lower	95% Conf. int. upper
1995	23	58	438	0.053	1.48	0.041	2505	102	0.33	54	193
1996	24	59	474	0.051	1.54	0.041	2505	103	0.33	55	193
1997	26	92	493	0.053	1.62	0.045	2505	112	0.3	63	199
1998	20	62	432	0.046	1.40	0.034	2505	85	0.31	47	155
2000	23	70	504	0.046	2.09	0.050	2505	125	0.32	67	234
2002	72	43	305	0.236	1.81	0.224	1953	562	0.21	375	841
Total	188	384	2646								

fully identified of which 191 were unique individuals (Table 2). Of these 191, 83 (44%) had been seen in this area in more than one year within this time period. The proportion of animals seen more than one year changed over the course of the study (Fig. 4). The proportion of whales identified each year that had been seen in others years decreased annually (Fig. 4, regression $r^2=0.63$, $P=0.002$); the most dramatic drop occurred between 1998 and 1999.

Photographs of humpback whales documented animal movements within the study area and provided some insight into possible reasons for the high sighting rates during the 2002 ship surveys. On two occasions, the same humpback whale was identified on different days in a slightly different area and represented a duplicate sighting of this animal from the ship survey. It is possible that shifting humpback whale distribution during the course of the 2002 survey could have occurred in a manner that resulted in the same animals being encountered multiple times and that elevated the sighting rate and line-transect abundance estimate (Fig. 3). We cannot test this hypothesis because other animals may have shifted in a manner that they avoided being detected at all.

Abundance of humpback whales from capture-recapture models yielded estimates of 89 to 343 whales (Table 5, Fig. 3). These estimates tended to increase over the course of the study from a low of 89 whales for 1994–95 to a high of 343 for 2000–2001 and 230 for 2001–2002 (regression $r^2=0.60$, $P=0.02$). There was fairly good agreement between the capture-recapture and line-transect estimates until 2002 (Fig. 3).

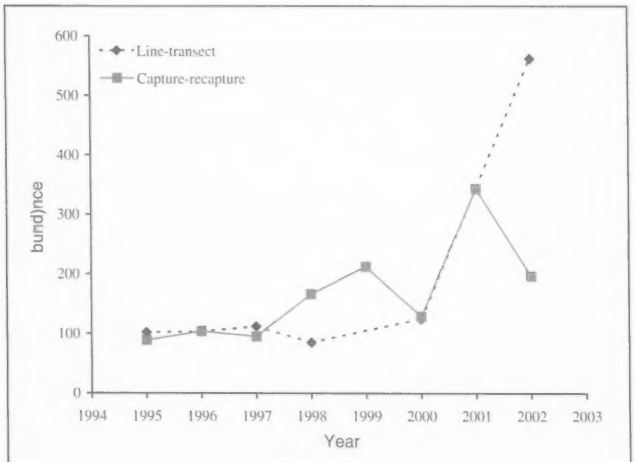

Figure 3

Line-transect (dashed line) and capture-recapture (solid line) estimates for humpback whale (*M. novaeangliae*) abundance between 1995 and 2002.

A total of 17 of the 191 (9%) whales that we identified off northern Washington had also been photographed off California and Oregon (Table 6). Interchange of whales seen off northern Washington and other feeding areas to the south decreased as distance among feeding areas increased. About 10% (10 of 105) of the whales that were identified off Oregon were also photographed off northern Washington. This rate of matching dropped below 3% (8 of 313) off northern California and continued to decrease to no interchange seen for whales photographed off southern California.

The proportion of whales that were seen in areas to the south appeared to change over the course of the study. From 1989 to 1998, when resighting rates between years within our study area were highest, we also had a higher proportion of interchange with feeding areas to the south (13 of 109 whales or 12%). From 1999 to 2002, after resightings within our region decreased, there was also a decrease

Table 5

Estimates of humpback whale abundance (Est.) off northern Washington obtained with the Petersen capture-recapture model. Each estimate was based on the identifications obtained (n) in each of two adjacent years.

	Sample 1		Sample 2				
Period	Year	n	Year	n	Match	Est.	CV
1994–95	1994	14	1995	35	5	89	0.27
1995–96	1995	35	1996	34	11	104	0.19
1996–97	1996	34	1997	21	7	95	0.24
1997–98	1997	23	1998	48	6	167	0.28
1998–99	1998	48	1999	60	13	213	0.19
1999–2000	1999	60	2000	31	14	129	0.16
2000–01	2000	40	2001	41	4	343	0.36
2001–02	2001	41	2002	32	5	230	0.32

in the proportion of these whales that had also been seen off California and Oregon (7 of 136 whales or 5%). This difference falls just short of statistical significance (χ^2=3.71, P<0.10) but is in the reverse direction from what would be expected if immigration from the south were to increase over time.

Between 1989 and 2002, 15 different mothers were seen with 16 calves (one mother seen with a calf in two different years). Mothers with calves represented 4.2% of the individual whales identified each year (15 of 356 unique annual identifications, Table 2). For each year only a small proportion of the calves were identified because calves raise their flukes less often.

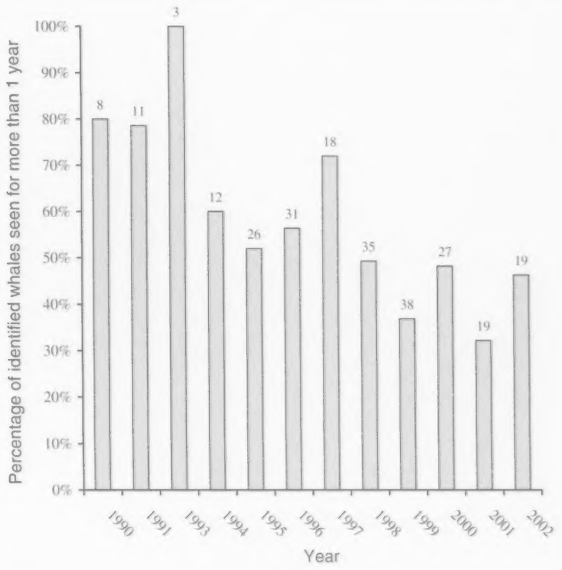

Figure 4

The proportion of humpback whales (*M. novaeangliae*) seen in more than one year during annual surveys off northern Washington from 1989 to 2002.

Killer whales

One other large cetacean species (killer whales) was also seen every year; there were a total of 14 sightings of 124 animals from ship surveys (Table 3). Three of these sightings were of large groups between 20 and 35 animals, and the rest were in groups fewer than ten (14 sightings, mean=8.9, SD=11.2). Killer whales were widely distributed across different habitats; there were sightings of animals both close to and far from shore and in fairly shallow and deep water (Fig. 5).

All three ecotypes of killer whales (namely, 1) southern and northern residents, 2) transients, and 3) offshore residents) were observed off the northern Washington coast. Of the 15 groups identified photographically between 1989 and 2002, there were sightings of animals from the southern resident (2 groups), northern resident (3), transient (5) and offshore (3) groupings (Table 7). Other sightings appeared to be northern residents (1) and offshore (1) animals but the quality of the photographs were too poor for us to be certain. Large groups of killer whales (20–40 animals) were seen on five occasions during small boat surveys.

Dall's porpoises

Dall's porpoises were the most frequently sighted small cetacean; there were 115 sightings of 406 animals and Dall's porpoises were observed every year (Table 3). No

Table 6

Number of humpback whales identified in different regions along the U.S. west coast and the number and percentage of these that matched with northern Washington. For northern Washington, we report the number of whales that were seen in that region in more than one year.

Region	No. of individuals	No. of matches with N. Wash.	% of whales that match with those in N. Wash.
Northern Washington	191	83	43.5%
Oregon	105	10	9.5%
N. California	313	8	2.6%
N. Central California	921	13	1.4%
S. Central California	666	3	0.5%
S. California	303	0	0.0%

Table 7

Summary of killer whale sightings off northern Washington between 1989 and 2002 where identifiable photographs were taken.

Date	No. of animals estimated	Lat. °N	Long. °W	Community	Pod or ID	Comments
13 Sep 89	3	48 23.0	124 48.5	Resident—southern	L10, L28,L41	
15 Jul 94	4	48 20.9	125 20.0	Transient	CA195	
25 Jul 95	7	47 49.8	124 59.5	Transient	CA195	
26 Jul 95	8	47 53.7	125 03.3	Transient	CA20,CA27	
17 Mar 96	6	46 58.2	124 15.7	Resident—southern	L26, L83	outside Grays Harbor
31 Mar 96	7	46 55.0	124 09.7	Transient—probably	T50?	Grays Harbor entrance
5 Jul 96	3	48 13.1	124 55.0	Transient	T185	
6 Jul 96	40	48 26.7	125 43.2	Resident—northern	C, D, G1s, G12s	
15 Jul 97	30	48 19.4	125 09.5	Offshore		
18 Jul 97	10	48 18.3	125 23.6	Offshore	CA105	
10 Aug 97	8	48 21.0	125 34.6	Transient	T36, T99, T36A?, T137?	
27 Aug 98	40	48 28.0	125 17.0	Offshore	O44,O30, O31,O172, O14, O158, O218	
10 Oct 99	30	48 22.0	125 38.1	Resident—northern	I11	
18 Jun 00	20	48 03.8	125 04.3	Probably resident—northern		not southern residents
6 Sep 01	12	47 01.8	124 46.6	Resident—northern	G12s, G17s, G29s	

Table 8

Results of line-transect analysis for Dall's porpoise off northern Washington. All on-effort sightings during regular transects (not including deadheads [areas between transect lines] and opportunistic sightings) within 2.5 nmi of the ship were included. The best detection model fit (AIC scores) was the hazard rate with no cosine adjustment, yielding $f(0)=2.60$. Effective strip width of 0.38 nmi with CV=0.12. The group size for 96–97 was adjusted to account for a significant group size bias with distance from the trackline.

Year	Sightings n	Survey effort: lines	Survey effort: nmi	Encounter rate	Group size	Density (per nmi^2)	Area (nmi^2)	Estimated abundance	CV	95% Conf. int.: lower	95% Conf. int.: upper
1995	16	58	438	0.037	2.25	0.100	2505	268	0.32	143	501
1996	14	59	474	0.030	2.65	0.102	2505	255	0.32	138	472
1997	13	92	493	0.026	2.28	0.078	2505	197	0.38	95	405
1998	9	62	432	0.021	2.67	0.072	2505	181	0.49	72	453
2000	13	70	504	0.026	3.46	0.116	2505	291	0.42	132	644
2002	17	43	305	0.056	4.82	0.350	2505	876	0.3	487	1576
Total	82	384	2646								

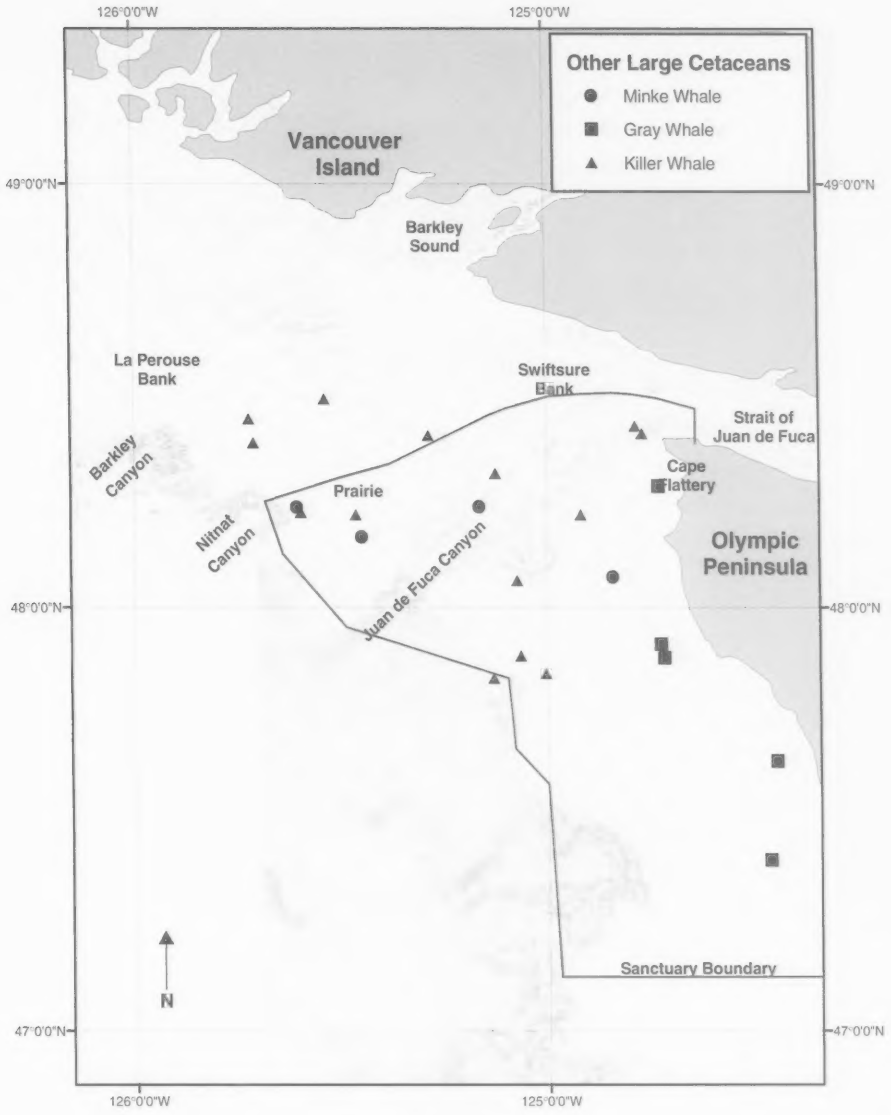

Figure 5

Locations of other large cetaceans seen during ship surveys off the northern Washington coast between 1995 and 2002.

calves were recorded during the surveys. Dall's porpoises were widely distributed in the study area but were not as commonly seen in more shallow coastal waters or in the southern portion of the study area (Fig. 6). Group size ranged between 1 and 12 individuals (mean=3.5, SD=2.2). Harbor porpoises were observed each year (except 2002) and there were a total of 38 sightings for the entire study period. Group size ranged between 1 and 6 individuals except for one sighting of a group of 20 animals (mean=2.3, SD=3.1). The distribution range for harbor porpoises was more restricted to coastal waters and showed only a small overlap with the distribution range for Dall's porpoises (Fig. 6).

Line-transect analysis allowed estimation of Dall's porpoise density and abundance (Table 8). Similar to those for humpback whales, results for Dall's porpoises were fairly consistent for the first five surveys (1995 to 2000): annual abundances were estimated between 181 and 291. For 2002, the encounter rate and corresponding density and abundances increased dramati-

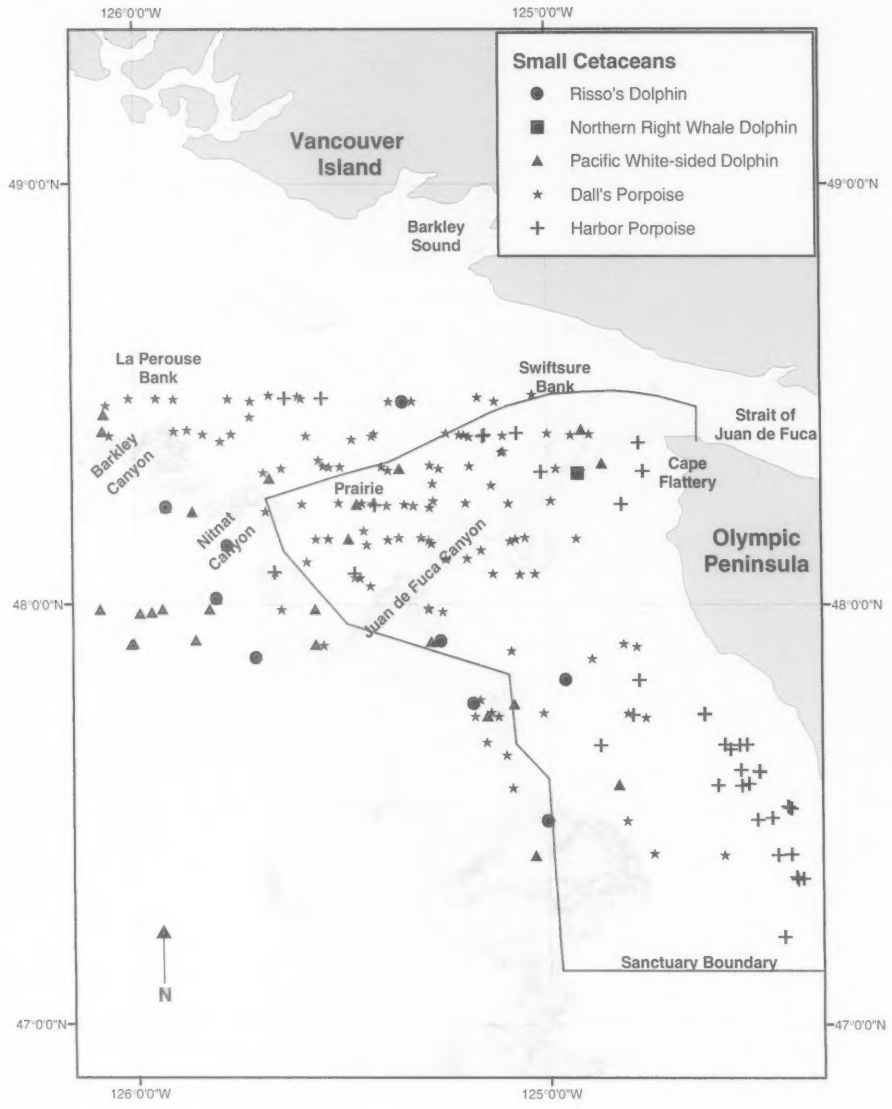

Figure 6

Locations of small cetaceans seen during ship surveys off the northern Washington coast between 1995 and 2002.

cally yielding an estimated abundance of 876 porpoises (CV=0.30, Table 8). Confidence intervals for some of the annual estimates overlapped among years.

Pinnipeds

Pinnipeds were not as frequently observed as cetaceans (Table 3, Fig. 7). The two most pelagic species observed in this region, northern fur seals and elephant seals, were the most commonly seen pinnipeds. Northern fur seals were observed every year except 2002 on a total of 28 occasions. All but one of these sightings were of a single animal. Elephant seals were seen in all years except 1998 and 2002.

Habitat differences

A number of broad habitat patterns emerged for different groups of species based on their association with water depth and distance from shore during the ship surveys from 1995 to 2000 (Table 9, data were not available for 2002). Five species were seen in shallow waters

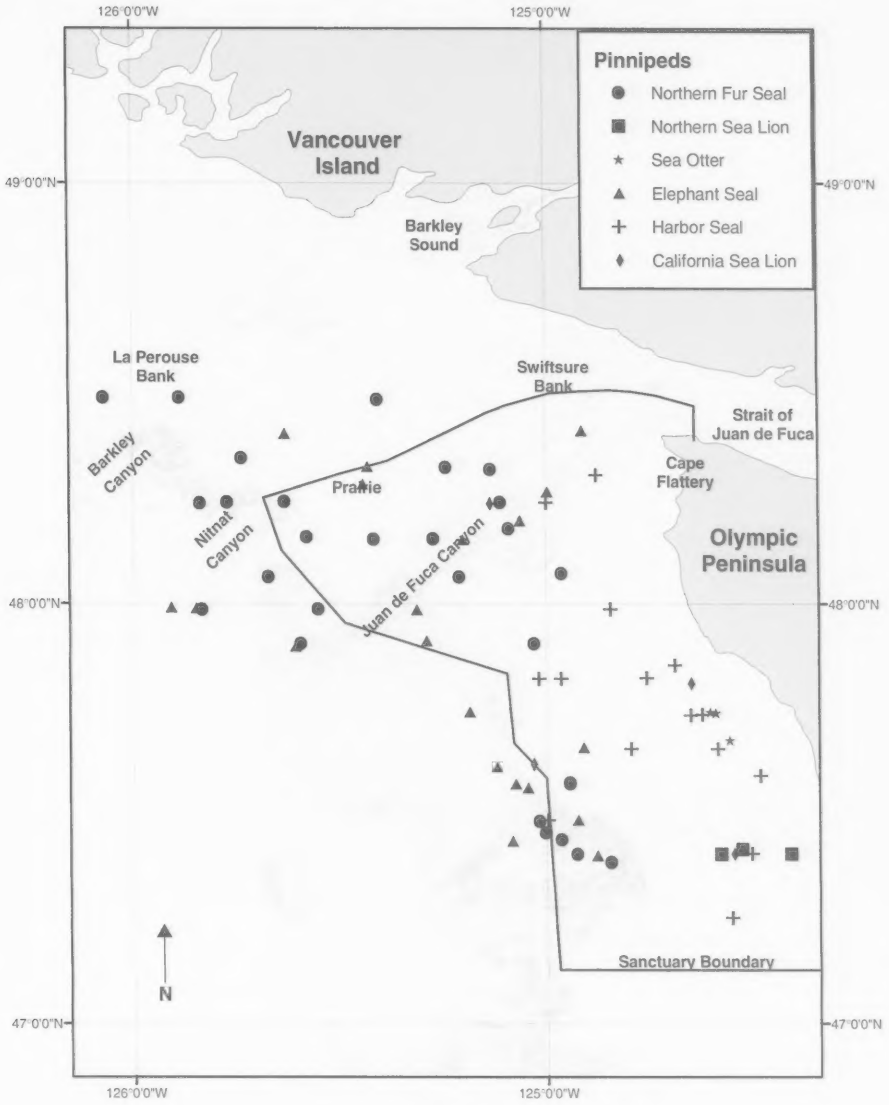

Figure 7

Locations of pinnipeds and sea otters (*Enhydra lutris*) seen during ship surveys off the northern Washington coast between 1995 and 2002.

(<100 m). Gray whales and sea otters were seen in the shallowest water of all species with average water depths of just 20 and 22 m, respectively; they also were the only two species for which sightings averaged less than 10 km from shore. The three other species—harbor porpoise, California sea lions, and northern sea lions (*Eumetopias jubatus*)—were seen in slightly deeper waters (averaging 34 to 91 m) and farther from shore (averaging 11 to 23 km). The five species that were predominantly found at mid-shelf depths (mean depths at 100–200 m) were humpback whales, killer whales, Dall's porpoises, harbor seals, and minke whales (*Balaenoptera acutorostrata*). Species seen far from shore (>40 km) and also in deepest waters (>200 m) included Pacific white-sided dolphins, Risso's dolphins, elephant seals, and northern fur seals. All of these species are known to feed along the continental slope or off the shelf.

Distances from the shelf break for different species did not fall into as clear a pattern as water depth and distance from shore (Table 9). This disparity may be the result of the varied habitat (with canyons cutting through the study area) and the lack of much effort off

Table 9

Summary of habitat and oceanographic parameters for sightings of different species during ship surveys from 1995 to 2000.

	Water depth (m)			Distance from shore (km)			Distance from shelf (km)			Sea surface temp. (°C)		
Species	*n*	Mean	SD	*n*	Mean	SD	*n*	Mean	SD	*n*	Mean	SD
Baleen whales												
Humpback whale	153	144	87	153	43.8	14.9	153	8.4	6.7	101	13.9	1.6
Gray whale	5	20	8	5	5.0	2.0	5	26.1	8.1	5	14.4	1.9
Minke whale	3	106	67	3	41.2	27.7	3	8.0	6.5	3	16.1	0.9
Unidentified large whale	21	189	280	21	40.5	18.4	21	8.0	7.3	18	15.4	1.3
Unidentified whale	1	197	—	1	36.3	—	1	0.1	—	1	13.0	—
Odontocetes												
Dall's porpoise	90	167	118	90	40.1	14.9	90	5.6	5.5	72	14.3	1.7
Harbor porpoise	38	58	70	38	16.3	15.6	38	17.2	11.6	29	13.9	1.7
Pacific white-sided dolphin	24	689	505	24	65.6	25.7	24	8.3	8.7	20	15.0	0.8
Northern right-whale dolphin	1	259	—	1	16.2	—	1	0.7	—			
Risso's dolphin	9	552	310	9	55.4	21.4	9	4.9	5.2	8	14.4	1.3
Killer whale	12	148	58	12	28.8	15.0	12	5.9	4.7	7	14.1	1.1
Unidentified delphinid	19	219	253	19	37.4	17.4	19	5.7	6.7	19	14.5	1.5
Pinnipeds and otters												
Harbor seal	15	102	154	15	17.3	11.0	15	15.5	12.0	14	14.2	1.4
Elephant seal	20	466	370	20	46.2	18.5	20	3.8	5.0	16	14.7	1.8
California sea lion	4	91	74	4	22.8	15.2	4	9.3	14.2	1	13.9	—
Steller sea lion	4	34	18	4	11.3	5.4	4	18.5	6.6	3	13.6	0.4
Northern fur seal	22	382	349	22	47.1	17.1	22	3.1	3.7	21	14.3	1.4
Sea otter	3	22	1	3	8.9	0.5	3	25.5	18.1	3	12.6	0.4
Unidentified pinniped	13	170	144	13	30.5	18.4	13	8.0	8.1	11	14.5	1.9
All sightings	457	205	251	457	39.1	20.1	457	8.4	8.4	352	14.3	1.6

the continental shelf. Despite most of our effort being on the continental shelf, the presence of several deep canyons in addition to the shelf edge, resulted in all species being an average of less than 11 km from the 200 m depth contour. The average surface water temperature for species that were seen also varied and was likely both a function of distance from shore and association with upwelling areas (Table 9). Sea otters were seen in the coldest waters (12.6°C) where they are predominantly found. Among the more offshore species, humpback whales, tended to be seen in colder waters (13.9°C) than most other offshore species, probably because of their association with offshore upwelling areas.

Discussion

Although humpback whales were the most abundant large cetacean seen in our study, their numbers of a few hundred still appear to be substantially lower than numbers found prior to whaling. Commercial hunting of humpback whales occurred in the 1900s from coastal whaling stations in northern California, Washington, and British Columbia. In these areas, thousands of humpback whales were killed over a relatively short time period (less than 10 years) before catches dropped precipitously with the depletion of the population. At the south end of our study area, 1933 humpback whales were taken from a station at Bay City (in Grays Harbor), Washington, from 1911 to 1925 (Scheffer and Slipp, 1948). To the north, 5638 humpback whales were taken from British Columbia stations from 1908 to 1967, of which 60% (3393) were taken from 1908 to 1917 from the two southernmost whaling stations on Vancouver Island closest to our study area (Gregr et al., 2000; Nichol et al., 2002). Additionally, 1871 humpback whales were taken from two stations in northern California from 1919 to 1926 (Clapham et al., 1997). Although these hunts encompassed areas larger than our study area, the number killed in short periods dwarfs even the sum of our abundance estimates for Washington and British Columbia and the estimate of under 1000 whales estimated in the 1990s for California, Oregon, and Washington (Calambokidis and Barlow, 2004). Moreover, humpback whales have not returned to some of the areas where they were once found prior to commercial

whaling; humpback whales were commonly observed in the inside waters of Washington and British Columbia (Scheffer and Slipp, 1948; Webb, 1988) and have not returned to these areas in any numbers (Calambokidis and Steiger, 1990).

The distribution of humpback whales within our study area was not uniform and indicated that some specific areas were important feeding habitat for this recovering species. The region between the Juan de Fuca Canyon and the shelf edge (the Prairie)—the mouth of Barkley Canyon and Swiftsure Bank—was the area where humpback whales were concentrated. In monthly aerial surveys in 1989–90 by Green et al.,[5] there were only a total of 13 sightings of 25 humpback whales along the entire Washington coast between July and September. Over half of those sightings were in the Prairie area.

Our line-transect estimates revealed that about 100 humpback whales inhabit the northern Washington coast waters each summer; substantially more (over 500), however, were present in 2002. Although this is a small number compared to estimates of just under 1000 humpback whales for California, Oregon, and Washington (Calambokidis and Barlow, 2004), our study area encompasses a relatively small area and reflects a high density of animals. Additionally our line-transect estimates were not corrected for any missed animals; therefore they are probably biased slightly downward.

Despite the relatively high density of humpback whales in this region, the photographic identification data indicated that a relatively small number of individuals use the area consistently. Both the line-transect and the photographic identification data (increasing capture-recapture estimates, as well as decreased proportions of animals sighted multiple years) showed that the number of whales using this region has increased in recent years. The growing number of whales in this region could be either the result of births or immigration into this area. Births alone could not account for this increase, especially because the proportion of whales that were mothers with calves seen in this region was not high. There did not appear to be a shift in distribution of animals from areas to the south because interchange with those areas dropped from 1999 to 2002. The most likely explanation for these changes is that there was a shift of animals from feeding areas from the north into this region beginning in the late 1990s.

This interchange of humpback whales with feeding areas to the south provides new insight into the structure of humpback whale feeding aggregations. In a study that examined interchange rates of humpback whales along the west coast, Calambokidis et al. (1996) identified northern Washington as a demographic boundary between the whales feeding area along California, Oregon, and Washington and those to the north. The larger sample reported here shows the same general pattern of decreasing interchange with distance from a feeding area as that reported previously for whales off California (Calambokidis et al., 1996). The decreasing rate of interchange with distance among feeding areas does not allow for a clear demarcation between feeding areas, however, as suggested by Calambokidis et al. (1996). Although humpback whales demonstrate site fidelity to specific feeding locations, their feeding aggregations may not have clear boundaries and may occupy overlapping ranges.

The commercial whaling data also tended to support the existence of somewhat discrete feeding areas off the west coast of the United States and British Columbia. Commercial whaling resulted in the depletion of humpback whales off British Columbia by 1917, whereas the numbers taken off Washington and California did not decline until the mid-1920s (Scheffer and Slipp, 1948; Clapham et al., 1997; Gregr et al., 2000).

The relatively small proportion of mothers with calves identified in our study is consistent with findings off California and Oregon (Steiger and Calambokidis, 2000). Steiger and Calambokidis reported reproductive rates along the California, Oregon, and Washington coasts that are lower than those reported for other regions in southeastern Alaska and the North Atlantic (Clapham and Mayo, 1987, 1990; Baker et al., 1992; von Ziegesar et al., 1994). In aerial transect surveys, no humpback whale calves were seen among the 68 humpbacks observed off the Oregon and Washington coasts in 1989–90 (Green et al.[5]). If geographic segregation is occurring by humpback mothers and calves, as was suggested by Steiger and Calambokidis (2000), this northern region is not the area where mothers and calves are congregated. It is interesting to note, however, that mothers and calves were distributed around the periphery of the main feeding region—a finding that suggests that a more local segregation may be occurring. A bias in sampling would occur if large concentrations of whales are targeted and mother with calves feeding on the perimeter of these groups were underrepresented.

In contrast to humpback whales, no other large rorquals (blue, fin, or sei whales) were observed during any of our ship or small boat surveys. Likewise, these species were absent in other recent surveys of Washington waters (Wahl, 1977; Von Saunder and Barlow, 1999; Shelden et al., 2000; Green et al.[5]), although they were seen in surveys farther offshore in surveys in July 1994 (Thomason et al.[6]). Fin whales were common

[5] Green, G. A., J. J. Brueggeman, R. A. Grotefendt, and C. E. Bowlby. 1992. Cetacean distribution and abundance off Oregon and Washington, 1989–1990. *In* Oregon and Washington marine mammal and seabird surveys (J. J. Brueggeman, ed.), 100 p. Final report of OCS Study MMS 91-0093 by Ebasco Environmental, Bellevue, Washington, and Ecological Consulting, Inc., Portland, Oregon, for the Minerals Management Service, Pacific OCS Region, U.S. Dept. of Interior, 770 Paseo Camarillo, Camarillo, CA 93010.

[6] Thomason, J., M. Dahlheim, S. E. Moore, J. Braham, K. Stafford, and C. Fox. 1997. Acoustic investigations of large cetaceans off Oregon and Washington: NOAA ship *Surveyor* (21 July–1 August 1994), 27 p. Final report by the National Marine Mammal Laboratory, 7600 Sand Point Way NE F/AKC3, Seattle, WA 98115.

in Washington waters in the early 1900s when they were the second most commonly killed species by Bay City whalers (Scheffer and Slipp, 1948). Blue and sei whales were less common, although they were present historically (Scheffer and Slipp, 1948). Although Bay City whaling stations (in Grays Harbor, Washington) were closed after humpback whales were depleted, serial depletion of whale populations continued off British Columbia waters, beginning with humpback and blue whales, then with fin and sperm whales, and finally with sei whales (Gregr et al., 2000).

No sperm whales or beaked whales were seen during our surveys, although our study area did not include the deeper waters where we would expect to find these species. Most of the sperm whales (90%) seen by Green et al.[5] off Washington and Oregon were present in deeper offshore waters outside of our study area.

The other cetacean species not seen in our surveys that have been reported to occur off Washington historically included northern right whale (*Eubalaena japonica*), pygmy sperm whale (*Kogia breviceps*), false killer whale (*Pseudorca crassidens*), short-finned pilot whale (*Globicephala macrorhynchus*), and striped dolphin (*Stenella coeruleoalba*) (Scheffer and Slipp, 1948). Sightings of northern right whales throughout the eastern North Pacific are scarce; there have been only a small number of sightings since the 1960s (Brownell et al., 2001). Several of these sightings, however, have been off the northern Washington coast (Fiscus and Niggol, 1965; Osborne et al., 1988; Rowlett et al., 1994). The primary reason for the paucity of sightings in the eastern North Pacific in recent decades is due to the illegal take of 372 right whales in the early to mid-1960s by the USSR (Brownell et al., 2001; Doroshenko[7]).

Although some small cetacean species such as Pacific white-sided dolphins and Risso's dolphins were sighted frequently on our surveys, they were not as common as in some previous surveys (Green et al.[5]), probably because our coverage was concentrated in shallower waters inside the shelf break. In contrast to our findings of a number of species seen near the shelf edge, Wahl (1977) reported that most marine mammal species off central Washington tended to be in either inshore or in deeper offshore waters and only killer whales and Dall's porpoises regularly used the slope waters (13–45 km offshore).

It is difficult to make abundance estimates of Dall's porpoise because of their proclivity to approach ships (Buckland and Turnock, 1992). If they begin to approach the ship before the observer sights them, the estimate is biased upwards, which would be the case with our estimate. Our estimate would also have a downward bias because we did not attempt to adjust for animals missed even if they were on the track line.

All three types of killer whales (residents [both northern and southern], transients, and offshore type) were identified in the waters off northern Washington. These sightings are interesting because of concerns about killer whale populations, especially the southern resident community that has declined in recent years. Although killer whales have been intensely studied in inside waters of the Pacific Northwest, little has been known about their use of outside waters, where they may spend large portions of their lives. Little is known about the offshore type of killer whales, which is believed to be a distinct race of killer whale that has only recently been described. These whales are believed to be found usually in large groups along the continental shelf but also have been seen in inland waters (Ford et al., 1994; Dahlheim et al., 1997). All three sightings of the offshore form were just west of the Juan de Fuca canyon on the Prairie; the closest sighting to shore was 37 km (30 animals on 15 July 1997).

Acknowledgments

We are grateful to those who assisted with this study. This work was supported by the Olympic Coast National Marine Sanctuary and Southwest Fisheries Science Center (Jay Barlow, COTR). Many people contributed to this study. Jennifer Quan, Richard Rowlett, Anne Nelson, and Annie Douglas worked on the ship surveys. We thank the ship personnel on board the *McArthur* and *Agate Passage*. Researchers who helped with small boat work included Joe Evenson and Todd Chandler. Photographs of whales from this area were also contributed by L. Baraff, R. Baird, P. Bloedel, V. Deeke, P. Ellifrit, G. Ellis, J. Evenson, B. Gisborne, B. Halliday, H. Hunt, S. Mizroch, K. Rasmussen, J. Wilson and SWFSC researchers. Permission to survey in Canadian waters was given by the Dept. of Fisheries and Oceans. Lisa Schlender, Kristin Rasmussen, and Annie Douglas organized and conducted the photographic matching with the help of many interns at Cascadia Research. DKE and Graeme Ellis identified the killer whales; Oscar Torres assisted with the photographic matching. Data analyses and mapping were conducted with the help of Scot McQueen at ESRI and Tom Williams.

Literature cited

Baker, C. S., A. Perry, and L. M. Herman.
1992. Population characteristics of individually identified humpback whales in southeastern Alaska: summer and fall 1986. Fish. Bull. 90:429–437.

Barlow, J., C. W. Oliver, T. D. Jackson, and B. L. Taylor.
1988. Harbor porpoise, *Phocoena phocoena*, abundance estimate for California, Oregon and Washington: II. Aerial surveys. Fish. Bull. 86:433–444.

Bigg, M. A., G. M. Ellis, J. K. B. Ford, and K. C. Balcomb.
1987. Killer whales. A study of their identification, genealogy and natural history in British Columbia and

[7] Doroshenko, N. V. 2000. Soviet whaling for blue, gray, bowhead and right whales in the North Pacific Ocean, 1961–1979. *In* Soviet whaling sata (1949–1979), p. 96–103. Center for Russian Environmental Policy, Vavilov St. 26, Moscow 117071, Russia.

Washington State, 79 p. Phantom Press and Publishers, Nanaimo, British Columbia, Canada.

Bigg, M. A., P. F. Olesiuk, G. M. Ellis, J. K. B. Ford, and K. C. Balcomb III.
1990. Social organization and genealogy of resident killer whales (*Orcinus orca*) in the coastal waters of British Columbia and Washington State. Rep. Int. Whal. Comm. (spec. issue 12):383–405.

Black, N. A., A. Schulman-Janiger, R. L. Ternullo, and M. Guerrero-Ruiz.
1997. Killer whales of California and western Mexico: a catalog of photo-identified individuals. NOAA Tech. Memo. NOAA-TM-NMFS-SWFSC-247, 174 p.

Brownell, R. L., Jr., P. J. Clapham, T. Miyashita, and T. Kasuya.
2001. Conservation status of North Pacific right whales. J. Cet. Res. Manag. (spec. issue 2):269–286.

Buckland, S. T., and B. J. Turnock.
1992. A robust line transect method. Biometrics 48:901–909.

Calambokidis, J., and J. Barlow.
2004. Abundance of blue and humpback whales in the eastern North Pacific estimated by capture-recapture and line-transect methods. Mar. Mamm. Sci. 20:63–85.

Calambokidis, J., J. C. Cubbage, G. H. Steiger, K. C. Balcomb, and P. Bloedel.
1990. Population estimates of humpback whales in the Gulf of the Farallones, California. Rep. Int. Whal. Commn (spec. issue 12):325–333.

Calambokidis, J., J. D. Darling, V. Deeke, P. Gearin, M. Gosho, W. Megill, C. M. Tombach, D. Goley, C. Toropova, and B. Gisborne.
2002. Abundance, range and movements of a feeding aggregation of gray whales (*Eschrichtius robustus*) from California to southeastern Alaska in 1998. J. Cet. Res. Manag. 4:267–276.

Calambokidis, J., and G. H. Steiger.
1990. Sightings and movements of humpback whales in Puget Sound, Washington. Northwestern Nat. 71:45–49.

Calambokidis, J., G. H. Steiger, J. R. Evenson, K. R. Flynn, K. C. Balcomb, D. E. Claridge, P. Bloedel, J. M. Straley, C. S. Baker, O. von Ziegesar, M. E. Dahlheim, J. M. Waite, J. D. Darling, G. Ellis, and G. A. Green.
1996. Interchange and isolation of humpback whales off California and other North Pacific feeding grounds. Mar. Mamm. Sci. 12:215–226.

Calambokidis, J., G. H. Steiger, K. Rasmussen, J. Urbán R., K. C. Balcomb, P. Ladrón de Guevara P., M. Salinas Z., J. K. Jacobsen, C. S. Baker, L. M. Herman, S. Cerchio, and J. D. Darling.
2000. Migratory destinations of humpback whales that feed off California, Oregon and Washington. Mar. Ecol. Prog. Ser. 192:295–304.

Clapham, P. J., and C. A. Mayo.
1987. Reproduction and recruitment of individually identified humpback whales, *Megaptera novaeangliae*, observed in Massachusetts Bay, 1979–85. Can. J. Zool. 65:2852–2863.
1990 Reproduction of humpback whales (*Megaptera novaeangliae*) observed in the Gulf of Maine. Rep. Int. Whal. Comm. (spec. issue 12):171–175.

Clapham, P. J., S. Leatherwood, I. Szczepaniak, and R. L. Brownell, Jr.
1996. Catches of humpback and other whales from shore stations at Moss Landing and Trinidad, California, 1919–1926. Mar. Mamm. Sci. 13:368–394.

Dahlheim, M. E., D. K. Ellifrit, J. D. Swenson.
1997. Killer whales of southeast Alaska: a catalogue of photo-identified individuals, 79 p. Day Moon Press, Seattle, WA.

Darling, J. D.
1984. Gray whales (*Eschrichtius robustus*) off Vancouver Island, British Columbia. *In* The gray whale, *Eschrichtius robustus* (M. L. Jones, S. Swartz, and S. Leatherwood, eds.), p. 267–287. Academic Press, Orlando, FL.

Fiscus, C. H., and K. Niggol.
1965. Observations of cetaceans off California, Oregon, and Washington. U.S. Fish and Wildl. Serv., Special Scientific Report-Fisheries 498, 27 p. U.S. Fish and Wildl. Serv., Washington, D.C.

Ford, J. K. B., G. M. Ellis, and K. C. Balcomb.
1994. Killer whales, 102 p. UBC Press, Vancouver, British Columbia.

Green, G. A., J. J. Brueggeman, R. A. Grotefendt, and C. E. Bowlby.
1995. Offshore distances of gray whales migrating along the Oregon and Washington coasts, 1990. Northwest Sci. 69:223–227.

Gregr, E. J., L. Nichol, J. K. B. Ford, G. Ellis, and A. W. Trites.
2000. Migration and populations structure of northeastern Pacific whales off coastal British Columbia: an analysis of commercial whaling records from 1908–1967. Mar. Mamm. Sci. 16:699–727.

Hammond, P. S.
1986. Estimating the size of naturally marked whale populations using capture-recapture techniques. Rep. Int. Whal. Comm. (spec. issue 8):253–282.

Huelsbeck, D. R.
1988. Whaling in the precontact economy of the central northwest coast. Arctic Anthropol. 25:1–15.

Jameson, R. J., K. W. Kenyon, S. Jeffries, and G. R. VanBlaricom.
1986. Status of a translocated sea otter population and its habitat in Washington. Murrelet 67:84–87.

Jameson, R. J., K. W. Kenyon, A. M. Johnson, and H. M. Wright.
1982. History and status of translocated sea otter populations in North America. Wildl. Soc. Bull. 10:100–107.

Jeffries, S., H. Huber, J. Calambokidis and J. Laake.
2003. Trends and status of harbor seals in Washington State: 1978–1999. J. Wildl. Manag. 67:201–219.

Kvitek, R. G., P. J. Iampietro, and C. E. Bowlby.
1998. Sea otters and benthic prey communities: a direct test of the sea otter as keystone predator in Washington state. Mar. Mamm. Sci. 14:895–902.

Kvitek, R. G., J. S. Oliver, A. R. DeGange, and B. S. Anderson.
1992. Sea otters and benthic prey communities in Washington State. Mar. Mamm. Sci. 5:266–280.

Nichol, L. M., E. J. Gregr, R. Flinn, J. K. B. Ford, R. Gurney, L. Michaluk, and A. Peacock.
2002. British Columbia commercial whaling catch data 1908 to 1967: a detailed description of the B.C. historical whaling database. Can. Tech. Rep. Fish. Aquat. Sci. 2396, vii +76 p.

Osborne, R., J. Calambokidis, and E. M. Dorsey.
1988. A guide to marine mammals of greater Puget Sound, 191 p. Island Publishers, Anacortes, WA.

Osmek, S., J. Calambokidis, J. Laake, P. Gearin, R. DeLong, S. Jeffries, and R. Brown.
1996. Assessment of the status of harbor porpoises (*Pho-*

coena phocoena) in Oregon and Washington waters. U.S. Dep. of Commerce, NOAA Tech. Memo., NMFS-AFSC-76, 46 p.

Rowlett, R. A., G. A. Green, C. E. Bowlby, and M. A. Smultea.
1994. The first photographic documentation of a northern right whale off Washington State. Northwestern Nat. 75:102–104.

Scheffer, V. B., and J. W. Slipp.
1948. The whales and dolphins of Washington State with a key to the cetaceans of the west coast of North America. Am. Midl. Nat. 39:257–337.

Seber, G. A. F.
1982. The estimation of animal abundance and related parameters, 2nd ed., 654 p. Griffin, London.

Shelden, K. E. W., D. J. Rugh, J. L. Laake, J. M. Waite, P. J. Gearin, and T. R. Wahl.
2000. Winter observations of cetaceans off the northern Washington coast. Northwestern Nat. 81:54–59.

Steiger, G. H., and J. Calambokidis.
2000. Reproductive rates of humpback whales off California. Mar. Mamm. Sci. 16:220–239.

Swan, J. G.
1868. The Indians of Cape Flattery, 109 p. Shorey Publications, Seattle, WA.

Von Saunder, A., and J. Barlow.
1999. A report of the Oregon, California and Washington line-transect experiment (ORCAWALE) conducted in West Coast waters during summer/fall 1996. NOAA Tech. Memo. NOAA-TM-NMFS-SWFSC-264, 49 p.

von Ziegesar, O., E. Miller, and M. E. Dahlheim.
1994. Impacts of humpback whales in Prince William Sound. *In* Marine mammals and the *Exxon Valdez* (T. R. Loughlin, ed.), p. 173–191. Academic Press, San Diego, CA.

Wahl, T. R.
1977. Sight records of some marine mammals offshore from Westport, Washington. Murrelet 58:21–23.

Webb, L. W.
1988. On the Northwest. Commercial whaling in the Pacific Northwest 1790–1967, 425 p. Univ. British Columbia Press, Vancouver, Canada.

Reproductive biology of male franciscanas (*Pontoporia blainvillei*) (Mammalia: Cetacea) from Rio Grande do Sul, southern Brazil*

Daniel Danilewicz

Grupo de Estudos de Mamíferos Aquáticos do Rio Grande do Sul (GEMARS)
Rua Felipe Neri, 382/203
Porto Alegre 90440-150, Brazil
Present address: Laboratório de Dinâmica Populacional–Pontificia Universidade Católica do Rio Grande do Sul (PUCRS)
Av. Ipiranga, 6681
Porto Alegre 90619-900, Brazil
Email address (for D. Danilewicz): Daniel.Danilewicz@terra.com.br

Juan A. Claver

Alejo L. Pérez Carrera

Area Histología y Embriología Facultad de Ciencias Veterinarias
Universidad de Buenos Aires
Ar. Chorroarín 280 C1427CWO
Buenos Aires, Argentina

Eduardo R. Secchi

Laboratório de Mamíferos Marinhos, Museu Oceanográfico "Prof. Eliézer C. Rios"
Fundação Universidade Federal do Rio Grande, Cx P. 379
Rio Grande 96200, Brazil

Nelson F. Fontoura

Laboratório de Dinâmica Populacional–Pontificia Universidade Católica do Rio Grande do Sul (PUCRS)
Av. Ipiranga, 6681
Porto Alegre 90619-900, Brazil

Abstract—The reproductive biology of male franciscanas (*Pontoporia blainvillei*), based on 121 individuals collected in Rio Grande do Sul State, southern Brazil, was studied. Estimates on age, length, and weight at attainment of sexual maturity are presented. Data on the reproductive seasonality and on the relationship between some testicular characteristics and age, size, and maturity status are provided. Sexual maturity was assessed by histological examination of the testes. Seasonality was determined by changes in relative and total testis weight, and in seminiferous tubule diameters. Testis weight, testicular index of maturity, and seminiferous tubule diameters were reliable indicators of sexual maturity, whereas testis length, age, length, and weight of the dolphin were not. Sexual maturity was estimated to be attained at 3.6 years (CI 95%=2.7–4.5) with the DeMaster method and 3.0 years with the logistic equation. Length and weight at attainment of sexual maturity were 128.2 cm (CI 95%=125.3–131.1 cm) and 26.4 kg (CI 95%=24.7–28.1 kg), respectively. It could not be verified that there was any seasonal change in the testis weight and in the seminiferous tubule diameters in mature males. It is suggested that at least some mature males may remain reproductively active throughout the year. The extremely low relative testis weight indicates that sperm competition does not occur in the species. On the other hand, the absence of secondary sexual characteristics, the reversed sexual size dimorphism, and the small number of scars from intrassexual combats in males reinforce the hypothesis that male combats for female reproductive access may be rare for franciscana. It is hypothesized that *P. blainvillei* form temporary pairs (one male copulating with only one female) during the reproductive period.

Manuscript submitted 4 October 2002 to the Scientific Editor's Office.

Manuscript approved for publication 18 May 2004 by the Scientific Editor.

Fish. Bull. 102:581–592 (2004).

The franciscana (*Pontoporia blainvillei*) is a small dolphin endemic to the coastal waters of the southwestern Atlantic Ocean. The distribution of this species ranges from Golfo Nuevo (42°35′S; 64°48′W), Chubut Province, Argentina (Crespo et al., 1998) to Itaúnas (18°25′S; 30°42′W), Espírito Santo, southeastern Brazil (Moreira and Siciliano, 1991) (Fig. 1).

The franciscana's coastal habitat makes it vulnerable to being caught as incidental catch in gill nets and trammel nets throughout most of the species range (e.g., Praderi et al., 1989; Corcuera et al., 1994; Secchi et al., 2003). Because of its vulnerability as bycatch, the franciscana has been considered the most impacted small cetacean in the southwestern Atlantic Ocean (Secchi et al., 2002). In the Rio Grande do Sul coast, southern Brazil, this species has been subject to an intense bycatch in gill nets for at least three decades (Moreno et al., 1997; Secchi et al., 1997; Ott, 1998; Ott et al., 2002). The annual mortality of franciscanas in this region was estimated to range from several hundred up to about a thousand individuals (Ott et al., 2002). Simulations

*Contribution 012 from the Grupo de Estudos de Mamíferos Aquáticos do Rio Grande do Sul (GEMARS), Rua Felipe Neri, 382/203, Porto Alegre 90440-150, Brazil.

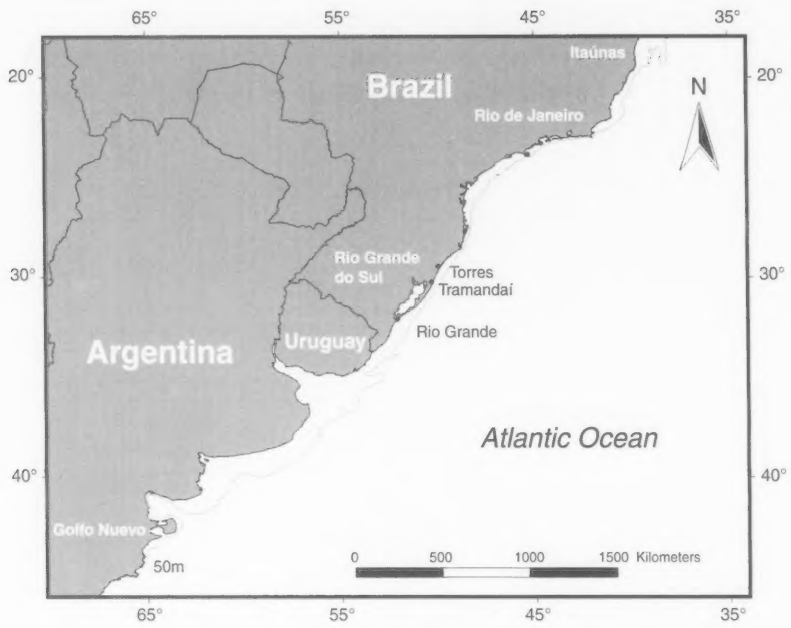

Figure 1

Map of the study area showing the locations along the southern coast of Brazil where franciscanas were caught as bycatch between 1992 and 1998.

studies on the effects of incidental captures on franciscanas in Rio Grande do Sul were carried out by using available data on vital rates, stock size, and bycatch estimates (e.g., Secchi, 1999; Kinas, 2002). All these studies showed that there is a decline in franciscana abundance in this region.

Although the reproductive biology of the female franciscanas have been studied in detail in Uruguay (Kasuya and Brownell, 1979; Harrison et al., 1981), Rio Grande do Sul (Danilewicz et al., 2000; Danilewicz, 2003), and Rio de Janeiro (Ramos, 1997), there are few data about male reproduction. Kasuya and Brownell (1979) presented information on male reproduction for Uruguay, although their small sample size precluded them from estimating age and size at attainment of sexual maturity.

In the Rio Grande do Sul coast, franciscanas are known to reproduce seasonally; births occur from October to early February (about 75% from October to December). Because the gestation period was estimated to last about 11.2 months, mating and conception may take place between November and early March (Danilewicz, 2003). Seasonal changes in testicular size and activity have been used to infer or corroborate mating seasons in some cetacean species (e.g., Neimanis et al., 2000). Nevertheless, it is not known if male franciscanas also undergo seasonal changes in the testicular activity.

In this study, we describe the reproductive biology of male franciscanas from Rio Grande do Sul and present evidences for the species' mating system.

Materials and methods

Sampling procedures

Data and samples collected from 121 specimens incidentally caught (88%) or beached (12%) along the Rio Grande do Sul coast between 1992 and 1998 were used for the analysis on reproduction of male franciscanas. The sampling of the incidentally caught animals was carried out through the monitoring of the commercial fishery fleet from Rio Grande (32°08′S; 52°05′W) and Tramandaí/Imbé (29°58′S, 50°07′W). Stranded dolphins were sampled from systematic beach surveys conducted in an area with an extension of 270 km of sandy beaches, between Torres (29°19′S, 49°43′W) and Lagoa do Peixe (31°15′S, 50°54′W).

Not all information could be collected from each carcass; therefore sample sizes varied among parameters. Standard length (SL, n=118) was measured by following the guidelines established by the American Society of Mammalogy (1961). The animals were weighed (n=97) and teeth were extracted and preserved dried or in a 1:1 mix of glycerin and alcohol (70%). Testes and epididymis were removed and fixed in 10% formalin.

Age determination

Age was estimated by counting the growth layer groups (GLGs) in thin, longitudinal sections of teeth (n=47). The teeth were decalcified in nitric acid or in RDO

(a commercial mixture of acids) and sectioned on a freezing microtome. The 15–20 μm sections were stained with Mayer's hematoxylin and mounted on microscope slides with Canadian balsam or in glycerin. Poor and off-center sections were discarded in favor of new preparations. Three readers counted independently the number of growth layer groups in both the dentine and cementum. When reader estimates differed, the sections were reexamined together and a best estimate was agreed upon. In this study, we considered one GLG to represent one year of age, which is the accepted model for the franciscana (Kasuya and Brownell, 1979; Pinedo, 1991; Pinedo and Hohn; 2000).

Reproduction

In the laboratory, the testes were separated from the epididymis, weighed to the nearest 0.01 g (n=107), and measured in three dimensions (length and two diameters perpendicular to each other in the middle of the testis) to the nearest 0.1 mm (n=104). The mean of these two diameters was called mean testis diameter. The weight of one of the gonads could not be recorded on some occasions (n=8) and we assumed that both testes had the same weight. Then, relative testis weight was determined as the ratio of the combined testis weight to the animal weight.

A 1-cm^3 subsample of each testis from the central portion of the organ was removed and examined by using standard histological preparations. The tissue was embedded in paraffin, sectioned in 4–10 μm thick slides through a manual microtome, and stained with hematoxylin and eosin (H&E). Male sexual maturity status was determined by examining the testicular sections at a magnification of 100×. In this study, we followed the classification criteria suggested by Hohn et al. (1985):

1 Immature—seminiferous tubules containing mainly spermatogonias. Abundant interstitial tissue present between the seminiferous tubules and lumen totally closed.
2 Pubertal—seminiferous tubules containing spermatogonias and spermatocytes. Less interstitial tissue present between the seminiferous tubules than in immature animals. The lumen is partially opened.
3 Mature—seminiferous tubules containing spermatogonias, spermatocytes, spermatids and, in many cases, spermatozoa. Interstitial tissue almost nonexistent between the seminiferous tubules. The lumen is totally opened.

The diameters of ten random circular seminiferous tubules were measured for each specimen (n=93) with a scale present in the lens of the microscope in order to calculate the seminiferous tubule mean diameter. A maturity index (MI) was calculated as the ratio of the combined testes weight by the combined testes length ($\Sigma W/\Sigma L$).

An analysis of the variation along the year of the values of relative and combined testes weight, and seminiferous tubule mean diameter, was employed to assess reproductive seasonality. Values of these parameters were compared between months when mating and conception occur ("reproductive months": November–March) and months when they not occur ("nonreproductive months": April–October). In order to increase the sample size of mature animals collected in reproductive months, data on testes weight from mature male franciscanas from Uruguay were included in the analysis (data supplied by Kasuya[1]).

The mean age at attainment of sexual maturity (ASM) was estimated through the DeMaster (1978) method and the logistic regression.

The DeMaster (1978) equation computes the mean as

$$ASM = \sum_{a=j}^{k} a(f_a - f_{a-1}),$$

where f_a = the fraction of sexually mature animals in the sample with age a;
j = the age of the youngest sexually mature animal in the sample; and
k = the age of the oldest sexually immature animal in the sample.

The variance of the DeMaster method estimate is calculated as

$$\mathrm{var}(ASM) = \sum_{a=j}^{k} \left[(f_a(1-f_a)/N_a - 1) \right],$$

where N_a = the total number of animals aged a.

The logistic regression approach fits a sigmoid curve representing the probability that a franciscana of age a is sexually mature to the distribution of sexually mature and immature animals by age as

$$Y = 1/(1+e^{a+bx}) \quad \text{or} \quad \ln(1/Y-1) = a + bx,$$

where x = the age of the dolphin;
b = the slope of the regression; and
a = the intercept.

To obtain the age when 50% of the animals are sexually mature (Y=0.5), the last equation is simplified as $ASM = -a/b$.

Mean length and weight at sexual maturity was also estimated by the DeMaster (1978) method, by substituting age for length and weight, respectively. The method was slightly modified, as suggested by Ferrero and Walker (1993), and was calculated as

[1] Kasuya, T. 1970–73. Unpubl. data. Teikyo University of Science and Technology. Uenohara, Yamanashi Prefecture, 409-0193, Japan.

$$LSM = \sum_{C\min}^{C\max} L(f_t - f_{t-1}),$$

where $Cmax$ = the length or weight class of the largest or heaviest sexually immature animal;
$Cmin$ = the length or weight class of the smallest or lightest sexually mature animal;
L = the lower value of the length or weight class t; and
f_t = fraction of mature animals in the length or weight class t.

The specimens were pooled into length and weight intervals of 4 cm and 4 kg, respectively.

The estimated variance of this method is also modified and is calculated as

$$\mathrm{var}(MS) = w^2 \sum_{C\min}^{C\max} \left[(f_i(1-f_i)/N_i - 1 \right],$$

where N_i = the number of specimens in the length or weight class t; and
w = the interval width, a constant equal to 4 in these cases.

For estimating age, length, and weight at sexual maturity, pubertal animals were grouped together with immature animals.

Results

The weight and length of the left testes ranged from 0.23 to 10.42 g ($\bar{x}$=2.60 g) and from 15.7 to 59.7 mm ($\bar{x}$=33.6 mm), respectively. The weight and length of the right testes ranged from 0.17 to 9.98 g ($\bar{x}$=2.62 g) and from 17.9 to 60.0 mm ($\bar{x}$=34.5 mm), respectively. The relationship of testes weight and testes length resulted in significant regression (P<0.0001) and correlation (r^2=0.91; F=823.9; P<0.0001; y=0.000012$x^{3.33}$). The male with the heaviest relative testes weight was 141.6 cm in length and 31.2 kg in weight, and its combined-testes weight was 20.1 g, which is 0.064% of its total weight. The mean of the relative testes weight from 23 mature males was 0.036% of their total weight.

The testes of the franciscana are characterized by a high lateral symmetry. There was no statistically difference in weight (t=−0.09; P=0.93; n=71) and length (t=−0.4; P=0.69; n=100) between testes of the same animal. A strong correlation was found between left and right testes length (b=0.95; F=1073.0; r^2=0.92; P<0.0001; n=100; y=1.232 $x^{0.95}$) and between left and right testes weight (b=0.99; F=7262.8; r^2=0.99; P<0.0001; n=71; y=1.02$x^{1.0}$), where x and y represent values of the left and right testis, respectively.

Seminiferous tubule diameter

A nonlinear regression demonstrated positive allometry (b>0.333) of the seminiferous tubule diameter to the combined testicular weight (b=0.39; 95% CI=0.35–0.44) (Fig. 2), and a strong correlation between these two variables (F=343.6; r^2=0.86; P<0.0001; y=59.4$x^{0.39}$).

The relationship between the seminiferous tubule diameter and testes length is shown in Figure 3 and the relationship between the seminiferous tubule diameter and standard length is shown in Figure 4. In immature males, there was almost no increase in the seminiferous tubule diameter with the increase of standard length (0.26 μm/cm) and total weight (0.5 μm/kg). In mature males, however, seminiferous tubule diameter was significantly correlated with standard length (b=1.06; F=4.4; r^2=0.18; P=0.048; y=1.4775x−43.572) and there was no correlation with total weight (b=0.23; F=1.28; r^2=0.07; P=0.27; y=1.6132x+108.54).

The differences of the seminiferous tubule mean diameters were statistically significant between immature, pubertal, and mature male franciscanas (ANOVA, Fs=255.4; df=87; P<0.001).

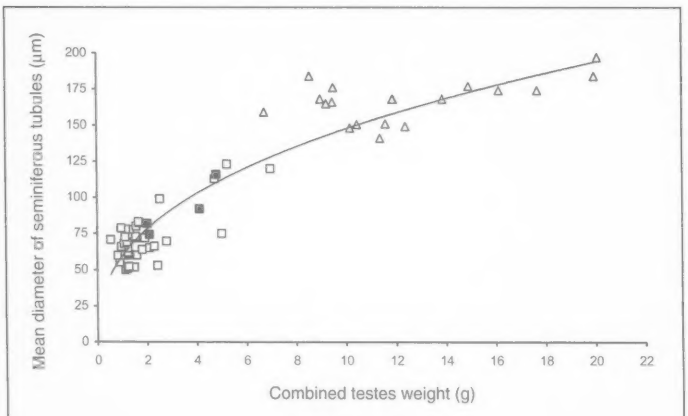

Figure 2

Relationship between combined-testes weight and mean seminiferous tubule diameter in immature (open boxes), pubertal (filled boxes), and mature (triangles) male franciscanas (*Pontoporia blainvillei*) from Rio Grande do Sul (n=59).

Combined-testes weight and length, and sexual maturity

There was almost no increment in mass of the combined-testes weight in immature dolphins. An increment of only about 2.0 g in the combined-testes mass was observed in animals of 70.0 to 125.0 cm in length. For dolphins about 120.0–130.0 cm in length, the combined-testes mass suddenly increased (Fig. 5), indicating the

attainment of sexual maturity. The rate of testes-mass gain was 0.05 g/cm for immature and 0.28 g/cm for mature dolphins. All animals with combined-testes weight higher than 5.0 g were sexually mature, and this finding may indicate that this parameter can be used as a reliable indicator of sexual maturity in male franciscanas from Rio Grande do Sul (Table 1). However, the large variation in testes weight after the attainment of sexual maturity precludes a correlation between testes mass and standard length.

Although testes length increases progressively as standard length increases (Fig. 6), there is no abrupt increase in testes length at the moment of attainment of sexual maturity, as observed in the testes mass. A nonlinear regression (exponential) best fits this relationship (y=4.5444 e0.0163x). As opposed to testes mass, there is a considerable overlap in the values of testes length of immature, pubertal, and mature franciscanas (Table 1), which makes testes length a less reliable predictor of sexual maturity than testes mass.

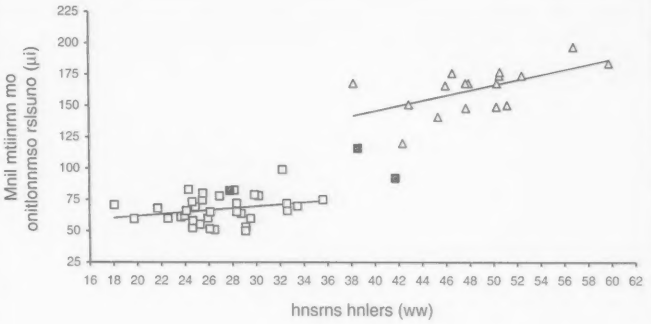

Figure 3

Relationship between testes length and mean diameter of seminiferous tubules in immature (open boxes), pubertal (filled boxes), and mature (triangles) male franciscanas (*Pontoporia blainvillei*) in Rio Grande do Sul (n=54). Data from pubertal animals are not included in the curves.

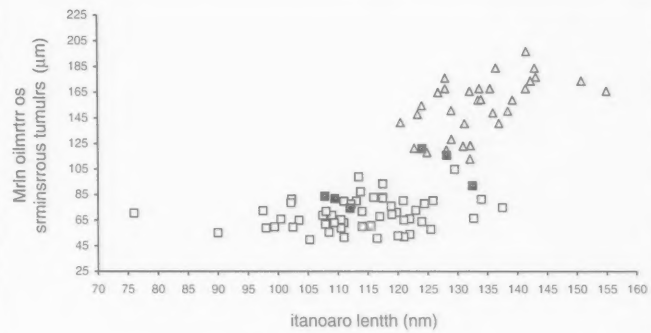

Figure 4

Relationship between standard length and mean diameter of seminiferous tubules in immature (open boxes), pubertal (filled boxes), and mature (triangles) male franciscanas (*Pontoporia blainvillei*) in Rio Grande do Sul (n=91).

Age, length, and weight at sexual maturity

Forty-seven specimens in the sample provided information on age and reproductive status (35 immature or pubertal, and 12 mature). The oldest immature animal was 5 years old and the youngest mature was 2 years old (Table 1). Average age at attainment of sexual maturity was estimated to be 3.6 years by the DeMaster method (SD=0.47; 95% CI =2.7–4.5) and 3.0 years by the logistic equation $Y = 1/(1+e^{0.74-2.23x})$. The age structure of the sample studied is presented in Figure 7.

Sexual maturity in relation to standard length was estimated for 110 males. The smallest mature and the largest immature males were 120.5 and 137.5 cm long, respectively. The average length at sexual maturity was 128.2 cm (SD=1.49; 95% CI=125.3–131.1 cm). Sexual maturity in relation to total weight was estimated for 90 males. The lightest mature and the heaviest immature males were 20.3 and 29.7 kg, respectively. The average weight at sexual maturity was 26.4 kg (SD=0.88; 95% CI=24.7–28.1 kg).

Index of testicular maturity

The differences of the mean index of testicular maturity between immature (0.03), pubertal (0.04), and mature (0.11) dolphins were statistically significant (ANOVA, Fs=210.0 df=101, P<0.001). There was almost no overlap in the values of this index between mature specimens and immature and pubertal specimens (Table 1). All males with an index value higher than 0.07 were sexually mature. These results indicate that the index of testicular maturity is a very good indicator of sexual maturity for franciscanas.

Reproductive seasonality

The null hypothesis that the combined and relative testis weight would be higher in the months when the females are reproductively active is rejected. No increase in the testes weight was observed during the months when most mating occurs (Fig. 8). There were no statistically significant differences in the combined-testes weight (ANOVA, Fs=2.28; df=34; P=0.48; n=35) and relative

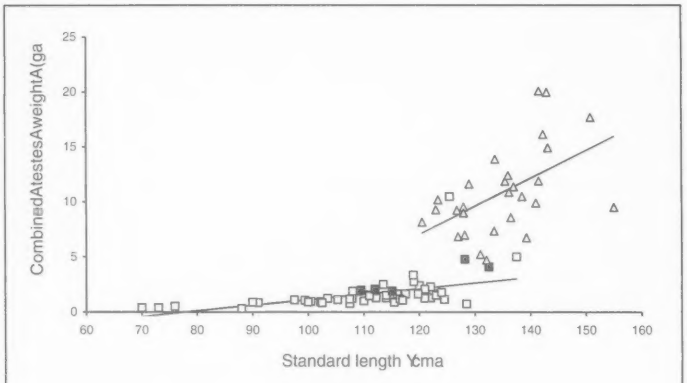

Figure 5

Relationship between standard length and combined-testes weight in immature (open boxes), pubertal (filled boxes), and mature (triangles) male franciscanas (*Pontoporia blainvillei*) in Rio Grande do Sul (n=79). Data from pubertal animals are not included in the curves.

testes weight (ANOVA, Fs=2.42; df=29; P=0.76; n=30) between reproductive and nonreproductive months.

The analyses of the variation in the diameter of the seminiferous tubules throughout the year also did not indicate that the testes undergo seasonal changes. However, it is important to view this result with caution because the sample size of mature males (and therefore the information on tubules diameter collected in reproductive months) was small (n=3). However, the presence of spermatids or spermatozoa (or both) in the seminiferous tubules may be also regarded as a direct evidence of testicular activity. Three mature males (11%) in the sample presented seminiferous tubules with spermatids or spermatozoa (or both) and were collected in nonreproductive months (May, June, and August). Although the epididymis of

Table 1

Summarized information on age, length, mass, and testicular characteristics for male franciscanas (*Pontoporia blainvillei*) in the Rio Grande do Sul at different sexual maturity stages.

Characteristics and maturity state	n	Mean	Standard deviation	Range
Age (years)				
Immature	31	1.29	1.01	0–5
Pubertal	4	2.0	0.82	1–3
Mature	12	3.8	1.14	2–6
Standard length (cm)				
Immature	62	111.2	13.62	70.0–137.5
Pubertal	7	118.5	9.75	107.8–132.5
Mature	37	133.7	7.71	120.5–155.0
Total mass (kg)				
Immature	53	19.0	5.6	4.95–29.7
Pubertal	6	21.4	4.62	17.1–28.0
Mature	30	29.9	5.22	20.25–41.5
Mean diameter of seminiferous tubules (μm)				
Immature	54	69.6	12.2	50.0–105.0
Pubertal	6	95.0	19.2	74.5–121.2
Mature	33	154.1	21.7	113.0–197.0
Combined testes mass (g)				
Immature	63	1.59	0.84	0.33–4.78
Pubertal	7	2.73	1.28	1.30–4.8
Mature	37	10.24	3.94	4.27–20.08
Testes length (mm)				
Immature	62	27.2	4.9	15.7–35.5
Pubertal	7	32.6	6.2	25.0–41.0
Mature	35	45.4	5.6	31.6–59.7
Index of testicular maturity				
Immature	61	0.03	0.01	0.01–0.06
Pubertal	7	0.04	0.01	0.02–0.06
Mature	36	0.11	0.03	0.05–0.18

a subsample of 10 mature males were examined histologically, we did not find any sign of spermatozoa.

Discussion

The high bilateral uniformity in testicular weight and length presented by the franciscana is a characteristic shared with many other cetacean species. Studies on the striped dolphin, *Stenella coeruleoalba* (Miyazaki, 1977), the common dolphin, *Delphinus delphis* (Collet and Saint Girons, 1984), the sperm whale, *Physeter macrocephalus* (Mitchell and Kozicki, 1984), and the dusky dolphin, *Lagenorhynchus obscurus* (van Waerebeek and Read, 1994), among others, demonstrate the same pattern of testis symmetry. Given the similar dimensions of both testes in franciscanas, it is possible to extrapolate the combined-testes weight by weighing only one testis without introducing bias in the analysis. It is recommended, however, that the weight of the testes should be presented without the epididymis weight, as it was presented in the most extensive comparative study on the subject (Kenagy and Trombulak, 1986).

There is a negative allometry of the seminiferous tubule diameter in relation to testis length, standard length, and total weight. This pattern is accentuated in immature males, in which the tubule diameters remain almost unchanged with the increase of the other variables. The lack of values for tubule diameters in the testes weight interval (2.5–6.0 g) and testes length interval (34–42 mm) just before the attainment of sexual maturity (Figs. 2 and 3) indicates that the increase in tubule size in relation to sexual maturity must occur very quickly, probably when the tubules are between 85 and 125 μm in diameter.

Attainment of sexual maturity

Length and weight at attainment of sexual maturity of male franciscanas in Rio Grande do Sul are very similar to those values estimated in previous estimates for Uruguay (Table 2). In contrast to the present study, Kasuya and Brownell (1979) calculated mean length at sexual maturity for Uruguay as the

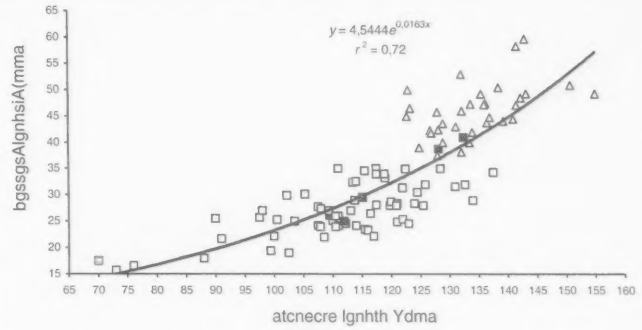

Figure 6

Relationship between standard length and testes length in immature (open boxes), pubertal (filled boxes), and mature (triangles) male franciscanas (*Pontoporia blainvillei*) in Rio Grande do Sul (n=99).

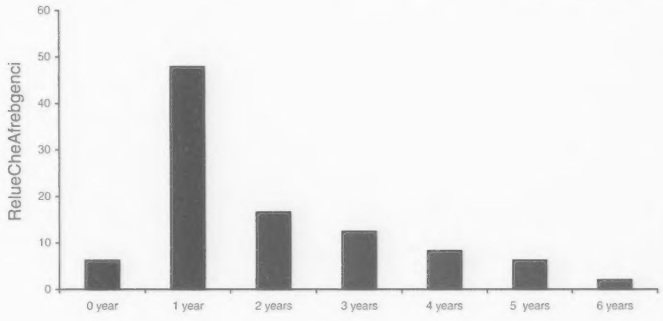

Figure 7

Age structure of male franciscanas (*Pontoporia blainvillei*) collected in Rio Grande do Sul (n=48).

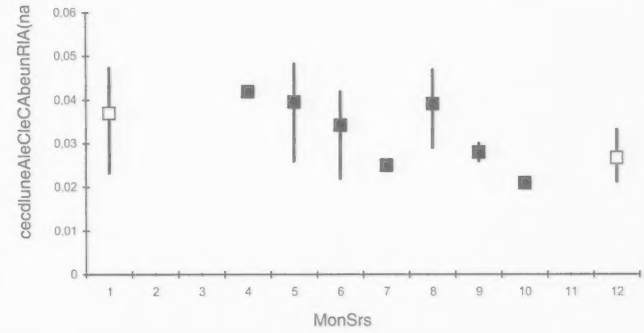

Figure 8

Relationship between month and relative testes weight in mature male franciscanas (*Pontoporia blainvillei*) (n=31) (1=January, 12=December; filled boxes=the nonreproductive months, open boxes=reproductive months). Bars indicate 25% and 75% percentiles.

Table 2

Comparison between average age, weight, and length at sexual maturity between male and female franciscanas from Rio Grande do Sul and Uruguay. The means of the animals from Rio Grande do Sul were estimated by using the DeMaster method (modified) and those from Uruguay were estimated by using a linear regression to determine the moment when 50% of the animals are mature.

	Rio Grande do Sul		Uruguay[1]	
	Males	Females[2]	Males	Females
Age	3.6	3.7	2–4	2.7
Weight (kg)	26.6	32.6	25.0–29.0	33.0–34.0
Length (cm)	127.4	138.9	131.4	140.3

[1] Data from Uruguay were compiled from Kasuya and Brownell (1979).

[2] Data from Danilewicz (2003).

length where 50% of the dolphins were mature through a linear regression. Applying this same approach, a LSM of 125.4 cm was estimated for Rio Grande do Sul—a value still very similar to the Uruguay estimate. Male franciscanas attain sexual maturity at less length and weight than do females in Rio Grande do Sul (Danilewicz, 2003), as observed previously in Uruguay (Kasuya and Brownell, 1979) and Rio de Janeiro (Ramos et al., 2000).

This is the first estimate of mean age at sexual maturity presented for male franciscanas. Kasuya and Brownell (1979) could not calculate ASM for Uruguay because of their small sample size (n=25). Nevertheless, Kasuya and Brownell suggested that sexual maturity is attained when males are between 2 and 4 years of age. Franciscanas from Rio de Janeiro were considered mature when they were older than 2 years of age and larger than 115.0 cm in length (Ramos et al., 2000). However, histological analysis of the testes was not performed and Ramos et al. employed indirect methods to determine sexual maturity. Nevertheless, despite the uncertainties produced by the use of different criteria to determine sexual maturity, it was evident that there was substantial difference in the size at maturity between males from Rio de Janeiro and those from Rio Grande do Sul and Uruguay. This difference is probably the result of the well-known distinct growth patterns of the franciscanas from these two regions (Pinedo, 1991) and does not necessarily reflect an early attainment of sexual maturity in males from the Rio de Janeiro population.

The trade-off between growth and reproduction is the best-documented phenotypic trade-off in nature (Stearns, 1992) and has been studied in a wide range of taxa. Because animals from Rio de Janeiro invest less in growth than do animals from Rio Grande do Sul, it is still an open question whether the franciscanas from the Rio de Janeiro have higher reproductive rates or start reproducing earlier than those from Rio Grande do Sul.

The oldest male and female franciscana ever aged were 16 and 21 years-old, respectively (Kasuya and Brownell, 1979; Pinedo, 1994). These ages contrasts with the age distribution found in the present study, where the oldest specimen analyzed was 6 years old. Similar to what is observed in catches for several other small cetacean species (e.g., Hector's dolphins—Slooten and Lad, 1991; harbor porpoise—Read and Hohn, 1995), a general feature of incidental catches for these species is the high entanglement rate of immature animals. In all fishing communities studied in Argentina, Uruguay, and Brazil, a large proportion (>50%) of the specimens caught were less than three years old (e.g., Kasuya and Brownell, 1979; Corcuera et al., 1994; Ott, 1998; Di Beneditto and Ramos, 2001). Although the precise reason for biased catch rates towards immature individuals is not well understood, it could be a combination of factors, including the imbalanced age-structure of local populations (where there are fewer older individuals because of an extensive history as bycatch) and a behavior-related higher vulnerability to bycatch for immature individuals (i.e., juveniles can be more inquisitive and have less ocean experience so that they rove into the area increasing the chances of being entangled). The typically low proportion of old animals in bycatches may explain the characteristics of the data used in this study.

Index of testicular maturity

An index of testicular maturity may be very useful in studies where it is necessary to know the sexual maturity of a large sample of animals without the need of histological analysis, which is time consuming and requires expertise. Although Hohn et al. (1985) recommended the investigation of the applicability of this indirect index of sexual maturity for male cetaceans, the research on this subject has shown no progress. To date, the index of sexual maturity has been calculated only for the common dolphin, *Delphinus delphis* (Collet and Saint Girons, 1984), and from the pantropical spotted dolphin, *Stenella attenuata* (Hohn et al., 1985). For both species, this index distinguished satisfactorily the mature from the immature and pubertal dolphins. Given the results presented, we also recommend the use of the index of testicular maturity as an alternative, nonhistological method, to determine the sexual maturity of male franciscanas. Males with index values lower than 0.05 can be safely classified as immature, and males with index values above 0.08 can be classified as mature. It is recommended that for animals with intermediate values their testes be analyzed histologically so that their reproductive status may be determined definitively.

Besides making intra- and inter-populational comparisons possible, the index of testicular maturity also permits interspecific comparisons because size differences between species are eliminated. The mean index of testicular maturity of mature franciscanas (0.12) is

considerably lower than mature pantropical spotted dolphins (1.9) (Hohn et al., 1985). This difference is a consequence of the relatively small increase of the testes weight of male franciscanas when sexual maturity is attained. Although male spotted dolphin show a marked increase of about 25-fold in testes weight at this moment, franciscanas show an increment in testes weight of about ninefold only.

Reproductive seasonality

The reproductive activities in male mammals are usually restricted to the periods when the females are in estrus (Lincoln, 1992). Reproductive seasonality in males has been reported for several cetacean species and populations through the identification of temporal variations in the testes weight and histological characteristics. In species where the reproductive period is restricted for a few months, as with the dusky dolphin (*Lagenorhynchus obscurus*) and the harbor porpoise (*Phocoena phocoena*), the testes weight presents marked fluctuations accompanying the reproductive period (Read, 1990; van Waerebeek and Read, 1994; Neimanis et al., 2000). Even in species with a diffuse reproductive period (i.e., with more than one peak for births per year) as in the case of dolphins of the genus *Stenella* in the tropical Pacific, it was possible to detect seasonal variation in the male reproductive rhythm (Perrin et al., 1976, Hohn et al., 1985).

Because of the known seasonality for births for franciscana (Kasuya and Brownell, 1979, Harrison et al., 1981, Danilewicz, 2003), it would be expected that the males would accompany the female rhythm, decreasing or even ceasing testicular activity in autumn and winter months. Kasuya and Brownell (1979) examined the seasonal change in testes weight in the months of January, June, and December. From our knowledge of the species' reproduction period, testes weight would be expected to be higher in December and January. However, the authors could not confirm this prediction and attributed the lack of seasonality to the small sample size of mature animals. Nevertheless, the lack of seasonality, even when the testes weight of the mature males from Rio Grande do Sul are included, may indicate what is occurring in the population, and not be a bias introduced by a small sample size.

In species that possess small testes, as in the case of the franciscana, the variation in the testicular activity may be better reflected by changes in the diameter of the seminiferous tubules and the rate of spermatogenesis rather than by changes in the testes weight. Nevertheless, the preliminary results about these characteristics (mature males with spermatids or spermatozoa [or both] in the seminiferous tubules in nonreproductive months and little monthly variation in the diameter of the seminiferous tubules) also do not support the hypothesis of a male reproductive seasonality. The combination of results presented here indicates that testicular activity is not completely interrupted in all males within the population, and that at least some of them may remain capable of fertilizing females during the year. This conclusion is supported by the observation of pregnancies outside the normal gestation season and that the births resulting from these pregnancies were estimated to take place in September and in late March (Danilewicz, 2003).

The hormone and sperm production by the testes during periods when the females are not able to reproduce may represent an unnecessary energetic expense by the male (Dewsbury, 1982) and may be an explanation for the period of reproductive inactivity for males of several mammal species. In species with large relative testes weight, the maintenance of high levels of sperm production in the testes is a considerable energetic cost for the individual. However, as discussed earlier, this is definitely not the case for the franciscana. For this reason, we suggest that the small energy investment in producing sperm all over the year, due to the small testicular mass, may be an evolutionary advantage for male franciscanas in case of the appearance of off-season reproductive females.

Franciscana reproductive strategy

Although important advances in the knowledge of franciscana behavior in the wild have been made (e.g., Bordino et al., 1999; Bordino, 2002), there is no information on the species' reproductive behavior and its mating strategy remains unknown. Relative testis weight, sexual size dimorphism, and secondary sexual characteristics may provide indirect clues regarding mating strategy in franciscana and are discussed below.

Relative testis weight In mammals, there is a functional relationship between relative testis weight and the species' mating system (Kenagy and Trombulak, 1986). Testes are relatively small in species presenting monogamy or extreme poliginy (several females + few males), i.e., where a male copulates with all females of a group or harem. Comparative studies have demonstrated that males tend to be larger than females and show secondary sexual characteristics in species presenting extreme poliginy. On the other hand, the relative testis weight is high and the sexual size dimorphism is reduced or nonexistent in species where several males copulate with only one estrus female (polyandry). In this case, the evolution for a large testis is attributed to the sperm competition in a system where different males attempt to fertilize the same female and where a higher copulatory frequency and higher levels of sperm production are required (Harcourt et al., 1981; Kenagy and Trombulak, 1986).

Using the data on 133 mammal species, Kenagy and Trombulak (1986) presented a function describing the relationship between body weight and combined-testes weight without epididymis. Applying their equation for the adult male franciscanas, we discovered that mature franciscanas have testes 3 to 12 times lighter than expected (mean=6 times) for a mammal of its body weight. Indeed, among the 133 species analyzed,

the relative testes weight of the franciscana is heavier than that of gorilla (*Gorilla gorilla*), humpback whales (*Megaptera novaeangliae*), and fin whales (*Balaenoptera physalus*), indicating that sperm competition does not occur in franciscanas.

Sexual size dimorphism Males are larger than females in most mammal species. Nevertheless, the reversed sexual size dimorphism (RSSD) (i.e., females are larger than males) is more common than previously thought and has been documented for 12 out of the 20 orders of mammals (Ralls, 1976, 1977). Among the odontocetes, four (Ziphidae, Pontoporiidae, Phocoenidae, and Delphinidae) out of the eight families present RSSD.

Although sexual selection may be the main reason why males are the larger sex in most mammal species, it has been systematically refused as an explanation in the cases where females are the larger sex (Ralls, 1976, 1977; Andersson, 1994). In species with RSSD, females do not mate with many males, they are not dominant, and are not more aggressive than males of the same species. Moreover, they do not show secondary sexual characteristics associated with intrasexual selection (e.g., horns in Artiodactyla and large canine teeth in Primates). Therefore, the occurrence of RSSD in mammals may be explained more satisfactorily by natural selection (Andersson, 1994).

Slooten (1991) proposed an interesting hypothesis for the occurrence of RSSD in cetaceans, suggesting that a minimum size may be necessary for a newborn cetacean to survive. In odontocetes, the smallest mean sizes at birth are about 70–80 cm. Because the size of the newborn is directly related to the size of the mother, in species of small dimensions the females would suffer a selective pressure to be a larger size, so that they could produce offspring with the minimum viable size. This hypothesis is reinforced by the fact that most of the odontocete species with RSSD (e.g., *Pontoporia blainvillei*, *Cephalorhynchus hectori*, *Cephalorhynchus commerssoni*, *Phocoena phocoena*, *Phocoena sinus*) are the smallest species within the group. Moreover, species presenting RSSD also have larger relative size at birth than the other species within the taxonomic group (Ralls, 1976).

The degree and direction of SSD (sexual size dimorphism) in mammals is the result of the difference of the sum of all selective pressures affecting the female's size and the sum of all selective pressures affecting the male's size (Ralls, 1976). Thus, it is very probable that more than one factor may act selectively on animals of both sexes in *Pontoporia*, molding the degree and direction of SSD. We propose that the requirement of a neonate minimum viable size (70–80 cm in length) is one of the main selective pressures acting on female franciscanas. It is important to emphasize that other factors may also be influencing SSD in franciscana, and in some species it was evident that different selective pressures could affect body size in opposing directions in males and females and in different age classes (Grant, 1986; Andersson, 1994). Among the factors that may be simultaneously acting on franciscana body size are intrinsic genetic and physiological limitations, and the requirement of maintaining an optimum size for the species' ecological niche.

Secondary sexual characteristics The presence and intensity of secondary sexual characteristics in males is a more precise indication of the degree of intrasexual selection than is body size (Andersson, 1994). In odontocete males, these characteristics are present in the form of "weapons," such as the tusk of the narwhal (*Monodon monoceros*) and the teeth in species of the genus *Grampus*, *Physeter*, *Berardius*, *Hyperoodon*, and *Mesoplodon* used in male-male combats (MacLeod, 1998). In species of these genus, the teeth were reduced in number, enlarged in size, and their form was modified (specially in males of Ziphiidae). The teeth of these species also lost their function in feeding because of a diet comprising almost exclusively cephalopods and were used uniquely in intrasexual combats. There is no evidence that the same evolutionary process occurred in male franciscanas because their teeth are very small and numerous (around 200), their diet is primarily fish, and the number of combat scars is apparently low. These characteristics support the hypothesis that male-male combat must be very rare or even nonexistent in franciscanas.

The sexual features presented in this study (extremely low testis weight, reversed sexual size dimorphism, absence of secondary sexual characteristics in males, and a low number of scars in males) indicate the absence of sperm competition in the franciscana, and these features differ drastically from those characteristics of odontocete species where males combat each other for copulation. This finding may indicate that franciscanas form temporary reproductive pairs during the reproductive period, where a male pairs and copulate with only one female. Recently, Valsecchi and Zanelatto (2003) provided molecular evidence suggesting that franciscanas may travel in kin groups that include mothers with their calves and the father of the youngest offspring. The authors also suggested that male franciscanas may prolong their bond with their reproductive partner, providing some form of paternal care. For a better understanding of franciscana social structure and mating system, the following suggestions are proposed: 1) an increase in the efforts of behavioral studies of free-ranging franciscanas; 2) quantification of the intraspecific teeth scars in franciscanas of different sexes and reproductive status in order to confirm the absence of intrassexual aggressions among males; 3) investigation of the relationship of relative testis weight, SSD, and reproductive strategies in cetaceans, by phylogenetic methods (see Harvey and Pagel, 1991) to understand the evolution of these characters in this group.

Acknowledgments

This study could not be made without the cooperation and friendship of the fishermen from Tramandaí/Imbé

and Rio Grande. Many people collaborated in the collection and necropsy of the dolphins, and the authors wish to thank Paulo Ott, Ignacio Moreno, Márcio Martins, Glauco Caon, Larissa Oliveira, Manuela Bassoi, Alexandre Zerbini, Luciana Möller, Luciano Dalla Rosa, Lilia Fidelix, and numerous volunteers for helping in this task. Gonad histology was partially done in Laboratório de Histologia e Embriologia Comparada of Universidade Federal do Rio Grande do Sul and we thank Sônia Garcia and Nívea Lothhammer for their instructions and encouragement on this subject. Paulo Ott, Enrique Crespo and Silvana Dans participated in the age determination procedures. Part of the age determination was also done in the Rio Grande and the first author thanks Cristina Pinedo and Fernando Rosas for their instruction. The authors also thanks Norma Luiza Würdig, Irajá Damiani Pinto (CECLIMAR-UFRGS), and Lauro Barcellos (Director of the Museu Oceanográfico) for their constant logistical support and for encouraging marine mammal studies in southern Brazil. Márcio Martins, Ignacio Moreno, Luiz Malabarba, and Mônica Muelbert reviewed an early draft of this paper. We wish to thank Renata Ramos and three anonymous reviewers for their suggestions regarding the manuscript. Financial support was given by Cetacean Society International, Fundação O Boticário de Proteção à Natureza, The MacCarthur Foundation, World Wildlife Fund, CNPq, UNEP, Yaqu Pacha Organization, and Whale and Dolphin Conservation Society. This paper is part of the first author's M.S. thesis, and The Coordenação de Aperfeiçoamento de Pessoal de Nível Superior (CAPES) has granted him a graduate fellowship. The Conselho Nacional de Desenvolvimento Científico e Tecnológico of the Brazilian Government (CNPq) has granted graduate fellowships to E.R. Secchi (Grant no. 200889/98-2).

Literature cited

American Society of Mammalogy.
1961. Standardized methods for measuring and recording data on the smaller cetaceans. J. Mamm. 42: 471–476.

Andersson, M.
1994. Sexual selection. Monographs in behavior and ecology, 599 p. Princeton Univ. Press. Princeton, NJ.

Bordino, P.
2002. Movement patterns of franciscana dolphin (*Pontoporia blainvillei*) in Bahia Anegada, Buenos Aires, Argentina. LAJAM (special issue) 1:71–76.

Bordino, P., G. Thompson, and M. Iñiguez.
1999. Ecology and behaviour of the franciscana (*Pontoporia blainvillei*) in Bahía Anegada, Argentina. J. Cetacean Res. Manag. 1 (2):213–222.

Collet, A., and H. Saint Girons.
1984. Preliminary study of the male reproductive cycle in common dolphins, *Delphinus delphis*, in the eastern North Atlantic. Rep. Int. Whal. Comm. (special issue) 6:355-360.

Corcuera, J., F. Monzon, E. A. Crespo, A. Aguilar, and J. A. Raga.
1994. Interactions between marine mammals and the coastal fisheries of Necochea and Claromecó (Buenos Aires Province, Argentina). Rep. Int. Whal. Comm. (special issue) 15:283–290.

Crespo, E. A., G. Harris, and R. González.
1998. Group size and distribution range of the franciscana, *Pontoporia blainvillei*. Mar. Mamm. Sci. 14 (4):845–849.

Danilewicz, D.
2003. Reproduction of female franciscana (*Pontoporia blainvillei*) in Rio Grande do Sul, southern Brazil. LAJAM 2 (2):67–78.

Danilewicz, D., E. R. Secchi., P. H. Ott, and I. B. Moreno.
2000. Analyses of the age at sexual maturity and reproductive rates of franciscanas (*Pontoporia blainvillei*) from Rio Grande do Sul, Southern Brazil. Comum. Mus. Ciênc. Tecnol. PUCRS 13(1):89–98.

DeMaster, D. P.
1978. Calculation of the average age of sexual maturity in marine mammals. J. Fish. Res. Board Can. 35 (6):912–15.

Dewsbury, D. A.
1982. Ejaculate cost and male choice. Am. Nat. 119: 601–610.

Di Beneditto, A. P. M., and R. M. A. Ramos.
2001. Biology and conservation of the franciscana (*Pontoporia blainvillei*) in the north of Rio de Janeiro State, Brazil. J. Cetacean Res. Manag. 3:185–192.

Ferrero R. C., and W. A. Walker.
1993. Growth and reproduction of the northern right whale dolphin, *Lissodelphis borealis*, in the offshore waters of the North Pacific Ocean. Can. J. Zool. 71 (12):2335–2344.

Grant, P. R.
1986. Ecology and evolution of Darwin's finches. Princeton Univ. Press, Princeton, NJ.

Harcourt, A. H., P. H. Harvey, S. G. Larson, and R. V. Short.
1981. Testis weight, body weight and breeding system in primates. Nature 293:55–57.

Harrison, R. J., M. M. Bryden, D. A. McBrearty, and R. L. Brownell Jr.
1981. The ovaries and reproduction in *Pontoporia blainvillei* (Cetacea: Platanistidae). J. Zool. 193:563–580.

Harvey, P., and M. Pagel.
1991. The comparative method in evolutionary biology, 239 p. Oxford series in ecology and evolution. Oxford Univ. Press, Oxford, England.

Hohn, A., S. J. Chivers, and J. Barlow.
1985. Reproductive maturity and seasonality of male spotted dolphins, *Stenella attenuata*, in the eastern tropical Pacific. Mar. Mamm. Sci., 1(4):273–293.

Kasuya, T., and R. L. Brownell Jr.
1979. Age determination, reproduction, and growth of the franciscana dolphin, *Pontoporia blainvillei*. Sci. Rep. Whales Res. Inst. 31:45–67.

Kinas, P. G.
2002. The impact of the incidental kills by gillnets on the franciscana dolphin (*Pontoporia blainvillei*) in southern Brazil. Bull. Mar. Sci. 70:409–421.

Kenagy , G. K., and S. C. Trombulak.
1986. Size and function of mammalian testes in relation to body size. J. Mamm. 67(1):1–22.

Lincoln, G. A.
1992. Biology of seasonal breeding in deer. *In* The biology of deer (R. D. Brown, ed.), p. 565–574. Springer-Verlag, New York, NY.

MacLeod, C.D.
1998. Intraspecific scarring in odontocete cetaceans: an indicator of male 'quality' in agressive interactions? J. Zool. 244:71–77.
Mitchell, E. D., and V. M. Kozicki.
1984. Reproductive condition of male sperm whales, *Physeter macrocephalus*, taken off Nova Scotia. Rep. Int. Whal. Comm. (special issue) 6:243–48.
Miyazaki, N.
1977. Growth and reproduction of *Stenella coeruleoalba* off the Pacific coast of Japan. Sci. Rep. Whales Res. Inst. 29:21–48.
Moreira, L. M., and S. Siciliano.
1991. Northward extension range for *Pontoporia blainvillei*, p. 8. Abs. Ninth Bienn. Conf. Biol. Mar. Mamm. Chicago, IL.
Moreno, I. B., P. H. Ott, and D. Danilewicz.
1997. Análise preliminar do impacto da pesca artesanal costeira sobre *Pontoporia blainvillei* no litoral norte do Rio Grande do Sul, sul do Brasil. *In* Proceedings of the second workshop for the research coordination and conservation of the franciscana (*Pontoporia blainvillei*) in the Southwestern Atlantic (M. C. Pinedo A. and Barreto, eds.), p. 31–41. Editora da FURG, Rio Grande, Rio Grande do Sul, Brazil.
Neimanis, A. S., A. J. Read, R. A. Foster, and D. E. Gaskin.
2000. Seasonal regression in testicular size and histology in harbour porpoises (*Phocoena phocoena*, L.) from the Bay of Fundy and Gulf of Maine. J. Zool. 250:221–229.
Ott, P. H.
1998. Análise das capturas acidentais da toninha, *Pontoporia blaivillei*, no litoral norte do Rio Grande do Sul, sul do Brasil. MSc. Thesis, 120 p. Pontifícia Universidade Católica do Rio Grande do Sul, Porto Alegre, Brazil.
Ott, P. H., E. R. Secchi, I. B. Moreno, I.B., D. Danilewicz, E. A. Crespo, P. Bordino, R. Ramos, A, P. Di Beneditto, C. Bertozzi, R. Bastida, R. Zanelatto, J. Perez, and P. G. Kinas.
2002. Report of the working group of fishery interactions. LAJAM (special issue) 1:55–64.
Perrin, W. F., J. M. Coe, and J. R. Zweifel.
1976. Growth and reproduction of the spotted porpoise, *Stenella attenuata*, in the offshore eastern tropical Pacific. Fish. Bull. 74:229–269.
Pinedo, M. C.
1991. Development and variation of the franciscana, *Pontoporia blainvillei*. Ph.D. diss., 406 p. Univ. California, Santa Cruz, CA.
1994. Impact of incidental fishery mortality on the age structure of *Pontoporia blainvillei* in southern Brazil and Uruguay. Rep. Int. Whal. Comm. (spec. issue 15):261–264.
Pinedo, M. C., and A. Hohn.
2000. Growth layer patterns in teeth from the franciscana, *Pontoporia blainvillei*: developing a model for precision in age estimation. Mar. Mamm. Sci. 16 (1):1–27.
Praderi, R., M. C. Pinedo, and E. A. Crespo.
1989. Conservation and management of *Pontoporia blainvillei* in Uruguay, Brazil and Argentina. *In* Biology and conservation of river dolphins (W. F. Perrin, R. L. Brownell, Z. Kaya, and L. Jiankang (eds.), p. 52–56. Allen Press, Lawrence, KS.
Ralls, K.
1976. Mammals in which females are larger than males. Q. Rev. Biol. 51:245–276.
1977. Sexual dimorphism in mammals: avian models and unanswered questions. Am. Nat. 111:917–937.
Ramos, R.
1997. Determinação de idade e biologia reprodutiva de *Pontoporia blainvillei* e da forma marinha de *Sotalia fluviatilis* no litoral norte do Rio de Janeiro. M.S. thesis, 95 p. Universidade Estadual do Norte Fluminense, Rio de Janeiro, Brazil.
Ramos, R., A. P. Di Beneditto, and N. R. W. Lima.
2000. Growth parameters of *Pontoporia blainvillei* and *Sotalia fluviatilis* (Cetacea) in northern Rio de Janeiro, Brazil. Aquat. Mamm. 26 (1):65–75.
Read, A.
1990. Reproductive seasonality in harbour porpoises, *Phocoena phocoena*, from the Bay of Fundy. Can. J. Zool. 68:284–288.
Read, A., and A. Hohn.
1995. Life in the fast lane: the life history of the harbour porpoises from the Gulf of Maine. Mar. Mamm. Sci. 11:423–440.
Secchi, E. R.
1999. Taxa de crescimento potencial intrínseco de um estoque de franciscanas, *Pontoporia blainvillei* (Gervais & D'Orbigny, 1846) (Cetacea, Pontoporiidae) sob o impacto da pesca costeira de emalhe. M.S. thesis, 152 p. Fundação Universidade Federal do Rio Grande, Rio Grande, do Sul, Brazil. [In Portuguese.]
Secchi, E. R., A. N. Zerbini, M. Bassoi, L. Dalla Rosa, L. M. Moller, and C. C. Rocha-Campos.
1997. Mortality of franciscanas, *Pontoporia blainvillei*, in coastal gillnetting in southern Brazil. Rep. Int. Whal. Comm. 47:653–658.
Secchi, E. R., Ott, P. H., and Danilewicz, D.
2002. Report of the fourth workshop for the coordinated research and conservation of the franciscana dolphin (*Pontoporia blainvillei*) in the western South Atlantic. LAJAM (special issue) 1:11–20.
2003. Effects of fishing bycatch and the conservation status of the franciscana dolphin, *Pontoporia blainvillei*. *In* Marine mammals: fisheries, tourism and management issues (N. Gales, M. Hindell, and R. Kirkwood, eds.), p. 174–191. CSIRO Publishing, Collingwood, Victoria, Australia.
Slooten, E.
1991. Age, growth, and reproduction in Hector's dolphins. Can. J. Zool. 69:1689–1700.
Slooten, E., and F. Lad.
1991. Population biology and conservation of Hector's dolphin. Can. J. Zool. 69:1701–1707.
Stearns, S. C.
1992. The evolution of life histories, 249 p. Oxford, Univ. Press, New York, NY.
Valsecchi, E., and R. C. Zanelatto.
2003. Molecular analysis of the social and population structure of the franciscana (*Pontoporia blainvillei*): conservation implications. J. Cetacean Res. Manag. 5(1):69–75.
Van Waerebeek, K., and A. Read.
1994. Reproduction of dusky dolphins, *Lagenorhynchus obscurus*, from coastal Peru. J. Mamm. 75 (4):1054–1062.

Red snapper (*Lutjanus campechanus*) demographic structure in the northern Gulf of Mexico based on spatial patterns in growth rates and morphometrics

Andrew J. Fischer
Coastal Fisheries Institute
School of the Coast and Environment
Louisiana State University
Baton Rouge, Louisiana 70803-7503
E-mail address: afische@lsu.edu

M. Scott Baker Jr.
Coastal Fisheries Institute
School of the Coast and Environment
Louisiana State University
Baton Rouge, Louisiana 70803-7503

Charles A. Wilson
Coastal Fisheries Institute and
Department of Oceanography and Coastal Sciences
School of the Coast and Environment
Louisiana State University
Baton Rouge, Louisiana 70803-7503

Abstract—Red snapper (*Lutjanus campechanus*) in the United States waters of the Gulf of Mexico (GOM) has been considered a single unit stock since management of the species began in 1991. The validity of this assumption is essential to management decisions because measures of growth can differ for nonmixing populations. We examined growth rates, size-at-age, and length and weight information of red snapper collected from the recreational harvests of Alabama (n=2010), Louisiana (n=1905), and Texas (n=1277) from 1999 to 2001. Ages were obtained from 5035 otolith sections and ranged from one to 45 years. Fork length, total weight, and age-frequency distributions differed significantly among all states; Texas, however, had a much higher proportion of smaller, younger fish. All red snapper showed rapid growth until about age 10 years, after which growth slowed considerably. Von Bertalanffy growth models of both mean fork length and mean total weight-at-age predicted significantly smaller fish at age from Texas, whereas no differences were found between Alabama and Louisiana models. Texas red snapper were also shown to differ significantly from both Alabama and Louisiana red snapper in regressions of mean weight at age. Demographic variation in growth rates may indicate the existence of separate management units of red snapper in the GOM. Our data indicate that the red snapper inhabiting the waters off Texas are reaching smaller maximum sizes at a faster rate and have a consistently smaller total weight at age than those collected from Louisiana and Alabama waters. Whether these differences are environmentally induced or are the result of genetic divergence remains to be determined, but they should be considered for future management regulations.

Manuscript submitted 6 May 2003
to the Scientific Editor's Office.

Manuscript approved for publication
19 April 2004 by the Scientific Editor.

Fish. Bull. 102:593–603 (2004).

Red snapper (*Lutjanus campechanus*) in the United States waters of the Gulf of Mexico (GOM) are heavily exploited by both recreational and commercial fishermen (Wilson and Nieland, 2001; Shirripa and Legault[1]). Harvest, however, has not proceeded without detrimental affects on the population. Commercial landings have declined substantially from 6048 metric tons (t) in 1964 to 1207 t in 1990; recreational landings exhibited similar declines from 1937 t in 1981 to 481 t in 1990 (NMFS[2]). In 1991, harvest restrictions including reef fish permits, seasonal fishing, fish quotas, creel limits, and minimum size limits were placed upon the red snapper fishermen by the Gulf of Mexico Fishery Management Council (GMFMC[3]) to increase the spawning potential ratio to 20%, which is indicative of recovery. These regulations have also been adopted for state waters in Alabama, Louisiana, and Texas. Despite the management actions, GOM red snapper remain overfished (Goodyear[4]; Schirripa and Legault[1]).

[1] Shirripa, M. J., and C. M. Legault. 1999. Status of the red snapper in the U. S. waters of the Gulf of Mexico: updated through 1998, 44 p. + appendices. Contribution rep. SFD-99/00-75 from Sustainable Fisheries Division, Miami Laboratory, Southeast Fisheries Science Center, National Marine Fishery Service, 75 Virginia Beach Drive, Miami, FL 33149-1099. [Not available from NTIS].

[2] NMFS (National Marine Fisheries Service). 2003. Fisheries Statistics and Economics Division. Website: www.nmfs.noaa.gov.

[3] GMFMC (Gulf of Mexico Fishery Management Council). 1991. Amendment 3 to the reef fishery management plan for the reef fish resources of the Gulf of Mexico, 38 p. Gulf of Mexico Fishery Management Council, 3018 N. U.S. Hwy 301 Suite 1000, Tampa, FL. 33619-2272. [Not available from NTIS].

[4] Goodyear, C. P. 1995. Red snapper in U.S. waters of the Gulf of Mexico. Stock assesment report MIA-95/96-05, 171 p. Miami Laboratory, Southeast Fisheries Science Center, National Marine Fisheries Service, 75 Virginia Beach Dr., Miami, FL, 33149-1099. [Not available from NTIS].

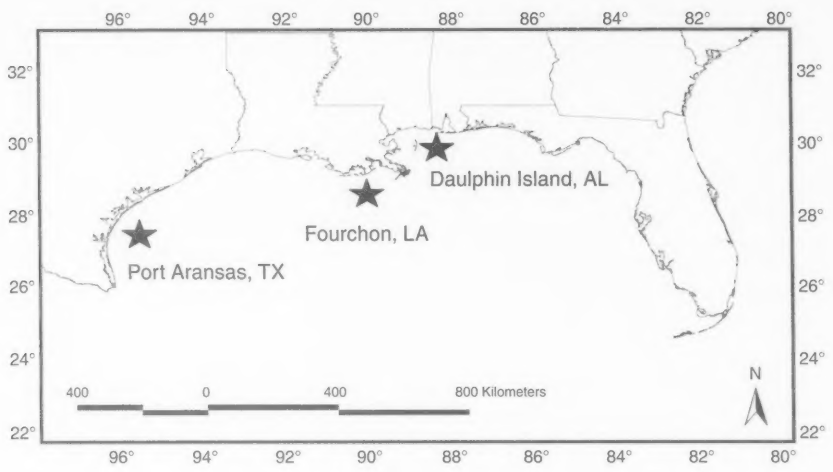

Figure 1

Map of the northern Gulf of Mexico showing the three red snapper (*Lutjanus campechanus*) sampling locations.

An underlying assumption crucial to a fishery management plan is that the fish species being managed is a unit stock (Gulland, 1965). A stock is defined as the part of a fish population that is under consideration as an actual or potential resource (Ricker, 1975). Since management began in 1991, red snapper in the northern GOM have been considered a unit stock. Genetic studies to date have shown that there is little evidence to dispute this assumption (Camper et al., 1993; Gold et al., 1997, Heist and Gold, 2000). On the other hand, tag-recapture studies indicate that red snapper have the capacity to move great distances, making it possible for separate stocks to develop (Patterson et al., 2001).

The validity of an assumption of a single stock of red snapper is essential to management decisions because measures of growth, natural mortality, reproductive capacity, and recruitment can differ among nonmixing populations. Should separate red snapper stocks exist, management plans would have to be enacted for each defined stock in order to follow federal guidelines. Even if a single large red snapper stock exists, management should be sensitive to both the diversity of habitats and user groups within the species area of occurrence. Because red snapper are arguably the most important recreational and commercial offshore fishery from Florida to southern Texas, every effort should be undertaken to develop the most effective and productive management plan.

The objective of this study was to evaluate the stock structure of GOM red snapper based on growth rates and size-at-age information. We hypothesized that red snapper sampled from across the northern GOM would be indistinguishable in their growth rates and size at age—a uniformity indicative of a single unit stock.

Methods and materials

Red snapper were collected from the recreational harvests of 1999, 2000, and 2001 from the northern GOM at Dauphin Island, Alabama, at Port Fourchon, Louisiana, and at Port Aransas, Texas (Fig. 1). A maximum of 75 fish were randomly selected and sampled from the daily catch of each charter boat or head boat while the captains and deck hands cleaned fish. These fish were not selected by size. Larger individuals (>6.8 kg) were opportunistically sampled from spear fishing and hook-and-line fishing tournaments in Alabama and Louisiana. In addition, a number of smaller fish (<406 mm, <457 mm during summer 1999) were randomly sampled during red snapper tagging cruises in Alabama. Morphometric measurements were recorded (fork length [FL] in mm, total weight [TW] in kg, and eviscerated body weight [BW] in kg), sex was determined by macroscopic examination of gonads, and both sagittal otoliths were removed, rinsed, and stored in coin envelopes until processed. Fish weights were not recorded for 1999 Texas samples.

A transverse thin section (containing the core) was taken from the left sagittal otolith of each individual. Sections were made with the Hillquist model 800 thin-sectioning machine equipped with a diamond embedded wafering blade and precision grinder (Cowan et al., 1995). When the left otolith was unavailable, the right otolith was sectioned. Examinations of otolith sections were made with a dissecting microscope with transmitted light and polarized light filter at 20× to 64× magnification Opaque annulus counts were made along the ventral side of the sulcus acousticus from the core to the proximal edge (Wilson and Nieland, 2001). Annulus counts were performed by two independent readers (AJF

and MSB) without knowledge of either date of capture or morphometric data. The appearance of the otolith section edge condition was coded as opaque or translucent after Beckman et al. (1989). Annuli were counted a second time when initial counts disagreed. In instances where a consensus between the two readers could not be reached, annulus counts of the more experienced reader (AJF) were used. Between-reader differences in annulus counts were evaluated with the coefficient of variation (CV), index of precision (D) (Chang, 1982), and average percent error (APE) (Beamish and Fournier, 1981). The periodicity of opaque zone formation was verified for each sampling location with edge analysis after Wilson and Nieland (2001). Ages of red snapper were estimated from opaque annulus counts and capture date with the equation described by Wilson and Nieland (2001):

$$Day\ age = -182 + (\text{opaque increment count} \times 365) + ((m-1) \times 30) + d,$$

where m = the ordinal number (1–12) of month of capture; and
d = the ordinal number (1–31) of the day of the month of capture.

The 182 days subtracted from each age estimate are to account for the uniform hatching date assigned for all specimens (Render, 1995; Wilson and Nieland, 2001). Age in years was assigned by dividing day age by 365.

Fork length–TW relationships were fitted with linear regression to the model $FL = a\ TW^b$ from $\log_{10}$-transformed data for Alabama, Louisiana, and Texas specimens. Analysis of covariance (ANCOVA) was used to compare slopes and intercepts among sampling locations (SAS, 1985). Variability in age, FL, and TW frequency distributions of red snapper were compared among states with the Komolgorov-Smirnov two-sample test (Tate and Clelland, 1957).

Growth of red snapper was modeled for FL and TW with the von Bertalanffy growth equations. Because of differences in sample population size among states, weighted mean FL and mean TW at age were fitted for each state with nonlinear regression in the forms:

$$FL_t = L_\infty(1 - e^{[-k(t)]})$$
$$TW_t = W_\infty(1 - e^{[-k(t)]})^b,$$

where FL_t = FL at age t;
TW_t = TW at age t;
L_∞ = the FL asymptote;
W_∞ = the TW asymptote;
k = the growth coefficient;
t = age in years; and
b = exponent derived from our length–weight regressions (SAS, version 5, 1985, SAS Inst, Cary, NC).

Because of a lack of smaller individuals in all sample populations, no y-intercepts for t_0 were specified and models were forced through 0. Larger individuals and juveniles selectively sampled by size were excluded from the models to more accurately reflect a random sample. Likelihood ratio tests (Cerrato, 1990) were used to test for differences among states in models and in growth parameter estimates. Differential growth was evaluated for red snapper in the first 10 years of life when somatic growth is most rapid (Szedlmayer and Shipp, 1994; Patterson et al., 2001; Wilson and Nieland, 2001). Linear regressions of mean FL and mean TW at age for fishes aged 1 to 10 years were compared among states with analysis of covariance (ANCOVA) and tested for homogeneity of slopes.

Table 1

Numbers of red snapper (*Lutjanus campechanus*) sampled from recreational sources by state and year.

State	Males	Females	Unknown sex		Total
Alabama					
1999	434	396	5		835
2000	355	415	7		777
2001	189	209	0		398
				Total	2010
Louisiana					
1999	367	339	31		737
2000	399	397	8		804
2001	160	179	25		364
				Total	1905
Texas					
1999	268	293	14		575
2000	278	284	22		584
2001	52	56	10		118
				Total	1277

Results

During the three-year study period, 5192 red snapper were sampled from the recreational harvest of the northern GOM (Table 1): 642 individuals from fishing tournaments, 71 undersize fish from tagging cruises, and 4479 random samples from recreational catches. The samples included 2502 males, 2568 females, and 122 individuals of undetermined sex. The resultant male-to-female ratios were 0.96:1 for Alabama, 1:0.99 for Louisiana, 0.94:1 for Texas, and 0.97:1 for all states combined. A chi-square test indicated no significant difference in the number of males to females (χ^2=0.78, P=0.38). Fork lengths ranged from 237 to 916 mm (Fig. 2A). Specimens from Alabama ranged from 237 to 916 mm FL, Louisiana specimens ranged from 282 to 913 mm FL, and Texas specimens ranged from 266 to 846 mm FL. The FL frequency distributions of the random samples were different among all states (AL and LA, maximum difference (MD)=5.26; AL and TX, MD=51.86; LA and TX, MD=51.77)(Fig. 2A).

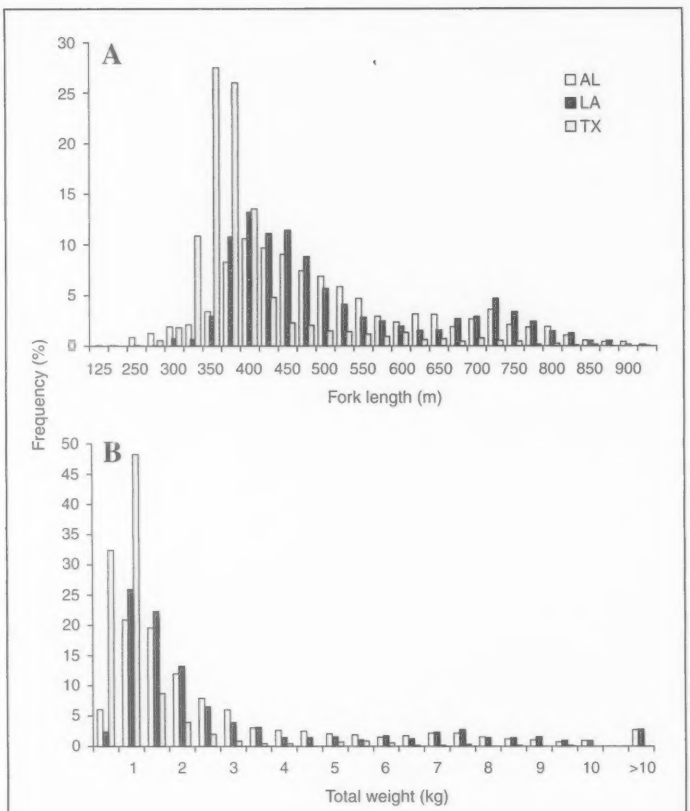

Figure 2

Distributions of (**A**) fork length in mm (n=5177) and (**B**) total weight in kg (n=4531) for red snapper (*Lutjanus campechanus*) sampled from the 1999–2001 recreational harvests of Alabama, Louisiana, and Texas.

Total weights of all fish sampled ranged from 0.11 to 17.35 kg (Fig. 2B). Specimens from Alabama ranged from 0.22 to 15.42 kg TW, Louisiana specimens were 0.42 to 17.35 kg TW, and Texas specimens ranged from 0.33 to 9.42 kg TW. Total weight-frequency distributions (in 0.5 kg increments) differed significantly between all states (AL and LA, MD=5.37; AL and TX, MD=53.68; and LA TX, MD=52.28)(Fig. 2B). Significant differences in red snapper FL-TW regression models were detected among states (ANCOVA test of homogeneity of slopes, $F_{5,\ 4522}$=23.36; P<0.001; r^2=0.98; ANCOVA test for equal intercepts, $F_{5,\ 4522}$=22.77, P<0.001, r^2=0.98); therefore, separate models were fitted for each state. The resultant equations were

$$AL\ TW = 1.51 \times 10^{-5}\ (FL^{3.03})$$
$$(F_{1;1965}=102740;\ P<0.0001;\ r^2=0.98);$$

$$LA\ TW = 1.02 \times 10^{-5}\ (FL^{3.09})$$
$$(F_{1;1856}=77981;\ P<0.0001;\ r^2=0.98);$$

$$TX\ TW = 2.88 \times 10^{-5}\ (FL^{2.92})$$
$$(F_{1;699}=13345;\ P<0.0001;\ r^2=0.95).$$

Ages were obtained from 5035 transverse otolith sections. Thirty fish had otolith sections deemed unreadable by both readers. The age estimates determined by the two readers were evaluated for reader agreement, precision, and average percent error for first and second readings of otolith sections by sample year. Table 2 gives APE, CV, D, percentage agreement (O), and percentages of differences in age estimates (±1, 2, and 3 years). The readers agreed on age estimates for 4053 otoliths (80.5%) after the initial reading. Re-examination of the 982 otolith sections for which annulus counts differed produced agreement for 5007 individuals.

We compared the timing of opaque annulus formation among red snapper sample sites by plotting the monthly occurrence of maximum and minimum proportions of opaque otolith edges. Sample limitations of red snapper in Texas, however, prevented meaningful comparisons of

opaque annulus formation for this state. However, minimum proportions of opaque edges during the months of April through October may indicate that red snapper from Texas form an opaque annulus during the winter months. Proportions of opaque edges for Alabama and Louisiana were essentially the same: maximum proportions of opaque edges during the months of February and March followed by a decrease to minimum proportions during the months of May through November (Fig. 3). These findings are consistent with previous age and growth studies on red snapper in the northern GOM (Patterson et al., 2001; Wilson and Nieland, 2001), indicating that the formation of one opaque annulus in the winter months is followed by the formation of one translucent annulus in summer. Annulus-based age estimates of red snapper from the northern GOM have also been validated to 55 years with otolith radiocarbon chronologies based on accelerator mass spectrometry ^{14}C measurements (Baker and Wilson, 2001).

Red snapper ages ranged from 1 to 45 years and the majority (90%) of individuals were between 2 and 6 years (Fig. 4). Alabama fish ranged from 1 to 35 years (n=1985), Louisiana fish ranged from 2 to 37 years (n=1864), and Texas fish ranged from 1 to 45 years (n=1186). Modal ages were 4 years for Alabama and 3 years for Louisiana and Texas red snapper. We found significant differences among age-frequency distributions from all states (AL and LA, MD=9; AL and TX, MD=33.84; and LA and TX, MD=24.84). Texas had a much higher proportion of younger individuals; 63% of sampled fish were aged at 3 years or less compared to only 30% of Alabama and 39% of Louisiana fish aged at 3 years or less.

Red snapper growth was modeled from weighted mean FL at age and mean TW at age by using the von Bertalanffy growth equation (Fig. 5, A and B). Resultant von Bertalanffy growth equations were

$$AL\ FL_{\infty} = 839(1 - e^{(-0.38(t))}) \quad (F_{1;15} = 2824.9;\ P<0.0001;\ r^2=0.95);$$

$$LA\ FL_{\infty} = 847.8(1 - e^{(-0.25(t))}) \quad (F_{1;13}=5024.4;\ P<0.0001;\ r^2=0.76);$$

$$TX\ FL_{\infty} = 778.2(1 - e^{(-0.49(t))}) \quad (F_{1;19}=1452.1;\ P<0.001;\ r^2=0.85);$$

$$AL\ TW_{\infty} = 17.05(1 - e^{(-0.15(t))})^{3.03} \quad (F_{1;15}=457.9;\ P<0.0001;\ r^2=0.89);$$

$$LA\ TW_{\infty} = 12.61(1 - e^{(-0.32(t))})^{3.03} \quad (F_{1;14}=122.02;\ P<0.0001;\ r^2=0.18);$$

$$TX\ TW_{\infty} = 8.89(1 - e^{(-0.21(t))})^{2.84} \quad (F_{1;12}=613.01;\ P<0.0001;\ r^2=0.96).$$

Models of mean red snapper FL at age for Alabama and Louisiana were markedly similar with likelihood ratio tests indicating no significant differences between red snapper from the two states (Table 3). However, the Texas model differed from both Alabama and Louisiana models. The Texas model displayed significant differences from the other models in both L_{∞} and in k. A comparison of the models of mean TW at age indicated no significant differences between Alabama and Louisiana red snapper (Table 3). Differential growth in TW was found when comparing Alabama and Louisiana with the Texas model; significant differences were manifested in both W_{∞} and in k. The model failed to converge for estimating a common value of k for both Louisiana and Texas.

We recognized that the larger red snappers from Louisiana might bias the data; therefore we compared growth for fish from 2 to 10 years of age—a time period when red snapper have demonstrated rapid linear growth (Szedlmayer and Shipp, 1994; Patterson et al., 2001; Wilson and Nieland, 2001). Linear regressions of mean FL at age for all individuals 2 to 10 years (Fig. 6A) were compared among states. We found no significant differences among states (ANCOVA test of homogeneity of slopes, $F_{2;28}$=2.7; P=0.08; ANCOVA test for equal intercepts, $F_{2;28}$=0.52; P=0.6).

Table 2

Differences between two readers in average percent error (APE), coefficient of variation (CV), index of precision (D), and in percentages of agreement (O) for counts of opaque annuli in red snapper (*Lutjanus campechanus*) otoliths after first and second readings for each sample year. n=number of otoliths sampled.

Year	1st reading	2nd reading
1999 (n=2100)		
APE	0.483	0.499
CV	0.014	0.0008
D	0.010	0.0006
O	89.48%	99.43%
±1	8.62%	0.48%
±2	1.19%	0.095%
±3	0.71%	
2000 (n=2069)		
APE	0.487	0.499
CV	0.034	0.0006
D	0.024	0.0004
O	73.79%	99.47%
±1	22.49%	0.53%
±2	1.78%	
±3	1.93%	
2001 (n=866)		
APE	0.459	0.498
CV	0.032	0.0005
D	0.023	0.0003
O	74.73%	99.42%
±1	22.06%	0.58%
±2	2.27%	
±3	0.94%	

Mean TW at age was also examined among states for red snapper 2 to 10 years in age as above (Fig. 6B). No significant differences were found between Alabama and Louisiana (ANCOVA test of homogeneity of slopes, $F_{1;17}$= 0.1; P=0.75; ANCOVA test for equal intercepts, $F_{1;17}$= 0.26; P=0.66 for intercepts). However, a significant difference between slopes was detected when comparing Alabama and Texas red snapper (ANCOVA test of homogeneity of slopes, $F_{1;16}$=19.68; P<0.0007; ANCOVA test for equal intercepts, $F_{1;16}$=2.74; P<0.12). The same was found when comparing slopes for Louisiana and Texas red snapper (ANCOVA test of homogeneity of slopes, $F_{1,\ 16}$=9.62; P<0.008) but not when comparing intercepts ($F_{1,\ 16}$=0.64; P<0.44).

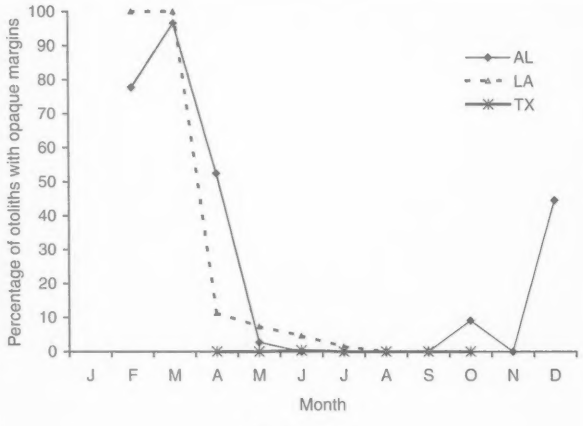

Figure 3

Marginal increment analysis of red snapper (*Lutjanus campechanus*) otoliths for specimens from Alabama (n=1985), Louisiana (n=1864), and Texas (n=1186).

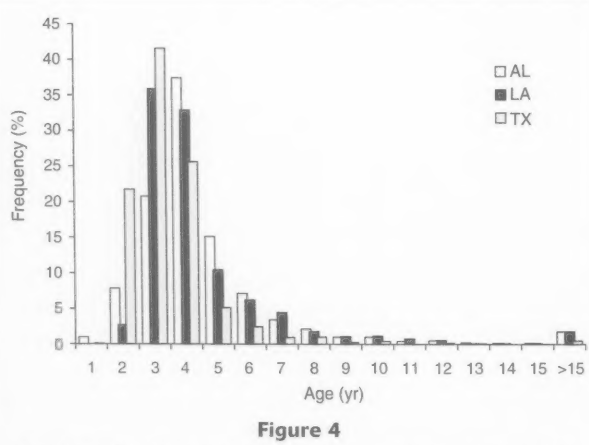

Figure 4

Age distributions for red snapper (*Lutjanus campechanus*) sampled from the 1999–2001 recreational harvests from Alabama, Louisiana, and Texas.

Discussion

Demographic variations in growth rates and in size-frequency distributions may indicate the existence of isolated management units of red snapper in the northern GOM. The recreational harvests of Alabama and Louisiana red snapper were dominated by individuals ranging from 375 to 425 mm FL, whereas the majority of Texas fish (69%) were 375 mm FL or less. It was within this size range (375–400 mm FL) that the significant differences in red snapper among states were detected. The FL distribution of red snapper sampled in Texas also differed from those for Alabama and Louisiana; there were very few large fish represented in the Texas sample population, partly because fishing tournaments (where larger individuals are targeted) were not sampled in Texas. Significant differences in TW frequencies among states were also detected at approximately 1 kg (the approximate weight of a red snapper 375–400 mm FL); 86% of Texas fish weighed 1 kg or less, compared to only 27% of Alabama fish and 28% of Louisiana fish in this size range.

One factor possibly contributing to the modal size class difference was the type of fishing vessel used to catch the fish. The majority of Texas specimens (~95%) were sampled from headboats; whereas Louisiana and Alabama fish were obtained almost exclusively from charterboats. This is not to say that charterboats were purposely excluded from the Texas survey. On the contrary, red snapper were sampled from any and all available recreational fishing parties at the three individual sampling locations. Differences in modal size and number of red snapper caught per person onboard charterboats versus headboats may be inconsequential considering that both trip types used similar gear and targeted similar or the same fishing locations. It should be noted however that in the Texas study area, charterboats routinely frequented a wider array of fishing spots (rigs, hardbottom, wrecks, etc.) than did headboats, which typically return to the same few rigs and large structures over and over again (Tolan[5]).

Our von Bertalanffy growth models on FL at age showed that red snapper from all three states exhibit a pattern of rapid, linear growth to approximately 10 years, after which maximum theoretical (asymptotic) FL is soon

[5] Tolan, J. 2003. Personal commun. Texas Parks and Wildlife Department, Resource Protection, 6300 Ocean Dr., Corpus Christi, TX 78412.

Table 3

Chi-square (χ^2), degrees of freedom (df), and *P*-values for likelihood ratio tests for comparing FL and TW von Bertalanffy growth models and parameters among sample locations (states). AL= Alabama; LA= Louisiana; and TX=Texas. n/a=not available.

	AL–LA	AL–TX			LA–TX		
	FL model	FL model	*L*	*k*	FL model	*L*	*k*
χ^2	2.54	5.14	13.67	21.53	5.8	10.16	9.8
df	1, 28	1, 34	1, 34	1, 34	1, 32	1, 32	1, 32
P	0.11	0.023	0.0002	3.48×10^{-6}	0.015	0.001	0.002
	TW model	TW model	*L*	*k*	TW model	*L*	*k*
χ^2	2.15	38.8	21.3	37.8	16.77	15.1	n/a
df	1, 29	1, 27	1, 27	1, 27	1, 26	1, 26	n/a
P	0.14	4.7×10^{-6}	3.9×10^{-6}	7.97×10^{-10}	4.2×10^{-5}	0.001	n/a

reached and growth in length becomes negligible. This pattern of rapid growth was similar to that reported in previous studies (Szedlmayer and Shipp, 1994; Manooch and Potts, 1997; Patterson, 1999; Wilson and Nieland, 2001). However, our models predicted smaller L_∞ and higher values of k. Because of the minimum size limits on the recreational fishery, very few fish under age 2 years (>300 mm FL) were included in our sample populations. We forced our models through t_0=0 to more accurately predict juvenile growth, which in turn increased our estimates of k. In addition, we had a much larger sample population that included more older, larger fish than most of the previously cited studies. These larger fish pulled the curve down, driving the lesser estimations of L_∞. The lack of significant differences in growth parameters between the Alabama and Louisiana models supports the findings of previous research, which indicates that Alabama and Louisiana red snapper grow at similar rates and reach comparable sizes (Patterson et al., 2001). However, values of L_∞ for Texas red snapper were significantly smaller than parameters predicted for Alabama and Louisiana red snapper. Interestingly, Texas had a value of k that was significantly larger then that for Alabama and Louisiana and this would indicate that Texas fish obtain a smaller maximum theoretical FL but reach it at a faster rate then fish from Alabama and Louisiana.

Von Bertalanffy growth models of mean weight at age produced similar results, indicating that Texas red snapper obtain significantly smaller maximum theoretical TW than fish from Alabama and Louisiana. Fish sampled from tournaments were excluded from all growth models to more accurately reflect

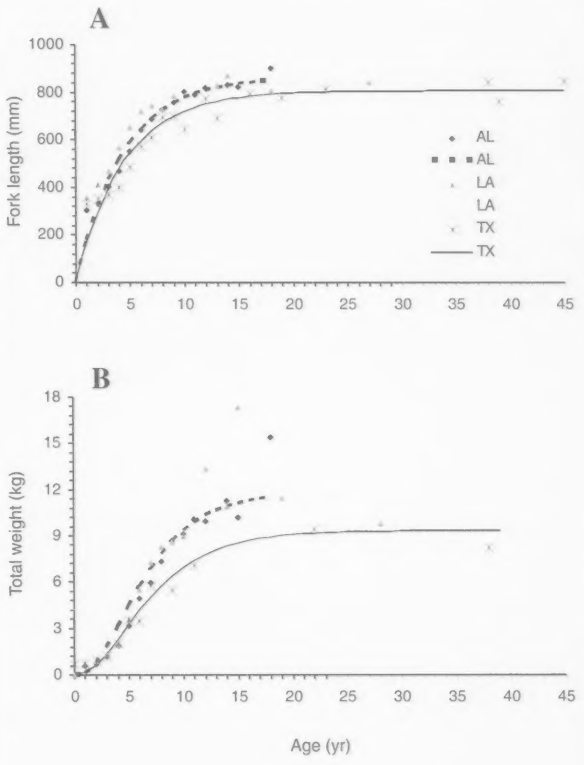

Figure 5

Observed (**A**) mean fork length (mm) at age and (**B**) mean total weight (kg) at age for red snapper (*Lutjanus campechanus*) from Alabama, Louisiana, and Texas. Plotted lines are weighted von Bertalanffy growth functions fitted to the data.

growth of a random population. Tournament anglers target large fish, possibly the fastest growing individuals at a given age, and their catches may bias growth estimates (Ottera, 1992; Vaughan and Burton, 1993; Goodyear, 1995). Without these tournament fish, however, the Alabama red snapper TW model did not reach an asymptote. Therefore the growth parameters for that model were poorly estimated. Notwithstanding, Alabama and Louisiana models did not differ significantly. Estimates of W_∞ and k predicted for Louisiana red snapper were slightly larger than previously reported for fish from the Louisiana commercial and recreational catches (Render, 1995). Although the Texas model predicted a value of W_∞ that was significantly less than those for both Alabama and Louisiana red snapper, Texas had a growth coefficient (k) that was larger then that for Alabama. It appears that, as in the length models, Texas fish reach a smaller theoretical maximum weight but at a faster rate than Alabama fish. Louisiana fish attained maximum weight at a faster rate than Alabama or Texas red snapper. Our growth models indicate that although Texas red snapper grow in mass at a faster rate than Alabama fish, Texas red snapper are consistently smaller at age and reach smaller maximum sizes than those from Alabama and Louisiana and that there is a veritable difference in size at age and growth rates among regions. Similar demographic variations in growth rates among populations have been previously noted for other marine fish species of the South Atlantic and GOM, such as gray snapper (Johnson et al., 1994; Burton 2001), and king mackerel (DeVries et al, 1990; DeVries and Grimes, 1997).

Linear regressions of mean FL and mean TW at age for red snapper aged one to 10 years indicated that only TW was significantly different among sample regions. Texas red snapper were shown to differ significantly from both Alabama and Louisiana red snapper in regressions of mean weight at age. Although comparisons of FL at age for all regions were not significantly different, Texas fish were significantly smaller in mass (TW) at age than fish from Alabama and Louisiana. This difference was observed in all age classes.

Our research efforts indicate that there is mounting evidence for discrete differences in size at age and in overall growth rates between red snapper sampled from the north central GOM (Louisiana and Alabama) and the southwest GOM (Texas). Texas red snapper are clearly reaching smaller maximum sizes and are consistently smaller (TW) at age than those collected from Louisiana and Alabama waters. Although the reasons behind these differences remain uncertain, logic indicates that factors such food availability, habitat preference, and actual population size may cause these differences between regions.

The more productive, nutrient-rich waters of the Mississippi River and north-central GOM off Louisiana and Alabama may be more conducive to faster growth than the less fertile waters off Texas. Approximately 70–80% of GOM fishery landings come from the waters surrounding the Mississippi River delta (Grimes, 2001). The western GOM (including the sampling area of Port Aransas, TX) is devoid of a contributing river system anything remotely similar to the Mississippi River. Draining 43% of the continental United States, the Mississippi River is the largest river system in North America and provides an enormous amount of nutrient-laden fresh water to the shallow continental shelf of the northern GOM. Although the mechanics by which the Mississippi River enhances fishery production remain uncertain, Grimes (2001) postulated that the discharge from the Mississippi primarily influences recruitment in the plume field. Increased growth rates associated with the Mississippi River plume compared with other regions of the GOM have been noted for a number of species, such as gulf menhaden (Warlen, 1988), king mackerel (DeVries et al., 1990), striped anchovy (Day, 1993), and yellowfin tuna (Lang et al., 1994).

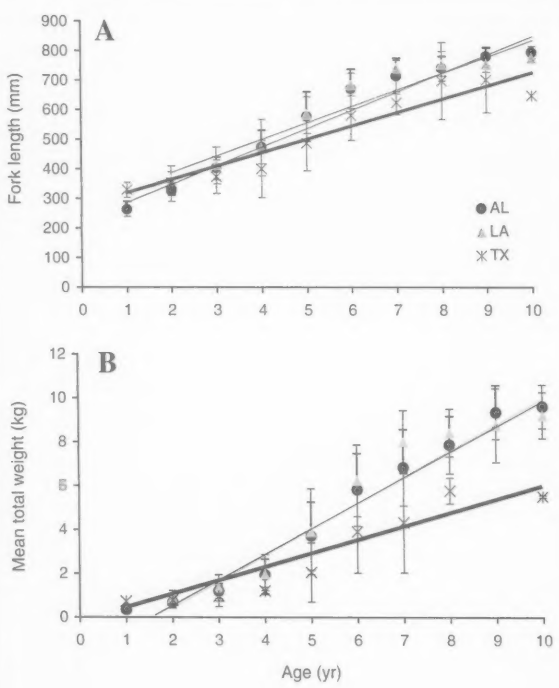

Figure 6

Scattergram with linear regression lines for relationships (**A**) between age (yr) and mean fork length (mm) and (**B**) age (yr) and mean total weight (kg) for red snapper (*Lutjanus campechanus*) aged 1 to 10 years from the 1999–2001 recreational harvests of Alabama, Louisiana, and Texas. Error bars represent standard deviations from the mean.

In addition to increased food availability off of the north-central GOM, the amount and condition of preferred habitat may have some effect on the observed differences in growth rates for Texas and those for Louisiana and Alabama. Approximately 95% of all Louisiana fishes sampled in this study were harvested from waters surrounding nearshore (<50 km) oil and gas platforms. Similarly, about 95% of all Alabama fishes sampled were caught over artificial reef sites. The fact that there was no detectable difference in size at age and overall growth rates between Louisiana and Alabama red snapper therefore is not surprising, given the similarity in the habitats sampled and the proximity of both locations to the Mississippi River discharge plume. Texas was the only area in which samples were routinely obtained from natural hard bottoms (40%), as well as from oil and gas platforms and artificial reefs (60%). Given that more than half of the Texas specimens were captured in the waters immediately surrounding artificial structures (i.e., oil and gas platforms), we can assume that habitat type is not be the sole source for the observed differences in growth rates among regions.

Despite the current acceptance of a unit stock hypothesis for GOM red snapper, the species is not, and to our knowledge never has been, uniformly distributed across the northern GOM. The fishery for red snapper began in northwest Florida approximately 20 years before the Civil War (Collins, 1887) and during that time period was centered between Mobile, AL, and Fort Walton, FL (Camber, 1955). One hundred years of landings data indicate that the fishery, and possibly the population, has undergone a major shift from the natural outcroppings of the West Florida Shelf to oil and gas platforms of the north-central portion of the GOM (Shirripa and Legault[1]). Fishery-dependent data indicate that currently there is a center of abundance of red snapper off southwest Louisiana and a second, smaller center off Alabama (Patterson et al., 2001; Goodyear[4]; Shirripa and Legault[1]). Patterson et al. (2001) stated that Louisiana and Alabama accounted for 32.6% and 11.4%, respectively, of the combined recreational and commercial GOM landings from 1981 to 1998. This is especially surprising for Alabama, considering that its coastline accounts for only 3% of the GOM coastline from the Texas-Mexico border to the southern tip if Florida (Patterson et al., 2001).

Red snapper have never been reported to be plentiful in Texas waters, despite the availability of suitable habitat in the form of natural hard bottom and the current high concentration of oil and gas platforms. In a historical report on red snapper fishing in the GOM, Camber (1995) reported that although a few red snapper were taken from the "Galveston Lumps" or the "Western" fishing grounds off Texas, the fishery never fully developed in this region during the latter part of the nineteenth century. Commercial landings for red snapper from the GOM indicated that Texas accounted for approximately only 18% of the total catch during the time period 1981–95 (Goodyear[6]). In a recent fishery-dependent survey of recreational headboat discards and landings in Texas coastal waters, red snapper less than the minimum legal size (15 inches) made up 64% of the catch (Dorf, 2000). In the latter study, Galveston, Port Aransas, and Port Isabel were surveyed to canvas a large portion of the Texas coast. Discard-to-landing ratios were as high as 211:1 in the waters off Galveston and were possibly indicative of the paucity of legal-size red snapper in Texas waters. Of the three sampling locations, Port Aransas had the lowest discard-to-landing ratio (5.2:1) and the largest mean fish length and weight (387 mm, 0.9 kg)—length and weight data that are consistent with a 3-yr-old fish from our Texas (Port Aransas) specimens. The majority of Texas fish (63%) were aged at 3 years or less. Age distribution, along with FL and TW distributions, may indicate that red snapper are being harvested from Texas waters just as they reach legal size. Given the vast differences in historical landings data between the northern and southwest GOM, the highly disproportionate discard-to-landing ratio reported for headboats in Texas waters (Dorf, 2000), and the large number of young fish sampled in Texas, it is not inconceivable to speculate that there are fewer red snapper available for harvest in Texas waters.

Demographic variation in growth rates may indicate the existence of separate management units of red snapper in the GOM. Our data indicate that the red snapper inhabiting the waters off Texas are reaching smaller maximum sizes at a faster rate, but are consistently smaller (TW) at age than those collected from Louisiana and Alabama waters. Whether these differences are environmentally induced or result from genetic divergence remains to be determined. The more productive, nutrient-rich waters of the Mississippi River and north-central GOM off Louisiana and Alabama may be more conducive to faster growth than the less fertile waters off Texas. Fishing pressure and its effects on population size may also be leading to the observed differences in growth rates. Fishery-dependent landing data and disproportionate discard-to-landing ratios in Texas waters loosely support the concept that fewer red snapper are available for harvest in the southwest GOM. Regardless of the cause, the existence of demonstrable demographic differences argues for the delineation of multiple red snapper management units in the GOM.

Acknowledgments

Funding for this research was provided by the U.S. Department of Commerce Marine Fisheries Initiative (MARFIN) program (grant number NA87FF0424). We

[6] Goodyear, C. P. 1996. An update of red snapper harvest in U.S. waters of the Gulf of Mexico. Report MIA-95/96-60, 21 p. Miami Laboratory, Southeast Fisheries Center, National Marine Fisheries Service, 75 Virginia Beach Dr. Miami, FL., 33149-1099. [Not available from NTIS].

thank Forrest Davis, John Gold, Jessica McCawley, Linda Richardson, Jim Tolan, Melissa Woods, Candace Aiken, and many others for help with sampling red snapper. We also thank Josh Maier and Brett Blackman for otolith sectioning. We thank Steve Tomeny and his boat captains and crew (Port Fourchon, LA), as well as all boat captains and crews in Dauphin Island, Alabama, and Port Aransas, Texas, for graciously allowing us to sample fish from their charter fishing vessels. We also thank Yvonne Allen for providing the map in Figure 1. Finally we would like to thank Dave Nieland for time spent fielding questions concerning statistical analysis and for a constructive review of this manuscript.

Literature cited

Baker, M. S. Jr., and C. A. Wilson.
2001. Use of bomb radiocarbon to validate otolith section ages of red snapper *Lutjanus campechanus* from the northern Gulf of Mexico. Limnol. Oceanogr. 46:1819–1824.

Beamish, R. J., and D. A. Fournier.
1981. A method for comparing the precision of a set of age determinations. Can. J. Fish. Aquat. Sci. 38:982–983.

Beckman, D. W., C. A. Wilson, and A. L. Stanley.
1989. Age and growth of red drum, *Sciaenops ocellatus*, from offshore waters of the northern Gulf of Mexico. Fish. Bull. 87:17–28.

Burton, M. L.
2001. Age, growth, and mortality of gray snapper, *Lutjanus griseus*, from the east coast of Florida. Fish. Bull. 99:254–265.

Camber, C. I.
1955. A survey of the red snapper fishery of the Gulf of Mexico, with special reference to the Campeche banks. Fla. Board Conserv. Tech. Ser. No. 12:1–64.

Camper, J. D., R. C. Barber, L. R. Richardson, and J. R. Gold.
1993. Mitochondrial DNA variation among red snapper (*Lutjanus campechanus*) from the Gulf of Mexico. Mol. Mar. Biol. Biotech. 2:154–161.

Cerrato, R. M.
1990. Interpretable statistical tests for growth comparisons using parameters in the von Bertalanffy equation. Can. J. Fish. Aquat. Sci. 47:1416–1426.

Chang, W. B.
1982. A statistical method for evaluating the reproducibility of age determination. Can. J. Aquat. Sci. 39:1208–1210.

Collins, J. W.
1887. Report on the discovery and investigation of fishing grounds made by the Fish Commision Steamer *Albatross* during a cruise along the Atlantic Coast and in the Gulf of Mexico. Rep. U.S. Comm. Fish. 13:217–311.

Cowan, J. H. Jr., R. L. Shipp, H. K. Bailey IV, and D. W. Haywick.
1995. Procedure for rapid processing of large otoliths. Trans. Am. Fish. Soc. 124:280–282.

Day, G. R.
1993. Distribution, abundance, growth and mortality of striped anchovy, *Anchoa hepsetus*, about the discharge plume of the Mississippi River. M.S. thesis, 45 p. Univ. West Florida, Pensacola, FL.

DeVries, D. A., and C. B. Grimes.
1997. Spatial and temporal variation in age and growth of king mackerel, *Scomeromorus cavalla*, 1977–1992. Fish. Bull. 95:694–708.

Devries, D. A., C. B. Grimes, K. C. Lang, and D. B. White.
1990. Age and growth of king and Spanish mackerel larvae and juveniles from the Gulf of Mexico and U.S. south Atlantic. Environ. Biol. Fishes 29:135–143.

Dorf, B. A.
2003. Red snapper discards in Texas coastal waters: a fishery-dependent onboard survey of recreational headboat discards and landings. *In* Fisheries, reefs, and offshore development (D. R. Stanley and A. Scarborough-Bull, eds.), p. 155–166. Am. Fish. Soc. Symposium 36. Am. Fish. Soc., Bethesda, MD.

Gold J. R., F. Sun, and L. R. Richardson.
1997. Population structure of red snapper from the Gulf of Mexico as inferred from analysis of mitochondrial DNA. Trans. Am. Fish. Soc. 126:386–396.

Goodyear, C. P.
1995. Mean size at age: an evaluation of sampling strategies using simulated red grouper data. Trans. Am. Fish. Soc. 124:746–755.

Grimes, C. B.
2001. Fishery production and the Mississippi River discharge. Fisheries 26:7–26.

Gulland, J. A.
1965. Fish stock assessment: a manual of basic methods, 223 p. John Wiley & Sons, New York, NY.

Heist, E. J., and J. R. Gold.
2000. DNA microsatellite loci, and genetic structure of red snapper in the Gulf of Mexico. Trans. Am. Fish. Soc. 129:469–475.

Johnson, A. G., L. A. Collins, and C. P. Kelm.
1994. Age-size structure of gray snapper from the Southeastern United States: a comparison of two methods of back-calculating size at age from otolith data. Proc. Annu. Conf. Southeast Assoc. Fish and Wildl. Agencies 48:592–600.

Lang, K. L., C. B. Grimes, and R. F. Shaw.
1994. Variations in the age and growth of yellowfin tuna larvae, *Thunnus albacares*, collected about the Mississippi River plume. Environ. Biol. Fishes 39:259–270.

Manooch, C. S., III, and J. C. Potts
1997. Age and growth of red snapper, *Lutjanus campechanus*, *Lutjanidae*, collected along the southeastern United States from North Carolina through the east coast of Florida. J. Elisha Mitchell Sci. Soc. 113:111–122.

Ottera, H.
1992. Bias in calculating growth rates in cod (*Gadus morhua L.*) due to size selective growth and mortality. J. Fish Biol. 40:465–467.

Patterson, W. F. III.
1999. Aspects of the population ecology of red snapper *Lutjanus campechanus* in an artificial reef area off Alabama. Ph.D. diss., 164 p. Univ. South Alabama, Mobile, AL.

Patterson, W. F. III, James H. Cowan Jr., Charles A. Wilson, and Robert L. Shipp.
2001. Age and growth of red snapper, *Lutjanus campechanus*, from an artificial reef area off Alabama in the northern Gulf of Mexico. Fish. Bull. 99:617–627.

Render, J. H.
1995. The life history (age, growth, and reproduction) of red snapper (*Lutjanus campechanus*) and its affinity

for oil and gas platforms. Ph.D. diss., 76 p. Louisiana State Univ., Baton Rouge, LA.

Ricker, W. E.
1975. Computation and interpretation of biological statistics of fish populations, 382 p. Bull. Fish. Res. Board Can., Ottawa.

Szedlmayer, S. T., and R. L. Shipp.
1994. Movement and growth of red snapper, *Lutjanus campechanus*, from an artificial reef area in the northeastern Gulf of Mexico. Bull. Mar. Sci. 55(2–3): 887–896.

Tate, M. W., and R. C. Clelland.
1957. Non-parametric and shortcut statistics in the social, biological, and medical sciences, p. 93–94. Interstate Printers and Publishers, Inc., Danville, IL.

Vaughan, D. S., and M. L. Burton.
1993. Estimation of von Bertalanffy growth parameters in the presence of size-selective mortality: a simulated example with red grouper. Trans. Am. Fish. Soc. 123:1–8.

Warlen, S. M.
1988. Age and growth of larval gulf menhaden, *Brevoortia patronis*, in the northern Gulf of Mexico. Fish. Bull. 86:77–90.

Wilson, C. A., and D. L. Nieland.
2001. Age and Growth of red snapper, *Lutjanus campechanus*, from the northern Gulf of Mexico off Louisiana. Fish. Bull. 99:653–664.

Elemental signatures in otoliths of larval walleye pollock (*Theragra chalcogramma*) from the northeast Pacific Ocean*

Jennifer L. FitzGerald
Simon R. Thorrold
Biology Department, MS 35
Woods Hole Oceanographic Institution
Woods Hole, Massachusetts 02543
E-mail address (for J. L. FitzGerald): jfitzgerald@whoi.edu

Kevin M. Bailey
Annette L. Brown
NOAA Alaska Fisheries Science Center
7600 Sand Point Way NE
Seattle, Washington 91185

Kenneth P. Severin
Department of Geology and Geophysics
University of Alaska Fairbanks
P.O. Box 755780
Fairbanks, Alaska 99775-5780

Abstract—The population structure of walleye pollock (*Theragra chalcogramma*) in the northeastern Pacific Ocean remains unknown. We examined elemental signatures in the otoliths of larval and juvenile pollock from locations in the Bering Sea and Gulf of Alaska to determine if there were significant geographic variations in otolith composition that may be used as natural tags of population affinities. Otoliths were assayed by using both electron probe microanalysis (EPMA) and laser ablation inductively coupled plasma mass spectrometry (ICP-MS). Elements measured at the nucleus of otoliths by EPMA and laser ablation ICP-MS differed significantly among locations. However, geographic groupings identified by a multivariate statistical approach from EPMA and ICP-MS were dissimilar, indicating that the elements assayed by each technique were controlled by separate depositional processes within the endolymph. Elemental profiles across the pollock otoliths were generally consistent at distances up to 100 μm from the nucleus. At distances beyond 100 μm, profiles varied significantly but were remarkably consistent among individuals collected at each location. These data may indicate that larvae from various spawning locations are encountering water masses with differing physicochemical properties through their larval lives, and at approximately the same time. Although our results are promising, we require a better understanding of the mechanisms controlling otolith chemistry before it will be possible to reconstruct dispersal pathways of larval pollock based on probe-based analyses of otolith geochemistry. Elemental signatures in otoliths of pollock may allow for the delineation of fine-scale population structure in pollock that has yet to be consistently revealed by using population genetic approaches.

Manuscript submitted 4 August 2003 to the Sceintific Editor's Office.

Manuscript approved for publication 28 May 2004 by the Scientific Editor.

Fish. Bull. 102:604–616 (2004).

The "stock" concept is a central tenet of modern fisheries science because it represents the fundamental management unit of marine fisheries (Begg and Waldman, 1999). This emphasis, in turn, places a premium on accurate identification of groups of fish whose population statistics are largely independent of other groups. However, stock identification has often proved problematic in marine fishes. For instance, the stock structure of walleye pollock (*Theragra chalcogramma*) across the North Pacific Ocean has been a topic of investigation for many years. Early studies were based on phenotypic characteristics of pollock, such as meristics and morphometrics (Serobaba, 1977; Hinckley, 1987; Temnykh, 1994). Other studies have focused on genotypic markers, such as DNA and allozyme analyses (Grant and Utter, 1980; Mulligan et al., 1992; Shields and Gust, 1995). These approaches resulted in only the broadest characterization of pollock stock structure but have been able to distinguish populations from the eastern and western Pacific (Bailey et al., 1999). Quasi-isolated subpopulations may be at least demographically isolated on smaller spatial scales. For instance, within the Gulf of Alaska, spawning pollock aggregate at specific locations in Shelikof Strait, Prince William Sound, and in the Shumagin Islands region (Bailey et al., 1999). However, the extent of larval dispersal from the spawning sites and the degree of spawning site fidelity of adult pollock to these locations remains unknown.

The difficulties associated with determining stock structure in fishes are essentially the same ones that currently limit our ability to determine population connectivity in marine systems (Thorrold et al., 2002). Tag-recapture studies using tags have limited applicability in the case of pollock. Adults are located deep in the water column and are sensitive to barotrauma during the process of being caught, brought to the surface, and tagged. Traditional population genetic approaches may be similarly

*Contribution 11219 from the Woods Hole Oceanographic Institution, Woods Hole, MA 02543.

ineffective because of the low level of exchange required to maintain genetic homogeneity, at least over ecological time scales, and the low level of genetic drift associated with large populations (Waples, 1998; Hellberg et al., 2002). However, preliminary studies have indicated that otolith geochemistry may prove to be a useful natural tag of population structure in walleye pollock (Severin et al., 1995). Otoliths are accretionary crystalline structures located within the inner ear of teleost fish. They are formed through concentric additions of alternating protein and aragonite layers around a central nucleus. The use of otoliths as natural geochemical tags is contingent on the metabolically inert nature of the otolith and the fact that once deposited, otolith material is neither resorbed nor metabolically reworked (Campana and Neilson, 1985; Campana, 1999). The chemical composition of otoliths also reflects to some degree the physicochemical characteristics of the ambient water (Bath et al., 2000). If the water where pollock reside has distinct oceanographic characteristics, then many of the elements incorporated into the otoliths should differ among locations. Migrations between water masses at some age will, therefore, be recorded in the chemical composition of the otolith at the appropriate daily increment. Natural geochemical signatures in otoliths may therefore be useful markers of environmental history throughout the life of the individual and in turn, fish stock composition (e.g., Campana et al., 1995).

The use of geochemical signatures in otoliths as natural tags requires accurate and precise assays of otolith composition. Electron probe micro-analysis (EPMA) has been commonly used for probe-based analyses of otolith chemistry (Gunn et al., 1992). However, detection limits of approximately 100 μg/g limit the technique to a relatively small number of minor elements in otoliths, including Na, Cl, K, and Sr (Campana et al., 1997). Most of the elements measured by EPMA are probably controlled by physiological rather than environmental factors, which may limit their usefulness in stock identification studies (Campana, 1999). Nonetheless, a number of researchers using EPMA have reported geographic differences in otolith chemistry (e.g., Thresher et al., 1994). More recently, attention has focused on inductively coupled plasma mass spectrometry (ICP-MS) to assay elements that are typically below the detection limits of EPMA. Laser ablation ICP-MS uses focused Nd:YAG or excimer lasers to ablate specific locations on the otolith. The vaporized material is then swept up by a carrier gas into a plasma torch and analyzed by mass spectrometry. Limits of detection of the technique are typically on the order of 0.1–1μg/g, allowing for quantification of several elements that cannot be assayed by using EPMA including Mg, Mn, Ba, and Pb (Thorrold et al., 1997; Thorrold and Shuttleworth, 2000). These observations led Campana et al. (1997) to conclude that EPMA and laser ablation ICP-MS were complementary and that there is little overlap in the elements that are accurately measured by the two techniques. Yet few studies of otolith geochemistry have attempted to use both approaches on the same samples.

The objectives of this study are to determine if larval walleye pollock from different geographic localities can be distinguished based on elemental signatures in their otoliths. By analyzing sagittal otoliths with both EPMA and laser ablation ICP-MS, we hoped to identify greater differences among locations than would have been possible by using either technique in isolation. If successful, the study may provide a powerful tool for determining stock structure and tracing migration pathways of walleye pollock in the north Pacific. These data could then be used by managers of one of the world's largest single species fisheries to direct the sustainable harvest of this considerable natural resource.

Materials and methods

All fish used in the study were collected in the spring and summer of 1999 from Alaska Fisheries Science Center research cruises in the Bering Sea and Gulf of Alaska (Fig. 1, Table 1). Fish of birth year 1999 were collected within three months of spawning time to minimize the likelihood of larval transport from other regions. In the case of the Yakutat samples, fresh juvenile pollock were removed from Pacific cod guts. Samples were collected only when the pollock were readily identifiable and heads were intact. Otoliths showed no visible sign of degradation from digestive processes. Juvenile pollock were frozen whole and transported to the laboratory for otolith removal.

Otoliths were removed from the fish and mounted on petrographic slides in LR White resin (acrylic, hard-grade). Larval otoliths were ground on one side to expose the nucleus by using 500-grit paper and were polished with 0.25-μm grit diamond paste. Juvenile otoliths were ground and polished in the sagittal plane on both sides to maximize clarity of the nucleus during microanalysis.

Electron probe microanalysis

After having been polished, the otoliths were cleaned with Formula 409® and coated with a 30-nm layer of carbon. They were subsequently analyzed with a Cameca SX-50 electron microprobe equipped with four wavelength dispersive spectrometers. A 15keV, 10 nA, 4-μm diameter beam was used for all analyses. Counting times, standards, detection limits, and analytical errors are summarized in Table 2. Although Mg was analyzed in all otoliths, in most cases it was below detection limits and was therefore not used in the statistical analysis.

Laser ablation ICP-MS

After having been ground and polished, otolith sections were decontaminated before elemental analysis by using laser ablation ICP-MS. Sections were rinsed in ultrapure water, scrubbed with a nylon brush in a solution of ultrapure H_2O, triple rinsed with ultrapure 1%HNO_3,

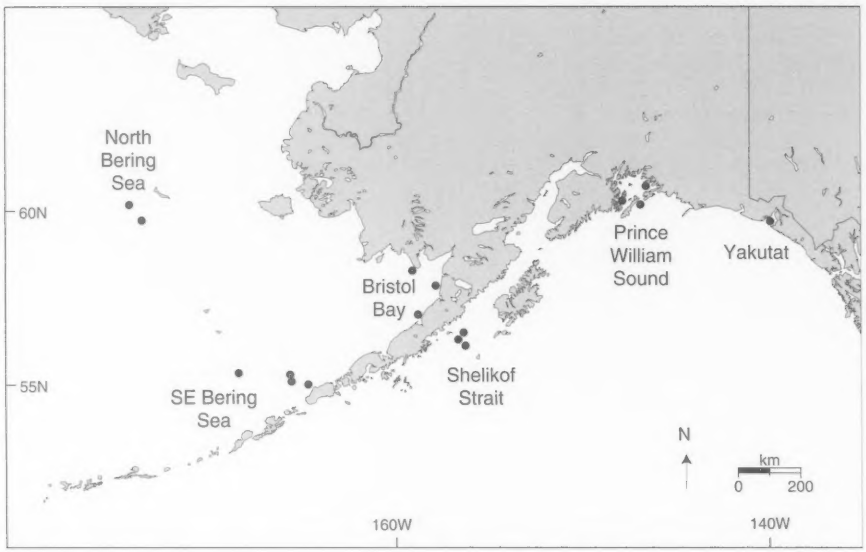

Figure 1

Locations of sampling sites for larval and juvenile walleye pollock (*Theragra chalcogramma*) in the Gulf of Alaska and Bering Sea.

sonified for 5 minutes in ultrapure H_20, and finally triple rinsed again with Milli-Q water. The section was dried under a positive flow hood for 24 hours and stored in a polyethylene bag.

Elemental analyses were conducted with a Finnigan MAT Element2 magnetic sector field ICP-MS and Merchantek EO LUV266X laser ablation system (Thorrold and Shuttleworth, 2000). Instrument set-up was similar to that outlined by Günther and Heinrich (1999). An Ar gas stream was used to carry ablated material from the laser cell to the ICP-MS. The carrier gas was then mixed with the Ar sample gas and a wet aerosol (1% HNO3) in the concentric region of the quartz dual inlet spray chamber. The wet aerosol was supplied by a self-aspirating PFA micro-flow (20 μL/min) nebulizer attached to a CETAC ASX100 autosampler. Diameter of the 266-nm laser beam was nominally 5 μm, repetition rate was 5 Hz, and the scanning rate was set at 5 μm/sec.

A typical run for an individual otolith consisted of a blank sample (1%HNO_3 only), a standard sample, five laser samples, and then another blank and standard. The number of laser samples in a run ranged from 5 to 15, depending upon the size of the otolith. All laser runs began with a 70 μm × 70 μm raster, centered on the otolith nucleus. The laser software was then used to trace out concentric lines, 720 μm in length and approximately 40 μm apart, which followed the contour of individual growth increments from the raster to the otolith edge. This approach produced reasonably high spatial resolution (30–50 μm) for life history scans across otoliths while allowing sufficient acquisition time to maintain measurement precision.

We examined Mn/Ca, Sr/Ca, and Ba/Ca ratios in the pollock otoliths by monitoring ^{48}Ca, ^{55}Mn, ^{86}Sr, and ^{138}Ba. Quantification followed the approach outlined by Rosenthal et al. (1999) for precise element/Ca ratios using sector field ICP-MS (Thorrold et al., 2001). Quality control was maintained by assaying a dissolved aragonite standard (Yoshinaga et al., 2000) every five samples. The standard was introduced at the appropriate time by moving the autosampler probe from the solution containing the 1% HNO_3 to the standard solution, while maintaining the carrier gas flow through the ablation cell. Elemental mass bias was calculated by reference to known values of the standard, and a correction factor was then interpolated and applied to the laser samples bracketed between adjacent standard measurements. Average (n=40) within-run precisions (RSD) of the standard measurements were all less than 1% (Mn/Ca: 0.16%, Sr/Ca: 0.16%, and Ba/Ca: 0.33%). Long-term (5-month) estimates of the standard measurements (n=40), again uncorrected for changes in mass bias over time, were less precise (Mn/Ca: 5.6%, Sr/Ca: 3.7%, and Ba/Ca: 5.6%). However, laser samples were corrected for changes in mass bias by using the laboratory standard. Precision of the technique was approximately 1% for all the ratios that we measured.

Statistical analyses

All elemental data were initially examined for normality and homogeneity of variance by using residual analysis (Winer, 1971) and were found to conform to the assumptions of ANOVA without the need for data transformation. We therefore assumed that require-

Table 1

Location, collection date, standard length range (mm), and sample sizes (n) of larval and juvenile walleye pollock (*Theragra chalcogramma*) captured from the southeast Bering Sea (SE Bering), North Bering Sea (N Bering), Bristol Bay, Shelikof Strait, Prince William Sound (PWS), and Yakutat, and analyzed by laser ablation ICP-MS (ICP-MS) and electron probe microanalysis (EPMA).

Area	Date	SL range (mm)	n (total)	n (ICP-MS)	n (EPMA)
SE Bering	23 May–27 July 1999	5.3–42.2	117	8	30
N Bering	18–23 July 1999	15.6–30.7	45	9	25
Bristol Bay	22–24 July 1999	85.1–135.7	75	11	28
Shelikof	27–28 May 1999	3.6–7.9	46	—	25
PWS	7 July–19 August 1999	35.2–66.0	11	4	6
Yakutat	15 July,1999	—	50	6	24

Table 2

Counting times for each element (time [seconds], standards, limits of detection [LOD, %weight, 99% confidence limits] and analytical errors [Error, %weight, 1 standard deviation]) for electron probe microanalysis (EPMA). Detection limits and analytical errors were calculated by following the procedures of Scott et al. (1995). N/A = not applicable.

Element	Time	Standard	LOD	Error
Na	60	Halite (CM Taylor)	0.029	0.023
Mg	60	Osumilite (USNM 143967)	0.019	0.022
P	60	Apatite (Wilberforce)	0.036	0.027
S	60	Gypsum (CM Taylor)	0.023	0.017
Cl	46	Halite (CM Taylor)	0.027	0.015
K	46	Osumilite (USNM 143967)	0.019	0.012
Ca	20	Calcite (NMNH 136321)	N/A	0.245
Sr	120	Strontianite (Smithsonian R-10065)	0.036	0.019

ments for the MANOVA were also met by the data. Among-location differences in the elemental composition of larval pollock in specific regions of the otoliths were compared by using one-factor multivariate analysis of variance (MANOVA) and one-factor analysis of variance (ANOVA). We treated location as a fixed factor in both MANOVA and ANOVA tests. Because of difficulties collecting pollock larvae, we were unable to achieve equal replication of sites within locations. We therefore pooled samples from collections within a location by randomly selecting fish from each location for subsequent analysis. However, the lack of replication at the within-location level necessarily restricted our ability to draw general conclusions concerning spatial variability in otolith composition beyond the samples analyzed in the present study. All *a posteriori* comparisons among locations were performed by using Tukey's honestly significant difference (HSD) test (experimentwise error rate=0.05). Multivariate differences in elemental signatures from the MANOVA were visualized by using canonical discriminant analyses (CDA). All analyses were conducting by using the SAS statistical program (SAS, version 6, 1990, SAS Inst. Inc., Cary, NC).

Comparisons of elemental profiles across otoliths were made with repeated measures ANOVA. We tested the following null hypotheses: 1) there was no variation in trace element profiles across individual otoliths (i.e., from the nucleus to the edge), 2) there were no differences in mean element concentrations among locations, determined by averaging data across individual otolith profiles, and 3) there were no differences in the pattern of element profiles across otoliths among locations. Otolith profiles with missing values were removed, and therefore we were able to use MANOVA for the repeated measures analysis. The multivariate approach to repeated measures is generally more conservative than univariate repeated measures analysis. However, the multivariate test does not assume sphericity of orthogonal components, requiring only that the data conform to multivariate normality with a common covariance matrix for individual larvae at each location (Littell et al., 1991). The approach still requires that adjacent points on the trajectories be equidistant. Therefore samples from EPMA were assigned to a distance category at intervals of 15 μm (0 μm, 15 μm, 30 μm , 45 μm, 60 μm, 75 μm, and 90 μm) across the otolith, to a distance of 90 μm from the nucleus. Samples were averaged when more than one measurement was available within a distance category. Laser ablation ICP-MS samples were assigned to a distance category at intervals of approxi-

Table 3

EPMA results of one-factor ANOVA (degrees of freedom [df]; sums of squares [SS]; mean square [MS]) at two positions (0–20 μm and 20–45 μm from the nucleus) in otoliths of larval walleye pollock (*Theragra chalcogramma*) collected from six locations: three locations in the Bering Sea (southeast Bering Sea [SB]; North Bering Sea [NB]; Bristol Bay [BB]) and three in the Gulf of Alaska (Prince William Sound [PW]; Shelikof Strait [SH]; and Yakutat [YK]). ***= significant at $\alpha = 0.05$; ns = nonsignificant. *A posteriori* multiple comparisons among locations were conducted by using Tukey's honestly significant difference (HSD). Locations are ordered (left to right) from lowest to highest concentrations, and lines link locations that are not significantly different (experimentwise error rate=0.05).

Element	Source	df	SS	MS	F	$P < F$	Tukey's HSD
0–20 μm							
Na	Location	5	24.7	4.9	16.37	***	PW BB YK NB SB SH
	Error	113	34.1	3.0×10^{-1}			
P	Location	5	18.3	3.7	14.93	***	BB SH NB SB PW YK
	Error	113	27.7	2.5×10^{-1}			
S	Location	5	2.0	3.9×10^{-1}	5.04	***	PW BB NB YK SH SB
	Error	113	8.8	7.8×10^{-2}			
Cl	Location	5	10.2	2.0	3.93	***	PW NB BB YK SB SH
	Error	113	58.6	5.2×10^{-1}			
K	Location	5	2.4	4.8×10^{-1}	4.01	***	SH NB SB PW BB YK
	Error	113	13.51	1.2×10^{-1}			
Sr	Location	5	7.1	1.4	6.66	***	YK NB BB SH PW SB
	Error	113	24.1	2.1×10^{-1}			
20–45 μm							
Na	Location	4	15.9	4.0	26.66	***	BB PW YK SB NB
	Error	93	13.9	1.5×10^{-1}			
P	Location	4	14.9	3.7	17.07	***	BB NB SB PW YK
	Error	93	20.3	2.2×10^{-1}			
S	Location	4	1.1	2.8×10^{-1}	4.62	***	BB PW SB NB YK
	Error	93	5.7	6.1×10^{-2}			
Cl	Location	4	8.4×10^{-1}	2.1×10^{-1}	1.61	ns	PW SB NB BB YK
	Error	93	12.1	1.3×10^{-1}			
K	Location	4	1.9	4.7×10^{-1}	5.65	***	NB PW BB SB YK
	Error	93	7.7	8.3×10^{-2}			
Sr	Location	4	9.0×10^{-1}	2.2×10^{-1}	3.75	***	NB YK BB PW SB
	Error	93	5.6	6.0×10^{-2}			

mately 40 μm (nucleus, 40–80 μm, 80–120 μm, 120–160 μm, and 160–200 μm) across the otolith, to a distance of 200 μm from the nucleus.

Results

Electron probe microanalysis

A total of six elements (Na, P, S, Cl, K, and Sr) were quantified in the otoliths of pollock larvae by using EPMA. Average concentrations of the elements ranged from approximately 4 mg/g (otolith weight) for Na to less than 1 mg/g for Cl, S, and K. We found significant differences in the elemental composition both among sampling locations and across positions on the otoliths. Multivariate analyses of elemental signatures revealed significant differences among locations from samples 0–20 μm from the nucleus (MANOVA; Pillai's trace=1.18; $F_{30,560}=5.74$; $P<0.0001$), and 20–45 μm from the nucleus (MANOVA; Pillai's trace=1.47; $F_{24,364}=8.86$; $P<0.0001$).

Analysis of variance and Tukey's HSD *a posteriori* multiple comparison tests identified the individual elements contributing to differences in the multivariate signatures among locations. All six elements showed significant differences among locations at 0–20 μm from the otolith nucleus (Table 3). Multiple comparisons for each of the elements indicated relatively subtle differences among locations. Phosphorus concentrations were, however, significantly higher in samples from Yakutat than any of the other locations. Results of the ANOVA from samples at distances 20–45 μm from the nucleus were generally comparable with samples closer to the nucleus (Table 3). Although only Cl showed no significant variation among locations (Table 3), multiple comparisons of mean values for each element revealed little geographic patterns among locations. Note that Shelikof Strait samples were removed from this analysis because of a small sample size in this distance category.

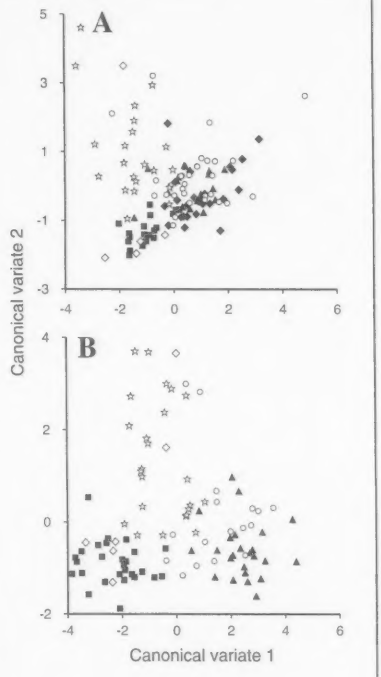

Figure 2

Plot of first two canonical variates contrasting multivariate elemental signatures in otoliths of walleye pollock (*Theragra chalcogramma*) determined by using electron probe microanalysis, at 0–20 μm from the nucleus (**A**) and 20-40 μm from the nucleus (**B**). Larvae were collected from the North Bering Sea (▲), southeast Bering Sea (○), Bristol Bay (■), Shelikof Strait (◆), Prince William Sound (◇), and Yakutat (☆).

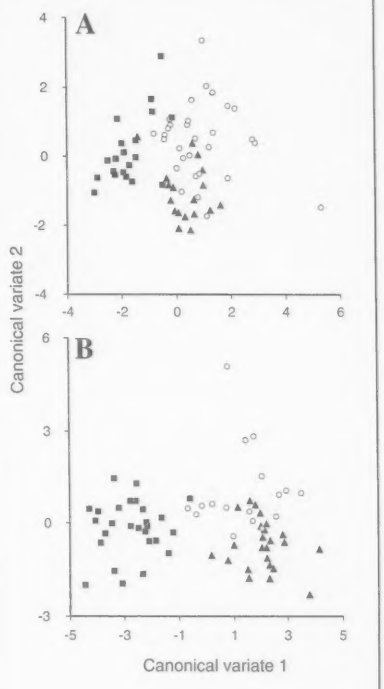

Figure 3

Plot of first two canonical variates contrasting multivariate elemental signatures in otoliths of walleye pollock (*Theragra chalcogramma*) determined by electron probe microanalysis at 0–20 μm from the nucleus (**A**) and 20–40 μm from the nucleus (**B**). Larvae were collected from the North Bering Sea (▲), southeast Bering Sea (○), and Bristol Bay (■).

We used CDA to visualize multivariate differences among locations in reduced dimensional space. Three groups were readily discernible in a plot of the first two canonical variates (Fig. 2). Samples from the North Bering Sea, the southeast Bering Sea, and Shelikof Strait formed one group separated from Yakutat, Bristol Bay, and Prince William Sound samples along the first canonical variate. The second canonical variate separated Yakutat samples from Bristol Bay and Prince William Sound individuals. Elemental signatures at 20–45 μm from the otolith nucleus were distributed similarly in canonical space to samples from the otolith nucleus (Fig. 2). Three groupings were apparent in the canonical plot, and Bering Sea larvae were separated from Bristol Bay and Prince William samples on canonical variate one, and Yakutat samples were separated from all other locations on canonical variate two. We then conducted a similar analysis with only samples from the southeast and North Bering Sea and Bristol Bay. Elemental signatures of larvae from the Bering Sea separated from Bristol Bay on canonical variate one. The southeast Bering Sea samples separated from the North Bering Sea along canonical variate two, although not as clearly as with the elemental signatures from the Bering Sea and Bristol Bay (Fig. 3).

Elemental profiles across otoliths varied significantly, as determined by repeated measures ANOVA, among the five locations for Na, P, S, and Sr (Table 4). Both S and Sr concentrations declined from high values at the nucleus to significantly lower values towards the edge of the otolith (Fig. 4). Repeated measures ANOVA also provided a test of the differences among locations when data were averaged over the otolith profiles. Significant differences among locations were detected for

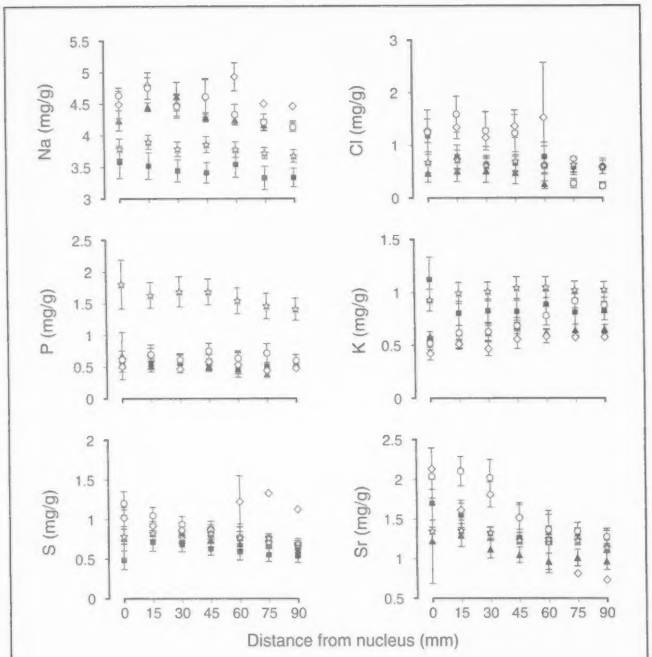

Figure 4

Profiles of elemental concentrations, determined by electron probe microanalysis, from the nucleus out to a distance of approximately 90 μm in the otoliths of larval walleye pollock (*Theragra chalcogramma*) collected from the North Bering Sea (▲), southeast Bering Sea (○), Bristol Bay (■), Prince William Sound (◇), and Yakutat (☆). Individual points are mean (±SE) values grouped at 15-μm intervals.

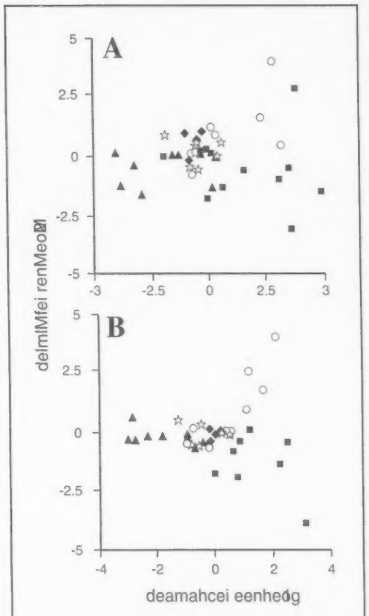

Figure 5

Plot of the first two canonical variates contrasting multivariate elemental signatures in otoliths of walleye pollock (*Theragra chalcogramma*) determined with laser ablation ICP-MS, at 0–40 μm from the nucleus (**A**) and 40–80 μm from the nucleus (**B**). Larvae and juveniles were collected from the North Bering Sea (▲), southeast Bering Sea (○), Bristol Bay (■), Prince William Sound (◆), and Yakutat (☆).

five elements (Sr, K, S, P, and Na). Finally, the interaction term (position×location) in the repeated measures ANOVA tested the hypothesis that the shape of the elemental profiles differed among locations. There was a significant interaction between profile and location for K.

Laser ablation ICP-MS

We quantified Mn/Ca, Sr/Ca, and Ba/Ca ratios in the otoliths of larval walleye pollock using laser ablation ICP-MS. Both Mn and Ba were found at trace levels in otoliths, with average values of approximately 3 μmol/mol and 6 μmol/mol, respectively. Strontium was present in the otoliths at an average concentration of approximately 2.2 mmol/mol. A MANOVA detected significant differences among locations from a raster centered on the nucleus (MANOVA; Pillai's trace=0.85; $F_{12,99}$=3.26; P<0.0005), and from the average values of lines 40–80 μm from the nucleus (MANOVA; Pillai's trace=0.99; $F_{12,99}$=4.1; P<0.0001).

Univariate ANOVA and *a posteriori* multiple comparisons by using Tukey's HSD revealed that Mn/Ca, Sr/Ca, and Ba/Ca ratios varied significantly among locations at the otolith nucleus and at positions 40–80 μm from the nucleus (Table 5). Samples from the North Bering Sea had consistently lower Sr/Ca and Ba/Ca ratios than those from the southeast Bering Sea at both positions. However, we noted only subtle differences among the Gulf of Alaska and Bristol Bay samples.

We found a total of three groupings in canonical plots of multivariate elemental signatures from the otoliths of larval walleye pollock (Fig. 5). Samples from the North Bering Sea and Bristol Bay were separated along canonical variate one. A third grouping, including larvae from the southeast Bering Sea, Prince William Sound, and Yakutat, clustered together in the center of the canonical plot. Samples from the nucleus and 40–80 μm outside the nucleus showed very similar geographic patterns.

Repeated measures ANOVA detected significant differences in both Mn/Ca and Ba/Ca profiles from the nu-

Table 4

EPMA results from repeated-measures ANOVA of elemental profiles across otoliths from walleye pollock (*Theragra chalcogramma*) larvae collected at five locations in the Bering Sea and the Gulf of Alaska. Within-subject effects (profile and profile×location) tested by using MANOVA (Pillai's trace), and between subjects effect (location) tested by using ANOVA (degrees of freedom [df]; sums of squares [SS]; mean squares [MS]). *** = significant at $\alpha = 0.05$; ns = nonsignificant.

Element	Source	df	Pillai's trace or SS	MS	*F*	*P* < F
Na	Profile	6, 41	4.9×10^{-1}		6.67	***
	Profile×location	24, 176	5.3×10^{-1}		1.12	ns
	Location	4	43.8	10.9	10.35	***
	Error	46	48.7	1.1		
P	Profile	6, 40	3.0×10^{-1}		2.91	***
	Profile×location	24, 172	4.6×10^{-1}		0.93	ns
	Location	4	55.0	13.8	8.07	***
	Error	45	76.8	1.7		
S	Profile	6, 41	3.6×10^{-1}		3.92	***
	Profile×location	24, 176	5.3×10^{-1}		1.12	ns
	Location	4	3.8	9.6×10^{-1}	4.56	***
	Error	46	9.7	2.1×10^{-1}		
Cl	Profile	6, 39	1.8×10^{-1}		1.41	ns
	Profile×location	24, 168	3.7×10^{-1}		0.72	ns
	Location	4	8.0	2.0	1.6	ns
	Error	44	55.3	1.3		
K	Profile	6, 41	8.3×10^{-2}		0.62	ns
	Profile×location	24, 176	8.5×10^{-1}		1.98	***
	Location	4	4.3	1.1	2.61	***
	Error	46	19.1	4.1×10^{-1}		
Sr	Profile	6, 40	4.5×10^{-1}		5.51	***
	Profile×location	24, 172	7.7×10^{-1}		1.72	ns
	Location	4	6.4	1.6	3.96	***
	Error	45	18.2	4.0×10^{-1}		

Table 5

Laser ablation ICP-MS results of one-factor ANOVA (degrees of freedom [df]; sums of squares [SS]; mean square [MS]) at two positions (0–40 μm and 40–80 μm from the nucleus) in walleye pollock (*Theragra chalcogramma*) otoliths collected at five locations: the southeast Bering Sea [SB], North Bering Sea (NB), Bristol Bay (BB), Prince William Sound (PW), and Yakutat (YK). ***= significant at $\alpha = 0.05$; ns=nonsignificant. Multiple comparisons among locations were conducted by using Tukey's honestly significant difference (HSD). Locations were ordered (left to right) from lowest to highest ratios; lines link locations that were not significantly different (α=0.05).

Element	Source	df	SS	MS	*F*	*P* < F	Tukey's HSD
0–40 μm (nucleus)							
Mn/Ca	Locations	4	19.3	4.82	3.5	***	PW NB SB YK BB
	Error	33	45.5	1.38			
Sr/Ca	Locations	4	1.07	0.27	3.43	***	NB YK BB PW SB
	Error	33	2.58	0.08			
Ba/Ca	Locations	4	219	54.8	3.35	***	NB BB PW YK SB
	Error	33	540	16.4			
40–80 μm							
Mn/Ca	Locations	4	30.7	7.68	3.24	***	NB PW SB YK BB
	Error	33	78.3	2.37			
Sr/Ca	Locations	4	0.99	0.25	3.70	***	NB YK PW BB SB
	Error	33	2.21	0.07			
Ba/Ca	Locations	4	397	99.2	5.50	***	NB BB PW YK SB
	Error	33	595	18.0			

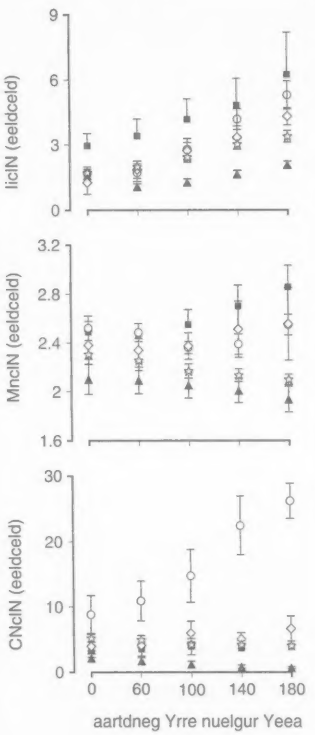

Figure 6

Profiles of elemental ratios, determined with laser ablation ICP-MS, from the nucleus out to a distance of approximately 200 μm in the otoliths of larval and juvenile walleye pollock (*Theragra chalcogramma*) collected from the North Bering Sea (▲), southeast Bering Sea (○), Bristol Bay (■), Prince William Sound (◇), and Yakutat (☆). Individual points are mean (±SE) values grouped at 40-μm intervals.

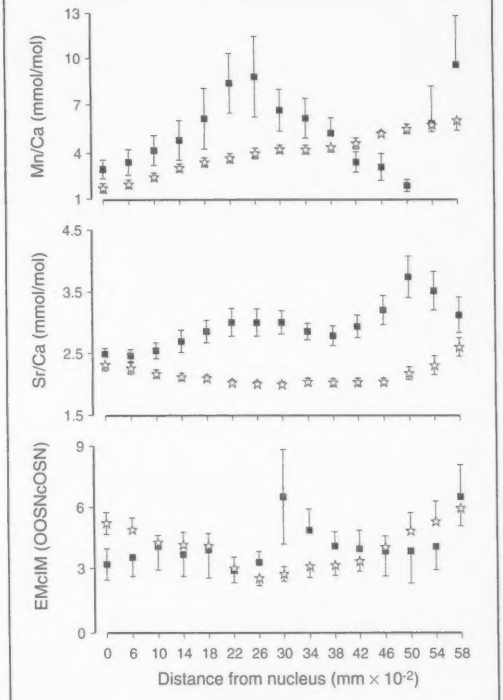

Figure 7

Profiles of elemental ratios, determined by using laser ablation ICP-MS, from the nucleus out to a distance of approximately 600 μm in the otoliths of juvenile walleye pollock (*Theragra chalcogramma*) collected from Bristol Bay (■) and Yakutat (☆). Individual points are mean (± SE) values grouped at 40-μm intervals.

cleus out to a distance of approximately 200 μm in the walleye pollock otoliths (Fig. 6, Table 6). The univariate test of location, averaged over the individual otolith profiles, was significant for both Sr/Ca and Ba/Ca. We also found significant interactions between profile and location for Mn/Ca, Sr/Ca, and Ba/Ca ratios (Table 6). Manganese values increased from the nucleus to the otolith edge at all locations, indicating that the significant interaction was generated by the observation that the profile from the North Bering Sea was considerably flatter than profiles from Bristol Bay and southeast Bering Sea. Strontium trajectories were more dynamic; profiles from some locations increased from the nucleus to the edge (Bristol Bay and Prince Williams Sound), profiles from other locations decreased (North Bering Sea and Yukatat), and a single location (southeast Bering Sea) showed no obvious trend. Finally, profile variations in Ba/Ca ratios among locations were dominated by a sharp increase in Ba/Ca ratios across the otoliths in the southeast Bering Sea samples. Profiles were effectively horizontal for the other four locations.

Otoliths in walleye pollock collected from Bristol Bay and Yakutat were significantly larger than those from the other four locations. We were, therefore, able to conduct extended profiles in these otoliths out to a distance of approximately 600 μm (Fig. 7). After starting at similar values at the nucleus, Mn/Ca and Sr/Ca profiles from the two locations quickly diverged and appeared to vary largely independently over the remaining time periods. The Ba/Ca profiles also appeared to be varying independently between the two locations, although the relative magnitude of differences between the two locations was smaller than for either Mn/Ca or Sr/Ca profiles.

Table 6

Laser ablation ICP-MS results from repeated-measures ANOVA of elemental profiles across otoliths from walleye pollock (*Theragra chalcogramma*) larvae collected at five locations in the Bering Sea and the Gulf of Alaska. Within-subject effects (profile and profile×location) were tested by using MANOVA (Pillai's trace), and between subjects effect (location) tested by using ANOVA (degrees of freedom [df]; sums of squares [SS]; mean squares [MS]). *** = significant at $\alpha = 0.05$; ns = nonsignificant.

Element	Source	df	Pillai's trace or SS	MS	*F*	*P* < F
Mn/Ca	Profile	4, 30	3.0×10^{-1}		17.1	***
	Position×location	16, 132	7.4×10^{-1}		1.9	***
	Location	4	1.99×10^{2}	49.7	2.49	ns
	Error	33	6.61×10^{-2}	20.1		
Sr/Ca	Profile	4, 30	2.18×10^{-1}		2.09	ns
	Position×location	16, 132	9.19×10^{-1}		2.46	***
	Location	4	1.05×10^{1}	2.62	6.02	***
	Error	33	1.44×10^{1}	0.44		
Ba/Ca	Profile	4, 30	6.92×10^{-1}		16.83	***
	Position×location	16, 132	1.04		2.9	***
	Location	4	5.83×10^{3}	1459	15.25	***
	Error	33	3.16×10^{3}	95.6		

Discussion

Quantifying dispersal pathways of larval fishes in marine environments is a difficult proposition. Marine fishes typically produce on the order of 10^4–10^6 eggs in a single spawning episode. These propagules are quickly dispersed in large volumes of seawater, making recovery of marked individuals difficult even if it were possible to introduce an artificial tag into the larvae at the time of spawning (Jones et al., 1999). Natural geochemical signatures in otoliths offer a useful alternative to artificial tagging approaches (Thorrold et al., 2002). The technique relies upon the assumption that larvae spawned at any given location retain a unique elemental or isotopic signature in their otoliths that can be recovered some time afterwards, and that variations in otolith geochemistry are sufficient to distinguish among geographic locations of interest. We found that elemental signatures in the otoliths of larval walleye pollock differed significantly geographically and with ontogeny. Samples at specific points on the otoliths, at the nucleus, and shortly after hatching, showed very similar patterns of variability, suggesting that the technique will likely be a robust method for identifying natal origins of walleye pollock after suitable groundtruthing of known spawning locations (e.g., Thorrold et al., 2001; Gillanders, 2002).

Elemental signatures in the otoliths of the larval pollock were assayed by using EPMA and laser ablation ICP-MS. Campana et al. (1997) noted that the two techniques were largely complementary in terms of elements that could be reliably assayed, and indeed only Sr was able to be quantified by both instruments in our study. Patterns of geographic variability presumably reflected the elements that were used in generating the multivariate signatures produced by each instrument. Elemental signatures from the EPMA data clustered into a Bering Sea group that included Shelikof Strait but excluded Bristol Bay, a coastal grouping that included Bristol Bay and Prince William Sound, whereas samples from Yakutat were separated from all other locations. Although sample sizes were smaller for the laser ablation ICP-MS assays, the data identified a grouping of locations in multivariate space that included the southeast Bering Sea, Prince William Sound, and Yakutat, whereas samples from both the north Bering Sea and Bristol Bay were separated from each other and the other locations. The observation that locations did not cluster into similar geographic groupings was probably a function of different mechanisms of elemental incorporation in otoliths. Elements assayed by ICP-MS in the present study substitute for Ca in the aragonitic lattice, and are believed to primarily reflect ambient physicochemical differences among natal locations (Bath et al., 2000; Milton and Chenery, 2001; Bath Martin et al, 2003). However, with the exception of Sr, the elements assayed by EPMA are likely under physiological regulation and therefore probably do not directly reflect either water chemistry or temperature (Campana, 1999). In either case, the application of elemental signatures in otoliths as natural tags of natal origins requires only that the signatures allow accurate classification of the natal origins of an unknown fish. A final caveat is necessary because it remains possible that preservation effects, particularly for labile elements that are not incorporated into the aragonite lattice, may also have contributed to at least some of the differences among locations (Milton and Chenery, 1998; Proctor et al., 1998). If present, such effects would clearly confound attempts to use elemental signatures as a natural tag of natal origins (Thresher, 1999).

It is important to note that although EPMA and laser ablation ICP-MS provided complementary information

on elemental composition, the spatial scale on which the data were gathered was different. Our laser ablation ICP-MS method required that we ablate a 70 μm × 70 μm raster, or a 720-μm line, in order to enable sufficient time to generate precise estimates of otolith composition. The EPMA analysis was less destructive than laser ablation ICP-MS, and therefore it was possible to sample individual points at a much finer spatial resolution (~5 μm), albeit with considerably less sensitivity and precision. For instance, using EPMA we were able to sample five points across a transect ending approximately 90 μm from the nucleus. In contrast, only a single raster could be sampled along this profile with laser ablation ICP-MS. Although the diameter of laser probes is approaching that of EPMA, ICP-MS is unlikely to match the spatial resolution of EPMA without further development of truly simultaneous mass analyzers such as time-of-flight ICP mass spectrometry (Mahoney et al., 1996). However, we were able to program the laser probe to trace out growth increments once the otolith radius had reached 120 μm and we found that the total length of a daily ring was approximately 700 μm. This finding, in turn, allowed us to construct elemental profiles at reasonable spatial resolution across the otoliths of larval pollock without sacrificing instrument precision by limiting acquisition times. Although it has not been used before with otoliths, our approach provides significant advantages over previous methods of using a raster to create elemental profiles (e.g., Thorrold et al., 1997; Thorrold and Shuttleworth 2000).

Previous work on pollock otolith chemistry was somewhat successful at distinguishing fish from locations in the Bering Sea and the Gulf of Alaska. Severin et al. (1995) used EPMA to sample the outer margin of otoliths from juvenile pollock collected along the Alaska Peninsula in the Gulf of Alaska and in Bristol Bay. We generated elemental profiles across otoliths from the nucleus out to approximately 90 μm for the EPMA samples, and up to 600 μm for the laser ablation ICP-MS assays. The profiles revealed some interesting differences between the elements assayed by each instrument. For instance, only one of the elements (K) from the EPMA analysis showed a significant interaction between profile and location, yet significant profile×location interactions were detected for Mn/Ca, Sr/Ca, and Ba/Ca ratios with laser ablation ICP-MS. We were also struck by the similarity of profiles from individuals sampled at the same location, as evidenced by the size of standard errors around mean values at specific distances across the otolith. For instance, the extended profiles from pollock collected in Bristol Bay and Yakutat show independent patterns of variation for all three elements from the nucleus out to 600 μm. Taken together, these data indicate that larvae from several spawning locations are indeed encountering water masses with differing physicochemical properties through their larval lives, and at approximately the same time. We lack, however, a sufficient understanding of the mechanisms controlling otolith chemistry to be able to relate the profiles to specific properties of different water masses in the study area. This knowledge will be necessary before it is possible to reconstruct dispersal pathways of larval pollock based on probe-based analyses of otolith geochemistry. Nonetheless, the among-location variability in elemental profiles revealed by both instruments is encouraging and justifies further investigations of otolith geochemistry in larval pollock.

Past attempts at identifying stock structure of walleye pollock in the North Pacific Ocean based on genetic techniques have been inconclusive (Bailey et al., 1999). In the most recent study, Olsen et al. (2002) were unable to distinguish between pollock from the Kamchatka Peninsula and several locations within the Gulf of Alaska based on three polymorphic microsatellite loci. Allozyme and MtDNA markers showed significant differences between North American and Asian populations, and among Gulf of Alaska locations. These data were difficult to reconcile because both markers showed temporal instability within locations. Adult tagging studies shed little light on the population structure of pollock because they address questions of repeat spawning, whereby adult fish return to the same area to spawn in subsequent years, rather than homing to natal spawning locations (Tsugi, 1989). It has proved impossible, except in rare circumstances (Jones et al., 1999), to artificially mark larvae before they are dispersed from spawning grounds, and therefore natural geochemical tags remain the most promising avenue for determining natal origins in walleye pollock. The ability to determine natal origins of individual fish is critical in the case of migratory marine fishes because it allows quantification of population connectivity through straying of adults as well as through larval dispersal (Thorrold et al., 2001). These data, in turn, identify the spatial extent of fish stocks that are demographically isolated or alternatively provide connectivity rates that are necessary to parameterize spatially explicit models if the species is usefully viewed as a metapopulation (Hanski and Gilpin, 1997; Smedbol and Wroblewski, 2002).

In summary, the elemental composition of otolith material deposited during early larval life in walleye pollock differed significantly among locations in the Gulf of Alaska and Bering Sea. These results imply that the larvae originated from different spawning locations, not that they constitute separate stocks. Nonetheless, these data represent the necessary first steps in using elemental signatures in otoliths as natural tags of natal origins in walleye pollock. Elemental profiles across otoliths were also unique to specific locations, suggesting that individuals collected at a location had experienced similar environmental conditions throughout their larval lives. This observation raised the possibility of reconstructing larval dispersal pathways based on high-resolution sampling of otolith chemistry. Although further work is needed to understand the processes influencing elemental uptake in pollock otoliths, we suggest that the potential information available from such studies would be invaluable for effective management of commercial pollock fisheries (Bailey et al., 1999). The approach appears to be particularly appropriate for in-

vestigating the potential existence of fine-scale population structure throughout the species range. Significant fine-scale population structure has been linked to the failure of northern cod stocks to recover from exploitation, even in the face of fishing moratoriums (Frank and Brickman, 2000; Hutchings, 2000). Analogous demographic processes acting in northern cod populations are clearly possible in walleye pollock, given the phyologenetic and life history similarities between the two species. The structure of pollock stock complexes within the major basins of the North Pacific Ocean remains, therefore, a critical gap in the knowledge necessary for the sustainable management of one of the world's largest marine fisheries.

Acknowledgments

This work was funded by North Pacific Marine Research Program to KMB, SRT and KPS, and was supported in part by NSF grants OCE-9871047 and OCE-0134998 to SRT. We thank the MACE, FOCI and groundfish task scientists who collected samples, and C. Latkoczy for assistance with the laser ablation ICP-MS analyses. This is Fisheries-Oceanography Coordinated Investigations collection number 0471-00A-0.

Literature cited

Bailey, K. M., T. J. Quinn, II, P. Bentzen, and W. S. Grant.
1999. Population structure and dynamics of walleye pollock, *Theragra chalcogramma*. Adv. Mar. Biol. 37:179–255.

Bath, G. E., S. R. Thorrold, C. M. Jones, S. E. Campana, J. W. McLaren, and J. W. H. Lam.
2000. Strontium and barium uptake in aragonitic otoliths of marine fish. Geochim. Cosmochim. Acta 64: 1705–1714.

Bath Martin, G. E., S. R. Thorrold, and C. M. Jones.
2004. The influence of temperature and salinity on strontium uptake in the otoliths of juvenile spot (*Leiostomus xanthurus*). Can. J. Fish. Aquat. Sci. 61:34–42.

Begg, G. A., and J. R. Waldman.
1999. An holistic approach to fish stock identification. Fish. Res. 43:1–3.

Campana, S. E.
1999. Chemistry and composition of fish otoliths: pathways, mechanisms and applications. Mar. Ecol. Prog. Ser. 188:263–297.

Campana, S. E., J. A. Gagne, and J. W. McLaren.
1995. Elemental fingerprinting of fish otoliths using ID-ICPMS. Mar. Ecol. Prog. Ser. 122:115–120.

Campana, S. E., and J. D. Neilson.
1985. Microstructure of fish otoliths. Can. J. Fish. Aquat. Sci. 42:1014–1032.

Campana, S. E., S. R. Thorrold, C. M. Jones, D. Guenther, M. Tubrett, H. Longerich, S. Jackson, N. M. Halden, J. M. Kalish, P. Piccoli, H. De Pontual, H. Troadec, J. Panfili, D. H. Secor.
1997. Comparison of accuracy, precision, and sensitivity in elemental assays of fish otoliths using the electron microprobe, proton-induced X-ray emission, and laser ablation inductively coupled plasma mass spectrometry. Can. J. Fish. Aquat. Sci. 54:2068–2079.

Frank, K. T., and D. Brinkman.
2000. Allee effects and compensatory population dynamics within a stock complex. Can. J. Fish. Aquat. Sci. 57:513–517.

Gillanders, B. M.
2002. Connectivity between juvenile and adult fish populations: do adults remain near their recruitment estuaries? Mar. Ecol. Prog. Ser. 240:215–223.

Grant, W. S., and F. M. Utter.
1980. Biochemical genetic variation in walleye pollock, *Theragra chalcogramma* population structure in the southeastern Bering Sea and the Gulf of Alaska. Can. J. Fish. Aquat. Sci. 37: 093–1100.

Gunn, J. S. H., I. R. Harrowfield, C. H. Proctor and R. E.Thresher.
1992. Electron probe microanalysis of fish otoliths--evaluation of techniques for studying age and stock discrimination. J. Exp. Mar. Biol. Ecol. 158:1–36.

Günther, D., and C. A. Heinrich.
1999. Enhanced sensitivity in laser ablation-ICP mass spectrometry using helium-argon mixtures as aerosol carrier. J. Anal. At. Spectrom 14:1363–1368.

Hanski, I., and M. Gilpin (eds.).
1997. Metapopulation dynamics. Academic Press, San Diego, CA.

Hellberg, M. E., R. S. Burton, J. E. Neigel, and S. R. Palumbi.
2002. Genetic assessment of connectivity among marine populations. Bull. Mar. Sci. 70273–290.

Hinckley, S.
1987. The reproductive biology of walleye pollock, *Theragra chalcogramma*, in Bering Sea, with reference to spawning stock structure. Fish. Bull. 85:481–498.

Hutchings, J. A.
2000. Collapse and recovery of marine fishes. Nature 406:882–885.

Jones, G. P., M. J. Milicich, M. J. Emslie, and C. Lunow.
1999. Self-recruitment in a coral reef fish population. Nature 402:802–804.

Littel, R. C., R. J. Freund, and P. C. Spector.
1991. SAS systems for linear models, 3rd ed. SAS Inst., Inc., Cary, NC.

Mahoney, P. P., G. Li, and G. M. Hieftje.
1996. Laser ablation-inductively coupled plasma mass spectrometry with a time-of-flight mass analyzer. J. Anal. At. Spectrom. 11:401–405.

Milton, D. A., and S. R. Chenery.
1998. The effect of otolith storage methods on the concentrations of elements detected by laser-ablation ICPMS. J. Fish Biol. 53:785–794.
2001. Sources and uptake of trace metals in otoliths of juvenile barramundi (*Lates calcarifer*). J. Exp. Mar. Biol. Ecol. 264:47–65

Mulligan, T. J., R. W. Chapman, and B. L. Brown.
1992. Mitochondrial DNA analysis of walleye pollock, *Theragra chalcogramma* , the eastern Bering Sea and Shelikof Strait, Gulf of Alaska. Can. J. Fish. Aquat. Sci. 49:319–326.

Olsen, J. B., S. E. Merkouris, and J. E. Seeb.
2002. An examination of spatial and temporal genetic variation in walleye pollock (*Theragra chalcogramma*) using allozyme, mitochondrial DNA, and microsatellite data. Fish. Bull. 100:752–764.

Proctor, C. H. and R. E. Thresher.
1998. Effects of specimen handling and otolith prepara-

tion on concentration of element in fish otoliths. Mar. Biol. 131: 681–694.

Rosenthal, Y., P. M. Field, and R. M. Sherrell.
1999. Precise determination of element/calcium ratios in calcareous samples using sector field inductively coupled plasma mass spectrometry. Anal. Chem. 71:3248–3253.

Scott, V. D., G. Love, and S. J. B. Reed.
1995. Quantitative electron-probe analysis. Ellis Horwood Limited, Hemel Hempstead, Hertfordshire, England.

Serobaba, I. I.
1977. Data on the population structure of the walleye pollock, *Theragra chalcogramma*, from the Bering Sea. J. Ichthyol. 17:219–231.

Severin, K. P., J. Carroll and B. L. Norcross.
1995. Electron microprobe analysis of juvenile walleye pollock, *Theragra chalcogramma*, otoliths from Alaska: a pilot stock separation study. Environ. Biol. Fishes 43:269–283.

Shields, G. F., and J. R. Gust.
1995. Lack of geographic structure in mitochondrial DNA sequences of Bering walleye pollock, *Theragra chalcogramma*. Molecular Mar. Biol. Biotechnol. 4:69–82.

Smedbol, R. K., and J. S. Wroblewski.
2002. Metapopulation theory and northern cod population structure: interdependency of subpopulations in recovery of a groundfish population. Fish. Res. 55: 161–174.

Temnykh, O. S.
1994. Morphological differentiation of walleye pollock *Theragra chalcogramma* the western Bering Sea and Pacific Kamchatka waters. Voprosy ikhtiologii 34: no. 2.

Thorrold, S. R., C. M. Jones, and S. E. Campana.
1997. Response of otolith microchemistry to environmental variations experienced by larval and juvenile Atlantic croaker (*Micropogonias undulatus*). Limnol. Oceanogr. 42:102–111.

Thorrold, S. R., G. P. Jones, M. E. Hellberg, R. S. Burton, S. E. Swearer, J. E. Neigel, S. G. Morgan, and R. R. Warner.
2002. Quantifying larval retention and connectivity in marine populations with artificial and natural markers. Bull. Mar. Sci. 70:291–308.

Thorrold, S. R., C. Latkoczy, P. K. Swart, and C. M. Jones.
2001. Natal homing in a marine fish metapopulation. Science 291:297–299.

Thorrold, S. R., and S. Shuttleworth.
2000. In situ analysis of trace elements and isotope ratios in fish otoliths using laser ablation sector field inductively coupled plasma mass spectrometry. Can. J. Fish. Aquat. Sci. 57:232–242.

Thresher, R. E.
1999. Elemental composition of otoliths as a stock delineator in fishes. Fish. Res. 43:165–204.

Thresher, R. E., C. H. Proctor, J. S. Gunn, and I. R. Harrowfield.
1994. An evaluation of electron-probe microanalysis of otoliths for stock delineation and identification of nursery areas in a southern temperature groundfish, *Nemadactylus macropterus*. Fish. Bull. 92:817–840.

Tsugi, S.
1989. Alaska pollock population, *Theragra chalcogramma*, of Japan and its adjacent waters: Japanese fisheries and population studies. Mar. Behav. Physiol. 15:147–205.

Waples, R. S.
1998. Separating the wheat from the chaff: patterns of genetic differentiation in high gene flow species. J. Heredity 89:438–450.

Winer, B.
1971. Statistical principles in experimental design, 2nd ed. McGraw-Hill, New York, NY.

Yoshinaga, J., A. Nakama, M. Morita, and J. S. Edwards.
2000. Fish otolith reference material for quality assurance of chemical analyses. Mar. Chem. 69:91–97.

A sudden collapse in distribution of Pacific sardine (*Sardinops sagax*) off southwestern Australia enables an objective re-assessment of biomass estimates

Daniel J. Gaughan
Timothy I. Leary
Ronald W. Mitchell
Ian W. Wright

Western Australian Marine Research Laboratories
Department of Fisheries
West Coast Drive
Waterman, Western Australia 6020, Australia
E-mail address (for D. J. Gaughan): dgaughan@fish.wa.gov.au

Abstract—Fishery-independent estimates of spawning biomass (B_{SP}) of the Pacific sardine (*Sardinops sagax*) on the south and lower west coasts of Western Australia (WA) were obtained periodically between 1991 and 1999 by using the daily egg production method (DEPM). Ichthyoplankton data collected during these surveys, specifically the presence or absence of *S. sagax* eggs, were used to investigate trends in the spawning area of *S. sagax* within each of four regions. The expectation was that trends in B_{SP} and spawning area were positively related. With the DEPM model, estimates of B_{SP} will change proportionally with spawning area if all other variables remain constant. The proportion of positive stations (PPS), i.e., stations with nonzero egg counts—an objective estimator of spawning area—was high for all south coast regions during the early 1990s (a period when the estimated B_{SP} was also high) and then decreased after the mid-1990s. There was a decrease in PPS from the mid-1990s to 1999. The particularly low estimates in 1999 followed a severe epidemic mass mortality of *S. sagax* throughout their range across southern Australia. Deviations from the expected relationship between B_{SP} and PPS were used to identify uncertainty around estimates of B_{SP}. Because estimation of spawning area is subject to less sampling bias than estimation of B_{SP}, the deviation in the relation between the two provides an objective basis for adjusting some estimates of the latter. Such an approach is particularly useful for fisheries management purposes when sampling problems are suspected to be present. The analysis of PPS undertaken from the same set of samples from which the DEPM estimate is derived will help provide information for stock assessments and for the management of purse-seine fisheries.

Manuscript submitted 5 December 2002 to the Scientific Editor's Office.

Manuscript approved for publication 27 April 2004 by the Scientific Editor.

Fish. Bull. 102:617–633 (2004).

As a stock of small pelagic fish decreases, biomass assessment becomes problematic because of such factors as patchy distribution (Fletcher and Sumner, 1999) and continuing high catchability as a result of the schooling behavior of some fish (Uphoff, 1993). In these circumstances, ichthyoplankton surveys can provide a useful means of estimating spawning biomass, B_{SP}, for some pelagic fish species. Mangel and Smith (1990) used a technique that assessed the presence or absence of sardine (*Sardinops sagax*) eggs in a known spawning area. They found that changes in adult biomass were more accurately predicted by using presence-absence of eggs in sampling surveys than mean egg abundance because of misleading results arising from the spatial patchiness of eggs. In their presence-absence analysis, the spatial distribution of eggs is the key determinant of B_{SP} estimates and is used in a model with a series of other parameters to provide an estimate of B_{SP} (Mangel and Smith, 1990). Although this technique provides an objective indication of stock size that is not subjected to the inherent problems in estimating B_{SP} with the daily egg production method (DEPM, e.g., Ward et al., 2001), the modeling requires substantial prior knowledge of adult and egg production parameters. More recently, Zenitani and Yamada (2000) developed an optimal relationship between B_{SP} and spawning area for the Japanese sardine (*Sardinops melanostictus*) using a nonlinear model that assumed patchy egg distribution. In their case, biomass was estimated by using virtual population analysis with catch-at-age data from the commercial fishery.

The purse seine fishery for *Sardinops sagax* in Western Australia (WA) operates along the south coast around the port regions of Esperance, Bremer Bay, and Albany; and on the lower West Coast in the regions of Fremantle and Dunsborough (Fig. 1). A level of spatial distinctness among adult *Sardinops* populations necessitates that three south coast regions and the west coast region be managed as separate fisheries (Gaughan et al., 2002). Unlike the case with Japanese sardine (Zenitani and Yamada, 2000), it has not been possible to estimate the B_{SP} of *Sardinops* in each fishery in WA using only an age-based approach. Although Gaughan et al. (2002) considered the catch-at-age data for the WA *Sardinops* fisheries to be reasonable, the data span a relatively short time series, commencing in 1988 at Albany and Bremer Bay and later at the other regions. Therefore, both age-structure data and estimates of spawning biomass (B_{SP}) obtained with the DEPM have provided the biological basis for managing the *Sardinops* fisheries in WA for over a decade (Fletcher, 1991, 1995; Fletcher et al., 1996,

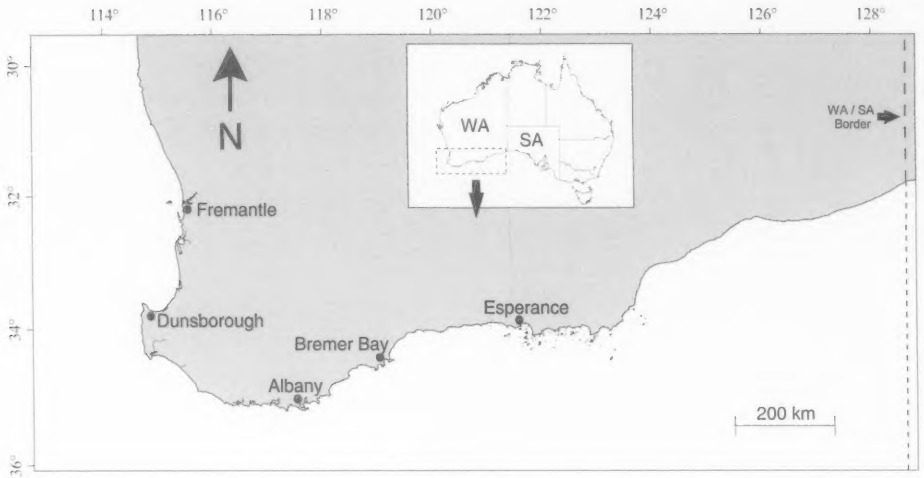

Figure 1

Map of southwestern Australia showing Pacific sardine fishing ports. North of Dunsborough to Fremantle constitutes the west coast fishery and the other regions constitute the south coast fishery. WA = Western Australia, SA = South Australia.

1996[1]; Cochrane[2]). A population model that integrates age-structure information and DEPM-derived estimates of B_{SP} ($B_{SP\text{-}DEPM}$) has recently been developed by Hall (2000) for each of the three south coast regions.

Although the DEPM is able to provide relatively robust estimates of B_{SP} for a variety of species (Alheit, 1993; Hunter and Lo, 1997), it is not without problems (Cochrane, 1999; Ward et al., 2001). The $B_{SP\text{-}DEPM}$ estimates for *Sardinops* in WA are presented at Management Advisory Committee (MAC) meetings and, in turn, are provided to the relevant government minister. The $B_{SP\text{-}DEPM}$ estimates therefore undergo critical scrutiny by industry representatives. The shortcomings of the DEPM (e.g., sensitivity of precision for small sample sizes) are well understood by the members of the management committee; industry recognizes that onshore infrastructure and fleet capacity must be matched to long-term average B_{SP} and that industry should not capitalize at levels that require maximal stock sizes to meet financial expectations. Inasmuch, a level of conservatism has been adopted by the Management Advisory Committee when setting quotas. Nonetheless, the accuracy of estimates has been a contentious issue; industry members typically believe that the scientific advice presented often underestimates the B_{SP}. Likewise, wide confidence intervals around biomass estimates introduce doubt in the minds of industry members regarding the reliability of scientific advice, which can therefore stall the implementation of management measures. However, the lack of a formal and objective means of dealing with suspect and imprecise $B_{SP\text{-}DEPM}$ estimates (e.g., because of problems with sampling spawning fish) has previously not been rigorously addressed.

Following the progression along the southern WA coast in early 1999 of a mass mortality of *Sardinops*, estimates of the quantity killed at Albany appeared to be very low (Gaughan et al., 2000). That is, very few dead *Sardinops* were found in comparison to the other regions where fisheries occur. Mortality rates for Esperance and Bremer Bay were 69.6% and 74.5% of the B_{SP}, respectively, whereas that for Albany was estimated to be only 2.4%. Estimates of the mortality rate of *Sardinops* in South Australia (SA, Fig. 1) for the same epizootic event were independently found to also be around 70% (Ward et al., 2001). The inconsistency with Albany could not be attributed to different weather conditions; the weather conditions at Albany were similar to those at Esperance and Bremer Bay and would be expected to result in equally visible evidence of mortality. Gaughan et al. (2000) contended that the true epizootic mortality rate of *Sardinops* in Albany was similar to that for the other regions, but that the very low mortality estimate was likely seen as such in view of the previous overestimation of B_{SP}.

In this study we aimed to address the problem of poor precision, while also developing a technique to identify particularly poor estimates of $B_{SP\text{-}DEPM}$, i.e., those for

[1] Fletcher, W. J., K. V. White, D. J. Gaughan, and N. R. Sumner. 1996. Analysis of the distribution of pilchard eggs off Western Australia to determine stock identity and monitor stock size. Final Report to Fisheries Research and Development Corporation. Project No. 92/95, 109 p. Department of Fisheries, Government of Australia, 168-170 St. Georges Tce, Perth, WA 6000, Australia.

[2] Cochrane, K. L. 1999. Review of Western Australia pilchard fishery, 12–16 April 1999. Fisheries Management Paper 129, 32 p. Department of Fisheries, Government of Western Australia, 168-170 St. Georges Tce, Perth, WA 6000, Australia.

Table 1

Estimates of spawning biomass (metric tons) of *Sardinops sagax* obtained by using the daily egg production method ($B_{SP\text{-}DEPM}$) for each of four regions in southwestern Australia. In those cases where data were sufficient to estimate a coefficient of variation (CV), the range around the $B_{SP\text{-}DEPM}$ estimate (Min./Max.) was calculated as ±1 standard deviation (SD); otherwise, the $B_{SP\text{-}DEPM}$ range was calculated by using assumed (AS) values for one or more of the DEPM parameters (see text). The numbers of adult *S. sagax* and plankton samples used in these calculations are shown.

Year	Min.	$B_{SP\text{-}DEPM}$	Max.	CV	±1 SD	Adult *n*	Plankton *n*
Albany							
1991	12,088	19,300	30,700	—	AS	10	41
1992	9006	16,994	24,981	0.44	±1 SD	10	31
1993	16,402	23,432	30,4620	0.30	±1 SD	9	61
1994	15,440	31,330	55,000	—	AS	10	107
1995	7720	17,544	27,368	0.56	±1 SD	10	83
1997	13,018	18,597	24,176	0.30	±1 SD	27	94
1999	0	89	531	4.99	±1 SD	2	263
Bremer Bay							
1992	12,000	19,280	79,000	—	AS	—	25
1993	16,170	44,010	63,608	—	AS	—	32
1994	15,700	28,458	42,500	—	AS	—	102
1999	2161	4156	6150	0.48	±1 SD	3	256
Esperance							
1993	14,326	32, 252	61, 800	—	AS	5	50
1994	10,700	20,080	40,100	—	AS	—	150
1995	10,900	31,900	45,647	—	AS	6	105
1999	3454	17,396	31,793	0.80	±1 SD	8	257
West coast							
1993	14,500	41,250	78,000	—	AS	—	55
1994	3100	8714	29,000	—	AS	—	133
1996	43,300	60,228	77,200	0.28	±1 SD	4	96
1998	9112	18,985	28,951	0.52	±1 SD	28	240
1999	3948	5275	6651	0.25	±1 SD	4	396

which accuracy was suspect. However, because of the small size of the fishery and the difficulty in securing additional research funds, no fishery-independent method of estimating biomass other than the DEPM was undertaken. We recognized that this study could not, therefore, unequivocally determine whether or not any improvement in accuracy had been achieved; therefore, we focused on improving the consistency between available data sets (in terms of the broader economic environment) in order to improve the decision-making process for what is a small-scale fishery.

We examine the relationship between relative trends in the $B_{SP\text{-}DEPM}$ and spawning area of *Sardinops* in each of four regional fisheries. We propose a method of using the relationship between spawning area and egg presence-absence data as an indicator of B_{SP} that is simpler than the methods of Mangel and Smith (1990) and Zenitani and Yamada (2000). We specifically chose to keep the retrospective analysis simple in recognition of data limitations, i.e., short time series and low numbers of samples for some DEPM surveys. In particular, our analyses did not rely on substantial knowledge of various parameters associated with estimating $B_{SP\text{-}DEPM}$. This investigation (an objective re-assessment of *Sardinops* $B_{SP\text{-}DEPM}$) was undertaken because of the contrast provided by the significant collapse in distribution, coupled with the sudden and substantial decrease in $B_{SP\text{-}DEPM}$ that followed mass mortality in 1998–99. Although problems in obtaining accurate B_{SP} estimates with the DEPM will not be resolved by the present study, greater consistency between indicators of the magnitude of B_{SP} and the development of a transparent and objective technique to identify apparent discrepancies between the two will facilitate better management of this key pelagic resource.

Methods

Estimates of spawning biomass with the DEPM

The estimates of B_{SP} used in this study (Table 1) were obtained by using the DEPM, which relies on ichthyoplankton surveys to estimate egg production and temporally concurrent samples of adult fish to estimate the adult parameters of fecundity, sex ratio, and weight.

The egg and adult data were subsequently combined in the DEPM model (Parker, 1985), as follows, to estimate spawning biomass:

$$B_{SP\text{-}DEPM} = (APWk)/(SFR),$$

where A = spawning area;
P = egg production (numbers of eggs before losses due to mortality);
W = weight of adult fish;
k = conversion factor to bring the various units to a value in metric tons;
S = spawning fraction; the proportion of females that spawn per day;
F = fecundity; number of eggs produced by a female; and
R = ratio of females to males by weight.

The DEPM provides a point estimate of spawning biomass, with upper and lower statistical bounds. In those individual surveys where all parameters could be estimated, estimates of coefficient of variation (CV) for $B_{SP\text{-}DEPM}$ were undertaken by using the delta method to sum the CV of the component parameters (Parker, 1985). In turn, the CV was used to provide an estimate of variability around the point estimate; specifically, we used ± 1 standard deviation to indicate the upper and lower bounds around the point estimates. In several surveys, particularly when the DEPM was initially being applied in WA, few adult samples meant that values for adult parameters (spawning fraction, sex ratio, fecundity, weight) could not be estimated and therefore a CV for the final estimate of $B_{SP\text{-}DEPM}$ could likewise not be estimated. Although sex ratio and weight could be reasonably estimated from the regular sampling of commercial catches around the survey period and fecundity could be estimated from a relatively small sample (e.g., 70–100 fish), estimating the spawning fraction was more difficult. In this latter case, the upper and lower bounds for the $B_{SP\text{-}DEPM}$ estimate were not based on a statistical measure but rather on what were thought to be likely low and high values of spawning fraction, respectively, for *Sardinops* from other surveys in WA and elsewhere (e.g., Alheit, 1993, Fletcher et al. 1996). Prior knowledge of likely $B_{SP\text{-}DEPM}$ values when applying the DEPM, specifically for the purpose of providing expert management advice, has recently been used successfully for *Sardinops* in South Australia (Ward et al. 2001).

Adult samples

Twenty DEPM surveys were conducted between 1991 and 1999 to identify stocks and to estimate spawning biomass of *Sardinops* of southwestern Australia (Fletcher et al., 1996a, 1996b; Fletcher et al.[3]; senior author's unpubl. data). The surveys were performed during the peak spawning months for *Sardinops* off the west coast, Albany, Bremer Bay, and Esperance regions. The timing of the DEPM survey cruises in each region was based on gonadosomatic indices for samples obtained from commercial catches, as described in Gaughan et al. (2002). The aim was to obtain samples from 35 catches of adult fish, as recommended by Alheit (1993), but this number was never achieved and in some cases no samples were obtained (Table 1). For each catch sampled, the ovaries from 15–50 females were immediately placed in 10% formalin and subsequently prepared histologically for microscopic examination. The remainder of the subsample was processed to obtain mean female weight and sex ratio by weight. Mature ovaries were retained for estimation of fecundity.

Plankton sampling and estimation of egg production

Plankton sampling extended from nearshore waters to the edge of the continental shelf (Fig. 2). Sampling stations were generally spaced uniformly, typically 2–4 nautical miles apart, along transects perpendicular to the shore. Analysis of *Sardinops* egg distribution from surveys conducted in the early 1990s indicated that these surveys sufficiently covered the distribution of the spawning stock (Fletcher and Tregonning, 1992; Fletcher et al., 1994), and later geostatistical analyses of *Sardinops* egg distribution patterns confirmed that the spacing of transects and stations were adequate to effectively represent the spatial distribution (Fletcher and Sumner, 1999). The earlier surveys were used to refine the spatial range of subsequent surveys. The number of plankton samples taken in each survey has generally increased since the early 1990s (Table 1).

Sardinops eggs were collected by using vertical tows that allowed the water column to be sampled from a maximum depth of 70 m to the surface; Fletcher (1999) showed that *Sardinops* eggs off southern Australia are typically restricted to the upper 70 m. Bongo nets with diameters of either 60 or 26 cm and constructed of either 500- or 300-micron mesh were used; the change to smaller nets was made to reduce sample volume and hence sorting time, whereas the change to smaller mesh was made to increase efficiency in capturing yolksac larvae; these changes did not affect the sampling efficiency for *Sardinops* eggs. Tow speed was standardized at 1 m/s. All samples were collected between 0630 and 1800 hours and immediately preserved in 5–10% formalin and seawater.

Plankton samples were examined under a dissecting microscope. *Sardinops* eggs were identified, classified into 12 developmental stages (White and Fletcher[4]), and

[3] Fletcher W. J., B. Jones, A. F. Pearce, and W. Hosja. 1997. Environmental and biological aspects of the mass mortality of pilchards (Autumn 1995) in Western Australia. Fisheries Research Report, Fisheries Department Western Australia 106, 115 p. Department of Fisheries, Government of Western Australia, 168-170 St. Georges Tce, Perth, WA 6000, Australia.

[4] White, K. V., and W. J. Fletcher. 1998. Identifying the developmental stages for eggs of the Australian pilchard, Sardinops sagax. Fisheries Research Division WA, Fisheries Research Report 103, 21 p. Department of Fisheries, Government of Western Australia, 168-170 St. Georges Tce, Perth, WA 6000, Australia.

Table 2

Correlations between 1) proportion of positive stations (PPS) and proportional spawning area (PSA) and 2) PPS and estimated spawning area (km^2) resulting from surveys of *Sardinops sagax* eggs at four regions in southwestern Australia. PPS is the proportion of the total number of plankton sampling stations that contained at least one *S. sagax* egg that had been spawned on the previous night. PSA is the proportion of the total survey area that consisted of spawning area. The values for spawning area are also provided.

	Survey	PPS	PSA (%)	Correlation I	Area (km^2)	Correlation II
Albany	Jul 91	0.46	37		1806	
	Jul 92	0.58	51		2686	
	Jul 93	0.52	36		2391	
	Jul 94	0.60	60		6672	
	Jul 95	0.33	28		1977	
	Jul 97	0.19	21		2224	
	Jul 99	0.15	1	0.94	107	0.68
Bremer Bay	Jul 92	0.61	64		2807	
	Jul 93	0.72	67		2809	
	Jul 94	0.70	71		4474	
	Jun 99	0.12	12	0.99	908	0.86
Esperance	Jul 93	0.50	44		5715	
	Jul 94	0.57	73		9796	
	Apr 95	0.61	36		5277	
	May 99	0.09	3	0.81	7840	0.83
West coast	Jul 93	0.53	62		8012	
	Jul 94	0.30	38		5199	
	Aug 96	0.23	16		2202	
	Aug 98	0.10	7		1835	
	Aug 99	0.12	10	0.98	1836	0.96

counted. Estimation of egg production was undertaken by fitting a negative exponential model (Picquelle and Stauffer, 1985) and was derived from the *y*-axis intercept of the regression model, representing time 0. The number of stages used to fit the model depended on the egg abundance for each stage; the best fitting model was chosen visually from an iterative sequence of fits. The best fit was not necessarily that with the smallest CV but rather that which intuitively did not violate our understanding of natural mortality rates as determined from the literature. For example, the slope of the regression model must be negative and egg mortality rates should fall within the broad range of 0.9–3.9/d (e.g., Smith et al., 1989).

Estimation of spawning area

According to water temperatures during each survey and the stage of egg development, *Sardinops* eggs were determined to have been spawned either the previous night ("day-1") or two nights previous ("day-2") as described by Fletcher et al. (1996). The total survey area was estimated by constructing a polygon around all stations. The spawning area was defined as the area in which day-1 *Sardinops* eggs were found (Fletcher et al., 1996a). The areas of the polygons around stations that had day-1 eggs, referred to as positive stations, were summed to estimate the spawning area for each zone. When positive stations occurred on the margin of the sampling area, polygons for these positive stations were drawn as for the embedded positive stations, but the areas of these polygons were extended by a standardized amount beyond the sampling areas (Wolf and Smith, 1986).

The proportion of positive stations (PPS) was calculated for each survey. The proportion of the survey area (PSA) that consisted of spawning area was also evaluated in each case. PPS and PSA were positively correlated at each region (Table 2); this result was expected and indicated that PPS provides a realistic representation of changes in spawning area. The relationships between PPS and the areal estimates of spawning area were not as strong, but these latter estimates suffered as potential predictors of biomass in our study because of the large differences in numbers of plankton samples collected between surveys (Table 1). PPS is thus not only an objective measure but can also be considered as an index of spawning area.

Modeling of spawning biomass

The collapse in distribution of *Sardinops* at each of four locations in southern Western Australia in 1999 is shown by the decline in spawning area (Fig. 2). The importance of this collapse in providing contrast for model fitting in otherwise poor data sets (few points with either flat or clumped distributions) is evident from linear fits of

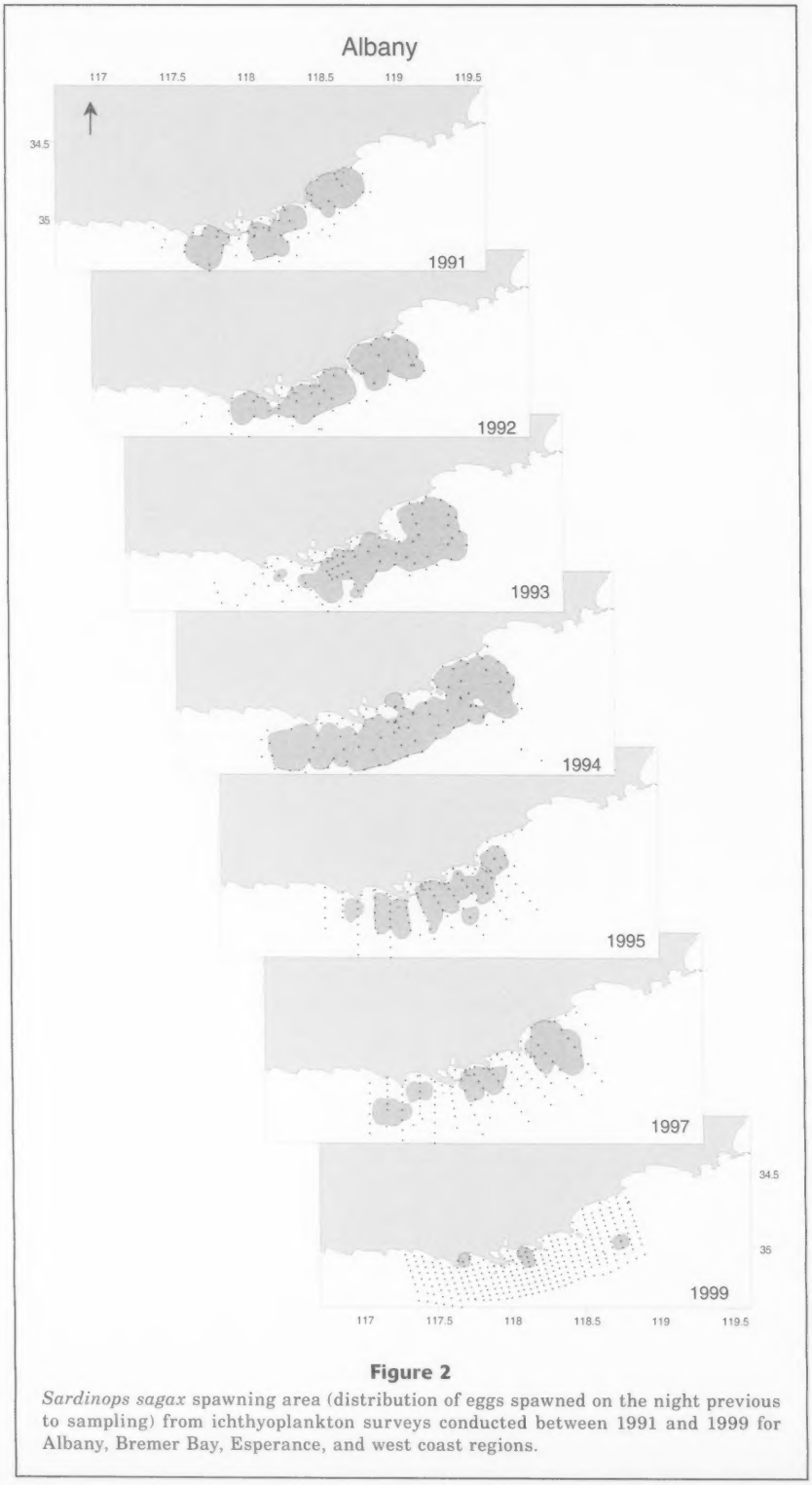

Figure 2

Sardinops sagax spawning area (distribution of eggs spawned on the night previous to sampling) from ichthyoplankton surveys conducted between 1991 and 1999 for Albany, Bremer Bay, Esperance, and west coast regions.

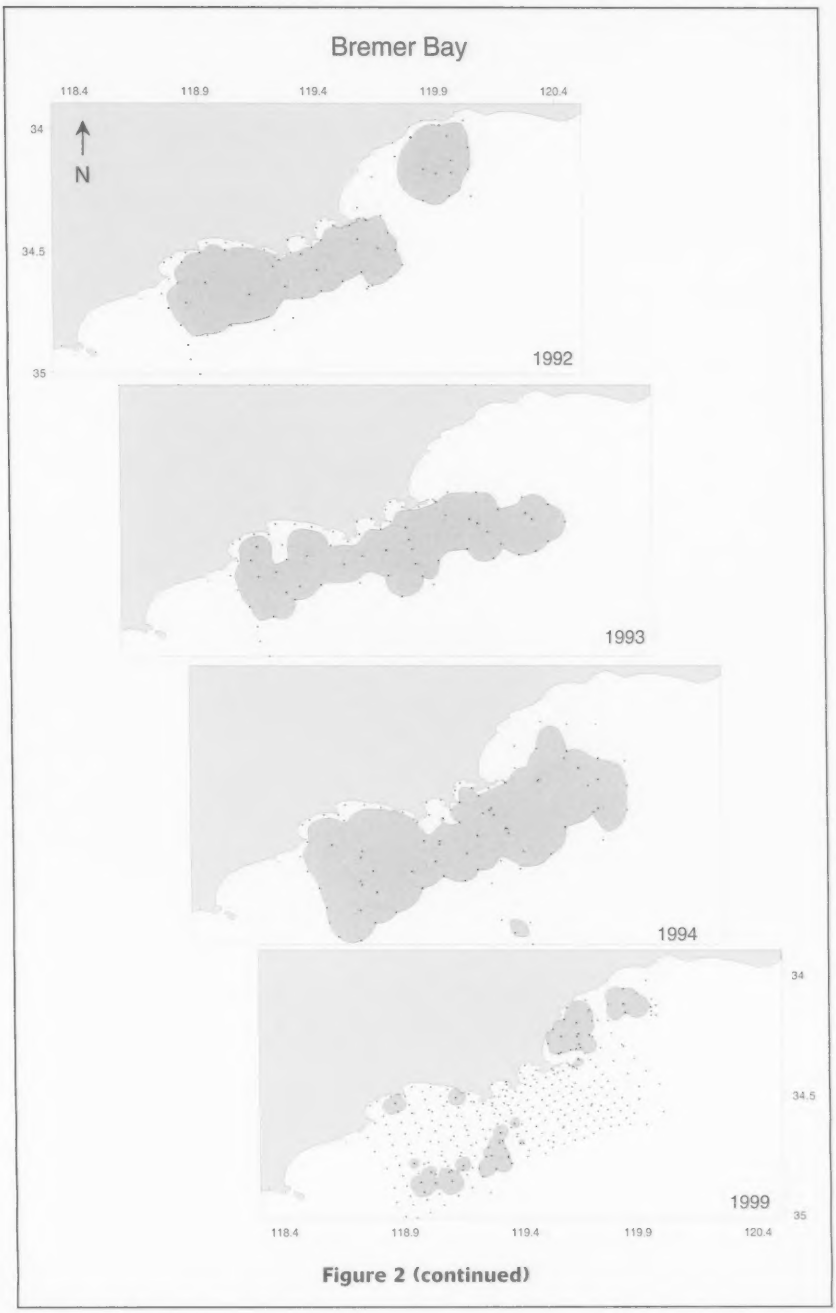

Figure 2 (continued)

$B_{SP\text{-}DEPM}$ against PPS for the south coast locations (Fig. 3). Because we wished to examine the relationship between trends in DEPM-based estimates of B_{SP} and PPS with the aim of improving estimates of B_{SP}, the development of an appropriate model is described here from first principles, followed by a selectivity analysis of error variance to choose the optimal estimator of B_{SP}. Given that we did not have a means of assessing the level of accuracy of the "adjusted" estimates, and the aim was therefore to improve consistency between data sets for the purpose of enhancing the decision-making process, our criteria in choosing an optimal estimator was to

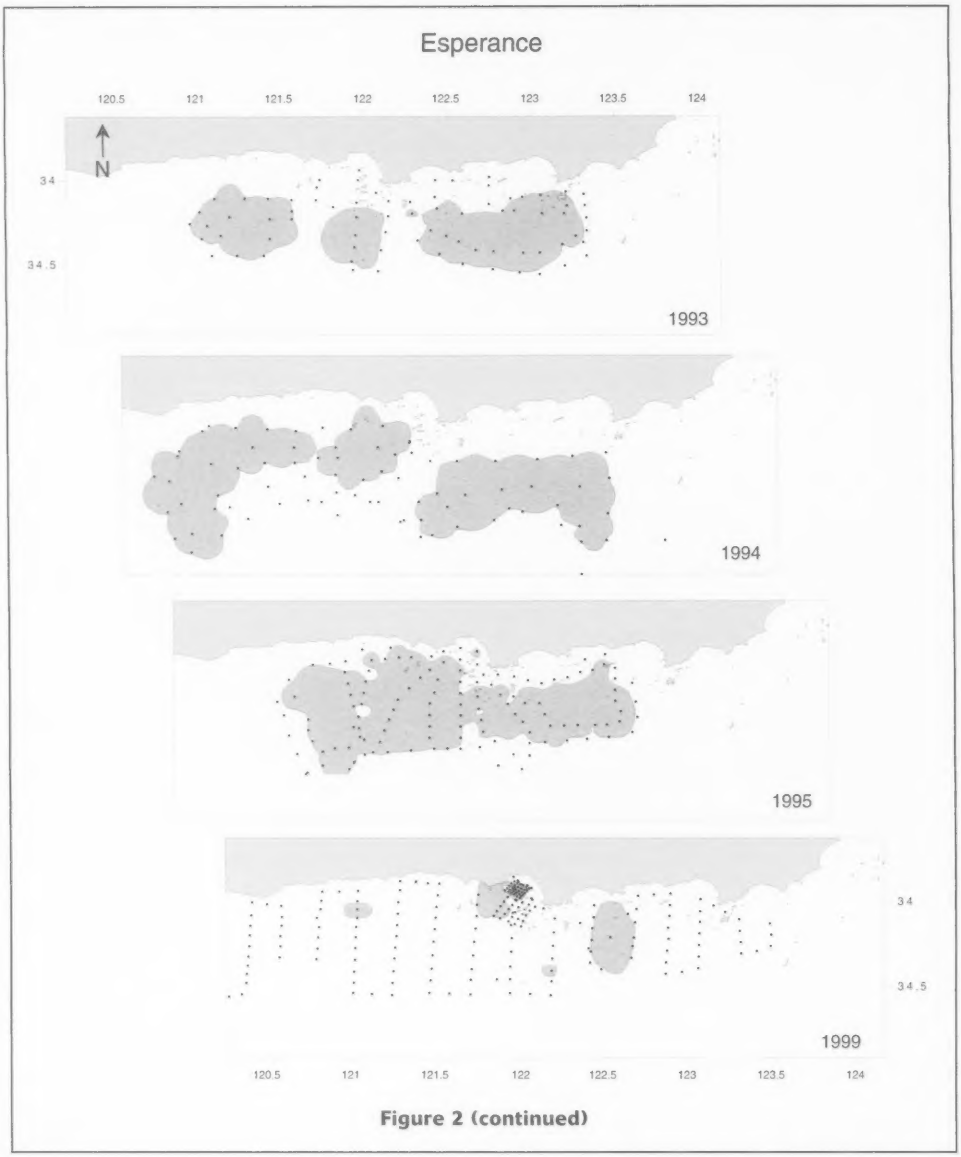

Figure 2 (continued)

minimize variance. In terms of improving management of the *Sardinops* fisheries in southwestern Australia, we considered this approach appropriate because of the relatively conservative exploitation rates that have been adopted by the Management Advisory Committee.

Model selection

The procedure used in the present study was to first invoke a general model and then use the data to drive a simplification process in order to avoid a specification error. Thus, for each of the fishery regions, we first considered the following general relationship between $B_{SP\text{-}DEPM}$ and PPS holding over time:

$$(B_{SP\text{-}DEPM})_t = \alpha_0 \, (PPS_t)^{\lambda} + \alpha_2 + e_t, \quad (1)$$

where λ is common for all areas, α_0 and α_2 are area specific constants, and the error term e_t is independent, homoscedastic and normal with a mean of zero. This model was chosen specifically in order to be amenable to Taylor series expansion during the simplification process. In satisfying dimensional and conservational

Figure 2 (continued)

arguments, α_2 must be zero; therefore the above family of models reduces to

$$(B_{SP\text{-}DEPM})_t = \alpha_0 (PPS_t)^{\lambda} + e_t \,. \quad (2)$$

An attempt to fit the linear regression model, composed of the natural logarithms of either side of the above relation, to the observed data was unsuccessful because of heterogeneity of error variance.

Direct estimation of model II with a nonlinear regression procedure gave estimates of λ that were near 1 and with large standard errors on account of the small size of the data sets. However, residual diagnostics were satisfactory. Because the observed PPS values fell between

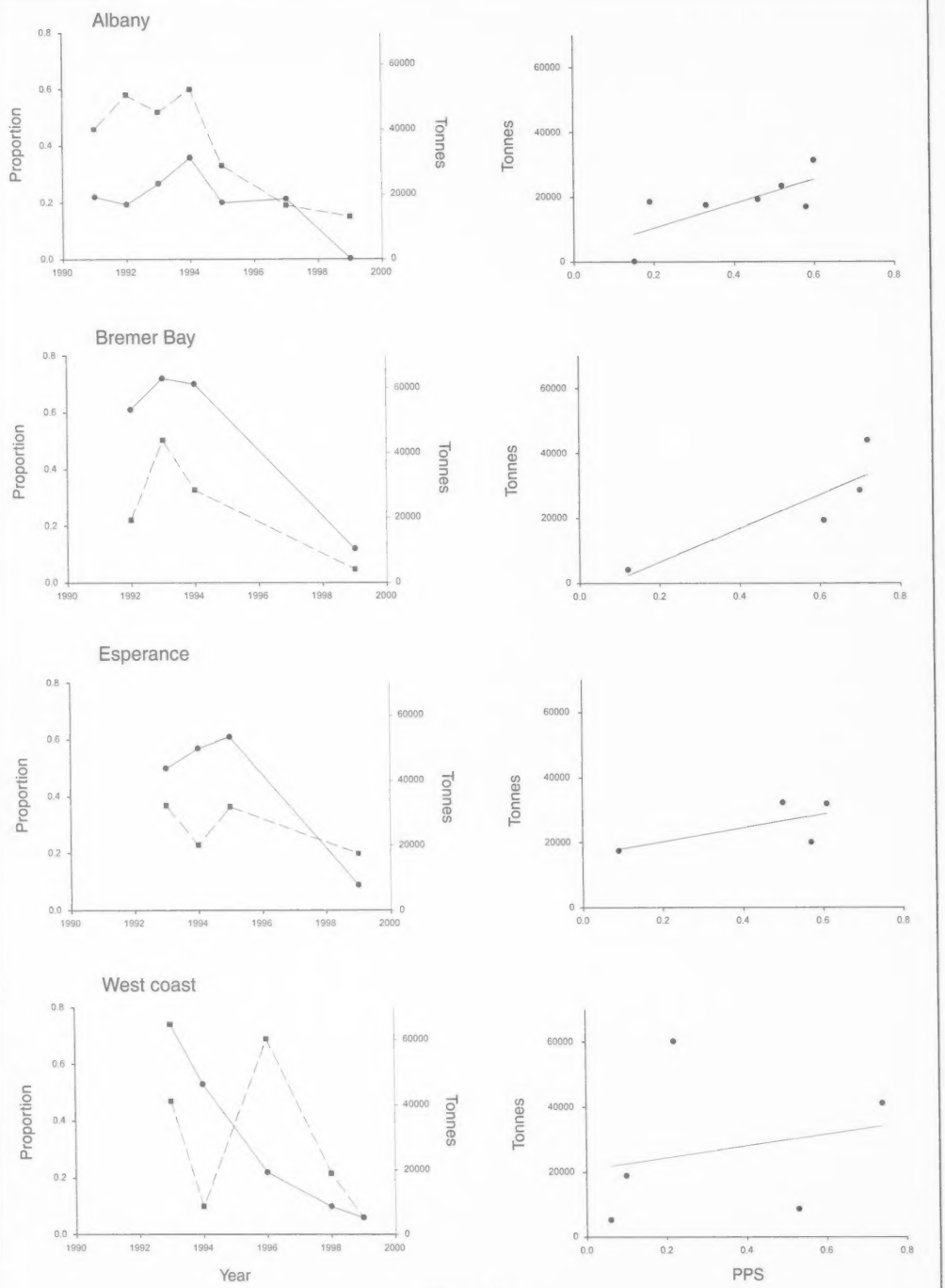

Figure 3

Plots of the proportions of positive stations (–●–) and $B_{SP\text{-}DEPM}$ estimates (--■--) for the four *Sardinops sagax* fisheries in southwestern Australia. The right-hand panel shows linear fits of the relationship between proportion of positive stations and $B_{SP\text{-}DEPM}$ estimates.

Table 3

Parameter estimates for two models (III and IV, see text for details) of *Sardinops sagax* spawning biomass, including tests for zero coefficients, at each of four regions in southwestern Australia.

Model III

Albany				
SE of estimate: 6011				
	B_{SP}	*SE* of B_{SP}	$t(22)$	*P*-level
Intercept	−4597.15	2419.94	−1.90	0.070661
PPS	56,780.19	6638.90	8.55	1.91E-08
Bremer Bay				
SE of estimate: 4016				
	B_{SP}	*SE* of B_{SP}	$t(14)$	*P*-level
Intercept	−1436.88	1573.94	−0.91	0.37674
PPS	45,341.85	3638.2	12.46	5.75E-09
Esperance				
SE of estimate: 4639				
	B_{SP}	*SE* of B_{SP}	$t(20)$	*P*-level
Intercept	15,840.52	1751.38	9.045	0.000317
PPS	17,790.27	4097.73	4.34	1.66E-08
West coast				
SE of estimate: 15,280				
	B_{SP}	*SE* of B_{SP}	$t(32)$	*P*-level
Intercept	5316.10	4826.58	1.10	0.278929
PPS	63,192.69	23,161.29	2.73	0.010251

Model IV

Albany				
SE of estimate: 6343				
	B_{SP}	*SE* of B_{SP}	$t(23)$	*P*-level
PPS	45,910.11	3552.36	12.92	4.96E-12
Bremer Bay				
SE of estimate: 3994				
	B_{SP}	*SE* of B_{SP}	$t(18)$	*P*-level
PPS	42,784	2308.30	18.53	9.47E-12
Esperance				
SE of estimate: 10,214				
	B_{SP}	*SE* of B_{SP}	$t(21)$	*P*-level
PPS	48,377.13	5095.09	9.49	4.76E-09
West coast				
SE of estimate: 15,330				
	B_{SP}	*SE* of B_{SP}	$t(33)$	*P*-level
PPS	84,615.52	12,615.76	6.71	1.22E-07

zero and one, and λ was also close to 1, model II was able to be recast in a more tractable form by using the Taylor series expansion of the RHS of model II about PPS = 1, leading to the relationship

$$(B_{SP\text{-}PPS})_t = \alpha_0 PPS_t + \delta + e_t, \quad (3)$$

where the expected value of δ is approximately $-0.25\alpha_0(\lambda-1)$. Details of the derivation are provided in Appendix 1.

Fitting the regression model III to the DEPM-based estimates of B_{SP} gave the estimated coefficients shown in the left hand column of Table 3. Residual diagnostics showed that model III was satisfactory. Because none of the intercept terms were significantly different from zero, the parsimonious model

$$(B_{SP\text{-}PPS})_t = \alpha_0 (PPS)_t + e_t \quad (4)$$

was fitted, giving the results in the right hand column of Table 3. Residual diagnostics were also satisfactory for these models.

Optimal estimation of spawning biomass

We now have available two unbiased estimates of B_{SP}: estimator 1 (i.e., $B_{SP\text{-}DEPM}$) with associated error e', which has an expected value of 0 and variance $\mathrm{Var}(e') = \sigma_1^2$; and estimator 2 (i.e., $B_{SP\text{-}PPS}$) which model IV of the previous section fitted to the values of $B_{SP\text{-}DEPM}$ with error e, which had an expected value of 0 and variance $\mathrm{Var}(e) = \sigma^2$. Thus estimator 2 can be seen to be unbiased and with full error term $(e+e')$. In order to obtain an optimal predictor, i.e., with minimum variance, of spawning biomass ($B_{SP\text{-}Optimal}$), we considered the weighted average of the two estimators above:

$$B_{SP\text{-}Optimal} = ((w)\ estimator\ 1 + (1-w)\ \text{estimator 2}),$$
$$\text{with weight } w\text{: } 0<w<1.$$

We must choose the weight w of estimator 1 in order to minimize the variance ($\mathrm{Var}(B_{SP\text{-}Optimal})$) of the estimator $B_{SP\text{-}Optimal}$.

$$\begin{aligned}\mathrm{Var}(B_{SP\text{-}Optimal}) &= \mathrm{Var}(we+(1-w)(e+e')) \\ &= \mathrm{Var}(e+(1-w)e') \\ &= \mathrm{Var}(e) + (1-w)^2\mathrm{Var}(e') + 2(1-w)\\ &\quad \mathrm{covariance}(e,e') \\ &= \sigma^2+(1-w)^2\sigma_1^2+2(1-w)\sigma\sigma_1\rho\end{aligned}$$

where ρ = correlation between e and e'. For Var ($B_{SP\text{-}Optimal}$) to be a minimum, the w derivative must be zero, yielding

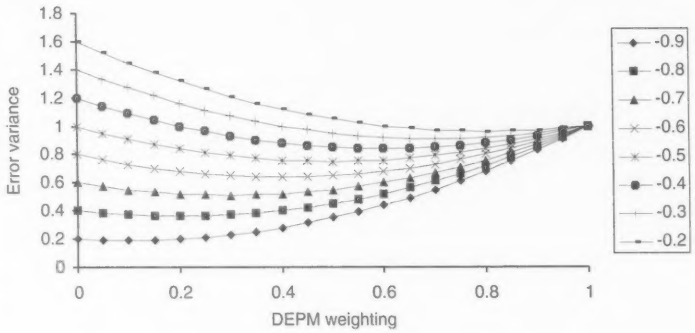

Figure 4

The relationship between error variance between the two estimators for spawning biomass ($B_{SP\text{-}DEPM}$ and $B_{SP\text{-}PPS}$) and the DEPM weighting required to give the optimally weighted estimate of B_{SP} (i.e., $B_{SP\text{-}OPTIMAL}$). Error variance is shown for a range of error correlations from $r = -0.9$ to -0.2.

$$0 = (1-w)\sigma_1 + \sigma\rho,$$

which requires $w = 1 + \sigma\rho/\sigma_1$.

In the event of $\rho = -\sigma_1/\sigma$, $B_{SP\text{-}Optimal}$ will have $w = 0$, i.e., the optimal estimator will just be estimator 2 alone.

The limited sample information available indicates that σ_1 is approximately equal to σ, which we therefore assume in order to simplify the next analysis. Because $B_{SP\text{-}PPS}$ is based on estimates of PPS, which can be estimated with more confidence than $B_{SP\text{-}DEPM}$, it must be expected that often, if not always, Variance($B_{SP\text{-}PPS}$) < Variance($B_{SP\text{-}DEPM}$).

i.e., $\mathrm{Var}(e+e') < \mathrm{Var}(e) + \varepsilon$, for small $\varepsilon > 0$;

i.e., $\sigma^2 + \sigma_1^2 + 2\rho\,\sigma_1\sigma < \sigma^2 + \varepsilon$;

i.e., $2\rho < (-\sigma_1^2 + \varepsilon)/\sigma_1\sigma$.

This requires $\rho < -0.5$ when $\sigma_1 = \sigma$, and ε is small. This relation has an important role in our decision of what is the best estimator.

In Figure 4 the error variance for the estimator $B_{SP\text{-}OPTIMAL}$ is shown for various DEPM weightings and a theoretical range of error correlations (i.e., between e and e') from $r = -0.9$ to -0.2. Our aim was to choose a DEPM weighting that provides minimal error variance along the most stable regions of the suite of error correlation curves, i.e., where the error correlation curves are flattest. The error correlation curves from -0.4 to -0.7 were the most stable and across these the DEPM weightings from 0.3 to 0.7 had the smallest error variance. Therefore we choose 0.5 as our preferred DEPM weighting, which lies centrally within a stable part of the range of theoretical error correlations.

Results

The decline in spawning area in each region (Fig. 2) corresponded to declines in $B_{SP\text{-}DEPM}$ (Table 1), which in turn were reflected by the $B_{SP\text{-}OPTIMAL}$ estimates (Fig. 5). We recognize that imbalance in the intensity of samples between years poses a problem for the interpolation of data between sampling stations but we contend that the collapse in distribution observed is of sufficient contrast to be a reliable reflection of the estimated 70% decrease in *Sardinops* biomass that resulted from the 1998–99 epidemic (Gaughan et al., 2000; Ward et al., 2001). Note that we have used Albany (Fig. 2A) as the primary support for this contention because of the larger data set. The same pattern was observed at all regions, although it was not so marked for the west coast *Sardinops* (Fig. 2D) because estimated B_{SP} (this term hereafter is used generically) had already declined substantially between 1996 and 1998.

Despite sometimes large intervals between consecutive surveys, there were two broad patterns in the trends for *Sardinops* B_{SP} during the 1990s (Fig. 5). Within each region on the south coast (Albany, Bremer Bay, and Esperance), $B_{SP\text{-}DEPM}$ remained relatively high in the early to mid 1990s before decreasing substantially by 1999. In contrast to the results from south coast DEPM surveys, the west coast estimated $B_{SP\text{-}DEPM}$ fluctuated widely (Table 1). This fluctuation resulted in a relatively poor fit of the optimal model and correspondingly wide CIs. Since 1996, when substantially more samples were routinely collected during each survey on the west coast, there has also been a decrease in B_{SP} consistent with that observed on the south coast.

Inconsistency in the determination of variability estimates around some $B_{SP\text{-}DEPM}$ estimates precludes any definitive statements about the relative precision of the

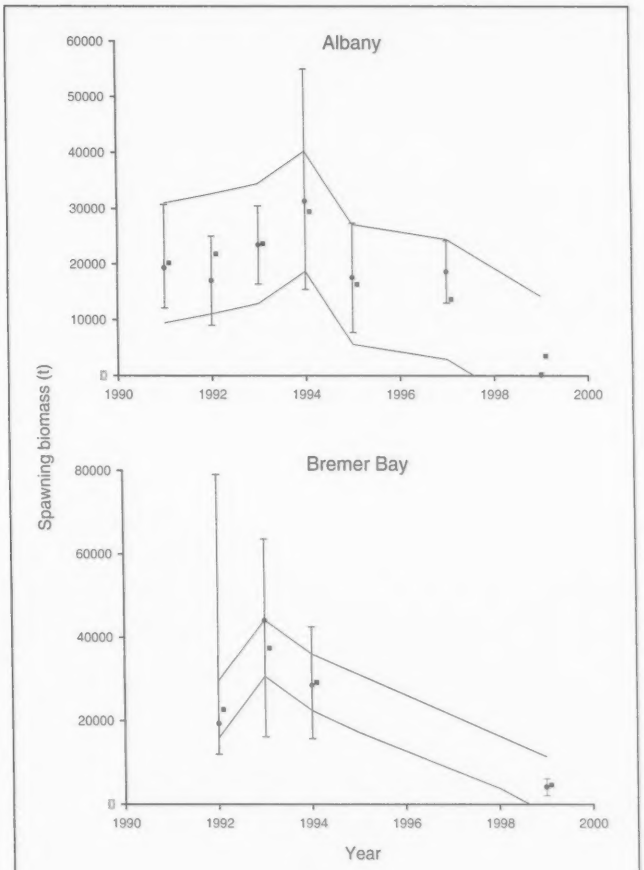

Figure 5

Sardinops sagax $B_{SP\text{-}DEPM}$ estimates (circles with error bars) and $B_{SP\text{-}OPTIMAL}$ estimates (squares with accompanying 95% confidence interval boundaries) at four regions of southwestern Australia. In each case the confidence intervals that extend below the *x*-axis have not been shown.

$B_{SP\text{-}OPTIMAL}$ estimates. Notwithstanding this, the CIs for the optimal estimates always encompassed the DEPM point estimates. Because the CIs were so broad in relation to the point estimates, only the point estimates for $B_{SP\text{-}DEPM}$ and $B_{SP\text{-}OPTIMAL}$ are further compared.

The estimated $B_{SP\text{-}OPTIMAL}$ indicates that for Albany the spawning biomasses were underestimated in 1992 and 1999 and overestimated in 1997 and that the difference between estimates in each case was greater than 25% (Fig. 5, Table 4). Although the DEPM estimated that the Albany B_{SP} remained steady between 1995 (17,544 t) and 1997 (18,597 t), the PPS almost halved from 0.33 to 0.19 for these same surveys (Tables 1 and 2). For Bremer Bay the estimates for $B_{SP\text{-}DEPM}$ and the $B_{SP\text{-}OPTIMAL}$ were within 20% (Fig. 5, Table 4). In Esperance the $B_{SP\text{-}OPTIMAL}$ estimate indicates that the DEPM underestimated B_{SP} by 19% in 1994, but overestimated B_{SP} by 37% in 1999.

The DEPM estimates of *Sardinops* B_{SP} on the west coast had the poorest fit against PPS. Thus, the optimal estimates of B_{SP} differed by >30% in four of the five DEPM-based B_{SP} estimates. In particular, the 1994 and 1999 DEPM estimates were too low, and those for 1996 and 1998 were too high.

Discussion

Egg presence-absence analysis, i.e., proportion of positive stations (PPS), was used to objectively assess changes in the spawning area of *Sardinops* along the south and lower west coasts of WA between 1991 and 1999. The

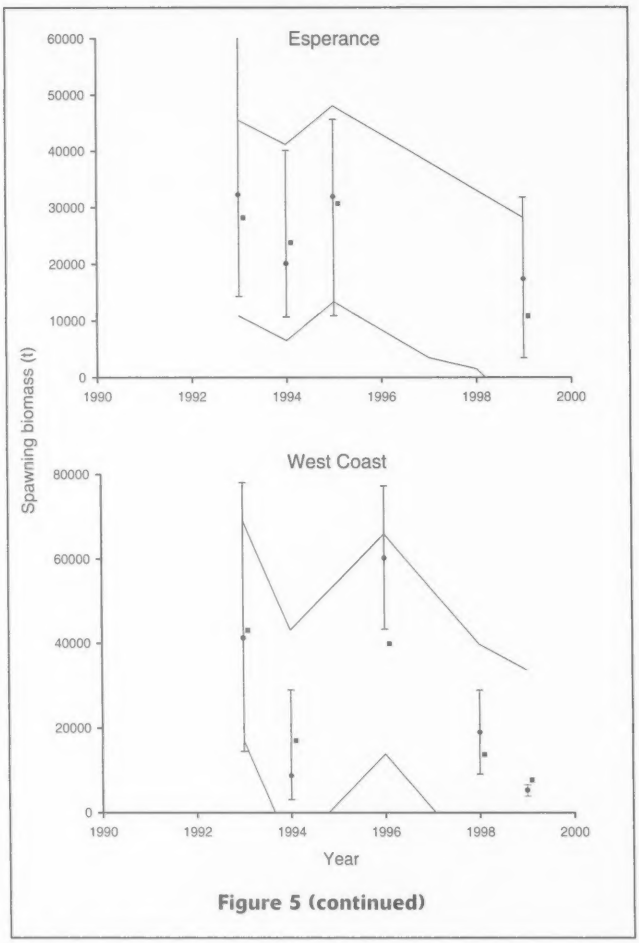

Figure 5 (continued)

collapse in distribution was evident in 1999 for three of the four regions examined and has been attributed to a combination of fishing mortality, several years of poor recruitment, and two mass mortality events (Murray and Gaughan, 2003). The spawning stock in Albany and Bremer Bay decreased to a point where the annual total allowable catch (TAC) in these fisheries was reduced to zero. The concurrent decreases in $B_{SP\text{-}DEPM}$ and PPS at the south coast regions in 1999, estimated shortly after the progression of an epidemic mass mortality (Gaughan et al., 2000), indicates a positive relationship between $B_{SP\text{-}DEPM}$ and PPS. This widespread response provides support for the concept of using the $PPS\text{-}B_{SP\text{-}DEPM}$ relationship to objectively detect, albeit retrospectively, particularly suspect estimates of $B_{SP\text{-}DEPM}$.

The marked decline in B_{SP} in 1999 to a very low level at Albany provided sufficient contrast in the time series of data to allow detection of an overestimation of spawning biomass in 1997. Although the difference may not appear to be overly large, the critical factor in this particular case is that the B_{SP} of 18,597 metric tons (t) was seen to be healthy, whereas an estimate of 13,660 t would have clearly indicated to the Management Advisory Committee a downward trend in *Sardinops* B_{SP}. In turn, such a result would have supported the contention that the stock was in decline, which was expected because of several years of poor recruitment, as evidenced by catch-at-age data (Gaughan et al., 2002). Furthermore, in 1998, during the 6 months prior to the mass mortality, the purse-seine fleet in Albany experienced significant difficulties in meeting catch expectations, which also indicated that the stock was at a low level. Although we cannot assess precision of the revised estimates of B_{SP}, it is likely that the $B_{SP\text{-}OPTIMAL}$ for 1997 still overestimates the actual stock size.

The evidence for a decline in B_{SP} at Bremer Bay from 1994 to 1999, as suggested by the decline in PPS, was supported by trends in catch curves for that period, which showed very low levels of recruitment (Gaughan et al., 2002). The recruitment trends ensured that the annual TACs for Bremer Bay after the mid 1990s did not increase but instead were gradually reduced. The

Table 4

Comparison of estimates of spawning biomass for *Sardinops sagax* from four regions in southwestern Australia. Estimates obtained by using the daily egg production method (DEPM) were re-estimated by using a model that considered the proportion of positive stations (PPS, see text and Table 2) during each of the DEPM surveys. In turn, a weighted, or optimal, estimate was derived from the previous two estimates. The difference and ratio between the optimal and the DEPM estimates are provided for comparison. Optimal estimates that fall outside the 95% confidence intervals for the DEPM estimates and optimal:DEPM ratios that differ from 1 by greater than 0.25 are shown in bold type.

	DEPM estimate	PPS estimate	Optimal estimate	DEPM–PPS estimate	Optimal:DEPM
Albany					
1991	19,300	20,190	20,209	−890	1.05
1992	16,994	25,456	21,811	−8462	**1.28**
1993	23,432	22,823	23,653	609	1.01
1994	31,330	26,334	29,438	4996	0.94
1995	17,544	14,484	16,347	−1197	0.93
1997	18,597	8339	13,660	10,258	**0.73**
1999	89	6584	**3488**	−6495	**39.19**
Bremer Bay					
1992	19,280	21,346	22,689	−2066	1.18
1993	44,010	25,195	37,407	−6603	0.85
1994	28,458	24,495	29,204	3963	1.03
1999	4156	4199	4645	−43	1.12
Esperance					
1993	32,252	23,542	28,220	−4032	0.88
1994	20,080	26,838	23,827	−6758	1.19
1995	31,900	28,721	30,705	3179	0.96
1999	17,396	4238	10,875	13,158	**0.63**
West coast					
1993	41,250	48,318	43,048	−7068	1.04
1994	8714	27,350	17,049	−18,636	**1.96**
1996	60,228	20,968	**39,845**	39,260	**0.66**
1998	18,985	9117	13,723	9868	**0.72**
1999	5725	10,940	**7714**	−5665	**1.35**

very poor fit for Esperance may reflect the low sample size or may be indicative of a certain level of decoupling of B_{SP} and PPS not evident in the other south coast regions.

The 1996 estimate for the west coast was hampered by poor estimation of adult parameters resulting from a low number of adult samples obtained; the $B_{SP\text{-}DEPM}$ estimate for that year appeared to be much too high and, intuitively, was not used as the basis for making management decisions at that time. The precautionary decision to use the lower bound rather than the "best" estimate from the 1996 west coast DEPM survey was therefore justified. In contrast, the estimate of $B_{SP\text{-}DEPM}$ of 8714 t in 1994 for the west coast *Sardinops* stock appears to have been too low. The lack of an obvious collapse in distribution off the west coast was partly due to the marked changes in the intensity and distribution of sampling after 1996. Another contributing factor may have been a change in the distribution of the spawning adults because of the anomalously warm water in the Indian Ocean in the late 1990s (Webster et al., 1999) during the last major La Niña. The PPS of only 0.10 in 1998, before the epidemic mortality, may therefore have been the result of behaviorally mediated changes in the distribution of *Sardinops* in response to the warmer than average water temperatures (Gaughan et al., 2000). We recognize that other factors may also have influenced the distribution of *Sardinops* off the west coast but our relatively short time series of data precluded development of more definitive, alternative hypotheses at this time. The potential for unusual environmental conditions to influence spawning behavior applies equally to the south coast *Sardinops*; interpretation of PPS data therefore also requires consideration of environmental conditions in each case. As our time series of biomass estimates is extended through further DEPM surveys, hypotheses regarding the influence of the environment will be further developed. Preliminary hypotheses have already been presented to the Management Advisory Committee and thus form part of current management deliberations.

The results from this retrospective analysis will immediately be used to reassess the B_{SP} estimates obtained for *Sardinops* in WA during the 1990s before

refitting them to Hall's (2000) integrated models for the three adult assemblages on the south coast of WA. The integrated model is tuned with $B_{SP\text{-}DEPM}$ estimates. Therefore, replacing $B_{SP\text{-}DEPM}$ estimates with $B_{SP\text{-}OPTIMAL}$ estimates will result in a model that better simulates the size of the *Sardinops* stocks off southern WA. Although the changes may appear trivial, it is important that re-estimating the most deviant estimates of $B_{SP\text{-}DEPM}$ can be undertaken in a manner that satisfies demands by stakeholders, including industry, for openness and clarity in the provision of scientific advice.

As further DEPM surveys are conducted to assess the status of the *Sardinops* stocks in the five to six years following the 1998–99 mortality event, more reliable relationships between PPS and $B_{SP\text{-}DEPM}$ will be developed. To assist this process, the relative merits of the data for individual DEPM surveys can also be re-examined, particularly those data that this study has indicated to have resulted in poor estimates of $B_{SP\text{-}DEPM}$. An ongoing iterative approach that employs retrospective analyses will be undertaken in an attempt to continuously reduce the variance of the PPS-$B_{SP\text{-}DEPM}$ relationship. This approach will permit further refinement of Hall's (2000) integrated model, a process already in progress (Stephenson et al.[5]) and will therefore contribute to increased confidence in the scientific advice that is provided for management of the *Sardinops* fisheries in WA. Eventually, PPS alone may be sufficient to provide an indication of spawning biomass with an acceptable level of precision.

Besides contributing to the integrated model, the $B_{SP\text{-}OPTIMAL}$ point estimates obtained over nearly a decade in each of four management regions now provide a clearer indication of potential maximum biomass levels against which industry members can plan their businesses. Because of the highly variable recruitment of many small pelagic fish, purse-seine businesses that target fish such as *Sardinops* should not invest at levels that require an economic return based on maximum biomass sizes. For the purse-seine fishing zones in southern WA the maximum spawning biomass from which purse-seine industry members can expect their TACS to be determined are as follows: west coast 40,000 t, Albany 29,000 t, Bremer Bay 37,000 t, and Esperance 30,000 t. Although these values provide an upper limit to business planning, maximum biomasses should not represent investment targets. These values provide an indication of the maximum size for the industry but, because of the "natural and social disarray" that can result "from harvesting marine fish species at the crest of their production" (Smith 2000), the industry should be structured at a level that focuses on longer-term average biomass and that includes industry's ability to survive during periods of low stock size. Maximum and average B_{SP} for *Sardinops* at each of the four management regions in southwestern Australia will be further investigated during ongoing development of the integrated model and as more information becomes available.

[5] Stephenson, P., N. Hall, and D. Gaughan. 2004. Unpubl. data. Department of Fisheries, Western Australian Marine Laboratories, North Beach, Western Australia 6920, Australia.

Conclusion

Even large numbers of plankton samples can result in imprecise estimates of egg production for use in DEPM calculations (e.g., Mangel and Smith, 1990). Relative trends in spawning area that can be obtained from the same survey by using egg presence-absence analysis provide a secondary means of assessing trends in the status of stocks. This egg presence-absence analysis will be particularly useful for stocks already assessed by using DEPM surveys and more so for those that do not have large amounts of ancillary information, such as long time-series of catch-at-age data, or meaningful effort data.

Detection of either upwards or downwards bias in estimates of B_{SP} will be considered in the integrated model and also communicated to industry members to increase their understanding of the stock in each region. Although this review of biomass trends of *Sardinops* during the 1990s cannot change how *Sardinops* were managed during that period, an increased understanding of both the stock sizes and the science behind the biomass assessments will facilitate ongoing management processes.

Acknowledgments

The authors sincerely thank all Department of Fisheries staff involved with the collection and analysis of historical ichthyoplankton-survey data, in particular Stuart Blight, Gary Buckenara, Cameron Dawes-Smith, Rick Fletcher, Kieren Gosden, Matt Robinson, Rob Tregonning, Ken White, Bruce Webber, and other personnel on PV *Baudin* and PV *McLaughlan*. We also thank Kevern Cochrane (FAO) for a detailed review of an earlier version of this manuscript. We are grateful to the Fisheries Research and Development Corporation (Canberra) that provided funding through Project 92/25 for the earlier DEPM surveys.

Literature cited

Alheit, J.
1993. Use of the daily egg production method for estimating biomass of clupeoid fishes: a review and evaluation. Bull. Mar. Sci. 53:750–767.

Fletcher, W. J.
1991. A test of the relationship between otolith weight and age for the pilchard *Sardinops neopilchardus*. Can. J. Fish. Aquat. Sci. 48:35–38.
1995. Application of the otolith weight-age relationship for the pilchard, *Sardinops sagax neopilchardus*. Can. J. Fish. Aquat. Sci. 52:657–664.
1999. Vertical distribution of pilchard (*Sardinops sagax*)

eggs and larvae off southern Australia. Mar. Freshw. Res. 50:117–122.

Fletcher, W. J., N. C. H. Lo, E. A. Hayes, R. J. Tregonning, and S. J. Blight.
1996. Use of the daily egg production method to estimate the stock size of Western Australian sardines (*Sardinops sagax*). Mar. Freshw. Res. 47:819–825.

Fletcher W. J., and N. R. Sumner.
1999. Spatial distribution of sardine (*Sardinops sagax*) eggs and larvae: an application of geostatistics and resampling to survey data. Can. J. Fish. Aquat. Sci. 56:907–914

Fletcher, W. J., and R. J. Tregonning.
1992. The distribution and timing of spawning by the Australian pilchard (*Sardinops sagax neopilchardus*) off Albany, Western Australia. Aust. J. Mar. Freshw. Res. 46:1437–1449.

Fletcher, W. J., R. J. Tregonning, and G. J. Sant.
1994. Interseasonal variation in the transport of pilchard eggs and larvae off southern Western Australia. Mar. Ecol. Prog. Ser. 111:209–224.

Gaughan, D. J., W. J. Fletcher, and J. P. McKinlay.
2002. Functionally distinct adult assemblages within a single breeding stock of the sardine, *Sardinops sagax*: management units within a management unit. Fish. Res. 59:217–231.

Gaughan, D. J., R. W. Mitchell, and S. J. Blight.
2000. Impact of mortality, possibly due to herpes virus, on pilchard *Sardinops sagax* stocks along the south coast of Western Australia in 1998–99. Mar. Freshw. Res. 51:601–612.

Hall, N. G.
2000. Modelling for fishery management, utilising data for selected species in Western Australia. Ph.D. diss.,199 p. Murdoch Univ., Perth, Australia.

Hunter, J. R., and N. C. H. Lo.
1997. The daily egg production method of biomass estimation: some problems and potential improvements. Ozeanografika 2:41–69.

Mangel, M., and P. E. Smith.
1990. Presence-absence sampling for fisheries management. Can. J. Fish. Aquat. Sci. 47:1875–1887.

Murray, A. G., and D. J. Gaughan.
2003. Using an age-structured model to simulate the recovery of the Australian pilchard (*Sardinops sagax*) population following epidemic mass mortality. Fish. Res. 60:415–426.

Parker, K.
1985. Biomass model for the egg production model. *In* An egg production method for estimating spawning biomass of pelagic fish: application to the northern anchovy, *Engraulis mordax* (R. M. Lasker, ed.), p. 5–6. NOAA Tech. Rep. NMFS 36.

Picquelle, S., and G. Stauffer.
1985. Parameter estimation for an egg production method of anchovy biomass assessment. *In* An egg production method for estimating spawning biomass of pelagic fish: application to the northern anchovy, *Engraulis mordax* (R. M. Lasker, ed.), p. 7–15. NOAA Tech. Rep. NMFS 36.

Smith, P. E.
2000. Pelagic fish early life history: CalCOFI overview. *In* Fisheries oceanography: an integrated approach to fisheries ecology and management (P. J. Harrison and T. R. Parsons, eds.), p. 8–28. Blackwell Science, Oxford, UK.

Smith, P. E., H. Santander, and J. Alheit.
1989. Comparison of the mortality rates of pacific sardine, *Sardinop sagax*, and Peruvian anchovy, *Engraulis ringens*, eggs off Peru. Fish. Bull. 87:497–508.

Uphoff, J. H.
1993. Determining striped bass spawning stock status from the presence or absence of eggs in ichthyoplankton survey data. N. Am. J. Fish. Manag. 13:645–657.

Ward T. M., F. Hoedt, L. McLeay, W. F. Dimmlich, M. Kinloch, G. Jackson, R. McGarvey, P. J. Rogers, and K. Jones.
2001. Effects of the 1995 and 1998 mass mortality events on the spawning biomass of sardine, *Sardinops sagax*, in South Australian waters. ICES J. Mar. Sci. 58(4):865–875.

Webster P. J., A. M. Moore, J. P. Loschnigg, and R. R. Leben.
1999. Coupled ocean-atmosphere dynamics in the Indian Ocean during 1997–98. Nature 401:356–360.

Wolf, P., and P. E. Smith.
1986. The relative magnitude of the 1985 Pacific sardine spawning biomass off southern California. CalCOFI Rep. 27:25–31.

Zenitani, H., and S. Yamada.
2000. The relation between spawning area and biomass of Japanese pilchard, *Sardinops melanostictus*, along the Pacific coast of Japan. Fish. Bull. 98:842–848.

Appendix 1—Derivation of model III from model II

We start with model II

$$B_{SP\_DEPM} = \alpha_0 PPS^{\lambda} + e_t.$$

For brevity, y is used to denote PPS. We first note that $y^{\lambda}=yy^{(\lambda-1)}$. Now we obtain the Taylor series expansion of $y^{(\lambda-1)}$ about $y=1$ giving

$$y^{(\lambda-1)} = 1 + (\lambda-1)(y-1) + (\lambda-1)(\lambda-2)/2!(y-1)^2 + (\lambda-1)(\lambda-2)(\lambda-3)/3!(y-1)^3 + \ldots .$$

Multiplying this expression through by y gives

$$y^{\lambda} = y + y(y-1)(\lambda-1) + y[\text{terms involving second and higher powers of } (y-1)].$$

Because y is a proportion, it satisfies $0<y<1$ so that the higher powers of $(y-1)$ will be individually and collectively small. If y is close to 0.5, a further algebraic simplification of the second term is possible, giving the identity

$$y(y-1) = -0.25 + (y-0.5)^2.$$

When y is in the range $0.25<y<0.75$, the right-hand side of this identity remains close to -0.25. Thus model II may be simplified to

$$B_{SP\_PPS} = \alpha_0(PPS) - 0.25\alpha_0(\lambda-1) + e_t,$$

which is the form of model III.

Fish recolonization in temperate Australian rockpools: a quantitative experimental approach

Shane P. Griffiths
Environmental Science
and
Institute for Conservation Biology
University of Wollongong
Wollongong, New South Wales, Australia
Present address: CSIRO Marine Research
233 Middle Street
Cleveland, Queensland 4163 Australia
Email address: shane.griffiths@csiro.au

Ron J. West
Environmental Science
University of Wollongong
Wollongong, New South Wales, Australia

Andy R. Davis
Institute for Conservation Biology
University of Wollongong
Wollongong, New South Wales, Australia

Ken G. Russell
School of Mathematics and Applied Statistics
University of Wollongong
Wollongong, New South Wales, Australia

Abstract—Understanding recolonization processes of intertidal fish assemblages is integral for predicting the consequences of significant natural or anthropogenic impacts on the intertidal zone. Recolonization of experimentally defaunated intertidal rockpools by fishes at Bass Point, New South Wales (NSW), Australia, was assessed quantitatively by using one long-term and two short-term studies. Rockpools of similar size and position at four sites within the intertidal zone were repeatedly defaunated of their fish fauna after one week, one month, and three months during two short-term studies in spring and autumn (5 months each), and every six months for the long-term study (12 months). Fish assemblages were highly resilient to experimental perturbations—recolonizing to initial fish assemblage structure within 1–3 months. This recolonization was primarily due to subadults (30–40 mm TL) and adults (>40 mm TL) moving in from adjacent rockpools and presumably to abundant species competing for access to vacant habitat. The main recolonizers were those species found in highest numbers in initial samples, such as *Bathygobius cocosensis*, *Enneapterygius rufopileus*, and *Girella elevata*. Defaunation did not affect the size composition of fishes, except during autumn and winter when juveniles (<30 mm TL) recruited to rockpools. It appears that Bass Point rockpool fish assemblages are largely controlled by postrecruitment density-dependent mechanisms that indicate that recolonization may be driven by deterministic mechanisms.

Manuscript submitted 28 April 2003 to the Scientific Editor's Office.
Manuscript approved for publication 5 May 2004 by the Scientific Editor.
Fish. Bull. 102:634–647 (2004).

Rocky intertidal fishes are faced with many biotic (competition and food availability) and abiotic (temperature and salinity) factors that can influence their distribution and abundance (Gibson, 1982). Despite occupying a dynamic environment, the fish assemblages in intertidal rockpools have been widely shown to remain persistent through time (Grossman, 1982, 1986; Collette, 1986). These communities can also rapidly return to their original state after major or even catastrophic perturbations (Moring, 1996). Such resilience is less common among assemblages of invertebrates (Connell, 1972; Astles, 1993) because recolonization of substrata is normally dependent upon successful larval settlement (Paine and Levin, 1981). In contrast, fish can rapidly colonize available habitat by larval recruitment from the plankton (Willis and Roberts, 1996, Beckley, 2000; Griffiths 2003a) but also by the relocation of subadults and adults from adjacent rockpools (Beckley, 1985a; Griffiths, 2003a). Under natural conditions rockpools can be defaunated by events such as hurricanes (Moring, 1996) and, in some regions, by seasonal freezing of rockpool water (Thomson and Lehner, 1976; Moring, 1990). These events can create new microhabitats or open existing ones for fish to colonize, and therefore have the potential to change fish assemblage structure.

Understanding recolonization processes of intertidal fish assemblages is integral for predicting the consequences of natural or anthropogenic impacts on the intertidal community. The role of disturbance and recolonization processes in structuring inter-

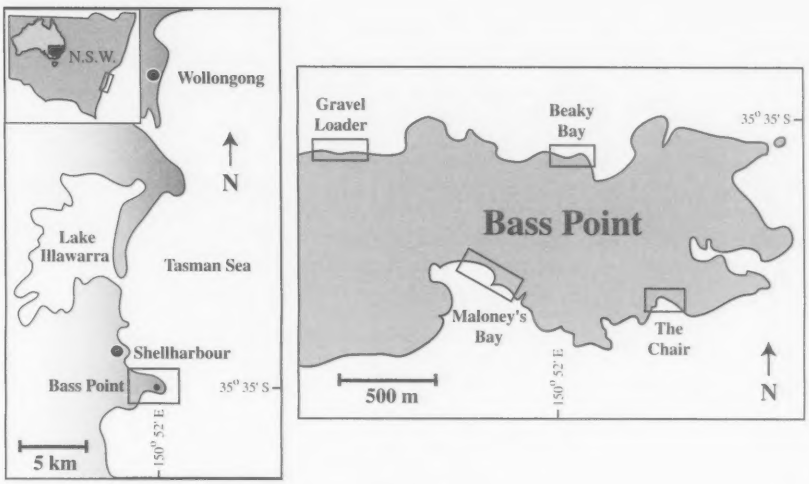

Figure 1

Map illustrating the four sampling sites at Bass Point and the location of the study location in the Illawarra region, New South Wales, Australia.

tidal rockpool fish assemblages has received considerable attention in many countries of the world (Bussing, 1972; Matson et al., 1986; Yoshiyama et al., 1986; Prochazka and Griffiths, 1992; Lardner et al., 1993; Prochazka, 1996; Faria and Almada, 1999; Silberschneider and Booth, 2001). Such studies have identified patterns in the rates of recovery, variation in species and size composition of recolonizing fish assemblages (Polivka and Chotkowski, 1998; Beckley, 2000), and homing abilities of many intertidal fishes (Green 1971; Yoshiyama et al., 1992; Griffiths, 2003b).

Rockpools can be regarded as "island' habitats (Underwood and Skilleter, 1996) among an inhospitable rocky landscape. Therefore, there is probably a balance between immigration (recruitment and relocation) and emigration (mortality) of fishes after a disturbance, *sensu* the equilibrium theory of island biogeography (MacArthur and Wilson, 1967). After a period of time, the number of species and individuals in a defaunated rockpool can be expected to reach an asymptote when a carrying capacity is reached. It is difficult to generalize about recolonization rates of rockpools by fishes from the current literature mainly owing to the diversity of methods used, their differing effectiveness in sampling fish, and the varying intensity of the sampling regime. For example, most studies have used only small sample sizes (<10 pools) and have sampled at a range of time intervals from days (Mistry et al., 1989; Matson et al., 1986; Polivka and Chotkowski, 1998) to years (Thomson and Lehner, 1976; Lardner et al., 1993; Mahon and Mahon, 1994). A second problem in measuring and comparing fish recolonization patterns between studies is that many researchers have sampled fish using an anesthetic (Mahon and Mahon, 1994; Pfister, 1995, 1997) or ichthyocide (Beckley, 1985a, 1985b, 2000; Willis and Roberts, 1996; Silberschneider and Booth, 2001), which may affect subsequent catches (Yoshiyama et al., 1986) and possibly result in fish assemblages never reaching preperturbation conditions (see Mok and Wen, 1985; Lockett, 1998).

Nonetheless, recolonization of rockpools by fishes is generally a rapid process, beginning within days, or even hours, after defaunation (Collette, 1986), and complete recolonization to preperturbation levels can take a few weeks (Collette, 1986; Faria and Almada, 1999) to several months (Mok and Wen, 1985; Willis and Roberts, 1996; Polivka and Chotkowski, 1998).

The aims of this study were to quantitatively determine 1) the period required for intertidal rockpools to recover to preperturbation levels, 2) the fish species (permanent residents, opportunist, or transients) responsible for recolonizing rockpools, 3) whether recolonization patterns differ between the four sites at Bass Point and between the times of year when defaunation took place, and 4) whether fish comprise different life-history stages before and after a disturbance (sampling)—by examination of length-frequency distributions.

Methods

Study site and experimental design

Spatial and temporal variation in fish recolonization patterns were investigated in three separate studies undertaken along the north- and south-facing rocky platforms at Bass Point (34°58′S, 150°93′E), New South Wales, Australia (Fig. 1). Bass Point is a large rocky headland that extends approximately 3 km into the Tasman Sea. Two short-term recolonization studies (each around 5

months in duration) were undertaken in spring–summer and autumn–winter (hereafter referred to as spring and autumn studies, respectively), and a long-term recolonization study spanned a 12-month period. Rockpools for each of the three studies were selected at four sites at Bass Point, NSW, which are named Maloney's Bay (MB), The Chair (TC), Gravel Loader (GL), and Beaky Bay (BB) (Fig. 1). Each of the four sites are separated by about 1 km. Rockpools were selected at each site (50–200 m apart) according to similar physical parameters (i.e., volume, surface area, and substrate type) and particularly according to their vertical elevation on the rock platform. Because higher pools might have less chance of fish recolonization because they are less frequently inundated by seawater (Griffiths et al., 2003), every effort was made to select pools located in the mid-intertidal zone (1–1.5 m above MLLW [mean lower low water]) and, although pools were visually similar, they varied in volume, ranging from 762 to 2160 liters (or 0.76–2.16 m^3). The bottom of the rockpools consisted of pebbles, cobbles, and small boulders.

For the short-term studies, four rockpools were sampled and fish removed at each of the four sites. In the spring study (beginning 7 September 1999), they were then resampled 1 week, 1 month, and 3 months after the preceding sampling date (referred to as the "1-week," "1-month," and "3-month" samples in this article). This study ended on 8 February 2000, after a period of 5 months. After this date a period of at least three months was given for pools to re-establish fish assemblages before beginning the autumn study on 15 May 2000. Rockpools were sampled in exactly the same manner as for the spring study, with sampling ending on 17 September 2000. For each study, 64 samples were taken giving a total of 128 samples for the short-term studies. It is important to note that although every effort was made to resample pools after exactly the same time intervals, this was not possible because of daily time and height of tides and wave heights. For example, for the "1 week" samples, the number of days between samples was actually between 7 and 10 days.

To determine whether frequent sampling in the short-term studies affected the structure of rockpool fish assemblages, a long-term study was undertaken by using four different rockpools at the same four sites that were sampled in the short-term studies. Four rockpools at each site were considered adequate because Griffiths (2003a) was able to detect significant differences in the numbers of fish species and individuals in rockpools between sites and months using four rockpools per site in the same region that was surveyed in our study. Rockpools were initially sampled on 22 September 1999 and then resampled twice at intervals of six months (20 April 2000 and 11 September 2000). A total of 48 samples were taken for this study.

Data collection

Fish were collected by hand after completely emptying each rockpool with a VMC 12V battery-powered bilge pump of 9029 L/h capacity by using the methods of Griffiths (2000). A thorough search of each pool was conducted by overturning all rocks and boulders, searching all crevices and shaking algal fronds until all fish that could be seen were removed. Fishes were identified and total lengths (TL) were measured. Fork length (FL) was also measured for economically significant species. Fish were categorized as being juveniles (<30 mm), subadults (30–40 mm), or adults (>40 mm). Fish were then released alive into rockpools or the shallow subtidal 10–30 m away from the rockpool being sampled, which was considered to be the approximate distance that fish may be displaced by waves and surge during significant natural disturbances, such as storms. Each species was categorized by its residential status in rockpool habitats according to the definitions of Griffiths (2003c) in order to better understand the types of fish responsible for recolonization. These categories were "permanent residents," "opportunists," and "transients."

Statistical analyses

A repeated-measures ANOVA (RM-ANOVA) was used (SPSS vers. 6.1; SPSS, Chicago, IL) to test for significant differences in the numbers of species and individuals between sampling intervals (within-subjects factor) and sites (among-subjects factor). Short- and long-term experiments were analyzed with two separate RM-ANOVAs. For the short-term study a third factor of season (i.e., spring or autumn; among-subjects factor) was added. All factors were considered fixed. Assumption of sphericity of the variance-covariance matrix was tested by using Mauchly's criterion and, if violated, F tests were performed with Greenhouse-Geisser–adjusted degrees of freedom. Student-Newman-Keuls (SNK) tests were used for *a posteriori* comparisons among means (numbers of species and individuals) in RM-ANOVAs.

Nonmetric multidimensional scaling (nMDS) was used to examine similarities in fish assemblage structure between sampling intervals and sites. Data were fourth-root transformed, to reduce the influence of highly abundant taxa, and a similarity matrix was constructed by using the Bray-Curtis similarity coefficient (Clarke, 1993). Stress values are given for all ordination plots; these values describe the quality of the representation of multidimensional relationships of the data in a two-dimensional plane. Stress factors of less than 0.2 (<0.2 is considered to give a good representation of sample "relatedness" and to prevent the prospect of drawing false inferences) were obtained for each ordination (Clarke, 1993).

Analysis of similarities (ANOSIM) was used to test whether fish assemblages in *a priori* groups differed statistically (Clarke, 1993). Abundance data for each species were pooled for the four rockpools at each site and time. Each ANOSIM comparison involved generating 4999 random permutations of the data to calculate the probability that observed differences in the structure of the fish assemblages among *a priori* groups could arise

by chance. Similarity percentages (SIMPER) were used to determine which species were responsible for differences between selected groups. This analysis involved calculating the average contribution of each species in each pair of groups and comparing this contribution to the overall dissimilarity of fish assemblages between the groups. All multivariate analyses were carried out with PRIMER (Plymouth routines in multivariate ecological research) software (version 5.2.2, PRIMER-E Ltd., Roborough, Plymouth, UK).

Results

Composition of rockpool fish assemblages

A total of 3658 fish representing 38 species and 19 families was caught in 176 samples from 32 rockpools at Bass Point between 7 September 1999 and 22 September 2000 (Table 1), corresponding to densities of 0.5 and 19 species/m^3 (mean 4.4 [±2.9] /m^3) and 0.5 and 80 fish/m^3 (mean 15.6 [±14.6] /m^3), respectively. The most numerically abundant taxa were permanent rockpool residents representing the families Gobiidae (*Bathygobius cocosensis*), Tripterygiidae (*Enneapterygius rufopileus*), Clinidae (*Heteroclinus whiteleggi* and *H. fasciatus*), Blenniidae (*Parablennius intermedius*), and Gobiesocidae (*Aspasmogaster costatus*), although the temporary resident *Girella elevata* was the third most abundant species. The ten most numerically abundant species represented 92% of the catch (Table 1). Three species, *G. elevata*, *Scorpis lineolatus*, and *Myxus elongatus*, represented by 504 fish were considered to be of economic significance. All economically important fishes were caught as juveniles in the rockpools and 89% of the fish measured less than 100 mm FL.

Numbers of species and individuals

For the short-term studies, the mean number of species differed significantly between sampling intervals and sites (RM-ANOVA, Table 2). With respect to the site factor, there were significantly more species caught at BB than at the other three sites and the latter three sites did not differ from each other (SNK test). Only the "1-week" samples accounted for significantly fewer species than the initial samples (Fig. 2). However, the mean number of species caught in the "1-month" and "3-month" samples did not differ significantly from the initial samples at all sites (Fig. 2).

The mean number of individuals differed significantly between sampling intervals and sites, although there was also a significant *time*×*site* interaction (RM-ANOVA, Table 2). A close investigation of the significant *interval*×*site* interaction, with primary interest in the interval factor, revealed that the number of individuals in the initial samples did not differ significantly from samples taken after three months at the exposed sites (MB and TC), but they did differ significantly at sheltered locations (GL and BB) (Fig. 2). It appeared that the Loader and Beaky Bay sites initially supported unusually high numbers of individuals and these high numbers may have accounted for significantly fewer individuals caught in the subsequent samples (Fig. 2).

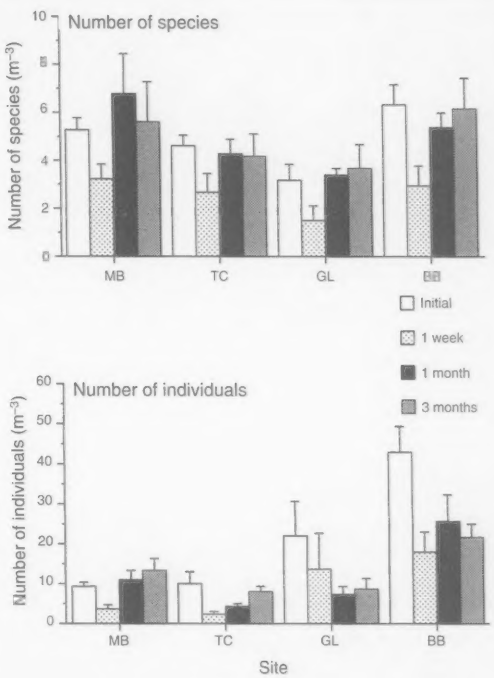

Figure 2

Mean (±SE) numbers of species and individuals (m^{-3}) caught in rockpools at Bass Point, New South Wales between 7 September 1999 and 17 September 2000 during the short-term recolonization studies (combined for spring and autumn) between sampling intervals separated by 1 week, 1 month, and 3 months. Key to sites: Maloney's Bay (MB), The Chair (TC), Gravel Loader (GL), Beaky Bay (BB).

For the long-term study, the number of individuals significantly differed among sampling times but did not for number of species (RM-ANOVA, Table 3). The significant difference in the mean number of individuals was due to fewer individuals caught in the "12-month" samples when fish numbers were pooled for all sites (SNK test, Fig. 3).

Variation in abundance of major recolonizing species

The rank abundances of the numerically dominant species were consistent for *B. cocosensis* and *E. rufopileus* across all sampling intervals for all studies, even though their relative abundances varied considerably (Table 4). In contrast, the ranks of the least common of the six species, namely *H. whiteleggi*, *P. intermedius*,

Table 1

Numbers of fish for each species caught from rockpools at four sites at Bass Point, NSW, during short-term (spring and autumn) and long-term recolonization studies conducted between 7 September 1999 and 22 September 2000. * = species of commercial or recreational significance (or both).

Family and scientific name	Spring study	Autumn study	Long-term study	Total
Muraenidae				
Gymnothorax prasinus	41	13	16	70
Gymnothorax cribroris	1	—	—	1
Plotosidae				
Cnidoglanis macrocephalus	1	—	—	1
Gobiesocidae				
Alabes dorsalis	—	2		2
Aspasmogaster costatus	134	41	65	240
Aspasmogaster liorhyncha	5	20	4	29
Syngnathidae				
Urocampus carinirostris	1	—	—	1
Scorpaenidae				
Scorpaena cardinalis	1	—	—	1
Serranidae				
Acanthistius ocellatus	33	35	16	84
Epinephelus daemelii	—	2	—	2
Plesiopidae				
Trachinops taeniatus	1	—	—	1
Girellidae				
*Girella elevata**	210	93	74	377
Scorpididae				
Microcanthus strigatus	1	—	—	1
*Scorpis lineolatus**	94	10	16	120
Pomacentridae				
Abudefduf vaigiensis	1	—	—	1
Parma microlepis	—	1	—	1
Chironemidae				
Chironemus marmoratus	30	11	10	51
Mugilidae				
*Myxus elongatus**	3	4	—	7
Labridae				
Halichoeres nebulosus	—	1	—	1
Notolabrus gymnogenis	—	1	—	1
Blennidae				
Parablennius intermedius	102	78	47	227
Istiblennius meleagris	8	10	4	22
Tripterygiidae				
Lepidoblennius haplodactylus	22	26	22	70
Norfolkia clarkei	7	4	3	14
Enneapterygius rufopileus	354	188	157	699
Clinidae				
Heteroclinus fasciatus	59	48	38	145
Heteroclinus nasutus	1	—	—	1
Heteroclinus heptaeolus	24	—	1	25
Heteroclinus johnstoni	—	2	—	2
Heteroclinus whiteleggi	138	66	39	243
Ophiclinus gracilis	15	16	6	37

continued

Table 1 (continued)

Family and scientific name	Spring study	Autumn study	Long-term study	Total
Gobiidae				
Bathygobius cocosensis	583	293	285	1161
Callogobius depressus	6	2	7	15
Callogobius mucosus	1	—	—	1
Priolepis cincta	1	—	—	1
Gobiidae sp.	1	—	—	1
Microdesmidae				
Gunnellichthys monostigma	1	—	—	1
Tetraodontidae				
Torquigener pleurogramma	—	1	—	1
Totals	1880	968	810	3658

Table 2

Results of repeated-measures ANOVAs for significant differences in numbers of species and number of individuals (/m^3) caught at Bass Point during two short-term recolonization studies among sampling intervals (time) (within-subjects factor), seasons (spring and autumn) and sites (among-subjects factors). Both numbers of species and individuals data were $\log_{10}(x+1)$ transformed before analysis, which removed heteroscedasticity in the data. Mauchly's criterion for sphericity of variances was violated for number of species (P=0.025); therefore the analysis was performed with Greenhouse-Geisser–adjusted degrees of freedom. Mean squares (MS) and significance levels are shown and significant results are given in boldface. * = P<0.05; ** = P<0.01; *** = P<0.001.

	Number of species		Number of fish	
Source	df	MS	df	MS
Among subjects				
Season (*Se*)	1	14.94	1	1292.24
Site (*S*)	3	**46.80****	3	**2782.52****
S×*Se*	3	3.66	3	63.53
Residual	24	9.38	24	370.27
Within subjects				
Time (*T*)	2.16	**18.03*****	3	**825.70*****
T×*S*	6.47	2.93	9	**247.99****
T×*Se*	2.16	2.54	3	94.86
T×*S*×*Se*	6.47	1.89	9	137.84
Residual	51.75	1.41	72	79.71
Mauchly's criterion *W*		**0.569***		0.625

Table 3

Results of repeated-measures ANOVAs for significant differences in numbers of species and number of individuals (/m^3) caught at Bass Point during the long-term recolonization study among sampling intervals (within-subjects factor) and sites (among-subjects factors). Both numbers of species and individuals data were $\log_{10}(x+1)$ transformed before analysis, which removed heteroscedasticity in the data. Mean squares (MS) and significance levels are shown and significant results are given in bold. ** = P<0.01.

	Number of species		Number of individuals
Source	df	MS	MS
Among subjects			
Site (*S*)	3	86.93	176.18
Residual	12	27.49	169.67
Within subjects			
Time (*T*)	2	3.26	**451.38****
T×*S*	6	4.44	111.82
Residual	24	2.84	55.45
Mauchly's criterion *W*		0.622	0.705

and *A. costatus*, varied considerably among sampling intervals for each study. This result probably reflects their generally low abundances, because differences in ranks can be a result of a few incidences of low individual counts.

The mean number of the six most abundant recolonizing species showed considerable variability in space and time. For the short-term study, densities of these species differed significantly among sites and among time intervals or at least for higher order interactions containing these effects (Table 5). No definitive conclusions could be made regarding the effects of defaunation on these species because short-term recolonization patterns for each species were clearly variable within and among seasons (Fig. 4). However, the mean number of fish was generally highest in initial samples and low-

Table 4

Ranked abundances of the six most abundant species overall for each sampling interval in the spring, autumn, and long-term experiments. Total numbers of fish caught during each sampling occasion from 16 rockpools from four sites are shown in parentheses. 1=initial samples; 2=samples taken after 1 week; 3=samples taken after 1 month; 4=samples taken after 3 months. Species having equally ranked abundances are denoted by an "=" sign.

	Spring study				Autumn study				Long-term study		
Species	1	2	3	4	1	2	3	4	1	2	3
Bathygobius cocosensis	1 (153)	1 (69)	1 (73)	1 (59)	2 (81)	1 (20)	1 (58)	1 (41)	1 (115)	1 (114)	1 (63)
Enneapterygius rufopileus	2 (109)	2 (50)	4 (33)	2 (46)	1 (84)	2 (12)	2 (29)	3 (25)	2 (73)	2 (43)	2 (41)
Girella elevata	3 (46)	3 (36)	3 (40)	3 (38)	3 (34)	3 (10)	3 (16)	5 (13)	5 (5)	6 (3)	4 (12)
Heteroclinus whiteleggi	6 (11)	=4 (7)	2 (51)	5 (35)	6 (9)	=4 (5)	6 (7)	2 (37)	6 (4)	4 (27)	6 (8)
Parablennius intermedius	4 (27)	=4 (7)	6 (10)	6 (23)	=4 (14)	=4 (5)	4 (15)	4 (23)	4 (14)	5 (14)	3 (19)
Aspasmogaster costatus	5 (21)	=4 (7)	5 (13)	4 (36)	=4 (14)	6 (3)	5 (8)	6 (7)	3 (22)	3 (34)	5 (9)

est in the 1-week samples at each site for the majority of dominant species. For the long-term study only the mean number of *B. cocosensis* and *E. rufopileus* differed significantly among sampling times (Table 5), and this difference was due to lower numbers being caught in the 12-month samples (Fig. 4).

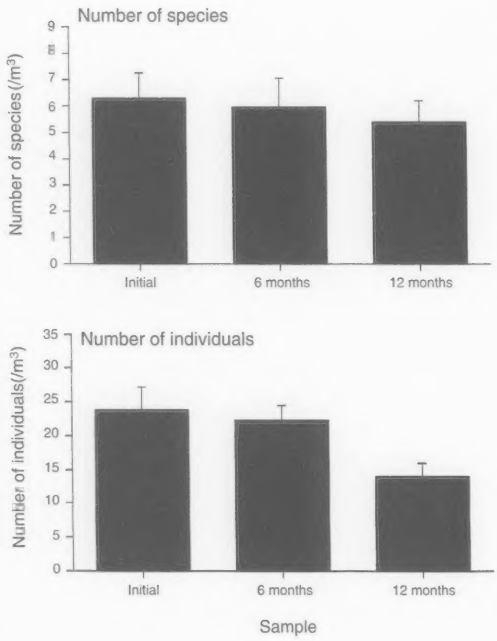

Figure 3

Mean (±SE) numbers of species and individuals (/m³) caught in rockpools at Bass Point, New South Wales, between 22 September 1999 and 11 September 2000 (pooled for all four sites) during the long-term recolonization study. Intervals between sampling for the long-term study were six months.

Fish assemblage structure

No clear patterns emerged in the nMDS ordination plots, with the exception of separation of the "1 week" samples from all other samples at BB during the autumn study (Fig. 5). ANOSIM supported these visual interpretations of ordination plots and revealed that fish assemblages did not differ significantly among sampling times at any of the four sites for the spring and long-term studies (Table 6) because abundant species *E. rufopileus*, *B. cocosensis*, *H. fasciatus*, and *P. intermedius* were common in all samples (SIMPER analysis). For the autumn study, the results of ANOSIM complemented those of RM-ANOVA in that significant differences among sampling intervals were detected only at BB (Table 6). At this site the initial samples and "1-week" samples differed significantly in their fish assemblages, which was due to higher numbers of *G. elevata* and *B. cocosensis* in the initial samples (SIMPER analysis).

Length-frequency distributions

Removal of fishes from rockpools did not have any apparent effects on the length-frequency distributions for at least two species (*B. cocosensis* and *E. rufopileus*) for which there were sufficient data to construct length-frequency histograms. Unfortunately, the less abundant recolonizing species, namely *P. intermedius*, *A. costatus*, and *H. whiteleggi*, were caught in too few numbers to ascertain the impacts of defaunation on their size compositions. Rockpools were mainly recolonized by subadults and adults for *B. cocosensis* and *E. rufopileus* in all three studies (Figs. 6 and 7). However, cohorts of small juveniles (15–30 mm) were evident in the "3-month" samples during spring and the initial autumn studies (February to June), which could then be clearly identified in subsequent samples (Figs. 6 and 7).

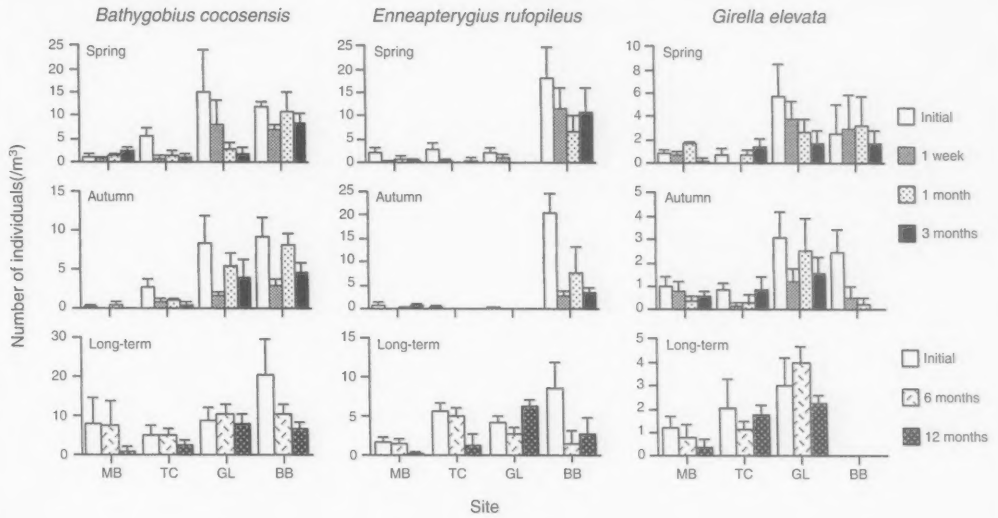

Figure 4

Mean (±SE) numbers of fish (/m^3) for the six most abundant species caught from rockpools at four sites (MB=Maloney's Bay, TC=The Chair, GL=Gravel Loader, BB=Beaky Bay) during short-term (spring and autumn) (four sampling events) and long-term (three sampling events) recolonization studies undertaken between 7 September 1999 and 22 September 2000.

Table 5

Results of repeated-measures ANOVAs for significant differences in numbers of individuals (/m^3) representing the six most abundant species caught at Bass Point during the short-term recolonization studies among sampling intervals (within-subjects factor) and sites and seasons (among-subjects factors). Data were $\log_{10}(x+1)$ transformed before analysis to remove heteroscedasticity in the data. Mauchly's criterion for sphericity of variances was violated ($P<0.001$) for species denoted by ^{G}; therefore analysis was performed using Greenhouse-Geisser–adjusted degrees of freedom. Greenhouse-Geisser degrees of freedom used for within-subjects factors where Mauchly's criterion for sphericity of variances was violated ($P<0.001$): *Time* (T) = 1.55; $Se\times T$ = 1.55; $S\times T$ = 4.64; $Se\times S\times T$ = 4.64; Residual = 34.14. Mean squares and significance levels are shown and significant results are given in bold. Degrees of freedom are shown in parentheses. * = $P<0.05$; ** = $P<0.01$; *** = $P<0.001$.

	Among-subjects factors				Within-subjects factors				
Species	Season (*Se*) (1)	Site (*S*) (3)	*Se*×*S* (3)	Residual (24)	Time (*T*) (3)	*Se*×*T* (3)	*S*×*T* (9)	*Se*×*S*×*T* (9)	Residual (72)
Bathygobius cocosensis^G	5.20	**24.50*****	3.62	2.18	**43.99*****	2.21	**10.68****	3.22	1.70
Enneapterygius rufopileus^G	0.66	**4.38*****	0.01	0.17	**0.70*****	0.05	**0.08***	**0.07***	0.04
Girella elevata	0.22	0.49	0.03	0.28	**0.12****	0.07	**0.05***	**0.07****	0.03
Heteroclinus whiteleggi^G	12.09	**20.77***	1.65	4.90	**18.99*****	**6.61***	**4.31***	4.22	1.72
Parablennius intermedius	0.00	**4.85***	0.20	1.20	**7.88****	0.20	1.92	0.29	1.07
Aspasmogaster costatus	0.37	**0.54****	0.15	0.10	**0.11***	0.09	0.03	**0.07***	0.03

Discussion

This study has shown that fish assemblages can quickly return to preperturbation levels after significant disturbance. This resilience appears to be driven mainly by postsettlement movements of fishes, although recruitment may periodically play a significant role in population replenishment. Not only does this provide an insight into the ecology of rockpool fish assemblages, but this information may also provide a basis for future sampling protocols where the confounding effects of sampling may be minimized.

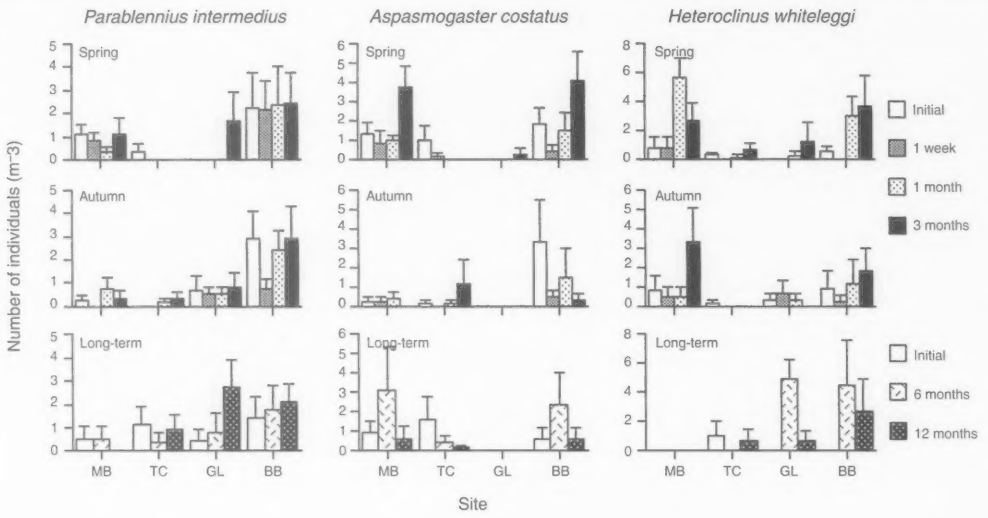

Figure 4 (continued)

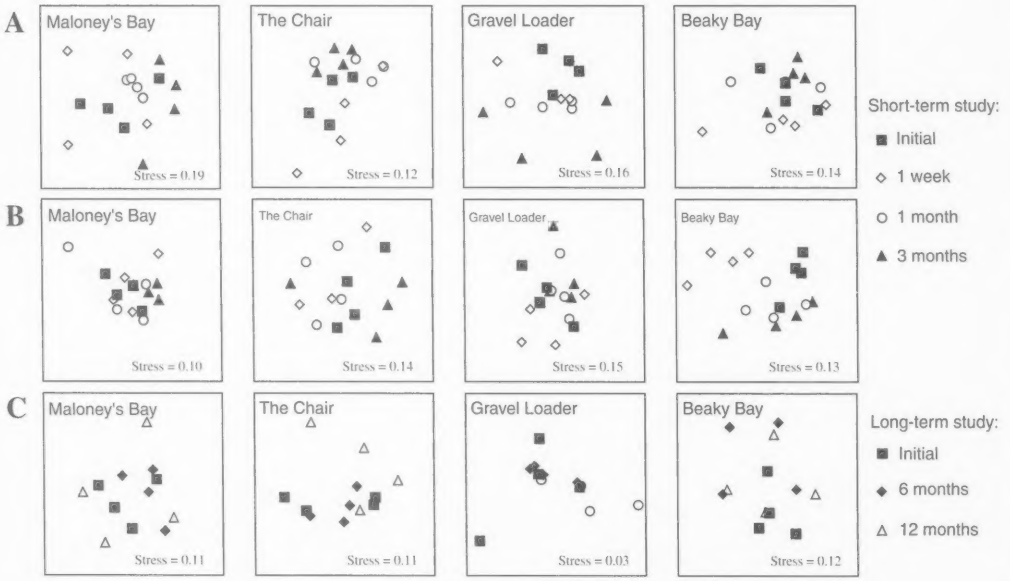

Figure 5

Nonmetric multidimensional scaling (MDS) plots for comparison of fish assemblages from four sites at Bass Point in respect to initial samples and those taken after 1 week, 1 month, and 3 months during (**A**) spring and (**B**) autumn short-term studies, and after 6 months and 12 months during (**C**) the long-term study. Each coordinate represents a single rockpool sample. Stress values are shown.

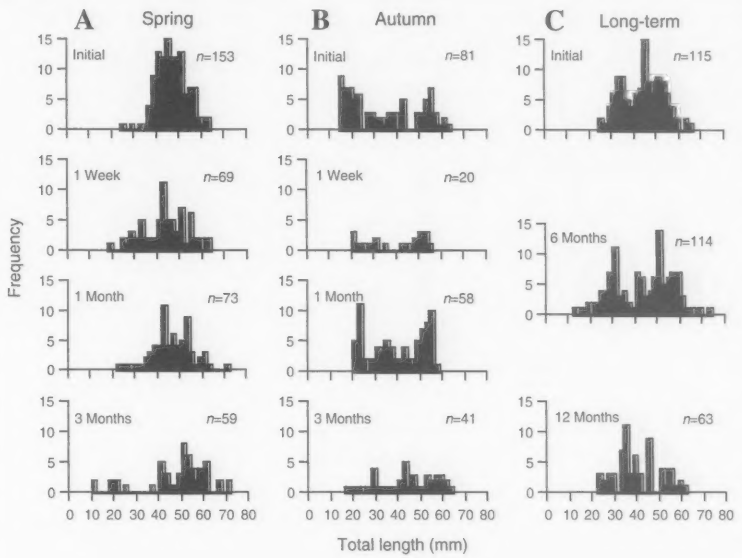

Figure 6

Length-frequency distributions (in 2-mm intervals) for *Bathygobius cocosensis* caught in the initial samples and after 1 week, 1 month, and 3 months later in the short-term study and caught in the initial sampling and 6 months and 12 months later in the long-term study. Samples were pooled for all sites during the (**A**) spring and (**B**) autumn short-term recolonization studies and for all sites during (**C**) the long-term recolonization study. Studies were conducted between 7 September 1999 and 22 September 2000. Samples sizes are shown.

Table 6

Results of ANOSIM testing for differences in fish assemblage structure among sampling intervals at four sites at Bass Point during the spring, autumn, and long-term recolonization studies. Significant results are shown in bold.

	Spring		Autumn		Long-term	
Site	*R*	*P* value	*R*	*P* value	*R*	*P* value
Maloney's Bay	0.002	0.474	0.029	0.393	−0.101	0.752
The Chair	0.185	0.057	0.014	0.422	0.063	0.284
Gravel Loader	0.083	0.165	0.027	0.389	0.190	0.051
Beaky Bay	0.025	0.383	0.726	**0.000**	0.044	0.348

For rockpool fish assemblages in southeastern Australia, a period of one week appears insufficient for recolonization of all species if fish are removed during sampling, whereas intervals of one to three months appear sufficient for rockpool fish assemblages at most Bass Point locations to recolonize to preperturbation levels. It is possible that recolonization times may be decreased if all fish are returned to rockpools immediately after sampling. However, this should not provide a foundation for subsequent studies with other defaunation methods, such as anesthetics or ichthyocides. The possible residual effects of these other sampling methods, such as the mortality of mobile and sessile invertebrates or the residues from chemical anesthetics and ichthyocides are possible factors that may complicate fish recolonization patterns (see Lockett, 1998) and certainly require additional investigation. Nonetheless, in recolonization studies with chemical sampling methods similar recolonization times as those of the present study were found. For example, recolonization of rockpools defaunated by ichthyocides was shown to be complete within 1 month (Grossman, 1982; Prochazka, 1996) and 3 months (Beckley, 1985a; Willis and Roberts, 1996; Polivka and Chotkowski, 1998).

Spatial variability in fish recolonization patterns was not definitive with regard to species composition

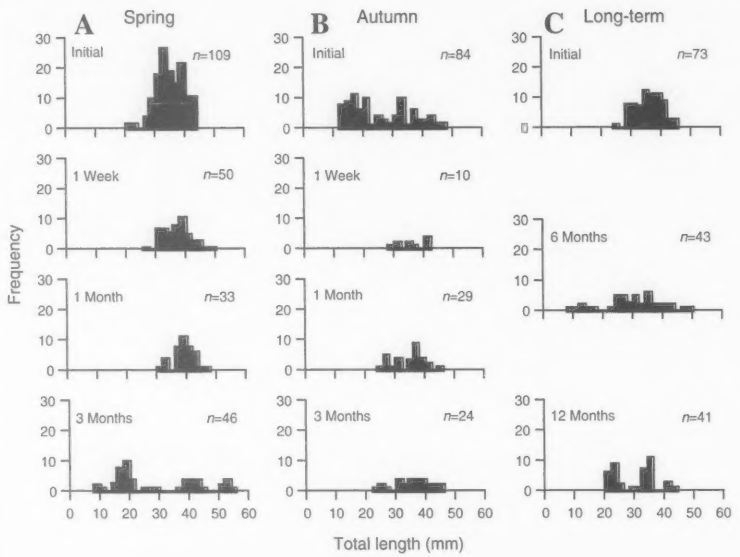

Figure 7

Length-frequency distributions (in 2-mm intervals) for *Enneapterygius rufopileus* caught in the initial samples and after 1 week, 1 month, and 3 months later in the short-term study and caught in the initial sampling and 6 months and 12 months later in the long-term study. Samples were pooled for all sites during the (**A**) spring and (**B**) autumn short-term recolonization studies and for all sites during (**C**) the long-term recolonization study. Studies were conducted between 7 September 1999 and 22 September 2000. Samples sizes are shown.

because samples were generally widely dispersed in nMDS ordination plots. The relatively low stress values (<0.2) indicate that high variability in fish assemblages at the level of individual rockpools is probably responsible for the patterns observed. However, some spatial variability in fish recolonization patterns was evident (Fig. 2) and appeared to be dependent to some extent on exposure of sites to predominant swell. There is evidence to suggest that wave exposure can affect the distribution of intertidal fishes (Gibson, 1972; Ibanez et al., 1989), although there is apparently no study that has investigated this effect in relation to fish recolonization in rockpools. In the present study, recolonization appeared more rapid at wave-exposed sites (MB and TC) compared to more sheltered sites. This may have been the result of the close distance between rockpools at exposed sites (within meters of each other), whereas at both sheltered sites, rockpools were significantly farther apart. Consequently, defaunated rockpools at exposed sites may recolonize more quickly if the major recolonizers are derived from neighboring rockpools as has been documented elsewhere (Beckley, 1985a; Polivka and Chotkowski, 1998).

Fish recolonization patterns were not influenced by the time of year that rockpools were defaunated in either short-term or long-term studies. The numbers of species and individuals consistently returned to pre-perturbation levels within a few weeks, but this return to previous levels may partially be a consequence of the relatively small number of species that are normally found in rockpools at any given time. In such situations a significant differences could only occur if large-scale changes in abundances were recorded. The lack of temporal variation in recolonization rates was surprising because recolonization was expected to be more rapid during summer, when the larvae of residents and warm water transients are expected to be available for settlement (Beckley, 1985a; Willis and Roberts, 1996). Recruitment was not the major mechanism driving fish recolonization in the present study because the majority of recolonizers were subadults and adults that would have relocated from nearby rockpools. Although many of the fish captured in each pool were tagged, the vast majority of fish caught in the same rockpool in subsequent sampling events were not tagged. Griffiths (2003b) showed that the common recolonizing species in the present study moved between a few rockpools within a limited home range. Therefore, postsettlement fishes from surrounding rockpools were probably moving into the study rockpools between each sampling event.

The movement of postsettlement fishes from adjacent rockpools also appears to control the resilience of rock-

pool fish assemblages. Therefore, the composition of species in newly recolonized rockpools is probably dependent upon the relative abundances of species in nearby rockpools. Species having the highest local abundances, such as *B. cocosensis* and *E. rufopileus*, are therefore more likely to be the primary recolonizers because vacant habitats have a higher probability of being located by these species during high-tide excursions throughout the intertidal zone (also see Polivka and Chotkowski, 1998). These species are also versatile and can exploit a range of microhabitats and, as a result, can occupy almost any rockpool within the intertidal zone (Griffiths et al., 2003). This is particularly true for *B. cocosensis*. In contrast, less abundant species such as *H. whiteleggi* often occupy more specific, and perhaps less abundant, microhabitats such as algal cover (see Marsh et al., 1978; Bennett and Griffiths, 1984) that may require longer periods to locate than more abundant habitats, such as cobble-covered substratum.

Processes regulating fish assemblages

The structure of multispecies assemblages can be regarded as being regulated by either deterministic or stochastic processes (see Grossman, 1982). Assemblages regulated by deterministic processes generally occur in environments where conditions are constant or fluctuate consistently over time. The structure of these assemblages is generally predictable. This can be maintained through a number of factors including partitioning of resources in finite supply (Schoener, 1974; Behrents, 1987) and interspecific competition, which prevents any single species being competitively dominant (Buss and Jackson, 1979).

In contrast, assemblages regulated by stochastic processes generally exist in unpredictable environments. Here, the resources are available on a random or periodic basis, which prevents superior competitors from dominating the assemblage (Sale, 1977, 1978). The success of particular species can be compared to winning a "lottery" for living space (Sale, 1977, 1978, 1982). Consequently, stochastically regulated assemblages are generally species rich (Sale, 1977).

Rockpool fish assemblages are often persistent for lengthy periods, even after catastrophic natural disturbances, such as hurricanes (Moring, 1996), and continual experimental eliminations (Grossman, 1982; Collette, 1986). For example, Collette (1986) found two species—*Pholis gunnellus* and *Tautogolabrus adspersus*—to be dominant over 19 years of study in two New England rockpools, whereas the rank of dominant species in the rockpools of Barbados showed no evidence of change over six years (Mahon and Mahon, 1994). Similar stability and persistence were evident in the present study, where *B. cocosensis*, *E. rufopileus* and *G. elevata* were consistently the highest ranked species in each collection for all three studies, regardless of the period between sampling. This finding may indicate that deterministic processes probably regulate the Bass Point fish assemblage. If this is the case, it may seem ironic because the intertidal zone is subjected to a high frequency of stochastic events. It would be easy to assume that such events could eliminate fishes from rockpools and thus leave microhabitats for other species to exploit. This kind of process has been documented for some sessile intertidal invertebrate assemblages that rely on the availability of vacant substrata for successful recruitment of larvae (see examples by Raffaelli and Hawkins, 1996). However, the locomotory capabilities and morphological and physiological adaptations of resident intertidal fishes allow them to cope with such disturbances by being able to cope temporarily with adverse conditions (Martin, 1995). As a result, the abundance of resident species may be little affected under normal disturbance regimes.

Conclusions

The results of this study have significantly increased an understanding of the patterns of recolonization of rockpools by fishes and some of the processes that underpin these patterns. Such an understanding of recolonization processes may improve our ability to predict the consequences of significant natural and anthropogenic disturbances on not only the fish assemblages but also on other intertidal community assemblages that may be maintained by the presence of fish (see Coull and Wells, 1983; Connell and Anderson, 1999).

On a more technical note, the recolonization rates observed in the present study may provide insight for other researchers aiming to study natural temporal variation of rockpool fish assemblages by minimizing the possibility of confounding effects of sampling. This may be particularly important for long-term monitoring programs, such as for marine protected areas (MPAs), that may require detection of changes in community structure over time. Finding sufficient numbers of similar-size pools at a single location for monitoring can be difficult; therefore repeated visits to the same rockpools may often be required. For southeastern Australian rockpools, we feel that a period of one to three months is required before resampling the same rockpools with the methods employed in this study. Although fish were not returned to rockpools immediately after sampling in the present study, we feel that this practice may significantly increase recolonization rates. However, the results of the present study should not provide a foundation for studies using other defaunation methods, such as anesthetics or ichthyocides, because other factors, such as chemical residues remaining in rockpools, may complicate fish recolonization patterns. Further investigation into these other factors will be necessary in the future.

Acknowledgments

We sincerely thank Jade Butler and Alan Griffiths for help with fieldwork. This paper is partly based upon

research included in a Ph.D. by S. P. Griffiths funded by an Australian Postgraduate Award. Additional funding was granted by the Institute for Conservation Biology, University of Wollongong, Shellharbour City Council, The Ecology Lab. Pty. Ltd., and Ocean Beach Hotel Fishing Club. S. P. Griffiths would like to thank CSIRO Marine Research for support during the preparation of this article.

Literature cited

Astles, K. L.
1993. Patterns of abundance and distribution of species in intertidal rockpools. J. Mar. Biol. Assoc. U.K. 73:555–569.

Beckley, L. E.
1985a. Tide-pool fishes: recolonization after experimental elimination. J. Exp. Mar. Biol. Ecol. 85:287–295.
1985b. The fish community of East Cape tidal pools and an assessment of the nursery function of this habitat. S. Afr. J. Zool. 20:21–27.
2000. Species composition and recruitment of tidal pools fishes in KwaZulu-Natal, South Africa. Afr. Zool. 35:29–34.

Behrents, K. C.
1987. The influence of shelter availability on recruitment and early juvenile survivorship of *Lythrypnus dalli* Gilbert (Pisces: Gobiidae). J. Exp. Mar. Biol. Ecol. 107:45–59.

Bennett, B. A., and C. L. Griffiths.
1984. Factors affecting the distribution, abundance and diversity of rock-pool fishes on the Cape Peninsula, South Africa. S. Afr. J. Zool. 19:97–104.

Buss, L. W., and J. B. C. Jackson.
1979. Competitive networks: nontransitive competitive relationships in cryptic coral reef environments. Am. Nat. 113:223–234.

Bussing, W. A.
1972. Recolonization of a population of supratidal fishes at Eniwetok Atoll, Marshall Islands. Atoll Res. Bull. 154:1–4.

Clarke, K. R.
1993. Non-parametric multivariate analyses of changes in community structure. Aust. J. Ecol. 18:117–143.

Collette, B. B.
1986. Resilience of the fish assemblage in New England tidepools. Fish. Bull. 84:200–204.

Connell, J. H.
1972. Community interactions on marine rock intertidal shores. Ann. Rev. Ecol. Syst. 3:169–192.

Connell, S. D., and M. J. Anderson.
1999. Predation by fish on assemblages of intertidal epibiota: effects of predator size and patch size. J. Exp. Mar. Biol. Ecol. 241:15–29.

Coull, B. C., and J. B. J., Wells.
1983. Refuges from fish predation: experiments with phytal meiofauna from the New Zealand rocky intertidal. Ecology 64:1599–1609.

Faria, C., and V. Almada.
1999. Variation and resilience of rocky intertidal fish in western Portugal. Mar. Ecol. Prog. Ser. 184:197–203.

Gibson, R. N.
1972. The vertical distribution and feeding relationships of intertidal fish on the Atlantic coast of France. J. Anim. Ecol. 41:189–207.
1982. Recent studies on the biology of intertidal fishes. Oceanogr. Mar. Biol. Ann. Rev. 20:363–414.

Green, J.M.
1971. High tide movements and homing behaviour of the tidepool sculpin *Oligocottus maculosus*. J. Fish. Res. Can. 28:383–389.

Griffiths, S. P.
2000. The use of clove oil as an anaesthetic and method for sampling intertidal rockpool fishes. J. Fish Biol. 57:1453–1464.
2003a. Spatial and temporal dynamics of temperate Australian rockpool ichthyofaunas. Mar. Freshw. Res. 54:163–176.
2003b. Homing behaviour of intertidal rockpool fishes in south-eastern New South Wales, Australia. Aust. J. Zool. 51:387–398.
2003c. Rockpool ichthyofaunas of temperate Australia: species composition, residency and biogeographic patterns. Estuar. Coast Shelf Sci. 58:173–186.

Griffiths, S. P., R. J. West, and A. Davis.
2003. Effects of intertidal elevation on the rockpool ichthyofaunas of temperate Australia. Environ. Biol. Fishes 68:197–204

Grossman, G. D.
1982. Dynamics and organisation of a rocky intertidal fish assemblage: the persistance and resilience of taxocene structure. Am. Nat. 119:611–637.
1986. Long term persistence in a rocky intertidal fish assemblage. Environ. Biol. Fishes 15:315–317.

Ibanez, M., I. Miguel, D. San Millan, and I. Ripa.
1989. Intertidal ichthyofauna of the Spanish Atlantic coast. Sci. Mar. 53:451–455.

Lardner, R., W. Ivantsoff, and L. E. L. M. Crowley.
1993. Recolonization by fishes of a rocky intertidal pool following repeated defaunation. Aust. Zool. 29: 85–92.

Lockett, M. M.
1998. The effect of Rotenone on fishes and its use as a sampling technique: a survey. Z. Fischkd. 5:13–45.

MacArthur, R. H., and E. O. Wilson.
1967. The theory of island biogeography, 224 p. Princeton Univ. Press, Princeton, NJ.

Mahon, R., and S. D. Mahon.
1994. Structure and resilience of a tidepool fish assemblage at Barbados. Environ. Biol. Fishes 41:171–190.

Marsh, B., T. M. Crowe, and W. W. Siegfried.
1978. Species richness and abundance of clinid fish (Teleostei: Clinidae) in intertidal rock pools. S. Afr. J. Zool. 13:283–291.

Martin, K. L. M.
1995. Time and tide wait for no fish: intertidal fishes out of water. Environ. Biol. Fishes 44:165–181.

Matson, R. H., C. B. Crabtree, and T. R. Haglund.
1986. Ichthyofaunal composition and recolonization in a central California tidepool. Calif. Fish and Game 72:227–231.

Mistry, S. D., E. K. Lizerbram, and E. R. Parton.
1989. Short-term ichthyofaunal recruitment in northern California tidepools. Copeia 1989:1081–1084.

Mok, H., and P. Wen.
1985. Intertidal fish community ecology on Lu Tao Island (Green Island), Taiwan. J. Taiwan Mus. 38:81–118.

Moring, J. R.
1990. Seasonal absence of fishes in tidepools of a boreal environment (Maine, USA). Hydrobiologia 194: 163–168.
Moring, J. R.
1996. Short-term changes in tidepools following two hurricanes. Hydrobiologia 328:155–160.
Paine, R. T., and S. A. Levin.
1981. Intertidal landscapes: disturbance and the dynamics of pattern. Ecol. Monogr. 47:37–63.
Pfister, C.A.
1995. Estimating competition coefficients from census data: a test with field manipulations of tidepool fishes. Am. Nat. 146:271–291.
1997. Demographic consequences of within year variation in recruitment. Mar. Ecol. Prog. Ser. 153: 229–238.
Polivka, K. M., and M. A.Chotkowski.
1998. Recolonization of experimentally defaunated tidepools by northeast Pacific intertidal fishes. Copeia:456–462.
Prochazka, K.
1996. Seasonal patterns in a temperate intertidal fish community on the west coast of South Africa. Environ. Biol. Fishes 45:133–140.
Prochazka, K., and C. L. Griffiths.
1992. The intertidal fish fauna of the west coast of South Africa—species, community and biogeographic patterns. S. Afr. J. Zool. 27:115–120.
Raffaelli, D., and S. Hawkins.
1996. Intertidal ecology, 372 p. Chapman and Hall, London.
Sale, P. F.
1977. Maintenance of high diverity in coral reef fish communities. Am. Nat. 111:337–359.
1978. Coexistance of coral reef fishes—a lottery for living space. Environ. Biol. Fishes 3: 85–102.
1982. Stock-recruit relationships and regional coexistance in a lottery competitive system: a simulation study. Am. Nat. 120:139–159.
Schoener, T. W.
1974. Resource partitioning in ecological communities. Science 185:27–39.
Silberschneider, V., and D. J., Booth.
2001. Resource use by *Enneapterygius rufopileus* and other rockpool fishes. Environ. Biol. Fishes 61:195–204.
Thomson, D. A., and C. E. Lehner.
1976. Resilience of a rocky intertidal fish community in a physically unstable environment. J. Exp. Mar. Biol. Ecol. 22:–29.
Underwood, A. J., and G. A. Skilleter.
1996. Effects of patch-size on the structure of assemblages in rock pools. J. Exp. Mar. Biol. Ecol. 197: 63–90.
Willis, T. J., and C. D. Roberts.
1996. Recolonization and recruitment of fishes to intertidal rockpools at Wellington, New Zealand. Environ. Biol. Fishes 47:329–343.
Yoshiyama, R. M., C. Sassaman, and R. N. Lea.
1986. Rocky intertidal fish communities of California: temporal and spatial variation. Environ. Biol. Fishes 17:23–40.
Yoshiyama, R. M., K. B. Gaylord, M. T. Philippart, T. R. Moore, J. R. Jordan, C. C. Coon, L. L. Schalk, C. J. Valpey, and I. Tosques.
1992. Homing behaviour and site fidelity in the intertidal sculpins (Pisces: Cottidae). J. Exp. Mar. Biol. Ecol. 160:115–130.

Factors influencing the timing and frequency of spawning and fecundity of the goldlined seabream (*Rhabdosargus sarba*) (Sparidae) in the lower reaches of an estuary

S. Alexander Hesp
Ian C. Potter
Centre for Fish and Fisheries Research
School of Biological Sciences and Biotechnology
Murdoch University
South Street
Murdoch, Western Australia 6150, Australia
E-mail address (for I. C. Potter, contact author): i.potter@murdoch.edu.au

Sonja R. M. Schubert
Ernst-Moritz Arndt Universitaet, Hansestadt Greifswald
F.-L.-Jahn Straße 15a
17487 Greifswald, Germany

Abstract—We have studied the reproductive biology of the goldlined seabream (*Rhabdosargus sarba*) in the lower Swan River Estuary in Western Australia, focusing particularly on elucidating the factors influencing the duration, timing, and frequency of spawning and on determining potential annual fecundity. Our results demonstrate that 1) *Rhabdosargus sarba* has indeterminate fecundity, 2) oocyte hydration commences soon after dusk (ca. 18:30 h) and is complete by ca. 01:30–04:30 h and 3) fish with ovaries containing migratory nucleus oocytes, hydrated oocytes, or postovulatory follicles were caught between July and November. However, in July and August, their prevalence was low, whereas that of fish with ovaries containing substantial numbers of atretic yolk granule oocytes was high. Thus, spawning activity did not start to peak until September (early spring), when salinities were rising markedly from their winter minima. The prevalence of spawning was positively correlated with tidal height and was greatest on days when the tide changed from flood to ebb at ca. 06:00 h, i.e., just after spawning had ceased. Because our estimate of the average daily prevalence of spawning by females during the spawning season (July to November) was 36.5%, individual females were estimated to spawn, on average, at intervals of about 2.7 days and thus about 45 times during that period. Therefore, because female *R. sarba* with total lengths of 180, 220, and 260 mm were estimated to have batch fecundities of about 4500, 7700, and 12,400 eggs, respectively, they had potential annual fecundities of about 204,300, 346,100 and 557,500 eggs, respectively. Because spawning occurs just prior to strong ebb tides, the eggs of *R. sarba* are likely to be transported out of the estuary into coastal waters where salinities remain at ca. 35‰. Such downstream transport would account for the fact that, although *R. sarba* exhibits substantial spawning activity in the lower Swan River Estuary, few of its early juveniles are recruited into the nearshore shallow waters of this estuary.

Manuscript submitted 9 June 2003
to the Scientific Editor's Office.
Manuscript approved for publication
28 April 2004 by the Scientific Editor.
Fish. Bull. 102:648–660 (2004).

The goldlined seabream (*Rhabdosargus sarba*) is an important recreational and commercial fish species in numerous regions throughout the Indo-west Pacific (van der Elst, 1988; El-Agamy, 1989; Kuiter, 1993). Although this species is a protandrous hermaphrodite in certain regions, e.g., the waters of Hong Kong and South Africa (Yeung and Chan, 1987; Garratt, 1993), it is a rudimentary hermaphrodite in a range of environments in Western Australia (Hesp and Potter, 2003). Rudimentary hermaphrodites are those species in which the juveniles possess gonads consisting of both immature testicular and ovarian tissues that, in adults, develop permanently into either functional testes with rudimentary ovarian tissue or functional ovaries with rudimentary testicular tissue (Buxton and Garratt, 1990). In Western Australia, *R. sarba* attains similar maximum lengths, i.e., 346–370 mm, in temperate marine coastal waters and the lower reaches of the Swan River Estuary on the lower west coast of Australia and in a large subtropical embayment ca. 800 km farther north (Hesp et al., 2004). However, the maximum age recorded for this species in the estuary, 7 years, was far less than that for the other two environments: temperate marine coastal waters (11 years) and a large subtropical embayment (13 years) (Hesp et al., 2004).

Although *R. sarba* is typically regarded as a marine species that frequently uses estuaries as a nursery area (e.g., Wallace, 1975; Potter and Hyndes, 1999; Smith and Suthers, 2000), it spawns in the lower Swan River Estuary as well as in coastal waters outside this estuary (Hesp and Potter, 2003). However, this sparid attains maturity later in the estuary than in those nearby coastal marine waters. If this indication that the onset of spawning for *R. sarba* in the Swan River Estuary is related to the attainment of higher salinities in the spring, it would parallel the situation recorded for the spotted seatrout (*Cynoscion nebulosus*) in the estuaries of the Gulf of Mexico where this species completes its entire life cycle (Brown-Peterson et al., 2002).

Despite the importance and widespread occurrence of *R. sarba*, and the great value of fecundity data for stock assessments (Hunter et al., 1992; Nichol and Acuna, 2001), only one attempt has apparently been made to estimate the annual fecundity of wild populations of this sparid (El-Agamy, 1989). Although El-Agamy (1989) recognized that *R. sarba* is a "fractional" spawner and has a

protracted spawning season, he recorded the fecundity of this species as the number of larger eggs (diameter >180 μm) estimated to be present in the ovaries of mature females just prior to the commencement of the spawning period. Thus, the very strong possibility that some eggs with diameters <180 μm would have been destined to have become fully mature and released at some stage during the protracted spawning season, i.e., the species has indeterminate fecundity, was not taken into account.

In species with indeterminate fecundity, the distribution of oocyte diameters essentially forms a continuum, reflecting the continuous maturation of oocytes throughout the spawning season and thus the progression through to maturity of some of the small and previtellogenic oocytes that were present at the beginning of the spawning period. Consequently, counts of the standing stock of larger oocytes found just prior to the onset of spawning will result in an underestimate of the potential annual fecundity of such species (Hunter et al., 1985, 1992; Lisovenko and Andrianov, 1991). Estimation of the annual fecundity of species with indeterminate fecundity thus requires a combination of data on batch fecundity and spawning frequency (Hunter et al., 1985). Batch fecundity, i.e., the number of oocytes released during a single spawning event, can be estimated by counting the number of hydrated oocytes present in ovaries immediately prior to that spawning (Hunter et al., 1985). The frequency with which a fish spawns during the spawning period can be determined from the frequency of mature female fish possessing ovaries with either hydrated oocytes or postovulatory follicles (POFs) of a known age (Hunter and Macewicz, 1985).

The spawning of many marine species of teleosts and invertebrates is correlated with lunar periodicity and the associated tidal cycles (e.g., Schwassmann, 1971; Taylor, 1984; Greeley et al., 1986; Hoque et al., 1999), with the spawning of such fish species typically peaking around the full or new moon (or both) (e.g., Johannes, 1978; Taylor and DiMichele, 1980; Greeley et al., 1986). Many fish and invertebrates with pelagic eggs spawn on high or ebb tides that enable eggs and the subsequent larval stages to be transported away from spawning areas, in which planktivorous predators are concentrated. This process thus reduces the likelihood of those early life cycle stages being subjected to predation (Taylor, 1984; Johnson et al., 1990; Morgan, 1990). The fact that there is very little recruitment of the early 0+ individuals of *R. sarba* into the lower Swan River Estuary, where extensive spawning occurs, indicates that tides transport the eggs of this species from spawning areas in the estuary into coastal marine waters (Hesp and Potter, 2003; Hesp et al., 2004).

This investigation, which involved a detailed study of the females of *R. sarba* in the lower Swan River Estuary, had the following aims: 1) to test the hypothesis that *R. sarba* has indeterminate fecundity; 2) to establish the period during the day when the oocytes of *R. sarba* become hydrated and when ovulation and spawning occur; 3) to establish whether *R. sarba* spawns mainly when salinities are high and thus approach those of the marine waters in which this species typically breeds and whether spawning is correlated with the strength and type (ebb vs flood) of tide in the lower reaches of the Swan River Estuary; 4) to estimate the average frequency of spawning for *R. sarba* during the spawning period; 5) and to determine the relationship between batch fecundity and fish length, and to use this relationship, in combination with the average spawning frequency, to calculate the potential annual fecundity of *R. sarba* of different sizes.

Materials and methods

Tide, lunar phase, and salinity

The maximum daily tidal heights at the mouth of the Swan River Estuary were calculated by using the tidal prediction data of the Coastal Data Centre at the Department of Planning and Infrastructure, Government of Western Australia (http://www.coastaldata.transport.wa.gov.au). The maximum tidal range at the mouth of the Swan River Estuary is small, i.e., ≤0.8 m, and tides can be diurnal or semidiurnal, depending on the time of year (Spencer, 1956). Salinity was measured on each sampling occasion by using a Yellow Springs Instruments salinity meter (YSI model number 30, Yellow Springs Instrument Co., Inc., Yellow Springs, OH).

Sampling

During 2001 and 2002, female *Rhabdosargus sarba* were collected by seine netting in nearshore shallow waters at distances of ca. 2.5 to 5 km from the mouth of the Swan River Estuary, and by rod and line fishing in water depths of 10–12 m at a distance of ca. 150 m from the shore (for details of sampling region and seine net, see Hesp and Potter, 2003). Sampling was undertaken at least once weekly between July and November, the period when *R. sarba* reach maturity in the lower Swan River Estuary (Hesp and Potter, 2003). It was restricted to the hours between dusk (ca. 18:00 h) and dawn (ca 06:00 h) because extensive seine netting and angling during the day in our earlier study failed to yield any *R. sarba*. The failure to capture *R. sarba* by these methods during daylight reflected the offshore movement of this species from the shallows prior to dawn and a far stronger targeting of bait by the large numbers of the banded toadfish (*Torquigener pleurogramma*) that feed in the offshore waters of the lower estuary during the day. Because the lower reaches of the Swan River Estuary act as a shipping harbor, alternative sampling methods, such as gill netting and spearing, could not be used to catch *R. sarba* during the day. The data for 2000 and 2001 were augmented by those derived from fish collected from the same location by using the same methods in 1998 and 1999 (Hesp and Potter, 2003). In total, the results of the present study are based on an examination of over 2000 *R. sarba*, of which 510 were

Table 1

Characteristics of each macroscopic stage in the development of the ovaries of *Rhabdosargus sarba*, and its corresponding histological characteristics. Adapted from Laevastu (1965). Terminology for oocyte stages follows Wallace and Selman (1989).

Stage	Macroscopic characteristics	Histological characteristics
I Virgin	Ovary is very small and strand-like.	*Rhabdosargus sarba* is a rudimentary hermaphrodite, *sensu* Hesp and Potter (2003). Thus, the gonads of small juveniles contain only connective tissue. Larger juveniles possess gonads (ovotestes) in which each ovarian lobe consists of an immature ovarian and testicular zone, separated by connective tissue. The ovotestes develop later into gonads containing almost entirely ovarian tissue (functional ovaries) or, in the case of males, gonads containing almost entirely testicular tissue (functional testes).
II Immature and resting	Small and transparent. Yellowish-orange in color. Oocytes not visible through ovarian wall.	Ovigerous lamellae highly organized. Chromatin nucleolar and perinucleolar oocytes dominate the complement of oocytes. Oogonia sometimes present. Chromatin nucleolar oocytes present in all subsequent ovarian stages.
III Developing	Slightly larger than stage II. Reddish color. Oocytes visible through ovarian wall.	Chromatin nucleolar, perinucleolar and cortical alveolar oocytes present.
IV Maturing	Larger than stage III. Reddish-orange in color. Yolk granule oocytes visible through ovarian wall.	Cortical alveolar and yolk granule oocytes abundant.
V Mature	Larger than stage IV, occupying half to two thirds of body cavity. Extensive capillaries visible in ovarian wall.	Yolk granule oocytes predominant.
VI Spawning	Hydrated oocytes visible through ovarian wall. Note that fish with ovaries in "spawning condition" can only be detected macroscopically when caught during the hydration period.	Migratory nucleus oocytes, hydrated oocytes, or postovulatory follicles present.
VII Spent	Smaller than V and VI and flaccid. Some yolk granule oocytes visible through ovarian wall.	Some remnant yolk granule oocytes present, all or almost all of which are typically undergoing atresia.
VIII Spent and recovering	Small and dark red.	Extensive scar tissue present. Ovarian lamellae becoming reorganized. No yolk granule oocytes present.

females with stage-V (mature) or stage-VI (spawning) ovaries (see Table 1 for definitions of these stages).

During the above sampling, *R. sarba* was collected for up to 2 hours at intervals commencing at 18:30, 21:30, 00:30, and 03:30 h on 1–2 September 2001 and for up to 2 hours at intervals commencing at 18:30 and 22:30 h on 13 September 2001. One of the ovarian lobes of up to five fish caught during each of these above time intervals was cut into several pieces, preserved in 10% neutrally buffered formalin solution and used for determining the distributions of oocyte diameters at the above different times. The other lobe was used for histology to determine the oocyte stages present in that lobe, and thus, by extrapolation, also the stages of the oocytes in the lobe that had been preserved in formalin. The resultant comparisons were used, in conjunction with data from other times, to elucidate the pattern of oocyte development during hydration and the duration of hydration and timing of ovulation.

Gonadal staging and histology of ovaries

The sex, total length (to the nearest 1 mm), and total weight and gonad weight (to the nearest 0.01 g) of each fish were recorded. From its macroscopic appearance, each gonad was assigned to one of the following stages in maturation, based on the scheme of Laevastu (1965), i.e., I = virgin, II = immature and resting, III = developing, IV = maturing, V = mature, VI = spawning, VII = spent, VIII = spent and recovering. The corresponding histological characteristics of each macroscopic stage are shown in Table 1. When hydrated oocytes could be seen through the ovarian wall of a fish, a note was made as to whether they were distributed throughout the ovary or were in

the ovarian duct and thus whether or not ovulation had commenced at the time of capture of that fish.

For all histological studies of the gonads, part of the mid region of one of the ovarian lobes was placed in Bouin's fixative for ca. 48 hours, dehydrated in a series of ethanols, embedded in paraffin wax, cut into 6-μm sections, and stained with Mallory's trichrome. The ovaries were fixed within 1–3 hours of capture of the fish.

To test the hypothesis that *R. sarba* has indeterminate fecundity, the diameters of 100 oocytes in histological sections of stage-VI ovaries of two fish caught during the spawning period were measured to the nearest 10 μm by using an eyepiece graticule in a compound microscope and the stage of each of those oocytes was recorded. Measurements were restricted to oocytes in which a nucleus was visible in their center to ensure that the oocytes had been sectioned through their center and that the diameters were thus measured accurately. This approach could not be used to measure the oocyte diameters of hydrated oocytes in histological sections because the nucleus of these oocytes undergoes germinal vesicle breakdown.

Histological sections of numerous ovaries were used to determine the timing of the formation and degeneration of postovulatory follicles (POFs). An age was assigned to the POFs found in ovaries of fish caught at different times of the day, based on the timing of ovulation and the degree to which those POFs had degenerated (Hunter and Goldberg, 1980; Hunter and Macewicz, 1985). Histological sections were also used to determine the relative abundance of the different stages of atresia in ovaries at different times during the spawning period.

The jars containing the ovarian lobes that had been preserved in formalin at the different time intervals on 1, 2, and 13 September 2001 (see earlier) were shaken until the oocytes of each ovary had become evenly suspended in the solution. The resultant solution from each ovary was then passed through a 125-μm sieve to remove the smallest oocytes, and we were able thus to focus our study more specifically on the vitellogenic oocytes. Comparisons of the appearance of the larger oocytes under a dissecting microscope with those of the different oocyte stages in histological sections of the other ovarian lobe of the same fish were used to allocate the oocytes observed under the dissecting microscope to a specific stage in oocyte development. Each oocyte in a representative subsample of 100 oocytes from each formalin-preserved ovarian lobe was measured under a dissecting microscope with an eyepiece graticule. This approach enabled the diameters of hydrated oocytes to be measured accurately, which was not possible with histological sections (see earlier).

Categorization of stages in atresia, fecundity estimates, and spawning frequency

On the basis of their histological characteristics, atretic oocytes were allocated to either the α or β stages, by using the criteria of Hunter and Macewicz (1985). Mature ovaries were categorized according to the proportions of their α and β atretic oocytes (Hunter and Macewicz, 1985). Thus, atretic state 0 = ovaries with yolked oocytes but no α atretic oocytes; atretic state 1 = ovaries in which less than 50% of the yolked oocytes are in the α stage of atresia; atretic state 2 = ovaries in which less than 50% of the yolked oocytes are α atretic and atretic state 3 = ovaries which contain no yolked oocytes but do possess β atretic oocytes. During the present study, atretic state 1 ovaries were further divided into three categories on the basis of the percentage of α atretic yolk granule oocytes in histological sections, namely early (<10%), mid (10–35%) and late (36–50%) atretic state 1, an approach similar to that adopted by Farley and Davis (1998).

The batch fecundities of 31 *R. sarba* were estimated from the number of hydrated oocytes in one of the ovarian lobes of fish that had been preserved in 10% neutrally buffered formalin. These fish were chosen because histological examination of their other ovarian lobe demonstrated that the ovaries were in atretic state 0 or early state 1, i.e., less than 10% of their yolk granule oocytes were atretic and newly formed POFs were not present (Hunter et al., 1992; Nichol and Acuna, 2001). The formalin-preserved ovarian lobe was dried with blotting paper and ca. 180–200 mg of tissue was removed from each of its anterior, middle, and posterior regions and weighed to the nearest 1 mg. These pieces of tissue were placed on separate slides, covered with 30% glycerol and examined under a dissecting microscope. The oocytes were then teased apart and the number of hydrated oocytes recorded. The number of hydrated oocytes in each of the three pieces of ovarian tissue of known weight were then used, in conjunction with the weight of both ovarian lobes, to estimate the total number of hydrated oocytes (=batch fecundity) that would have been present in the pair of ovarian lobes of each fish. The prevalence of spawning on any given night is expressed as the percentage of female fish with hydrated eggs (ovarian stage VI) among all female fish with stage-V (mature) and stage-VI (spawning) ovaries. These estimates were based on an examination of samples collected between 22:00 and 01:30 h, when it was possible to determine which female fish were going to spawn in the ensuing few hours (see Hunter et al., 1985, for further details of this method).

Results

Although mean monthly salinities in the lower Swan River Estuary in late spring to early winter were close to that of full strength sea water (35‰), they fell precipitously to a minimum of 23‰ (minimum individual value=14‰) in August, and then rose sharply in early to mid-spring (Fig. 1).

Staging of the ovaries and confirmation of indeterminate fecundity

The characteristics of each macroscopic stage of the ovaries of *R. sarba* and the corresponding histologi-

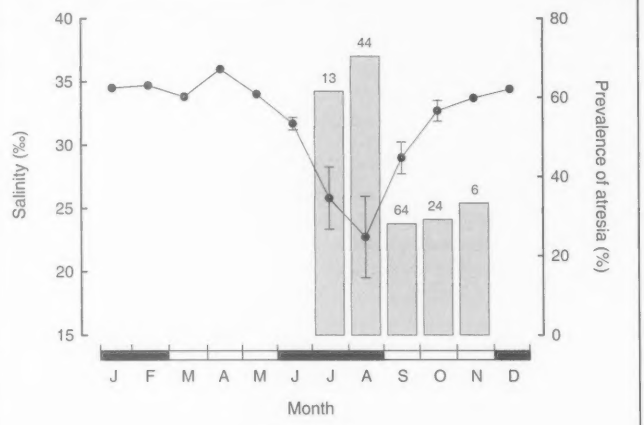

Figure 1

Mean monthly salinities (±1SE) at the bottom of the water column in the lower Swan River Estuary throughout the year and the prevalences of atresia in mature ovaries of *Rhabdosargus sarba* between July and November, which are shown as histograms, together with the number of fish examined. Closed rectangles on the horizontal axis refer to summer and winter months, and the open rectangles to autumn and spring months.

cal characteristics are presented in Table 1. Because stages V and VI could be distinguished macroscopically only during the period of oocyte hydration, the macroscopic data for these two stages had to be combined for other times. The diameters of the oocytes in histological sections of an ovarian lobe from each of two mature female *R. sarba* caught during the spawning season—oocyte diameters that were typical of those from mature *R. sarba* during this period—formed an essentially continuous distribution (Fig. 2). This distribution reflected the presence of oocytes at all stages in development from chromatin nucleolar oocytes to yolk granule oocytes and demonstrated that *R. sarba* has indeterminate fecundity *sensu* Hunter et al. (1985). Thus, the potential annual fecundity is not fixed prior to the commencement of the spawning period and consequently the potential annual fecundity of *R. sarba* has to be estimated by using a combination of batch fecundity and spawning frequency.

Period of hydration and spawning

The diameters of oocytes in ovaries of fish collected at intervals on 1–2 September 2001 and 13 September 2001 and which had been retained on the 125-μm sieve, produced a modal class that, for each time interval, fell between 420 and 600 μm (Fig. 3). At ca. 18:30 h on 1 September 2001, the oocyte diameters formed a single mode, and the vast majority of oocytes were less than 720 μm and produced a modal class at 420–539 μm (Fig. 3). However, by ca. 21:30 h on the same evening, the maximum diameter of the oocytes had increased markedly and the distribution of the oocyte diameters was beginning to become bimodal, with modal classes at 480–539 and 780–839 μm. By 00:30 h on 2 September, the oocyte diameter distributions had become markedly bimodal, and the modal diameter class of the largest oocytes at this time, and also at 03:30 h, lay between 840 and 959 μm (Fig. 3). The oocyte diameter frequencies on 13 September were essentially the same as those at similar times on 1 September; the distributions were unimodal at 18:30 h and bimodal at 22:30 h (Fig. 3). The oocyte diameters of each fish within a given time slot on 1, 2, and 13 September exhibited essentially the same distribution.

Histological sections showed that, at 18:30 h on 1 September 2001, most of the mature ovaries contained migratory nucleus stage oocytes, i.e., oocytes in which the nucleus was migrating towards the edge of the cytoplasm and a conspicuous lipid droplet was present in the cytoplasm (Fig. 4A). However, it was difficult at this time to distinguish migratory nucleus oocytes from yolk granule oocytes under a dissecting microscope (Fig. 4B). By 21:30 h, the yolk and lipid of the larger oocytes had begun to coalesce and the nucleus could sometimes be seen near the edge of the cytoplasm (Fig. 4C). Their relatively larger size, translucent appearance, and one's ability to detect their lipid droplet enabled these hydrating oocytes to be far more readily distinguished from yolk granule oocytes under a dissecting microscope than was the case earlier in the evening (cf. Fig. 4, B and D). By 00:30 h, the largest oocytes had increased

further in size and all of their lipid and yolk material had coalesced (Fig. 4E). Under the dissecting microscope, these hydrated oocytes were of similar appearance to the corresponding oocytes at 21:30 h (Fig. 4F). Although mature fish with ovaries containing the above stages in oocyte hydration were frequently found in nearshore shallow waters, the numbers of such fish in these waters declined markedly after about 00:30 h and none of the few fish caught there after this time contained recently formed POFs. However, fish with ovaries containing newly formed POFs were caught in offshore deeper waters.

Histological examination demonstrated that, when hydrated oocytes were present in the ovarian duct, the ovary contained recently formed POFs, which are formed by the thecal and granulosa layers of the oocytes that surround the zona radiata externa (Fig. 5A). Newly formed POFs (0–6 h old) possess a conspicuous lumen and their granulosa cells contain prominent darkly stained nuclei (Fig. 5B). These newly formed postovulatory follicles were first observed in the ovaries of females caught at ca. 01:30 h and were present in the ovaries of several fish caught in the ensuing four hours. In contrast, no newly formed POFs were found in the ovaries of *R. sarba* at dusk, i.e., ca. 18:30 h. At this time, the POFs comprised one of two morphological forms. The first and least degenerate form was less well organized than newly formed POFs and its nuclei were becoming pycnotic (Fig. 5C); the second form was smaller and highly degenerate and its nuclei had become far less visible or undetectable (Fig. 5D). The least degenerate of the two forms of POFs in ovaries of fish caught at ca. 22:00 and 01:00 h (Fig. 5, D and E) represents stages in degeneracy that are intermediate between those of the two different forms described above for the ovaries of fish caught at 18:30 h. These POFs were thus compact and, although some of their nuclei were still detectable, they were markedly pycnotic.

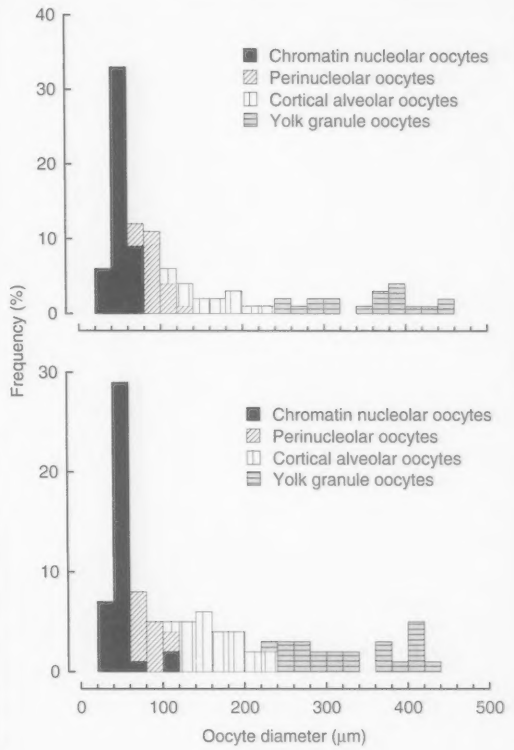

Figure 2

Percent frequency distributions for the oocyte diameters of different oocyte stages in histological sections of stage-VI ovaries of two female *Rhabdosargus sarba*.

Influence of salinity and tides on spawning

Both α and β atretic oocytes were frequently observed in the ovaries of *R. sarba*. The chorion (zona radiata) of the early α atretic vitellogenic oocyte was distorted, fragmented, and had moved inwards (Fig 6A). By the β atretic stage, the yolk and lipid had been resorbed and a large proportion of the oocyte volume was occupied by vacuoles (Fig. 6B).

Sixty-two percent and 72% of the stage-V and stage-VI ovaries sectioned in July and August, respectively, were at mid or late atretic state 1, i.e., 11–50% of their yolk granule oocytes were α atretic (Fig. 1). However, the prevalence of these mid-late state-1 ovaries declined precipitously to 28% in September, as salinities rose markedly, and remained at a similar level until the end of spawning in late November.

Histological sections showed that, in July and August, only 39% of the 57 pairs of ovarian lobes of *R. sarba* that were macroscopically assigned as stage V and stage VI contained migratory nucleus oocytes, hydrated oocytes, or POFs, i.e., were at stage VI. However, in the following two months, 76% of the 88 pairs of ovarian lobes of *R. sarba*, that were macroscopically assigned as stage V or stage VI, were shown by histology to be at stage VI.

During September, when spawning activity was greatest, the prevalence of spawning (PS) was positively correlated ($P<0.05$) with maximum daily tidal height (T). $PS = 91.72T + 20.73$ ($r^2=0.46$, number of sampling occasions=10) (Fig. 7A).

Data for the same days as those used to provide the points shown in Fig. 7A demonstrated that the prevalence of spawning (PS) is inversely correlated with the difference in hours between the time when spawning is believed to cease (ca. 06:00 h, see later) and the time of high tide. $PS = -8.26(T) + 78.22$ ($r^2=0.49$, number of sampling occasions=10) (Fig. 7B). Thus, the prevalence of these "spawning" females was greatest on those days when the time that the tide was about to change from flood to ebb coincided with the time when *R. sarba* is considered to cease spawning.

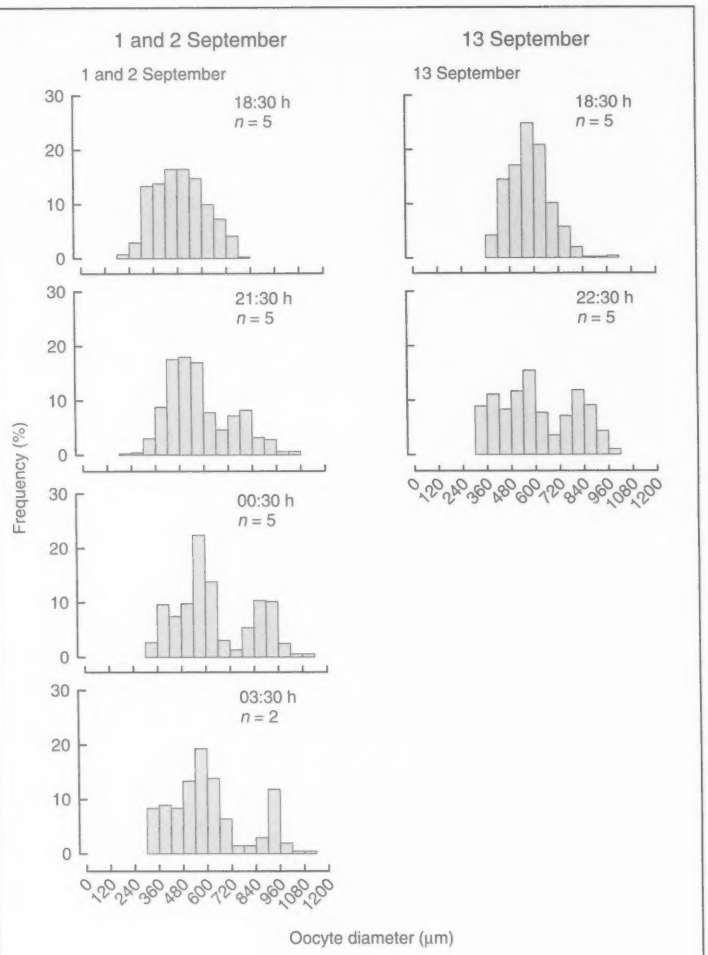

Figure 3

Frequency distributions for the oocyte diameters in mature ovaries of *Rhabdosargus sarba* caught on 1–2 and 13 September 2001. The ovaries had been preserved in formalin and their oocytes had been passed through a 125-µm sieve. The time of commencement of each 2-hour sampling interval is shown. *n* = number of fish used for oocyte diameter measurements.

Batch fecundity, spawning frequency, and potential annual fecundity

The relationship between batch fecundity (*BF*) and total length (*TL*) shown in Figure 8, and between batch fecundity and somatic weight (*W*) are described by the following equations:

$$\ln BF = 5.0025 \ln TL - 17.557 \quad (P<0.001;\ r^2=0.52,\ n=30),$$

$$BF = 1997e^{0.0105W} \quad (P<0.001;\ r^2=0.55,\ n=30).$$

The batch fecundities of *R. sarba*, predicted by the above equations for fish with lengths of 180, 220, and 260 mm, were ca. 4500, 7700, and 12,400, eggs, respectively, and for fish with somatic weights of 100, 150, and 200 g were ca. 5700, 9600, and 16,300 eggs, respectively. The average daily prevalence of spawning during the spawning period was 36.5%. Thus, during this period, individual females spawned, on average, once every 2.7 days and therefore about 45 times during the spawning season. The potential annual fecundities of female *R. sarba* with lengths of 180, 220, and 260 mm were thus estimated to be ca. 204,300, 346,100, and 557,500 eggs, respectively.

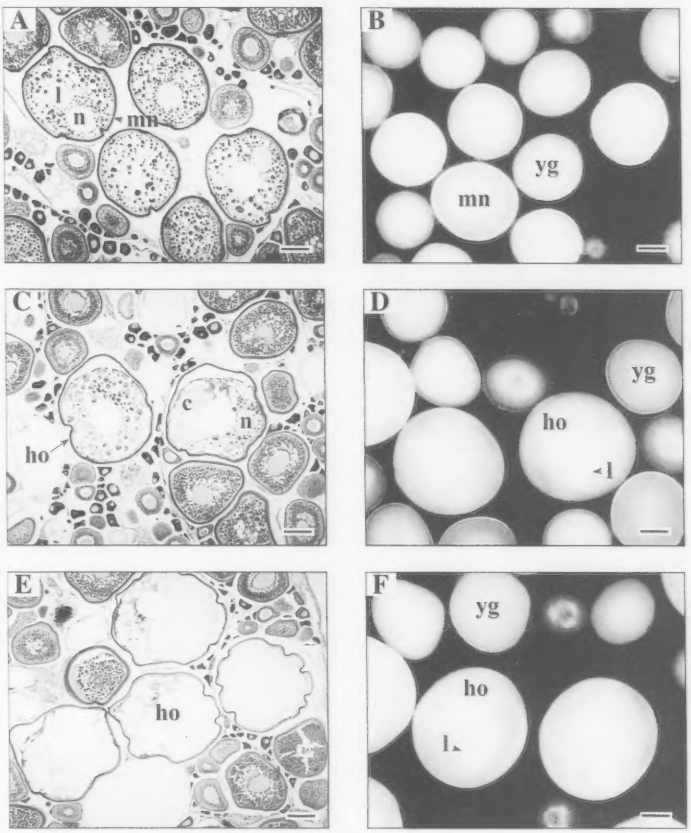

Figure 4

Histological sections of ovaries of individual *Rhabdosargus sarba* caught on 1 and 2 September 2001 at ca. 18:30 h (**A**), 21:30 h (**C**) and 00:30 h (**E**) and photographs of the oocytes from the other lobe of the ovary of the same three fish (**B, D ,F**). c=coalescing yolk and lipid; ho=hydrating oocyte; l=lipid droplet; mn=migratory nucleus oocyte; n=nucleus; yg=yolk granule oocyte. Scale bars = 200 μm in A, C, and D and 250 μm in B, D, and F.

Discussion

Oocyte hydration, ovulation, and spawning periods

Because histological studies showed that the ovaries of numerous fish caught on different occasions between 18:30 and 20:30 h did not contain recently formed POFs, we deduced that these fish had not spawned in the previous few hours. However, at this time, the ovaries of many fish, that were designated macroscopically as at stage V and stage VI, often contained numerous migratory nucleus-stage oocytes and, towards the end of this period, often a few oocytes in the early stages of hydration. Although the frequency distributions of the oocyte diameters of fish examined on both 1 and 13 September were still unimodal at 18:30 to 20:30 h, they had become bimodal by 21:30 to 23:30 h (Fig. 3), reflecting the fact that, by this time, numerous oocytes had become markedly enlarged through hydration. The above data demonstrate that hydration typically commences soon after dusk. Furthermore, because a number of *R. sarba* caught between 01:30 and 04:30 h, and particularly towards the end of this time interval, contained ovaries undergoing ovulation and had newly formed POFs, the period between the onset of hydration and commencement of ovulation typically lasts about 7–10 hours, which is very similar to the duration estimated for species such as the black sea anchovy (*Engraulis encrasicholus*) (Lisovenko and Andrianov, 1991) and ballyhoo (*Hemiramphus brasiliensis*) (McBride et al., 2003). Although we

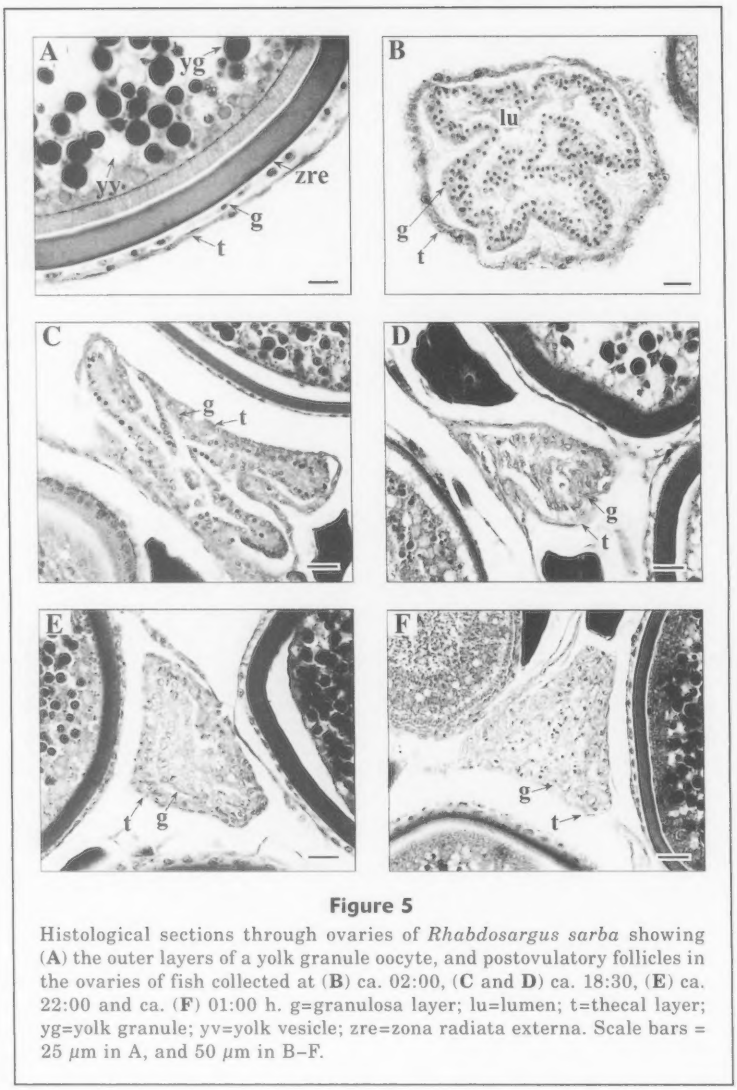

Figure 5

Histological sections through ovaries of *Rhabdosargus sarba* showing (**A**) the outer layers of a yolk granule oocyte, and postovulatory follicles in the ovaries of fish collected at (**B**) ca. 02:00, (**C** and **D**) ca. 18:30, (**E**) ca. 22:00 and ca. (**F**) 01:00 h. g=granulosa layer; lu=lumen; t=thecal layer; yg=yolk granule; yv=yolk vesicle; zre=zona radiata externa. Scale bars = 25 μm in A, and 50 μm in B–F.

caught several *R. sarba* with new POFs in their ovaries and hydrated oocytes in their oviducts, we were able to catch only one individual of this species in which the ovaries possessed new POFs and no hydrated oocytes. The latter fish, which had clearly just completed spawning, was caught between 05:00 and 06:00 h.

Several species are known typically to complete spawning in the 10–14 hours after the time when their oocytes commence hydration, e.g., the northern anchovy (*Engraulis mordax*) (Hunter and Macewicz, 1985), the spotted seatrout (*Cynoscion nebulosus*) (Brown-Peterson et al., 1988) and the horse mackerel (*Trachurus trachurus*) (Karlou-Riga and Economidis, 1997). Furthermore, spawning is typically completed 2–5 hours after the commencement of ovulation, e.g., the spotted seatrout (*Cynoscion nebulosus*) (Brown-Peterson et al., 1988), the Black Sea anchovy (*Engraulis encrasicholus*) (Lisovenko and Andrianov, 1991) and the weakfish (*Cynoscion regalis*) (Taylor and Villoso, 1994). These consistent data, when considered in conjunction with the similar duration of hydration of *R. sarba*, and the capture of a very recently spawned fish between 05:00 and 06:00 h, provide very strong circumstantial evidence that, in the lower Swan River Estuary, *R. sarba* spawns mainly between 02:00 and 06:00 h.

The newest POFs in the ovaries of *R. sarba* caught at dusk, i.e., at 18:30 h, had degenerated to an extent similar to those of ca. 12-h-old POFs in the ovaries of other species, e.g. the skipjack tuna (*Katsuwonus pelamis*) (Hunter et al., 1986) and the whitemouth croaker

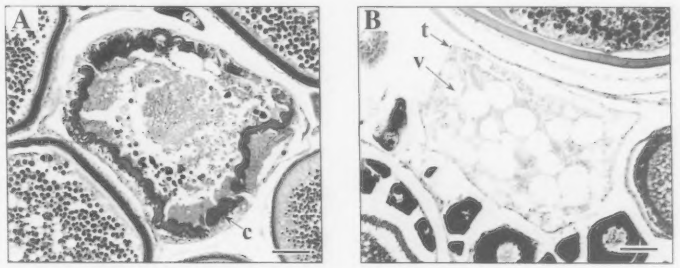

Figure 6

Histological sections of ovaries of *Rhabdosargus sarba* showing an oocyte at the (**A**) α and (**B**) β stages of atresia. c=chorion; t=thecal layer; v=vacuole. Scale bars = 100 μm in A and 50 μm in B.

(*Micropogonias furnieri*) (Macchi et al., 2003). This finding provides further evidence that *R. sarba* spawns close to dawn. Certainly, the state of degeneration of the newest POFs in mature ovaries of *R. sarba* at dusk provides very strong circumstantial evidence that spawning could not have occurred during at least most of the previous daylight hours.

Our results demonstrate that the prevalence of fish with ovaries at mid to late atretic state 1 declined precipitously as salinities increased from their winter minima in July and August and that this decrease was accompanied by an increase in the prevalence of migratory nucleus oocytes, hydrated oocytes or POFs. The implication that the oocytes of *R. sarba* are often inhibited from undergoing final oocyte maturation when salinities are low parallels the conclusions drawn for the influence of salinity on the gonadal development of *Cynoscion nebulosus* in estuaries entering the Gulf of Mexico (Brown-Peterson et al., 2002). The resorption of yolk granule oocytes by the ovaries of *R. sarba* in July and August would help conserve energy at a time when, if those oocytes progressed through to final maturation and were released, they would be exposed to salinities that are known to be lower than those required for optimal development (Mihelkakis and Kitajima, 1994).

Frequency of spawning

Because ovulation lasts for ca. 2–5 hours, the POFs that were present in ovulating ovaries and that showed no detectable signs of degeneration were presumably <3 hours old. It then follows that, when POFs at intermediate and advanced stages of degeneration were present in those same ovaries, those POFs were presumably ca. 24 and ca. 48 hours old, respectively. Thus, the presence of these three very distinct forms of POFs in the same ovary of a fish implies that individual *R. sarba* are capable of spawning on at least three successive days during that part of the month when spawning activity is greatest.

The estimated average frequency of spawning by *R. sarba*, i.e., once every 2.7 days, is essentially the same as that recorded for several other species, including e.g., spotted seatrout (*Cynoscion nebulosus*) (Brown-Peterson et al., 1988, 2002), red drum (*Sciaenops ocellatus*) (Wilson and Nieland, 1994), and common snook (*Centropomus undecimalis*) (Taylor et al., 1998). The resultant conclusion that *R. sarba* spawns about 45 times during a spawning period is comparable to that estimated for black sea anchovy (*Engraulis encrasicholus*) (Lisovenko and Andrionov, 1991) and cobia (*Rachycentron canadum*) (Brown-Peterson et al., 2001). However, spawning frequency does vary markedly among species.

Relationship between spawning time and tidal cycle

Although seine netting between 00:30 and 05:30 h on a number of days yielded no female *R. sarba* with newly formed POFs, rod-and-line angling in deeper water between 01:30 and 04:30 h yielded several females in which the ovaries contained both newly formed POFs and concentrations of hydrated oocytes in their oviducts, and also running ripe males. This finding provides strong circumstantial evidence that, just prior to ovulation, *R. sarba* moves from nearshore shallows to offshore deeper waters.

Because *R. sarba* typically spawns just prior to the commencement of a relatively strong ebb tide, the fertilized eggs would likely be transported downstream and out of the estuary. The conclusion that eggs are swept out of the estuary is supported by the fact that only 15 larvae of *R. sarba* were caught during extensive sampling of the lower Swan River Estuary and that virtually all of these larvae were caught at its mouth (Gaughan et al., 1990). A downstream movement of eggs would be further facilitated by *R. sarba* spawning in deeper waters, where the current is greatest. Emigration of eggs from the estuary would enhance the chances of survival of the eggs of this essentially marine species by ensuring that they would develop in

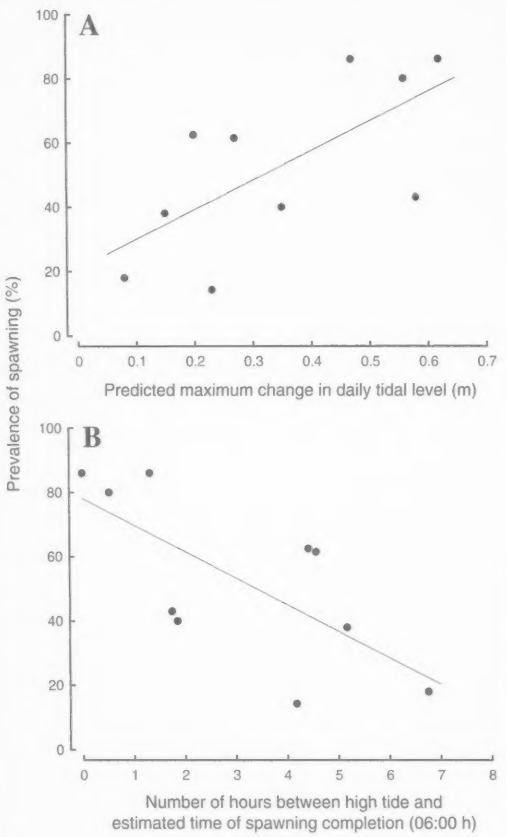
A
Prevalence of spawning (%)
Predicted maximum change in daily tidal level (m)
B
Number of hours between high tide and
estimated time of spawning completion (06:00 h)

Figure 7

Relationship between prevalence of spawning and (**A**) the predicted maximum change in daily tidal level and (**B**) the difference between the time of high tide and the time at which spawning in *Rhabdosargus sarba* is estimated to be completed in the lower Swan River Estuary (06:00 h). Each point represents the data for a separate sampling occasion.

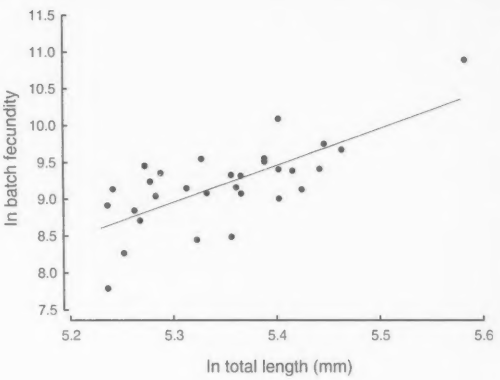

Figure 8

Relationship between batch fecundity (=number of hydrated oocytes) and total length (mm) for *Rhabdosargus sarba*.

a marine environment in which salinity remained constantly at ca. 35‰, rather than in one in which sudden rainfall could result in sudden marked declines in salinity. However, the possession of spawning cycles linked to lunar and tidal periodicities can reduce the likelihood of predation (Taylor, 1984). For example, Johannes (1978) pointed out that, because the spawning of many reef-dwelling fishes is synchronized with the lunar cycle and occurs on high or ebbing tides, their eggs would be transported away from reefs, where the concentration of predators is high, and consequently the likelihood of predation during the early stages of life would be reduced. Because planktivorous fishes are abundant in estuaries (Johnson et al., 1990; Morgan, 1990), including the Swan River Estuary where the planktivorous *Spratelloides robustus* was particularly numerous in some of our seine-net catches, a movement of the eggs of *R. sarba* out of the estuary would also enhance their chances of avoiding predation by that species.

A downstream transport of eggs would account for the relatively few young 0+ juveniles that are recruited into the nearshore shallow waters of the estuary (Hesp et al., 2004). Indeed, substantial recruitment into these nearshore waters, presumably as a result of immigration from coastal marine waters, does not occur until *R. sarba* is about one year old and about 140 mm in length (Hesp et al., 2004). Because *R. sarba* settles at a length of ca. 12 mm (Hesp et al., 2004) and ca. 30 days of age (Neira[1]), this immigration back into the estuary does not occur until 11 months after settlement. In contrast to the situation in the Swan River Estuary, *R. sarba* elsewhere typically spawns in marine waters and their larvae often enter estuaries on flood tides (e.g., Miskiewicz, 1986; Neira and Potter, 1992).

Potential annual fecundity

The estimates of potential annual fecundity derived for *R. sarba* during the present study, which ranged from 109,000 to 2,417,000 eggs for fishes of 188 and 266 mm total length, respectively, greatly exceed those of El-Agamy (1989), which ranged from 23,000 to 99,000 eggs for fishes of 170 and 260 mm total length, respectively. However, because El-Agamy (1989) based his estimates on the number of large oocytes present in the ovaries of individual *R. sarba*, he did not take into account the fact

[1] Neira, F. J. 2004. Personal commun. Australian Maritime College, Faculty of Fisheries and Marine Environment, PO Box 21, Beaconsfield, Tasmania 7270, Australia.

that this species has indeterminate fecundity. Thus, the values recorded for the annual fecundity of *R. sarba* in the Arabian Gulf almost certainly represent a marked underestimate of the true annual fecundity of this species in that region.

Acknowledgments

Our gratitude is expressed to colleagues and friends for help with sampling—to G. Thomson for preparing the histological sections, to F. J. Neira for information on the larval phase of *R. sarba,* and to D. Fairclough and two anonymous reviewers for invaluable comments on the manuscript. Financial support was provided by Murdoch University.

Literature cited

Brown-Peterson, N. J., R. M. Overstreet, J. M. Lotz, J. S. Francis, and K. M. Burns.
2001. Reproductive biology of cobia, *Rachycentron canadum*, from coastal waters of the southern United States. Fish. Bull. 99:15–28.

Brown-Peterson, N. J., M. S. Peterson, D. L. Nieland, M. D. Murphy, R. D. Taylor, and J. R. Warren.
2002. Reproductive biology of female spotted seatrout, *Cynoscion nebulosus*, in the Gulf of Mexico: differences among estuaries? Environ. Biol. Fishes 63:405–415.

Brown-Peterson, N., P. Thomas, and C. R. Arnold.
1988. Reproductive biology of the spotted seatrout, *Cynoscion nebulosus*, in south Texas. Fish. Bull. 86:373–388.

Buxton, C. D., and P. A. Garratt
1990. Alternative reproductive styles in seabreams (Pisces: Sparidae). Environ. Biol. Fishes 28:113–124.

El-Agamy, A. E.
1989. Biology of *Sparus sarba* Forskål from the Qatari water, Arabian Gulf. J. Mar. Biol. Assoc. India. 31:129–137.

Farley, J. H., and T. L. O. Davis.
1998. Reproductive dynamics of southern bluefin tuna, *Thunnus maccoyii*. Fish. Bull. 96:223–236.

Gaughan, D. J., F. J. Neira, L. E. Beckley and I. C. Potter.
1990. Composition, seasonality and distribution of the ichthyoplankton in the lower Swan Estuary, south-western Australia. Aust. J. Mar. Freshw. Res. 41:529–543.

Garratt, P. A.
1993. Comparative aspects of the reproductive biology of seabreams (Pisces: Sparidae). Ph.D. thesis, vol. 1, 175 p. Rhodes Univ., Grahamstown, South Africa.

Greeley, M. S., D. R. Marion, and R. MacGregor III.
1986. Semilunar spawning cycles of *Fundulus similes* (Cyprinodontidae). Environ. Biol. Fishes 17:125–131.

Hesp, S. A., N. G. Hall and I. C. Potter.
2004. Size-related movements of *Rhabdosargus sarba* in three different environments and their influence on estimates of von Bertalanffy growth parameters. Mar. Biol.

Hesp, S. A., and I. C. Potter.
2003. Reproductive biology of the tarwhine *Rhabdosargus sarba* (Sparidae) in Western Australian waters, in which it is a rudimentary hermaphrodite J. Mar. Biol. Assoc. U.K. 83:1333–1346.

Hoque, M. M., A. Takemura, M. Matsuyama, S. Matsuura, and K. Takano.
1999. Lunar spawning in *Siganus canaliculatus*. J. Fish Biol. 55: 1213-1222.

Hunter J. R., and S. R. Goldberg.
1980. Spawning incidence and batch fecundity in northern anchovy, *Engraulis mordax*. Fish. Bull. 77:641–652.

Hunter, J. R., N. C. H. Lo, and R. J. H. Leong.
1985. Batch fecundity in multiple spawning fishes. *In* An egg production method for estimating spawning biomass of pelagic fish: application to the northern anchovy (*Engraulis mordax*) (R. Lasker, ed.), p. 67–77. NOAA Tech. Rep. NMFS 36.

Hunter, J. R., and B. J. Macewicz.
1985. Measurement of spawning frequency in multiple spawning fishes. *In* An egg production method for estimating spawning biomass of pelagic fish: application to the northern anchovy (*Engraulis mordax*) (R. Lasker, ed.), p. 79–94. NOAA Tech. Rep. NMFS 36.

Hunter, J. R., B. J. Macewicz, L. N. Chyan-huei, and C. A. Kimbrell.
1992. Fecundity, spawning, and maturity of female Dover sole *Microstomus pacificus*, with an evaluation of assumptions and precision. Fish. Bull. 99:101–128.

Hunter J. R., B. J. Macewicz, and J. R. Sibert.
1986. The spawning frequency of skipjack tuna *Katsuwonus pelamis*, from the South Pacific. Fish. Bull. 84:895–903.

Johannes, R. E.
1978. Reproductive strategies of coastal marine fishes in the tropics. Environ. Biol. Fishes 3:65–84.

Johnson, W. S., D. M. Allen, M. V. Ogburn, and S. E. Stancyk.
1990. Short-term predation responses of adult bay anchovies *Anchoa mitchilli* to estuarine zooplankton availability. Mar. Ecol. Prog. Ser. 64:55–68.

Karlou-Riga C., and P. S. Economidis.
1997. Spawning frequency and batch fecundity of horse mackerel, *Trachurus trachurus* (L.), in the Saronikos Gulf (Greece). J. Appl. Ichthyol. 13:97–104.

Kuiter, R. H.
1993. The complete diver's and fishermen's guide to coastal fishes of south-eastern Australia, 437 p. Crawford House Press, Bathurst, Australia.

Laevastu, T.
1965. Manual of methods in fisheries biology. FAO, Rome.

Lisovenko, L. A., and D. P. Andrianov.
1991. Determination of absolute fecundity of intermittently spawning fishes. Vop. Ikhtiol. 31:631–641.

Macchi, G. J., E. M. Acha and M. I. Militelli.
2003. Seasonal egg production of whitemouth croaker (*Micropogonias furnieri*) in the Río de la Plata estuary, Argentina-Uruguay. Fish. Bull. 101:332–342.

McBride, R. S., J. R. Styer and R. Hudson.
2003. Spawning cycles and habitats for ballyhoo (*Hemiramphus brasiliensis*) and balao (*H. balao*) in south Florida. Fish. Bull. 101:583–589.

Mihelkakis, A., and C. Kitajima.
1994. Effects of salinity and temperature on incubation period, hatching rate, and morphogenesis of the silver sea bream, *Sparus sarba* (Forskål, 1775). Aquaculture 126:361–371.

Miskiewicz, A. G.
1986. The season and length at entry into a temper-

ate Australian estuary of the larvae of *Acanthopagrus australis*, *Rhabdosargus sarba* and *Chrysophrys auratus* (Teleostei: Sparidae). *In* Indo-Pacific fish biology: proceedings of the second international conference on Indo-Pacific fishes (T. Uyeno, A. R. Taniuchi and K. Matsuura, eds.), p. 740–747. Ichthyological Society of Japan, Tokyo.

Morgan, S. G.
1990. Impact of planktivorous fishes on dispersal, hatching, and morphology of estuarine crab larvae. Ecology 71:1639–1652.

Neira, F. J., and I. C. Potter.
1992. Movement of larval fishes through the entrance channel of a seasonally open estuary in Western Australia. Estuar. Coast. Shelf Sci. 35:213–224.

Nichol, D. G., and E. I. Acuna.
2001. Annual and batch fecundities of yellowfin sole, *Limanda aspera,* in the eastern Bering Sea. Fish. Bull. 99:108–122.

Potter, I. C., and G. A. Hyndes.
1999. Characteristics of the ichthyofauna of southwestern Australian estuaries, including comparisons with holarctic estuaries and estuaries elsewhere in temperate Australia: areview. Aust. J. Ecol. 24:395–421.

Schwassmann, H. O.
1971. Biological rhythms. *In* Fish physiology, vol. VI (W. S. Hoar and D. J. Randall, eds.), p 371–428. Academic Press Inc., New York, NY.

Smith, K. A., and I. M. Suthers.
2000. Consistent timing of juvenile fish recruitment to seagrass beds within two Sydney estuaries. Mar. Freshw. Res. 51:765–776.

Spencer, R. S.
1956. Studies in Australian estuarine hydrology. 2. The Swan River. Aust. J. Mar. Freshw. Res. 7:193–253.

Taylor, M. H.
1984. Lunar synchronisation of fish reproduction. Trans. Am. Fish. Soc. 113:484–493.

Taylor, M. H., and L. DiMichele.
1980. Ovarian changes during the lunar spawning cycle of *Fundulus heteroclitus*. Copeia 1980:118–125.

Taylor, M. H., and E. P. Villoso.
1994. Daily ovarian cycles in weakfish. Trans. Am. Fish. Soc. 123:9–14.

Taylor, R. G., H. J. Grier, and J. A. Whittington.
1998. Spawning rhythms in common snook in Florida. J. Fish Biol. 53:502–520.

van der Elst, R.
1988. A guide to the common sea fishes of Southern Africa, 2nd ed., 398 p. Struik Publishers, Cape Town, South Africa.

Wallace, J. H.
1975. The estuarine fishes of the east coast of South Africa. III. Reproduction. South African Association for Marine Biological Research, Oceanographic Research Institute, Investigational Report 41. The Oceanographic Research Inst., Durban, South Africa.

Wallace, R. A., and K. Selman.
1989. Cellular and dynamic aspects of oocyte growth in teleosts. Am. Zool. 21:325–343.

Wilson, C. A., and D. L. Nieland.
1994. Reproductive biology of red drum, *Sciaenops ocellatus*, from the neritic waters of the northern Gulf of Mexico. Fish Bull. 92:841–850.

Yeung, W. S. B., and S. T. H. Chan.
1987. The gonadal anatomy and sexual pattern of the protandrous sex-reversing fish, *Rhabdosargus sarba* (Teleostei: Sparidae). J. Zool. Lond. 212:521–532.

Fishery dynamics of the California market squid (*Loligo opalescens*), as measured by satellite remote sensing

Michael R. Maxwell
University of California
c/o Southwest Fisheries Science Center
8604 La Jolla Shores Drive
La Jolla, California 92037
Present address: Department of Biology
University of San Diego
5998 Alcalá Park
San Diego, California 92110
E-mail address: maxwellm@sandiego.edu

Annette Henry
California Department of Fish and Game
8604 La Jolla Shores Drive
La Jolla, California 92037

Christopher D. Elvidge
NOAA National Geophysical Data Center
325 Broadway
Boulder, Colorado 80305

Jeffrey Safran
Vinita R. Hobson
Ingrid Nelson
Benjamin T. Tuttle
Cooperative Institute for Research in Environmental Sciences
University of Colorado
Boulder, Colorado 80303

John B. Dietz
Cooperative Institute for Research on Atmosphere
Colorado State University
Fort Collins, Colorado 80523

John R. Hunter
Southwest Fisheries Science Center
NOAA National Marine Fisheries Service
8604 La Jolla Shores Drive
La Jolla, California 92037

Abstract—Novel data on the spatial and temporal distribution of fishing effort and population abundance are presented for the market squid fishery *(Loligo opalescens)* in the Southern California Bight, 1992–2000. Fishing effort was measured by the detection of boat lights by the Defense Meteorological Satellite Program (DMSP) Operational Linescan System (OLS). Visual confirmation of fishing vessels by nocturnal aerial surveys indicated that lights detected by satellites are reliable indicators of fishing effort. Overall, fishing activity was concentrated off the following Channel Islands: Santa Rosa, Santa Cruz, Anacapa, and Santa Catalina. Fishing activity occurred at depths of 100 m or less. Landings, effort, and squid abundance (measured as landings per unit of effort, LPUE) markedly declined during the 1997–98 El Niño; landings and LPUE increased afterwards. Within a fishing season, the location of fishing activity shifted from the northern shores of Santa Rosa and Santa Cruz Islands in October, the typical starting date for squid fishing in the Bight, to the southern shores by March, the typical end of the squid season. Light detection by satellites offers a source of fine-scale spatial and temporal data on fishing effort for the market squid fishery off California, and these data can be integrated with environmental data and fishing logbook data in the development of a management plan.

Manuscript submitted 24 February 2003 to the Scientific Editor's Office.
Manuscript approved for publication 17 June 2004 by the Scientific Editor.
Fish. Bull. 102:661–670 (2004).

The market squid *(Loligo opalescens)* (also known as the opalescent inshore squid, FAO [Roper et al., 1984]) is currently the largest revenue fishery for California (Vojkovich, 1998; CDFG, 2000). The fishery's importance rose steadily in the 1980s and 1990s, in response to increased demand in Asia coupled with declines in other fisheries off the U.S. West Coast. Market squid is a short-lived species (Jackson, 1994; Butler et al., 1999) whose abundance appears to be readily impacted by environmental variability. For example, squid landings plummeted during the 1997–98 El Niño but reached a record high in the following year (CDFG, 2000). Considered an integral component of California's pelagic fishery, the market squid was included in the Coastal Pelagic Species Fishery Management Plan as approved by the Pacific Fisheries Management Council in 1998. In this plan, federal authority is invoked to monitor the fishery to ensure the provisions of the Magnuson-Stevens Fishery Conservation and Management Act of 1996. If a resource is estimated as overfished, the Council is to consider implementing active management measures.

The lack of records of fishing effort, such as vessel logbooks or observer data, hampered initial attempts to formulate a management plan for the market squid. The nature of the fishery, however, suggested an alternative measure of fishing effort: the detection of boat lights by satellites. The market squid is typically harvested on shallow nearshore spawning grounds in the Southern California Bight and Monterey Bay (Vojkovich, 1998). At night, specialized lightboats shine high intensity (c. 30,000 watt) lights on the water, which attract and congregate the squid near the surface. Seiner boats then capture the concentrated squid with purse-seine nets (Vojkovich, 1998). The lights of the fishing boats are detected and recorded by the U.S. Air Force Defense Meteorological Satellite Program (DMSP) Operational Linescan System (OLS).

DMSP-OLS satellites continuously orbit the planet, acquiring data on

meteorology and, incidentally, nighttime light sources (Croft, 1978; Elvidge et al., 1997, 2001b). Nighttime light detection by satellites has proven useful for various environmental questions, such as identifying the extent of forest fires (Elvidge et al., 2001a) and the effects of urban lighting on sea turtle nest selection and hatchling survivorship (Salmon et al., 2000). Compilation of light data for the global light-fishing squid fleet has contributed to examinations of the fishery's ecosystem impacts (Rodhouse et al., 2001). For local squid fisheries, the locations of boat lights over space and time are particularly valuable in cases where national boundaries pose constraints on the collection of effort data (e.g., *Illex argentinus* in the southwestern Atlantic, Waluda et al., 2002).

In this study, we used boat lights to quantify the spatial and temporal patterns of market squid fishing activity in the Southern California Bight over the period 1992–2000. The bight has come to represent the great majority of squid landings off California (Vojkovich, 1998; Butler et al., 1999; CDFG, 2000). An important component of our study is ground-truthing work that validates the feasibility of using light data as a measure of fishing effort. This estimate for fishing effort enables us to present novel landings-per-unit-of-effort (LPUE) data for the market squid. A companion paper analyzes the light detection properties of the DMSP-OLS satellites over the Southern California Bight (Elvidge et al.[1]).

Materials and methods

Light detection by satellites

The DMSP is a polar orbiting satellite system that acquires daytime and nighttime data during each orbit. The OLS is an oscillating scan radiometer designed for cloud imaging. A full technical description of image acquisition by the DMSP-OLS system, and the subsequent processing of images, appears in a companion paper (Elvidge et al.[1]). Briefly, the DMSP-OLS acquired nighttime data for over 2200 satellite orbits over the Southern California Bight (i.e., 117° to 122° W, 32°30′ to 34°30′N) between 26 April 1992 and 4 April 2001. Four different satellites were employed during this time. Three overlapped in operation dates, producing multiple images for some dates. On all dates, images were acquired between 18:30 and 22:00 Pacific Standard Time (PST), with 20:21 PST being the average time. The satellite images were processed into geo-referenced images of boat lights and clouds. This process involved superimposing a field of grid cells onto the satellite image, which quantified the satellite's "field of view," the extent of detected clouds, and the area available for light detection. Image pixels of lights were taken directly from the satellite image. Pixels were identified as lights by their visible band digital number. The images were subjected to quality-control procedures to correct for atmospheric noise and to eliminate images overly contaminated by solar glare, sunlight, heavy lunar illumination, or those containing missing data. Fixed sources of lights, such as city lights along the southern California coast, the city of Avalon (Santa Catalina Island), off-shore oil platforms, and naval installations, were masked from the light detection algorithm.

Data deliveries were irregular during 1992, resulting in gaps in the early part of the time series. For 1992–98, only data collected during the dark half of the lunar cycle were available. To control for lunar illumination throughout the time series, we restricted analysis of fishery data to images for which lunar illumination was less than 0.02 lux (lumens per square meter). Images for analysis were evaluated against additional criteria. For a given image, we calculated the number of total grid cells that were not used for light detection because of glare, missing data, or the masking of known nonboat lights. If the resulting number of grid cells left available for light detection was at least 50% of the original number of cells, we retained the image for analysis. Cloud coverage can obscure light sources[1]; therefore we used only images from nights when clouds covered less than 25% of the grid cells available for light detection. For nights with multiple acceptable images, we averaged the percent cloud coverage and the number of detected light pixels.

Ground-truthing: aerial observations of boat activity

To determine the relationship between detected light pixels and the number of squid fishing vessels on the water, 35 aerial surveys were conducted from 10 June 1999 to 18 May 2000. Each survey took place in a Cessna 337 Skymaster flown at an average altitude of 1160 m above sea level. The path of each survey covered the main areas of squid fishing activity within the Southern California Bight (Fig. 1): from San Diego, over the Channel Islands, to Point Conception, and back down the coastline to San Diego. Each survey took approximately four hours to complete, occurring between 18:00 h and midnight PST. These times encompassed the time that the DMSP-OLS satellites were over the bight. The 35 surveys produced 26 nights of usable data. Survey data were discarded if satellite images were unavailable, if flights were aborted because of weather, or if heavy fog obscured boat visibility. We note that, for this ground-truthing work, we did not restrict our analysis to nights with lunar illumination of less than 0.02 lux. Rather, we used all of the acceptable 26 nights, and quantified lunar illumination as a proportion of the moon's phase, where 0.00 denoted a new moon and 1.00 denoted a full moon.

All vessels on the water were identified by using Fujinon 10×50 gyroscopic binoculars, and the GPS positions of all vessels were recorded. Vessel type was identified as either a nonsquid vessel or as a squid fishing vessel.

[1] Elvidge, C. D., J. Safran, M. R. Maxwell, K. E. Baugh, A. Henry, and J. R. Hunter. Unpubl. data. Satellite based indices of lightboat fishing effort.

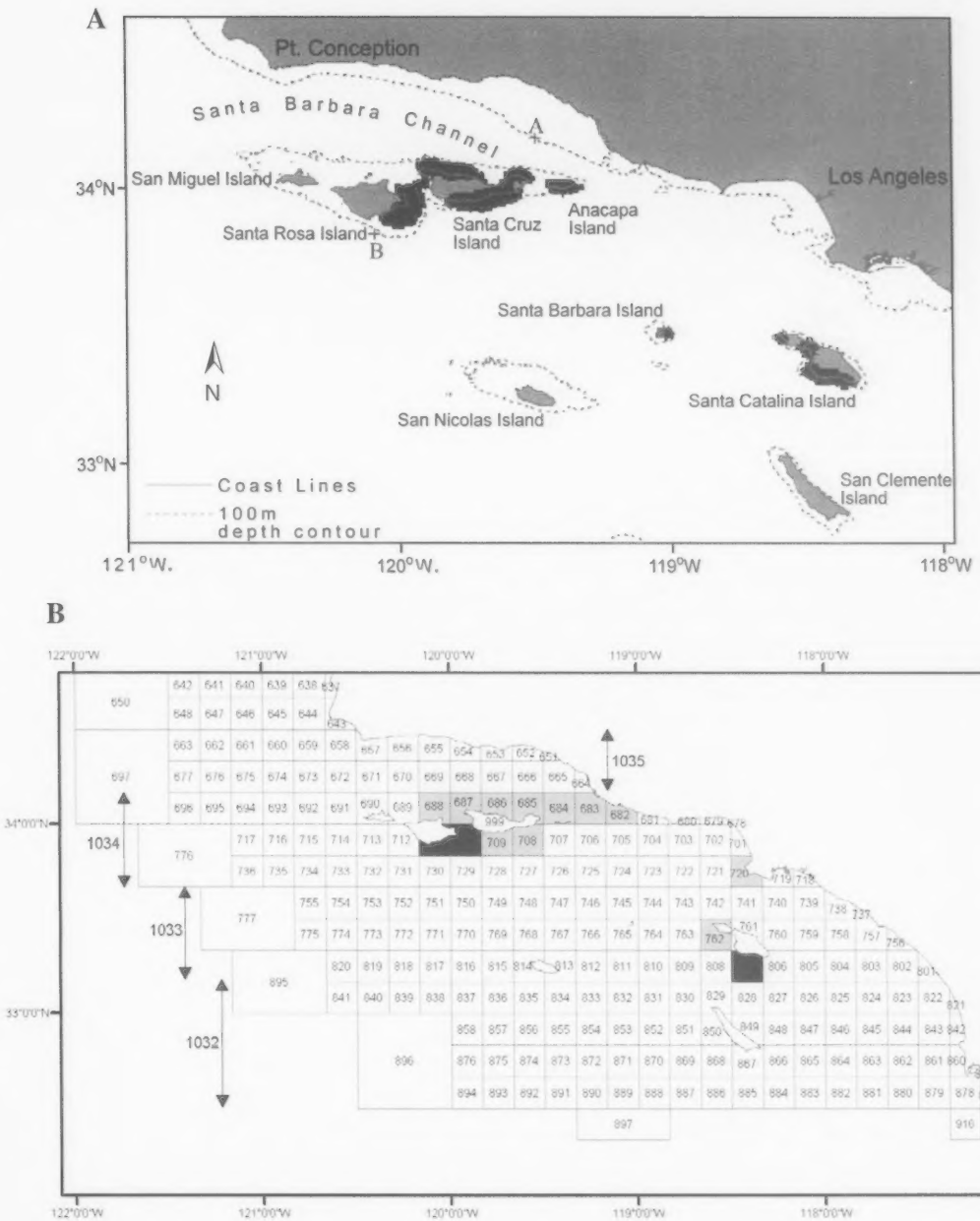

Figure 1

Fishing activity for the market squid in the Southern California Bight, from 26 April 1992 to 28 May 2000. (**A**) Composite satellite image of squid fishing vessel lights (black marks). Permanent sources of lights (e.g., city lights, offshore oil platforms, naval installations) are removed. CalCOFI stations 83.42 ("A"; 34.18°N, 119.51°W) and 83.51 ("B"; 33.88°N, 120.13°W) are indicated. (**B**) Squid landings as reported by California Dept. Fish and Game fishing blocks. Gray: blocks that account for 6.8 million kg (2%) or more of the landings from blocks 651–896. Black: blocks that account for 20.5 million kg (6%) or more. Latitudinal blocks 1032–1035 are indicated. Santa Cruz Island is marked "999" to aid correspondence with A.

Squid fishing vessels could not always be distinguished as light boats or seiners and therefore were recorded as "squid fishing vessels."

The numbers of squid fishing vessels showed large skew in their frequency distribution. These data were transformed by $x' = \log_{10}(x+1)$. Similarly, proportion lunar phase was transformed by $x' = \arcsin(\sqrt{x})$, and detected light pixels were transformed by $x' = \log_{10}(x+1)$ to correct for skew (Zar, 1984). These transformations produced normally distributed data acceptable for regression analysis. With these transformed variables, multiple stepwise regression (forward selection) was performed with the software S-Plus 2000 (MathSoft Inc., Cambridge, MA) to examine the effects of squid fishing vessels and the proportion lunar phase on detected light pixels. Squid fishing vessels and proportion lunar phase showed very little correlation (r=–0.09).

Fishery characteristics, 1992–2000

For quantitative analysis of the fishery data, we aggregated the nightly satellite data (i.e., light pixels detected on the water) into calendar quarters, as suggested by the within-year distribution of squid landings in the bight (Butler et al., 1999). To standardize conditions of light detection, we excluded all data after 28 May 2000, because this was the starting date of mandatory shielding of the high intensity lights of the lightboats. This regulation was enforced by California's Department of Fish and Game to reduce light pollution by the lightboats. The shields did not totally obscure the lightboats from detection by the satellites (authors' pers. obs.) but made the emitted light less bright, and, hence, less detectable by the satellites. Thus, our data for fishing effort spanned calendar quarters from Jul–Sep 1992 to Jan–Mar 2000. We included a quarter for analysis if it contained 10 or more nights of acceptable images. By these criteria, we described effort for 24 of the 31 calendar quarters. The mean number of nights per quarter was 26 (range=10–72 nights).

The quantity (kg) and location of landed market squid were recorded by California Department of Fish and Game (CDFG) throughout the 1992–2000 study period and were made available to the authors. During this study period, squid fishing in the bight occurred exclusively at night (Vojkovich, 1998). The squid were landed at port within several hours after being caught; therefore the landings for a given day corresponded to the previous night's effort. Squid fishermen reported the locations of their hauls by CDFG fishing blocks. We defined catch taken from the Southern California Bight as that from blocks 651–896 and 1032–1035 (Fig. 1). Blocks 651–896 are typically 10′ latitude × 10′ longitude and can be used to locate regions of high catch. Blocks 1032–1035 are large latitudinal bands, generally 30' wide, that encompass blocks 651–896. We used blocks 1032–1035 in calculating the total catch in the bight, but not in depicting the location of the catch.

To construct the abundance index of landings per unit of effort (LPUE), we first estimated the number of squid fishing vessels for each night of satellite data, using the regression results of the ground-truthing work (see "Results" section). We then summed the nightly estimated number of vessels for each calendar quarter. For those nights for which we had estimated numbers of vessels, we also summed the landed catch within each calendar quarter. To arrive at LPUE for the quarter, we divided the summed landings by the corresponding summed effort.

Environmental data

We used the multivariate ENSO index (MEI) to indicate overall environmental conditions over the course of the 1992–2000 study period. The MEI is a multivariate index that incorporates sea level pressure, surface zonal and meridional wind components, sea surface temperature, surface air temperature, and cloudiness (Wolter and Timlin, 1998). The MEI index is calculated for the tropical Pacific (i.e., between 10°N and 10°S, from Asia to the Americas), and its monthly values appear on the website http://www.cdc.noaa.gov/~kew/MEI/table.html.[2]

Analysis of the location of fishing effort over the course of the traditional squid fishing season in the bight led to an investigation of oceanographic data for waters surrounding Santa Cruz Island in March. Specifically, we examined sea temperature from two sources. First, we obtained sea surface temperature for all satellite nights in March 1993–2000 from the Physical Oceanography Distributed Active Archive Center (PO.DAAC) at California Institute of Technology (Pasadena, CA). These data were reported for 18×18 km grids, which were approximately the size of the 10′×10′ fishing blocks. We selected the grid that covered block 686 to represent the northern shore of the island, and that which covered block 708 to represent the southern shore (Fig. 1B). For each year in the 1993–2000 period, we calculated mean March temperature for both blocks.

The second source of sea temperature was the database maintained by the California Cooperative Oceanic Fisheries Investigations (CalCOFI). Since 1950, the CalCOFI program has conducted quarterly survey cruises along transects perpendicular to the southern California coast. This system of transects incorporates 66 geographically fixed stations. At each station, a conductivity-temperature-depth (CTD) instrument is deployed. Details on survey methods appear on the website http://www-mlrg.ucsd.edu/calcofi.html,[3] along with the publicly accessible database. For April 1993–2000, we obtained temperatures at sea surface and at 75 meters depth at two stations (Fig. 1A): 83.42 (northeast of Santa Cruz Island; 34.18°N, 119.51°W) and 83.51 (southwest of Santa Cruz Island; 33.88°N, 120.13°W).

[2] NOAA-CIRES Climate Diagnostics Center website. [Accessed 3 November 2003.]

[3] California Cooperative Oceanic Fisheries Investigations website. [Accessed 3 November 2003.]

One measurement was made at each station at sea surface and at 75 meters depth during April (n=8 for both depths).

Results

Ground-truthing: aerial observations of boat activity

Nonsquid vessels used weak lights (i.e., much less than 30,000 watts), which did not show in the satellite images. On average, 23 squid fishing vessels were observed each night by the aerial surveys (range=0–64 vessels, n=26 nights). The 20:00-midnight observation period was the peak time for attraction of squid by the light boats. Although the squid vessels did change location during this time, they typically left their lights running to continue searching for squid. The number of squid vessels explained much of the variation in detected light pixels; proportion lunar phase failed to enter the analysis as a significant variable (Table 1). Detected light pixels increased with the number of squid vessels (Fig. 2).

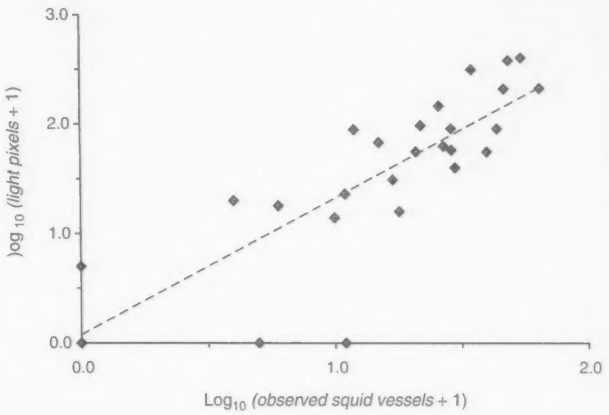

Figure 2

Plot of $\log_{10}$-transformed number of squid vessels and detected light pixels. Regression line taken from the statistics in Table 1.

The regression analysis yields the following simplified equation:

$$\log_{10}(p_t+1)=1.25\times\log_{10}(x_t+1), \quad (1)$$

where x_t = observed number of squid vessels; and
p_t = detected light pixels for night t.

We used inverse prediction to estimate the number of squid vessels for each satellite night ($\hat{E}_t$) in the 1992–2000 period (Zar, 1984). The estimated number of squid vessels was found by the equation

$$\hat{E}_t=10^{\log_{10}(p_t+1)/1.25}-1=\sqrt[1.25]{p_t+1}-1. \quad (2)$$

The ground sample distance of the satellite data is 2.7 km, which means that multiple squid vessels may potentially fit into one pixel of detected light. This could result in an underestimation of effort. The severity of this problem can be assessed by examining the coefficient of the simple linear regression of log-transformed variables represented by Equation 1. One of four scenarios is possible: 1) boats are not aggregated (coefficient=1), 2) boats are aggregated regardless of the number of boats on the water (coefficient=1), 3) boats are aggregated only when many boats are on the water (coefficient<1), or 4) boats are aggregated only when few boats are on the water (coefficient>1). The coefficient in Equation 1 is 1.25, which fails to significantly differ from 1.00 (t-test for regression coefficient: t = 1.305, β_0 = 1, df = 24, P > 0.2, two-tailed; power < 0.5, retrospectively calculated; Zar, 1984). This result suggests that very little clumping of the boats occurred (scenario 1), or that the degree of clumping was independent of the number of boats on the water (scenario 2). Although the statistical power of this t-test is not high (power<0.5), we conclude that the data provide more support for scenarios 1 and 2 over scenarios 3 and 4. Either scenario, 1 or 2, allows for a comparison of the relative values of estimated effort and LPUE within a time series.

Table 1

Multiple stepwise (forward selection) regression of detected light pixels on squid fishing vessels (transformed: $x'=\log_{10}(x+1)$ and proportion lunar phase (transformed: $x'=\arcsin(\sqrt{x})$. r^2=0.64; ANOVA: $F_{1,24}$=42.66, P<0.0001.

Variable	Coefficient ±SE	P
Squid fishing vessels	1.25 ±0.19	<0.0001
INTERCEPT	0.07 ±0.24	>0.75
Proportion lunar phase	not entered	not entered

Fishery characteristics, 1992–2000

A composite satellite image of all squid fishing activity in the Southern California Bight during the 1992–2000 study period revealed major concentrations of effort off the Channel Islands, especially Santa Rosa, Santa Cruz, Anacapa, and Santa Catalina (Fig. 1A). Squid fishing occurs close to the island shores and is bounded by the 100-m contour. During the study period, 379.2 billion kg of squid were landed in the bight: 341.2 billion from blocks 651–896 (Fig. 1B), and the remainder from the large blocks 1032–1035. The main areas of fishing activity, as indicated by satellite, are consistent with the blocks of high catch (Fig. 1B). We note that blocks 682

and 720, although areas of high catch, do not appear on the satellite composite because the mainland shore was excluded from light detection. Further, much activity was evident around Santa Barbara Island (block 765). Although this block represented 4.0 million kg (18th out of the 127 blocks), it did not rank highly enough for inclusion in Fig. 1B.

Analysis of temporal trends in the fishery showed peaks in landed catch for the bight in the fall and winter quarters (Oct–Dec and Jan–Mar, respectively; Fig. 3A). There was a near absence of catch during most of 1997–98 (Fig. 3A), which corresponded to the strong El Niño event during this period (Fig. 4). Effort data revealed surges in the Oct–Dec quarters before the 1997–98 El Niño (Fig. 3B). The Oct–Dec quarter of 1998 signalled a resumption of fishing effort following El Niño, but effort levels for 1999 and early 2000 were lower than pre-El Niño levels. Interestingly, squid abundance, as measured by landings per unit of effort (LPUE), showed a rapid increase from the El Niño lows, and squid abundance for 1999–2000 reached the highest values of the time series (Fig. 3C).

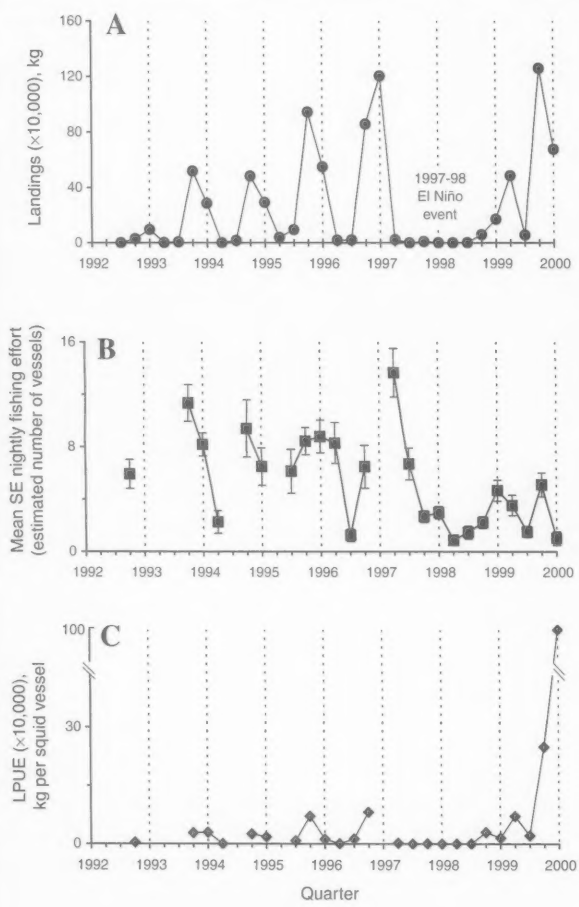

Figure 3

Time series of market squid fishery data in Southern California Bight, by calendar quarter (Jul–Sep 1992 to Jan–Mar 2000). The Jan–Mar quarters are marked by dashed vertical lines. (**A**) Landings are in kg (blocks 651–896, 1032–1035). (**B**) Mean ±SE nightly fishing effort, in estimated number of squid vessels. (**C**) Landings per unit of effort (LPUE): summed landings (kg) on satellite nights were divided by summed effort (estimated number of squid vessels) on the corresponding nights.

Analysis of boat locations along the Channel Islands revealed a shift over the course of the fishing season. Compiling the satellite data to yield composite images in multiyear sets, we found that fishing activity in October consistently included the north shore of Santa Cruz Island (Fig. 5, A,C,E). In contrast, fishing activity in March showed considerable reduction along the north side of Santa Cruz Is., but activity continued along the island's southern shore (Fig. 5, B,D,F). Composite images for December and January were also examined for all of the multiyear sets. December marked a transitional stage from the activity in October to reduction of fishing in March along the northern shores. In all multiyear sets, the December lights along northern Santa Cruz Island were more scattered and less dense than those in October. January images were very similar to those for March. Although data from March 1993–95 indicated little fishing activity, a composite image for January 1993–95 was very similar to that for March 1999–2000: light banks occurred off southern Santa Cruz, southeastern Santa Rosa, and around Anacapa, but were virtually absent from northern Santa Cruz and Santa Rosa.

Water temperatures around Santa Cruz Island did not consistently differ between northern and southern waters. March sea surface temperatures, measured by satellite, were very similar for the island's northern and southern shores (Table 2). April sea surface temperatures, measured at CalCOFI stations, were slightly warmer to the northeast of the island (Table 2). Temperatures at 75 meters, however, were nearly identical for the two CalCOFI stations (Table 2).

Discussion

The satellite images and landings data corroborated spatial and temporal patterns of fishing activity for the market squid. For the period 1992–2000, both data sets indicated intense harvesting along the Channel Islands of Santa Rosa, Santa Cruz, Anacapa, and Santa Catalina. The satellite images captured additional information, such as fishing activity being

Table 2

Water temperature (°C) for the northern and southern waters around Santa Cruz Island, March and April, 1993–2000.

	Northern waters				Southern waters			
Depth (m)	Location	Mean	Min	Max	Location	Mean	Min	Max
March sea surface temperature, as measured by satellite (PO.DAAC data)[1]								
0	Block 686	14.5	12.8	15.7	Block 708	14.7	13.2	15.9
April temperature, measured at CalCOFI stations[2]								
0	Station 83.42	13.6	11.6	16.7	Station 83.51	12.8	11.2	14.5
75	Station 83.42	9.9	9.3	11.2	Station 83.51	10.3	9.3	11.2

[1] Measurements made on multiple nights per month of March (range of measured nights per month of March: 6–26). "Mean" is the overall average of the mean March temperatures; "Min" is the minimum of the mean values, "Max is the maximum, of the mean values.

[2] One measurement made at each station at each depth per month of April (n=8 for both depths).

clearly delimited by the 100-m contour. The landings data, reported by fishing blocks, were much cruder in geographic scale and failed to catch this subtlety.

The ground-truthing work conducted by aerial surveys indicated that detected light pixels are useful in estimating the number of squid vessels in operation. This result is consistent with examination of the fishery for the squid *Illex argentinus* in the southwestern Atlantic, where vessels use powerful lamps to attract the squid to lures (Waluda et al., 2002). In the latter fishery, analysis of images acquired by the DMSP-OLS satellites revealed a good fit between the recorded number of vessels in operation on a given night and the number of light pixels detected (Waluda et al., 2002).

In the present study, the fishery data showed a strong response to the 1997–98 El Niño event, which was one of the strongest events on record (Wolter and Timlin, 1998). Fishing effort and landings tended to peak in the Oct–Dec and Jan–Mar quarters before the 1997–98 El Niño. Both data series dramatically dropped during the 1997–98 El Niño and showed recovery afterwards. Squid abundance, measured as LPUE, also showed a pronounced drop and rapid increase in response to the El Niño. It is interesting to note that another index of market squid abundance, the occurrence of squid beaks in the scat of sea lions, showed similar responses to earlier El Niño events (Lowry and Carretta, 1999). Squid beak occurrence dropped steeply during the strong 1983–84 El Niño, and increased afterwards. Beak occurrence also dipped and rose in response to a milder El Niño in 1992–93. Significantly, Lowry and Carretta (1999) examined southern Channel Islands: Santa Barbara, San Clemente, and San Nicolas. Our present study reflects squid abundance primarily around northern Channel Islands (e.g., Santa Rosa, Santa Cruz, Anacapa). Taken together, these studies may indicate that El Niño exerts a bight-wide influence on squid abundance.

We suggest that a strong El Niño event changes the reproductive conditions for the market squid in the Southern California Bight. With regard to spawning, the spawning population becomes less abundant on the traditional shallow-water spawning grounds. Research on a congener, the South African chokka squid (*Loligo vulgaris reynaudii*), points to possible environmental influences on spawning for loliginid squid (Roberts and Sauer, 1994). Off South Africa, a strong El Niño can lead to reduced upwelling and increased turbidity. In normal years, upwelling, presumably detected by the squid as an influx of cold water, may trigger spawning behavior (Roberts and Sauer, 1994). In El Niño years off South Africa, reduced upwelling and increased turbidity on the inshore spawning grounds are thought to force the spawners into deeper water, beyond the reach of the fishery (Roberts and Sauer, 1994). In a recent study, catch for the chokka squid increased with strong easterly winds, which caused upwelling, and decreased with increased turbidity (Schön et al., 2002). In the California Current System, upwelling decreases during strong El Niño events (Schwing et al., 2000). Upwelling

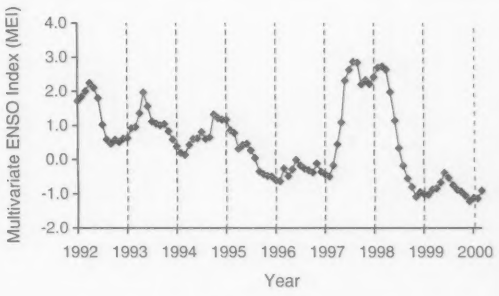

Figure 4

Multivariate ENSO index (MEI) for the tropical Pacific (between 10°N and 10°S), by month. Data were obtained from http://www.cdc.noaa.gov/~kew/MEI/table.html.

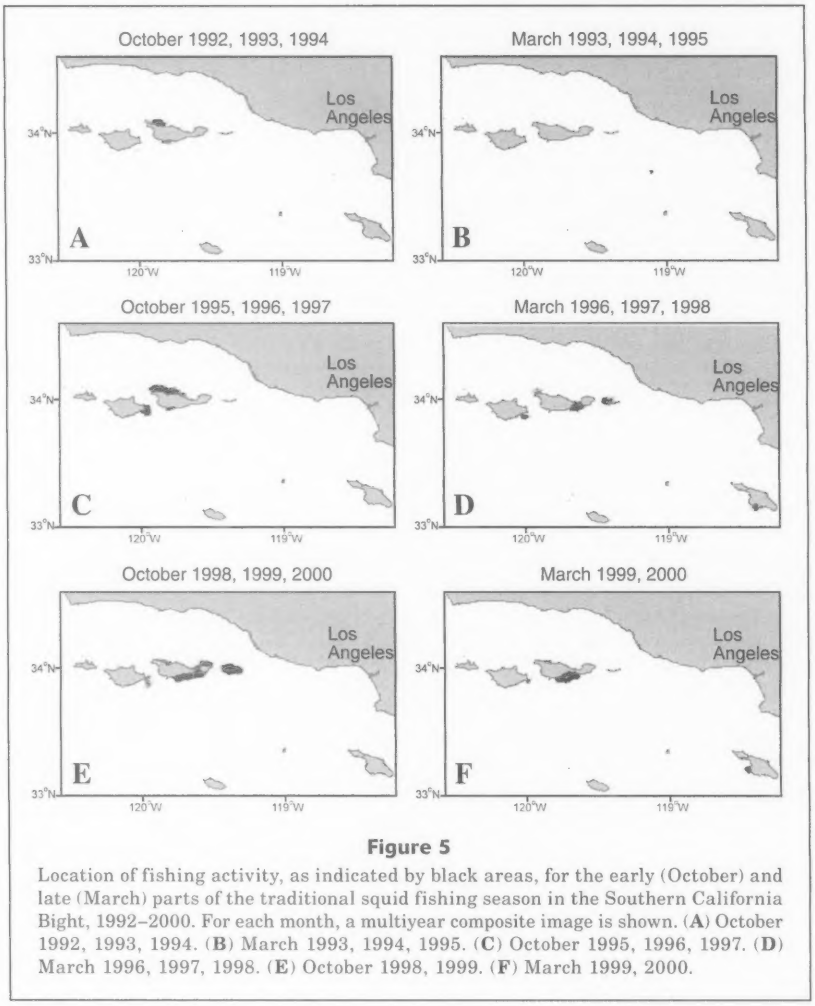

Figure 5

Location of fishing activity, as indicated by black areas, for the early (October) and late (March) parts of the traditional squid fishing season in the Southern California Bight, 1992–2000. For each month, a multiyear composite image is shown. (**A**) October 1992, 1993, 1994. (**B**) March 1993, 1994, 1995. (**C**) October 1995, 1996, 1997. (**D**) March 1996, 1997, 1998. (**E**) October 1998, 1999. (**F**) March 1999, 2000.

in the Southern California Bight was reduced during the 1997–98 El Niño (Hayward, 2000). It is not known how market squid adults respond to changes in water temperature or turbidity, or whether spawning fish shift to other habitats during El Niño events.

A strong El Niño event can also alter feeding and developmental conditions for squid. During the 1997-98 El Niño, macrozooplankton abundance substantially decreased in the Southern California Bight and off Baja California (Lynn et al., 1998; Hayward, 2000; Lavaniegos et al., 2002). Food availability affects growth rates of loligind squid (Jackson and Moltschaniwskyj, 2001). Recently, Jackson and Domeier (2003) indicated lower growth rates for the market squid in the Southern California Bight during the 1997–98 El Niño.

In the present study, fishing effort following the 1997–98 El Niño was generally below pre-El Niño levels. The subsequent high levels of catch in late 1999 and early 2000 may indicate that squid were in great abundance, thereby requiring less overall catch effort to meet market demand. A strong La Niña succeeded the 1997–98 El Niño (Lynn and Bograd, 2002; Schwing et al., 2002), with strong upwelling and high macrozooplankton abundance in the Southern California Bight by spring 1999 (Schwing et al., 2000; Hayward, 2000). Indeed, the high LPUE in the present study in late 1999 and early 2000 points to increased squid abundance in response to a more productive environment. Alternatively, one could argue that increased fishing efficiency, not increased squid abundance, resulted in high LPUE. One manifestation of higher fishing efficiency could be a contracted fishing range, where especially productive pockets are identified and targeted. An overall comparison of fishing location in October and March before and after El Niño did not support this explanation: the total spatial extent of fishing activity was not greatly

reduced in post-El Niño October or March. A noticeable concentration of fishing effort off the southern shore of Santa Cruz Island was evident in the post-El Niño period, however. The landings data may indicate that this southern shore, represented by blocks 708 and 709, was indeed productive. In the pre-El Niño period (1992–96), blocks 708 and 709 represented 3% of the landings in the bight. In the post-El Niño period (1999 to early 2000), these two blocks came to represent 12% of the landings.

The spatial distribution of fishing activity appears to shift over the course of the squid fishing season. In the Southern California Bight, October and March mark the traditional beginning and end of the squid fishing season, respectively (Butler et al., 1999). In the present study, fishing activity along the Santa Rosa and Santa Cruz Islands moved largely to the southern shores by March, leaving the northern shores relatively unfished. This spatial shift may reflect change in local squid habitat or changes in the fishermen's behavior. As a rough indicator of habitat quality, water temperature did not consistently differ between the northern and southern waters around Santa Cruz Island in March and April, both at sea surface and at 75 meters depth. Wind conditions, on the other hand, change considerably from October to March. The northern shores of Santa Rosa and Santa Cruz lie on the rim of the Santa Barbara Channel. Wind speed and wind stress are relatively low through the channel in the fall and early winter but increase significantly in March to remain high throughout the spring and summer (Winant and Dorman, 1997; Harms and Winant, 1998; Dorman and Winant, 2000). It remains unresolved whether the high winds in the Channel in March and April create ocean-floor turbulence and turbidity that discourage squid spawning (cf., Roberts and Sauer, 1994), or whether fishermen simply eschew the rocky Channel in favor of the southern shores of the islands.

Although satellite remote sensing can generate a "neutral party" record of fishing effort, we note three caveats associated with satellite data. First, large stationary sources of light, such as coastal cities, must be excluded when quantifying fishing vessel activity. The exclusion of urban light sources can result in underestimating effort, because boats that work near large light sources can be excluded from analysis. We were concerned that an underestimation of effort along the mainland coast would explain this study's post-El Niño increase in LPUE. Landings data, however, may indicate that effort in coastal blocks actually declined after the 1997–98 El Niño. Coastal blocks accounted for 19% of the landings in the pre-El Niño years (1992–96), dropping to 11% of landings in the post-El Niño years (1999 to early 2000).

Second, the spatial resolution of the satellite images may be large enough to allow multiple boats to fit into one "pixel" of detected light. Thus, effort may be underestimated. Analysis of the ground-truthing fly-overs, however, did not indicate a strong interaction between boat aggregation and nightly fleet size. Boats may have indeed aggregated over the course of our study, but our analysis indicates that such aggregation was independent of nightly fleet size. In this case, the absolute values of estimated effort and LPUE would be underestimated across all dates. The relative values of effort and LPUE, however, will be only slightly affected within a time series; therefore we place confidence in our examinations of the temporal patterns of the effort-based data. A third caveat is specific to the present study. The ground-truthing work occurred during a period of relatively low fishing effort (1999–2000). Future fly-overs during periods of greater effort will be useful in corroborating our observed relationship between fly-over and satellite data.

The present study demonstrates that light detection by satellite remote sensing is useful for examining temporal and spatial patterns of fishing effort and population abundance, as measured by LPUE. Light detection by satellite has certain drawbacks, but these are not insurmountable. Importantly, geo-referenced satellite images provide an independent source of fishing effort, which can be feasibly integrated with environmental data through GIS analysis. With regard to market squid off California, satellite data can help provide fine-scale data on fishing location for this fishery's ongoing management efforts[4,5] (see also Mangel et al., 2002). Although mandatory shielding of the boat lights went into effect in May 2000, these lights are still detectable by the satellites (authors' pers. obs.). Recently, effort logbooks have become mandatory for squid fishermen off California. This requirement points to a unique opportunity to collect and corroborate fishery-dependent and independent measures of fishing effort.

Acknowledgments

We owe much gratitude to personnel of California's Department of Fish and Game for their assistance in the ground-truthing work. In particular, we thank the pilots Jeff Veal and Tom Evans, and the following aerial observers: D. Bergen, T. Bishop, S. Carner, D. Hanan, C. Kong, J. Kraus, A. Lohse, S. MacWilliams, D. Ono, M. Songer, J. Wagner, and E. Wilson. We also thank Paul Crone for collaboration on this project, Chris Reiss for extracting CalCOFI water temperature data, Rich Cosgrove for assistance with mapping, Kevin Hill for information about the Pacific Fisheries Management Council, and George Watters and anonymous reviewers for constructive comments. This project was funded by the California Department of Fish and Game and U.S. Department of Commerce (NOAA NESDIS Ocean Remote Sensing Program).

[4] California Department of Fish and Game. 2003. Draft: Market squid fishery management plan. [Available from: Calif. Dept. Fish Game, 4949 Viewridge Avenue, San Diego, CA 92123.]

[5] Maxwell, M. R., L. D. Jacobson, and R. Conser. Manuscript in review. Eggs-per-recruit model for management of the California market squid (*Loligo opalescens*) fishery.

Literature cited

Butler, J., D. Fuller, and M. Yaremko.
1999. Age and growth of market squid (*Loligo opalescens*) off California during 1998. Calif. Coop. Oceanic Fish. Invest. Rep. 40:191–195.

CDFG (California Department of Fish and Game).
2000. Review of some California fisheries for 1999: market squid, Dungeness crab, sea urchin, prawn, abalone, groundfish, swordfish and shark, ocean salmon, nearshore finfish, Pacific sardine, Pacific herring, Pacific mackerel, reduction, white seabass, and recreational. Calif. Coop. Oceanic Fish. Invest. Rep. 41:8–25.

Croft, T. A.
1978. Nighttime images of the earth from space. Sci. Am. 239:68–79.

Dorman, C. E., and C. D. Winant.
2000. The structure and variability of the marine atmosphere around the Santa Barbara Channel. Month. Weather Rev. 128:261–282.

Elvidge, C. D., K. E. Baugh, E. A. Kihn, H. W. Kroehl, and E. R. Davis.
1997. Mapping city lights with nighttime data from the DMSP Operational Linescan System. Photogram. Engin. Remote Sens. 63: 727–734.

Elvidge, C. D., V. R. Hobson, K. E. Baugh, J. Dietz, Y. E. Shimabukuro, Y. E. Krug, E. M. L. M. Novo, and F. R. Echavarria.
2001b. DMSP-OLS estimation of rainforest area impacted by ground fires in Roraima, Brazil: 1995 versus 1998. Int. J. Remote Sens. 22:2661–2673.

Elvidge, C. D., M. L. Imhoff, K. E. Baugh, V. R. Hobson, I. Nelson, J. Safran, , J. B. Dietz, and B. T. Tuttle.
2001a. Night-time lights of the world: 1994–1995. ISPRS J. Photogram. Remote Sens. 56:81–99.

Harms, S., and C. D. Winant.
1998. Characteristic patterns of circulation in the Santa Barbara Channel. J. Geophys. Res. 103:3041–3065.

Hayward, T. L.
2000. El Niño 1997–98 in the coastal waters of southern California: a timeline of events. Calif. Coop. Oceanic Fish. Invest. Rep. 41:98–116.

Jackson, G. D.
1994. Statolith age estimates of the loliginid squid *Loligo opalescens* (Mollusca: Cephalopoda): corroboration with culture data. Bull. Mar. Sci. 54:554–557.

Jackson, G. D., and M. L. Domeier.
2003. The effects of an extraordinary El Niño / La Niña event on the size and growth of the squid *Loligo opalescens* off Southern California. Mar. Biol. 142:925–935.

Jackson, G. D., and N. A. Moltschaniwskyj.
2001. The influence of ration level on growth and statolith increment width of the tropical squid *Sepioteuthis lessoniana* (Cephalopoda: Loliginidae): an experimental approach. Mar. Biol. 138:819–825.

Lavaniegos, B. E., L. C.-Pérez, and G. Gaxiola-Castro.
2002. Plankton response to El Niño 1997–1998 and La Niña 1999 in the southern region of the California Current. Progress Oceanog. 54:33–58.

Lowry, M. S., and J. V. Carretta.
1999. Market squid *(Loligo opalescens)* in the diet of California sea lions *(Zalophus californianus)* in Southern California (1981–1995). Calif. Coop. Oceanic Fish. Invest. Rep. 40:196–207.

Lynn, R. J., T. Baumgartner, J. García, C. A. Collins, T. L. Hayward, K. D. Hyrenbach, A. W. Mantyla, T. Murphree, A. Shankle, F. B. Schwing, K. M. Sakuma, and M. J. Tegner.
1998. The state of the California Current, 1997–1998: transition to El Niño conditions. Calif. Coop. Oceanic Fish. Invest. Rep. 39:25–49.

Lynn, R. J., and S. J. Bograd.
2002. Dynamic evolution of the 1997–1999 El Niño-La Niña cycle in the southern California Current System. Progress Oceanog. 54:59–75.

Mangel, M., B. Marinovic, C. Pomeroy, and D. Croll.
2002. Requiem for Ricker: unpacking MSY. Bull. Mar. Sci. 70:763–781.

Roberts, M. J., and W. H. H. Sauer.
1994. Environment: the key to understanding the South African chokka squid *(Loligo vulgaris reynaudii)* life cycle and fishery? Antarctic Sci. 6:249–258.

Rodhouse, P. G., C. D. Elvidge, and P. N. Trathan.
2001. Remote sensing of the global light-fishing fleet: an analysis of interactions with oceanography, other fisheries and predators. Adv. Mar. Biol. 39:261–303.

Roper, C. F. E., M. J. Sweeney, and C. E. Nauen.
1984. Cephalopods of the world. An annotated and illustrated catalogue of species of interest to fisheries. FAO species catalogue, vol. 3, 277 p. FAO Fish Synop. 125.

Salmon, M., B. E. Witherington, and C. D. Elvidge.
2000. Artificial lighting and the recovery of sea turtles. *In* Sea turtles of the Indo-Pacific: research management and conservation (N. Pilcher and G. Ismail, eds.). p. 25–34. ASEAN Academic Press, London.

Schön, P-J., W. H. H. Sauer, and M. J. Roberts.
2002. Environmental influences on spawning aggregations and jig catches of chokka squid *Loligo vulgaris reynaudii:* a "black box" approach. Bull. Mar. Sci. 71:783–800.

Schwing, F. B., C. S. Moore, S. Ralston, and K. M. Sakuma.
2000. Record coastal upwelling in the California Current in 1999. Calif. Coop. Oceanic Fish. Invest. Rep. 41:148–160.

Schwing, F. B., T. Murphree, L. deWitt, and P. M. Green.
2002. The evolution of oceanic and atmospheric anomalies in the northeast Pacific during the El Niño and La Niña events of 1995–2001. Progress Oceanog. 54:459–491.

Vojkovich, M.
1998. The California fishery for market squid *(Loligo opalescens).* Calif. Coop. Oceanic Fish. Invest. Rep. 39:55–60.

Waluda, C. M., P. N. Trathan, C. D. Elvidge, V. R. Hobson, and P. G. Rodhouse.
2002. Throwing light on straddling stocks of *Illex argentinus*: assessing fishing intensity with satellite imagery. Can. J. Fish. Aquat. Sci. 59:592–596.

Winant, C. D., and C. E. Dorman.
1997. Seasonal patterns of surface wind stress and heat flux over the Southern California Bight. J. Geophys. Res. 102:5641–5653.

Wolter, K., and M. S. Timlin.
1998. Measuring the strength of ENSO events: how does 1997/98 rank? Weather 53:315–324.

Zar, J. H.
1984. Biostatistical analysis, 2nd edition, 718 p. Prentice-Hall, Englewood Cliffs, NJ.

Magnitude and distribution of sea turtle bycatch in the sea scallop (*Placopecten magellanicus*) dredge fishery in two areas of the northwestern Atlantic Ocean, 2001–2002

Kimberly T. Murray

Northeast Fisheries Science Center
National Marine Fisheries Service
166 Water Street
Woods Hole, Massachusetts 02543
E-mail address: Kimberly.Murray@noaa.gov

Abstract—In May 2001, the National Marine Fisheries Service (NMFS) opened two areas in the northwestern Atlantic Ocean that had been previously closed to the U.S. sea scallop (*Placopecten magellanicus*) dredge fishery. Upon reopening these areas, termed the "Hudson Canyon Controlled Access Area" and the "Virginia Beach Controlled Access Area," NMFS observers found that marine turtles were being caught incidentally in scallop dredges. This study uses the generalized linear model and the generalized additive model fitting techniques to identify environmental factors and gear characteristics that influence bycatch rates, and to predict total bycatch in these two areas during May–December 2001 and 2002 by incorporating environmental factors into the models. Significant factors affecting sea turtle bycatch were season, time-of-day, sea surface temperature, and depth zone. In estimating total bycatch, rates were stratified according to a combination of all these factors except time-of-day which was not available in fishing logbooks. Highest bycatch rates occurred during the summer season, in temperatures greater than 19°C, and in water depths from 49 to 57 m. Total estimated bycatch of sea turtles during May–December in 2001 and 2002 in both areas combined was 169 animals (CV=55.3), of which 164 (97%) animals were caught in the Hudson Canyon area. From these findings, it may be possible to predict hot spots for sea turtle bycatch in future years in the controlled access areas.

Manuscript submitted 1 December 2003 to the Scientific Editor's Office.

Manuscript approved for publication 27 May 2004 by the Scientific Editor.

Fish. Bull. 102:671–681 (2004).

Five species of sea turtles in the northwestern Atlantic Ocean are protected under the U.S. Endangered Species Act of 1973. The loggerhead turtle (*Caretta caretta*) is listed as a threatened species, and the leatherback (*Dermochelys coriacea*), hawksbill (*Eretmochelys imbricata*), Kemp's ridley (*Lepidochelys kempii*), and certain populations of the green sea turtle (*Chelonia mydas*) are listed as endangered. Populations of each of these species have declined principally as a result of human activities (NRC, 1990).

The incidental capture, or bycatch, of sea turtles in commercial fisheries is a major source of mortality (NRC, 1990; Turtle Expert Working Group, 2000). These turtles are captured incidentally in pelagic longlines (Lewison et al., 2004), trawls (Epperly, 2003), gill nets (Julian and Beeson, 1998), pound nets, weirs, pots, and traps (NMFS and USFWS, 1991; Allen, 2000). Such threats occur at various life stages of a population and at different intensities, and consequently have implications for management policy (Heppell et al., 2003).

The U.S. National Marine Fisheries Service (NMFS) has implemented management measures in both the Atlantic and the Pacific in the form of gear modifications or time and area closures to reduce sea turtle bycatch. For example, since the early 1990s, turtle excluder devices (TEDs) have been required in all inshore and offshore shrimp trawl nets in southeastern U.S. waters (Epperly, 2003) to reduce sea turtle mortality (Henwood and Stuntz, 1987). Bycatches of sea turtles in the U.S. pelagic longline fisheries for swordfish and tuna (Witzell, 1999) led to a year-round closure of a 2.6 million nmi^2 area in the northwestern Atlantic Ocean to these fisheries beginning in 2002.

In recent years, documented interactions have occurred between sea turtles and sea scallop dredges, a previously unidentified threat in recovery planning efforts (NMFS, 1991). During 2001 and 2002, fisheries observers aboard commercial sea scallop vessels documented the bycatch of sea turtles in two small regions of the Mid-Atlantic Bight (MAB). These areas, termed the "Hudson Canyon Controlled Access Area" (approximately 3150 km^2) and the "Virginia Beach Controlled Access Area" (approximately 900 km^2) were closed to scallop fishing in April 1998 but reopened in May 2001 on a conditional basis (Fig. 1). This study uses the generalized linear and generalized additive models to identify environmental factors and gear characteristics affecting the bycatch rate of sea turtles in these two areas and to predict total bycatch by sea scallop dredge vessels in these two areas in 2001 and 2002.

Methods

The fishery

In 2001 and 2002, 137 and 93 commercial vessels, respectively, participated in the Controlled Area Access Program sea scallop fishery. Although

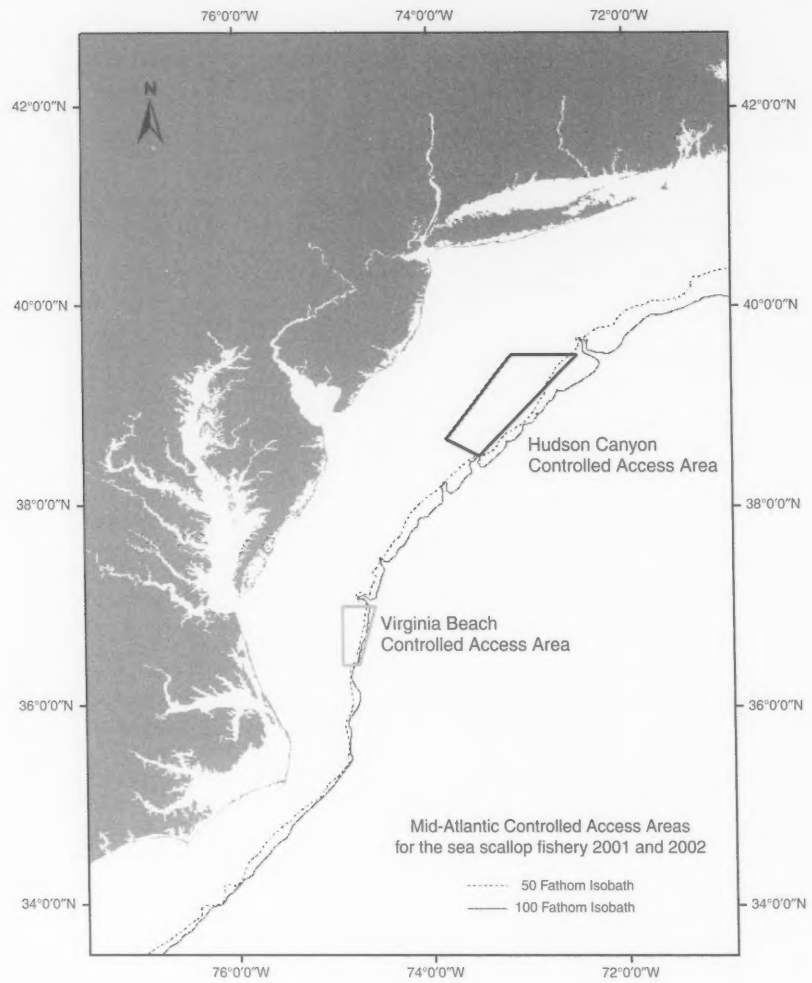

Figure 1

Mid-Atlantic controlled access areas for the sea scallop fishery 2001 and 2002.

the U.S. commercial scallop fishery operates year-round, the area access program in 2001 began on 1 May, and in 2002 on 1 March, and ended on 28 February following the respective fishing year (1 March–28 February). Vessels in the controlled access areas fished around the clock for approximately 5–12 days, accomplishing between 40 and 160 hauls per trip. Dredges in the controlled areas were generally fished at depths between 45 and 75 m. The average haul duration was about 1 hour. Most vessels fished two dredges simultaneously (one from each side of the vessel), which were generally either 3.9 or 4.5 m (13 or 15 ft) wide.

Vessels in the Mid-Atlantic typically fish with a New Bedford style scallop dredge equipped for soft-bottom substrates. In this configuration, tickler chains strung from the sweep chain run horizontally between the dredge frame and the ring bag and are designed to raise scallops off the bottom and into the bag. Turtles become entrapped in the ring bag or on the dredge frame. For dredging on hard bottom, such as in New England, vertical up and down chains hang over the tickler chains, preventing boulders from entering the ring bag (Smolowitz, 1998). New Bedford style scallop dredges have also been used in U.S. fisheries in the Pacific (PSMFC[1]).

[1] Pacific States Marine Fisheries Commission (PSMFC). 2003. Description of fishing gears used on the Pacific Coast. http://pcouncil.org/habitat/geardesc.pdf. [Accessed 6 April 2004.]

Data sources

Observer data Observers were placed on randomly selected vessels fishing in the controlled areas to record the bycatch of turtles and other protected species. From May to December in 2001 and 2002, observers sampled 11% of the commercial fishing effort in the Hudson Canyon region, and in October 2001, 16% of the effort in Virginia Beach. No trips were observed in the Virginia Beach region during 2002 because of low commercial fishing effort in the area. Observers were on- and off-watch on an irregular schedule throughout a 24-hour period, observing on average 65% of the hauls on a trip. When a dredge was hauled on board, observers recorded the haul location, time, depth, tow speed, tow duration, number of dredges observed, and the presence or absence of turtle bycatch. In 2001, observers identified 20% of the turtles that came aboard as loggerhead sea turtles but were unable to identify the remaining 80%. As a result of improved observer training (NMFS 2003), observers identified 88% of the turtles as loggerhead sea turtles in 2002, but they were unable to identify the remaining 12%. Given that observers document the loggerhead species most commonly in the Mid-Atlantic area, and that all sea turtles positively identified were loggerhead sea turtles, bycatch estimates in this analysis are considered to be those of loggerhead sea turtles. Although some turtles may have been released alive or injured, this analysis does not differentiate between live, dead, and injured animals.

Fishing effort data Under the 1982 Atlantic Sea Scallop Fishery Management Plan, all vessels targeting scallops must complete a vessel trip report (VTR) log (as of 1994) indicating area fished, kept and discarded catch, and fishing effort. These data were used to estimate the total fishing effort of the fleet. In calculating fishing effort, one unit of effort equals a single dredge haul because vessels may fish one or two dredges simultaneously on each haul. Because a preliminary analysis showed that tow duration or dredge length does not significantly affect the probability of turtle capture, dredge haul effort was not standardized for these two variables. All VTR trips from May to December in the controlled areas were used in the analysis. Because completion of vessel trip reports is mandatory and trips to the controlled areas were closely monitored, it was assumed that the VTR data represented 100% of total fishing effort.

Sea surface temperature Sea surface temperature at each position reported in the observer and VTR databases was extracted from NOAA AVHRR (advanced very high resolution radiometer) coastwatch satellite images. A Visual Basic (Microsoft Corp., Redmond, WA) routine was used to extract temperatures from 7-day composite images (3 days forward and backward from the haul date), by using a 3×3 cell window at 1-km resolution. Therefore, a 9-km^2 area of coverage around each coordinate position was used to extract sea surface temperature. Within the 3×3 cell search radius, the pixel representing the warmest temperature was used to avoid temperatures affected by cloud coverage.

Data analysis

Missing temperature data Sea surface temperature values could not be obtained for 33% of the VTR data and 10% of the observer data because of either missing coordinate positions on the VTR logs or bad satellite images. For these fishing events, sea surface temperature was predicted by using a linear regression based on year, month, and area. For the observer data, area was defined as either Hudson Canyon or Virginia Beach access areas (r^2=0.88). For the VTR data, the vessel's home state served as a proxy for area fished because most of the missing temperature values were due to missing coordinate positions (r^2=0.86).

Modeling approach Generalized linear model (GLM) and generalized additive model (GAM) fitting techniques were used to understand and predict bycatch rates of sea turtles in relation to environmental variables, fishing practices, and gear characteristics in the commercial sea scallop fishery. Unlike classic linear regression models, GLMs and GAMs allow for nonlinearity and nonconstant variance structures in the data (Guisan et al., 2002). GAMs differ from GLMs in that smooth functions replace the linear predictors in GLMs (Hastie and Tibshirani, 1990). Smooth functions, or "smoothers," summarize the trend of a response measurement as a function of multiple predictors (Hastie and Tibshirani, 1990) and therefore some form of parametric relationship between the response and explanatory variables is not assumed (Guisan et al. 2002). Both frameworks have been used to model abundance or probability events as a function of environmental variables (Frost et al., 1999; Denis et al., 2002; Guisan et al., 2002; Hamazaki, 2002).

A modeling approach to estimate bycatch of sea turtles in the sea scallop dredge fishery was preferred over the ratio method (Cochran, 1977) that has been used to estimate bycatch of marine mammals and turtles in other fisheries (Epperly et al., 1995; Rossman and Merrick, 1999). With the ratio method, the observed number of sea turtles divided by the observed effort is used to calculate a bycatch rate, and this rate is then multiplied by total commercial fishing effort to derive a bycatch estimate. Bycatch data in the sea scallop dredge fishery violate the underlying assumptions of the ratio method (Cochran, 1977), largely because sea turtle bycatch is binomially distributed with a nonconstant variance. An analyis of binary response data derived from a statistical model allows bycatch rates to be predicted by using factors that account for variability in bycatch. Moreover, stratifying bycatch rates according to these factors will reduce variability in total bycatch estimates. For the sea turtle data analyzed in the present study, the GLM approach provided a more accurate and less biased mortality estimate than that derived using the ratio method.

GAM smoothers Before a GLM was constructed, a GAM helped group continuous variables into categories. Fitting the GLM model with categorized variables was necessary to extrapolate bycatch rates in order to derive a total estimate of the bycatch of sea turtles in scallop dredges in the controlled access areas. All of the variables tested in the GLM model were first fitted to a GAM, in which the parameters of the continuous prediction variables were estimated by a smoothing spline. Variable values were grouped according to whether they had a positive or negative influence on the bycatch rate (i.e., the group explained more or less of the bycatch rate).

Development of a GLM bycatch model Because bycatch events were counts ranging from zero or one, a logistic regression was used to model the probability of sea turtle bycatch (GLM function, SPLUS 6.1, Seattle, WA). Each dredge haul is a data point and the response was whether turtle bycatch was zero or one. Probability of sea turtle bycatch (p) was calculated as

$$p = e^y / 1 + e^y$$
$$y = \beta_0 + \beta_1 x_1 + \beta_2 x_2 + \ldots + \beta_i x_i,$$

where β_i is a parameter coefficient;
x_i is a predictor variable; and
y is a sea turtle bycatch event.

Dredge hauls are assumed to be independent because turtles were never simultaneously caught in both dredges operating from a vessel during a single haul.

A forward stepwise selection method was used to determine the best fitting model. Model parameters were estimated by maximizing the log-likelihood function. The null model was the first model in the stepwise process and was specified with a single intercept term as

$$H_0: \log(turtle\ bycatch) = 1.$$

At each step, a new variable was added to the null model (Appendix 1) and tested against the former model formulation (ANOVA function, chi-square test) to determine the better fitting model. A preliminary assessment of a broad suite of gear characteristics and environmental factors indicated that 10 variables could significantly affect bycatch rates. The main effects of each variable were tested in the stepwise selection process as well as the interaction between season and temperature. Because the order of the predictor variables affects their significance, main effects were entered in various orders. If a P-value was less than 0.05, then the additional variable was considered to explain more of the variability in bycatch than a model without that variable. Each new model was also compared against the former model by using the Akaike information criterion (AIC), which is defined as

$$AIC = -2\log(L(\theta \mid y)) + 2K,$$

where $\log(L(\theta \mid y))$ = the numerical value of the log-likelihood at its maximum point; and
K = the number of estimable parameters (Burnham and Anderson, 2002).

The AIC is a measure of the level of parsimony, defined as a model that fits the data well and includes as few parameters as necessary (Palka and Rossman, 2001). If the AIC value decreases, the new combination of variables in the model fit the data better.

To investigate whether the bycatch data are over-dispersed, that is, where the sampling variance exceeds the theoretical variance, the GLM model was refitted by using a quasi-likelihood function. When data are over-dispersed, the estimated over-dispersion parameter is generally between 1 and 4 (Burnham and Anderson, 2002). The over-dispersion parameter fitted to the global model was 0.61, indicating these data were not over-dispersed and error assumptions of the binomial model were appropriate for analyzing these data.

Alias patterns in the final model were examined to assess correlation among the explanatory variables. The fit of the final model was assessed by plotting the observed turtle bycatch against the predicted turtle bycatch. The r^2 value indicated how well predictions from the linear model fit the actual data.

Bycatch rate estimates The spatial and temporal stratification of bycatch rates in each of the controlled access areas was determined by the explanatory variables in the best-fitting GLM. Parameter estimates from the model were used to predict the bycatch rate for each stratum.

The coefficient of variation (CV) for each bycatch rate was estimated by bootstrap resampling (Efron and Tibshirani, 1993). The resampling unit was a scallop dredge haul. Replicate bycatch rates were generated with the best-fitting GLM model, by sampling with replacement 1000 times from the original data set. The CV was defined as the standard deviation of the bootstrap replicate bycatch rates in a stratum divided by the bycatch rate for that stratum estimated from the original data. Variances and CVs of combined estimates were based on means weighted by their respective variances (Wade and Angliss, 1997).

Total bycatch The total estimated turtle bycatch in each stratum was calculated as the product of predicted bycatch per dredge haul (i.e., the predicted bycatch rate) for that stratum and the total number of dredge hauls accomplished by the commercial fishery in that stratum:

$$\frac{\sum Predicted\ bycatch}{\sum Dredge\ hauls_i} \times (Total\ dredge\ hauls)_i,$$

where i = stratum

Table 1

Analysis of deviance for significant factors affecting sea turtle bycatch. Significant factors were used to stratify bycatch rates and to contruct a model to predict total bycatch. AIC = Akaike information criterion.

Model	df	Deviance	Residual df	Residual deviance	*P* (chi)	AIC
null model only		18,071	405.29	407.2989		
null + year	1	–2.33	18,070	402.96	0.12626	406.9611
null + season	2	19.81	18,069	385.48	0.00004	391.4807
null + season + temp	1	9.34	18,068	376.13	0.00223	384.1319
null + season + temp + depth	2	17.23	18,066	358.89	0.00018	370.8983
null + season + temp + depth + time of day	1	7.86	18,065	351.03	0.00503	365.0318
null + depth + time of day + season (temp)	1	1.64	18,064	349.39	0.20011	365.3903
null + season + temp + depth + time of day + state	4	3.77	18,061	347.25	0.43746	369.2579
null + season + temp + depth + time of day + dredge frame width	2	3.27	18,063	347.76	0.19487	365.7611
null + season + temp + depth + time of day + number of up and down chains	1	0.54	18,064	350.48	0.45955	366.4849
null + season + temp + depth + time of day + number of tickler chains	1	3.18	18,064	347.84	0.07436	363.8480

Annual bycatch was the sum of the stratified bycatch estimates. The finite population correction factor (Cochran, 1977) was applied to bycatch estimates in stratas where the observer coverage was greater than 10%.

Number of dredge hauls in the VTR database without coordinate positions (32%) were prorated between the stratified areas according to the percentage of dredge hauls with known coordinates from the same year, state, and stratified areas.

Results

Observed bycatch

Nine and 16 turtle bycatch were observed in 2001 and 2002, respectively, in the Hudson Canyon controlled access area. Of the 25 turtles taken in the Hudson Canyon area across both years, 21 (84%) were taken during summer months. Two turtle bycatch were observed in the Virginia Beach access area during fall 2001—the only time when there was observer coverage in this area across both years.

GAM smoothers

Plots of the smoothed functions in the GAM revealed whether the continuous variable in the model explained any error in the bycatch rate estimates. For example, a plot of the smooth function for depth as a covariate revealed that bycatch rates may be higher between 49 m (27 fm) and 57 m (31 fm) and lower around this zone (Fig. 2). Likewise, a plot of the smooth function for temperature as a covariate revealed that bycatch rates may be higher above 19°C. These plots helped bin the continuous variables into categories (Appendix 1) which could then be tested in the GLM. All continuous variables in the GAM were categorized in a similar manner.

GLM bycatch model

Significant factors affecting sea turtle bycatch were season, sea surface temperature, depth zone, and time-of-day (Table 1). These variables were significant despite the order in which they were tested in the model. The model with the lowest AIC value was considered the "best" model, although time-of-day could not be included in the final model to predict bycatch rates. This level of information is not recorded in commercial fisheries logbooks; therefore bycatch rates based on time-of-day could not be extrapolated to total bycatch. Width of the scallop dredge frame, number of tickler chains, and number of up and down chains were not significant variables.

Model fit

The number of predicted sea turtle bycatch closely matched the observed bycatch in both years in all bycatch strata (Table 2). Strata were defined according to variables identified in the GLM as having a significant effect on bycatch rates. The relationship between actual and observed takes was strong (r^2=0.93), indicating that the predictions from the model fitted the data well.

Bycatch rate estimates

Bycatch rates were stratified by season, temperature interval, and depth zone (Table 3). Because year was not a

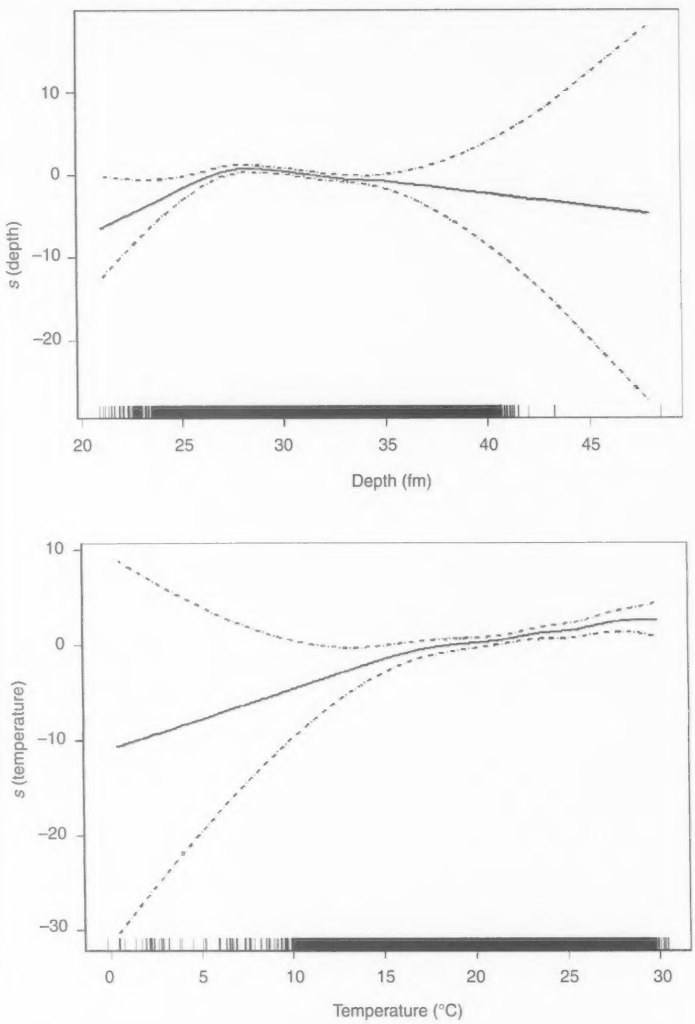

Figure 2

Partial fits for the general additive model (GAM) of sea turtle bycatch with depth and temperature as covariates, showing the relationship estimated by a smoothing spline. Depths between 27 fm (49 m) and 31 fm (57 m), and temperatures above 19°C, have a positive influence on the bycatch rate. 95% confidence bands are also shown. All continuous variables in the GAM were categorized in a similar manner. The "s" on the y-axis represents a smoothed function for each variable and explains the effect of each variable on sea turtle bycatch per haul.

significant factor in the final model, predicted bycatch rates were the same for 2001 and 2002. Highest sea turtle bycatch rates occurred during the summer season (Aug–Sep), in temperatures warmer than 19°C, in water depths from 49 to 57 m. Lowest bycatch rates occurred during the fall (Oct–Dec) and spring (May–June), in temperatures cooler than 19°C, and in water depths less than 49 m.

Total bycatch

The total estimated bycatch of sea turtles in the Mid-Atlantic controlled access areas in 2001 and 2002 combined was 169 animals (CV=55.3) (Table 4). Of this total, 164 animals (97%) were caught in the Hudson Canyon area: 69 (42%) in 2001 and 95 (58%) in 2002. Total esti-

Table 2

Observed versus predicted number of turtle bycatch, by stratum, 2001 and 2002. Obs.=observed; Pred.=predicted.

		Spring		Summer		Fall	
Water depth	Temp.	Number of obs. turtle bycatch	Number of pred. turtle bycatch	Number of obs. turtle bycatch	Number of pred. turtle bycatch	Number of obs. turtle bycatch	Number of pred. turtle bycatch
Shallow	High	0	0	0	0	0	0
	Low	0	0	0	0	0	0
Mid-depth	High	2	1	17	16	1	2
	Low	0	0	0	0	1	0
Deep	High	1	1	4	5	1	0
	Low	0	0	0	0	0	0

Table 3

Stratification of turtle bycatch rates with associated CVs. N.C.E.=no commercial effort.

Water depth	Temperature	Spring (May–June)	Summer (Aug–Sep)	Fall (Oct–Dec)
Shallow (<49 m)	High (>19°C)	0.0000027 (82.5)	0.0000052 (62.1)	0.0000030 (87.7)
	Low (<19°C)	0.0000002 (99.5)	N.C.E.	0.0000002 (106.6)
Mid-depth (49–57 m)	High (>19°C)	0.0032018 (64.9)	0.0061179 (25.4)	0.0035838 (57.2)
	Low (<19°C)	0.0002117 (95.4)	N.C.E.	0.0002371 (98.3)
Deep (>57 m)	High (>19°C)	0.0007578 (73.8)	0.0014512 (41.9)	0.0008485 (80.5)
	Low (<19°C)	0.0000500 (92.9)	N.C.E.	0.0000560 (103.8)

Table 4

Total bycatch estimates by year and season with weighted CVs (%) N.C.E.=no commercial effort.

		Spring	Summer	Fall	Total
Hudson Canyon	2001	10 (89.2)	50 (61.5)	9 (105.8)	69
	2002	13 (89.2)	78 (61.5)	4 (105.8)	95
Virginia Beach	2001	N.C.E.	N.C.E.	5 (105.8)	5
	2002	0	0	N.C.E.	0
Totals		23	128	18	169 (55.3)

mated bycatch of turtles in the Virginia Beach area was five animals in 2001 and zero animals in 2002.

Across both areas, the highest bycatches occurred in summer (128 turtles; 76%), followed by spring (23 turtles; 14%) and fall (18 turtles; 10%) (Table 5). One hundred thirty-two (78%) (CV=49.6) sea turtles were caught in the mid-depth zone from 49 to 57 m, whereas 37 (22%) (CV=59.6) sea turtles were caught in waters deeper than 57 m. One-hundred fifty-eight (93%) (CV=51.2) sea turtles were caught in waters warmer than 19°C, and 11 (7%) (CV=74.9) in waters cooler than 19°C.

Discussion

Use of bycatch models

Generalized linear and generalized additive models help to identify environmental variables or fishing practices that influence the probability of sea turtle bycatch. In estimating total mortality, bycatch rates can then be stratified according to these factors, reducing unexplained variability in the total estimate. Moreover, understanding factors that lead to a high or low

Table 5

Total bycatch estimates by season, depth, and temperature strata in Hudson Canyon and Virginia Beach controlled access areas in 2001 and 2002 with 95% confidence intervals. Spring=May–Jun; Summer=Jul–Sep; Fall=Oct–Dec. N.E.C.= no commercial effort; N.O.=no observer coverage.

		2001			2002			
Water depth	Temperature	Spring	Summer	Fall	Spring	Summer	Fall	Total
Shallow (<49 m)	High (>19°C)	0	0	0	0	0	0	0
	Low (<19°C)	0	N.O.	0	0	N.C.E.	0	0
Mid–Depth (49–57 m)	High (>19°C)	6 (0–13)	37 (21–59)	2 (0–5)	8 (0–21)	65 (34–96)	5 (0–9)	123
	Low (<19°C)	2 (0–8)	N.C.E.	4 (0–19)	1 (0–2)	N.C.E.	2 (0–10)	9
Deep (>57 m)	High (>19°C)	2 (0–5)	13 (4–25)	2 (0–5)	4 (0–11)	13 (4–24)	1 (0–1)	35
	Low (<19°C)	0 (0–1)	N.C.E.	1 (0–6)	0 (0–1)	N.C.E.	1 (0–2)	2
Total		10	50	9	13	78	9	169

probability of bycatch can motivate bycatch mitigation research. Finally, the ability to predict bycatch on the basis of explanatory variables allows one to examine the relative effectiveness of different management measures designed to reduce bycatch (Kobayashi and Polovina[2]). Ultimately this framework can improve the assessment of threats to turtles and broaden conservation options.

Magnitude of bycatch

During May–December in 2001 and 2002, an estimated 169 animals were captured incidentally by commercial sea scallop dredge vessels in two areas of the Mid-Atlantic Bight. Throughout the entire Mid-Atlantic Bight, the magnitude of bycatch was probably larger, particularly because the factors associated with the high bycatch rates were not specific to the controlled access areas. Of the 11 observed turtles measured for size, 9 (82%) were between 70–80 cm straight carapace length (the large juvenile stage). Stage class models indicate that the long-term survivability of loggerhead sea turtles is sensitive to mortality at this life stage (Crouse et al., 1987).

Factors influencing bycatch

The incidental capture of turtles occurs where there is overlap between fishing effort and turtle habitat. The elevated probability of turtle bycatch occurring in warm waters, during summer, at depths between 50 and 60 m is consistent with the habitat regime of loggerhead sea turtles in the Mid-Atlantic (Shoop and Kenney, 1992; Epperly et al., 1995; Coles and Musick, 2000). During the oceanic phase of their life cycle, sea turtles occupy habitats at specific temperatures or with bathymetric features that concentrate prey and other areas of enhanced productivity (Polovina et al., 2000). In Mid-Atlantic waters, high aggregations of loggerhead sea turtes have been observed in the summer, in waters 22–49 m deep, at temperatures from 20° to 24°C (Shoop and Kenney, 1992). In the Hudson Canyon and Virginia Beach controlled access creas, the bycatch of sea turtles was associated with habitat conditions rather than gear characteristics. From these findings, it may be possible to predict future hotspots for sea turtle bycatch in the controlled access areas where fishing effort and sea turtles overlap in time and space. These hotspots may be centered over the portion of the Hudson Canyon where depths are between 50 and 60 m, after waters warm to 19°C.

Because of the low amount of observer data in the Virginia Beach area, predicted bycatch rates for this area were based largely on conditions within the Hudson Canyon area. Sea scallop fishing effort occurs year-round both north and south of the Hudson Canyon, and high concentrations of loggerhead sea turtles (determined from migratory patterns) exist in spring and fall from North Carolina to northern Maryland (Shoop and Kenney, 1992). It is probable that the distribution of turtles and scallop fishing effort co-occur in other regions of the Mid-Atlantic, particularly south of the Hudson Canyon. The scallop dredge fishery in the Mid-Atlantic is a complex, dynamic system; there may be other factors influencing the bycatch of sea turtles in the fishery south of the Hudson Canyon that were not observed. However, without additional data on turtle interactions in these areas, it is unwise to extrapolate bycatch estimates beyond the scope of the data in this analysis.

Conservation management options

Time and area closures Models of turtle migrations can be used to predict interactions with fisheries in time and space to maximize the efficiency of time and area

[2] Kobayashi, D. R., and J. J. Polovina. 2000. Time/area closure analysis for turtle take reductions. Appendix C, Environmental Impact Statement, FMP for Pelagic Fisheries of the Western Pacific, 44 p. NMFS Honolulu, Hawaii, 96822.

closures (Morreale, 1996). The results of this analysis indicate that bycatch rates are affected by season, depth, and sea surface temperature. Within certain months and depth zones, therefore, the time when sea surface temperature reaches a threshold level may be the time to trigger an area closure. For example, this type of management approach has been taken in the southeastern United States to regulate turtle bycatch in the large-mesh gill-net fishery.[3] The timing of seasonally adjusted area closures is based upon analyzing sea surface temperatures in relation to the presence or absence of sea turtles throughout the area (Epperly et al., 1995; Epperly and Braun-McNeill[4]). In addition, temperature thresholds currently trigger area closures in the southern California driftnet fishery during El Niño conditions to prevent the incidental capture of loggerhead sea turtles.[5]

Results from the present study can be used to help evaluate potential bycatch reduction under different management scenarios, given certain assumptions. For example, had the portion of the Hudson Canyon controlled access area between depths of 49 and 57 m been closed after surface waters reached 19°C in the summer (the stratum with highest bycatch), the closure would have reduced bycatch by 39%. For this estimate, it is assumed that surface temperatures remain above 19°C throughout the summer and drop below 19°C thereafter. Further, this bycatch reduction scenario also assumes that fishing effort shifts proportionately to the fall and spring season within the same depth zone and that bycatch rates remain the same as those that are calculated. Alternatively, fishing effort could shift within a season to shallow and deep depth zones if scallop catch-per-unit-of-effort were not affected. Under this assumption, bycatch would be reduced by 60% under the same time and area closure. However, unless there are concurrent reductions in fishing effort, bycatch reductions achieved by these measures could well be offset by increases in bycatch in other depth strata and seasons.

Gear or fishing modifications Management actions to modify gear or fishing practices can be evaluated in a similar manner. For instance, this analysis indicates that bycatch rates are influenced by the time-of-day when dredges are in the water. Time-of-day was not used to stratify bycatch rates or to extrapolate total bycatch estimates because of limitations in the fishing effort data (VTR records). If time-of-day had been incorporated into the bycatch model, the model would have predicted higher bycatch rates when dredges were set between 4 am and 4 pm (day tows). If the stratum with the highest bycatch rate (summer, high surface temperatures, and depths between 49 and 57 m), had been further stratified by time-of-day, the model would have predicted a bycatch rate of 0.008 sea turtles/dredge hauls during the day, and 0.002 turtles/dredge hauls during the night. If all the commercial vessels had been fishing during the day in this stratum (n=6352 dredges in 2001), the estimated bycatch would have been 51 turtles. If the vessels had been fishing during the night, the total estimated bycatch would have been 13 turtles. According to these rates and effort, restricting vessels to night-time tows between the hours of 4 pm and 4 am has the potential to reduce bycatch by 75% in this particular stratum.

Although specific gear characteristics did not show a strong relationship to sea turtle bycatch in this analysis, further work should be conducted to evaluate whether specific gear characteristics could be modified to decrease bycatch. For example, the near significance with the model incorporating number of tickler chains (P=0.07) warrants further testing of this gear characteristic. Tickler chains cover the mouth of the dredge in a grid-like configuration with the vertical up and down chains. The number of chains on the bag and distance between the chains may help to prevent sea turtles from entering the dredge bag. This dredge configuration is currently being tested for sea turtle bycatch reduction in the Hudson Canyon area (DuPaul and Smolowitz[6]). Further research should also examine the behavior of sea turtles in relation to dredge gear for a more complete understanding of how and when turtles are entrapped.

Sea turtles and scallop dredge interactions cannot be viewed in isolation from other gear types and conservation measures. Some fisheries that co-occur with sea turtles may have an equal, if not greater, impact on turtles than do scallop dredges (e.g., the shrimp trawl fishery in the Gulf of Mexico [Henwood and Stuntz, 1987]). Changes in sea turtle abundance, or shifts in fishing effort, may increase the likelihood of encounters in both net and dredge fisheries. If environmental conditions associated with high bycatch rates in the Hudson Canyon and Virginia Beach areas are consistent across years, it may be possible to anticipate and deter future interactions from occurring.

Acknowledgments

I would like to thank Debra Palka and Marjorie Rossman for help with analytical and statistical approaches to bycatch estimation. Andy Solow and Andy Beet at the Marine Policy Center, Woods Hole Oceanographic Institute, also provided guidance in the statistical analysis. David Mountain provided invaluable help in acquiring

[3] Final Rule, FR 67: 71895-71900, 3 December 2002.

[4] Epperly, S. P. and J. Braun-McNeill. 2002. Unpubl. data. The use of AVHRR Imagery and the management of sea turtle interactions in the Mid-Atlantic Bight. NMFS Southeast Fisheries Science Center, Miami, Florida, 33149.

[5] Final Rule, FR 68: 69962-69967, 16 December 2003.

[6] DuPaul, W. P., and R. Smolowitz. 2003. Unpubl. data. Industry trials of a modified sea scallop dredge to minimize the catch of sea turtles. Virginia Institute of Marine Science, Gloucester Point, Virginia, 23062, and Coonamessett Farm, East Falmouth, Massachusetts, 02536.

sea surface temperature for the Observer and VTR data. Frederic Serchuk, Richard Merrick, Debra Palka, Marjorie Rossman, and Paul Rago at the Northeast Fisheries Science Center all provided initial reviews of the manuscript. Jeffrey Seminoff and two anonymous reviewers provided valuable comments during peer review. Finally, I wish to thank the observers who collected data on interactions between turtles and the sea scallop dredge fishery.

Literature cited

Allen, L. K.
2000. Protected species and New England fisheries: an overview of the problem and conservation strategies. Northeastern Naturalist 7(4):411–418.

Burnham, K. P. and D. R. Anderson.
2002. Model selection and multimodel inference: a practical information-theoretic approach, 2nd ed., 488 p. Springer-Verlag, New York, NY.

Cochran, W.G.
1977. Sampling techniques, 3rd ed., 428 p. John Wiley & Sons, New York, NY.

Coles, W. C. and J. A. Musick.
2000. Satellite sea surface temperature analysis and correlation with sea turtle distribution off North Carolina. Copeia 2:551–554.

Crouse, D. T., L. B. Crowder, and H. Caswell.
1987. A stage-based population model for loggerhead sea turtles and implications for conservation. Ecology 68(5):1412–1423.

Denis, V., J. Lejeune, and J. P. Robin.
2002. Spatio-temporal analysis of commercial trawler data using General Additive models: patterns of Loliginid (*sic*) squid abundance in the north-east Atlantic. ICES J. Mar. Sci., 59:633–648.

Efron, B. and R. J. Tibshirani.
1993. An introduction to the boostrap, 436 p. Chapman & Hall, New York, NY.

Epperly, S. P.
2003. Fisheries-related mortality and turtle excluder devices (TEDs). *In* The biology of sea turtles, vol. II (P. L. Lutz, J. A. Musick, and J. Wyneken, eds.), p. 339–353. CRC Press, Boca Raton, FL.

Epperly, S. P., J. Braun, A. J. Chester, F.A. Cross, J. V. Merriner, and P. A. Tester.
1995. Winter distribution of sea turtles in the vicinity of Cape Hatteras and their interactions with the summer flounder trawl fishery. Bull. Mar. Sci. 56(2): 547–568.

Frost, K. J., L. F. Lowry, and J. M. Ver Hoef.
1999. Monitoring the trend of harbor seals in Prince William Sound, Alaska, after the *Exxon Valdez* oil spill. Mar. Mamm. Sci. 15(2):494–506.

Guisan, A., T. C. Edwards, and T. Hastie.
2002. Generalized linear and generalized additive models in studies of species distributions: setting the scene. Ecol. Model. 157:89–100.

Hamazaki, T.
2002. Spatiotemporal prediction models of cetacean habitats in the mid-western North Atlantic ocean (from Cape Hatteras, North Carolina, USA to Nova Scotia, Canada). Mar. Mamm. Sci. 18(4):134–151.

Hastie, T. J., and R. J. Tibshirani.
1990. Generalized additive models, 329 p. Chapman and Hall, London.

Henwood, T. A., and W. E. Stuntz.
1987. Analysis of sea turtle captures and mortalities during commercial shrimp trawling. Fish. Bull. 85: 813–817.

Heppell, S. S., L. B. Crowder, D. T. Crouse, S. P. Epperly, and N. B. Frazer.
2003. Population models for Atlantic loggerheads. *In* Loggerhead sea turtles (A. Bolten and B. Witherington, eds.), pp. 255–273. Smithsonian Books, Washington, D.C..

Julian, F., and M. Beeson.
1998. Estimates of marine mammal, turtle, and seabird mortality for two California gillnet fisheries: 1990–1995. Fish. Bull. 96:271–284.

Lewison, R. L., S. A. Freeman, and L. B. Crowder.
2004. Quantifying the effects of fisheries on threatened species: the impact of pelagic longlines on loggerhead and leatherback sea turtles. Ecology Letters 7:221–231.

Morreale, S. J., E. A. Standora, J. R. Spotila, and F. V.Paladino.
1996. Migration corridor for sea turtles. Nature 384: 319–320.

NMFS (National Marine Fisheries Service).
2003. Fisheries observer program manual, 217 p. Northeast Fisheries Observer Program, Northeast Fisheries Science Center, Woods Hole, MA.

NMFS and USFWS (National Marine Fisheries Service and U.S. Fish and Wildlife Service).
1991. Recovery plan for U.S. population of loggerhead turtle, 64 p. National Marine Fisheries Service, Washington, D.C.

NCR (National Research Council).
1990. Decline of the sea turtles: causes and prevention, 259 p. National Academy Press, Washington, D.C.

Palka, D. L., and M. C. Rossman.
2001. Bycatch estimates of coastal bottlenose dolphin (*Tursiops truncatus*) in U.S. Mid-Atlantic gillnet fisheries for 1996–2000. Northeast Fisheries Science Center Reference Document 01-15, 77 p.

Polovina, J. J., D. R. Kobayashi, D. M. Parker, M. P. Seki, and G. H. Balazs.
2000. Turtles on the edge: movement of loggerhead turtles (*Caretta caretta*) along oceanic fronts, spanning longline fishing grounds in the central North Pacific, 1997–1998. Fish. Oceanogr. 9:71–82.

Rossman, M. C., and R. L. Merrick.
1999. Harbor porpoise bycatch in the Northeast multispecies sink gillnet fishery and the Mid-Atlantic coastal gillnet fishery in 1998 and during January–May 1999. Northeast Fish. Sci. Cent. Ref. Doc. 99-17, 36 p.

Shoop, R. C. and R. D. Kenney.
1992. Seasonal distributions and abundances of loggerhead and leatherback sea turtles in waters of the northeastern United States. Herpetol. Monogr. 6:43–67.

Smolowitz, R.
1998. Bottom tending gear used in New England. *In* Effects of fishing gear on the sea floor of New England (E. Dorsey and J. Pederson, eds.), p. 46–52. Conservation Law Foundation, Boston, MA.

Turtle Expert Working Group.
2000. Assessment update for the Kemp's ridley and loggerhead sea turtle populations in the western North Atlantic. U.S. Dep. Commer. NOAA Tech. Memo. NMFS-SEFSC-444, 115 p.

Wade, P. R., and R. P. Angliss.
1997. Guidelines for assessing marine mammal stocks: report of the GAMMS workshop April 3–5, 1996, Seattle, Washington. U.S. Dep. Commer., NOAA Tech. Memo. NMFS-OPR-12, 93 p.

Witzell, W. N.
1999. Distribution and relative abundance of sea turtles caught incidentally by the U.S. pelagic longline fleet in the western North Atlantic Ocean, 1992–1995. Fish. Bull. 97:200–211.

Appendix 1

Categorical variables examined in an analysis of factors affecting sea turtle bycatch in the sea scallop dredge fishery. Frequency of observed dredges in each category is also shown.

Variable	Category	Number of observed dredges in Hudson Canyon 2001	Number of observed dredges in Virginia Beach 2001	Number of observed dredges in Hudson Canyon 2002	Number of observed dredges in Virginia Beach 2002
Year	2001 or 2002	9493	520	8059	0
Season	Spring = May and June	3919	0	1987	0
	Summer = July, August, September	2719	0	3764	0
	Fall = October, November, December	2855	520	2308	0
State in which scallops were landed	Connecticut	199	0	595	0
	Massachusetts	4925	0	5628	0
	New Jersey	2849	0	740	0
	Rhode Island	112	0	474	0
	Virginia	1408	520	622	0
Frame width[1] category	Small = 3.0–3.9 m (10–13 ft)	560	0	443	0
	Medium = ≥3.9 m and <4.5 m (15 ft)	3987	122	3013	0
	Large = <4.5 m–4.8 m (15–16 ft)	4946	398	4603	0
Number of up and down chains used[2]	Code 1 = 0 chains	4256	520	2171	0
	Code 2 = 1–4 chains	4089	0	5378	0
	Code 3 = >4 chains	1148	0	510	0
Number of tickler chains used[3]	Code 1 = ≤2 chains	6890	520	4469	0
	Code 2 = >2 chains	2603	0	3590	0
Time-of-day	Day = 4 am–4 pm	5514	346	4854	0
	Night = 4 pm–4 am	3979	174	3205	0
Sea surface temperature	Hi = >19°C	3910	518	4883	0
	Low = ≤19°C	5583	2	3176	0
Depth	Shallow = 40–<49 m (22–27 fm)	1089	42	782	0
	Mid-Depth = 49–57 m (27–31 fm)	3371	280	3642	0
	Deep = >57–88 m (31–48 fm)	5033	198	3635	0

[1] Width of the dredge frame.

[2] Vertical chains attached to the sweep on the bottom of the dredge that prevent rocks from entering the chain bag. Number of up and down chains were influenced by bottom type.

[3] Horizontal chains attached to the sweep on the bottom of the dredge that help stir up contents of the sea bottom. Number of tickler chains were influenced by bottom type.

Validation and interpretation of annual skeletal marks in loggerhead (*Caretta caretta*) and Kemp's ridley (*Lepidochelys kempii*) sea turtles

Melissa L. Snover

Duke University Marine Laboratory
135 Duke Marine Lab Road
Beaufort, North Carolina 28516
Present addresss: Pacific Fisheries Environmental Laboratory
1352 Lighthouse Ave.
Pacific Grove, California 93950
E-mail address: melissa.snover@noaa.gov

Aleta A. Hohn

Center for Coastal Fisheries and Habitat Research
National Marine Fisheries Service, NOAA
101 Pivers Island Road
Beaufort, North Carolina 28516

Abstract—Numerous studies have applied skeletochronology to sea turtle species. Because many of the studies have lacked validation, the application of this technique to sea turtle age estimation has been called into question. To address this concern, we obtained humeri from 13 known-age Kemp's ridley (*Lepidochelys kempii*) and two loggerhead (*Caretta caretta*) sea turtles for the purposes of examining the growth marks and comparing growth mark counts to actual age. We found evidence for annual deposition of growth marks in both these species. Corroborative results were found in Kemp's ridley sea turtles from a comparison of death date and amount of bone growth following the completion of the last growth mark (n=76). Formation of the lines of arrested growth in Kemp's ridley sea turtles consistently occurred in the spring for animals that strand dead along the mid- and south U.S. Atlantic coast. For both Kemp's ridley and loggerhead sea turtles, we also found a proportional allometry between bone growth (humerus dimensions) and somatic growth (straight carapace length), indicating that size-at-age and growth rates can be estimated from dimensions of early growth marks. These results validate skeletochronology as a method for estimating age in Kemp's ridley and loggerhead sea turtles from the southeast United States.

Manuscript submitted 15 August 2003 to the Scientific Editor's Office.

Manuscript approved for publication 3 June 2004 by the Scientific Editor.

Fish. Bull. 102:682–692 (2004).

The basic tenet of skeletochronology is that bone growth is cyclic and has an annual periodicity in which bone formation ceases or slows before new, relatively rapid bone formation resumes (Simmons, 1992; Castanet et al., 1993; Klevezal, 1996). This interruption of bone formation is evidenced within the primary periosteal compacta by histological features, which take two forms in decalcified and stained thin-sections. The most common form is a thin line that appears darker than the surrounding tissue, termed the "line of arrested growth" (LAG) (Castanet et al., 1977). The second, less-common form is a broader and less distinct line that also stains darker, referred to as an annulus (Castanet et al., 1977). Alternating with LAGs or annuli are broad zones that stain homogeneously light, and represent areas of active bone formation. Together, a broad zone followed by either a LAG or an annulus represents a skeletal growth mark (GM) (Castanet et al., 1993). To apply skeletochronology to a species, the annual periodicity of the GM must be validated.

Validation studies are necessary not only to confirm the annual nature of the GM but also to identify and interpret anomalous LAGs. Anomalous LAGs that are a common problem in skeletochronology studies of reptiles and amphibians include double (Chinsamy et al., 1995; El Mouden et al., 1997; Guarino et al., 1998), splitting (Guarino et al., 1995; 1998; Coles et al., 2001), and supplemental (Guarino et al., 1995; Lima et al., 2000; Trenham et al., 2000) lines. In addition to anomalous LAGs, there are two other difficulties typical in skeletochronology studies; compression of LAGs at the periphery of the bone and resorption of the innermost LAGs. In older animals the GMs are compressed at the outer periphery of the bone as a result of decreased growth. Francillon-Vieillot et al. (1990) term this phenomenon "rapprochement" and it is a problem when the LAGs become too close together to be differentiated —usually in the small phalangeal bones used in amphibian studies (Eggert and Guyetant, 1999; Lima et al., 2000; Leclair et al., 2000).

In addition to anomalous and compressed LAGs, the loss of early GMs through endosteal resorption is another problem with skeletochronology. Although this does not present a problem with most amphibian species (Kusano et al., 1995; Castanet et al., 1996; Sagor et al., 1998), the problem is extreme in skeletochronology studies of loggerhead (*Caretta caretta*; Klinger and Musick, 1995; Zug et al., 1995; Parham and Zug, 1997), green

Table 1

Species and history of known-age sea turtles analyzed in this study.

Sample	Species	History during captivity	Age (yr)
LK-1	*Lepidochelys kempii*	Captive for first year, then released	5.0
LK-2	*L. kempii*	Captive for first year, then released	6.5
LK-3	*L. kempii*	Captive for first year, then released	4.5
LK-4	*L. kempii*	Tagged and released after hatching	1.27
LK-5	*L. kempii*	Tagged and released after hatching	1.70
LK-6	*L. kempii*	Tagged and released after hatching	1.72
LK-7	*L. kempii*	Tagged and released after hatching	2.37
LK-8	*L. kempii*	Tagged and released after hatching	2.37
LK-9	*L. kempii*	Tagged and released after hatching	3.25
LK-10	*L. kempii*	Tagged and released after hatching	2.0
LK-11	*L. kempii*	Tagged and released after hatching	2.75
LK-12	*L. kempii*	Tagged and released after hatching	3.0
LK-13	*L. kempii*	Tagged and released after hatching	4.25
CC-1	*Caretta caretta*	Captive during entire life	29.4
CC-2	*C. caretta*	Captive for first two years, then released	8.0

(*Chelonia mydas*; Zug and Glor, 1998; Zug et al., 2002) and Kemp's ridley (*Lepidochelys kempii*; Zug et al., 1997) sea turtles. In each of these studies, the authors used various protocols to estimate the number of layers lost. Any protocol estimating the number of layers lost to resorption relies on the concept that the spatial pattern of the LAGs is representative of the growth of the animal. To confirm this assumption, researchers must establish a correlation between bone dimensions and body size (Hutton, 1986; Klinger and Musick, 1992; Leclair and Laurin, 1996).

Two of the studies that have applied skeletochronology to sea turtles have demonstrated annual GMs in both juvenile (Klinger and Musick, 1992) and adult (Coles et al., 2001) loggerhead sea turtles. Numerous additional studies have applied skeletochronology to sea turtles. To date, the technique has been applied to loggerhead (Zug et al., 1986; Zug et al., 1995; Bjorndal et al., 2003), green (Bjorndal et al., 1998; Zug and Glor, 1998; Zug et al., 2002), Kemp's ridleys (Zug et al., 1997), and leatherback (*Dermochelys coriacea*) (Zug and Parham, 1996) sea turtles. What is needed for the appropriate application of skeletochronology to sea turtle species is additional validation of annual GMs and a guide to their interpretation. Furthermore, because resorption is a problem in sea turtle bones, the validation of a proportional allometry between bone and somatic growth is necessary to enable back-calculation.

In this study, we address each of these issues for Kemp's ridley and loggerhead sea turtles by examining humeri from known-age animals. We analyzed each humerus without prior knowledge of the animal's age and we present the results of our analyses, including reinterpretations of bones for which we were incorrect in our age assessments. The purpose of this study was to use known-age samples both to validate the likelihood that GMs are annual and as a learning tool for the best guide to interpreting GM in wild animals.

Materials and methods

We obtained samples from two known-age loggerhead and 13 known-age Kemp's ridley sea turtles (Table 1). In addition, we collected samples from 240 wild loggerhead and 262 wild Kemp's ridley sea turtles. With the exception of one loggerhead, CC-1, all of the sea turtles died in the wild and samples were retrieved from the carcasses. Sample CC-1 died in captivity.

Sample preparation

Zug et al. (1986) analyzed skeletal elements of the cranium and right forelimb of loggerhead sea turtles and determined that the humerus was most suited to skeletochronology studies. Therefore, we also used the humerus. Specimens arrived as either dried bones or whole flippers. For flippers, we dissected out the humerus, which was then flensed, boiled, and air-dried for at least two weeks. We cross-sectioned each humerus at a site just distal to the deltopectoral crest. At this site, the ratio of cortical to cancellous bone is highest (Zug et al., 1986), and the region immediately distal to the insertion scar of the deltopectoral muscle on the ventral side of the bone maximizes that ratio (see Zug et al., 1986 for diagrams of the loggerhead sea turtle humerus). This site also provided a landmark that allowed us to section at equivalent sites on every humerus.

We removed 2–3 mm thick sections at that site using a Buehler® isomet low speed saw. This section was

fixed in 10% formalin then decalcified by using a commercial decalcifying agent (RDO, Apex Engineering Products Corporation, Calvert City, Kentucky). Time to decalcification varied with the size of the bone and the strength of the solution, usually between 12 and 36 hours. Following decalcification, 25-μm thick cross-sections were made by using a freezing-stage microtome. Sections were stained in Erlich's hematoxylin diluted 1:1 with distilled water (Klevezal, 1996) and mounted on slides in 100% glycerin.

Known-age sea turtles

We received the humeri from each of two captive, known-age loggerhead sea turtles after they died (Table 1). The first specimen, CC-1, was held in an outdoor tank during the summer months and inside a greenhouse during the winter months (this turtle was the same captive female noted in Swartz, 1997). The second, CC-2, was raised in captivity for two years then released from Panama City, Florida, into the Gulf of Mexico.

For the Kemp's ridley sea turtles, we received humeri from 13 dead known-age animals (Table 1). The head-start Kemp's ridleys were raised in captivity for one year, then released as part of a binational program operated jointly by state and federal U.S. agencies and the Instituto Nacional de la Pesca (INP) of Mexico (Klima and McVey, 1995). The coded-wire–tagged (CWT) Kemp's ridley sea turtles were tagged and released as hatchlings. This tagging program is operated jointly by the U.S. National Marine Fisheries Service (NMFS) Galveston Laboratory and the INP of Mexico as a means of gaining a better understanding of the early life history of the Kemp's ridley sea turtle (Caillouet et al., 1997).

Using the methods described previously, we prepared stained thin-sections from the humeri. Without prior knowledge of the animal's history, the number of visible LAGs was quantified for each bone and a minimum age estimated. Our age estimates were then compared to the age information available for each animal.

Indirect validation of annual growth marks

Peabody (1961) and Castanet et al. (1993) suggested that the correlation between the width of the last zone formed and the date of death provided an indirect means of validating that deposition of the LAG occurs annually and at the same time of year for an individual population. We applied this method to 76 wild Kemp's ridley sea turtles for which humeri displayed between one and five LAGs. Each of these animals had stranded dead along the Atlantic coast between Maryland and North Carolina. Thin-sections were prepared of the humeri as described above. We quantified the width of the last zone formed by measuring the outside diameter of the whole section (D_O) and the diameter of the last competed LAG (D_L), between the lateral edges of the bone on an axis parallel to the dorsal edge. The amount of bone growth after the last LAG (D_O–D_L) was plotted against the Julian stranding date, with the assumption that stranding date approximated date of death. Least-squares linear regressions were fitted to the data.

Validation of the relationship between LAG diameter and body size

In order to relate GM diameters to somatic growth rates, there must be a constant proportionality between bone growth and somatic growth (Chaloupka and Musick, 1997). To address this proportionality, we took eight morphometric measurements of 240 wild loggerhead and 262 wild Kemp's ridley humeri, using digital calipers or a tape measure when dimensions were beyond the range of the calipers. Measurements of maximum length, longitudinal length, proximal width, distal width, deltopectoral crest width, lateral diameter at sectioning site, ventral to dorsal thickness at sectioning site, and mass were recorded. We compared these measurements with the carapace length, measured as standard straight-line length (SCL) from the nuchal notch to the posterior end of the posterior marginal, using a least-squares linear regression. For mass, the data were natural-log transformed to form a linear regression.

Results

Known-age Kemp's ridley sea turtles

Three Kemp's ridley sea turtles captive for one year and then released were recovered 4.5 to 6.5 years after hatching (Table 1). Sample LK-1 had minimal resorption and four complete GMs, each comprising one zone followed by a LAG. An additional zone was seen at the periphery and the LAG that would complete this last GM was not yet visible at the outer edge of the humerus cross-section. From GM counts and death date, we estimated the age of this animal accurately at five years (Fig. 1). Sample LK-2 retained five completed and one incomplete GM; however, we observed a large area of resorption in the interior region of the cross-section that potentially obscured additional GMs. We aged this animal at a minimum of 5.5 years, the actual age being 6.5 years. Sample LK-3 displayed four completed GMs and one incomplete mark. Without prior knowledge of this animal's age, we estimated the age accurately at 4.5 years based on layer count and time of death.

Ten of the Kemp's ridley sea turtle samples were tagged and released after hatching, and no time was spent in captivity (Table 1). Results from these ten recovered animals allowed us the opportunity to study and interpret the early GM patterns in noncaptive animals. The first year mark for Kemp's ridley sea turtles appeared to be a poorly defined annulus, as evidenced by LK-4 (Fig. 2A). In turtles greater than two years old, similar first year marks also appeared more or less distinctly (Figs. 2B and 3). Additional marks, which can only be interpreted as supplemental lines given the age of the animal, appeared between GM one and the outer edge of the bone in LK-6 (Fig. 2B) and LK-10. Specimens

LK-7 and LK-8 were difficult to interpret and in our initial assessment we underestimated age by one year. In both of these samples, the LAG representing the end of the second GM was very close to the outer edge of the bone cross-section and was difficult to differentiate from the edge. Hence these samples were not counted in the initial assessment. Because both of these animals died in the fall, there would have been a full growing season, and hence a growth zone, following the completion of the second GM. Both of these animals were recovered dead in Cape Cod, Massachusetts, during the fall of 1999 when record numbers of cold-stunned sea turtles stranded in that region.

Humerus cross-sections from LK-9 through LK-13 (Fig. 3) showed poorly defined annuli at the end of the first GM—annuli similar to the poorly defined annulus in LK-4 (Fig.2A). Subsequent GMs in these humerus cross-sections contained well-defined LAGs. Without prior knowledge of these animals' history we accurately aged each of them from GM counts and stranding date. Specimens LK-9 through LK-13 demonstrated clearly that well-defined LAGs were deposited at the end of year two and in subsequent years, providing evidence that any lines between the year-one annulus and the year-two LAGs were supplemental.

Known-age loggerhead sea turtles

The first known-age loggerhead sea turtle, CC-1, was 29.4 years old. Eleven LAGs were discernible around the circumference of the bone cross-section (Fig. 4A), although the LAGs become too compressed on the lateral edges of the bone to be differentiated; hence counts were made on the ventral and dorsal edges.(Fig. 4). Tracing the LAGs from the lateral to the ventral edge of the bone, we observed that these LAGs at some point became bifurcating and splitting LAGs and we interpreted each branch as a separate LAG. An additional nine LAGs can still be seen within the resorption zone in most areas of the bone (Fig. 4B). On the dorsal side of the cross-section, at least four less-distinct LAGs or annuli could still be observed; these had been

Figure 1

Image of a humerus cross-section from a headstart Kemp's ridley (*Lepidochelys kempii*, LK-1) sea turtle. GM-1 refers to growth mark one; LAG-2, LAG-3, and LAG-4 refer to the lines of arrested growth ending growth marks two, three, and four. Curved dashed lines highlight GM-1 and the LAG. Black bar represents 1 mm in length. This specimen was 5.0 years old.

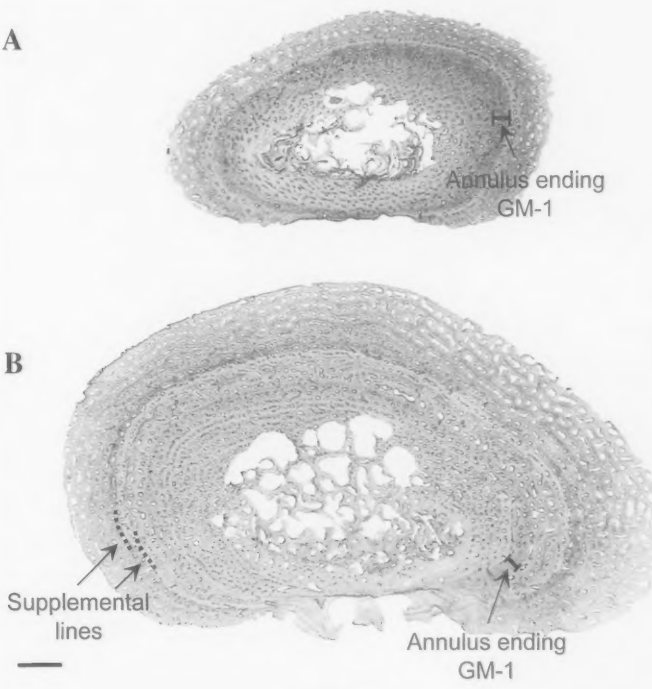

Figure 2

Images of humeri cross-sections of two coded-wire–tagged Kemp's ridley sea turtles (*L. kempii*). GM-1 refers to growth mark one. Black bar represents 1 mm for both images. (**A**) Specimen LK-4 was 1.27 years old. (**B**) Specimen LK-6 was 1.72 years old.

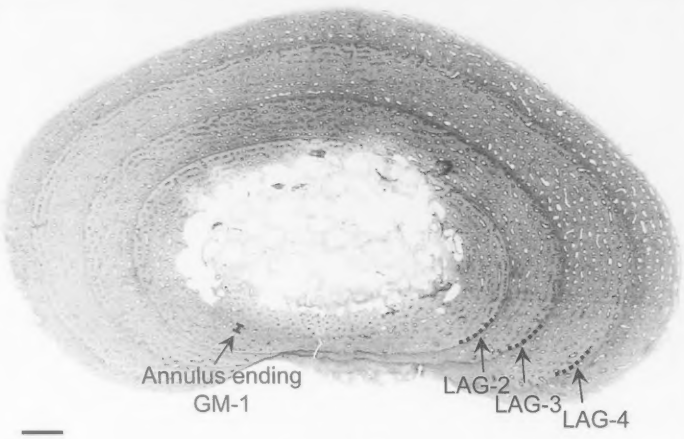

Figure 3

Image of humerus cross-section from a coded-wire–tagged Kemp's ridleys (*L. kempii*). Black bar represent 1 mm in length. GM-1 refers to growth mark one; LAG-2, LAG-3, and LAG-4 refer to the lines of arrested growth ending growth marks two, three, and four. Curved black lines highlight LAGs or annuli. This specimen, LK-13, was 4.75 years old.

resorbed in all other parts of the bone (Fig. 4C). There had been a great deal of remodeling within the bone and much of the inner portion of the bone had been resorbed. Summing all of these GMs, we gave a minimum age estimate of 24 years without prior knowledge of the history of the animal. The outermost 20 GMs contained well-defined LAGs that were spaced close together, whereas the four interior-most visible GMs contained LAGs or annuli that were spaced farther apart (Fig. 4). The number of layers completely resorbed was five.

A second known-age loggerhead sea turtle, CC-2, was eight years old. We assigned a minimum age estimate of five years. Just outside of the resorption area was a series of three LAGs that were very close together (Fig. 5). In our initial analysis, we assumed that three LAGs so close together could not each be deposited annually and we interpreted the triple LAGs as a single LAG with an anomalous appearance. We re-evaluated this assumption after learning its history. The animal was in captivity for two years and then released at 42.7 cm SCL in October 1994. Counting back from the outside of the bone, the outermost of the triplet LAGs would represent spring 1996. Given this evidence, our best interpretation of this bone section was that the innermost of the triplets of LAGs indicated release and was therefore not an annual mark. The next LAG was likely deposited the following spring (1995) and was likely an annual mark. The third of the closely spaced LAGs likely represented spring 1996, indicating that the animal did not grow significantly in its first year in the wild (Fig. 5). Following the three closely spaced LAGs, there were four additional indistinct LAGs or annuli that represented the remaining years at large. The outermost of these was very close to the edge of the bone, indicating that the animal did not grow much, if at all, during the last summer of its life.

Indirect validation of annual growth marks

For Kemp's ridley sea turtles, there was a significant increase in the amount of bone deposited after the last LAG from 20 June to 30 November (Fig. 6). The LAGs near the outer edges of the bones were fully visible in strandings that occurred after 20 June. Earlier detection of the outer LAGs was unlikely because a certain amount of bone formation must occur following the LAG before it can be discerned from the edge. There was not a significant relationship between bone growth and date from 1 December to 19 June. The slope of this regression was very close to zero (b=−0.003), indicating no trend, either increasing or decreasing, in the amount of bone deposited during this time (Fig. 6).

Validation of the relationship between LAG diameter and body size

The regressions of the eight morphometric measurements of loggerhead and Kemp's ridley sea turtle humeri against SCL revealed high correlations between bone dimension and body size (Table 2). Most importantly for purposes of back-calculation, the lateral diameter at the sectioning site of the humerus (distal to the insertion scar of the deltopectoral muscle) and the body length of the animal was highly correlated.

Discussion

Validation of the annual nature of growth marks

Our results supported annual deposition of GMs in loggerhead and Kemp's ridley sea turtles. The headstarted and older CWT Kemp's ridley sea turtles in particular highlighted the likelihood of annual marks. These animals displayed sharp and regularly spaced LAGs that were consistent with the actual ages of the animals. The results from the CWT Kemp's ridley sea turtles also emphasized the difficulties in interpreting early GMs. From these animals we concluded that in general Kemp's ridley sea turtles deposit a poorly defined annulus in their first year and well-defined LAGs starting with the end of the second year and in following years.

For loggerhead sea turtles, only CC-2 spent any time in the wild. The number of GMs deposited after the animal was released (determined from the appearance of the anomalous triplet of LAGs) was consistent with the number of years for which the animal was at large, considering that the first mark was deposited at release. This indicated that not less than one GM was deposited per year, and that additional or supplemental LAGs or annuli indistinguishable from annual lines may be deposited under extreme conditions, such as at the time of release into the wild. Fortunately, in this case, these extreme conditions were not frequent enough to have a serious impact on age estimates. For the life-time captive animal, CC-1, our estimated minimum age was five years shorter than the actual age of 29.4 years and clearly demonstrated that not more than one GM was deposited each year. Because of the relatively large size of the sea turtle humerus, in comparison to phalanges of amphibians, rapprochement did not appear to be a problem in our attempts to discern LAGs. This bone was similar in appearance to adult wild loggerhead and Kemp's ridleys sea turtles with rapprochement of the peripheral LAGs and resorption of most of the interior GMs. Although accurate age estimates cannot be made of these bones through skeletochronology, if rapprochement correlates to the timing of sexual maturity, counts of the compressed GMs can provide valuable information on postreproductive longevity and adult survival. This information can be combined with average age at reproductive maturation for piecing together the life history of sea turtles. Although our sample size for loggerhead sea turtles was very small (two), the size complements a tetracycline-injection study that previously validated annual GMs for juvenile loggerhead sea turtles from Chesapeake Bay (Klinger and Musick, 1992). In addition, an adult loggerhead sea turtle from that same study stranded dead 8.25 years after injection and provided evidence of annual deposition of growth marks in adults (Coles et al., 2001).

The indirect validation results for Kemp's ridley sea turtles highlighted the cyclic nature of bone growth; bone deposition increases from late spring through early summer to fall and no bone deposition occurs from December to spring. From this information we inferred that LAGs form annually in the spring for Kemp's ridley sea turtles that strand along the mid- to southeast U.S. Atlantic coast and that these LAGs are visible at the edges of the bones by late spring to early summer.

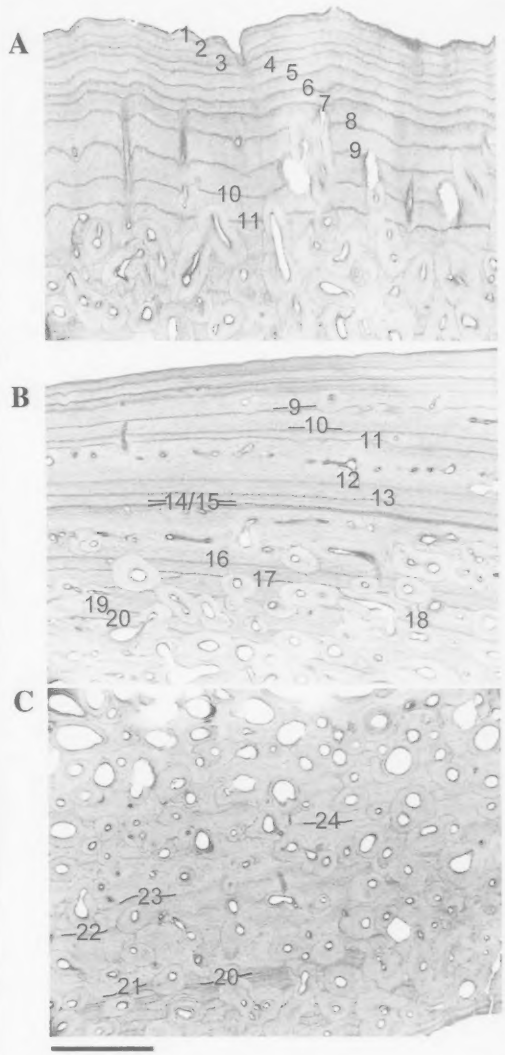

Figure 4

Images of different portions of the humerus cross-sections of CC-1 (*Caretta caretta*). Black bar represents 1 mm in length for all views. (**A** and **B**) The outer edge of the bone is at the top of the photo. (**C**) The outer edge of the bone is towards the bottom of the photo. For all views, lines of arrested growth (LAGs) are labeled with numbers; low numbers represent the most recently deposited LAGs (near the outer edge of the bone) and higher numbers represent the earlier LAGs.

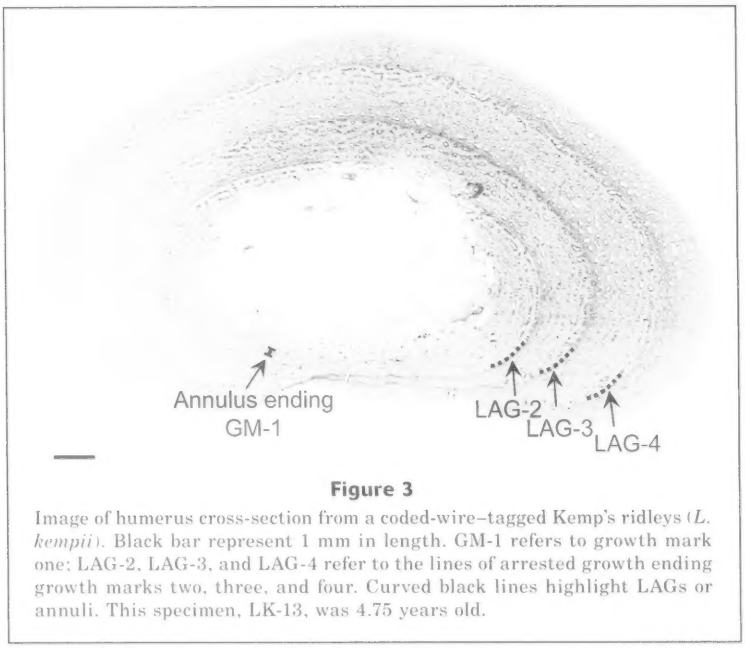

Figure 3

Image of humerus cross-section from a coded-wire–tagged Kemp's ridleys (*L. kempii*). Black bar represent 1 mm in length. GM-1 refers to growth mark one; LAG-2, LAG-3, and LAG-4 refer to the lines of arrested growth ending growth marks two, three, and four. Curved black lines highlight LAGs or annuli. This specimen, LK-13, was 4.75 years old.

resorbed in all other parts of the bone (Fig. 4C). There had been a great deal of remodeling within the bone and much of the inner portion of the bone had been resorbed. Summing all of these GMs, we gave a minimum age estimate of 24 years without prior knowledge of the history of the animal. The outermost 20 GMs contained well-defined LAGs that were spaced close together, whereas the four interior-most visible GMs contained LAGs or annuli that were spaced farther apart (Fig. 4). The number of layers completely resorbed was five.

A second known-age loggerhead sea turtle, CC-2, was eight years old. We assigned a minimum age estimate of five years. Just outside of the resorption area was a series of three LAGs that were very close together (Fig. 5). In our initial analysis, we assumed that three LAGs so close together could not each be deposited annually and we interpreted the triple LAGs as a single LAG with an anomalous appearance. We re-evaluated this assumption after learning its history. The animal was in captivity for two years and then released at 42.7 cm SCL in October 1994. Counting back from the outside of the bone, the outermost of the triplet LAGs would represent spring 1996. Given this evidence, our best interpretation of this bone section was that the innermost of the triplets of LAGs indicated release and was therefore not an annual mark. The next LAG was likely deposited the following spring (1995) and was likely an annual mark. The third of the closely spaced LAGs likely represented spring 1996, indicating that the animal did not grow significantly in its first year in the wild (Fig. 5). Following the three closely spaced LAGs, there were four additional indistinct LAGs or annuli that represented the remaining years at large. The outermost of these was very close to the edge of the bone, indicating that the animal did not grow much, if at all, during the last summer of its life.

Indirect validation of annual growth marks

For Kemp's ridley sea turtles, there was a significant increase in the amount of bone deposited after the last LAG from 20 June to 30 November (Fig. 6). The LAGs near the outer edges of the bones were fully visible in strandings that occurred after 20 June. Earlier detection of the outer LAGs was unlikely because a certain amount of bone formation must occur following the LAG before it can be discerned from the edge. There was not a significant relationship between bone growth and date from 1 December to 19 June. The slope of this regression was very close to zero (b=−0.003), indicating no trend, either increasing or decreasing, in the amount of bone deposited during this time (Fig. 6).

Validation of the relationship between LAG diameter and body size

The regressions of the eight morphometric measurements of loggerhead and Kemp's ridley sea turtle humeri against SCL revealed high correlations between bone dimension and body size (Table 2). Most importantly for purposes of back-calculation, the lateral diameter at the sectioning site of the humerus (distal to the insertion scar of the deltopectoral muscle) and the body length of the animal was highly correlated.

Discussion

Validation of the annual nature of growth marks

Our results supported annual deposition of GMs in loggerhead and Kemp's ridley sea turtles. The headstarted and older CWT Kemp's ridley sea turtles in particular highlighted the likelihood of annual marks. These animals displayed sharp and regularly spaced LAGs that were consistent with the actual ages of the animals. The results from the CWT Kemp's ridley sea turtles also emphasized the difficulties in interpreting early GMs. From these animals we concluded that in general Kemp's ridley sea turtles deposit a poorly defined annulus in their first year and well-defined LAGs starting with the end of the second year and in following years.

For loggerhead sea turtles, only CC-2 spent any time in the wild. The number of GMs deposited after the animal was released (determined from the appearance of the anomalous triplet of LAGs) was consistent with the number of years for which the animal was at large, considering that the first mark was deposited at release. This indicated that not less than one GM was deposited per year, and that additional or supplemental LAGs or annuli indistinguishable from annual lines may be deposited under extreme conditions, such as at the time of release into the wild. Fortunately, in this case, these extreme conditions were not frequent enough to have a serious impact on age estimates. For the life-time captive animal, CC-1, our estimated minimum age was five years shorter than the actual age of 29.4 years and clearly demonstrated that not more than one GM was deposited each year. Because of the relatively large size of the sea turtle humerus, in comparison to phalanges of amphibians, rapprochement did not appear to be a problem in our attempts to discern LAGs. This bone was similar in appearance to adult wild loggerhead and Kemp's ridleys sea turtles with rapprochement of the peripheral LAGs and resorption of most of the interior GMs. Although accurate age estimates cannot be made of these bones through skeletochronology, if rapprochement correlates to the timing of sexual maturity, counts of the compressed GMs can provide valuable information on postreproductive longevity and adult survival. This information can be combined with average age at reproductive maturation for piecing together the life history of sea turtles. Although our sample size for loggerhead sea turtles was very small (two), the size complements a tetracycline-injection study that previously validated annual GMs for juvenile loggerhead sea turtles from Chesapeake Bay (Klinger and Musick, 1992). In addition, an adult loggerhead sea turtle from that same study stranded dead 8.25 years after injection and provided evidence of annual deposition of growth marks in adults (Coles et al., 2001).

The indirect validation results for Kemp's ridley sea turtles highlighted the cyclic nature of bone growth; bone deposition increases from late spring through early summer to fall and no bone deposition occurs from December to spring. From this information we inferred that LAGs form annually in the spring for Kemp's ridley sea turtles that strand along the mid- to southeast U.S. Atlantic coast and that these LAGs are visible at the edges of the bones by late spring to early summer.

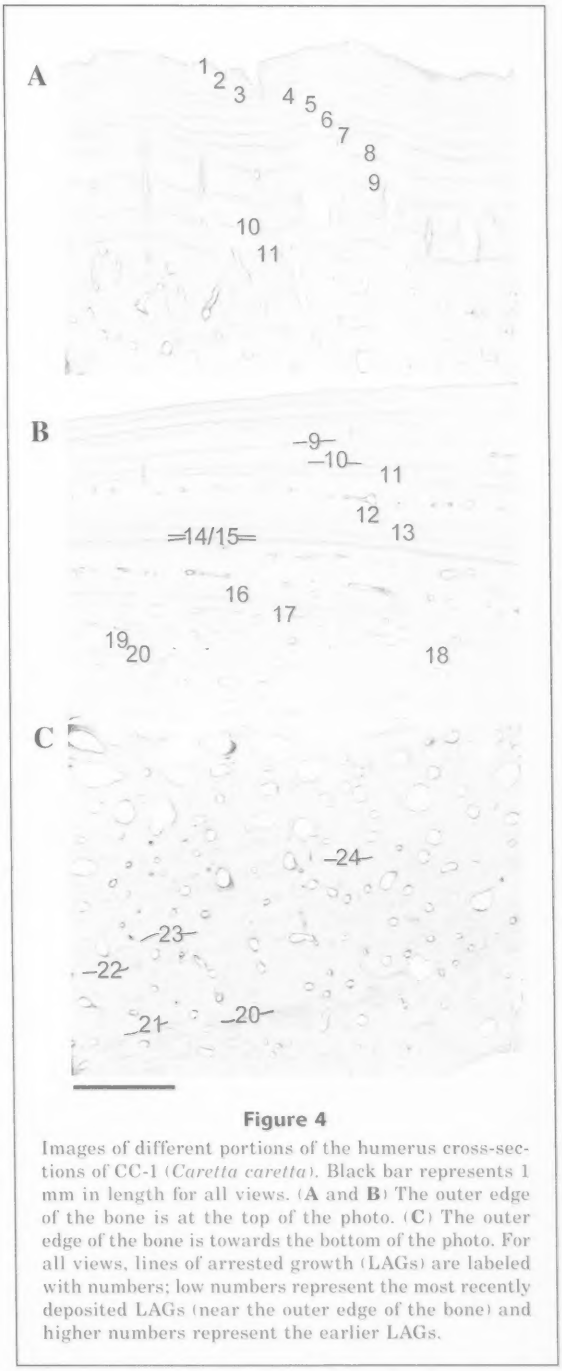

Figure 4

Images of different portions of the humerus cross-sections of CC-1 (*Caretta caretta*). Black bar represents 1 mm in length for all views. (**A** and **B**) The outer edge of the bone is at the top of the photo. (**C**) The outer edge of the bone is towards the bottom of the photo. For all views, lines of arrested growth (LAGs) are labeled with numbers; low numbers represent the most recently deposited LAGs (near the outer edge of the bone) and higher numbers represent the earlier LAGs.

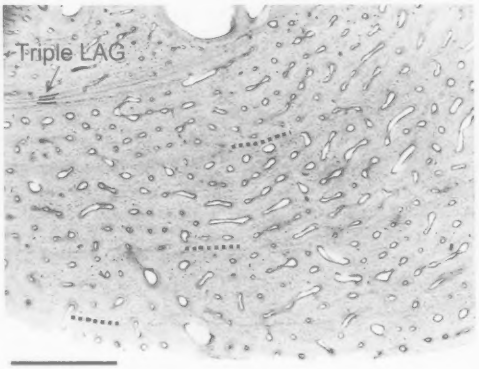

Figure 5

Image of a section of the humerus cross-section of CC-2 (*C. caretta*). Outer edge of bone is towards the bottom of the photo. Solid lines (upper left) highlight a series of triple lines of arrested growth (LAGs); curved dashed lines highlight the three diffuse LAGs. Black bar represents 1 mm in length.

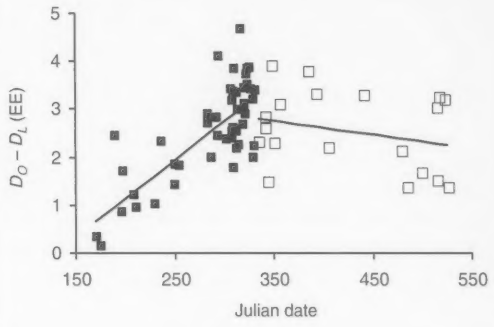

Figure 6

Julian date of stranding plotted against the amount of bone deposited peripherally to the last LAG in Kemp's ridley sea turtles (*L. kempii*; n=76). D_O represents the outside diameter of the humerus, D_L represents the diameter of the last LAG. Julian dates on x-axis equate to 20 June through 19 June; therefore numbers that are greater than 365 represent the Julian date plus 365. Solid lines represent linear regressions that were run separately for 6 months, 20 June to 31 November (filled squares) and 1 December to 19 June (open squares). The regression for the first six months was significant (P<0.006) and the regression for the second six months was not significant (P=0.27).

Most studied species of reptiles and amphibians deposit GMs within their bones (Castanet et al., 1993; Smirina, 1994). For some of these species, the annual nature of the GM has been validated (e.g., Tucker, 1997; de Buffrénil and Castanet, 2000; Trenham et al., 2000). For others, it is consistent with their ecology that the marks must represent annual events (Castanet et al., 1993). Growth marks observed in loggerhead (Zug et al., 1986; Zug et al., 1995; Coles et al., 2001), Kemp's ridley (Zug et al., 1997), and green (Zug and Glor, 1998; Zug et al., 2002) sea turtles are similar in structure to those observed in other species of reptiles and amphibians. Drawing on previous studies of reptiles and amphibians, validation studies on sea turtles, and the evidence presented in this article, we assert that GM in bones of sea turtles are likely deposited primarily with an annual periodicity.

Given these results, on the surface it seems contradictory that in two validation studies annual GMs could not be confirmed. For serpentine species, Collins and Rodda (1994) injected brown snakes with a fluorescent marker and kept them in captivity for one year under two different feeding regimes. Five or six GMs varying in distinctness were identified beyond the fluorescent marks in bone cross-sections. Statistical analyses showed that these marks may relate to shedding events. It is unclear if the GM pattern prior to captivity was similar to what was seen after the fluorescent mark. The forced feeding component of that study may have induced higher growth rates than would be found in nature, causing the shedding events to appear as histological marks in the bone.

In a sea turtle study, Bjorndal et al. (1998) did not find GMs in the humeri of green sea turtle bones. They suggested that the tropical marine habitat of the study population (approximately 21°07′N) allowed for continual activity and growth and inhibited GM formation. However, GMs have been clearly demonstrated in green sea turtles from the coastal waters of Florida (approximately 29°N) (Zug and Glor, 1998) and Hawaii (approximately 22°N) (Zug et al., 2002). Other studies of reptiles and amphibians in tropical and warm temporate climates have reported distinct GMs in species that remain active year-round (i.e., do not hibernate or estivate) (Patnaik and Behera, 1981; Estaban et al., 1996; Guarino et al., 1998).

Interpretation of anomalous LAGs

Although our sample sizes were small, especially for loggerhead sea turtles, several characteristics were noted in the analyses of the samples that would affect how anomalous LAGs are interpreted. Three interpretations of double and bifurcating LAGs are provided. The first interpretation is that if double LAGs appear frequently in individual bones and throughout the sample, they likely indicate an ecology that has two growth cycles per year (Castanet et al., 1993). In this case the two LAGs are distinct from each other over the entire bone cross-section. This pattern was observed in the newt *Triturus marmoratus* living at a high altitude where the animals had both winter and summer dormancy periods (Castanet and Smirina, 1990; Caetano et al., 1985; Caetano and Castanet, 1993). The second interpretation of double LAGs is that they result from a brief

Table 2

Regressions equations and statistics from correlations between dimensions of the humerus and notch-to-tip straight carapace length (SCL, cm) in loggerhead and Kemp's ridley sea turtles. All F statistics are significant at $P<0.005$.

Humeral measurement	Model equation	SE slope	F	r^2
Loggerhead sea turtles (n=243)				
Maximal length (ML, mm)	$SCL = 0.44 \times ML + 5.97$	0.0064	4814	0.95
Longitudinal length (LL, mm)	$SCL = 0.47 \times LL + 4.85$	0.0064	5381	0.96
Proximal width (PW, mm)	$SCL = 1.06 \times PW + 7.31$	0.015	4857	0.95
Deltopectoral crest width (DCW, mm)	$SCL = 1.69 \times DCW + 6.04$	0.026	4069	0.94
Site of sectioning width (SW, mm)	$SCL = 2.38 \times SW + 5.48$	0.037	4110	0.94
Site of sectioning thickness (ST, mm)	$SCL = 4.13 \times ST + 11.62$	0.080	2682	0.92
Distal width (DW, mm)	$SCL = 1.28 \times DW + 5.43$	0.021	3684	0.94
Mass (M, g)	$\ln(SCL) = 0.30 \times \ln(M) + 2.94$	0.0022	18905	0.99
Kemp's ridley sea turtles (n=262)				
Maximal length (ML, mm)	$SCL = 0.43 \times ML + 4.69$	0.0040	10970	0.98
Longitudinal length (LL, mm)	$SCL = 0.47 \times LL + 3.11$	0.0039	14772	0.98
Proximal width (PW, mm)	$SCL = 1.12 \times PW + 4.39$	0.010	12390	0.98
Deltopectoral crest width (DCW, mm)	$SCL = 1.69 \times DCW + 3.35$	0.017	10200	0.98
Site of sectioning width (SW, mm)	$SCL = 2.48 \times SW + 2.74$	0.033	5715	0.96
Site of sectioning thickness (ST, mm)	$SCL = 4.16 \times ST + 4.79$	0.072	3306	0.93
Distal width (DW, mm)	$SCL = 1.36 \times DW + 0.227$	0.013	11435	0.98
Mass (M, g)	$LN(SCL) = 0.30 \times LN(M) + 2.89$	0.0023	16305	0.98

interruption of hibernation (Hemelaar and van Gelder, 1980). In this instance little bone deposition would occur and the layers would not be distinct from each other over the entire bone, thus giving the appearance of a bifurcating LAG (Hemelaar and van Gelder, 1980). The third interpretation of double or bifurcating LAGs is that they result from extreme decreased growth over the active period, which places annual LAGs very close to each other and in some cases they appear to merge (de Buffrénil and Castanet, 2000).

With the first two interpretations, a double or bifurcating LAG would be counted as one for the purposes of age estimation, whereas the third interpretation would necessitate counting each LAG or bifurcating branch separately. Coles et al. (2001) interpreted a bifurcating LAG as one LAG in an adult loggerhead sea turtle that was recovered 8.25 years after it had been injected with oxytetracycline. In cross-sections of the humerus, Coles et al. (2001) reported seven LAGs following the tetracycline mark, six plus the bifurcating LAG. The animal was marked on 20 June 1989 and recovered dead on 22 September 1997. It is reasonable to assume that, as with Kemp's ridley sea turtles from the same region, the LAGs form in the spring, and Coles et al. (2001) showed that the oxytetracycline mark overlaid one of the LAGs—likely the LAG deposited in spring of 1989. Therefore, there should have been eight LAGs deposited after the tetracycline mark, not seven, each representing the spring of years 1990 through 1997. In this case, then, the bifurcating mark in this bone should be counted as two LAGs.

Similarly, for splitting LAGs, where numerous thinner LAGs branch out from what appears to be one thick LAG, Francillon-Vieillot et al. (1990) examined different bones from the same animal and determined whether each thin LAG comprising splitting LAGs should be counted as one LAG. In our analysis of the adult loggerhead sea turtle, CC-1, we observed several bifurcating and splitting LAGs, each of which eventually split into two or more thinner LAGs. We counted each of the thin LAGs as one. Because the LAG count was close to the actual age of the animal, this interpretation appears to have been appropriate for compressed LAGs in adult humeri.

The question remains as to whether this is the appropriate interpretation for double or bifurcating LAGs in juveniles. Wild loggerhead growth rates have been monitored in an ongoing mark-recapture study in Pamlico and Core Sounds in North Carolina (Epperly et al., 1995). Epperly et al. (1995) currently have 65 growth rates for 49 juvenile loggerhead sea turtles between 45.1 and 81.0 cm SCL at initial capture that were at-large for one year (±0.1 year). The mean annual growth rate for all of the animals is 2.09 cm/yr. However, of the 65 growth records, 11 of them displayed an annual increase of 0.3 cm or less in SCL (Braun-McNeill[1]). Hence it is not uncommon for juvenile loggerhead sea turtles to

[1] Braun-McNeill, J. 2004. Personal commun. Center for Coastal Fisheries and Habitat Research, National Marine Fisheries Service, NOAA, 101 Pivers Island Rd., Beaufort, NC 28516

grow little or not at all over the course of a year. Using the equation for width at sectioning site from Table 2, we found that the increase in bone diameter for these 11 animals was ≈0.13 mm or less, which places the LAGs very close together. Because it not uncommon for sea turtle to exhibit little or no growth over a year, LAGs spaced closely together very likely represent distinct years as also determined by de Buffrénil and Castanet (2000). Although the sample sizes are still small for a definitive answer, our results indicate that counting the LAGs individually is the correct interpretation of double or bifurcating LAGs in juvenile as well as adult loggerhead sea turtles.

Similarly, our results indicate the same interpretation for double or bifurcating LAGs in juvenile Kemp's ridley sea turtles. The CWT Kemp's ridley sea turtles, samples LK-7 and LK-8, displayed LAGs near the outer edge of the bone and a small amount of bone was deposited after the LAGs. These animals were each 2.25 years old and had one-year marks visible in the humeri but no LAGs or annuli other than those at the periphery. Other CWT samples clearly indicated that LAGs are deposited at the end of the second GM. The indirect validation results demonstrated that LAGs were visible in bone tissue by late spring or early summer. It seemed that the LAGs at the outer edge of the LK-7 and LK-8 bones were the LAGs ending the second GM and that very little growth occurred over the subsequent growing season. Both of these animals were recovered as dead strandings resulting from a major cold stun event in Cape Cod, Massachusetts, in 1999; hence their growth rates may have been anomalous in their last year of life. Had these animals survived the cold stun event, they would have deposited a year-three LAG very close to year two, giving the appearance of a double or bifurcating LAG.

Another anomaly in skeletochronology, supplemental lines, may form as a result of temporary stressful environmental events such as droughts. In support of this, Rogers and Harvey (1994) noted a supplemental line in 11 of 43 specimens of the toad *Bufo cognatus*, and in 10 of these animals the supplemental line was within a growth zone that corresponded to a drought year. Most skeletochronology studies that have noted the presence of supplemental lines have indicated that supplemental lines are easily identified as such because they are less distinct and do not appear around the entire circumference of the bone. In general, the same has been observed in sea turtles. Supplemental lines do appear but are generally easily differentiated from LAGs by appearance. An exception to this was the presence of supplemental marks in one- to two-year-old Kemp's ridley sea turtles. These marks were similar in appearance to the first year annuli. We were able to identify these marks as supplemental only by the observation of known-age animals. In addition, there appeared to be a supplemental line in CC-2 that represented when the animal was released; hence, highly stressful events may cause the deposition of nonannual lines, but these events are likely to be relatively rare in wild turtles and not likely to interfere significantly with age estimations.

Resorption of early growth marks

The loss of the early GMs due to endosteal resorption and remodeling of the interior region of the bone is a limiting factor in the application of skeletochronology to sea turtles. From our findings, it was possible to accurately age juvenile Kemp's ridley sea turtles up to at least 5 years from GM counts and this may be true for other sea turtle species (e.g., Bjorndal et al., 2003), with the possible exception of the leatherback sea turtle (Zug and Parham, 1996). Because sea turtles have distinct life-cycle stages, we suggest that in order to age a population of sea turtles, one must acquire an ontogenetic series of samples spanning all sizes and stages. Average duration can be determined for each ontogenetic stage and the approximate age of older animals with extreme resorption can be estimated. Because GM patterns appear to mimic somatic growth rates, once growth through each life-cycle stage is understood, backcalculation techniques can be used to estimate the number of layers resorbed.

Conclusions

For many species, skeletochronology is not a perfect method for age estimation. As GMs are histological expressions of variation in rates of osteogenesis (Castanet et al., 1993), external factors and individual variation will affect the appearance of the marks (Castanet et al., 1993, Esteban et al., 1996, Waye and Gregory, 1998). Endosteal resorption also serves to confound this technique and is the primary difficulty in the application of the technique to sea turtles. However, the evidence presented in the present study gives strong support to the concept that GMs are deposited on an annual basis in sea turtles and that the spatial pattern of the GMs correspond to the growth rates of the animal. The GMs therefore provide invaluable information on age and growth that cannot otherwise be easily obtained, and age determination by skeletocronology is valid and appropriate for the study of sea turtles.

Acknowledgments

We thank L. Crowder, S. Heppell, A. Read, and D. Rittschof for their valuable comments on earlier versions of this manuscript. A. Gorgone, B. Brown and J. Weaver provided assistance with the preparation of the humeri. Most of the humeri were received through the Sea Turtle Stranding and Salvage Network, a cooperative endeavor between the National Marine Fisheries Service, other federal and state agencies, many academic and private entities, and innumerable volunteers. We especially thank R. Boettcher and W. Teas. In addition, humeri were received from F. Swartz at the University of North Carolina–Chapel Hill Institute of Marine

Science, B. Higgins at the National Marine Fisheries Service–Galveston Lab, the Virginia Marine Science Museum Stranding Program, the Maryland Department of Natural Resources, and the Massachusetts Audubon Society in Wellfleet. Funding was provided by the National Marine Fisheries Service. All work was done under and complied with the provisions of the Sea Turtle Research Permit TE-676379-2 issued by the U.S. Fish and Wildlife Service.

Literature cited

Bjorndal, K. A., A. B. Bolten, R. A. Bennet, E. R. Jacobson, T. J. Wronski, J. J. Valeski, and P. J. Eliazar.
1998. Age and growth in sea turtles: limitations of skeletochronology for demographic studies. Copeia 1998: 23–30.

Bjorndal, K. A., A. B. Bolten, T. Dellinger, C. Delgado, and H. R. Martins.
2003. Compensatory growth in oceanic loggerhead sea turtles: response to a stochastic environment. Ecology 84:1237–1249.

Caetano, M. H., and J. Castanet.
1993. Variability and microevolutionary patterns in *Triturus marmoratus* from Portugal: age, size, longevity and individual growth. Amphibia-Reptilia 14:117–129.

Caetano, M. H., J. Castanet, and H. Francillon.
1985. Determination of the age of *Triturus marmoratus marmoratus* from the National Park of Peneda Geres, Portugal by means of skeletochronology. Amphibia-Reptilia 6:117–132.

Caillouet, C. W., B. A. Robertson, C. T. Fontaine, T. D. Williams, B. M. Higgins, and D. B. Revera.
1997. Distinguishing captive-reared from wild Kemp's ridleys. Marine Turtle News Letter 77:1–6.

Castanet, J., H. Francillon-Vieillot, and R. C. Bruce.
1996. Age estimation in desmognathine salamanders assessed by skeletochronology. Herpetologica 52:160–171.

Castanet, J., H. Francillon-Vieillot, F. J. Meunier, and A. De Ricqles.
1993. Bone and individual aging. *In* Bone, vol. 7: Bone growth B (B. B. K. Hall, ed.), p. 245–283. CRC press, Boca Raton, FL.

Castanet, J., F. J. Meumier, and A. de Ricqles.
1977. L'enregistrement de la croissance cyclique par le tissu osseux chez les Vertébrés poïkilothermes: données comparatives et essai de synthése. Bull. Biol. Fr. Belg. 111:183–202.

Castanet, J., and E. Smirina.
1990. Introduction to the skeletochronological method in amphibians and reptiles. Ann. Sci. Nat. Zool. 11:191–196.

Chaloupka, M. Y., and J. A. Musick.
1997. Age, growth, and population dynamics. *In* The biology of sea turtles (P. L. Lutz and J. A. Musick, eds.) p. 233–276. CRC Press, New York.

Chinsamy, A., S. A. Hanrahan, R. M. Neta, and M. Seely.
1995. Skeletochronological assessment of age in *Angolosaurus skoogi*, a cordylid lizard living in an aseasonal environment. J. Herpetol. 29:457–460.

Coles, W. C., J. A. Musick, and L. A. Williamson.
2001. Skeletochronology validation from an adult loggerhead (*Caretta caretta*). Copeia 2001:240–242.

Collins, E. P., and G. H. Rodda.
1994. Bone layers associated with ecdysis in laboratory-reared *Boiga irregularis* (Colubridae). J. Herpetol. 28:378–381.

de Buffrénil, V., and J. Castanet.
2000. Age estimation by skeletochronology in the Nile monitor (*Varanus niloticus*), a highly exploited species. J. Herpetol. 34:414–424.

Eggert, C., and R. Guyetant.
1999. Age structure of a spadefoot toad *Pelobates fucus* (Pelobatidae) population. Copeia 1999:1127–1130.

El Mouden, P. E., H. Francillon-Vieillot, J. Castanet, and M. Znari.
1997. Âge individuel maturité, croissance et longévité chez l'agamidé nord-africain, *Agama impalearis* Boettger, 1874, étudiés à l'aide de la squelettochronologie.

Epperly, S. P., J. Braun, and A. Veishlow.
1995. Sea turtles in North Carolina waters. Conserv. Biol. 9:384–394.

Esteban, M., M. Garcia-Paris, and J. Castanet.
1996. Use of bone histology in estimating the age of frogs (*Rana perezi*) from a warm temperate climate area. Can. J. Zool. 74:1914–1921.

Francillon-Vieillot, H., J. W. Arntzen, and J. Géraudie.
1990. Age, growth and longevity of sympatric *Triturus cristatus*, *T. marmoratus* and their hybrids (Amphibia, Urodela). A skeletochronological comparison. J. Herpetol. 24:13–22.

Guarino, F. M., F. Andreone, and F. Angelini.
1998. Growth and longevity by skeletochronological analysis in *Mantidactylus microtympanum*, a rainforest anuran from southern Madagascar. Copeia 1998:194–198.

Guarino, F. M., F. Angelini, and M. Cammarota.
1995. A skeletochronological analysis of three syntopic amphibian species from southern Italy. Amphibia-Reptilia 16:297–302.

Hemelaar, A. S. M., and J. J. van Gelder.
1980. Annual growth rings in phalanges of *Bufo bufo* (Anura, Amphibia) from the Netherlands and their use for age determination. Neth. J. Zool. 30:129–135.

Hutton, J. M.
1986. Age determination of living Nile crocodiles from the cortical stratification of bone. Copeia 1986: 332–341.

Klevezal, G. A.
1996. Recording structures of mammals: determination of age and reconstruction of life history, p. 49–52. A. A. Balkema, Rotterdam.

Klima, E. F., and J. P. McVey.
1995. Headstarting the Kemp's ridley turtle, *Lepidochelys kempi*. *In* The biology and conservation of sea turtles (K. A. Bjorndal, eds.), p. 481–487. Smithsonian Institution, Washington, D.C..

Klinger, R. C., and J. A. Musick.
1992. Annular growth layers in juvenile loggerhead turtles (*Caretta caretta*). B. Mar. Sci. 51:224–230.
1995. Age and growth of loggerhead turtles (*Caretta caretta*) from Chesapeake Bay. Copeia 1995:204–209.

Kusano, T., K. Fukuyama, and N. Miyashita.
1995. Age determination of the stream frog, *Rana sakuraii*, by skeletochronology. J. Herpetol. 29:625–628.

Leclair Jr., R., and G. Laurin.
1996. Growth and body size in populations of mink frogs *Rana septentrionalis* from two latitudes. Ecography 19:296–304.

Leclair Jr., M. H. Leclair, J. Dubois, and J-L. Daoust.
2000. Age and size of wood frogs, *Rana sylvatica*, from Kuujjuarapik, Northern Quebec. Can. Field. Nat. 114:381–387.

Lima, V., J. W. Arntzen, and N. M. Ferrand.
2000. Age structure and growth pattern in two populations of the golden-striped salamander *Chioglossa lusitanica* (Caudata Salamandra). Amphibia-Reptilia 22:55–68.

Parham, J. F., and G. R. Zug.
1997. Age and growth of loggerhead sea turtles (*Caretta caretta*) of coastal Georgia: an assessment of skeletochronological age-estimates. B. Mar. Sci. 61:287–304.

Patnaik, B. K., and H. N. Behera.
1981. Age-determination in the tropical agamid garden lizard, *Calotes versicolor* (Daudin), based on bone histology. Exp. Gerontol. 16:295–307.

Peabody, F. E.
1961. Annual growth zones in vertebrates (living and fossil). J. Morphol. 108:11–62.

Rogers, K. L., and L. Harvey.
1994. A skeletochronology assessment of fossil and recent *Bufo cognatus* from south-central Colorado. J. Herpetol. 28:133–140.

Sagor, E. S., M. Ouellet, E. Barten, and D. M. Green.
1998. Skeletochronology and geographic variation in age structure in the wood frog, *Rana sylvatica*. J. Herpetol. 32:469–474.

Simmons, D. J.
1992. Circadian aspects of bone biology. *In* Bone, vol. 6: Bone growth A (B. B. K. Hall, ed.), p. 91–128. CRC press, Boca Raton, FL.

Smirina, E. M.
1994. Age determination and longevity in amphibians. Gerontology 40:133–146.

Swartz, F. J.
1997. Growth, maturity, and reproduction of a long-term captive male loggerhead sea turtle, *Caretta caretta* (Chelonia, Reptilia) in North Carolina. Elisha Mitchell Scientific Society 133:143–148.

Trenham, P. C., H. B. Shaffer, W. D. Koenig, and M. R. Stromberg.
2000. Life history and demographic variation in the California tiger salamander (*Ambystoma californiense*). Copeia 2000:365–377.

Tucker, A. D.
1997. Validation of skeletochronology to determine age of freshwater crocodiles (*Crocodylus johnstoni*). Mar. Freshw. Res. 48:343–351.

Waye, H. L., and P. T. Gregory.
1998. Determining the age of garter snakes (*Thamnophis* spp.) by means of skeletochronology. Can. J. Zool. 76:288–294.

Zug, G. R, G. H. Balazs, and J. A. Wetherall.
1995. Growth in juvenile loggerhead sea turtles (*Caretta caretta*) in the north Pacific pelagic habitat. Copeia 1995:484–487.

Zug, G. R., G. H. Balazs, J. A. Wetherall, D. M. Parker, and S. K. K. Murakawa.
2002. Age and growth of Hawaiian green sea turtles (*Chelonia mydas*): and analysis based on skeletochronology. Fish. Bull. 100:117–127.

Zug, G. R, and R. E. Glor.
1998. Estimates of age and growth in a population of green sea turtles (*Chelonia mydas*) from the Indian River lagoon system, Florida: a skeletochronological analysis. Can. J. Zool., 76:1497–1506.

Zug, G. R, H. J. Kalb, and S. J. Luzar.
1997. Age and growth in wild Kemp's ridley sea turtles *Lepidochelys kempii* from skeletochronological data. Biol. Conserv. 80:261–268.

Zug, G. R, and J. F. Parham.
1996. Age and growth in leatherback sea turtles, *Dermochelys coriacea* (Testudines, Dermochelyidae): a skeletochronological analysis. Chelonian Conserv. Biol. 2:244–249.

Zug, G. R., A. H. Wynn, and C. Ruckdeschel.
1986. Age determination of loggerhead sea turtles, *Caretta caretta*, by incremental growth marks in the skeleton. Smithsonian Institution, Contrib. Zool. 427, Washington D.C.

The Hudson-Raritan Estuary as a crossroads for distribution of blue (*Callinectes sapidus*), lady (*Ovalipes ocellatus*), and Atlantic rock (*Cancer irroratus*) crabs

Linda L. Stehlik
Robert A. Pikanowski
Donald G. McMillan

James J. Howard Marine Sciences Laboratory
Northeast Fisheries Science Center
National Marine Fisheries Service, NOAA
74 Magruder Road
Highlands, New Jersey 07732
E-mail address (for L. L. Stehlik): Linda.Stehlik@noaa.gov

Abstract—Blue (*Callinectes sapidus*) (Portunidae), lady (*Ovalipes ocellatus*) (Portunidae), and Atlantic rock (*Cancer irroratus*) (Cancridae) crabs inhabit estuaries on the northeast United States coast for parts or all of their life cycles. Their distributions overlap or cross during certain seasons. During a 1991–94 monthly otter trawl survey in the Hudson-Raritan Estuary between New York and New Jersey, blue and lady crabs were collected in warmer months and Atlantic rock crabs in colder months. Sex ratios, male: female, of mature crabs were 1:2.0 for blue crabs, 1:3.1 for lady crabs, and 21.4:1 for Atlantic rock crabs.

Crabs, 1286 in total, were subsampled for dietary analysis, and the dominant prey taxa for all crabs, by volume of foregut contents, were mollusks and crustaceans. The proportion of amphipods and shrimp in diets decreased as crab size increased. Trophic niche breadth was widest for blue crabs, narrower for lady crabs, and narrowest for Atlantic rock crabs. Trophic overlap was lowest between lady crabs and Atlantic rock crabs, mainly because of frequent consumption of the dwarf surfclam (*Mulinia lateralis*) by the former and the blue mussel (*Mytilus edulis*) by the latter. The result of cluster analysis showed that size class and location of capture of predators in the estuary were more influential on diet than the species or sex of the predators.

Manuscript submitted 27 November 2000 to the Scientific Editor's Office.

Manuscript approved for publication 4 May 2004 by the Scientific Editor.

Fish. Bull. 102:693–710 (2004).

The blue crab (*Callinectes sapidus*) (Portunidae), the lady crab (*Ovalipes ocellatus*) (Portunidae), and the Atlantic rock crab (*Cancer irroratus*) (Cancridae) are the largest and most common brachyuran crabs inhabiting both estuaries and inner continental shelves of the northeast coast of North America. The centers of abundance of these three species overlap in estuarine and coastal waters from New York to Virginia, although their ranges along the northwest Atlantic coast are broad. The blue crab is nearly always an estuarine resident, except during its larval stages, and ranges from the waters off Nova Scotia to Argentina (Williams, 1984). The northernmost estuaries where the species is abundant enough for commercial harvest are in New Jersey and New York (Briggs, 1998; Stehlik et al., 1998). The lady crab is distributed from the waters off Prince Edward Island to those off Georgia but it is most numerous from Georges Bank to Cape Hatteras (Williams, 1984). The Atlantic rock crab (referred to as "rock crab" in this article) is distributed in waters from off Labrador to Florida but is most common in estuaries from Nova Scotia to Virginia (Williams, 1984; Stehlik et al., 1991). Seasonal migrations are common for all three species. Although Jonah crabs (*Cancer borealis*) are present on the continental shelf, they are not included in the present study because they are rare within the Hudson-Raritan Estuary where our study was conducted.

Physiological tolerances and habitat preferences of these crabs have been extensively studied. In eastern United States estuaries the blue crab occurs in shallow to deep, sandy to muddy estuaries and tributaries along marsh edges, and in seagrass (Van Engel, 1958; Milliken and Williams, 1984; Hines et al., 1987; Wilson et al., 1990; van Montfrans et al., 1991; Rountree and Able, 1992). In the colder portions of its range, it becomes less active at about 15°C (Leffler, 1972), and buries itself, without eating, when the temperature is <5°C (Auster and DeGoursey, 1994). It survives at 34°C (Leffler, 1972) and at salinities from 0 to 50 ppt (Guerin and Stickle, 1992). The lady crab is most common on sand substrates (Williams, 1984). It is present on the inner continental shelf from off Cape Cod to off the Carolinas throughout the year (Stehlik et al., 1991). Its temperature tolerance is unknown, but it does not survive in <21 ppt (Birchard et al., 1982). The rock crab's optimum temperature range for activity is 14–22°C (Jeffries, 1966); thus the species avoids high summer temperatures. It is found on many substrates, such as sand, mud, bare rock, cobble, and algal beds.

The diet of the blue crab is generally mollusks, crabs, and fish, depending on crab size (Virnstein, 1977; Laughlin, 1982; Ryer, 1987; Hines et al., 1990). The diet of the lady crab is mainly bivalves such as *Mya arenaria* and *Spisula solidissima*, and some crustaceans (McDermott, 1983; Ropes, 1989; Stehlik, 1993). The rock crab consumes mollusks, small crustaceans, crabs, urchins, and fish (Scarratt and Lowe, 1972; Drummond-Davis et al., 1982; Hudon and Lamarche, 1989; Ojeda and Dearborn, 1991; Stehlik, 1993). In some of the aforementioned studies these crabs have been considered opportunistic and as such may be competitors for the same prey taxa. However, differences in maximum body size, chela structure, and the presence or absence of swimming appendages among blue, lady, and rock crabs indicate that they may have differences in diet (Warner and Jones, 1976; Williams, 1984).

Within the Hudson-Raritan Estuary, blue, lady, and rock crabs are all abundant, providing an opportunity to study partitioning of habitat and food resources by these species. The objectives of our study were to determine the temporal and spatial overlap of blue, lady, and rock crabs in this estuary and to differentiate the composition of their diets by the species, sex, and size of predators, and by location of collection.

This study has potential practical applications. Resource managers could use the results to consider when and where crabs depend upon certain locations to complete their life cycles, if dredging, filling, or sanctuaries were proposed. Dietary analysis of these crabs could indicate if they are a cause of mortality for young stages of commercially important species. For instance, the northern quahog *(Mercenaria mercenaria)* and the soft-shell clam *(M. arenaria)* recently have supported and presently support commercial and recreational harvests in the Hudson-Raritan Estuary (MacKenzie, 1990; 1997) and when young these clams are consumed by crabs. The blue crab supports lucrative fisheries in the estuary (Stehlik et al., 1998) and predation by various species of crabs upon blue crab juveniles may affect recruitment.

Materials and methods

Study area

The Hudson-Raritan Estuary, bordered by New Jersey on the south and Staten Island and Brooklyn, New York, on the north (Fig.1), has a surface area of about 280 km^2. The Hudson, Raritan, and Navesink-Shrewsbury rivers flow into the estuary from the north, west, and south, respectively. The study area is bounded on the west by the 74°15′ longitude line; on the east by a line between the northeast corner of Sandy Hook, NJ, and the tip of Rockaway Point, NY; and on all sides by the-3 m contour. The area was divided into nine strata according to physiographic features (Wilk et al.[1]). Sandy-bottom strata included Sandy Hook Bay (stratum 1), Raritan Bay south of Raritan Channel (stratum 2), and Lower Bay north of Raritan Channel (stratum 3). Eastern strata of more irregular depths were Romer Shoals (stratum 4), East Bank between Ambrose Channel and Rockaway, NY (stratum 5), and Gravesend Bay at the mouth of the Hudson River (stratum 6). Three strata were channels: Ambrose (stratum 7), Chapel Hill (stratum 8), and Raritan (stratum 9). Raritan Channel is maintained at a depth of 13.7 m, and the average depth of adjacent nonchannel stations is 7.1 m. Gravesend Bay is more than 13 m deep in its center.

The bottom of the Hudson-Raritan Estuary consists mostly of soft sediments (Jones et al., 1979; Coch, 1986; Wilber[2]). The substrates in semi-sheltered southern strata 1 and 2 are predominantly fine sand, silt, and clay; those of stratum 3 are mainly medium sand, with a mixture of sand, silt, and clay near channels; those of ocean-exposed strata 4, 5, 6, and 7 are gravel, sand, silt, broken shell, and have beds of blue mussels *(Mytilus edulis)*. The bottom of Ambrose Channel is silt and clay near its head and fine sand toward the ocean. The sediments of the other two channels, and their immediate borders, are sand, silt, and clay. Based on physiographic form, temperature ranges, and sediments, strata 1, 2, 3, 8, and 9 were considered inner or riverward strata, whereas 4, 5, 6, and 7 were considered outer or oceanic-influenced strata.

Collections and analyses

Crabs were collected during monthly otter trawl surveys of the Hudson-Raritan Estuary from June 1991 to December 1994 (Wilk et al.[1]). Sampling was done from the 18-m research vessel *Gloria Michelle* by towing a 9.1-m otter trawl with a chain sewn to the bottom opening, and a 76-mm mesh net with a 51-mm codend liner. Wooden trawl doors were deployed to spread open the net. The net was towed once per station for 10 min at 5.6 km/h to cover a distance of approximately 1 km. All tows were made between 8 am and 2 pm. During 1991, fixed stations were towed (number of stations in 1991: 10 in June, 8 in July; 11 in August; 18 in September; 22 in October; 23 in November; 34 in December). Beginning in 1992, a stratified random sampling design was used, in which the nine strata were divided into 190 blocks of approximately 0.5 minutes latitude by 0.5 minutes longitude. Each month, 40 blocks were randomly sampled without replication, and the number of blocks in each stratum was proportional to the area of the stratum. Because of conflicting schedules, the vessel was not available in May or September 1992 or 1994. Temperature and salinity of water 1 m above the bottom were measured after each tow. During 1991

[1] Wilk, S. J., E. M. MacHaffie, D. G. McMillan, A. L. Pacheco, R. A. Pikanowski, and L. L. Stehlik. 1996. Fish, megainvertebrates, and associated hydrographic observations collected in the Hudson-Raritan Estuary, January 1992–December 1993, 95 p. Northeast Fish. Sci. Cent. Ref. Doc. 96-14, NMFS, Woods Hole, MA.

[2] Wilber, P. 2000. Unpubl. data. Coastal Services Center, National Ocean Survey, NOAA, 2234 Hobson Avenue, Charleston, SC, 29405.

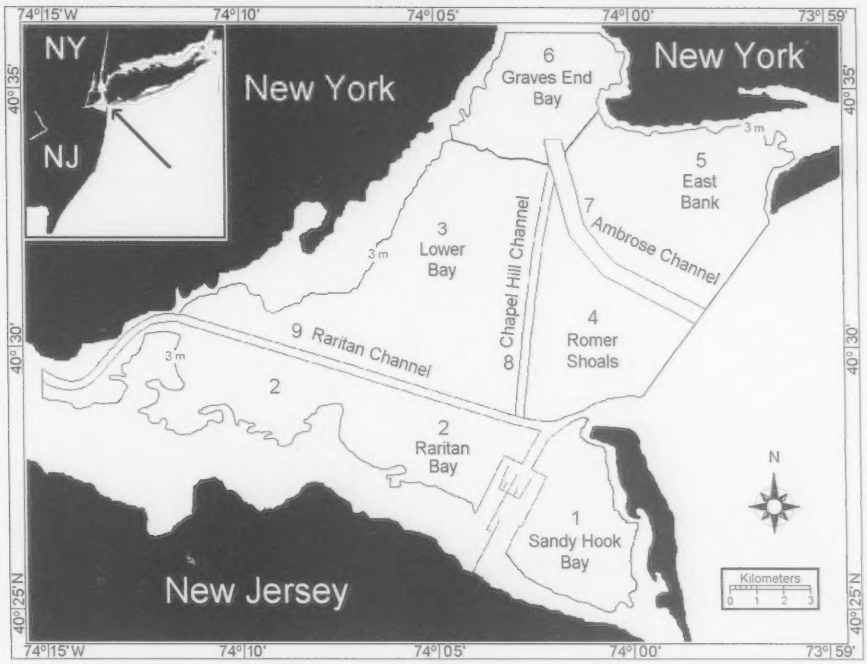

Figure 1

Hudson-Raritan Estuary, from New York to New Jersey, with 3-m contour, drawn boundaries, and the nine strata of the Hudson-Raritan Estuary trawl survey. The inset shows the location of the estuary on the United States coast off New York and New Jersey.

and 1992 temperature and salinity were determined by using a Niskin bottle, a thermometer, and an induction salinometer. Beginning in January 1993 a Hydrolab® Surveyor III multiprobe was used.

Fish and large invertebrates were counted, weighed, and measured (±1.0 cm), and sexes of the crabs were recorded. Catch per unit of effort or number per tow was used to estimate relative abundance. Crabs were measured by carapace width (CW) between the tips of the anterolateral teeth. Specimens were saved for dietary analysis from June 1991 through June 1992. These specimens were measured (±1.0 mm) and molt stages were classified as intermolt (hard-shelled), premolt (new skin separates easily from inside the carapace), soft-shelled, or postmolt (early and late papershell).

For some analyses, we separated crabs into two size classes based on maturity because preferred habitats, tolerances, or reproductive needs may be different for different life stages. Most researchers use a carapace width at which ≥50% or ≥80% of the individuals are mature (produce viable eggs or sperm) as a separation boundary. Maturity in males is determined by dissection or by allometric changes in growth of appendages (Hartnoll, 1978; Block and Rebach, 1998; de Lestang et al., 2003). Most female blue crabs in our study area and in Virginia had completed their pubertal molt and thus could reproduce by 12 cm CW (Van Engel, 1958; Fisher, 1999; Stehlik, unpubl. data). In Virginia, 80% of male blue crabs are mature by 11.9 cm (Van Engel, 1990). In lady crabs from the New York coast, nearly all males are mature at ≥6 cm, and females at about 5 cm (Briggs and Grahn[3]). In the middle-Atlantic portion of their range, male rock crabs mature at 5 cm (Haefner, 1976) and some females <5 cm bear eggs (Reilly and Saila, 1978). We chose the following CW boundaries for ≥80% maturity: blue crabs, ≥12 cm both sexes; lady crabs, ≥5 cm both sexes; and rock crabs, males ≥5 cm and females ≥4 cm.

Data on blue, lady, and rock crabs from NEFSC (Northeast Fisheries Science Center, NOAA) fall bottom trawl surveys on the northeast United States continental shelf, 1992–94, were used to expand the geographical viewpoint of our study. The presence of each species in each tow was plotted to show distributions in a representative year, 1992. The plots were made with Surfer® (version 6, Golden Software Inc., Golden, CO). Methods on the trawl surveys are described elsewhere (Azarovitz, 1981).

[3] Briggs, P. T., and C. M. Grahn. 1996. Aspects of the fishery biology of the lady crab (*Ovalipes ocellatus*) in New York waters, 8 p. An in-house paper, New York State Department of Environmental Conservation, 205 North Belle Mead Road, Suite 1, East Setauket, NY, 11733.

Foregut contents were analyzed as in Stehlik (1993). The foregut of each crab was removed and preserved in 70% ethanol. After opening the foregut, we estimated fullness of the gut (from 0% to 100%) visually, and prey items were identified to the lowest possible taxon. The proportion of the total volume of the foregut contents contributed by each prey taxon was estimated visually—a less labor-intensive modification of the methods of Williams (1981), Hyslop (1980), and Steimle et al. (1994). The volume of each prey taxon was multiplied by the percentage of gut fullness. Combining all foreguts, the volumes of prey taxa were listed in descending order. The top 12 prey categories on the list (with the exception of "unidentified" and nonexclusive categories such as Mollusca) were selected for use in most of the subsequent analyses. Foreguts that did not contain prey in any of the 12 categories were dropped from numerical analyses.

The dietary data were grouped in turn by predator species, sex, size class, and collection stratum, and the mean percentage volumes of each of the 12 mutually exclusive prey categories were calculated. For graphic representation of ontogenetic differences in diet, blue and rock crabs were grouped for convenience into 20-mm CW classes, and lady crabs were grouped in 10-mm CW classes because of their smaller size range. For numerical analyses, two maturity classes were used. We used Mann-Whitney tests to compare diets between sexes within predator species and between maturity stages within predator species. The test statistic was a chi square approximation.

Group average cluster analysis was used to graph the separation of diets by species, sexes, maturity stages, and strata by using the 12 prey categories as dependent variables. A Bray-Curtis similarity matrix was generated for each of the groupings, cluster analysis was performed by using Systat® (version 10, SPSS Inc., Chicago, IL), and dendrograms were generated by using the Bray-Curtis values as distance measures (Romesburg, 1984; Marshall and Elliott, 1997). A percent similarity level was chosen *a posteriori* that generated a reasonable number of classes.

Analysis of similarity (ANOSIM) was used to test for statistical significance of dietary differences among predator species and for sexes within species. Analysis of dissimilarity (SIMPER) was used to determine which prey taxa contributed most to the differences between species pairs (Clarke and Warwick, 1994).

Spatial, temporal, and trophic niche breadth and overlap indices were calculated from the number per tow (1992–94) and diets (June 1991–June 1992) of each crab species and sex. Temporal niche and overlap were calculated by month for combined years. Female rock crabs were dropped from consideration of trophic niche overlap due to low sample size.

Niche breadth (Colwell and Futuyama, 1971; Marshall and Elliot, 1997) is a measure of exploitation within a particular resource (for example, substrates or prey taxa within an estuary by a species). Niche breadth values are relative and can be compared only within one study. The highest value corresponds to the broadest niche, or to habitat or a diet generalist rather than to a specialist. Niche breadth (B) was calculated by the formula of Colwell and Futuyama (1971), and modified for measuring trophic niche breadth according to Hines et al. (1990):

$$B = 1/\sum(p_{kj})^2 \text{ from } j = 1 \text{ to } n,$$

where $p_{kj} = N_{kj} / Y_k$ (p_{kj} is the proportion of crabs of species k associated with resource state j);
j = resource states (months, strata, diet categories);
n = number of resource states;
N_{kj} = catch per tow of species k at resource state j; and
Y_k = catch per tow of species k over all resource states.

When trophic niche breadth was calculated,

N_{kj} = total volume of diet category j consumed by predator k;
Y_k = total volume of all diet categories consumed by predator k.

Niche overlap is a measure of the joint use of a resource by two species (Colwell and Futuyama, 1971). Niche overlap (C_{hi}) between species h and i was calculated by the following formula (Colwell and Futuyama, 1971; Hines et al., 1990):

$$C_{hi} = 1 - 0.5\left(\sum | p_{hj} - p_{ij} |\right) \text{ from } j = 1 \text{ to } n,$$

where p_{hj} and p_{ij} are calculated in the same manner as p_{kj} above.

This index ranges from 0 (no overlap) to 1 (complete overlap) and is independent of sample size and differential resource availability (Eggleston et al., 1998).

Results

Temperature and salinity

Bottom water temperature in the study area followed a temperate seasonal cycle. The range during 1992–94 was from 0° to 26.6°C. Using the monthly mean temperature below or above 10°C, and migration cycles of the crabs, we grouped the months into two seasons: winter (November through April) and summer (May through October). The mean temperature in the winter months 1992–94 was 5.5°C, and that for summer was 18.9°C. Temperature nearest the estuary mouth was usually a few degrees lower in summer months and higher in the winter months each year, compared with the average throughout the estuary.

Bottom salinity in the study area ranged from 15.0 to 33.5 ppt. The majority of stations had salinities between

Table 1

Species, sex, number collected (n), and sex ratio (SR, male:female) of all crabs collected during the Hudson-Raritan Estuary trawl survey, June 1991–December 1994. Maturity boundaries are explained in the text. For the subsample examined for stomach contents (June 1991–June 1992), number (n), number of non-empty stomachs, and the mean and range of carapace width (CW, mm) are presented.

Crab species, sex	n collected	SR (m:f) immature	SR (m:f) mature	n stomachs opened	n not empty	Subsample CW	
						Mean	(Range)
Blue, male	2803	1:1.13	1:1.97	167	120	112	(35–185)
Blue, female	4816			272	208	129	(21–169)
Lady, male	14,903	1:1.30	1:2.12	173	124	60	(34–88)
Lady, female	29,681			255	228	55	(30–89)
Atlantic rock, male	15,503	4.65:1	21.43:1	400	281	92	(28–130)
Atlantic rock, female	822			19	14	51	(29–80)
Total	68,528			1286	975		

25 and 30 ppt. Salinity decreased with distance from the bay mouth and in any one month, the difference in salinity between stations at the estuary mouth and those at the westernmost part of the study area was approximately 5–10 ppt.

Catch by species, size, and sex

From June 1991 through December 1994, more than 68,000 blue, lady, and rock crabs were caught in 1200 otter trawl tows (Table 1). Other mega-invertebrates in the tows included the northern moonsnail *(Euspira heros)*, the horseshoe crab *(Limulus polyphemus)*, the American lobster *(Homarus americanus)*, the portly spider crab *(Libinia emarginata)*, the flatclaw hermit crab *(Pagurus pollicaris)*, mud crabs (Xanthidae), and the sea star (*Asterias* sp.)

Catch per tow of crabs by size class increased as they became large enough to be retained by the mesh of the net (Fig. 2). Abundances of female blue and lady crabs in the study area were greater than those of the males. In rock crabs, males predominated (Table 1). Immature blue and lady crabs had sex ratios fairly close to 1:1 (male:female). Sex ratio in mature blue crabs, however, was 1:1.97, and in mature lady crabs, 1:2.12. In all sizes of rock crabs, sex ratio strongly favored males, particularly in mature crabs, in which the ratio was 21.43:1.

Temporal and spatial variation in catch

The maximum relative abundance of blue and lady crabs occurred during the warm months each year, whereas rock crabs were abundant only in the cold months (Fig. 3). Blue crabs were scarce in the otter trawls from January through May or June. We believe that many of them do remain in the study area, but are relatively inactive and are not accessible to otter trawls, as discussed below. Lady crabs migrated into the estuary in April and May and left in October and November.

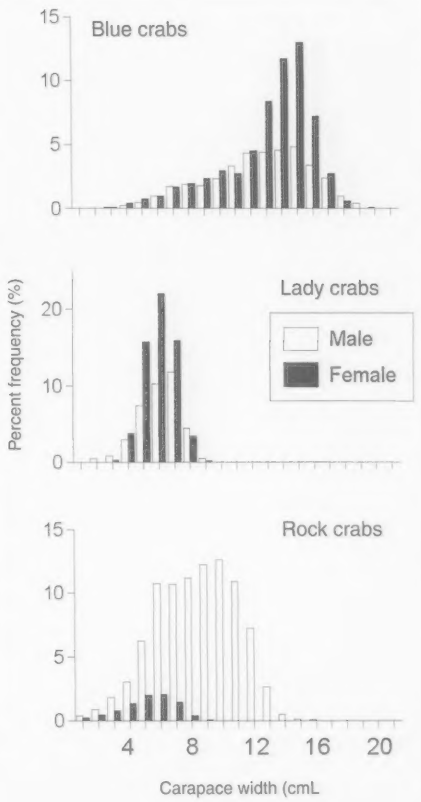

Figure 2

Carapace width (cm) frequencies for male and female blue, lady, and rock crabs collected during the Hudson-Raritan Estuary trawl survey, June 1991–December 1994, by percent frequency of the total catch of each species.

Rock crabs migrated into the estuary in November and gradually left during April, May, and June.

Hundreds of soft and postmolt male rock crabs were caught each winter in the study area (Fig. 4). The highest numbers of molting rock crabs were collected each December and January, and almost all of these crabs had completed molting by February. Very few molting or postmolt blue or lady crabs were caught.

The relative abundances of the three species varied by stratum (Fig. 5, A–C; Fig. 6). Blue crabs of both sexes were caught mainly in strata near river mouths (strata 1, 2, and 6), in the Chapel Hill and Raritan channels (strata 8 and 9) in summer, but mainly in stratum 6 and in the channels in winter. Lady crabs were widely distributed and were caught throughout the study area, including the outer strata close to the ocean. Male rock crabs were most frequently collected in and near the channels and in strata 1 and 6, whereas female rock crabs were sparsely scattered throughout the study area.

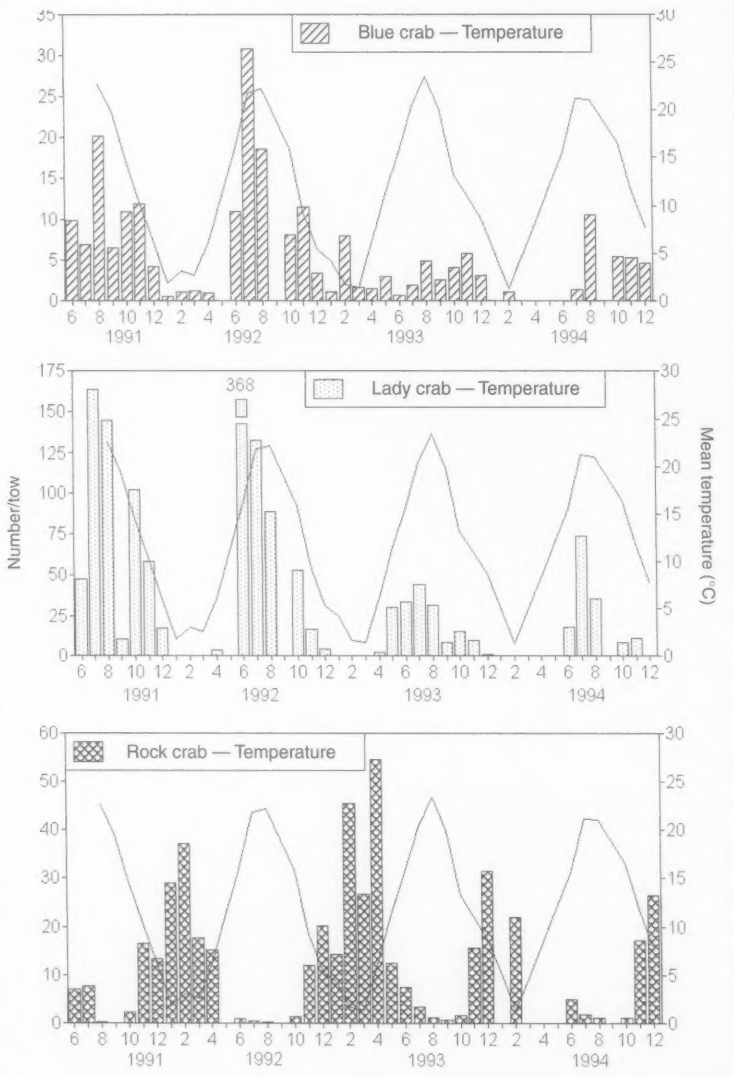

Figure 3

Catch per unit of effort (number/tow) of blue, lady, and rock crabs by month, graphed with mean bottom temperatures, June 1991–December 1994.

Foregut fullness

The total number of blue, lady, and rock crab foreguts examined was 1286. Foregut fullness varied by month in blue and rock crabs. The average fullness of blue crabs was 1% by volume from January through April, and 34% for the rest of the year. Ovigerous blue crabs (n=27) averaged 40% full. Lady crabs' average fullness was 41% during the months when they were present. The average fullness of rock crabs was 30% in all months when they were present; a minimum occurred in January when fullness was 7%. Of 419 rock crabs examined, intermolt crabs (n=293) were 33% full, premolt crabs (n=9) were empty, soft crabs (n=22) were empty, and postmolt crabs (n=95) were 20% full. Some rock crabs in the late postmolt stage were full even though their chelae were not completely calcified.

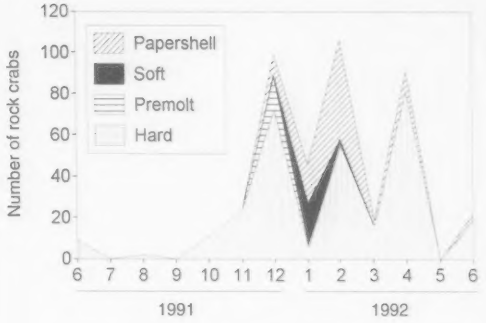

Figure 4

Number of rock crabs at each molt stage by month, 1991–92.

Diet composition

The number of crabs containing food was 975, and they consumed 44 identifiable taxa (Table 2). Most of the mollusks preyed upon were <15 mm in shell length. The crabs consumed were mud crabs (Xanthidae) and juvenile stages of other Anomura and Brachyura. When foreguts were only partially full, well-digested remains of prey frequently could be identified by pieces of shell or opercula, mandibles (for shrimp), or chela tips and carapace fragments (for crabs) (Elner et al., 1985). Recognizable prey taxa were grouped into 12 mutually exclusive categories (Table 3), which contributed 80.1% of the volume of all prey. The prey category "CRABS" represented pooled fragments of all crabs except Paguridae and Xanthidae. Crabs containing prey in one or more of the 12 categories numbered 713.

Differences in diet by predator species, sex, and size

Although the three predator species shared most prey taxa, there were differences in the proportions of the taxa consumed (Fig. 7). Mann-Whitney tests comparing diets of sexes within each species showed only two significant differences out of 36 comparisons. After cluster analysis upon the 12 prey types by species, sex, and size class (immature and mature), the resulting dendrogram showed that diets were most similar between size classes within a species (Fig. 8). Female rock crabs were not included because of their small sample size. When the diets of the three species were compared by analysis of similarity (ANOSIM) they were found to be different (P=0.067), but the data were extremely variable and not normally distributed. No significant differences were found between sexes within species and we therefore pooled sexes within species.

Pairwise comparisons of the species were performed by analysis of dissimilarity (SIMPER). Four taxa contributed significantly to the difference in diets of the first pair: the bivalves *M. edulis* and *M. lateralis* were more important in the diets of lady crabs, and Xanthidae and CRABS, were more important in the diets of blue crabs. The diets of blue crabs and rock crabs were significantly different in four taxa: CRABS and *M. lateralis* were more important for blue crabs, and *M. edulis* and Xanthidae for rock crabs.

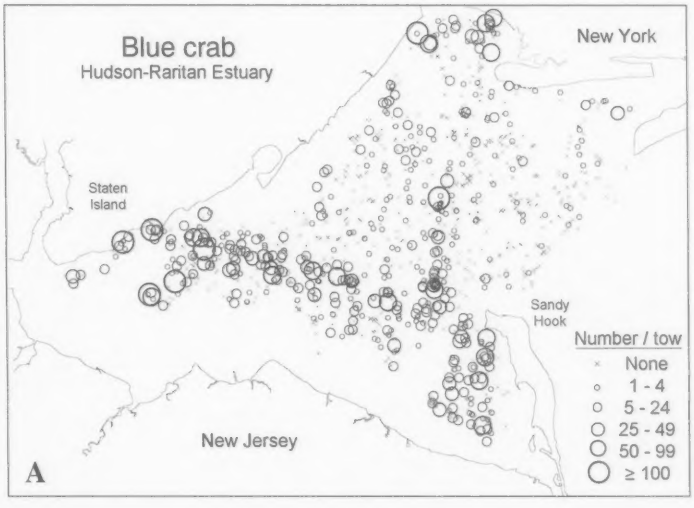

Figure 5

Catch per unit of effort of (**A**) blue, (**B**) lady, and (**C**) rock crabs, sexes combined, January 1992–December 1994, mapped by the midpoint of each tow.

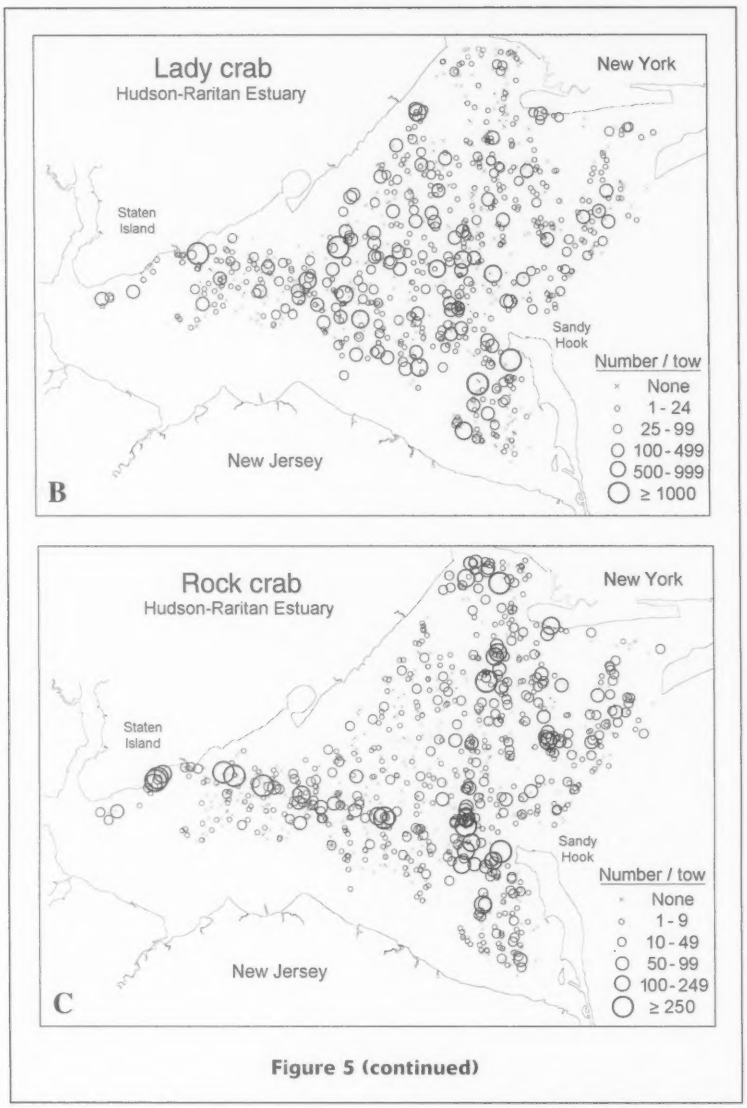

Figure 5 (continued)

The diets of lady crabs and rock crabs were significantly different in two taxa: *M. lateralis* for lady crabs and *M. edulis* for rock crabs.

Within the crab size ranges sampled adequately by our gear, we found some ontogenetic differences in diets (Fig. 9). Notably, amphipods and shrimp were consumed by smaller sizes of all three predators. Certain mollusks, such as *N. trivittatus* and the Atlantic jackknife clam *(Ensis directus)*, increased in occurrence in foreguts with increasing crab size. Smaller lady crabs primarily fed upon *M. lateralis*, but larger ones broadened their diets to include other mollusks such as slippersnails *(Crepidula* spp.) and *M. edulis*. Blue and rock crabs exhibited two peaks in consumption of *M. edulis*: the foreguts of small crabs contained recently settled mussels, whereas those of large crabs contained shell fragments and meat of larger mussels. Xanthidae and Paguridae, small in body size, were eaten mostly by intermediate-size predators.

Mann-Whitney tests showed that amphipods were the only prey significantly different ($P<0.01$) between maturity classes for all three crab species.

Spatial variability in diets

Cluster analysis of the diets by species and stratum defined six groups at 50% similarity (Fig. 10). Group A consisted of lady and rock crabs caught at oceanward

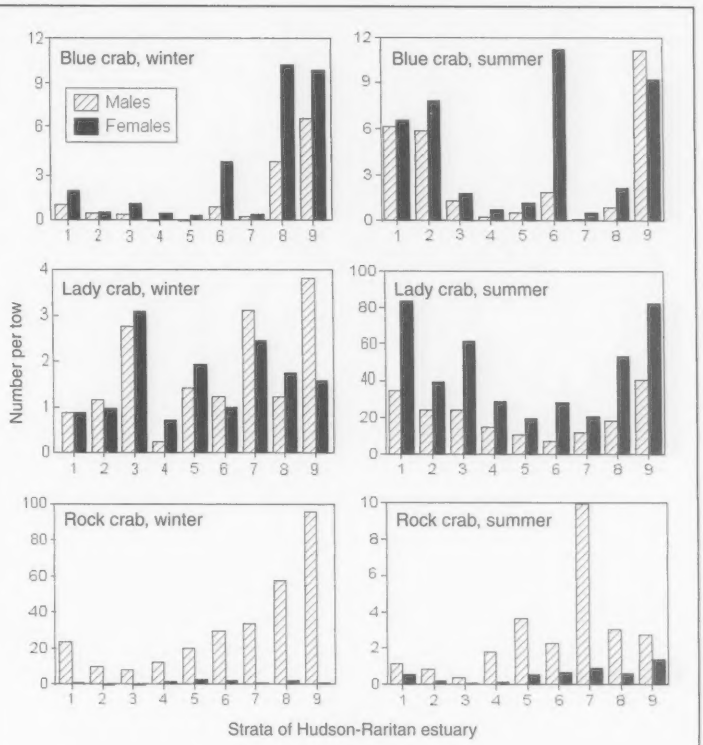

Figure 6

Catch per unit of effort for male and female crabs by seasons and strata, January 1992–December 1994. Note differences in scale among *y* axes.

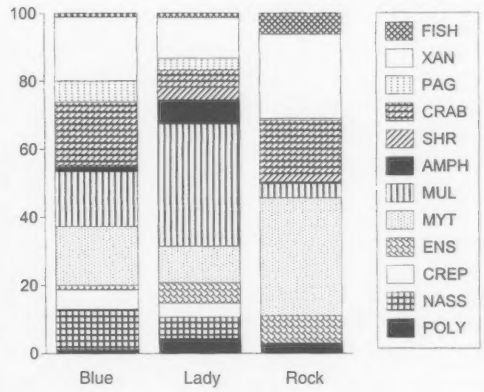

Figure 7

Percent volume of prey (of the 12 chosen categories) of blue, lady, and rock crabs from the Hudson–Raritan Estuary, including all strata and size classes, June 1991–June 1992. n=713. Codes for prey taxa are from Table 3.

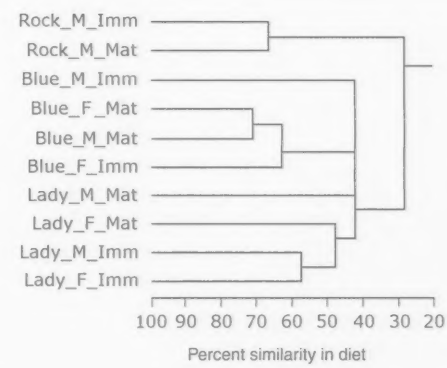

Figure 8

Cluster analysis dendrogram of similarities of the diets of species, sexes (M=male, F=female), and maturity stages (Imm=immature, Mat=mature) of blue, lady, and rock crabs, including all seasons and strata, June 1991–June 1992. Female rock crabs were not included because of the small sample size.

Table 2

Percent frequency of occurrence (%FRE) and percent volume (%VOL) of prey of blue, lady, and rock crabs collected during the trawl survey, June 1991–June 1992. Dashes mean that the dietary item was not found in any stomachs of that crab species. "Unid." means unidentified; "other" means uncommon identified taxa not listed below.

	Blue crab		Lady crab		Rock crab	
	%FRE	%VOL	%FRE	%VOL	%FRE	%VOL
Number of nonempty foreguts	328		352		295	
Plant material	1.5	<0.1	2.8	0.3	4.4	0.1
Hydrozoa	0.6	<0.1	1.4	<0.1	1.4	0.1
Mollusca, unid.	6.7	0.9	3.4	0.9	12.3	14.2
Bivalvia, unid., other	12.2	1.4	11.1	1.6	7.8	4.6
Anadara transversa	—	—	0.3	0.1	—	—
Ensis directus	2.4	0.8	9.9	4.8	8.2	6.2
Lyonsia hyalina	—	—	0.3	<0.1	—	—
Mercenaria mercenaria	0.3	<0.1	0.3	<0.1	—	—
Mulinia lateralis	9.3	13.6	43.5	33.1	6.8	1.4
Mya arenaria	—	—	0.3	0.4	—	—
Mytilus edulis	19.6	14.3	13.9	9.8	28.7	27.3
Nucula proxima	3.4	0.4	5.1	0.6	0.7	0.1
Petricola pholadiformis	1.2	0.1	2.3	0.8	—	—
Pitar morrhuanus	—	—	0.3	<0.1	—	—
Spisula solidissima	—	—	1.7	0.5	—	—
Tellina agilis	4.6	1.5	9.4	2.1	1.4	0.2
Gastropoda, unid., other	6.4	0.7	4.0	0.2	1.0	0.1
Crepidula fornicata, convexa	8.6	2.5	5.4	2.8	0.3	<0.1
Crepidula plana	0.6	<0.1	0.3	<0.1	—	—
Nassarius obsoletus	1.5	1.2	0.3	0.2	0.3	<0.1
Nassarius trivittatus	20.8	6.8	15.6	4.6	0.3	<0.1
Naticidae	—	—	0.6	<0.1	—	—
Rictaxis punctostriatus	—	—	0.9	0.1	0.3	<0.1
Cephalopoda	0.3	0.8	0.6	0.3	—	—
Polychaeta, unid., other	2.4	0.2	4.3	0.3	2.7	0.9
Glyceridae	—	—	0.9	0.3	—	—
Hydroides dianthus	—	—	0.3	<0.1	—	—
Nephtyidae	—	—	0.9	0.3	—	—
Nereidae	1.5	0.3	1.7	0.1	0.7	0.3
Pherusa affinis	—	—	—	—	0.3	0.1
Pectinaria gouldii	2.4	0.8	15.9	2.4	0.7	<0.1
Polynoidae	—	—	0.3	<0.1	1.4	0.1
Insecta	0.3	<0.1	—	—	—	—
Crustacea, unid., other	4.9	0.6	3.4	0.3	5.8	1.4
Amphipoda, unid., other	2.8	0.6	7.7	1.4	1.4	0.2
Ampelisca sp.	1.5	0.6	6.8	1.3	0.7	0.4
Corophium sp.	0.6	0.2	1.7	0.7	—	—
Gammarus sp.	—	—	3.1	3.3	—	—
Mysidacea	—	—	0.3	<0.1	—	—
Caridean shrimp, unid., other	0.6	<0.1	2.0	0.1	0.7	<0.1
Crangon septemspinosa	2.8	0.6	6.0	2.3	3.1	2.0
Crabs unid., other[1]	17.7	7.4	8.8	2.7	11.3	4.2
Callinectes sapidus	0.3	<0.1	0.6	0.1	1.4	1.8
Cancer irroratus	1.5	1.0	2.3	0.5	2.0	1.4
Libinia sp.	0.9	0.6	0.9	0.6	1.0	0.5

continued

Table 2 (continued)

	Blue crab		Lady crab		Rock crab	
	%FRE	%VOL	%FRE	%VOL	%FRE	%VOL
Crabs unid., other[1] (cont.)	0.6	<0.1	2.0	0.1	0.7	<0.1
Ovalipes ocellatus	3.4	3.6	0.6	0.2	1.0	1.0
Pagurus longicarpus	2.1	1.5	1.7	0.6	—	—
Pagurus sp.	8.0	4.3	5.4	2.3	1.7	0.1
Xanthidae	21.1	20.8	15.9	10.6	21.2	18.4
Fish remains and scales	2.1	0.9	3.4	0.7	6.4	3.7
Inorganic debris, sand, mud	0.9	<0.1	0.9	0.2	0.7	0.1
Shell hash	2.4	1.5	—	—	—	—
Human-made objects	4.0	<0.1	4.8	<0.1	1.7	<0.1
Unid. organic matter	—	9.2	—	5.3	—	9.0
Mytilus byssus	1.8	<0.1	2.0	<0.1	3.1	0.2

Table 3

Twelve mutually exclusive prey categories that contributed 80% of the prey volume of all crabs examined. Codes are used in Figures 7 and 9. "Other" means uncommon identified taxa.

CODE	Category	Identifiable species
NASS	mud snails	*Nassarius trivittatus, N. obsoletus*
CREP	slipper shells	*Crepidula fornicata, C. convexa, C. plana*
ENS	razor clam	*Ensis directus*
MYT	blue mussel	*Mytilus edulis*
MUL	dwarf surfclam	*Mulinia lateralis*
POLY	Polychaeta	all
AMPH	Amphipoda	all
SHR	shrimp	*Crangon septemspinosa,* unid., other
CRAB	crabs	*Libinia* sp., *Cancer irroratus, Ovalipes ocellatus, Callinectes sapidus,* crab unid., and others excluding Paguridae or Xanthidae
PAG	hermit crabs	*Pagurus acadianus, P. longicarpus,* unid., other
XAN	mud crabs	Xanthidae: *Dyspanopeus sayi,* unid., other
FISH	fish, fish scales	all

outer strata (4, 5, and 7) that consumed large quantities of *M. edulis*. Clumps of recently settled and larger mussels were frequently collected in trawl nets in these strata. Group B contained crabs from Gravesend Bay, (stratum 6) that ate primarily *M. edulis* and *M. lateralis*. Group C contained crabs caught in the siltier southern strata and nearby channel (strata 1, 2, and 9) that consumed mainly *M. lateralis*, *M. edulis*, and CRABS. Group D consisted of rock crabs collected at inner strata (2, 3, and 8) that fed primarily upon *E. directus* and Xanthidae. *Ensis directus* was most common in diets in the northern sandier strata (strata 3, 5, 6, and 7). Groups E and F consisted of lady and rock crabs that consumed mainly *M. lateralis*. Four species-stratum combinations did not cluster with any groups.

Temporal, spatial, and trophic niche breadth and overlap

Niche breadth and overlap were calculated for both sexes of the three crab species (Table 4). Lady crabs of both sexes had the narrowest temporal niches (3.896 and 4.592), reflecting their presence in the estuary strictly in warm months. The temporal niche breadth of female blue crabs (8.187) was greatest, reflecting their year-long presence in the study area, even in the cold months when many males remain in rivers. The temporal overlaps of

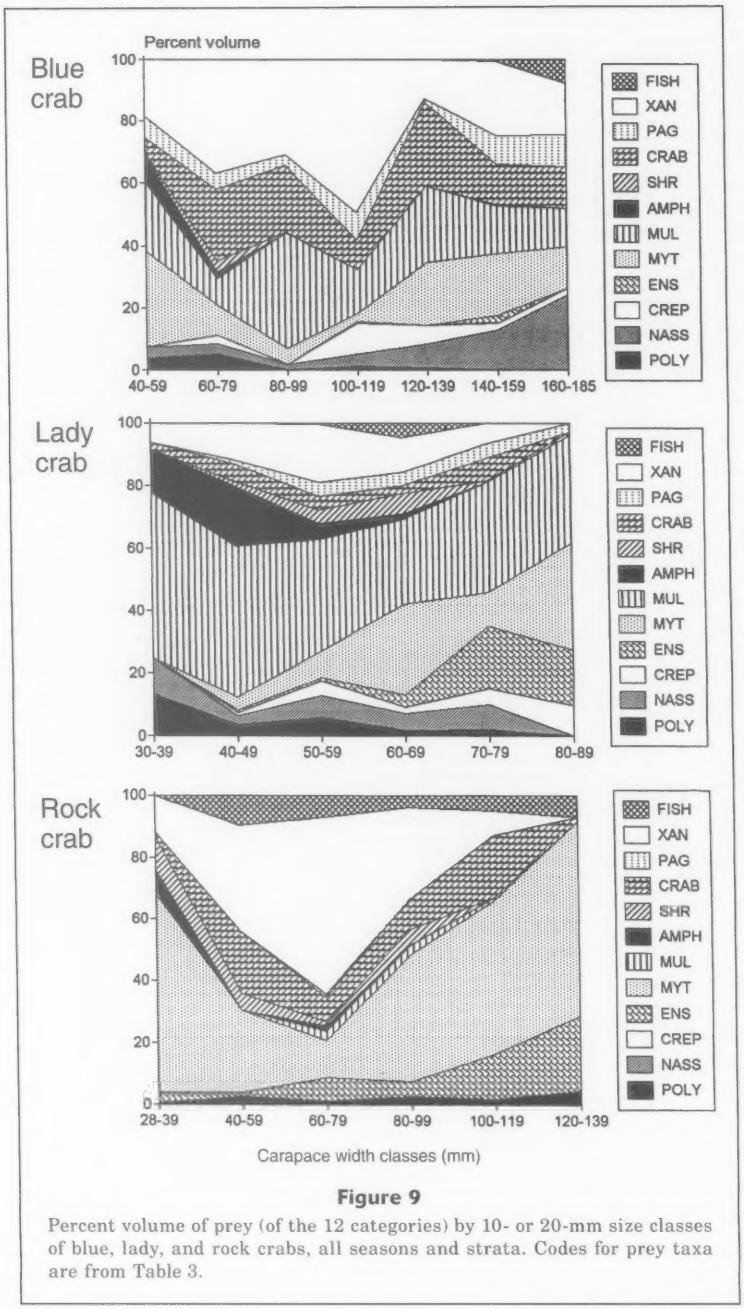

Figure 9

Percent volume of prey (of the 12 categories) by 10- or 20-mm size classes of blue, lady, and rock crabs, all seasons and strata. Codes for prey taxa are from Table 3.

male and female lady crabs with male rock crabs were the lowest in the matrix (0.149 and 0.186).

The spatial niche breadths of lady crabs were largest (7.320 and 7.324) (a result of their nonaggregative distribution throughout the study area), whereas the other two species tended to aggregate in certain locations, particularly in or near channels. Female rock crabs also had a broad spatial niche, although they were caught much less frequently than the other groups. Spatial overlap was highest within species, particularly between male and female lady crabs (0.908).

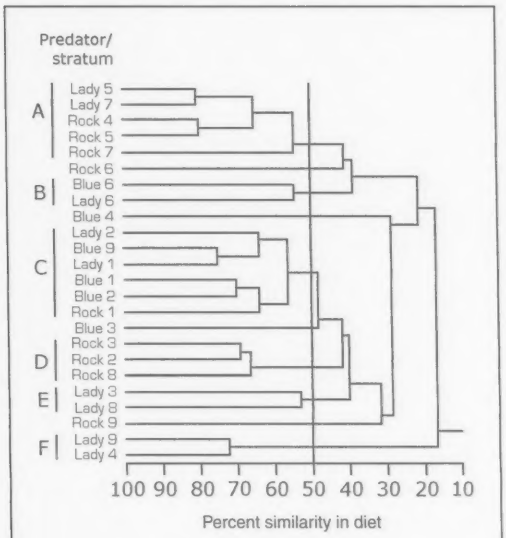

Figure 10

Cluster analysis dendrogram of the diets of blue, lady, and rock crabs from the nine strata of the Hudson-Raritan Estuary. The vertical line at 50% similarity defines groups A–F.

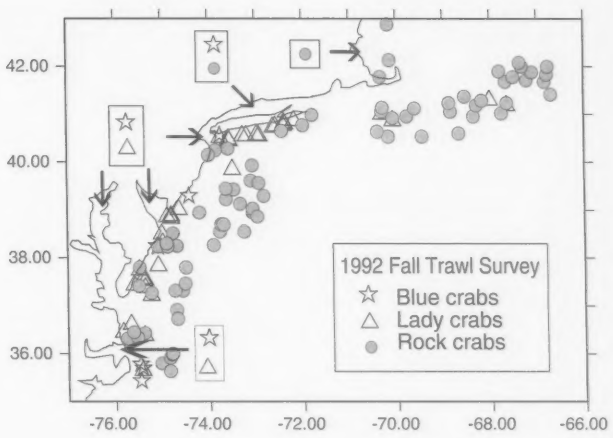

Figure 11

Presence of blue, lady, and rock crabs at stations from the fall 1992 bottom trawl survey, (Northeast Fisheries Science Center, Woods Hole, MA). Each point represents presence at a station. Occurrence inside the estuaries(boxed symbols) was derived from the literature cited in this article.

Trophic niche breadth was greatest in male and female blue crabs (5.234 and 6.563) and male lady crabs (6.166) (Table 4). It was narrowest for female rock crabs, but sample size was low. Overlap was highest within species: blue crab males and females (0.819), and lady crab males and females (0.861). Overlap was lowest between lady and rock crabs, sexes combined (0.427).

Discussion

Temporal and spatial overlap within the estuary

The scatter plots (Fig. 5) and spatial niche overlap indices indicate substantial likelihood of co-occurrence and encounter among blue, lady, and rock crabs in the Hudson-Raritan Estuary. However, the species were not all active in the study area at the same time. Seasonal migration and winter torpor are two mechanisms that, at times, prevent interspecies encounters. Rock crabs had low temporal overlaps with blue and lady crabs because when rock crabs migrate in from the coastal ocean, lady crabs migrate out and blue crabs become less active and sometimes bury themselves. Although otter trawling does not adequately sample buried blue crabs, commercial crab dredgers catch large numbers of overwintering blue crabs from December through March in and near the Raritan and Chapel Hill channels (Stehlik et al., 1998).

Temporal overlap between blue crabs and lady crabs was fairly high because of their co-occurrence in the warm months. It was expected that intra-estuarine spatial separation might minimize contact between these species because they are reported to prefer different substrates. The blue crab is known to occupy a variety of substrate types, including sand, mud, and submerged vegetation (Milliken and Williams, 1984; Wilson et al. 1990), whereas the lady crab is primarily collected on sand (Williams and Wigley, 1977). The lady crab buries itself in sand more readily than in mud (Barshaw and Able, 1990) and it is able to forage more efficiently in sand than in sand-gravel or sand-shell substrates (Sponaugle and Lawton, 1990). However, as shown in Figures 5 and 6, lady crabs were not confined to sandy strata but were most abundant on the fine-grained sediment strata 1, 2, and 9.

The pattern of seasonal estuarine use by blue and lady crabs is not unique to the Hudson-Raritan Estuary. Other estuaries in which the two Portunidae are abundant in summer months but uncommon in winter are Barnegat Bay, NJ (Milstein et al., 1977; pers. observ.), Delaware Bay (Winget et al., 1974), and Chesapeake Bay (Haefner and Van Engel, 1975).

Rock crabs undergo seasonal migrations from coastal waters into and out of estuaries, but the timing differs by latitude. In Canada, the Gulf of Maine, and northern Massachusetts, rock crabs are much more abundant in immediate coastal waters, estuaries, and in the intertidal zone in warmer months (Krouse, 1972; Scarratt and Lowe, 1972). Rock crabs are more numerous in Narragansett Bay, Rhode Island, in warmer months (Jeffries, 1966; Clancy[4]). Juveniles are present inside

[4] Clancy, M. 2002. Personal commun. Boston University, College of General Studies, Division of Natural Science, Boston, MA, 02115.

Table 4

Niche breadth and overlap for temporal, spatial, and trophic dimensions among blue, lady, and rock crabs. For temporal and spatial niches, all crabs (of all sizes) collected in 1992–94 are included. For trophic analyses, only the crabs containing one or more of the 12 prey categories were included. Female rock crabs were not included in trophic overlap because of the small sample size.

	Number of crabs	Mean CW, mm	Niche breadth		Overlap matrices				
Temporal niche									
(n=12 months, 1992–94)					BCF	LCM	LCF	RCM	RCF
Blue crab male (BCM)	2191	125	6.104	BCM	0.854	0.604	0.618	0.297	0.463
Blue crab female (BCF)	3483	129	8.187	BCF		0.649	0.576	0.376	0.564
Lady crab male (LCM)	11883	62	4.592	LCM			0.894	0.186	0.417
Lady crab female (LCF)	25312	61	3.896	LCF				0.149	0.339
Rock crab male (RCM)	14530	85	6.764	RCM					0.479
Rock crab female (RCF)	778	51	5.782						
Spatial niche									
(n=9 strata, 1992–94)					BCF	LCM	LCF	RCM	RCF
Blue crab male	2191	125	3.927	BCM	0.757	0.720	0.703	0.675	0.474
Blue crab female	3483	129	5.343	BCF		0.679	0.685	0.746	0.641
Lady crab male	11883	62	7.324	LCM			0.908	0.677	0.616
Lady crab female	25312	61	7.320	LCF				0.678	0.638
Rock crab male	14530	85	5.447	RCM					0.763
Rock crab female	778	51	7.191						
Trophic niche									
(n=12 prey categories, 1991–92)					BCF	LCM	LCF	RCM	
Blue crab male	84	111.0	5.234	BCM	0.819	0.570	0.580	0.576	
Blue crab female	139	127.9	6.563	BCF		0.629	0.651	0.609	
Lady crab male	98	59.4	6.166	LCM			0.861	0.437	
Lady crab female	200	54.9	4.655	LCF				0.417	
Rock crab male	181	88.8	4.139						
Rock crab female	11	53.7	2.620						
Trophic niche, sexes combined									
(n=12 prey categories, 1991–92)					LC	RC			
Blue crab (BC)	223	121.6	6.250	BC	0.628	0.623			
Lady crab (LC)	298	56.4	5.140	LC		0.427			
Rock crab (RC)	192	86.8	4.008						

that bay all year (Reilly and Saila, 1978). In contrast, in Delaware Bay and Chesapeake Bay they occur in coastal waters and estuaries mainly in colder months (Winget et al., 1974; Haefner and Van Engel, 1975; Haefner, 1976). Our data showed that rock crabs in the Hudson-Raritan Estuary conform to the pattern of migration typical of the latter southern bays.

A crossroads or overlap in distribution of the three crab species is more evident when a broader area on the continental shelf from Cape Cod to Cape Hatteras is considered. Crab presence was plotted by using data from the fall 1992 continental shelf trawl survey (Fig. 11). Fall surveys are done in September and October when waters are still warm. In the coastal waters off Raritan, Delaware, and Chesapeake Bays, blue and lady crabs were collected, whereas rock crabs were collected mainly on the central shelf. Estuarine presence in warm months, compiled from citations in the present study, is marked by symbols.

Sex ratios

In the Hudson-Raritan Estuary, sex ratios of blue, lady, and rock crabs were different from 1:1. In mature blue crabs, the sex ratio favored females because the study area is in the deeper oceanward portion of the estuarine system, where females release their eggs and overwinter. Many males spend their entire lives in water of relatively low salinity (Van Engel, 1958), such as is found in the nearby Hudson, Raritan, and Navesink-Shrewsbury rivers. In the Navesink River, the sex ratio of male to female blue crabs ≥12 cm over a two-year period was 2.6:1 (Meise and Stehlik, 2003).

In the Hudson-Raritan Estuary, female lady crabs ≥5 cm outnumbered males 2:1. Many of these females were ovigerous and therefore estuarine use may be related to reproduction. We were unable to locate published reports of lady crabs or other *Ovalipes* spp. mating locations, single-sex migrations, or locations of lar-

val release, any of which might be a reason for the use of the estuaries by female lady crabs.

The rock crabs that enter the estuary were predominantly males, and many females may never enter the estuary. Males use the estuary to molt, and possibly to avoid predators offshore. In comparison, on the northwest Atlantic continental shelf, the sex ratio in winter dredge collections was 1:2.2 males:females (Stehlik et al., 1991).

Feeding periodicity

Food consumption in crabs is affected by daily and seasonal cycles, temperature changes, reproductive rhythms, and molt (Warner, 1977; Stevens et al., 1982; Ryer, 1987; Mantelatto, 2001). In our study area, blue crabs ate little when inactive during the winter months, as reported above. Choy (1986) reported less feeding during egg-brooding in Portunidae, but in our study we found that fullness was about 40% in both egg-bearing and non-egg-bearing females in summer. A lack of feeding before and during molt, until calcification has sufficiently progressed, is typical of crabs (Warner, 1977). Empty stomachs in premolt and soft rock crabs in our study supported this observation.

Diet composition

We found that in the Hudson-Raritan Estuary, the most important prey items of blue crabs by volume were Xanthidae, then the mollusks *M. edulis* and *M. lateralis*, whereas only 2% of the prey volume was from cannibalism. In contrast, small blue crabs are of major importance in the diets of large blue crabs in Florida (Laughlin, 1982) and Maryland (Hines et al., 1990), and cannibalism is the source of more than 75% of the mortality of juveniles near estuarine shores (Hines and Ruiz, 1995). The major targets of cannibalism, early instars or molting juveniles, may be more abundant in rivers adjacent to our study area (Meise and Stehlik, 2003).

The diets of rock crabs in estuarine and coastal Canada and Maine usually contained a larger number of prey categories than did the diets in the present study (Scarratt and Lowe, 1972; Drummond-Davis et al., 1982; Hudon and Lamarche, 1989; Ojeda and Dearborn, 1991). These northern studies were done on rock, boulders, cobble, sand, and algal beds, where the diversity of habitats within a study area may offer a larger assortment of potential prey than the soft-bottom habitat of our estuary.

In the Hudson-Raritan Estuary, juveniles of commercially or recreationally harvested species were rarely consumed by the three species of crabs. Among mollusks, *M. arenaria* and *M. mercenaria* were scarce in crab stomachs, perhaps because other taxa such as *M. lateralis, N. trivittatus*, and Xanthidae provided abundant prey. The other commercially important species eaten by crabs was the blue crab juvenile, but infrequently as mentioned above.

Differences in diet among species, sexes, and size classes of predators

Our data did not support our hypotheses, based on existing studies, that blue, lady, and rock crabs would have different diets as a consequence of their species-specific body and chela structures. Blue and lady crabs (unlike rock crabs) swim, allowing them a greater foraging area than rock crabs. Chela structure affects the type and size of prey that can be crushed (Vermeij, 1978; Seed and Hughes, 1995; Behrens Yamada and Boulding, 1998). In Portunidae, the long chelae (in relation to their CW) have short muscle fibers better suited to quick grabbing than to prolonged crushing (Warner and Jones, 1976; Seed and Hughes, 1997). The chelae of Cancridae are monomorphic (same characteristics left and right sides), have relatively short, stout teeth, and close relatively slowly because of their muscle fibers (Warner and Jones, 1976). Chela crushing force (Newtons), measured with a force transducer, is positively correlated with chela height and thickness (Govind and Blundon, 1985; Block and Rebach, 1998). Although the chela structures of blue and rock crabs are quite different, the chelae of mature rock crabs (9–13.5 cm CW) generate crushing forces comparable to those of cutter and crusher chelae of mature male blue crabs (12–16 cm) (Govind and Blundon, 1985).

Chela crushing force in mature blue and rock crabs is likely to be more than sufficient for successful foraging upon all but the largest prey (Block and Rebach, 1998) and may not be a major determinant of diet. In fact, crabs often prey upon small or young bivalves rather than on large sizes, perhaps because the latter require more handling time and may damage chelae (Juanes, 1992; Seed and Hughes, 1995). Because Portunidae swim and have more versatile chelae, they may be expected to have broader trophic niches than Cancridae. In our study, blue crabs had the broadest trophic niche, lady crabs had an intermediate trophic niche, and rock crabs had the narrowest trophic niche.

We found no significant differences in diet by sex within species. Sexual dimorphism within a crab species accelerates after puberty (Hartnoll, 1978), but our study included many immature crabs. Some experimenters using force transducers found no significant difference in crushing force between the sexes of blue crabs of a broad size range (Blundon and Kennedy, 1982; Seed and Hughes, 1997), but in blue crabs >135 mm, males produced significantly more force than females (Eggleston, 1990). Sexual dimorphism is found in chela length, but not chela height, in lady crabs (significantly different slopes of CL/CW by regression; Stehlik, unpubl. data).

Carapace width and the proportion of chela height to carapace width are positively correlated with crushing force, which makes it possible for larger crabs to consume larger, harder-shelled mollusks or crustaceans (Hartnoll, 1978; Block and Rebach, 1998). The largest lady crabs do not grow to the carapace widths or chela lengths of mature blue crabs; therefore the force

of their chelae cannot match those of blue crabs. As they grow, Cancridae and Portunidae undergo shifts in diet, and may be divided into ontogenetically distinct trophic units (Laughlin, 1982; Stevens et al., 1982; Stoner and Buchanan, 1990; Rosas et al., 1994). In our study, larger crabs dropped amphipods and shrimp from their diets, but otherwise only minor changes occurred in prey identity and relative volumes of prey taxa among size classes (Fig. 9). An interesting ontogenetic shift was in the size of prey eaten: small crabs ate small individuals of prey taxa, such as *M. edulis*, and Xanthidae, and large crabs ate large individuals of the same taxa. Thus in our study the influence of physical structure upon diet was greater as body size increased within a species than among species.

Spatial variability and overlap in diets

The three predators were scattered throughout the cluster diagram of diet among strata of the estuary (Fig. 10), yet crabs from inner and outer groups of strata usually clustered separately. We concluded that location influenced diet more than did predator identity. The inner, outer, and channel strata differ in depth, sediment type, currents, and mean temperature, and therefore in benthic and epibenthic prey assemblages. Our results support the concept that these species are mainly opportunistic in diet, as was suggested for blue crabs (Laughlin, 1982), and rock crabs (Hudon and Lamarche, 1989). The Hudson-Raritan and other nearby coastal and estuarine areas from Long Island Sound to Chesapeake Bay are crossroads where blue, lady, and rock crabs share space and resources.

Acknowledgments

We thank those who helped design and carry out the Hudson-Raritan Estuary trawl surveys, especially Stuart Wilk, Anthony Pacheco, and Eileen MacHaffie. We also thank Fred Farwell, Sherman Kingsley, and the NOAA Corps captains and crew. Suellen Fromm was instrumental in obtaining data from NEFSC trawl surveys. We thank the scientists who shared their opinions and unpublished data. We are indebted to colleagues Mary Fabrizio, Clyde MacKenzie, John Manderson, Carol Meise, Frank Steimle, Allan Stoner, and anonymous reviewers who helped improve the manuscript. This paper is dedicated to the memory of Tony Pacheco.

Literature cited

Auster, P. J., and R. E. DeGoursey.
1994. Winter predation on blue crabs, *Callinectes sapidus*, by starfish *Asterias forbesi*. J. Shellfish Res. 13:361–366.

Azarovitz, T. A.
1981. A brief historical review of the Woods Hole Laboratory trawl survey time series. *In* Bottom trawl surveys (Doubleday, W.G., and D. Rivard, eds.), p. 62–67. Can. Spec. Publ. Fish. Aquat. Sci. 58.

Barshaw, D. E., and K. W. Able.
1990. Deep burial as a refuge for lady crabs, *Ovalipes ocellatus*: comparisons with blue crabs, *Callinectes sapidus*. Mar. Ecol. Prog. Ser. 66:75–79.

Behrens Yamada, S., and E. G. Boulding.
1998. Claw morphology, prey size selection and foraging efficiency in generalist and specialist shell-breaking crabs. J. Exp. Mar. Biol. Ecol. 220:191–211.

Birchard, G. F., L. Drolet, and L. H. Mantel.
1982. The effect of reduced salinity on osmoregulation and oxygen consumption in the lady crab, *Ovalipes ocellatus* (Herbst). Comp. Biochem. Physiol. 71A:321–324.

Block, J. D., and S. Rebach.
1998. Correlates of claw strength in the rock crab, *Cancer irroratus* (Decapoda, Brachyura). Crustaceana 71:468–473.

Blundon, J. A., and V. S. Kennedy.
1982. Mechanical and behavioral aspects of blue crab, *Callinectes sapidus* (Rathbun), predation on Chesapeake Bay bivalves. J. Exp. Mar. Biol. Ecol. 65:47–65.

Briggs, P. T.
1998. New York's blue crab *(Callinectes sapidus)* fisheries through the years. J. Shellfish Res. 17:487–491.

Choy, S. C.
1986. Natural diet and feeding habits of the crabs *Liocarcinus puber* and *L. holsatus* (Decapoda, Brachyura, Portunidae). Mar. Ecol. Prog. Ser. 31:87–99.

Clarke, K. R., and R. M. Warwick.
1994. Change in marine communities: an approach to statistical analysis and interpretation, 144 p. National Environmental Research Council, UK.

Coch, N. K.
1986. Sediment characteristics and facies distributions in the Hudson system. *In* Sedimentation in the Hudson system: the Hudson River and contiguous waterways (N. K.Coch and H. J. Bokuniewicz, eds.), p. 109–129. Northeastern Geology (spec. issue) 8.

Colwell, R. K., and D. J. Futuyama.
1971. On the measurement of niche breadth and overlap. Ecology 52:567–576.

de Lestang, S., N. G. Hall, and I. C. Potter.
2003. Reproductive biology of the blue swimmer crab (*Portunus pelagicus*, Decapoda: Portunidae) in five bodies of water on the west coast of Australia. Fish. Bull. 101:745–757.

Drummond-Davis, N. C., K. H. Mann, and R. A. Pottle.
1982. Some estimates of population density and feeding habits of the rock crab, *Cancer irroratus*, in a kelp bed in Nova Scotia. Can. J. Fish. Aquat. Sci. 39:636–639.

Eggleston, D. B.
1990. Functional responses of blue crabs *Callinectes sapidus* Rathbun feeding on juvenile oysters *Crassostrea virginica* (Gmelin): effects of predator sex and size, and prey size. J. Exp. Mar. Biol. Ecol. 143:73–90.

Eggleston, D. B., J. J. Grover, and R. N. Lipcius.
1998. Ontogenetic diet shifts in Nassau grouper: trophic linkages and predatory impact. Bull. Mar. Sci. 63:111–126.

Elner, R. W., P. G. Beninger, L. E. Linkletter, and S. Lanteigne.
1985. Guide to indicator fragments of principal prey taxa in the stomachs of two common Atlantic crab species: *Cancer borealis* Stimpson, 1859 and *Cancer irroratus* Say, 1817. Can. Tech. Rep. Fish. Aquat. Sci. 1403:1–20.

Fisher, M. R.
1999. Effect of temperature and salinity on size at maturity of female blue crabs. Trans. Am. Fish. Soc. 128:499–506.
Govind, C. K., and J. A. Blundon.
1985. Form and function of the asymmetric chelae in blue crabs with normal and reversed handedness. Biol. Bull. 168:221–231.
Guerin, J. L., and W. B. Stickle.
1992. Effect of salinity gradients on the tolerance and bioenergetics of juvenile blue crabs (*Callinectes sapidus*) from waters of different environmental salinities. Mar. Biol. 114:391–396.
Haefner, P. A., Jr.
1976. Distribution, reproduction and moulting of the rock crab, *Cancer irroratus* Say 1917, in the mid-Atlantic Bight. J. Nat. Hist. 10:377–397.
Haefner, P. A., Jr., and W. A. Van Engel.
1975. Aspects of molting, growth and survival of male rock crabs, *Cancer irroratus*, in Chesapeake Bay. Chesapeake Sci. 16:253–265.
Hartnoll, R. G.
1978. The determination of relative growth in Crustacea. Crustaceana 34:281–293.
Hines, A. H., R. N. Lipcius, and A. M. Haddon.
1987. Population dynamics and habitat partitioning by sex, size, and molt stage of blue crabs *Callinectes sapidus* in a subestuary of Chesapeake Bay. Mar. Ecol. Prog. Ser. 36:55–64.
Hines, A. H., A. M. Haddon, and L. A. Wiechert.
1990. Guild structure and foraging impact of blue crabs and epibenthic fish in a subestuary of Chesapeake Bay. Mar. Ecol. Prog. Ser. 67:105–126.
Hines, A. H., and G. M. Ruiz.
1995. Temporal variation in juvenile blue crab mortality: nearshore shallows and cannibalism in Chesapeake Bay. Bull. Mar. Sci. 57:884–901.
Hudon, C., and G. Lamarche.
1989. Niche segregation between American lobster *Homarus americanus* and rock crab *Cancer irroratus*. Mar. Ecol. Prog. Ser. 52:155–168.
Hyslop, E. J.
1980. Stomach contents analysis—a review of methods and their application. J. Fish. Biol. 17:411–429.
Jeffries, H. P.
1966. Partitioning of the estuarine environment by two species of *Cancer*. Ecology 47:477–481.
Jones, C. R., C. T. Fray, and J. R. Schubel.
1979. Textural properties of surficial sediments of Lower Bay of New York Harbor. Special Report 21, 113 p. Marine Sciences Research Center, State University of New York, Stony Brook, NY.
Juanes, F.
1992. Why do decapod crustaceans prefer small-sized molluscan prey? Mar. Ecol. Prog. Ser. 87:239–249.
Krouse, J. S.
1972. Some life history aspects of the rock crab, *Cancer irroratus*, in the Gulf of Maine. J. Fish. Res. Board Can. 29:1479–1482.
Laughlin, R. A.
1982. Feeding habits of the blue crab, *Callinectes sapidus* Rathbun, in the Appalachicola estuary, Florida. Bull. Mar. Sci. 32:807–822.
Leffler, C. W.
1972. Some effects of temperature on the growth and metabolic rate of juvenile blue crabs, *Callinectes sapidus*, in the laboratory. Mar. Biol. 14:104–110.
MacKenzie, C. L., Jr.
1990. History of the fisheries of Raritan Bay, New York and New Jersey. Mar. Fish. Rev. 52:1–45.
1997. The U. S. molluscan fisheries from Massachusetts Bay through Raritan Bay, N. J. and N. Y. *In* The history, present condition, and future of the molluscan fisheries of North and Central America and Europe. Volume I, Atlantic and Gulf Coasts (C. L. MacKenzie, Jr., V. G. Burrell Jr., A. Rosenfield, and W. L. Hobart, eds.), p. 87–118. NOAA Tech. Rep. 127.
Mantelatto, F. L. M, and R. A. Christofoletti.
2001. Natural feeding activity of the crab *Callinectes ornatus* (Portunidae) in Ubatuba Bay (Sao Paulo, Brazil): influence of season, sex, size and molt stage. Mar. Biol. 138:585–594.
Marshall, S., and M. Elliott.
1997. A comparison of univariate and multivariate numerical and graphical techniques for determining inter- and intraspecific feeding relationships in estuarine fish. J. Fish Biol. 51:526–545.
McDermott, J. J.
1983. Food web in the surf zone of an exposed sandy beach along the mid-Atlantic coast of the United States. *In* Sandy beaches as ecosystems (A. McLachlan and T. Erasmus eds.), p. 529–538. Dr. W. Junk, The Hague, Netherlands.
Meise, C. J., and L. L. Stehlik.
2003. Habitat use, temporal abundance variability, and diet of blue crabs from a New Jersey estuarine system. Estuaries 26:731–745.
Milliken, M. R., and A. B. Williams.
1984. Synopsis of biological data on the blue crab, *Callinectes sapidus* Rathbun. NOAA Tech. Rep. NMFS 1, 39 p.
Milstein, C. B., D. T. Thomas, and associates.
1977. Summary of ecological studies for 1972–1975 in the bays and other waterways near Little Egg Inlet and in the ocean in the vicinity of the proposed site for the Atlantic Generating Station, New Jersey. Bull. 18, 757 p. Ichthyological Associates, Inc., Ithaca, NY.
Ojeda, F. P., and J. H. Dearborn.
1991. Feeding ecology of mobile benthic predators: experimental analyses of their influence in Atlantic rocky subtidal communities of the Gulf of Maine. J. Exp. Mar. Biol. Ecol. 149:13–44.
Reilly, P. N., and S. B. Saila.
1978 Biology and ecology of the rock crab, *Cancer irroratus* Say, 1817, in southern New England waters (Decapoda, Brachyura). Crustaceana 34:121–140.
Romesburg, H. C.
1984. Cluster analysis for researchers, 334 p. Lifetime Learning Publications, Belmont, CA.
Ropes, J. W.
1989. The food habits of five crab species at Pettaquamscutt River, Rhode Island. Fish. Bull. 87:197–204.
Rosas, C., E. Lazaro-Chavez, and F. Buckle-Ramirez.
1994. Feeding habits and food niche segregation of *Callinectes sapidus*, *C. rathbunae* and *C. similis* in a subtropical coastal lagoon of the Gulf of Mexico. J. Crustacean Biol. 14:371–382.
Rountree, R. A., and K. W. Able.
1992. Fauna of polyhaline subtidal marsh creeks in southern New Jersey: composition, abundance and biomass. Estuaries 15:171–185.

Ryer, C. H.
1987. Temporal patterns of feeding by blue crabs (*Callinectes sapidus*) in a tidal-marsh creek and adjacent seagrass meadow in the lower Chesapeake Bay. Estuaries 10:136–140.
Scarratt, D. J., and R. Lowe.
1972. Biology of the rock crab (*Cancer irroratus*) in Northumberland Strait. J. Fish. Res. Board Canada 29:161–166.
Seed, R., and R. N. Hughes.
1995. Criteria for prey size-selection in molliscivorous crabs with contrasting claw morphologies J. Exp. Mar. Biol. Ecol. 193:177–195.
1997. Chelal characteristics and foraging behavior of the blue crab *Callinectes sapidus* Rathbun. Estuar. Coastal Shelf Sci. 44:221–229.
Sponaugle, S., and P. Lawton.
1990. Portunid crab predation on juvenile hard clams: effects of substrate type and prey density. Mar. Ecol. Prog. Ser. 67:43–53.
Stehlik, L. L.
1993. Diets of the brachyuran crabs *Cancer irroratus*, *C. borealis*, and *Ovalipes ocellatus* in the New York Bight. J. Crustacean Biol. 13:723–735.
Stehlik, L. L., C. L. MacKenzie Jr. and W. W. Morse.
1991 Distribution and abundance of four brachyuran crabs on the northwest Atlantic shelf. Fish. Bull. 89:473–492.
Stehlik, L. L., P. G. Scarlett, and J. Dobarro.
1998. Status of the blue crab fisheries of New Jersey. J. Shellfish Res. 17:475–485.
Steimle, F. W., D. Jeffress, S. A. Fromm, R. N. Reid, J. J. Vitaliano, and A. B. Frame.
1994. Predator-prey relationships of winter flounder, *Pleuronectes americanus*, in the New York Bight apex. Fish. Bull. 92:608–619.
Stevens, B. G., D. A. Armstrong, and R. Cusimano.
1982. Feeding habits of the Dungeness crab *Cancer magister* as determined by the index of relative importance. Mar. Biol. 72:135–145.
Stoner, A. W., and B. A. Buchanan.
1990. Ontogeny and overlap in the diets of four tropical *Callinectes* species. Bull. Mar. Sci. 46:3–12.
Van Engel, W. A.
1958. The blue crab and its fishery in Chesapeake Bay. Part I—Reproduction, early development, growth, and migration. Commer. Fish. Rev. 20:6–17.
1990. Development of the reproductively functional form in the male blue crab, *Callinectes sapidus*. Bull. Mar. Sci. 46:13–22.
van Montfrans, J., C. H. Ryer, and R. J. Orth.
1991. Population dynamics of blue crabs *Callinectes sapidus* Rathbun in a lower Chesapeake Bay tidal marsh creek. J. Exp. Mar. Biol. Ecol. 153:1–14.
Vermeij, G. J.
1978. Biogeography and adaptation, 332 p. Harvard University Press, Cambridge, MA.
Virnstein, R. W.
1977. The importance of predation by crabs and fishes on benthic infauna in Chesapeake Bay. Ecology 58:1199–1217.
Warner, G. F.
1977. The biology of crabs, 202 p. Van Nostrand Reinhold Co., New York, NY.
Warner, G. F., and A. R. Jones.
1976. Leverage and muscle type in crab chelae (Crustacea: Brachyura). J. Zool., Lond. 180:57–68.
Williams, A. B.
1984. Shrimps, lobsters, and crabs of the Atlantic coast of the eastern United States, Maine to Florida, 550 p. Smithsonian Institution Press, Washington, DC.
Williams, A. B., and R. L. Wigley.
1977. Distribution of decapod Crustacea off northeastern United States based on specimens at the Northeast Fisheries Center, Woods Hole, MA. NOAA Tech. Rep. NMFS Circ. 407, 44 p.
Williams, M. J.
1981. Methods for analysis of natural diet in portunid crabs (Crustacea, Decapoda, Portunidae). J. Exp. Mar. Biol. Ecol. 52:103–113.
Wilson, K. A., K. W. Able, and K. L. Heck Jr.
1990. Habitat use by juvenile blue crabs: a comparison among habitats in southern New Jersey. Bull. Mar. Sci. 46:105–114.
Winget, R. R., D. Maurer, and H. Seymour.
1974. Occurrence, size composition and sex ratio of the rock crab, *Cancer irroratus* Say and the spider crab, *Libinia emarginata* Leach in Delaware Bay. J. Nat. Hist. 8:199–205.

Radiometric validation of age, growth, and longevity for the blackgill rockfish (*Sebastes melanostomus*)

Melissa M. Stevens
Allen H. Andrews
Gregor M. Cailliet
Kenneth H. Coale

Moss Landing Marine Laboratories
8272 Moss Landing Road
Moss Landing, California 95039
E-mail address (for A. H. Andrews, contact author): andrews@mlml.calstate.edu

Craig C. Lundstrom

Department of Geology
University of Illinois–Urbana Champaign
255 Natural History Bldg.
1301 W. Green Street
Urbana, Illinois 61801

Abstract—As nearshore fish populations decline, many commercial fishermen have shifted fishing effort to deeper continental slope habitats to target fishes for which biological information is limited. One such fishery that developed in the northeastern Pacific Ocean in the early 1980s was for the blackgill rockfish (*Sebastes melanostomus*), a deep-dwelling (300–800 m) species that congregates over rocky pinnacles, mainly from southern California to southern Oregon. Growth zone-derived age estimates from otolith thin sections were compared to ages obtained from the radioactive disequilibria of ^{210}Pb, in relation to its parent, ^{226}Ra, in otolith cores of blackgill rockfish. Age estimates were validated up to 41 years, and a strong pattern of agreement supported a longevity exceeding 90 years. Age and length data fitted to the von Bertalanffy growth function indicated that blackgill rockfish are slow-growing (k=0.040 females, 0.068 males) and that females grow slower than males, but reach a greater length. Age at 50% maturity, derived from previously published length-at-maturity estimates, was 17 years for males and 21 years for females. The results of this study agree with general life history traits already recognized for many *Sebastes* species, such as long life, slow growth, and late age at maturation. These traits may undermine the sustainability of blackgill rockfish populations when heavy fishing pressure, such as that which occurred in the 1980s, is applied.

Manuscript submitted 9 June 2003 to the Scientific Editor's Office.

Manuscript approved for publication 18 June 2004 by the Scientific Editor.

Fish. Bull. 102:711–722 (2004).

The blackgill rockfish (*Sebastes melanostomus*) is a deep-water rockfish that is found mainly along the continental slope between 300 and 800 m depth off central and southern California (Moser and Ahlstrom, 1978; Cross, 1987; Williams and Ralston, 2002). Although not as heavily targeted in relation to other commercially important rockfish species, a directed commercial fishery for blackgill rockfish has existed since the mid-1970s, beginning off southern California (Point Conception area) and spreading northward (Monterey area) as stocks of other heavily fished rockfishes declined (Butler et al., 1999). Using acoustic sonar and set nets, the commercial fleet was able to catch large aggregations of previously unexploited blackgill rockfish. Landings peaked in 1983 with 1346 metric tons (t) caught coast-wide, but declined over the next decade, presumably because of the disappearance of the large concentrations that could be located with acoustical gear (Butler et al., 1999). In 2001, 141 t were reportedly landed along the entire west coast (PacFIN[1])—less than half of the allowable catch (343 t; NOAA, 2001) for blackgill rockfish that year.

The first stock assessment of blackgill rockfish was made by Butler et al. (1999). One objective of this assessment was to determine age and growth characteristics, which were then applied to estimate age-at-maturity, natural mortality, and stock biomass. Using conventional aging methods (i.e., otolith increments), we estimated that blackgill rockfish live at least 87 years and reach full (100%) maturity from 13 to 26 years for females, and from 13 to 24 years for males. Although such estimates are useful and should be considered whenever available, validation of the age-estimation procedure is needed to be certain of accurate age estimates (Beamish and McFarlane, 1983; Campana, 2001). Inaccurate age determinations in some cases have led to overharvesting of stocks such as Pacific ocean perch (*Sebastes alutus*)

[1] PacFIN (Pacific Fisheries Information Network). 2002. Commercial fisheries landing data. http://www.PacFIN.org. [Accessed 9 August 2002].

and orange roughy (*Hoplostethus atlanticus*; Beamish, 1979; Archibald et al., 1983; Mace et al., 1990). These historical examples of fishery collapses necessitate that age validation be achieved before age and growth information is applied to management.

In the last decade, radiometric age validation has been applied successfully to over 20 species of rockfishes and other marine teleosts (Burton et al., 1999; Kastelle et al., 2000; Andrews et al., 2002). The most common technique uses the disequilibria between two radioisotopes, radium-226 (^{226}Ra) and lead-210 (^{210}Pb), present in the otolith (Bennett et al., 1982; Smith et al., 1991). Radium-226 is a naturally occurring radioisotope and calcium analogue that is incorporated from the surrounding seawater into the aragonitic crystalline matrix of fish otoliths. Radium-226 decays through a series of short-lived radioisotopes to ^{210}Pb. Because the half-lives of these isotopes are known, the ratio of activity between them (^{210}Pb:^{226}Ra) gives a measure of elapsed time since the initial incorporation of ^{226}Ra into the otolith (Campana et al., 1990). Radium-226 decays very slowly (a 1600 year half-life) in relation to ^{210}Pb (a 22 year half-life), allowing the activity ratio of these radioisotopes to build into secular equilibrium (1:1 ratio; Smith et al., 1991). Based on this relationship (also referred to as ingrowth), the ^{210}Pb: ^{226}Ra activity ratio is suitable for age determination in fishes up to 5 half-lives of ^{210}Pb, or approximately 120 years of age (Andrews et al., 1999b; Campana, 2001). This approach is therefore ideally suited to the blackgill rockfish, whose longevity has been estimated at almost 90 years (Butler et al., 1999).

The objectives of this study were 1) to estimate age from otolith growth zone counts, 2) to describe growth, and 3) to validate the annual periodicity of growth zones used to estimate longevity for the blackgill rockfish with the radiometric aging technique. An ancillary objective was to create a reliable predictive relationship between average otolith weight and estimated age for use as a timesaving tool in the management of this species. Growth zones quantified in sectioned otoliths were used to estimate age, and growth was described by using the von Bertalanffy growth function. Final age estimates were directly compared to radiometric ages to evaluate agreement between the two methods and ultimately were used to validate age estimation procedures, age-at-maturity, and longevity for this species.

Materials and methods

Approximately 1210 blackgill rockfish sagittal otoliths were available for this study. Otoliths were collected by National Marine Fisheries Service (NMFS) personnel from commercial vessels in 1985 at ports along the California coastline (Long Beach to Fort Bragg), and during NMFS research surveys from 1998 to 2000 from central California to the Oregon-Washington border. Thirty-two juvenile blackgill rockfish, collected from spot prawn traps along the central California coast, were provided by Robert Lea of the California Department of Fish and Game (CDFG). Fish total length (TL; cm or mm), catch area (port or geographic location), and otolith weights (right and left, 1985 samples only) were provided. Otoliths were first considered for age estimation (sectioning), and the remainder were reserved for radiometric analysis. Otolith weights (left and right, male and female) were measured to the nearest milligram and compared with *t*-tests to determine if significant differences in mass existed between sides or sexes.

Estimation of age and growth

Based on previous aging studies and the need to conserve samples for radiometric analysis, approximately 310 otoliths (25% of the collection) were assumed to be sufficient for age estimation. The left otolith from 5 to 30 fish, depending upon the number available in each 50-mm size class (ranging from 100 mm to 600 mm), was randomly chosen by using a basic resampling tool. Otoliths were thin-sectioned and mounted onto glass slides. Approximately 50 otoliths were damaged in the sectioning process, leaving 260 otoliths available for age estimation.

Sections were viewed by three readers under magnification (25 and 40×) with transmitted or reflected light. Each reader obtained age estimates by inspecting all available growth axes, choosing the most discernible axis, and reading it three times consecutively. A growth zone (here termed an "annulus") was defined as one pair of translucent (winter-forming) and opaque (summer-forming) bands. A final age, based on each reader's most confident estimate, was chosen. Precision between and within readers was compared by using average percent error (APE; Beamish and Fournier, 1981), index of precision (D) and coefficient of variation (CV; Chang, 1982). Percent agreement among readers was also calculated. Reader 1 (author) determined the final age estimate for each section as described in Mahoney (2002). Ages that could not be confidently resolved (through re-examination or discussion) were removed from analysis.

Length and age estimates for males, females, and sexes combined were fitted to the von Bertalanffy growth function (VBGF). A small portion of juvenile samples (n=16) were included in each function. Because there was strong agreement between facility aging techniques (MLML and NMFS, La Jolla, Butler et al. 1999), additional aged samples were added to strengthen the VBGF and age prediction models (n=119). Estimates of age at first, 50%, and 100% maturity were calculated by inserting existing size at maturity data (Echeverria, 1987) into the VBGF and solving for age (t).

Age prediction, age group determination, and core extraction

Campana et al. (1990) was the first to circumvent the assumption of constant ^{226}Ra uptake throughout the life of the fish by eliminating younger growth layers from adult otoliths, leaving just the oldest layers of

otolith growth (i.e., the core, representing the first few years of life). Radium-226 is present at such low activity levels, however, that many otolith cores from fish of a similar age and same sex must be pooled to acquire the mass of material needed for detection (~0.5 to 1 gram; Andrews et al., 1999a, 1999b). Because we possessed a limited number of blackgill rockfish otoliths (~1200), an age prediction model was created to conserve otolith material for radiometric analysis. It was appropriate to assume from the results of Francis (2003) that within-sample heterogeneity with respect to otolith age and mass growth rate was negligible in the core material.

To determine age groups for radiometric analyses, final ages for fish whose otoliths were sectioned, along with their corresponding average otolith weight (left and right, n=2), were used to predict age for the remaining fish in the collection. Several parameters were regressed to determine a predictive relationship between average otolith weight (henceforth termed "otolith weight") and estimated age (i.e., section age). The following regressions were compared to estimated age by using Kruskal-Wallis (nonnormal) ANOVA: 1) otolith weight (to the nearest 0.001 g), 2) otolith weight and fish length (to the nearest 1 mm), and 3) otolith weight plus otolith length (to the nearest 0.001 mm) multiplied by otolith weight (as an interaction term). A power function was also investigated but did not result in a better fit than that provided by a simple linear regression (either log-transformed or normal). A paired sample t-test and student's t-test for slopes were used to determine if a significant difference existed between male and female otolith weight, and between male and female otolith weight-to-age regressions, respectfully. The final regression equations were applied to the average otolith weight for all individual remaining fish to obtain a predicted age. Age groups were created if there was sufficient otolith material from fish of the same sex and of a similar predicted age.

The predicted age range for each group was kept as narrow as possible while permitting enough material for analysis; approximately 25 to 50 otoliths were needed at a target core weight of 0.02 g. Fish that had both otoliths intact (not sectioned or broken) were preferred to reduce the number of fish for each radiometric sample. To better insure sample conformity, 90% confidence intervals with respect to fish length and otolith weight were used to eliminate from each group dissimilar fish that may have varied significantly from predicted age. In addition to this discriminating technique, groups were further confined by capture year and location. Only samples caught in the same year and similar geographic location (based on the majority of port locations within 300 miles) were included in the same group.

Core size was determined by viewing several whole juvenile blackgill rockfish otoliths with estimated ages between 1 and 7 years. The first annulus was determined to be approximately 2 mm wide, and a 3-year-old otolith was measured at 3 mm wide, 4 mm long, and 1 mm thick, and having a weight of 0.02 g. These dimensions were chosen as the target core size because a core of this size could be easily extracted, yet was young enough to minimize the possible error associated with variable ^{226}Ra uptake in the first few years of growth. Otoliths from adult fish were ground down to the target core size with a lapping wheel and 80- to 120-grit silicon-carbide paper. Otoliths from selected juveniles, if older than age 3 (core size), were also ground to the target core size.

Radiometric analysis

The radiometric analysis was conducted as described in Andrews et al. (1999a, 1999b). Because previous studies have revealed extremely low levels of ^{210}Pb and ^{226}Ra in otolith samples, trace metal precautions were employed throughout sample cleaning and processing (Bennett et al., 1982; Campana et al., 1990; Andrews et al.,1999a). Acids were double distilled (GFS Chemicals®, Powell, OH) and all dilutions were made using Millipore® filtered Milli-Q water (18 MΩ/cm). Samples were thoroughly cleaned, dried, and weighed to the nearest 0.0001 g prior to dissolution. Whole juvenile otoliths groups were analyzed first to determine if exogenous ^{210}Pb was a significant factor, and to determine baseline levels of ^{226}Ra activity.

Because of the low-level detection problems associated with (beta) β-decay of ^{210}Pb, the activity ^{210}Pb was quantified through the autodeposition and (alpha) α-spectrometric determination of its daughter proxy, polonium-210 (^{210}Po, half-life=138 days; Flynn, 1968). In preparation for ^{210}Po analysis, samples were dissolved in acid and spiked with a calibrated yield tracer, ^{208}Po, estimated to be 5 times the activity of ^{210}Po in the otolith sample. Polonium isotopes from the sample were autodeposited onto a purified silver planchet (A.F. Murphy Die and Machine Co., North Quincy, MA) held in a rotating Teflon™ holder over a 4-hour period (Flynn, 1968). The activity of ^{208}Po and ^{210}Po on the planchets was measured with ion-implant detectors in a Tennelec (Oak Ridge, TN) TC256 α-spectrometer interfaced with a multichannel analyzer and an eight channel digital multiplexer. Counts were recorded with Nucleus® software (Nucleus Personal Computer Analyzer II, The Nucleus Inc., Oak Ridge, TN) on an IBM computer. Counts measured over periods that ranged from 28 to 50 days accumulated from 160 to 919 total counts. Lead-210 activity, along with uncertainty, was calculated in a series of equations that corrected for background and reagent counts, as well as error associated with count statistics and procedure (pipetting error, yield-tracer uncertainty, etc; Andrews et al., 1999a). The remaining sample was dried and conserved for ^{226}Ra analysis.

Determination of ^{226}Ra employed an elemental separation procedure followed by isotope-dilution thermal ionization mass spectrometry (TIMS) as described in Andrews et al. (1999a, 1999b). The sample was spiked with a known amount of ^{228}Ra yield tracer estimated to produce a ^{226}Ra:^{228}Ra atom ratio close to one. The samples were dissolved in strong acid and dried repeatedly (~90–100°C) until the sample color was bright

white, indicating that most organic material had been removed. A three-step elemental separation procedure was used to remove calcium and barium, elements that interfere with the detection of radium in the TIMS process. This involved passing the samples through three cation exchange columns, two containing a slurry of BioRad AG® 50W-X8 resin (first and second column), and one containing EiChroM Sr® resin (third column). The samples were introduced to a highly acidic medium within the columns, which separated the elements according to elution characteristics (Andrews et al., 1999b).

Radiometric age for each group was determined by inserting the measured ^{210}Pb and ^{226}Ra activities into the secular equilibrium model (Smith et al., 1991) and correcting for the elapsed time between capture and autodeposition. Because these activities were measured from the same sample, the calculation was independent of sample mass (Andrews et al., 1999a, 1999b). Propagated uncertainty associated with the final ^{210}Pb activity was based on count statistics, and procedural error and uncertainty for the final ^{226}Ra activity was based on procedural error and an instrumental TIMS analysis routine (Wang et al., 1975; Andrews et al., 1999b). The combined errors were used to calculate high and low radiometric ages.

Accuracy of age estimates

Measured ^{210}Pb:^{226}Ra activity ratios for each age group, along with their total sample age (predicted age + time since capture), were plotted with the expected ^{210}Pb:^{226}Ra growth curve. Each age group range was widened by multiplying the minimum and maximum age in the range by the age estimate CV, which was determined from the variability in age estimates among three readers. Agreement between the measured ratio with respect to estimated age and the expected ratio (ingrowth curve) provided an indication of the age estimate accuracy. Radiometric age was compared to the average predicted age for each group by using two tests: 1) a paired sample *t*-test to determine if a significant difference existed between the two age estimates for the groups and 2) predicted age was plotted against radiometric age and the correlation was compared to a hypothetical agreement line (slope of 1) by using *t*-tests for slope and elevation.

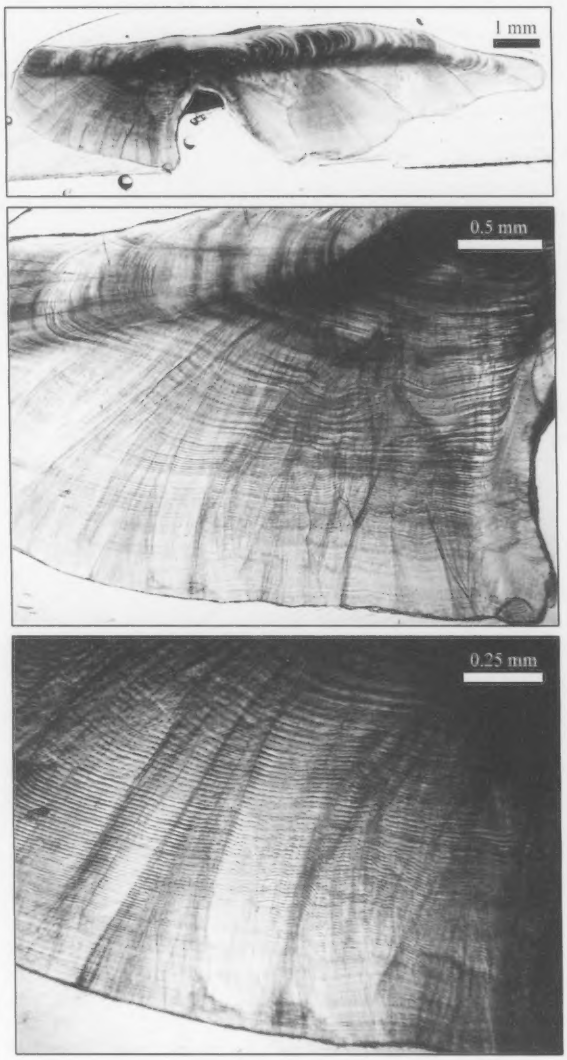

Figure 1

Three images of a blackgill rockfish (*Sebastes melanostomus*) otolith section viewed with transmitted light at 25× magnification (top), 40× (center), and 80× magnification (bottom). This section was aged most consistently as 90 years under a microscope, but because of finer digital resolution and contrast, the section pictured can be aged as high as 102 years.

Results

Estimation of age and growth

Growth zones observed within otolith sections of most blackgill rockfish were difficult to interpret. Distinction of the first annulus was often ambiguous, and the banding pattern during the first several years (1 to ~10) of growth was, in some sections, wide and inconsistent. After approximately 8 to 12 growth zones, the zone width transitioned to a narrower zone, which became extremely compressed after 20–40 growth zones. In some sections, these older zones were beyond optical resolution, whereas in others they were remarkably clear (Fig. 1).

Table 1

Comparison of von Bertalanffy growth function parameters for this study and Butler et al. (1999; in parentheses), for combined sexes, females, and males. All lengths are total lengths (mm). Note that the sample size for females and males does not sum to 332 because the same juvenile samples (n=16) were used for each sex, and only once for combined sexes. N.R.= not reported.

	Combined sexes	Females	Males
L_∞ (mm)	509 (524[1])	548 (554[1])	448 (467[1])
95% CI	491–528 (N.R.)	520–576 (N.R.)	434–462 (N.R.)
k	0.045 (0.040)	0.040 (0.040)	0.068 (0.060)
95% CI	0.038–0.052	0.033–0.047	0.058–0.078
t_0	−4.86 (−5.02)	−4.49 (−4.66)	−2.37 (−2.98)
95% CI	−6.60 to −3.12	−6.30 to −2.67	−3.55 to −1.19
n	332 (335)	181 (98)	167 (78)
r^2	0.81 (0.79)	0.87 (0.90)	0.87 (0.92)

[1] Total lengths from some samples in Butler et al., 1999 were estimated from fork length (FL in mm) by using an equation from Echeverria and Lenarz (1984).

The most consistent axis in the otolith section for which confident interpretations could be made was along either the sulcus ridge, or along the dorsoventral margin. Final age estimates were resolved for 197 fish, or approximately 76% of the 260 successfully sectioned otoliths. Agreement among readers was relatively low: approximately 24% of age estimates were within ±1 year, 61% were within ±5 years, and 87% were within ±10 years. The mean difference in age estimates between readers was 2.9 ±4.0 years. Among the three readers, APE was 10.7%, D was 8.4%, and CV was 14.6%. Average percent error, D, and CV estimates were comparable within readers; reader 1 APE was 5.2%, D was 4.1%, and CV was 7.0%. The two oldest fish to be aged were a 90-year-old male (450 mm TL) collected in 1999 and an 87-year-old female (546 mm TL) collected in 1985. Both individuals were caught south of Point Conception, California.

The VBGF fitted to age and length data resulted in distinct growth curves for male and female blackgill rockfish (Fig. 2). This difference is also represented by non-overlapping confidence intervals with respect to the primary VBGF parameters (L_∞, k; Table 1). The growth coefficient, k, ranged from 0.040 (±0.007, female) to 0.068 (±0.010, male), and asymptotic length was 448 ±14 mm for males to 548 ±28 mm for females. The asymptotic length for females was 32 mm less than the largest female fish sampled (580 mm TL), and for males, was 74 mm less than the largest male sampled (522 mm TL). The fit for all three functions was satisfactory (r^2=0.81, 0.87; Table 1, Fig. 2). Estimated ages at first, 50%, and 100% maturity, derived from inserting published estimates of length-at-maturity (Echeverria, 1987) into the growth model for each sex, were 15, 21, and 22 years for females and 13, 17, and 28 years for males (Table 2).

Table 2

Age at maturity estimates, in years, for male and female blackgill rockfish (95% confidence intervals are in parentheses). Maturity estimates were derived by inserting published estimates of length at maturity into the von Bertalanffy growth function.

	First maturity	50% maturity	100% maturity
Females	15 (12–22)	21 (16–31)	22 (17–33)
Length at maturity[1] (mm)	300	350	360
Males	13 (11–15)	17 (14–20)	27 (22–35)
Length at maturity[1] (mm)	290	330	390

[1] Echeverria (1987).

Age prediction, age group determination, and core extraction

A paired sample t-test indicated that there was a significant difference between male and female average otolith weight (t=4.54, P<0.001), and a student's t-test for slopes indicated a significant difference between male and female average otolith weight-to-age regressions (t_{crit}=1.967, t=2.87, P<0.05). Therefore, male and female age estimates and regressions were treated separately. There was no statistical difference between regressions involving fish length and average otolith weight (Kruskal-Wallis one-way ANOVA on ranks, H=4.834, P=0.089). A simple linear regression, with average otolith weight as the independent variable and estimated

age as the dependent variable, was sufficient to predict age. Log normalizing the regressions to stabilize the variance in older age estimates was unsuccessful (Cochran's test: α=0.05, 36 df, C=0.4748, P=0.486). The final regressions are given in Figure 3.

Fourteen age groups based on the predicted ages of unsectioned otoliths were chosen. These groups consisted of four juvenile groups, and five male and five female adult groups (Table 3). Fish lengths ranged from 82 mm to 580 mm TL, and predicted age ranged from 1 to 69 years. The number of otolith cores per age group ranged from 11 to 59, representing 7 to 32 fish per group. Total sample weight for each age group ranged from 0.4649 g to 1.6424 g. Whole otolith weight ranged from 0.041 to 0.842 g, and average individual core weight for the adult age groups ranged from 0.025 g to 0.028 g. The process of extracting the core inadvertently destroyed some otoliths in the grinding process, leading to smaller samples for some groups.

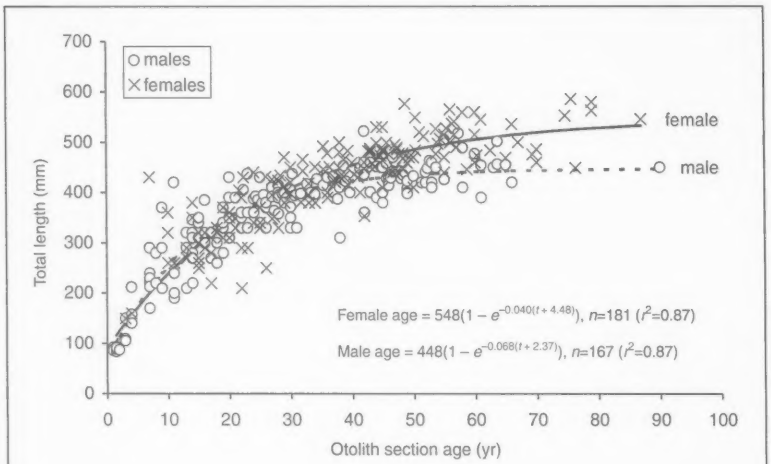

Figure 2

Blackgill rockfish (*Sebastes melanostomus*) von Bertalanffy growth functions plotted for males and females. Observed and expected values, as well as the parameters of the equations, are given. Note that the same juvenile samples (n=16) were included in both male and female equations.

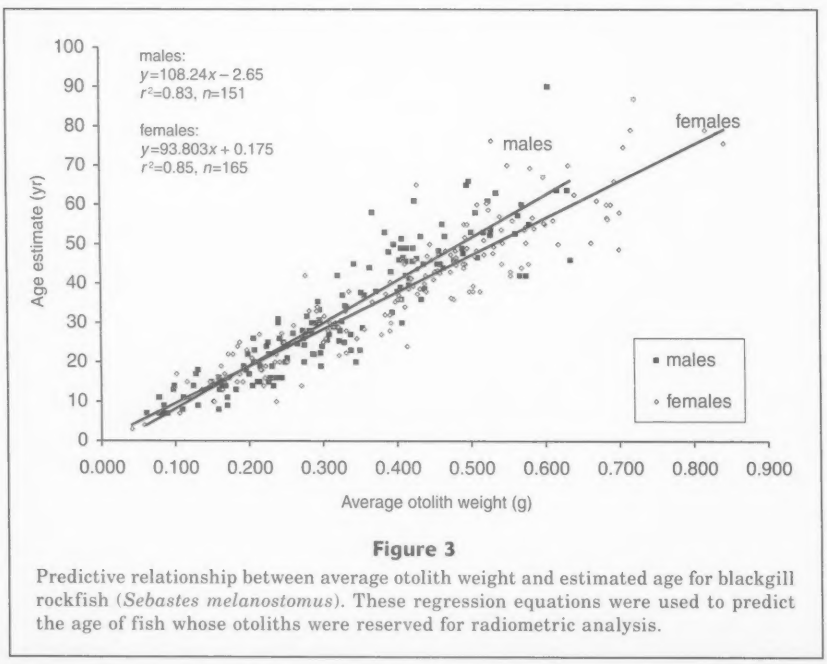

Figure 3

Predictive relationship between average otolith weight and estimated age for blackgill rockfish (*Sebastes melanostomus*). These regression equations were used to predict the age of fish whose otoliths were reserved for radiometric analysis.

Radiometric analysis

Radiometric analysis of all age groups (n=14) resulted in the successful determination of ^{210}Pb activity for all samples, and limited success for ^{226}Ra (Table 4). Activities of ^{210}Pb increased, as expected, fivefold from juvenile to adult age groups, and ranged from near 0.01 dpm/g for the juvenile samples to over 0.05 dpm/g for the oldest age groups. Error associated with these measurements ranged from 3.7 to 9.2 % (1s). The detection of ^{226}Ra activity was met with some technical difficulties. Because of poor radium recovery, radium measurements were unreliable in three samples and radium was lost in four samples. Therefore, an average of the reliable ^{226}Ra measurements was used because of the relative consistency of levels measured in these samples (0.0643 ±0.0035 dpm/g, n=7). The use of a single estimate for ^{226}Ra activity was acceptable prior to refinement of the technique (Andrews et al., 1999b). Calculated ^{210}Pb:^{226}Ra ratios increased as expected from 0.172 to 0.845 and 0.912 for the oldest groups (Table 4).

Age estimate accuracy

Radiometric ages were in agreement with predicted ages, as evidenced by concordance of ^{210}Pb:^{226}Ra activity

Table 3

Summary data for 14 pooled otolith age groups of blackgill rockfish. The age range and sample weight of each age group was based on the age prediction model and otolith availability. Groups were confined by year of capture, and for the 1985 samples, by port location. Mean total length (±1 standard deviation) of individuals per group is provided, along with the number of fish and otoliths, total sample weight, and average core weight.

Sample number	Age group (yr)	Sex	Capture year	Mean length ±σ (TL mm)	Number of fish,[1] number of otoliths	Sample weight (g)	Avg. core weight (g)
BG1	1–3	Juvenile	1998	154 ±26	7, 11[2]	0.4649	0.042
BG2	4	Juvenile	1998	200 ±8	10, 8[2]	1.1687	0.065
BG3	4–5	Juvenile	1999	217 ±9	15,19[2]	1.6630	0.088
BG4	1–7	Juvenile	2000	119 ±37	25, 36[2]	0.7854	0.022
BG5	29–31	Female	1985	400 ±20	25, 46	1.2510	0.027
BG6	26–28	Male	1985	379 ±19	22, 35	0.8866	0.025
BG7	11–17	Female	1998	276 ±20	22, 33	0.9018	0.027
BG8	39–41	Female	1985	458 ±22	31, 53	1.3332	0.025
BG9	48–54	Male	1985	459 ±21	25, 48	1.2491	0.026
BG10	60–69	Female	1985	525 ±30	19, 30	0.8254	0.028
BG11	19–23	Male	1998	329 ±16	21, 39	1.0313	0.026
BG12	56–59	Female	1985	502 ±28	13, 25	0.6989	0.028
BG13	39–41	Male	1985	428 ±24	31, 59	1.6424	0.028
BG14	42–47	Male	1998	423 ±26	32, 54	1.4267	0.026

[1] Both otoliths were not available for every fish chosen.

[2] Whole juvenile otoliths.

Table 4

Summary of radiometric results for pooled otolith age groups. Samples are listed in order of increasing age-group range. Activities are expressed as disintegrations per minute, per gram (dpm/g). Radium-226 activity was averaged among samples with low analytical error (<10%; n=7) and was determined to be 0.0643 (±0.0035) dpm/g. This value was then applied to all samples to gain an estimate of ^{226}Ra activity and radiometric age. Agreement between radiometric age and predicted age was qualified by the degree of overlap between the two age ranges. Radiometric age incorporates the time between capture and analysis.

Sample number	^{210}Pb activity (dpm/g) ±%s[1]	^{210}Pb:^{226}Ra activity ratio	Radiometric age (yr)	Radiometric age range (yr)	Predicted age group range[2]	Average age[3] (yr)	Age range agreement[4]
BG1	0.0154 ±8.6	0.234	7.1	5.4–8.7	0–3	2	Exceeds
BG2	0.0124 ±6.7	0.193	5.5	4.3–6.5	4–5	4	Overlaps
BG3	0.0118 ±5.5	0.184	5.5	4.5–6.4	4–6	4.5	Overlaps
BG4	0.0111 ±9.2	0.172	6.0	5.3–6.7	0–8	3.5	Encompasses
BG7	0.0300 ±5.6	0.467	18.0	15.2–21.4	9–19	14	Overlaps
BG11	0.0276 ±5.8	0.430	15.7	13.2–18.7	16–26	21	Overlaps
BG6	0.0440 ±4.7	0.684	22.3	16.2–30.3	22–32	27	Overlaps
BG5	0.0439 ±4.4	0.683	22.1	16.2–30.3	25–35	30	Overlaps
BG13	0.0481 ±3.8	0.749	29.3	21.8–40.4	33–47	40	Overlaps
BG8	0.0494 ±4.0	0.769	32.1	23.7–45.1	33–47	40	Overlaps
BG14	0.0499 ±3.8	0.777	45.8	37.3–59.1	36–54	45	Overlaps
BG9	0.0560 ±3.7	0.871	50.7	35.8–85.1	41–62	51	Encompasses
BG12	0.0586 ±4.7	0.912	62.9	40.7–undef.	48–67	57	Encompasses
BG10	0.0543 ±4.4	0.845	44.8	31.6 – 71.6	51–79	65	Overlaps

[1] Error calculation based on the standard deviation of ^{210}Pb activity (Wang et al., 1975).

[2] Predicted age range was extended by 14.6% of coefficient of variation (CV) associated with growth-zone–derived age estimates.

[3] The average predicted age of each radiometric age group.

[4] Definition of terms: Exceeds = radiometric age range is greater than predicted age range; Overlaps = radiometric age range partially agrees with predicted age range; Encompasses = radiometric age range was in agreement with predicted age range.

in otolith cores with expected ingrowth curves through time (Fig. 4). Of the 14 pooled otolith groups, three had radiometric age ranges that fully encompassed the predicted age range, ten resulted in overlapping age ranges, and one exceeded predicted age (Table 4). In addition, radiometric ages were in close agreement with predicted ages in a direct comparison (r^2=0.88; Fig. 5). Further t-tests indicated no significant difference in slope (t=1.92, P=0.092) or elevation (t=0.163, P=2.201) between the regression and a hypothetical agreement line (slope of 1), confirming the close agreement of radiometric age and predicted age.

Discussion

Estimation of age and growth

The growth pattern present in otoliths of blackgill rockfish was often difficult to interpret. Complications inherent to the growth pattern were the following: obscure growth zones up to age 10–15 (the ages when the otolith begins to thicken laterally), rapid transition to slower growth, conflicting or ambiguous growth patterns, and poor resolution of extremely compressed zones in old-age fish. Irregular patterns may have led to enumeration of false growth zones (checks), and the compression of the outer layers may have concealed growth zones present in older fish. This finding has been consistent among previous studies of rockfishes (Chilton and Beamish, 1982). Because of the difficulty involved in interpreting growth patterns, aging of blackgill rockfish otoliths involved a high degree of individual subjectivity, as evidenced by the relatively low precision (D=8.4%) and high variation (CV=15%) between readers. However, there were some remarkably clear otoliths and for these we were highly confident of age estimates (Fig. 1). Overall, 87% of between-reader age estimates were within 10 years, emphasizing that although the method of interpretation of growth can be imprecise, it provides a reasonable indication of the growth characteristics and longevity of this species.

The von Bertalanffy growth parameters for male and female blackgill rockfish appear to indicate that blackgill rockfish possess distinct patterns of growth (Table 1). Female blackgill rockfish exhibited a slower growth rate than males up to approximately 25–30 years of age (Fig. 2). At this point, the male growth rate slows and approaches an asymptotic length of 448 mm, but females continue to grow in length, reaching an asymptotic length of 548 mm. This trend of slower growing, but ultimately larger females has been observed in other slope-dwelling *Sebastes* species, such as the darkblotched (*S. crameri*; Rogers et al., 2000), and splitnose (*S. diploproa*; Wilson and Boehlert, 1990) rockfishes. For both sexes, the growth coefficient is low (k=0.040–0.068) when compared to shallower-dwelling (50–200 m) rockfishes, such as the greenstriped (*S. elongates*, 0.10–0.12; Love et al., 1990) and widow (*S. entomelas*, 0.20–0.25; Williams et al., 2000) rockfishes, but very similar to other deep-dwelling, long-lived species, such as the shortspine thornyhead (*Sebastolobus alascanus*, k=0.020; Cailliet et al., 2001), yelloweye (*S. ruberrimus*, k=0.046; Andrews et al., 2002), and bank (*S. rufus*, k=0.041; Cailliet et al., 2001) rockfishes.

Previous maturity estimates for blackgill rockfish (7–9 yr males, 6–10 yr females; Echeverria 1987), based on whole otolith counts, were much lower than estimates obtained from section ages in the present study (Table 2). Maturity estimates from our study support those derived by Butler et al. (1999), largely because the aging protocol was the same between facilities. Although our growth model included some age estimates (37%) from Butler et al. (1999), our results further confirm age at maturity (Table 2). Compared to other species of the genus, blackgill rockfish have a late maturity that resides at the upper end of the range for rockfishes (Cailliet et al., 2001; Love et al., 2002).

Extraordinarily old ages in average-size fish exhibited by the blackgill rockfish should not be dismissed as an anomaly. In this study the oldest blackgill rockfish was a 90-year-old male (aged as high as 102 years) that was 450 mm TL. This fish was 160 mm less than the maximum reported

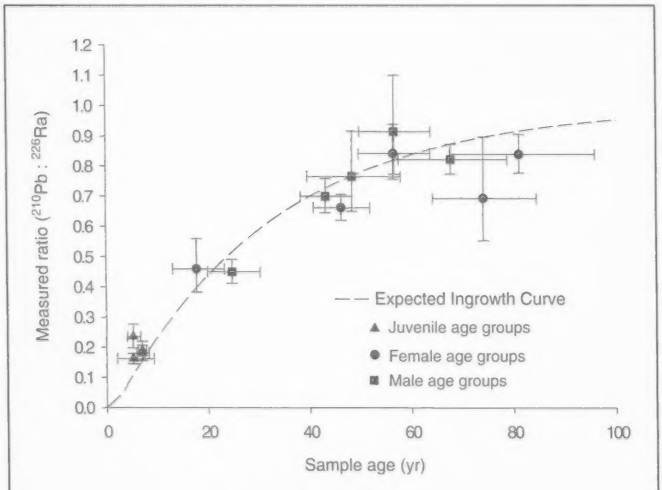

Figure 4

Measured ^{210}Pb:^{226}Ra ratio plotted against total sample age (mean predicted age plus time since capture) of blackgill rockfish (*Sebastes melanostomus*), with respect to the expected ^{210}Pb:^{226}Ra activity ratio. Horizontal error bars represent the predicted age range (based on age prediction model extended by 14.6% CV). Vertical error bars represent high and low activity ratios based on the analytical uncertainty associated with ^{210}Pb and ^{226}Ra measurements.

length (Love et al., 2002). According to an experienced rockfish age and growth researcher, "some of the oldest specimens [rockfish] are rarely the largest (lengthwise), and most, if not all, are males." (Munk[2]) The reasons for this age-length pattern are beyond the scope of this study, but the implications for stock dynamics and management are that it is worthy of further consideration.

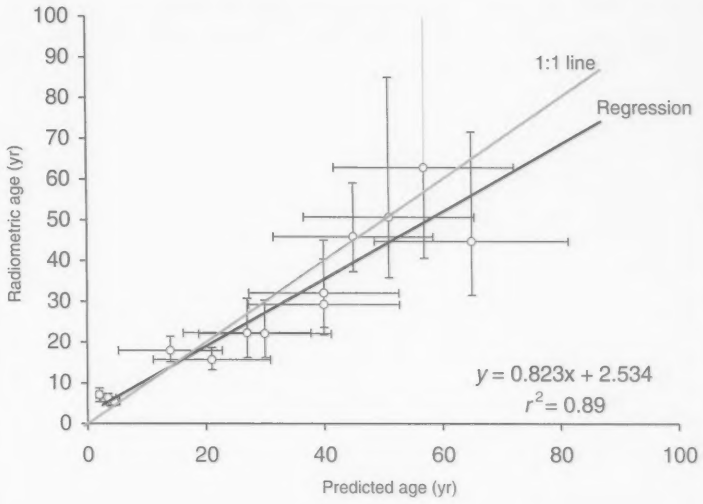

Figure 5

Direct comparison of mean predicted age and radiometric age for 14 pooled otolith age groups for blackgill rockfish (*Sebastes melanostomus*). A regression of the data points and 1:1 line of agreement are included for comparison. Horizontal error bars represent the error associated with age estimation (average predicted age multiplied by 14.6% CV), plus the standard error of the regression (1*s*) used to predict age for radiometric samples. Vertical error bars represent high and low radiometric age estimates based on the analytical uncertainty associated with ^{210}Pb and ^{226}Ra measurements.

Age prediction, age-group determination, and core extraction

The use of otolith weight as a proxy for age has benefits over conventional otolith aging methods by reducing cost, increasing sample size, and allowing greater objectivity (Boehlert, 1985; Pawson, 1990; Fletcher, 1991; Pilling et al., 2003). In this study, predicting ages from otolith weight increased the number of unsectioned otoliths that could be used in the radiometric analysis, but the prediction model also amplified the uncertainty associated with estimates of age, especially in older fish. The variance around the regression line increased with otolith weight, and log normalizing the data did not eliminate this problem. Older predicted ages, therefore, were more uncertain than younger ages (Fig. 3). Although limited to a specific otolith weight range, the prediction model presented here may provide managers with a more efficient and less costly way to investigate the age structure of blackgill rockfish stocks.

In an ideal study, otoliths from the entire estimated age range for blackgill rockfish would be available in the sample set. Otoliths from fish with predicted ages greater than 70 years, however, were not present in our study in sufficient numbers to allow age determination by radiometric methods. This was so, even though more than half of the 1200 otolith pairs obtained for ourstudy were sampled directly from commercial fishing vessels in 1985 along the coast of central and southern California, where the bulk of the fishery occurred. Because fishermen often target adult aggregations, the absence of these older individuals may be an indication that the population had already experienced depletion of older age classes at the time of sample collection, particularly if natural mortality is thought to be low for most rockfishes (Bloeser[3]). However, it is possible that the largest, oldest fish are naturally rare, even at the start of an intensive commercial fishery. Knowledge of blackgill rockfish pre-exploitation stock structure and population dynamics would help to elucidate which (depletion of older age classes or a natural situation of low numbers of older fish) is the more likely scenario.

Radiometric analysis

In previous studies the analytical uncertainty of ^{226}Ra was the limiting factor in radiometric age determination (Andrews et al., 1999a). Typically, TIMS determination of ^{226}Ra reduces error to less than 1–3% of the determined value, but technical difficulties (improperly mixed nitric acid) led to poor recovery and loss of radium in seven samples. The remaining seven samples were deemed reliable because of relatively high radium recovery, longer run times, and low analytical uncertainty as determined by the TIMS analysis routine. The ^{226}Ra activity determined for these samples was consistent

[2] Munk, K. 2002. Personal commun. Alaska Department of Fish and Game, P.O. 25526, Juneau, AK 99802.

[3] Bloeser, J. A. 1999. Diminishing returns: the status of West Coast rockfish, 94 p. Pacific Marine Conservation Council, P.O. Box 59, Astoria, OR 97103.

enough that we could assume that ^{226}Ra activities were similar among all samples and that use of an average was valid (0.0643 [±0.0035] dpm/g). This approach is acceptable because ^{226}Ra activities measured in previous radiometric studies on Pacific rockfishes were relatively constant. For example, the activity of cored yelloweye rockfish (*S. ruberrimus*) otoliths had a mean ^{226}Ra activity of 0.0312 (±0.0026) dpm/g (n=18; Andrews et al., 2002), and the rougheye rockfish (*S. aleutianus*), another deepwater species (to 730 m; Love et al., 2002), had a similar otolith core ^{226}Ra activity averaging 0.065 (±0.003) dpm/g (Kastelle et al., 2000).

Accuracy and uncertainty of ages estimates

Radiometric activities measured in blackgill rockfish otoliths generally agreed with expected activity ratios for ^{210}Pb and ^{226}Ra (Fig. 4), confirming the validity of growth-zone–derived age estimates. In addition, a direct comparison between radiometric age and predicted age resulted in a strong agreement (r^2=0.89; Fig. 5), which was further supported by slope and elevation tests that revealed no significant difference from a 1:1 agreement line.

The most critical sources of error involved in age estimation, prediction, and radiometric age determination were the following: 1) age estimate uncertainty, 2) regression error associated with predicted ages, and 3) analytical uncertainty associated with the radiometric aging technique (TIMS and α-spectrometry). Conventional aging techniques are inherently subjective (Boehlert, 1985; Campana, 2001) and thus create uncertainty associated with an estimated age. This uncertainty is transferred to the prediction model, where the natural variability associated with individual otolith weight must also be considered. For most samples, however, the error bars either overlapped or were in contact with the agreement line (Figs. 4 and 5), further confirming the concordance of radiometric age with predicted age.

Implications for management

When considering the longevity of rockfishes for which a maximum age has been reported (Munk, 2001; Cailliet et al., 2001), a longevity exceeding 90 years places the blackgill rockfish within the top 20% of long-lived rockfishes. There is a trend for rockfishes that may indicate that longevity increases as maximum depth of occurrence increases, and physiological adaptations to the environmental conditions of deep-sea living could provide an explanation (Cailliet et al., 2001). The confirmed longevity and the maximum depth of occurrence (~800 m) for the blackgill rockfish provide further support for this concept.

Longevity in the rockfishes has been central to its evolutionary success in relation to other marine teleosts. The suite of life history characters implicit with a long lifespan (slow adult growth, late age-at-maturity, low adult natural mortality) represent a "slow and steady" adaptive strategy, whereby the energy allocated towards individual growth is prolonged, eventually contributing to greater fecundity (due to larger size at maturity) over the lifespan of the individual. This reproductive strategy serves to propagate genetic material across several generations, as well as to diffuse the effect of mortality associated with each reproductive event (Leaman, 1991). In this sense, longevity may act to buffer the species against short-term (El Niño) and long-term environmental change (Pacific Decadal Oscillations), and the stochasticity inherent in the Pacific Ocean system (Moser et al., 2000).

In the absence of fishing pressure, the genetic contribution of a slow-growing, longer-lived species may be more conserved in the collective species' gene pool (Munk[2]). In the presence of fishing pressure, however, this "slow and steady" adaptation may be detrimental (Musick, 1999). Although modeling fish populations for the purpose of management typically involves some or all of these parameters, the focus is often on determining sustainable biomass and this approach largely ignores the unknown effects of changes in age structure due to removal of the oldest individuals from the population (Craig, 1985), as well as a loss of genetic diversity that could prevent full recovery of severely depleted populations (Hauser et al, 2002). Given the current depressed condition of many heavily fished rockfish stocks, species-specific life history characteristics, such as longevity, growth rate, and age-at-maturity estimates, should be given thorough consideration in the development of an effective management strategy. Management regulations that account for these characteristics, such as a limited fishing season, or designation of harvest refugia (Yoklavich, 1998), would provide a stronger basis for conservation and sustainability of the resource.

Acknowledgments

We wish to thank John Butler, Don Pearson, and Cindy Taylor of the Southwest Fisheries Science Center, Mark Wilkins, Jerry Hoff, Waldo Wakefield, and Bob Lauth of the Alaska Fisheries Science Center, and Bob Lea of CDFG for donating specimens for this study. Mary Yoklavich (NMFS), Di Tracey and Larry Paul (NIWA, New Zealand), Kristen Munk (ADFG), Don Pearson (NMFS), Tom Laidig (NMFS), and Steve Campana (DFO, Canada) provided valuable insight into blackgill rockfish growth patterns. Patrick McDonald of the Oregon Department of Fish and Wildlife aged otolith sections. Pete Holden at the University of California, Santa Cruz, measured radium in the refined samples using TIMS. The comments and suggestions of three anonymous reviewers were greatly appreciated. This work was supported by the National Sea Grant College Program of the U.S. Department of Commerce's National Oceanic and Atmospheric Administration under NOAA Grant number NA06RG0142, project number R/F-182, through the California Sea Grant College Program; and in part by the California State Resources Agency.

Literature cited

Andrews, A. H., G. M. Cailliet, and K. H. Coale.
1999a. Age and growth of the Pacific grenadier (*Coryphaenoides acrolepis*) with age estimate validation using an improved radiometric ageing technique. Can. J. Fish. Aquat. Sci. 56:1339–1350.

Andrews, A. H., K. H. Coale, J. Nowicki, C. Lundstrom, A. Palacz, and G. M. Cailliet.
1999b. Application of an ion-exchange separation technique and thermal ionization mass spectrometry to ^{226}Ra determination in otoliths for radiometric age determination of long-lived fishes. Can. J. Fish. Aquat. Sci. 56:1329–38.

Andrews, A. H., G. M. Cailliet, K. H. Coale, K. M. Munk, M. M. Mahoney and V. M. O'Connell.
2002. Radiometric age validation of the yelloweye rockfish (*Sebastes ruberrimus*) from south-eastern Alaska. Mar. Freshw. Res. 53:1–8.

Archibald, C. P., D. Fournier, and B. M. Leaman.
1983. Reconstruction of stock history and development of rehabilitation strategies for Pacific ocean perch in Queen Charlotte Sound, Canada. N. Am. J. Fish. Manag. 3:283–294.

Beamish, R. J.
1979. New information on the longevity of Pacific ocean perch (*Sebastes alutus*). J. Fish. Res. Board Can. 36:1395–1400.

Beamish, R. J., and D. A. Fournier.
1981. A method for comparing the precision of a set of age determinations. Can. J. Fish. Aquat. Sci. 38:982–983.

Beamish, R. J., and G. A. McFarlane.
1983. The forgotten requirement for age validation in fisheries biology. Trans. Am. Fish. Soc. 112(6):735–743.

Bennett, J. T., G. W. Boehlert, and K. K. Turekian.
1982. Confirmation of longevity in *Sebastes diploproa* (Pisces: Scorpaenidae) from $^{210}Pb/^{226}Ra$ measurements in otoliths. Mar. Biol. 71:209–215.

Boehlert, G. W.
1985. Using objective criteria and multiple regression models for age determination in fishes. Fish. Bull. 83:103–117.

Burton, E. J., A. H. Andrews, K. H. Coale, and G. M. Cailliet.
1999. Application of radiometric age determination to three long-lived fishes using ^{210}Pb:^{226}Ra disequilibria in calcified structures: a review. *In* Life in the slow lane: ecology and conservation of long-lived marine animals (J. A. Musick, ed.,), p. 77–87. Am. Fish. Soc. Symp. 23.

Butler, J. L., L. D. Jacobson, and J. T. Barnes.
1999. Stock assessment for blackgill rockfish. *In* Appendix to the status of the Pacific coast groundfish fishery through 1998 and recommended acceptable biological catches for 1999: stock assessment and fishery evaluation, 93 p. Pacific Fishery Management Council, 2130 SW Fifth Avenue, Suite 224, Portland, Oregon, 97201.

Cailliet, G. M., A. H. Andrews, E. J. Burton, D. L. Watters, D. E. Kline, and L. A. Ferry-Graham.
2001. Age determination and validation studies of marine fishes: do deep-dwellers live longer? Exp. Gerontology 36:739–764.

Campana, S. E.
2001. Accuracy, precision and quality control in age determination, including a review of the use and abuse of age validation methods. J. Fish Biology 59:197–242.

Campana, S. E., K. C. Zwanenburg, and J. N. Smith.
1990. $^{210}Pb/^{226}Ra$ determination of longevity in redfish. Can. J. Fish. Aquat. Sci. 47:163–165.

Chang, W. Y. B.
1982. A statistical method of evaluating the reproducibility of age determination. Can. J. Fish. Aquat. Sci. 48:734–750.

Chilton, D. E., and R. J. Beamish.
1982. Age determination methods for fishes studied by the Groundfish Program at the Pacific Biological Station, 102 p. Can. Spec.Pub. Fish. Aquat. Sci. 60.

Craig, J. F.
1985. Aging in fish. Can. J. Zoology 63:1–8.

Cross, J. N.
1987. Demersal fishes of the upper continental slope off southern California. CalCOFI Report 28:155–167.

Echeverria, T. W.
1987. Thirty-four species of California rockfishes: maturity and seasonality of reproduction. Fish. Bull. 85:229–249.

Echeverria, T. W., and W. H. Lenarz.
1984. Conversions between total, fork, and standard length in 35 species of *Sebastes* from California. Fish. Bull. 82:249–251.

Fletcher, W. J.
1991. A test of the relationship between otolith weight and age for the pilchard *Sardinops neopilchardus*. Can. J. Fish. Aquat. Sci. 48:35–38.

Flynn, W. W.
1968. The determination of low levels of polonium-210 in environmental materials. Anal. Chimica Acta. 43: 221–227.

Francis, R. I. C. C.
2003. The precision of otolith radiometric ageing of fish and the effect of within-sample heterogeneity. Can. J. Fish. Aquat. Sci. 60:441–447.

Hauser, L., G. J. Adcock, P. J. Smith, J. H. Bernal Ramirez, and G. R. Carvalho.
2002. Loss of microsatellite diversity and low effective population size in an overexploited population of New Zealand snapper (*Pagrus auratus*). Proc. Nat Acad. Sci. 99(18):11742–11747.

Kastelle, C. R., D. K. Kimura, and S. R. Jay.
2000. Using Pb^{210}/Ra^{226} disequilibrium to validate conventional ages in Scorpaenids (*sic*) (genera *Sebastes* and *Sebastolobus*). Fish. Res. 46:299–312.

Leaman, B. L.
1991. Reproductive style and life history variables relative to exploitation and management of *Sebastes* stocks. Environ. Biol. Fishes 30: 253–271.

Love, M. S., P. Morris, M. McCrae, and R. Collins.
1990. Life history aspects of 19 rockfish species (Scorpaenidae: Sebastes) from the southern California Bight, 38 p. NOAA Technical Report. NMFS 87.

Love, M. S., M. M. Yoklavich, L. Thorsteinson, and J. Butler.
2002. The rockfishes of the Northeast Pacific, 405 p. Univ. California Press, Berkeley, CA.

Mace, P. M., J. M. Fenaughty, R. P. Coburn, and I. J. Doonan.
1990. Growth and productivity of orange roughy (*Hoplostethus atlanticus*) on the north Chatham Rise. New Zealand J. Mar. Fresh. Res. 24:105–109.

Mahoney, M. M.
2002. Age, growth and radiometric age validation of the blackgill rockfish, *Sebastes melanostomus*. M.Sc. thesis, 70 p. California State Univ., San Francisco, CA. [Available from: Moss Landing Marine Labora-

tories, 8272 Moss Landing Road, Moss Landing, CA 95039.]

Moser, H. G., and E. H. Ahlstrom.
1978. Larvae and pelagic juveniles of blackgill rockfish, *Sebastes melanostomus*, taken in midwater trawls off southern California and Baja California. J. Fish. Res. Board Can. 35:981–996.

Moser, H. G. R. L. Charter, W. Watson, D. A. Ambrose, J. L. Butler, S. R. Charter, and E. M. Sandknop.
2000. Abundance and distribution of rockfish (*Sebastes*) larvae in the southern California Bight in relation to environmental conditions and fishery exploitation. CalCOFI Report 41:132–147.

Musick, J. A.
1999. Ecology and conservation of long-lived marine animals. *In* Life in the slow lane: ecology and conservation of long-lived marine animals (J. A. Musick, ed.), p. 1–10. Am. Fish. Soc. Symp. 23.

Munk, K. M.
2001. Maximum ages of groundfishes in waters off Alaska and British Columbia and considerations of age determination. Alaska Fish. Res. Bull. 8(1):12–21.

NOAA (National Oceanic and Atmospheric Administration).
2001. Magnuson-Stevens Act Provisions; Fisheries off West Coast states and in the western Pacific; Pacific coast groundfish fishery; annual specifications and management measures. Federal Register 66:8, 2338–2355.

Pawson, M. G.
1990. Using otolith weight to age fish. Fish. Biol. 36:521–531.

Pilling, G. M., E. M. Grandcourt, and G. P. Kirkwood.
2003. The utility of otolith weight as a predictor of age in the emperor *Lethrinus mahsena* and other tropical fish species. Fish. Res. 60:493–506.

Rogers, J. B., R. D. Methot, T. L. Builder, K. Piner, and M. Wilkins.
2000. Status of the darkblotched rockfish (*Sebastes crameri*) resource in 2000. *In* Appendix to the status of the Pacific Coast groundfish fishery through 2000 and recommended acceptable biological catches for 2001: stock assessment and fishery evaluation, 79 p. Pacific Fishery Management Council, 2130 SW Fifth Ave., Suite 224, Portland, OR 97201.

Smith, J. N., R. Nelson, and S. E. Campana.
1991. The use of Pb-210/Ra-226 and Th-228/Ra-228 disequilibria in the ageing of otoliths of marine fish. *In* Radionuclides in the study of marine processes (P. J. Kershaw and D. S. Woodhead, eds.), p. 350–359. Elsevier Applied Science, New York, NY.

Wang, C. H., D. L. Willis, and W. D. Loveland.
1975. Radiotracer methodology in the biological, environmental, and physical sciences, 480 p. Prentice Hall, Englewood Cliffs, NJ.

Williams, E. H., A. D. MacCall, S. V. Ralston, and D. E. Pearson.
2000. Status of the widow rockfish resource in 2000. *In* Appendix to the status of the Pacific Coast groundfish fishery through 1999 and recommended acceptable biological catches for 2000, 75 p. Pacific Fishery Management Council, 2130 SW Fifth Ave., Suite 224, Portland, OR 97201.

Williams, E. K., and S. R. Ralston.
2002. Distribution and co-occurrence of rockfishes (family: Sebastidae) over trawlable shelf and slope habitats of California and southern Oregon. Fish. Bull. 100:836–855.

Wilson, C. D., and G. W. Boehlert.
1990. The effects of different otolith ageing techniques on estimates of growth and mortality for the splitnose rockfish, *Sebastes diploproa*, and canary rockfish, *S. pinniger*. Calif. Fish Game 76:146–160.

Yoklavich, M. (ed).
1998. Marine harvest refugia for West Coast rockfish: a workshop, 162 p. NOAA-Tech. Memo. NMFS-SWFSC-255.

Descriptions of larval, prejuvenile, and juvenile finescale menhaden (*Brevoortia gunteri*) (family Clupeidae), and comparisons to gulf menhaden (*B. patronus*)

James M. Tolan
Texas Parks and Wildlife Department
6300 Ocean Dr., NRC 2501
Corpus Christi, Texas 78412
E-mail address: James.Tolan@tpwd.state.tx.us

David A. Newstead
Center for Coastal Studies
Texas A&M University–Corpus Christi
6300 Ocean Dr., NRC 3216
Corpus Christi, Texas 78412

Abstract—Larval and juvenile development of finescale menhaden (*Brevoortia gunteri*) is described for the first time by using wild-caught individuals from Nueces Bay, Texas, and is compared with larval and juvenile development of co-occurring gulf menhaden (*B. patronus*). Meristics, morphometrics, and pigmentation patterns were examined as development proceeded. An illustrated series of finescale menhaden is presented to show changes that occurred during development. For finescale menhaden, transformation to the juvenile stage was completed by 17–19 mm standard length (SL). By contrast, transformation to the juvenile stage for gulf menhaden was not complete until 23–25 mm SL. Characteristics useful for separating larval and juvenile finescale menhaden from gulf menhaden included 1) the presence or absence of pigment at the base of the insertion of the pelvic fins; 2) the standard length at which medial predorsal pigment occurs; 3) differences in the number of dorsal fin ray elements; and, 4) the number of vertebrae.

Manuscript submitted 9 September 2003 to the Scientific Editor's Office.

Manuscript approved for publication 14 June 2004 by the Scientific Editor.

Fish. Bull. 102:723–732 (2004).

Finescale menhaden (*Brevoortia gunteri* Hildebrand), one of three recognized species of menhaden (Reintjes, 1969; Hettler, 1984) found in the Gulf of Mexico, occurs in the northern and western Gulf of Mexico, from Chandeleur Bay, Louisiana, to Campeche Bay, west of Punto Morros (McEachran and Fechhelm, 1998). Despite their common occurrence in coastal and estuarine waters along the Texas and Mexico coasts (Simmons, 1957; Hellier, 1962; Hoese, 1965; Whitehead, 1985; Castillo-Rivera and Kobelkowsky, 2000), their early development has not been described. Early development of gulf menhaden (*B. patronus* Goode), on the other hand, has been well described (Suttkus, 1956; Hettler, 1984; Ahrenholz, 1991).

In coastal waters of the western Gulf of Mexico, finescale menhaden are spatially and temporally sympatric with gulf menhaden (Castillo-Rivera et al., 1996). Gulf menhaden are found throughout the northern gulf from Florida Bay to Campeche Bay. Yellowfin menhaden (*B. smithi* Hildebrand) are found in the eastern gulf from the Mississippi River Delta to Cape Lookout, North Carolina, and co-occur with finescale menhaden only in its extreme western range (Dahlberg, 1970; Hoese and Moore, 1977). A large amount of hybrid introgression occurs between gulf and yellowfin menhaden, although finescale hybrids (either finescalexgulf menhaden or finescalexyellowfin menhaden) have not been reported (Ahrenholz, 1991).

Both finescale and gulf menhaden are estuarine-dependent species inhabiting shallow nursery areas for their early development (Gunter, 1945; Shaw et al., 1985; Castillo-Rivera and Kobelkowsky, 2000). Gulf menhaden are intermittent or multiple spawners (Christmas and Waller, 1975; Lewis and Roithmayr, 1981), and adults move offshore in late summer and early fall. Spawning off the coast of Texas is protracted, and the spawning season begins at the end of August and continues through April (Shaw et al., 1985). Estuarine immigration of gulf menhaden ranging in size from 10 to 32 mm TL has been observed from late October through April (Copeland, 1965; Gallaway and Strawn, 1974; Allshouse, 1983). In Nueces Bay, the greatest densities of gulf menhaden larvae are seen from late February to early May, and the peak immigration of 19–26 mm TL individuals occurs from late April and early May (Newstead, 2003). Finescale menhaden spawn in estuarine or nearshore areas (Gunter, 1945; Simmons, 1957) and their spawning season has been reported from November to March (Ahrenholz, 1991). Hellier (1962) reported 25-mm-TL specimens taken from the Upper Laguna Madre

on the lower Texas coast during February, and Gunter (1945), Simmons (1957), and Hoese (1965) have reported postlarval finescale menhaden from the middle and lower Texas coasts from January to May. Gulf menhaden have received considerable attention in fishery science because of their large population sizes and resulting ecological and economic importance in the northern Gulf of Mexico (Nelson and Ahrenholz, 1981; Smith, 1991), whereas finescale menhaden are less numerous and not directly sought by any recognized fishery (Ahrenholz, 1991). Our study describes for the first time the development of postflexion (late larval), prejuvenile, and juvenile finescale menhaden.

Materials and methods

A total of 170 wild-caught finescale menhaden larvae and juveniles were used to describe early development. All specimens came from ichthyoplankton collections in Nueces Bay, Texas (27.87°N, 97.51°W), during May and June 2003. Individuals were collected in the tidal channels of Nueces Delta with a side-mounted push net (60-cm ring net, 0.505-mm mesh). For comparison, 357 wild-caught gulf menhaden larvae and juveniles collected during May and June of 1999, 2000, and 2002 from two nearby stations outside the delta (less than 1.5 km away), in addition to the tidal channel collections of 2003, were also studied. All individuals were initially fixed in either 10% formalin or 95% ethanol and transferred to fresh 95% ethanol after 48 hours.

Pigment patterns were recorded and specimens of finescale menhaden were illustrated. Gulf menhaden were not illustrated because the figures in Hettler (1984) are adequate.

Morphometrics

Body measurements were made to the nearest 0.1 mm with an ocular micrometer fitted to a dissecting microscope. All individuals collected were postflexion, prejuvenile, or juvenile stage as defined in Leis and Rennis (1983), and standard length (SL) was measured as the distance from the tip of the snout along the midline to a vertical line through the posterior edge of the hypural plate. All lengths are SL unless otherwise noted. Definitions and other terms are as follows:

BD = body depth; vertical depth at the pectoral symphysis.
CP = caudal peduncle; horizontal distance from the posterior edge of the dorsal fin base to the posterior edge of the hypural plate.
EYE = eye diameter; horizontal distance between the anterior and posterior edges of the fleshy orbit.
PAL = preanal length; distance from the tip of the snout to the origin of the anal fin, measured along the midline.

Ratios of these four body proportion measurements in relation to SL were fitted by means of nonlinear least squares regression techniques (SigmaPlot, version 5.0, SPSS Inc., Chicago, IL) in order to graphically illustrate any development differences between the two species. Increasing ratios (BD/SL, CP/SL, and EYE/SL) were described with an exponential rise-to-maximum equation:

$$y = a(1 - e^{-bx}),$$

whereas, the decreasing ratio of PAL/SL measurements were described with a exponential decay equation:

$$y = ae^{-bx}.$$

In both equations, y = body proportion ratio; x = SL; a = intercept; and b = SL specific exponential rate of change.

Meristics

Each specimen was examined to determine whether scale formation had been initiated, and a total count of ventral scutes for specimens in which they were sufficiently developed was obtained. A total of 37 finescale and 48 gulf menhaden from the 2003 collections were cleared and stained according to Potthoff (1984) and used for fin-ray and vertebrae counts. Because of the difficulty in accurately counting myomeres in transforming clupeids (Hettler, 1984; Ditty et al., 1994), we chose to count total vertebrae and use the number of postdorsal and preanal vertebrae instead of postdorsal and preanal myomeres as a potential diagnostic character. Fin-ray counts included dorsal, anal, and caudal fins (both principal and procurrent rays).

Results

Morphological development

Finescale menhaden larvae were first collected at 9.7 mm and ranged to 22.5 mm as transforming juveniles (Fig. 1). Transformation from the larval to the juvenile form began around 14 mm and was completed by around 20 mm (Fig 2). Ratios of body depth, caudal peduncle, and eye diameter all increased in relation to standard length as larvae grew, whereas snout-to-anal length decreased (Table 1). The decrease in snout-to-anal length reflected the transformation from the elongate fusiform shape of the larvae to the laterally compressed deep-bodied shape of the juvenile. Scales began to form at around 15 mm on the caudal peduncle region and progressed forward along the ventral and lateral surfaces towards the dorsal surface. None of the individuals examined had the enlarged and fringed median scales preceding the dorsal fin, which are an adult characteristic of the genus *Brevoortia*. Ventral scutes also began forming around 15 mm, and the full complement of 27–31 scutes (McEachran and Fechhelm, 1998) was found by 19 mm.

Gulf menhaden ranged from 11.7 mm as larvae to 40.4 mm juveniles. For gulf menhaden, body depth,

Table 1

Proportional measurements in relation to standard length (SL) used to describe finescale menhaden (*Brevoortia gunteri*) larval development.

Length class (mm, SL)	Number of specimens	Body depth: SL	Preanal length: SL	Caudal peduncle: SL	Eye diameter: SL
<11.0	1	0.100	0.804	0.256	0.054
11.1–12.0	2	0.108	0.798	0.259	0.059
12.1–13.0	5	0.119	0.778	0.251	0.059
13.1–14.0	15	0.139	0.764	0.263	0.064
14.1–15.0	28	0.136	0.756	0.269	0.062
15.1–16.0	25	0.168	0.735	0.281	0.074
16.1–17.0	23	0.208	0.711	0.302	0.082
17.1–18.0	17	0.220	0.705	0.311	0.085
18.1–19.0	3	0.239	0.700	0.327	0.080
19.1–20.0	2	0.219	0.700	0.304	0.078
>20.1	1	0.318	0.690	0.304	0.093

caudal peduncle, and eye diameter ratios all similarly increased in relation to standard length as larvae grew, whereas snout-to-anal length decreased (Table 2). Scale initiation in gulf menhaden was not seen until 19 mm, and ventral scutes did not begin forming until around 18 mm. The full complement of scutes (28–32 scutes; McEachran and Fechhelm, 1998) was seen by around 25 mm. No enlarged median dorsal scales were noted from the gulf menhaden individuals examined.

With little overlap in the 15–20 mm size range (see Fig. 1) and a limited number of juvenile-size finescale menhaden (SL>20 mm), it was not possible to effectively separate finescale and gulf menhaden morphometrically on the basis of BD:SL, PAL:SL, CP:SL, and EYE:SL ratios (Fig 3). By 25 mm, proportional body measurements had become nearly constant for gulf menhaden whereas body measurements were still changing for finescale menhaden even though they appeared to be fully transformed. For a fish of given size, finescale menhaden typically had a greater body depth, a shorter preanal length, and a greater caudal peduncle length than gulf menhaden.

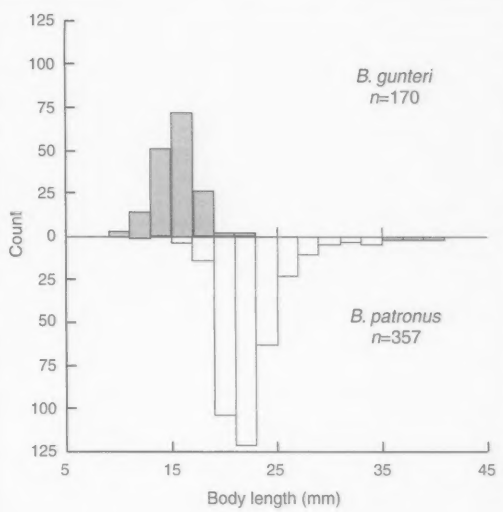

Figure 1

Length-frequency histograms for *Brevoortia gunteri* and *B. patronus* derived from ichthyoplankton collections in Nueces Bay, Texas, during May and June (1999–2003).

Meristic features

No recently hatched or preflexion finescale menhaden were examined and all postflexion individuals followed the fin development sequence identified for other clupeids (Houde et al., 1974; Hettler, 1984; Ditty et al., 1994). The caudal and dorsal fins are first to develop, followed by the pelvic fins, whereas the pectoral fins are the last to fully develop even though the pectorals are the first fins to form as nonrayed buds. Only vertebrae and dorsal-fin ray counts were useful in separating finescale and gulf menhaden, because most other meristics overlapped (Table 3). Finescale menhaden had fewer total vertebrae (=43 vs. 46) and fewer dorsal-fin rays (median value=18 vs. 21) than gulf menhaden. Postdorsal and preanal vertebrae also showed a high degree of overlap between the two species (Table 3). The forward movement of the anal fin in relation to the dorsal fin was most evident in fully transformed gulf menhaden, and the number of postdorsal-preanal vertebrae decreased from 4 to –3. The relative placement of the anal fin also

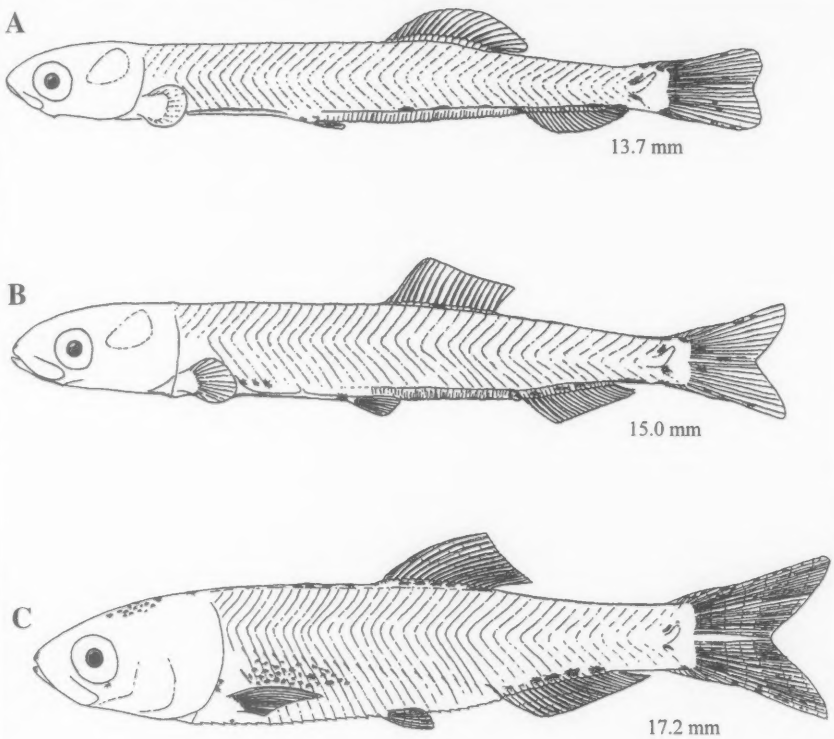

Figure 2

Developmental stages of *Brevoortia gunteri*. (**A**) Postflexion larva, 13.7 mm. (**B**) Postflexion larva, 15.0 mm. (**C**) Transforming larva, 17.2 mm. (**D**) Transforming larva, 19.0 mm. (**E**) Transformed juvenile, 23.9 mm.

Table 2

Proportional measurements relative to standard length (SL) used to describe gulf menhaden (*Brevoortia patronus*) larval development.

Length class (mm, SL)	Number of specimens	Body depth: SL	Preanal length: SL	Caudal peduncle: SL	Eye diameter: SL
<14.0	1	0.086	0.829	0.229	0.061
14.1–15.0	1	0.119	0.786	0.238	0.061
15.1–16.0	3	0.136	0.764	0.261	0.063
16.1–17.0	4	0.136	0.764	0.261	0.063
17.1–18.0	5	0.144	0.749	0.257	0.065
18.1–19.0	13	0.169	0.733	0.265	0.067
19.1–20.0	26	0.183	0.725	0.274	0.074
20.1–21.0	22	0.176	0.735	0.271	0.068
21.1–22.0	17	0.236	0.719	0.282	0.084
22.1–24.0	9	0.286	0.709	0.298	0.095
24.1–26.0	2	0.337	0.730	0.313	0.103
26.1–29.0	11	0.352	0.730	0.299	0.098
29.1–32.0	4	0.356	0.740	0.308	0.100
>32.1	3	0.380	0.736	0.294	0.097

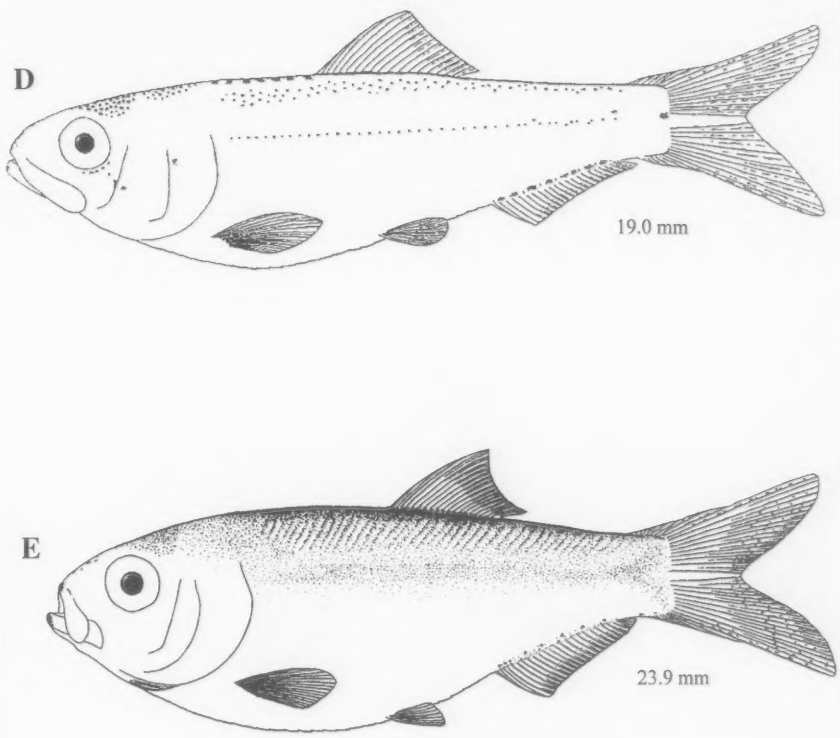

Figure 2 (continued)

Table 3

Meristics in finescale menhaden, *Brevoortia gunteri*, (37 specimens) and in gulf menhaden, *B. patronus*, (48 specimens). Median values are given in parentheses.

			Number in full complement	
Meristic	*B. gunteri*	*B. patronus*	*B. gunteri*	*B. patronus*
Caudal-fin rays				
Principal (dorsal)	10	10		10–11
(ventral)	9	9		9–10
Procurrent (dorsal)	7–9 (8)	8–9 (8)		8–9
(ventral)	7–8 (7)	5[1]–8 (7)		7–8
Dorsal-fin rays	17–20 (18)	16[1]–23 (21)	17–20	21–23
Anal-fin rays	18–24 (22)	20–23 (21)	20–25	18–22
Vertebrae	43–44 (43)	40[1]–46 (46)	42–44	45–46
Postdorsal and preanal vertebrae	0–3 (2)	–3[2]–4 (1)		2–4[3]

[1] *B. patronus* larva SL=11.7 mm.
[2] *B. patronus* fully transformed individual SL=40.4 mm.
[3] Postdorsal and preanal myomere counts in larvae 10–15 mm SL (Ditty et al., 1994)

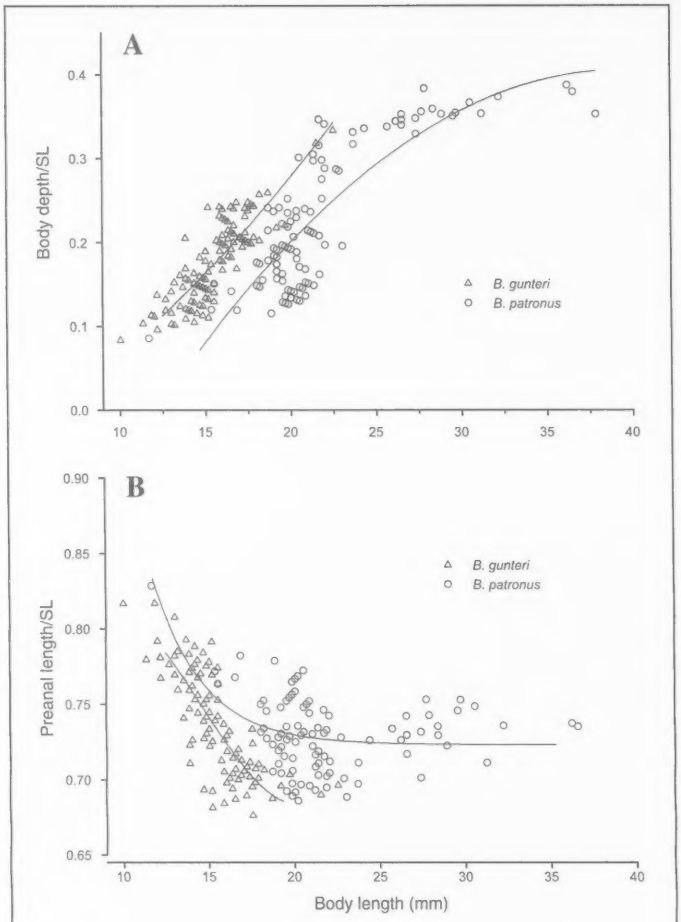

Figure 3

Morphometric comparisons (shown as a percentage of standard length [SL]) for wild-caught *Brevoortia gunteri* and *B. patronus*. (**A**) BD/SL. (**B**) PAL/SL. (**C**) CP/SL. (**D**) EYE/SL. Best fit nonlinear regression lines were fitted by least squares estimation.

changed in finescale menhaden, although the number of postdorsal-preanal vertebrae only decreased from three to zero.

Pigmentation

Early pigmentation patterns in finescale menhaden (Fig. 2) were similar, but not identical, to the pigmentation described for gulf menhaden (Suttkus, 1956; Hettler, 1984). Both dorsal and ventral notochord tip pigment, which are diagnostic for the genus *Brevoortia* (Fig. 2), were found in all individuals examined. In specimens <14 mm, pigmentation was sparse and found primarily along the ventral margin of the caudal peduncle, the base of the anal fin, at the end of the gut near the vent, and ventrally as two lines beginning at the pectoral fin bases below the foregut. Along the dorsal margin of the hindgut, 3–6 fine melanophores were usually present. At the base of the pelvic fins, 1–2 small, paired stellate melanophores were present. Additionally, all individuals had a medial melanophore along the isthmus (ventral midline anterior to the cleithrum) and most had an internal melanophore at the nape. Other pigment present in the smallest finescale larvae included a series of paired melanophores anterior to the dorsal fin base (seen in 26% of the larvae examined). This predorsal mid-line pigment series increased both in size and number as the larvae grew. The head was unpigmented.

By 16 mm, pigment increased along the dorsal surface of the hindgut, the base of the dorsal fin, and the

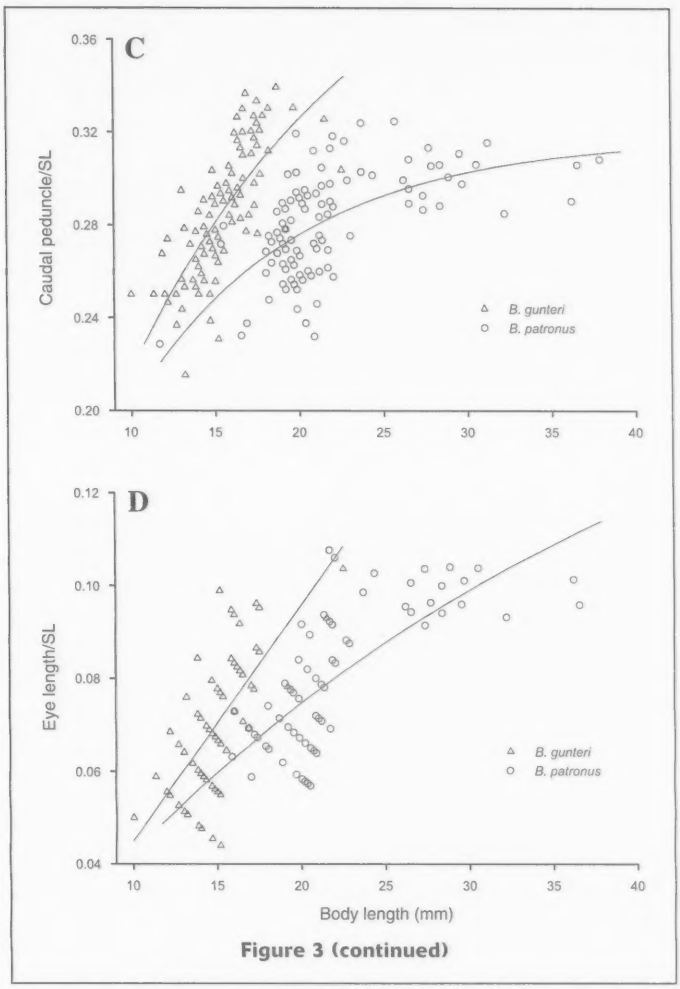

Figure 3 (continued)

base of the anal fin (Fig. 2). The predorsal midline melanophores series was more prominent (51% of the individuals displayed this pigment pattern). Additional pigmentation included paired lateral melanophores near the dorsal region of the brain cavity, internal pigment above the notochord from the posterior margin of the base of the dorsal fin to the caudal fin, and internal pigment over the gas bladder. A large melanophore was also present above the base of the pectoral fin.

By 18 mm, the dorsal surface of the head became highly pigmented with up to 25 small melanophores. The snout, lower jaw, and pelvic fins were also pigmented by this size. The dorsal and ventral surfaces of the caudal peduncle, as well as the medial predorsal region became more densely pigmented. Outstanding features at this size included 2–9 ventrolateral melanophores in a series along the digestive tract level with the pectoral fins, and isthmus pigment was separated into two spots in many individuals. By 20 mm, the head region was heavily pigmented and the mid-line predorsal pigment progressed fully to the head. Ventrolaterally, 10–30 melanophores forming a triangular pattern covered much of the digestive tract. New pigmentation features at this size included 1–3 small melanophores at the base of the eye and an internal series below the notochord from the base of the dorsal fin to the caudal fin. Pigmentation at the pelvic fin insertion was lost in some specimens, although it was still visible internally in all but one of the cleared and stained specimens. Isthmus pigmentation was also lost at this size.

Living juveniles (>20 mm) are silvery in color over most of the body. The head, back, and dorsal and caudal fins are all pigmented. In preservation, two dark, slash-like pigments spots were present on the posterior lateral body above and below the urostyle. In nearly all other aspects, juvenile finescale menhaden closely

resembled adults by this size. No humeral spots were noted in the two individuals examined.

Discussion

Finescale menhaden larvae resemble the larvae of other clupeids (Houde and Fore, 1973; Jones et al., 1978; McGowan and Berry, 1983; Hettler, 1984; Ditty et al., 1994) in having elongate, slender bodies, light pigmentation, and a small head lacking spines. They have a long, straight gut, often with striations along the hindgut, posteriorly placed dorsal and anal fins, and the vent is always posterior to the dorsal fin base (Jones et al., 1978). Hettler (1984) discussed the separation of individual species of *Brevoortia*, and Ditty et al. (1994) presented a synopsis of characters to separate clupeid larvae (<15 mm) based on meristic, morphometrics, and pigmentation. Finescale menhaden have 43–44 vertebrae, whereas gulf menhaden have 44–46. Yellowfin menhaden are reported to have 45–47 vertebrae (Houde and Swanson, 1975). The number of vertebrae, which should approximate the number of myomeres in larvae much smaller than those collected in this study, in conjunction with pigment differences have been shown to be useful in separating clupeid species complexes (Ditty et al., 1994). In the western gulf, counts of 43–44 vertebrae (=myomeres) would separate finescale menhaden from other clupeid larvae such as *Sardinella aurita* (45–47 vertebrae; Ditty et al., 1994), *Etrumeus teres* (48–50 vertebrae; Fahay, 1983), and *Opisthonema oglinum* (45–46 vertebrae; Richards et al., 1974). Species from the western gulf with similar vertebral counts (*Harengula jaguana*, 39–42; Houde et al., 1974; and *Jenkinsia lamprotaenia*, 39–42; Powles, 1977) can be distinguished from finescale menhaden by their larger PAL:SL ratio (>85% at 15 mm for *Harengula* vs. <85% for finescale menhaden, Table 1) and fewer anal rays (13–14 for *Jenkinsia* vs. 18–24 for finescale menhaden, Table 3). Although vertebral counts were used successfully in distinguishing finescale menhaden from gulf menhaden, the time necessary to clear and stain larvae makes this method impractical for distinguishing between large numbers of menhaden.

In larval and prejuvenile stages, finescale and gulf menhaden are morphologically very similar. Proportional body measurements overlapped too greatly to reliably distinguish the two species. Only the presence of medial predorsal pigment prior to transformation, stellate melanophores at the pelvic fin base, and the size at transformation were useful characters in distinguishing the two species. Hettler (1984) noted that gulf menhaden lack paired melanophores in the predorsal region until initiation of transformation. Pigment at the pelvic fin base appears to be a diagnostic character for the small-scale menhadens because Houde and Swanson (1975) also reported a similar feature in yellowfin menhaden as small as 12.3 mm. Although the presence of this pigment at the pelvic fin base is proposed to be diagnostic for the small-scale menhadens (present study), Hettler's (1984) illustration of a 16.5-mm gulf menhaden shows this pigment. Pigmentation descriptions for developing gulf menhaden have not specifically addressed melanophores at the pelvic fin insertion (Hettler, 1984). Finescale menhaden transform at a smaller size (17–19 mm) than any of the other Gulf of Mexico menhadens. Gulf menhaden did not complete transformation until around 25 mm, which is in agreement with the reported lengths of 25–28 mm for both laboratory reared and wild-caught individuals (Suttkus, 1956; Hettler, 1984). Yellowfin menhaden reach transformation at an intermediate size (20–23 mm; Houde and Swanson, 1975).

Even as adults, finescale menhaden very closely resemble gulf menhaden (Hoese and Moore, 1977) and few reliable characters effectively separate them. Only the absence of striations on the margin of the operculum, a single humeral spot (with no hint of trailing spots along the lateral margins), and more scale rows (60–77 in finescale vs. 36–50 in gulf menhaden; Hoese and Moore, 1977; McEachran and Fechhelm, 1998) distinguish finescale from gulf menhaden. All other meristics overlap greatly; i.e., counts of dorsal-fin rays, anal-fin rays, pectoral-fin rays, pelvic-fin rays, gill-raker counts, and ventral scutes. Although externally similar, significant differences in internal structure between finescale and gulf menhaden have been documented. Finescale menhaden have fewer branchiospinules and shorter intermediate gill rakers than gulf menhaden and, as such, filter mainly zooplankton from the water column; gulf menhaden, in contrast, feed primarily on phytoplankton and detritus (Castillo-Rivera et al., 1996).

Based on length-frequency differences seen between the two species (Fig. 1), the reported spawning season for finescale menhaden along the middle Texas coast could be extended to late May. We still do not know of characters that would distinguish finescale menhaden eggs, and yolksac, preflexion, and flexion larvae from other species in the genus *Brevoortia*. In order to fully describe the development of finescale menhaden, laboratory spawning and rearing experiments are needed to fully describe these early-life stages. Houde (1973) presented relatively simple rearing techniques that allow descriptions of the developmental stages of larval fish (from egg through transformation of larvae to the juvenile stage). These methods have been used successfully for Atlantic, gulf, and yellowfin menhaden, and presumably, finescale menhaden could be reared with these same techniques if their eggs could be obtained. The rearing of finescale menhaden would also allow the effectiveness of the proposed pigment characters used to separate finescale menhaden from gulf menhaden to be tested.

Acknowledgments

This work was performed with funding from the Coastal Bend Bays & Estuaries Program under contract 0203. The Texas Parks and Wildlife Department, Coastal

Studies Program, Resource Protection Division provided additional interagency cooperation in the form of equipment and field logistical support. This manuscript was improved by comments from two anonymous reviewers.

Literature cited

Ahrenholz, D. W.
1991. Population biology and life history of the North American menhadens, *Brevoortia* spp. Mar. Fish. Rev. 53(4):3–19.

Allshouse, W. C.
1983. The distribution of immigrating larval and postlarval fishes into the Aransas-Corpus Christi Bay complex. M.S. thesis, 118 p. Corpus Christi State Univ., Corpus Christi, Texas.

Castillo-Rivera, M., and A. Kobelkowsky.
2000. Distribution and segregration of two sympatric *Brevoortia* species (Teleostei:Clupeidae). Estuar. Coast. Shelf Sci. 50:593-598.

Castillo-Rivera, M., A. Kobelkowsky, and V. Zamayoa.
1996. Food resource partitioning and trophic morphology of *Brevoortia gunteri* and *B. patronus*. J. Fish Biol. 49:1102–1111.

Christmas, J. Y., and R. S. Waller.
1975. Location and time of menhaden spawning in the Gulf of Mexico, 20 p. Gulf Coast Res. Lab., Ocean Springs, MS.

Copeland, B. J.
1965. Fauna of the Aransas Pass Inlet, Texas: I. Emigration as shown by tide trap collections. Publ. Inst. Mar. Sci. Univ. Tex. 10:9–21.

Dahlberg, M. D.
1970. Atlantic and Gulf of Mexico menhadens, genus *Brevoortia* (Pisces:Clupeidae). Bull. Fla. State Mus., Biol. Sci. 15:91–162.

Ditty, J. G., E. D. Houde, and R. F. Shaw.
1994. Egg and larval development of Spanish sardine, *Sardinella aurita* (Family Clupeidae), with a synopsis of characters to identify clupeid larvae from the northern Gulf of Mexico. Bull. Mar. Sci. 54(2):367–380.

Fahay, M. P.
1983. Guide to the early stages of marine fishes occurring in the western North Atlantic Ocean, Cape Hatteras to the southern Scotian shelf. J. Northwest Atl. Fish. Sci. 4:1–423.

Gallaway, B. J., and K. Strawn.
1974. Seasonal abundance and distribution of marine fisheries at a hot-water discharge in Galveston Bay, Texas. Contr. Mar. Sci. 18:71–137.

Gunter, G.
1945. Studies on marine fishes of Texas. Publ. Inst. Mar. Sci. 1(1):1–190.

Hellier, T. R., Jr.
1962. Fish production and biomass studies in relation to photosynthesis in the Laguna Madre of Texas. Publ. Inst. Mar. Sci. Univ. Tex. 8:1–22.

Hettler, W. F.
1984. Description of eggs, larvae, and early juveniles of gulf menhaden, *Brevoortia patronus*, and comparisons with Atlantic menhaden, *B. tyrannus*, and yellowfin menhaden, *B. smithi*. Fish. Bull. 82:85–95.

Hoese, H. D.
1965. Spawning of marine fishes in the Port Aransas, Texas, area as determined by the distribution of young and larvae. Ph.D. diss., 144 p. Univ. of Texas, Austin, TX.

Hoese, H. D., and R. H. Moore.
1977. Fishes of the Gulf of Mexico: Texas, Louisiana, and adjacent waters, 327 p. Texas A&M Univ. Press, College Station.

Houde, E. D.
1973. Some recent advances and unsolved problems in the culture of marine fish larvae. Proc. World Mariculture Soc. 3:83–112.

Houde, E. D., and P. L. Fore.
1973. Guide to identify eggs and larvae of some Gulf of Mexico clupeid fishes. Fla. Dep. Nat. Resour. Mar. Res. Lab. Leafl. Ser. 4 (part 1, no. 23). 14 p.

Houde, E. D., W. J. Richards, and V. P . Sakensa.
1974. Descriptions of eggs and larvae of the scaled sardine, *Harengula jaguana*. Fish. Bull. 72:1106–1122.

Houde, E. D., and L. J. Swanson Jr.
1975. Descriptions of eggs and larvae of yellowfin menhaden, *Brevoortia smithi*. Fish. Bull. 73:660–673.

Jones, P. W., F. D. Martin, and J. D. Hardy Jr.
1978. Development of fishes of the Mid-Atlantic Bight: an atlas of egg, larvae, and juvenile stages. Vol. I: Acipenseridae through Ictaluridae, 340 p. U.S. Dep. Inter., Biol. Serv. Prog.

Leis, J. M., and D. S. Rennis.
1983. The larvae of Indo-Pacific coral reef fishes, 269 p. Univ. Hawaii Press, Honolulu, HI.

Lewis, R. M., and C. M. Roithmayr.
1981. Spawning and sexual maturity of gulf menhaden, *Brevoortia patronus*. Fish. Bull. 78:947–951.

McEachran, J. D., and J. D. Fechhelm.
1998. Clupeidae. *In* Fishes of the Gulf of Mexico. Vol. 1: Myxiniformes to Gasterosteiformes, p. 328–346. Univ. Texas Press, Austin, TX.

McGowan, M. F., and F. H. Berry.
1983. Clupeiforms: development and relationships. *In* Ontogeny and systematics of fishes, p. 108–126. Am. Soc. Ichthyol. Herpetol., Special Publ. 1.

Nelson, W. R., and D .W. Ahrenholz.
1981. Population and fishery characteristics of gulf menhaden, *Brevoortia patronus*. Fish. Bull. 84:311–325.

Newstead, D. J.
2003. Larval fish recruitment to isolated nursery grounds in Nueces Bay, Texas. M.S. thesis, 61 p. Texas A&M Univ.-Corpus Christi, Corpus Christi, TX.

Potthoff, T.
1984. Clearing and staining techniques. *In* Ontogeny and systematics of fishes, p. 35–37. Am. Soc. Ichthyol. Herpetol., Special Publ. 1.

Powles, H.
1977. Description of larval *Jenkinsia lamprotaenia* (Clupeidae, Dussumieriinae) and their distribution off Barbados, West Indies. Bull. Mar. Sci. 27:788–801.

Reintjes, J. W.
1969. Synopsis of the biological data on Atlantic menhaden, *Brevoortia tyrannus*, 30 p. U.S. Dep. Inter., Fish Wildl. Ser., Circ. 320.

Richards, W. J., R. V. Miller, and E. D. Houde.
1974. Egg and larval development of the Atlantic thread herring, *Opisthonema oglinum*. Fish. Bull. 72:1123–1136.

Shaw, R. F., J. H. Cowan and T. L. Tillman.
1985. Distribution and density of *Brevoortia patronus*

(gulf menhaden) eggs and larvae in the continental shelf waters of western Louisiana. Bull Mar. Sci. 36(1):96–103.

Simmons, E. G.
1957. An ecological survey of the upper Laguna Madre of Texas. Publ. Inst. Mar. Sci. Univ. Tex. 4:156–200.

Smith, J. W.
1991. The Atlantic and gulf menhaden purse seine fisheries: origins, harvesting technologies, biostatistical monitoring, recent trends in fisheries statistics, and forecasting. Mar. Fish. Rev. 53(4):28–41.

Suttkus, R. D.
1956. Early life history of the gulf menhaden, *Brevoortia patronus*, in Louisiana. Trans. North Am. Wild. Conf. 21:390–407.

Whitehead, P.J .
1985. FAO species catalogue. Vol. 7. Clupeoid fishes of the world. An annotated and illustrated catalogue of the herrings, sardines, pilchards, sprats, anchovies and wolfherrings. Part 1: Chirocentridae, Clupeidae and Pristigasteridae. FAO Fish. Synop. 125, vol 7, pt 1, 303 p. FAO, Rome.

Diet of the minimal armhook squid (*Berryteuthis anonychus*) (Cephalopoda: Gonatidae) in the northeast Pacific during spring

Kazuhisa Uchikawa
National Research Institute of Far Seas Fisheries
5-7-1 Shimizu-Orido
Shizuoka, 424-8633, Japan
E-mail address: stomyct@affrc.go.jp

John R. Bower
Northern Biosphere Field Science Center, Hakodate Branch
Hokkaido University
3-1-1 Minato-cho, Hakodate
Hokkaido 041-8611, Japan

Yasuko Sato
Department of Agriculture, Forestry and Fisheries, Niigata Prefecture
Agriculture Affairs Division
Shinko-cho
Niigata 950-8570, Japan

Yasunori Sakurai
Graduate School of Fisheries Sciences
Hokkaido University
3-1-1 Minato-cho, Hakodate
Hokkaido 041-8611, Japan

Abstract–The stomach contents of the minimal armhook squid (*Berryteuthis anonychus*) were examined for 338 specimens captured in the northeast Pacific during May 1999. The specimens were collected at seven stations between 145–165°W and 39–49°N and ranged in mantle length from 10.3 to 102.2 mm. Their diet comprised seven major prey groups (copepods, chaetognaths, amphipods, euphausiids, ostracods, unidentified fish, and unidentified gelatinous prey) and was dominated by copepods and chaetognaths. Copepod prey comprised four genera, and 86% by number of the copepods were from the genus *Neocalanus*. *Neocalanus cristatus* was the most abundant prey taxa, composing 50% by mass and 35% by number of the total diet. *Parasagitta elegans* (Chaetognatha) occurred in more stomachs (47%) than any other prey taxon. Amphipods occurred in 19% of the stomachs but composed only 5% by number and 3% by mass of the total prey consumed. The four remaining prey groups (euphausiids, ostracods, unidentified fish, and unidentified gelatinous prey) together composed <2% by mass and <1% by number of the diet. There was no major change in the diet through the size range of squid examined and no evidence of cannibalism or predation on other cephalopod species.

Manuscript submitted 2 September 2003 to the Scientific Editor's Office.
Manuscript approved for publication 29 June 2004 by the Scientific Editor.
Fish. Bull. 102:733–739 (2004).

The squid family Gonatidae plays an important role in the ecosystems of the North Pacific. In the Sea of Okhotsk, the annual production of gonatid squids is more than half that of fish production (Lapko, 1996), and in the western and central Bering Sea, gonatid production is thought to exceed that of the dominant fish families (Radchenko, 1992). In the subarctic North Pacific, the gonatids are an important link in the pelagic food web (Brodeur et al., 1999). To better understand the food web in the North Pacific and the processes influencing the production of gonatid squids in this region, information is needed on the feeding behavior of these squids.

The minimal armhook squid (*Berryteuthis anonychus*) (also known as the "smallfin gonate squid" [Roper et al., 1984]) is a small gonatid (maximum mantle length=150 mm) distributed mainly in the northeast Pacific (Roper et al., 1984; Bower et al., 2002). It is a major prey for fishes, squids, seabirds, and marine mammals (Ogi et al., 1980; Pearcy et al., 1988; Pearcy, 1991; Kuramochi et al., 1993; Pearcy et al., 1993; Ohizumi et al., 2003) but is not targeted by any fishery. Despite the importance of *B. anonychus* in the food web of the subarctic North Pacific, the only published reports on its feeding behavior are two abstracts in the Russian literature (Lapshina, 1988; Didenko, 1990). In this article, we provide further information on the feeding behavior of *B. anonychus* by describing the diet of a wide size range of squid collected from the northeast Pacific during late spring.

Methods

Berryteuthis anonychus was collected during a United States National

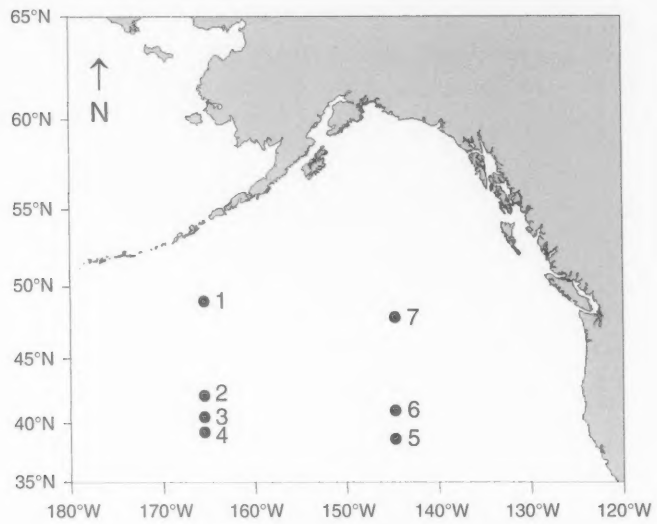

Figure 1

Sampling stations in the northeast Pacific where *Berryteuthis anonychus* were collected during May 1999. Numbers indicate station numbers.

Marine Fisheries Service (NMFS) survey of salmon in the northeast Pacific (Carlson et al., 1999; Bower et al., 2002). Samples were collected during 6–17 May 1999 at seven stations between 145–165°W and 39–49°N (Fig. 1). At each station, a midwater trawl modified to fish at the surface was towed for 1 hour. The trawl was 198 m long and had hexagonal mesh in its wings and body, and a 1.2-cm mesh liner was used in the codend. Trawling speeds were 7–9 km/h, and the average net dimensions while fishing were 16 m vertical spread and 45 m horizontal spread.

Squid samples were frozen on board to –20°C and preserved in 50% isopropyl alcohol in the laboratory. The mantle length (ML) of each squid was measured to the nearest 0.1 mm, and each squid was weighed to the nearest 0.01 g. The stomach contents of 338 squid (167 males, 144 females, 27 undetermined) ranging in ML from 10.3 to 102.2 mm (Fig. 2) were examined under a stereomicroscope. A total of 359 squid were collected during the survey (Bower et al., 2002), but 21 of these specimens were either damaged or lost, and thus excluded from our analyses. Most prey items were fragmented; therefore prey identification was usually based on diagnostic body parts as described in Brodsky (1950), Miller (1988), Baker et al. (1990), and Vinogradov et al. (1996), and by comparison with zooplankton specimens collected in the same area. The prey items were counted and weighed to the nearest 0.01 mg. These wet mass measurements presumably underestimated the initial wet masses because mass loss occurs in invertebrate samples preserved in isopropyl alcohol (e.g., Howmiller, 1972), and it was assumed all prey taxa were equally affected by the preservation. The numbers of individuals of each prey taxon were estimated from the numbers of prey parts, such as copepod mandibles, amphipod heads and chaetognath seizing hooks. Because of the difficulty in distinguishing the copepods *Neocalanus plumchrus* and *N. flemingeri*, they were grouped as a single taxon, *N. plumchrus+flemingeri*. Some calanoid copepods that could not be identified to genus level were identified as either a "specialized form" or a "generalized form"; characters of the specialized form included appendages that were greatly enlarged or strongly developed with chelae, spines on the posterior corners of the terminal thoracic segment,

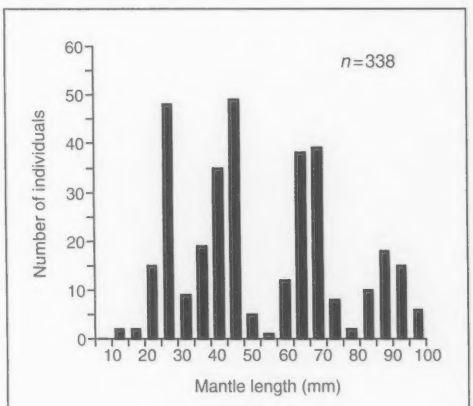

Figure 2

Length-frequency distribution for *Berryteuthis anonychus*.

Table 1

Numbers of *Berryteuthis anonychus* stomachs with identifiable prey remains, without identifiable remains, and without remains from the northeast Pacific. Station numbers refer to those shown in Figure 1.

Station no.	With identifiable remains	Without identifiable remains	Without remains	Total
1	25	0	0	25
2	29	19	45	93
3	33	0	2	35
4	12	1	2	15
5	51	9	6	66
6	44	18	16	78
7	26	0	0	26
Total	220	47	71	338

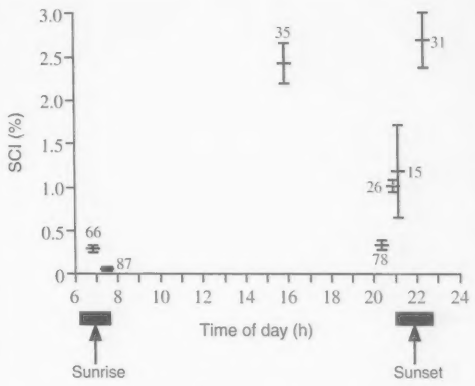

Figure 3

Mean stomach contents index (SCI) of *Berryteuthis anonychus* collected in the northeast Pacific during May 1999 at different times of day. SE = standard error of the mean. Numbers indicate squid sample size for each sampling.

and an asymmetrically swollen genital segment. The generalized form included calanoid copepods of the *Calanus* type that did not share any of these characters.

A stomach-contents index (SCI, %) was calculated as *SCI*=(*wet mass of total stomach contents/wet body mass*)×100. For each prey taxon, the percentages by number (*N*) and wet mass (*WM*) of the total prey, and the percentage frequency of occurrence (*F*) were determined. An index of relative importance (IRI) was calculated for each prey taxon as $IRI_i = F_i \times (N_i + WM_i)$ (Pinkas et al., 1971), where *i* denotes the taxon. The *IRI* for each major group of prey taxa was then standardized to *%IRI* (Cortés, 1997):

$$\%IRI_i = 100 \times IRI_i / \sum_i^n IRI_i,$$

where *n* is the total number of groups collected.

Copepod mandible size is directly related to the carapace length of several calanoid copepods in the North Atlantic (Karlson and Båmstedt, 1994); therefore mandible width was used as an indicator of relative prey size to compare copepod prey size with squid mantle size. A total of 87 mandibles were measured from the stomachs of 10 squid measuring 29–102 mm ML.

Results

Of the 338 stomachs examined, 267 (79%) contained prey, and 220 (65%) contained identifiable prey (Table 1). Individual SCI values ranged from 0% to 8.0% (station mean=1.0%). SCI values varied significantly among sampling times (Kruskal-Wallis test, $P<0.001$), and the two highest SCI values occurred in the afternoon and just after sunset (Fig. 3).

The diet of *B. anonychus* comprised seven major prey groups and was dominated by copepods (*N*=70%, *WM*=85%, *F*=74%, *%IRI*=87%) and chaetognaths (*N*=24%, *WM*=11%, *F*=48%, *%IRI*=12%) (Table 2). The five other prey groups (amphipods, euphausiids, ostracods, unidentified fish, and unidentified gelatinous prey) each had a *%IRI* value ≤1%.

Copepod prey comprised four genera, and 86% by number of the copepods were from the genus *Neocalanus*. *Neocalanus cristatus* was the most abundant prey taxa, composing 50% by mass and 35% by number of the total diet. The three *Neocalanus* taxa (*Neocalanus* spp., *N. plumchrus+flemingeri,* and *N. cristatus*) composed 85% by mass and 68% by number of the diet. *Neocalanus cristatus* was identified based on the presence of the head crest, which develops at the C5 copepodite stage (Brodsky, 1950). Thus, this taxon comprises only the C5 and C6 stages, and possible members of the *Neocalanus* spp. taxon include *N. plumchrus*, *N. flemingeri*, and earlier stages (C1–C4) of *N. cristatus*. Squid ≥60 mm ML fed mainly on *Neocalanus cristatus* (*N*=39%, *WM*=53%, *F*=50%) and *Neocalanus* spp. (*N*=29%, *WM*=31%, *F*=40%), whereas those <60 mm ML fed mainly on *Neocalanus* spp. (*N*=43%, *WM*=53%, *F*=29%) and *Neocalanus plumchrus+flemingeri* (*N*=8%, *WM*=10%, *F*=14%), and consumed few C5–C6 *Neocalanus cristatus* (*N*=4%, *WM*=4%, F=6%). The mandible size of copepod prey showed a clear positive relationship with ML (Fig. 4), indicating that the squid fed on larger copepods as the squid grew. Taxa from other copepod genera (i.e., *Candacia, Metridia,* and *Pleuromamma*) composed 0.5% of the total prey number and 0.1% of the total wet mass (Table 2).

Parasagitta elegans, the only identified chaetognath, occurred in more stomachs (47%) than any other prey taxon and in 58% of the stomachs from squid ≥60 mm

Table 2

Prey items identified from stomach contents of *Berryteuthis anonychus* collected in the northeast Pacific during May 1999. %IRI: standardized index of relative importance. *%IRI* values in parentheses are those for <60 mm ML and ≥60 mm ML squid. Frequency of occurrence was calculated from the number of stomachs containing food. "—" means prey taxon was not present in stomachs.

Taxon	Number (%)	Wet mass (%)	Frequency of occurrence (%)	*%IRI* (<60 mm ML, ≥60 mm ML)
Copepoda	70.2	85.3	74.2	86.5 (80.9, 84.8)
Candacia columbiae	0.2	0.1	1.9	
Candacia sp.	<0.1	<0.1	0.4	
Metridia pacifica	0.2	<0.1	2.2	
Neocalanus cristatus	35.0	50.4	23.2	
Neocalanus plumchrus+flemingeri	3.1	1.8	12.4	
Neocalanus spp.	30.0	32.3	33.3	
Pleuromamma spp.	0.1	<0.1	1.9	
Calanoida (generalized form)	0.5	0.3	4.9	
Calanoida (specialized form)	0.1	0.1	0.4	
Unidentified Calanoida	0.9	0.3	14.2	
Unidentified Copepoda	0.1	0.1	2.6	
Chaetognatha	23.9	10.8	47.6	12.4 (18.1, 13.9)
Parasagitta elegens	23.8	10.7	47.2	
Unidentified Chaetognatha	0.1	0.1	1.1	
Amphipoda	4.6	2.5	19.1	1.0 (1.0, 1.3)
Hyperia medusarum	0.8	0.9	2.2	
Themisto pacifica	2.5	0.9	7.5	
Unidentified Hyperiidae	0.4	0.5	0.7	
Unidentified Physocephalata	<0.1	<0.1	0.4	
Unidentified Hyperiidea	0.7	0.2	7.5	
Unidentified Amphipoda	0.1	<0.1	1.9	
Euphausiacea	0.5	0.9	4.5	<0.1 (<0.1, 0.1)
Euphausia pacifica	<0.1	0.4	0.5	
Thysanoessa sp.	<0.1	<0.1	0.4	
Unidentified Euphausiacea	0.5	0.5	3.7	
Ostracoda	<0.1	<0.1	1.1	<0.1 (<0.1, —)
Unidentified fish	<0.1	0.8	0.4	<0.1 (—, <0.1)
Unidentified gelatinous prey	<0.1	<0.1	0.4	<0.1 (<0.1, —)
Unidentified crustacea	0.1	<0.1	1.1	
Unidentified material	0.6	0.1	18.7	

Neocalanus plumchrus and *N. flemingeri* were grouped as a single taxon (*N. plumchrus+flemingeri*) because of difficulty in distinguishing these species in partly digested materials.

Neocalanus cristatus comprises stages C5 and C6 only.

Neocalanus spp. = *N. cristatus* (stages C1–C4), *N. plumchrus*, and *N. flemingeri*.

Calanoida (specialized form) = unidentified individuals with markedly enlarged appendages, strongly developed chelae, a spine on the posterior corner of the terminal thoracic segment, or asymmetrically swollen genital segments.

Calanoida (generalized form) = unidentified *Calanus*-type individuals that share none of the characters of the specialized form.

ML. *P. elegans* was the third most abundant prey taxon, composing 24% by number and 11% by mass of the total diet (Table 2).

Amphipods (mainly *Themisto pacifica* and *Hyperia medusarum*) were consumed by 19% of the squid but composed only 5% by number and 3% by wet mass of the total prey consumed. The four other prey groups combined composed <2% by mass and <1% by number of the diet. There were no major changes in *%IRI* values through the size range of squid examined (Table 1) and no evidence of cannibalism or predation on other cephalopod species.

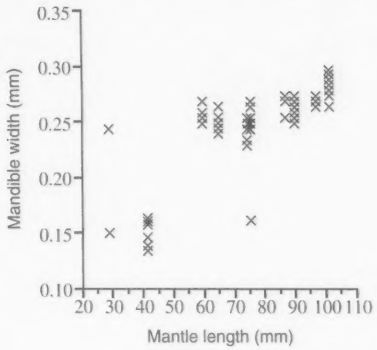

Figure 4

Relationship between mandible width of copepod prey and mantle length of *Berryteuthis anonychus*.

Discussion

The diet of *Berryteuthis anonychus* collected in the northeast Pacific during May was dominated by calanoid copepods and chaetognaths. During early July in this area, *B. anonychus* larger than those examined in the present study (ML: 75–127 mm vs. 10–102 mm) fed on a wider variety of prey, including primarily calanoid copepods, hyperiid amphipods, pteropods, and euphausiids (Lapshina, 1988). Possible causes for this change in diet include seasonal change in prey availability and an ontogenetic change in the squid's ability to capture prey.

The zooplankton composition in the upper 150 m of the subarctic North Pacific is highly seasonal. *Neocalanus* copepods, the major prey of *B. anonychus*, dominate the epipelagic zooplankton community during spring and early summer (Mackas and Tsuda, 1999). They then descend from the upper layer to spend the late summer, autumn, and early winter at 400–2000 m, well below the depth range of *B. anonychus* (0–200 m; Nesis, 1997). As a result of this ontogenetic descent, the upper ocean zooplankton biomass decreases greatly, and the community is then dominated by a different group of species. This group includes euphausiids (Mackas and Tsuda, 1999), which are consumed by more *B. anonychus* in July (28%; Lapshina, 1988) than in May (5%; present study). Other prey that show a large increase in frequency of occurrence between May and July are amphipods (19% in May, 52% in July) and pteropods (0% in May, 40% in July).

Oceanic squids such as *B. anonychus* generally feed on small crustaceans as juveniles and then shift their diet to larger fish and other cephalopods as they grow (Rodhouse and Nigmatullin, 1996). We observed no such ontogenetic shift within the size range examined, but copepod prey size was found to increase with growth. These data are consistent with those for other squids in that prey size increases during development (Nixon, 1987; Hanlon and Messenger, 1996). Most gonatids undergo ontogenetic vertical descent (Roper and Young, 1975; Nesis, 1997), and a clear shift in the diet can accompany this habitat shift (e.g., as seen in *Berryteuthis magister*; Nesis, 1997). Nesis (1997), however, suggested that *B. anonychus* does not undergo ontogenetic descent; therefore no such habitat-change–related shift in diet would be expected to occur in this species.

Highest feeding intensities were recorded in the afternoon and just after sunset, which would indicate that *B. anonychus* feeds both day and night. Such a feeding scenario is supported by the high overlap in depth distributions of *B. anonychus* (day: 50–200 m, night: 0–150 m; Nesis, 1997) and its main prey, *Neocalanus cristatus*; during spring, *N. cristatus* occurs mainly at 50–150 m, and like the other *Neocalanus* species, shows no evidence of diel vertical migration (Mackas et al., 1993). Therefore *B. anonychus* and *N. cristatus* occupy nearly the same depth range both day and night.

The chaetognath *Parasagitta elegans* was the third most abundant prey taxon and was consumed by more squid than any other taxon. *Parasagitta elegans* forms an important fraction of the springtime macrozooplankton community in the North Pacific (Brodeur and Terazaki, 1999) and inhabits mainly the epipelagic layer (0–200 m) (Kotori, 1976; Terazaki and Miller, 1986); therefore predation on *P. elegans* could also occur both day and night. Another gonatid squid, *Gonatus madokai*, has also been found to prey on *Parasagitta* sp. (Kubodera and Okutani, 1977).

There was no evidence of cannibalism, which commonly occurs in many gonatids, particularly *Berryteuthis magister* and *Gonatopsis borealis* (Lapko, 1996; Nesis, 1997). Cannibalism in squids appears to occur less frequently when prey are abundant (Shchetinnikov, 1992; Santos and Haimovici, 1997), as is the case in the North Pacific during spring. In addition, at nearly every station sampled, squid of a small size range were collected (Bower et al., 2002); therefore it seems that opportunities for intercohort cannibalism were limited.

The large stock size of *B. anonychus* in the North Pacific (Nesis, 1997) and its importance in the diet of higher predators may indicate that the food chain from copepods through squids and these higher predators is an important trophic pathway in the pelagic food web of the Subarctic Pacific during spring. The large seasonality in zooplankton composition in the upper 150 m may indicate that these trophic pathways will show similar seasonal variations.

Acknowledgments

We thank the late H. Richard Carlson for providing us with squids collected during the May 1999 NMFS salmon survey aboard the FV *Great Pacific*. We also thank Chingis Nigmatullin and the late Kir Nesis for translating two Russian abstracts into English, H. Sugi-

saki and M. Terazaki for helping identify prey, K. Ichige for helping in the laboratory, and the three anonymous reviewers of the manuscript.

Literature cited

Baker A. de C., B. P. Boden, and E. Brinton.
1990. A practical guide to the euphausiids of the world, 96 p. Natural History Museum, London.

Bower, J. R., J. M. Murphy, and Y. Sato.
2002. Latitudinal gradients in body size and maturation of *Berrytetuhis anonychus* (Cephalopoda: Gonatidae) in the northeast Pacific. Veliger 45:309–315.

Brodeur, R. D., and M. Terazaki.
1999. Springtime abundance of chaetognaths in the shelf region of the northern Gulf of Alaska, with observations on the vertical distribution and feeding of *Sagitta elegans*. Fish. Oceanogr. 8:93–103.

Brodeur, R., S. McKinnell, K. Nagasawa, W. Pearcy, V. Radchenko, and S. Takagi.
1999. Epipelagic nekton of the North Pacific subarctic and transition zones. Prog. Oceanogr. 43:365–397.

Brodsky, K.A.
1950. Calanoida of the far eastern seas and Polar basin of the U.S.S.R. Dokl. Akad. Nauk. SSSR. 35:1–442. USSR Israel Program Scient. Transl. (1967), Jerusalem. Transl. No. TT-65-51200, 440 p.

Carlson, H. R., J. M. Murphy, C. M. Kondzela, K. W. Myers, and T. Nomura.
1999. Survey of salmon in the northeastern Pacific Ocean, May 1999. North Pacific Anadromous Fish Commission, Document 450, 37 p. Natl. Mar. Fish. Serv., Juneau, AK.

Cortés, E.
1997. A critical review of methods of studying fish feeding based on analysis of stomach contents: application to elasmobranch fishes. Can. J. Fish. Aquat. Sci. 54:726–738.

Didenko, V. D.
1990. Prospects of fishery for the squid *Berryteuthis anonychus* in the north-eastern Pacific. *In* "Vth all-USSR conference on commercial invertebrates, Minsk–Naroch. Abstracts of Communications," p. 82–83. [In Russian.] VNIRO Publishing, Moscow, Russia.

Hanlon, R. T., and J. B. Messenger.
1996. Cephalopod behaviour, 232 p. Cambridge Univ. Press, Cambridge, UK.

Howmiller, R. P.
1972. Effects of preservatives on weights of some common macrobenthic invertebrates. Trans. Am. Fish. Soc. 101:743–746.

Karlson, K., and U. Båmstedt.
1994. Planktivorous predation on copepods. Evaluation of mandible remains in the predator guts as a quantitative estimate of predation. Mar. Ecol. Prog. Ser. 108:79–89.

Kotori, M.
1976. The biology of Chaetognatha in the Bering Sea and the northern North Pacific Ocean, with emphasis on *Sagitta elegans*. Mem. Fac. Fish. Hokkaido Univ. 23:95–183.

Kubodera, T., and T. Okutani.
1977. Description of a new species of gonatid squid, *Gonatus madokai* n.sp. from the north-west Pacific, with notes on morphological changes with growth and distribution in immature stages (Cephalopoda: Oegopsida). Venus Jap. J. Malacol. 36(3):123–151.

Kuramochi, T., T. Kubodera, and N. Miyazaki.
1993. Squids eaten by Dall's porpoises, *Phocoenoides dalli* in the northwestern North Pacific and in the Bering Sea. *In* Recent advances in cephalopod fisheries biology (T. Okutani, R. K. O'Dor, and T. Kubodera, eds.), p. 229–240. Tokai Univ. Press, Tokyo.

Lapko, V. V.
1996. The role of squids in the Sea of Okhotsk communities. Oceanology 35:672–677.

Lapshina, V. I.
1988. On the feeding of the squid *Berryteuthis anonychus* Pearcy and Voss from the area of north-eastern Pacific. Deposited MS, Dep. VINITI 25.10.88, No. 7673-B 88, 1–5. [In Russian.]

Mackas, D. L., H. Sefton, C. B. Miller, and A. Raich.
1993. Vertical habitat partitioning by large calanoid copepods in the oceanic subarctic Pacific during spring. Prog. Oceanogr. 32:259–294.

Mackas, D. L., and A. Tsuda.
1999. Mesozooplankton in the eastern and western subarctic Pacific: community structure, seasonal life histories, and interannual variability. Prog. Oceanogr. 43:335–363.

Miller, C. B.
1988. *Neocalanus flemingeri*, a new species of Calanidae (Copepoda: Calanoida) from the subarctic Pacific Ocean, with a comparative redescription of *Neocalanus plumchrus* (Marukawa) 1921. Prog. Oceanogr. 20:223–273

Nesis, K. N.
1997. Gonatid squids in the subarctic North Pacific: ecology, biogeography, niche diversity and role in the ecosystem. Adv. Mar. Biol. 32:243–324.

Nixon, M.
1987. Cephalopod diets. *In* Cephalopod life cycles, vol. II: comparative reviews (P. R. Boyle, ed.), p. 201–219. Academic Press, London.

Ogi, H., T. Kubodera, and K. Nakamura.
1980. The pelagic feeding ecology of the short-tailed shearwater *Puffinus tenuirostris* in the subarctic Pacific region. J. Yamashina Inst. Ornithol. 12:157–182.

Ohizumi, H., T. Kuramochi, T. Kubodera, M. Yoshioka, and N. Miyazaki.
2003. Feeding habits of Dall's porpoises (*Phocoenoides dalli*) in the subarctic North Pacific and the Bering Sea basin and the impact of predation on mesopelagic micronekton. Deep-Sea Res. (I Oceanogr. Res. Pap.). 50:593–610.

Pearcy, W. G.
1991. Biology of the transition region. *In* Biology, oceanography, and fisheries of the North Pacific Transition Zone and Subarctic Frontal Zone (J. A. Wetherall, ed.), p. 39–55. NOAA Tech. Rep. NMFS 105.

Pearcy, W. G., R. D. Brodeur, J. M. Shenker, W. W. Smoker, and Y. Endo.
1988. Food habits of Pacific salmon and steelhead trout, midwater trawl catches and oceanographic conditions in the Gulf of Alaska, 1980–1985. Bull. Ocean Res. Inst. Univ. Tokyo. 26:29–78.

Pearcy, W. G., J. P. Fisher, and M. M. Yoklavich.
1993. Biology of the Pacific pomfret (*Brama japonica*) in the North Pacific Ocean. Can. J. Fish. Aquat. Sci. 50:2608–2625.

Pinkas L., M. S. Oliphant, and I. L. K. Iverson.
1971. Food habits of albacore, bluefin tuna, and bonito in California waters. Calif. Dep. Fish Game Fish. Bull. 152:1–105.
Radchenko, V. I.
1992. The role of squids in the pelagic ecosystem of the Bering Sea. Oceanology 32:762–767.
Rodhouse, P. G., and Ch. M. Nigmatullin.
1996. Role as consumers. Phil. Trans. R. Soc. Lond. B. 351:1003–1022.
Roper, C. F. E., and R. E. Young.
1975. Vertical distribution of pelagic cephalopods. Smithson. Contrib. Zool. 209:1–51.
Roper, C. F. E., M. J. Sweeney, and C. E. Nauen.
1984. FAO species catalogue. Vol. 3. Cephalopods of the world. An annotated and illustrated catalogue of species of interest to fisheries. FAO Fish. Synop. 125, vol. 3, 277 p. FAO, Rome.
Santos, R. A., and M. Haimovici.
1997. Food and feeding of the short-finned squid *Illex argentinus* (Cephalopoda: Ommastrephidae) off southern Brazil. Fish. Res. 33:139–147.
Shchetinnikov, A. S.
1992. Feeding spectrum of squid *Sthenoteuthis oualaniensis* (Oegopsida) in the eastern Pacific. J. Mar. Biol. Assoc. U.K. 72:849–860.
Terazaki, M., and C. B. Miller.
1986. Life history and vertical distribution of pelagic chaetognaths at Ocean Station P in the subarctic Pacific. Deep-Sea Res. 33:323–337.
Vinogradov, M. E., A. F. Volkov, and T. N. Semenova.
1996. Hyperiid amphipods (Amphipoda, Hyperiidea) of the world oceans (D. Siegel-Causey, ed.), 632 p. Science Publishers, Lebanon, NH.

Capture probability of a survey trawl for red king crab (*Paralithodes camtschaticus*)

Kenneth L. Weinberg
Alaska Fisheries Science Center
National Marine Fisheries Service, NOAA
7600 Sand Point Way N.E.
Seattle, Washington 98115
E-mail address: ken.weinberg@noaa.gov

Robert S. Otto
Kodiak Fisheries Research Center
National Marine Fisheries Service, NOAA
301 Research Court
Kodiak, Alaska 99615

David A. Somerton
Alaska Fisheries Science Center
National Marine Fisheries Service, NOAA
7600 Sand Point Way N.E.
Seattle, Washington 98115

Abstract—The relative abundance of Bristol Bay red king crab *(Paralithodes camtschaticus)* is estimated each year for stock assessment by using catch-per-swept-area data collected on the Alaska Fisheries Science Center's annual eastern Bering Sea bottom trawl survey. To estimate survey trawl capture efficiency for red king crab, an experiment was conducted with an auxiliary net (fitted with its own heavy chain-link footrope) that was attached beneath the trawl to capture crabs escaping under the survey trawl footrope. Capture probability was then estimated by fitting a model to the proportion of crabs captured and crab size data. For males, mean capture probability was 72% at 95 mm (carapace length), the size at which full vulnerability to the survey trawl is assigned in the current management model; 84.1% at 135 mm, the legal size for the fishery; and 93% at 184 mm, the maximum size observed in this study. For females, mean capture probability was 70% at 90 mm, the size at which full vulnerability to the survey trawl is assigned in the current management model, and 77% at 162 mm, the maximum size observed in this study. The precision of our estimates for each sex decreased for juveniles under 60 mm and for the largest crab because of small sample sizes.

In situ data collected from trawl-mounted video cameras were used to determine the importance of various factors associated with the capture of individual crabs. Capture probability was significantly higher when a crab was standing when struck by the footrope, rather than crouching, and higher when a crab was hit along its body axis, rather than from the side. Capture probability also increased as a function of increasing crab size but decreased with increasing footrope distance from the bottom and when artificial light was provided for the video camera.

Manuscript submitted 5 September 2003 to the Scientific Editor's Office.
Manuscript approved for publication 28 April 2004 by the Scientific Editor.
Fish. Bull. 102:740–749 (2004)

Regulations limit the annual harvest of Bristol Bay red king crab (RKC; *Paralithodes camtschaticus*) to males ≥135 mm in carapace length[1] (6.5 inches carapace width), and the size of the harvest is dependent upon the estimated biomasses of mature males and females. For stock assessments of RKC, area-swept abundance estimates are determined from the data from annual eastern Bering Sea (EBS) bottom trawl surveys conducted by the National Marine Fisheries Service, Alaska Fisheries Science Center (AFSC), and these estimates are used as input into a length-based assessment model (Zheng et al., 1995) to compute the total allowable catch for each annual fishing season.

It is assumed with the current assessment model that all male RKC ≥95 mm and all female RKC ≥90 mm within the path of the survey trawl (wingtip to wingtip) are captured. This assumption seems reasonable because the survey trawl uses a small diameter footrope designed to stay close to the bottom and red king crab are quite large. However, video photography taken following the 2000 EBS survey revealed that a considerable number of large (≥90 mm) RKC pass under the footrope of the survey trawl.

To assess the potential impact of escaping crab on the calculation of crab biomass, we conducted an experiment to estimate the size-related capture efficiency of the standard survey bottom trawl for Bristol Bay RKC. In this experiment, crab passing beneath the survey trawl were subsequently captured with an auxiliary net that was attached underneath and behind the footrope of the survey trawl (Engås and Godø, 1989; Walsh, 1992). Experimental nets like the one used for this study have been used previously in trawl efficiency studies for flatfish (Munro and Somerton, 2002), as well as for snow *(Chionoecetes opilio)* and Tanner (*C. bairdi*) crabs (Somerton and Otto, 1999). Trawl catch data alone, however, tell little about the details involved with escapement. Therefore, we deployed a video camera on the trawl to observe crab behavior and analyzed a combination of trawl-per-

[1] All references to measured crab lengths are carapace length.

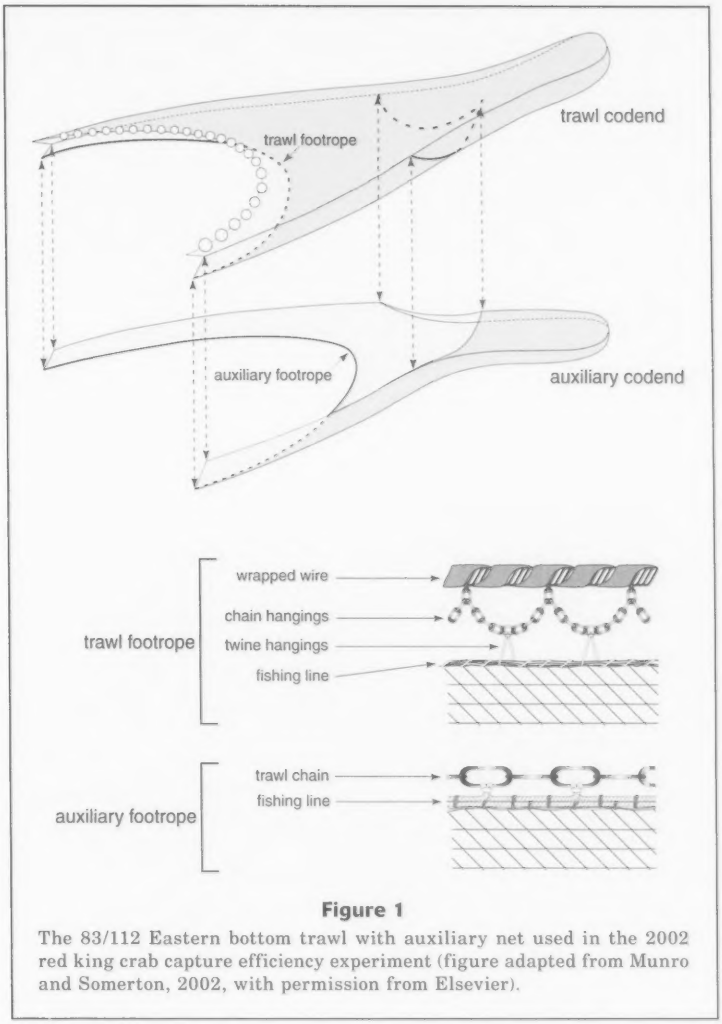

Figure 1

The 83/112 Eastern bottom trawl with auxiliary net used in the 2002 red king crab capture efficiency experiment (figure adapted from Munro and Somerton, 2002, with permission from Elsevier).

formance and crab-behavioral variables to help us understand the escapement process.

Materials and methods

Description of trawl gear

The 83/112 Eastern bottom trawl has been used by the AFSC in annual surveys to assess EBS crab and shelf groundfish stocks since 1982 (Armistead and Nichol, 1993). For the present experiment, an auxiliary net with an independent footrope constructed of heavy chain-link and a separate codend were attached to the bottom of the survey trawl to capture epibenthic animals passing beneath the trawl footrope (Fig. 1). Briefly, the 83/112 Eastern is a low-rise trawl that has a 25.3-m long headrope strung with 48 floats giving it approximately 102 kg of lift and a 34.1 m long, 5.2-cm diameter footrope constructed of 1.6-cm stranded wire rope protected with a single wrap of polypropylene line and split rubber hose. The net is constructed with nylon twine: 10.1-cm stretch mesh throughout the wing and throat sections; 8.9-cm stretch mesh in the intermediate section; a double layer of 8.9-cm stretch mesh in the codend; and a 3.1-cm stretch mesh liner in the codend. It is fished with a pair of 1.8×2.7-m steel V-doors weighing approximately 816 kg apiece.

The auxiliary net attaches to the wingtips and to the bottom of the survey trawl so that the bottom panel of the trawl serves as the top panel of the auxiliary net up to the beginning of the intermediate section. At this point, the two nets part and the auxiliary net then has a top panel of 8.9-cm stretch mesh and a double layer

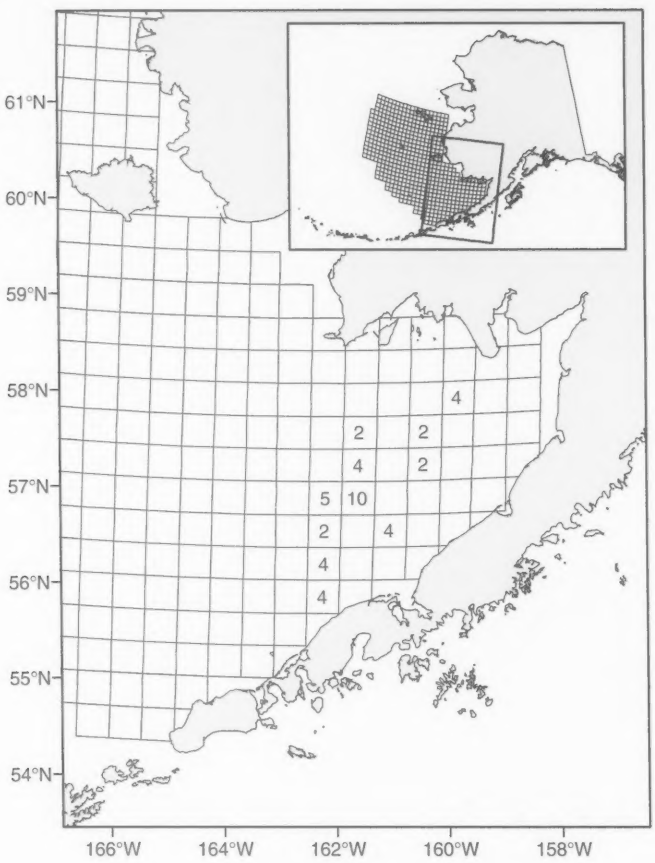

Figure 2

The annual eastern Bering Sea survey station grid showing the number of successful tows per station block made during the 2002 red king crab capture efficiency study. Each block represents a 400-nmi^2 area.

codend with a 3.1-cm stretch mesh liner. The 38.2 m long auxiliary footrope constructed of heavy 16-mm-long link trawl chain was designed to drag through soft bottom and presumably captures all escaping crabs. Munro and Somerton (2002) provided detailed construction plans of this experimental gear in their appendices.

Experimental design

Operations were conducted from 21 to 29 July 2002, aboard the FV *Arcturus*, one of two commercial stern trawlers chartered by the AFSC since 1993 to carry out annual Bering Sea groundfish surveys. Trawling took place in Bristol Bay (Fig. 2) at depths from 41 to 77 m and followed standardized survey protocols that included towing during daylight hours at a 1.5 m/sec (3 knots) vessel speed and using locked winches and standardized lengths of trawl warp (scope) at each towing depth. Acoustic net mensuration equipment was used to measure wing spread for each tow. Bottom contact sensors were used on the centers of both the trawl and auxiliary footropes to measure the distance (in centimeters) between the footropes and the bottom (Somerton and Weinberg, 2001). A silicon-intensified tube (SIT) camera, which uses ambient light, was attached to the center of the trawl to view RKC interaction with the footrope. On some of our trial tows, however, a 30-W quartz halogen light was also used to increase contrast between ambient light and the sea floor.

Two departures from standardized survey protocol were necessary for this experiment. First, 27.5-m long bridles were used instead of the survey standard 55-m long bridles to help offset the loss of wing spread caused by the added drag of the auxiliary net (Munro and Somerton, 2002). Second, tow length was shortened from the survey standard of 30 min to 20 min to minimize the decrease of path width over time due to increased drag from large catches in the auxiliary net.

Towing sites were selected according to catch rates and carapace lengths obtained from the recently completed 2002 EBS survey (Stevens[2]). Tows were made in pairs, one in a northerly direction, the other in a southerly direction and were offset to the east or west by a minimum of 0.1 nmi; the initial direction was chosen randomly in order to mitigate any bias that the current flow might have on footrope contact with the bottom (Weinberg, 2003). Increased effort was given to sites producing favorable numbers and crab lengths by adding additional towing pairs. For each tow the total catch of all species from each net was first weighed before all RKC were removed from the catch, weighed, coded by sex, and measured to the nearest millimeter.

Data analysis

Trawl geometry Trawl geometry for standard survey nets and experimental nets was measured to confirm that the two gear types fished similarly. Average wing spreads and footrope heights off-bottom for experimental tows were compared to those from 33 standard survey gear tows taken at the same or nearby sampling locations. Because the depth of sampling varied, wing spread and footrope height were linearly regressed on scope, a factor variable indicating gear type (i.e., survey or experimental), and their interaction. Two-tailed *t*-tests were used to test for the difference in the slopes and the intercepts between gear types. Significance of the interaction term indicated that slopes differed between gear types. For nonsignificant interaction, significance of the intercepts indicated that wing spread or footrope height differed between gear types by a constant amount.

Capture probability Capture probability for the experimental gear was estimated from catch data of the trawl and the auxiliary net as a function of carapace length (L) for both male and female crab. Based on the assumption that the auxiliary net allows no escapement, the probability of capture at the footrope was modeled as a logistic function (Munro and Somerton, 2002) by using SPLUS software (version 6.1, Insightful Corporation, Seattle, WA). Two models were considered: the first, a two-parameter model which reaches an asymptotic maximum of 1 (unity):

$$P(L)=\frac{1}{1+e^{-(\alpha+\beta L)}}; \quad (1)$$

and the second, a three-parameter model which reaches an asymptotic maximum less than 1:

$$P(L)=\frac{\gamma}{1+e^{-(\alpha+\beta L)}}. \quad (2)$$

[2] Stevens, B. G., R. A. Macintosh, J. A. Haaga, C. E. Armistead, and R. S. Otto. 2002. Report to industry on the 2002 eastern Bering Sea crab survey. AFSC Proc. Rep. 2002-5, 59 p. Alaska Fish. Sci. Cent., Natl. Mar. Fish. Serv., NOAA, Kodiak Fishery Research Center, 301 Research Court, Kodiak AK 99615.

Because crab capture at the footrope is a binomial process (i.e., crabs are either captured or they escape), the models were fitted to the capture and length data by using maximum likelihood (Millar, 1992; Munro and Somerton, 2001) and the data were pooled across tows. For each sex, both models were fitted to the data, and the best of the competing models was selected according to the lowest obtained value of the Akaike information criterion (AIC; Burnham and Anderson, 1998), defined as

$$AIC = -2(log\ likelihood) + 2(number\ of\ parameters).$$

After choosing a model for each sex, we examined whether the capture probability curves differed between sexes by fitting a model to the data for both sexes combined, and then comparing the value of AIC for this model to the sum of the AIC values for the models fitted to each sex, again using the minimum AIC value to objectively select the better of the two models.

Bootstrapped confidence intervals were constructed for the mean capture probability for each 1-mm length category, between the smallest and the largest individuals (Efron and Tibshirani, 1993) by resampling the catch-at-size data from individual hauls 1000 times. Empirical 95% confidence intervals were then determined as the range between the 25th highest and the 25th lowest of the bootstrap capture probability estimates.

Video data analyses

To understand the factors associated with crab escapement under the footrope, a video camera was mounted on the trawl to observe RKC interaction with the center of the trawl footrope. These *in situ* video observations included tows made in 2000 on the standard trawl and in 2002 on the experimental trawl. Artificial light was provided for all of the 2000 tows, and for some of the 2002 trial tows made before the capture efficiency experiment began. All the 2002 experimental tows were made under natural light conditions. RKC encounters observed on the videotapes were counted from the time the footrope settled to the bottom until the time the footrope was lifted off-bottom at the end of the tow. The probability of capture was predicted as a function of several explanatory variables. Variables observed and codes (in parentheses) for each individual included the following:

1 the capture event—the crab escaped beneath the footrope (0) or was captured (1);
2 use of artificial light—the tow was made with (0) or without artificial light (1);
3 estimated mean footrope height above the sea floor over the course of the entire tow was based on the bottom contact sensor and was expressed in centimeters (0–5);
4 body height—the crab was observed to be crouching with its legs either tucked beneath the carapace or stretched out so that the carapace was very close to the bottom (0) or standing upright on its dactyls (1);

Table 1

Regression coefficients of wing spread (width) and footrope distance from the bottom (footrope) as a function of scope and gear type based on tows from the capture efficiency experiment and tows using standard survey gear. Also provided are the results of two-tailed *t*-tests testing for the difference in intercept between gear types.

		Intercept		
	Slope	Experimental gear (n=43)	Standard gear (n=33)	P intercept
Width (m)	0.0038	15.3206	16.0713	<0.0000
Footrope (cm)	0.0087	−1.2582	−0.4241	0.0023

5 body orientation at the point of contact with the footrope—footrope contact occurred along the body axis (1) or from the side (2);

6 crab size—small (0), medium (1), or large (2), where size is expressed as an approximation based on visual comparison of carapace length to the dimensions of trawl parts, such as mesh or chain links. Corresponding length intervals were approximately ≤90 mm, 90–135 mm, and ≥135 mm.

As a general rule, crabs could be seen in the videos 1–2 seconds prior to contact with the footrope. Assignment of codes was typically straightforward. However, in some instances, several reviews of the encounter were necessary in order to determine a crab's position or orientation in relation to the footrope.

The probability of capture was estimated by using stepwise generalized linear modeling (GLM; Venables and Ripley, 1994) to fit a logistic model describing the probability of capture as a function of crab size, where body height, body orientation, average footrope distance from the bottom during the tow, the use of artificial light, and all possible first order interactions were considered as additional potential terms. The model fitting procedure (with data from crabs for which all variables were observed) entailed a stepwise backward model selection process. The process began with fitting the model to all interaction terms less one, and then calculating and comparing the resulting AIC values. The interaction producing the largest decrease in AIC was subsequently eliminated. Next, the procedure was repeated with the remaining terms until no interaction term could be eliminated without increasing the AIC. Then, the above process was repeated for the main effects. For the main effects having an interaction term, both the main effects and the interaction term were eliminated together as a unit. The final model chosen contained those terms that produced the minimum AIC value.

Results

Effect of the auxiliary net on trawl geometry

Regressions of wing spread and footrope height on scope, gear type, and their interaction were compared to determine how closely the two gear types fished. The interaction term was not significant for wing spread (P=0.08) nor for footrope height (P=0.82), indicating that the slopes did not differ between gear types. However, tests of the intercepts were significant for both wing spread and footrope height and indicated that trawl geometry differed between survey and experimental trawls (Table 1). Predicted standard survey wing spreads for the minimum (137 m), median (229 m), and maximum (320 m) scopes used were 16.6, 16.9, and 17.3 m —approximately 0.8 m more than the experimental gear at the same scopes. Predicted footrope distances off the bottom were 0.8, 1.6, and 2.4 cm, at the above three scope values—approximately 0.8 cm greater than the experimental gear. Although we detected statistical differences in the trawl geometry between the two gear types, the actual difference in physical measurements was small and presumably had only a nominal effect on the results of the capture efficiency experiment.

Our assumption that the auxiliary net caught all escaping crabs was reinforced by two observations: 1) the data from the bottom contact sensor on the chain footrope indicated consistent contact with the sea floor; and 2) the auxiliary net consistently had large catches of benthic organisms other than crab, such as starfish and shells, and produced enough drag on the system to reduce wing spread. The effectiveness of the auxiliary footrope at capturing escaping crab is in part due to its weight and small diameter that enable it to sweep beneath the crabs and in part due to the suspension of benthic organisms initiated by the turbulence created by the passing of the first footrope.

Length-based capture probability

Capture probability was estimated from length measurements (n=3233) collected from 43 successful experimental tows (21 north, 22 south) made within 11 standard EBS survey station blocks (Fig. 2). Male samples (n=1667) ranged in size from 23 to 184 mm (Fig. 3). Female samples (n=1566) ranged in size from 51 to 162 mm.

The two-parameter model (model 1) of capture probability was selected over the three-parameter model (model 2) because it had a lower AIC value for both male and female RKC (Table 2). For the comparison of

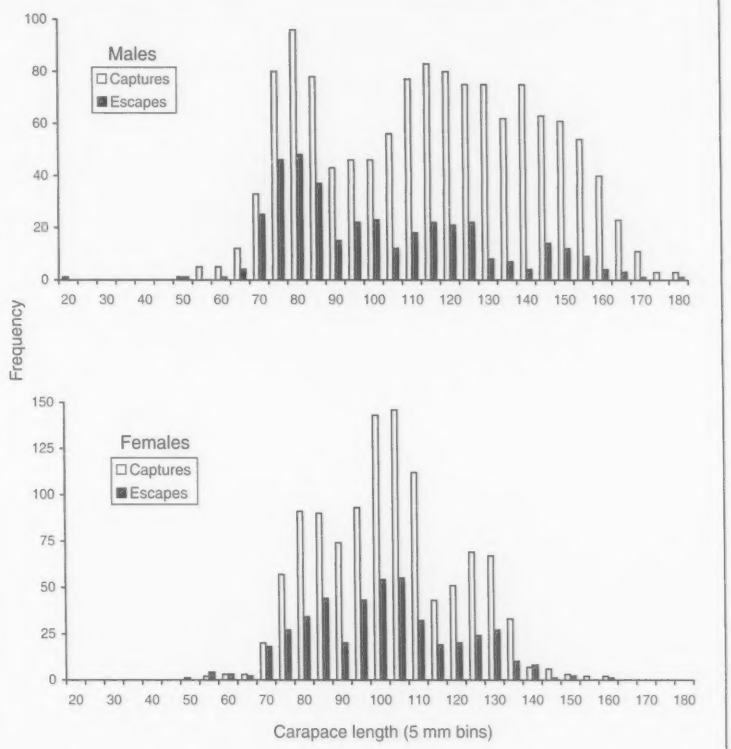

Figure 3

Size frequency of red king crabs taken in the survey trawl (captures) and the auxiliary net (escapes) during the 2002 capture efficiency study. Crab have been binned into 5-mm carapace length intervals.

Table 2

Estimated parameter and Akaike's information criterion (AIC) values for the maximum likelihood fit of the 2-parameter and the 3-parameter logistic models for males, females, and for sexes combined. Parameter variance estimates based on bootstrapping 1000 replicates are provided for the final model used to estimate red king crab capture probability for the 83/112 Eastern survey bottom trawl.

Sex	Model	α	β	γ	AIC	Var α	Var β	Covariance $\alpha\beta$
Male	$1/(1+e^{-(\alpha+\beta l)})$	−0.7366	0.0178	—	1725.3	0.113	1.28×10^{-5}	-1.14×10^{-3}
	$\gamma/(1+e^{-(\alpha+\beta l)})$	−0.8826	0.0209	0.9622	1727.1	—	—	—
Female	$1/(1+e^{-(\alpha+\beta l)})$	0.3540	0.0054	—	1875.7	0.279	2.58×10^{-5}	-2.63×10^{-3}
	$\gamma/(1+e^{-(\alpha+\beta l)})$	0.3540	0.0054	0.9999	1877.7	—	—	—
Combined sexes	$1/(1+e^{-(\alpha+\beta l)})$	−0.4569	0.0143	—	3612.7	—	—	—

selectivity curves for males and females with model 1, we found the summed AIC for separate curves to be lower than the AIC for sexes combined. Consequently, separate selectivity curves were estimated for males and females (Table 2).

The fitted model predicted male capture probability to be 41.9% at 23 mm (size of the smallest male observed); 72.2% at 95 mm (size at which full vulnerability to the survey trawl is assigned in the current management model); 80.2% at 120 mm (size assigned

in the current management model for male maturity); 84.1% at 135 mm (legal size for males); and 92.7% at 184 mm (size of the largest male crab encountered in our experiment [Fig. 4]). The fitted model predicted female capture probability to be 65.2% at 51 mm (size of the smallest female observed); 69.8% at 90 mm (size at which both full vulnerability to the survey trawl and 50% female maturity are assigned in the current management model); 74.7% at 135 mm (same size at which males enter the fishery); and 77.4% at 162 mm (size of the largest female crab encountered in our experiment [Fig. 5]). Estimated capture probability for both male and female crab was equal at 88 mm (69.9%). Model variability, as indicated by the 95% confidence bounds, was greatest at the extremes of our size ranges because of low sample frequency. This was especially true for small crabs, and the uncertainty was so large that extrapolation of the capture probability functions to either males or females below <60 mm is not recommended.

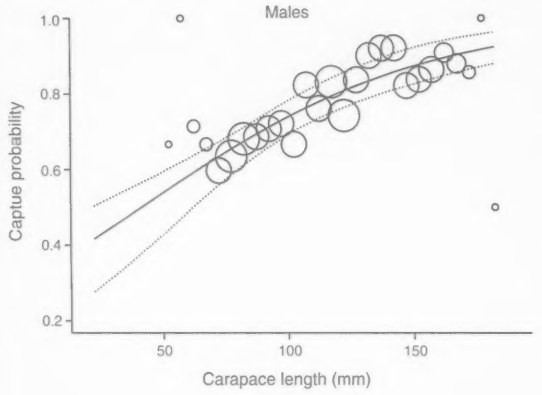

Figure 4

A 2-parameter logistic model (solid line) and 95% confidence bounds (dashed lines) estimating male red king crab capture probability for the 83/112 Eastern survey bottom trawl. Symbols are scaled to the sample length frequency summed over all tows and binned into 5-mm carapace length intervals. Symbols range in size from the smallest circle representing a single individual to the largest circle representing 138 males.

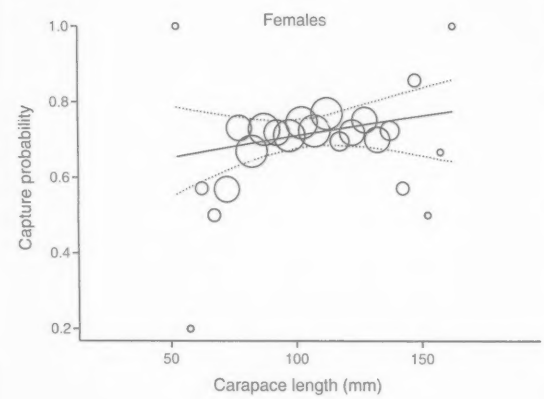

Figure 5

A 2-parameter logistic model (solid line) and 95% confidence bounds (dashed lines) estimating female red king crab capture probability for the 83/112 Eastern survey bottom trawl. Symbols are scaled to the sample length frequency summed over all tows and binned into 5-mm carapace length intervals. Symbols range in size from the smallest circle representing two individuals to the largest circle representing 206 females.

Factors influencing escapement

Modeling the effect of various factors on capture probability was based on observations of RKC (n=248) from videotapes collected during 28 EBS tows. Approximately two-thirds of the counted crabs were captured. The influence of artificial lighting, body height, footrope distance from the bottom, crab size, body orientation, and the interaction of body height and body orientation were significant (Table 3). Capture probability decreased when lights were used and when the distance between the footrope and the bottom increased. Capture probability increased when crabs were standing up on their legs, with increased body size, and when the footrope contact was made along the body axis rather than from the side of the crab.

Capture probability, based on direct observation, was predicted by the fitted logistic models to illustrate how the various explanatory variables affect the capture outcome. We present two examples. In the first case, capture probability in natural light

Table 3

Model coefficients for predicting red king crab capture probability from counts obtained with a trawl-mounted video camera.

	Value	Standard error
Intercept	−2.014	0.676
Light variable	−0.959	0.526
Body height variable	3.789	0.624
Body orientation variable	0.207	0.613
Crab size variable	1.506	0.315
Footrope height variable	−0.286	0.197
Body height and orientation interaction	−1.436	0.785

conditions and when crab are oriented sideways to the oncoming footrope, was predicted as a function of footrope distance off the bottom for each size class, and for both standing and crouching crab (Fig. 6). For all size groups, capture probability decreased with increasing footrope height from the bottom. The importance of whether a crab was standing or crouching diminishes with decreasing crab size because the footrope is more likely to pass completely over smaller crab. In contrast, the importance of standing was higher for large crab because they were more likely to be undercut by the footrope and captured, whereas crouching crab were more susceptible to having their legs first pinned down by the footrope, which exerted a downward pressure on their carapace and allowed the footrope to pass over the crab. Capture probability of medium-size individuals, which included a large proportion of egg-bearing females, was more dependent upon the body height of the crab. Footrope contact below the carapace typically resulted in capture; however contact above the legs often forced the crab's carapace down, causing the crab to roll forward and pass beneath the footrope.

In the second case, capture probability was predicted for natural light conditions when the footrope is 1 cm off-bottom, as a function of crab size, by body orientation to the footrope, and for standing and crouching individuals (Fig. 7). Under these conditions, capture probability was greater for crab contacted along their body axis than for crab hit from the side. In addition, capture probability increased with crab size for both standing and crouching crab, regardless of whether the footrope first contacted the crab along their body axis or from the side. When the footrope was 1 cm off bottom, the difference in the body-orientation effect on capture probability for standing crab was greater for smaller crab than for medium and larger individuals, but relatively equal for crouching crab of all sizes.

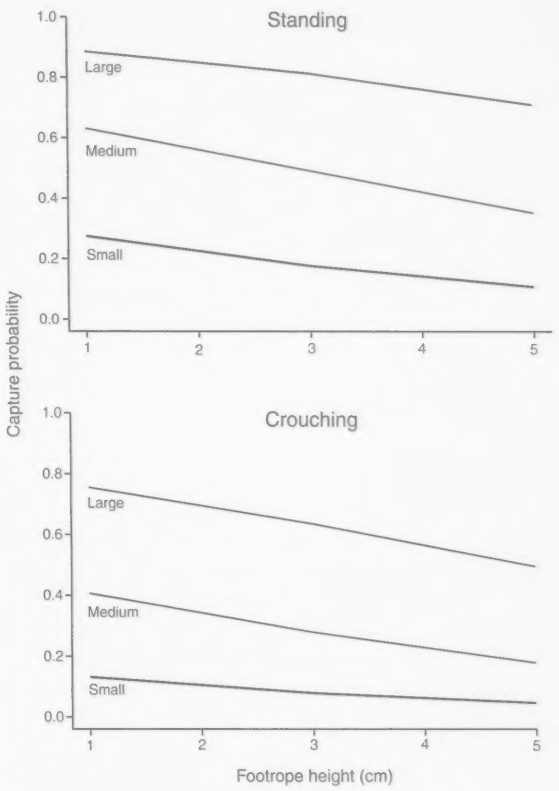

Figure 6

Estimated red king crab capture probability (based on direct observations) by size class as a function of footrope height above the bottom for standing and crouching individuals. For this model, it was assumed that no artificial light was used for the camera and that crab were oriented sideways to the footrope upon initial contact.

Discussion

Our observations confirmed that adult Bristol Bay red king crab can escape beneath the footrope of the AFSC's 83/112 Eastern survey bottom trawl under normal towing conditions. Capture probability increased with size but did not reach 100% for the largest crab caught. For the current management model used for RKC stock assessments, 100% capture probability is assumed for adult crabs and should be revised. A recruitment ogive is used in the calculation of the total spawning biomass for defining overfishing under the Magnuson-Stevens Fishery Conservation and Management Act (Stevens[2]). Revised computations of vulnerability will be required for this purpose as well. Survey trawl selectivity, although similar between the two sexes at prerecruit sizes, was generally 15% higher for legal-size males than for equal-size females. This between-sex difference in capture probability may be explained by behavioral differences (for instance, egg-bearing females stand differently from large males). Unfortunately, crab, when viewed from above, mask their gender; thus sex was excluded from our modeling exercise of video data.

Survey catch statistics for RKC are routinely included in the management modeling procedure to estimate the abundance of legal-size males (≥135 mm), male prerecruits (95–134 mm), the effective spawning biomass of males (≥120 mm), and the spawning biomass of females (≥90 mm, as determined from size at 50% maturity). We estimated capture probability for legal-size males (up to 184 mm) to range from 84% to 93%, for prerecruit males from 73% to 84%, and for the mature portion of the male spawning population (up to 184 mm) from

80% to 93% Our estimated capture probability for the survey trawl on the female portion of the spawning RKC population ranged from 70% to 77% for crab up to 162 mm. A review of the AFSC database for EBS crab surveys showed that the largest male and female crabs taken were 200 mm and 172 mm. Corresponding capture probabilities estimated by the model for these size crabs were 94% and 78%, respectively.

Two main factors affect the overall capture efficiency of epibenthic species by a bottom trawl: 1) horizontal herding, defined as movement into the path of the trawl between the wingtips in response to stimuli produced by the doors or bridles; and 2) escapement, defined as the avoidance of capture once the crab is within the path of the trawl. We believe herding is negligible because our observations of crab movement, which were consistent with those reported by Rose (1999), indicated that RKCs are slow-moving animals that can travel only slight distances before being overtaken by a trawl approaching at 1.5 m/sec. Our video observations of the trawl bridle revealed that RKCs consistently passed over the top of the bare cable, with one exception—where a few crabs were seen sliding along the bridle, legs entangled, to the wingtip before being cast outside the path of the trawl. Escapement is likely restricted to footrope escapement because mesh escapement is impeded by the spiny surface and long legs of the crab and could only occur for the smallest individuals, which we encountered in low numbers and which could not be predicted reliably by our model.

We recognize from the analysis of our *in situ* data that capture probability is influenced not only by trawl performance but also by crab behavior. For instance, crabs standing upright, such as moving or migrating individuals, are more susceptible to capture than those with their bodies resting on the substrate. Crab density could also affect capture probability as seen for some species of fish (Godø et al., 1999). The crabs we observed with our video cameras were fairly dispersed and the maximum number of crabs seen in any single video frame was two (twice observed). Crabs in relatively low abundance are likely to react directly to the gear, but in areas of high abundance, crabs may react to each other in response to the stimuli from the approaching gear, causing them to crouch or conversely move away from perceived danger. Both of these responses would result in a different capture probability.

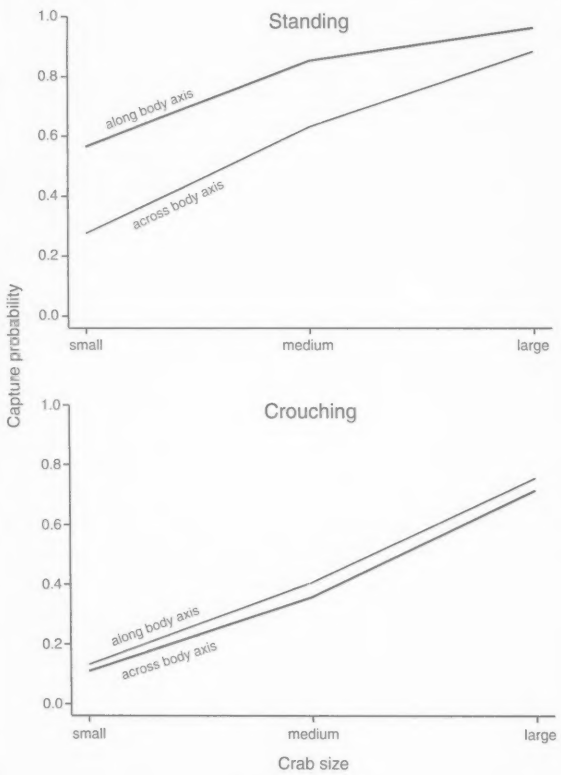

Figure 7

Estimated red king crab capture probability (based on direct observations) by body orientation at the time of footrope contact as a function of crab size for standing and crouching individuals. For this model, it was assumed that no artificial light was used for the camera and that the footrope was 1 cm off bottom.

Our estimates of capture probability apply to the conditions in which the EBS survey is conducted; that is, relatively disperse offshore populations encountered during daylight hours on sandy bottom during the summer months. There are other behavioral factors or environmental conditions that we did not consider in the present study but which could affect the efficiency of the survey trawl. These include, but are not limited to, the following: trawling where the substrate is substantially different; crabs that are either aggregated into pods or are buried (Dew[3]); and temperatures or tidal currents that would affect the migratory or feeding behavior, and therefore the body height of crab (Dew, 1990). Our estimates of capture probability are also based on the assumption that the auxiliary net is 100% efficient at capturing crab escaping beneath the footrope of the survey trawl. We have no direct evidence to believe otherwise. However, if crabs also escaped the auxiliary net, then our estimates of capture probability would be too large.

In conclusion, we wish to clarify to users of our findings that, although these experimentally determined selectivity models indicate an upward correction in spawning biomass of red king crab may be in order, we find no reason

[3] Dew, C. B. 2003. Personal commun. Alaska Fisheries Science Center, 7600 Sand Point Way NE, Seattle, WA 98115.

to claim that the stock is in any better condition than the condition that was determined by the most recent assessment. The foremost utility of the AFSC annual EBS surveys is to monitor distribution and abundance trends through time. The survey accomplishes this by maintaining strict protocols and consistency in trawling methods, in computation of area-swept abundance, and in nonenvironmentally affected trawl efficiency. The survey times series is designed to detect changes in abundance, signaling advances in the population's rebuilding processes, regardless of whether crab are 100% or 80% vulnerable to the survey trawl. We advocate that careful consideration be given to the other factors that drive the management model, along with the results of our capture efficiency experiment, to ensure that the stock rebuilding process remains uninterrupted.

Acknowledgments

We are thankful to Captain Glenn Sullivan and the crew of the FV *Arcturus* for their professional attitudes and relentless attention to detail; to scientists Chris Johnston, Frank Shaw, and Kerim Aydin for their assistance at sea following the 2002 survey; to Craig Rose and Scott McEntire for technical support; to Dave King and Jim Smart for preparation of the experimental trawl gear; and to Gary Walters, Braxton Dew, Doug Pengilly, Jie Zheng, and our anonymous reviewers for their helpful comments during the manuscript review process.

Literature cited

Armistead, C. E., and D. G. Nichol.
1993. 1990 bottom trawl survey of the eastern Bering Sea continental shelf. NOAA Tech. Memo. NMFS-AFSC-7, 190 p.

Burnham, K. P., and D. R. Anderson.
1998. Model selection and inference: a practical information-theoretic approach, 353 p. Springer-Verlag, New York, NY.

Dew, C. B.
1990. Behavioral ecology of podding red king crab, *Paralithodes camtschatica*. Can. J. Fish. Aquat. Sci. 47:1944–1958.

Efron, B., and R. Tibshirani.
1993. An introduction to the bootstrap, 436 p. Chapman and Hall, New York, NY.

Engås, A., and O. R. Godø.
1989. Escape of fish under the fishing line of a Norwegian sampling trawl and its influence on survey results. J. Cons. Int. Explor. Mer 45:269–276.

Godø, O. R., S. J. Walsh, and A. Engås.
1999. Investigating density-dependent catchability in bottom trawl surveys. ICES J. Mar. Sci. 56:292–298.

Millar, R. B.
1992. Estimating the size-selectivity of fishing gear by conditioning on the total catch. J. Am. Stat. Assoc. 87:962–968.

Munro, P. T., and D. A. Somerton.
2001. Maximum likelihood and non-parametric methods for estimating trawl footrope selectivity. ICES J. Mar. Sci. 58:220–229.
2002. Estimating net efficiency of a survey trawl for flatfishes. Fish. Res. 55:267–279.

Rose, C. R.
1999. Injury rates of red king crab, *Paralithodes camtschaticus*, passing under bottom-trawl footropes. Mar. Fish. Rev. 61(2):72–76.

Somerton, D. A., and R. S. Otto.
1999. Net efficiency of a survey trawl for snow crab, *Chionoecetes opilio*, and Tanner crab, *C. bairdi*. Fish. Bull. 97:617–625.

Somerton, D. A., and K. L. Weinberg.
2001. The affect of speed through the water on footrope contact of a survey trawl. Fish. Res. 53:17–24.

Venables, W. N., and B. D. Ripley.
1994. Modern applied statistics with S-plus, 452 p. Springer-Verlag, New York, NY.

Walsh, S. J.
1992. Size-dependent selection at the footgear of a groundfish survey trawl. N. Am. J. Fish. Manag. 12:625–633.

Weinberg, K. L.
2003. Change in the performance of a Bering Sea survey trawl due to varied trawl speed. Alaska Fish. Res. Bull. 10(1):42–49.

Zheng, J., M. C. Murphy, and G. H. Kruse.
1995. A length-based population model and stock-recruitment relationships for red king crab, *Paralithodes camtschaticus*, in Bristol Bay, Alaska. Can. J. Fish. Aquat. Sci. 52 (6):1229–1246.

Evidence of shark predation and scavenging on fishes equipped with pop-up satellite archival tags

David W. Kerstetter
School of Marine Science
Virginia Institute of Marine Science
College of William and Mary
Gloucester Point, Virginia 23062
E-mail address: bailey@vims.edu

Jeffery J. Polovina
Pacific Islands Fisheries Science Center
National Marine Fisheries Service
Honolulu, Hawaii 96822

John E. Graves
School of Marine Science
Virginia Institute of Marine Science
College of William and Mary
Gloucester Point, Virginia 23062

Over the past few years, pop-up satellite archival tags (PSATs) have been used to investigate the behavior, movements, thermal biology, and postrelease mortality of a wide range of large, highly migratory species including bluefin tuna (Block et al., 2001), swordfish (Sedberry and Loefer, 2001), blue marlin (Graves et al., 2002), striped marlin (Domeier and Dewar, 2003), and white sharks (Boustany et al., 2002). PSAT tag technology has improved rapidly, and current tag models are capable of collecting, processing, and storing large amounts of information on light level, temperature, and pressure (depth) for a predetermined length of time before the release of these tags from animals. After release, the tags float to the surface, and transmit the stored data to passing satellites of the Argos system.

A problem noted by several authors using early PSAT models was the occasional occurrence of tags that did not transmit data. Clearly, a tag attached to a moribund fish that would sink to a depth exceeding the pressure limit of the tag casing would be destroyed. To prevent the loss of tags due to mortality events, tag manufacturers and researchers have developed mechanisms that release tags from dead or dying fish before the structural integrity of the tag is compromised at depth. These mechanisms include both mechanical devices that sever the monofilament tether that attaches the tag to the fish upon reaching a given depth and internal software subroutines that activate the normal electronic release mechanism if the tag either reaches a certain depth or maintains a constant depth for a predetermined length of time.

Despite the addition of these release mechanisms to PSATs, some tags still fail to transmit data. Such failure could result from any of the following events or conditions: mechanical failure of a critical tag component; destruction by fishing crews unaware of or not participating in the present research; excessive epifaunal growth that makes the tag negatively buoyant or prevents the tag from floating with the antenna in a vertical position; or fouling of the tag on the fish, fishing gear, or flotsam. Another cause of failure is that the tags could be lost as a result of ingestion. For example, a free-swimming white marlin (*Tetrapturus albidus*) was observed mouthing and almost swallowing a free-floating PSAT off the Dominican Republic in May 2002 (Graves, personal observ.). Alternately, the tag could be ingested incidentally with part of the tagged fish, as described by Jolley and Irby (1979) who reported that an acoustic tag on a sailfish (*Istiophorus platypterus*) was eaten along with the fish by an undetermined species of shark. In this note, we present data from PSATs deployed on two white marlin in the western North Atlantic Ocean and on an opah (*Lampris guttatus*) in the central Pacific; the data from these tags indicate that the tags were consumed by sharks.

Materials and methods

White marlin 1 (WM1)

At approximately 10:00 am local time on 1 September 2002, a white marlin was observed on pelagic longline gear set during the night near the southeastern edge of Georges Bank. The fish, which had been caught on a slightly offset, straight-shank J-style hook (size 9/0), was manually guided with the leader alongside the vessel. A PTT-100 HR model PSAT (Microwave Telemetry, Inc., Columbia, MD) was attached to the dorsal musculature approximately 5 cm below the base of the dorsal fin with a large nylon anchor according to the procedure and tether design described in Kerstetter et al. (2003). The tag was activated shortly after the white marlin was first identified, although approximately one hour is required following activation for this tag model to begin collecting data. The tag was programmed to record point measurements of temperature, light, and pressure (depth) in four-minute time intervals and to detach from the animal after 10 days. After release from the fish, the positively buoyant tag was expected to float to the surface and transmit stored and real-time data. For both white marlin

Manuscript submitted 27 April 2003 to the Scientific Editor's Office.
Manuscript approved for publication 7 June 2004 by the Scientific Editor.
Fish. Bull. 102:750–756 (2004).

Table 1

Comparison of depths and temperatures recorded by three pop-up satellite archival tags (PSATs) before and after the tags were ingested by an organism.

	Before ingestion					After ingestion				
Animal	Depth range (m)	Depth mean (SD)	Temp. range (°C)	Temp mean (SD)	*n*	Depth range (m)	Depth mean (SD)	Temp range (°C)	Temp mean (SD)	*n*
WM1	145.2	145.2 (±0.00)	11.6–11	11.7 (±0.07)	179	0–564.9	130.0 (±237.50)	12.1–26.5	24.1 (±0.84)	2755
WM2	0–26.9	5.9 (±4.44)	19.8–27.8	24.7 (± 0.91)	207	0–699.3	131.0 (±162.61)	18.9–29.5	27.3 (±1.20)	1683
Opah	32–456	221.81 (±92.20)	8–25.6	16.68 (±4.21)	360	0–524	170.56 (±133.83)	26.2–30.6	28.64 (±0.67)	168

tags, minimum straight-line distances were calculated between the point of release and the first clearly transmitted location of the tag following its release (pop-off) (Argos location codes 0–3).

At the time of tagging, the longline hook used to capture the fish was not visible in the mouth of the white marlin. The leader was therefore cut as close as possible to the fish before the fish was released, following the standard operating procedure for the domestic pelagic longline fleet. The fish was maintained alongside the vessel for less than three minutes for the application of the PSAT and a conventional streamer tag. Although the white marlin was initially active at the side of the vessel, some light bleeding from the gills was noted. After release, the fish swam away slowly under its own power.

White marlin 2 (WM2)

At 9:05 am on 2 August 2003, a white marlin was observed on pelagic longline gear with the same configuration in the same approximate area of Georges Bank as WM1. The fish was caught by a circle hook (size 16/0) in the right corner of the mouth, and although the stomach was everted, the fish appeared to be in excellent physical condition. A PTT-100 HR tag had been activated at 6:30 am that morning, and was therefore collecting data at the time of tagging. After the fish was brought to the side of the vessel, both the PSAT and a conventional streamer tag were attached to this fish in less than three minutes by using the same protocol as that described for WM1, and the fish swam strongly away from the vessel after release without any evident bleeding.

Opah

At 5:52 pm local time on 21 November 2002, a female opah was observed on pelagic longline gear set during the day east of the Island of Hawaii. The fish was brought to the side of the fishing vessel and a Wildlife Computers (Redmond, WA) PAT2 model tag was attached through the dorsal musculature with a Wildlife Computers titanium anchor. The tag was programmed to record the temperature and depth occupied by the fish in binned histograms, and the minimum and maximum temperatures and depths for 12-hour time periods. However, these 12-hour bins encompassed both day and night periods. The tag was programmed to be released six months after deployment. In the event of a premature release, the tag was programmed to begin transmitting stored data if it remained at the surface for longer than three days. The opah was lively and quickly dived after it was released.

Results

WM1

Release of the PSAT was expected to occur on 10 September 2002 and the tag was expected to begin transmitting data on that date, but the first transmission was not received until almost two days later. At the time of first transmission, the PSAT was 81.3 km (43.9 nmi) west-southwest of the tagging location. A total of 81.5% of the archived light level, temperature, and pressure (depth) data was recovered.

The light level, temperature, and pressure (depth) readings over time are presented in Fig. 1 (A–C) and summarized in Table 1. The first light level measurements indicated that the fish was already in relatively dark waters within one hour following its release. Light levels continued to drop to almost zero during the next ten hours and remained at that level for the next nine days (Fig. 1A). During the next seven-day surface transmission period, the tag recorded real-time day and night differences in light levels, which indicated that the light sensor was functioning properly.

Sea surface temperatures in the area where the gear was set and hauled back, varied from 25.2° to 26.7°C (D. Kerstetter, unpubl. data) and the first temperature

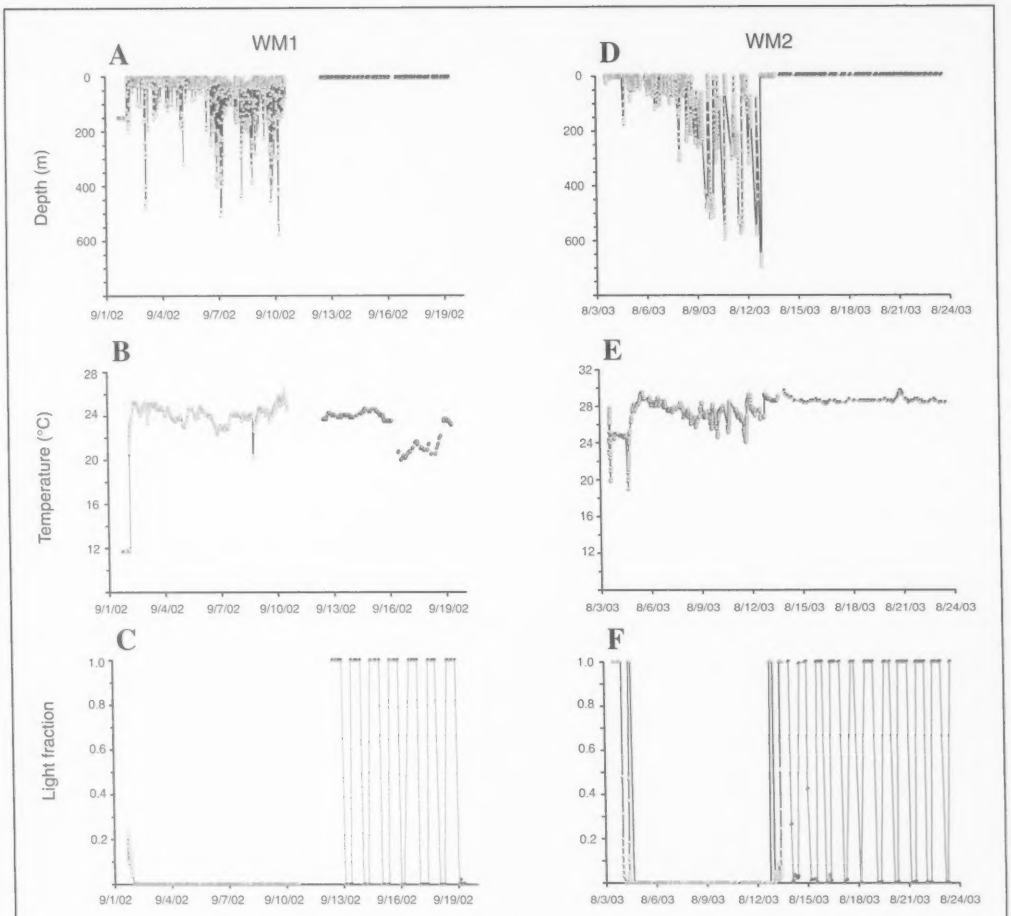

Figure 1

Graphs of data on and depth (**A** and **D**), temperature (**B** and **E**), and light index (**C** and **F**) for tags WM1 and WM2. Lighter lines and points are prior to programmed release date, whereas darker lines and points are "real-time" surface condition measurements transmitted by the tag in addition to the archived data.

recording by the PSAT (one hour after activation) was 11°C (Fig. 1B). The temperature remained fairly constant at 11°C for a period of approximately ten hours after which there was a rapid rise to 25°C. The temperature of the PSAT remained between 22.5° and 26.5°C for the next nine days (until the programmed release date), with the exception of one brief decrease to 20°C on 8 September. When the tag began transmitting on 12 September, the real-time surface temperature was 23.6°C.

The pressure data (Fig. 1C) indicated that the tag was at a depth of approximately 145 m at one hour following release. The PSAT remained at this depth for a little more than ten hours after which the data suggested that there was a rapid rise to the surface. For the next nine days, the tag reported considerable vertical movement between the surface and depths to 565 m. The tag was at the surface when it began transmitting both archived and real-time data on 12 September.

WM2

The tag reported data as expected on 13 August 2003 and transmitted 57.3% of the archived data. At the time of first transmission, the PSAT was 600.1 km (324.0 nmi) east-southeast of the tagging location. Summary depth and temperature data recorded by the PSAT are included in Table 1.

From the depth and temperature data, it appears that the fish survived for approximately 24 hours after release, at which point the light readings dropped to zero (see Fig, 1D) and remained at that level for

the next eight days. The depth record following this change in light level was marked by several discrete diving events, and depths (see Fig. 1F) ranged between the surface and over 699 m. Recorded temperatures for this period varied between 18.9° and 29.5°C, although sea surface temperatures in the area where gear was set and hauled back varied from 20.9° to 26.0°C (Kerstetter, unpubl. data). On 12 August, the light level returned to its maximum value and the tag remained at the surface for approximately one day until its scheduled release date (13 August) when it began transmitting data.

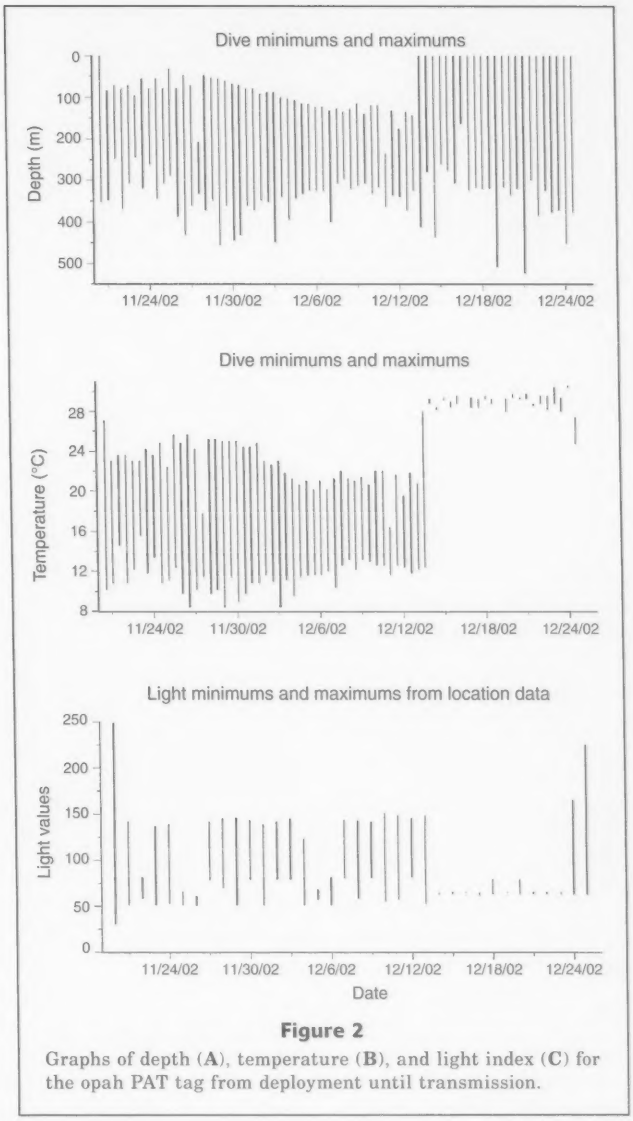

Figure 2

Graphs of depth (**A**), temperature (**B**), and light index (**C**) for the opah PAT tag from deployment until transmission.

Opah

The PAT2 satellite tag was expected to pop-up 6 months after deployment, but the first transmission was received after only 34 days from a location about 330 km (178 nmi) northwest of the deployment site. All the archived binned light level, temperature, and pressure (depth) data from this period were recovered (see Table 1). This tag model collected eight temperature and depth samples during each 12-hour period, resulting in 16 values per day or 528 total values for the deployment period. The two 12-hour blocks were removed from all analyses to more accurately represent the differences in data between specimens: 1) the 12-hour block after tagging in order to allow for the recovery of the animal, and 2) the 12-hour block during which the predation event putatively occurred in order to clarify the potentially distant depth and temperature characteristics of the ingesting animal.

The measured sea surface temperature during the tagging of the opah was 25.9°C. The ranges of dive depths, temperature, and light based on minimum and maximum values over the 12-hour day and night periods showed two distinct patterns (Fig. 2). During the first period (23 days), the dive depths ranged from about 32 to 456 m (Fig. 2A). Water temperatures encountered by the tag during this period ranged from 8.0° to 25.6°C (Fig. 2B) and the light index values ranged from about 50 to 150 (Fig. 2C). During the second period (11 days), the dive depths ranged from 0 to 524 m, temperature ranged from 26.2° to 30.6°C (higher than the 24.2–24.8°C SST recorded by the tag after it was released from the fish), and the light index recorded persistently low values.

Discussion

WM1

Our interpretation of these data is that the PSAT on WM1 was ingested by an animal scavenging the marlin carcass. The first PSAT readings for WM1, recorded about one hour after its release, indicated that the marlin was already dead or moribund by that time and was descending to the ocean floor. For the next ten hours, the tag and carcass remained at a constant depth of 145 m (the depth of the nearest sounding at the site of release, according to NOAA depth chart 13003 [1998], was approximately 160 m) and at a temperature of 11°C. The light level steadily decreased at approximately 4:30 pm, corresponding to changes in ambient light from the setting of the sun. At approximately 9:00 pm local time, there was a dramatic change in conditions when temperature rapidly rose to near 26°C and depths began to vary between the surface and 600 m.

We cannot attribute these changes to a resuscitation of the fish for three reasons. 1) The measured light levels indicated that the tag was in complete darkness for a period of ten days, even though it was at the surface during daylight hours. A malfunctioning light sensor cannot explain this observation because the tag recorded day and night differences in light levels at the surface during the seven-day transmission period after it was released from the fish. 2) After a rapid increase, the temperature remained relatively constant, between 23° and 26°C, even when the tag was at depths in excess of 300 m. Although dive behavior may be affected by location-specific conditions, previous PSAT observations of more than 20 other white marlin indicated that temperature ranges of individual dive events rarely exceed 8°C when, it is assumed, animals make foraging dives to depth (Horodysky et al., in press). 3) The PSAT recorded several dives in excess of 400 m, and previous observations of white marlin have revealed no dives in excess of 220 m (Horodysky et al., in press). Finally, the PSAT was scheduled to be released from WM1 after ten days on 10 September. Although archiving of light, temperature, and pressure data ceased on that date, the tag did not begin transmitting until 12 September.

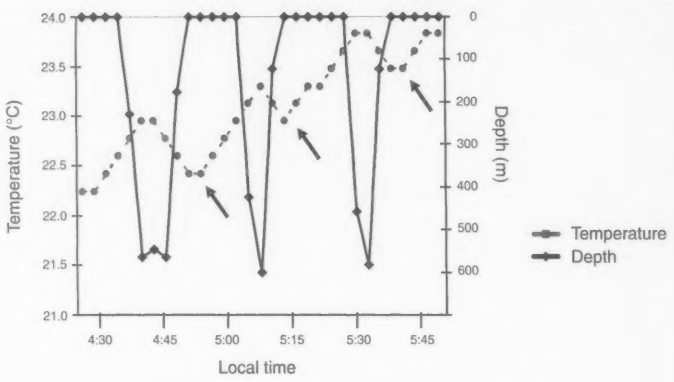

Figure 3

Delayed temperature changes recorded by tag WM1 following deep dive events on the morning of 2 September 2002. Arrows indicate the lowest temperatures recorded in association with a movement of the animal to depth; note that these temperatures were often recorded while the animal was at or near the surface and therefore represent a delay between depth and temperature.

WM2

The shallow dive patterns reported by this fish may indicate that it survived for approximately 24 hours following its release. Between 12:45 and 3:07 pm (local time), the light level fell abruptly from the maximum light level value to zero. At 3:08 pm, the temperature was 19.8°C at 166 m depth; by 4:37 pm, the temperature was above 24°C and remained above this value for the remainder of the deployment period. At 5:58 pm on 12 September, the light levels returned to maximum strength from zero—an indication that the tag had likely been egested. For the 19 hours remaining of the programmed deployment period prior to pop-off, the depth, light, and temperature data all indicated that the tag was floating at the surface.

Opah

Based on recovered data, our conjecture is that the tag was attached to the live opah for the first 23 days. Then, sometime during the 12-hour period from 2:00 pm 13 December to 2:00 am 14 December the tag was ingested. From our data, we cannot discern whether 1) the tag was detached prematurely from the opah and was floating on the surface when it was ingested, 2) an animal attacked the opah and ingested the tag incidentally, or 3) an animal ingested the tag alone. However, it is unlikely that the opah died, sank to the ocean floor, and was scavenged because the ocean floor in the area where the opah was tagged is below 2000 m. We have observed from other tags on opahs what we believe are mortalities; these occur shortly after tagging and show that the tag reaches depths in excess of 1000 m before detaching when the emergency pressure release in the tag is triggered. We did not observe depths below 600 m at any time during this record, and therefore the pressure-induced detachment mechanism on the tag was not triggered.

The ingestion hypothesis for the failure of these three tags to transmit data is supported by several lines of evidence. First, the light level readings were consistent with a tag residing in the complete darkness of an alimentary canal. Second, although temperature variations occurred during the deployment period, the delay in temperature changes during dives to depths indicates that the tags were not directly exposed to ambient water (see Fig. 3 for an example from WM1, as well as the comparisons in Table 1) and further may indicate that the scavenger was either endothermic or of large enough size to mitigate heat loss at depth.

There are several organisms that could have eaten these PSATs, whether by scavenging a carcass or attacking a moving fish. Clearly, each of these organisms was sufficiently large to ingest the tag without seriously damaging it. It is unlikely that a cetacean was responsible for any of these events because internal temperatures for odontocete whales (including killer whales, *Orcinus orca*) range between approximately 36° and 38°C (Whittow et al., 1974)—well above the range of temperatures recorded by the PSATs.

The only other natural predators of large pelagic fishes are various species of sharks. Several species of lamnid sharks maintain elevated body temperatures, including the shortfin mako (*Isurus oxyrinchus*) and the white shark (*Carcharodon carcharias)*, both of which are found in the area of Georges Bank (Cramer, 2000) and the Central Pacific (Compagno, 1984). Several shortfin makos were caught by the same longline vessel during the week following each white marlin PSAT deployment (WM1: n=4, 95–189 cm FL; WM2: n=3, 94–199 cm FL) (Kerstetter, unpubl. data). The opah tag record closely resembles the relatively constant temperature noted for lamnid sharks, despite the independence of stomach temperature with ambient water for these endothermic sharks as reported by Carey et al. (1981). It is also interesting to note that although precipitous temperature fluctuations were generally absent, a rapid drop in temperature from 24° to 20°C was observed with tag WM1 on 8 September at 32.3 m depth—a fluctuation that could have resulted from another feeding event that brought cool food matter into the stomach. Similar reductions in stomach temperatures due to feeding have been noted for white sharks (McCosker, 1987). The range of temperatures recorded by each of the two white marlin tags appears rather broad for an endothermic shark, however, and although the temperature at depth was not measured, the delay in stomach temperature closely resembles the pattern of blue shark internal temperatures (*Prionace glauca*) measured in the Mid-Atlantic (Carey and Scharold, 1990).

The diving behavior recorded by the three tags also corroborates ingestion of the tags by sharks. Carey et al. (1982) reported that a tagged white shark off Long Island, New York, made frequent dives to the bottom during a 3.5-day acoustic tracking period. White sharks are known to dive to depth while scavenging whale carcasses (Dudley et al., 2000; Carey et al., 1982). A juvenile white shark also tracked by Klimley et al. (2002) spent far more extended times at depth than either white marlin tag. Although the programming of the tag on the opah precludes such fine-scale analyses of diving behavior, the available data are not inconsistent with the mako tracks in the study of Klimley et al. (2002). However, the short duration dives with frequent returns to the surface seen with the two white marlin tags most closely resemble those of blue sharks (Carey and Scharold, 1990) and were notably missing from the tracks of three shortfin makos observed by Klimley et al. (2002).

If sharks were indeed the scavenging animals, it is likely that the tags were regurgitated, rather than egested through the alimentary canal, whereupon the PSAT floated to the surface and was able to transmit the archived data. The narrow diameter of the spiral valve in the elasmobranch gastrointestinal tract would likely be too narrow to allow the undamaged passage of an object the size of a PSAT, even for a large shark. Although the available literature describing regurgitation abilities of pelagic sharks is rather limited, Hazin et al. (1994) reported that 35% of blue sharks brought aboard for scientific study had everted and protruding stomachs. Economakis and Lobel (1998) also stated their belief that regurgitation of ingested ultrasonic tags was the primary cause of lost tracks for grey reef sharks (*Carcharhinus amblyrhynchos*) on Johnston Atoll in the central Pacific Ocean.

Conclusions

The temperatures and dive depths recorded by the opah tag and both white marlin tags after apparent ingestion share similarities, yet also contain sufficient information to indicate the different identities of the ingesting organisms. The dive depths in all cases ranged from the surface to over 500 m, whereas the temperatures remained relatively constant at several degrees above the background SST, even during deep dive events. Temperature ranges alone strongly indicate sharks rather than odontocete whales were the ingesting organisms. However, limited literature on the internal stomach temperatures of the various pelagic sharks forces us to rely on telemetered diving behavior data for further species identification, which we used in the present study to suggest that blue sharks ingested the two white marlin tags (on account of the broad range of recorded temperatures) and that an endothermic shark ingested the opah tag.

It is not possible to account for all of the factors that may result in the failure of satellite tags to transmit data, but the results from these three PSATs indicated that biological activities such as predation and scavenging may play an important role. We believe that the most consistent explanation for the data transmitted by these three tags is that they were ingested by large sharks. One cannot calculate the probability that a tag could be engulfed whole without physical damage to the tag, survive for several days in the caustic environment of a digestive system, and be regurgitated with sufficient battery power to transmit data to the Argos satellites, but we suspect that the probability is not very great. We expect that a far greater number of tags may have had similar fates, that is to say, they were damaged by predation or scavenging and digestion processes or were regurgitated later in the transmission cycle, when the PSAT batteries had insufficient remaining power for successful data transmission. The failure of satellite tag to transmit data is frequently considered to be the result of internal tag malfunction or user error. However, these three data sets clearly indicate that the failure of PSATs to function may also be due to predation or scavenging events.

Acknowledgments

The authors would like to thank the Captain of the FV *Sea Pearl* and Captain Greg O'Neill of the FV *Carol Ann*, Don Hawn (University of Hawaii), who deployed the tag on the opah, Evan Howell (PIFSC) for analyses of the opah data, Andrij Horodysky (VIMS), who provided a critical review of the manuscript, Melinda Braun (Wild-

life Computers), who suggested the predation hypothesis to explain the opah data, and Lissa Werbos (Microwave Telemetry, Inc.), who independently suggested the scavenging hypothesis for the WM1 data. This research was supported in part by the National Marine Fisheries Service, the NOAA Ocean Exploration Program, and the University of Hawaii Pelagic Fisheries Research Program (PFRP).

Literature cited

Block, B. A., H. Dewar, S. B. Blackwell, T. D. Williams, E. D. Prince, C. J. Farwell, A. Boustany, S. L. H. Teo, A. Seitz, A. Walli, and D. Fudge.
2001. Migratory movements, depth preferences and thermal biology of Atlantic bluefin tuna. Science 293:1310–1314.

Boustany, A. M., S. F. Davis, P. Pyle, S. D. Anderson, B. J. LeBoeuf, and B. A. Block.
2002. Expanded niche for white sharks. Nature 415: 35–36.

Carey, F. G., J. W. Kanwisher, O. Brazier, G. Gabrielson, J. G. Casey, and H. L. Pratt.
1982. Temperature and activities of a white shark, *Carcharodon carcharias*. Copeia 1982(2):254–260.

Carey, F. G., and J. V. Scharold.
1990. Movements of blue sharks (*Prionace glauca*) in depth and course. Mar. Biol. 106:329–342.

Carey, F. G., J. M. Teal, and J. W. Kanwisher.
1981. The visceral temperatures of mackerel sharks (Lamnidae). Physiol. Zool. 54(3):334–344.

Compagno, L. J. V.
1984. Sharks of the world: an annotated and illustrated catalogue of shark species known to date. Part 1. Hexanchiformes to Lamniformes. U.N. FAO species synopsis 125, vol. 4, pt. I, 249 p. FAO, Rome.

Cramer, J.
2000. Species reported caught in the U.S. commercial pelagic longline and gillnet fisheries from 1996 to 1998. NMFS Sustainable Fisheries Division SFD-99/00-78:1–33.

Domeier, M. L, and H. Dewar.
2003. Post-release mortality rate of striped marlin (*Tetrapterus audax*) caught with recreational tackle. Mar. Freshw. Res., 54(4):435–445.

Dudley, S. F. J., M. D. Anderson-Reade, G. S. Thompson, and P. B. McMullen.
2000. Concurrent scavenging off a whale carcass by great white sharks, *Carcharodon carcharias*, and tiger sharks, *Galeocerdo cuvier*. Fish. Bull. 98:646–649.

Economakis, A. E., and P. S. Lobel.
1998. Aggregation behavior of the grey reef shark, *Carcharhinus amblyrhynchos*, at Johnston Atoll, central Pacific Ocean. Environ. Biol. Fishes 51(2):129–139.

Graves, J. E., B. E. Luckhurst, and E. D. Prince.
2002. An evaluation of pop-up satellite tags for estimating post-release survival of blue marlin (*Makaira nigricans*) from a recreational fishery. Fish. Bull. 100:134–142.

Hazin, F., R. Lessa, and M. Chammas.
1994. First observations on stomach contents of the blue shark, *Prionace glauca*, from southwestern equatorial Atlantic. Revista Brasileira de Biologia 54(2):195–198.

Horodysky, A. Z., D. W. Kerstetter, and J. E. Graves.
In press. Habitat preferences and diving behavior of white marlin (*Tetrapturus albidus*) released from the recreational rod-and-reel and commercial pelagic longline fisheries in the western North Atlantic: implications for habitat-based stock assessment models. International Commission for the Conservation of Atlantic Tunas, Coll. Vol. Sci. Pap., SCRS 2003/033.

Jolley, J. W., Jr., and E. W. Irby Jr.
1979. Survival of tagged and released Atlantic sailfish (*Istiophorus platypterus*: Istiophoridae) determined with acoustical telemetry. Bull. Mar. Sci. 29(2):155–169.

Kerstetter, D. W., B. E. Luckhurst, E. D. Prince, and J. E. Graves.
2003. Use of pop-up satellite archival tags to demonstrate survival of blue marlin (*Makaira nigricans*) released from pelagic longline gear. Fish. Bull. 101(4):939–948.

Klimley, A. P., S. C. Beavers, T. H. Curtis, and S .J. Jorgensen.
2002. Movements and swimming behavior of three species of sharks in La Jolla Canyon, California. Environ. Biol. Fishes 63:117–135.

McCosker, J. E.
1987. The white shark, *Carcharodon carcharias*, has a warm stomach. Copeia 1987(1):195–197.

NOAA (National Oceanographic and Atmospheric Administration).
1998. Atlantic coast chart 13003: Cape Sable to Cape Hattaras. National Ocean Service, Washington, D.C.

Sedberry, G .R., and J. K. Loefer.
2001. Satellite telemetry of swordfish, *Xiphias gladius*, off of the eastern United States. Mar. Biol. 139:355–360.

Whittow, G. C., I. F. G. Hampton, D. T. Matsuura, C. A. Ohata, R. M. Smith, and J. F. Allen.
1974. Body temperature of three species of whales. J. Mammol. 55(3):653–656

Survival rates for rays discarded by the bottom trawl squid fishery off the Falkland Islands

Vladimir V. Laptikhovsky

Falkland Islands Government Fisheries Department
P.O. Box 598
Stanley, FIQQ 1ZZ
Falkland Islands

E-mail address: vlaptikhovsky@fisheries.gov.fk

Waters off the Falkland Islands are subject to a specialized multispecies ray fishery and were first fished by a Korean fleet in 1989. More than twenty different rajid species have been recorded from catches around the islands, and five species accounted for 87.04% of the total catch during 1993–2002. Catches peaked in 1993 at 8523 metric tons, and specific fishing licenses—R (second season) and F (first season)—were first introduced in 1994 and in 1995, respectively (Agnew et al. 2000; Falkland Islands Government, 2002; Wakeford et al., in press).

In addition to the licensed ray fishery, rays are taken as bycatch in the bottom trawl fishery that targets the squid *Loligo gahi* and, to a lesser extent, by the trawl fishery that targets finfish. A 10% bycatch of nontarget species is allowed in both these fisheries. In 2000–2002, the reported ray bycatch of trawlers not licensed to catch rays represented between 20.2% and 31.9% of the total ray catch. However, under-reporting of elasmobranch bycatch is a common practice for trawl fisheries where sharks and rays are discarded (Stevens et al., 2000), and the reported chondrichthyan catch is only about half of the estimated actual global catch (Bonfil, 1994). The actual ray bycatch in Falkland waters may be much higher than reported because only large rays are processed (and therefore, reported) onboard trawlers. This situation makes ray fishery management in the Falkland Islands, which is already difficult because of the nature of the multispecies target, even more complicated. However, good management is of primary importance because sharks and rays appear to be particularly vulnerable to over-exploitation because of their late attainment of sexual maturity, long life span, both low fecundity and natural mortality, and close relationship between recruitment and parental stock (Stevens et al., 2000). In the Falkland trawl fisheries (which includes most trawlers licensed to catch rays), rays smaller than approximately 30 cm disk width are discarded after spending between 5 min and 4 hours in the fish bin and passing through the factory sorting line together with other catch. Some rays that have been caught, stored, and then discarded still show signs of life. In contrast to other marine organisms whose survival after being discarded has been investigated, ray survival has been studied only in Australian waters (Stobutzki et al., 2002). The aim of this study was to investigate the survival rates of discarded rays onboard trawlers in the Falkland waters.

Materials and methods

The research was conducted onboard the Falkland Islands registered trawler *Sil* (length of 78.5 m, gross tons (GRT) of 2156 t, net tons (NT) of 647 t). The vessel used a bottom trawl with a vertical opening of 5 m, horizontal opening of 30 m, and a codend mesh size of 110 mm. Trawling speed varied between 3.8 and and 4.2 kn. Fishing occurred at a depth of 80–190 m during the day and the early part of the night. The surface temperature was 8.7–9.2°C; the near bottom temperature was 6.8–7.6°C. Up to four hauls occurred daily. Each catch was released from the codend into the fish bin, which had a continuous supply of sea water, and the catch immediately began to be sorted on a conveyor belt. Squids and commercial fish were separated from the noncommercial discarded bycatch and were frozen. Of a total of 4306.2 kg of rays caught during the observed period, 67.0% were discarded and only the large rays were processed. The time taken to sort the catch was between 1 and 3 hours.

A total of 66 rays that had been discarded by fishermen were sampled randomly from the conveyor belt and put into a 40-liter (44×35×26 cm) or a 60-liter (31×76×26 cm) fish box that contained running seawater. For each animal, the species and sex was identified and total length (TL) and disk width (DW) were measured within 1 cm. Their "stamina index" was assigned according to four major categories:

A alive, flapping wings.

I immobile, but alive, reacting to irritation, spiracles beginning to work actively after being placed in seawater.

D dead; immobile, but spiracles begin to move slowly and irregularly after being placed in seawater.

DD dead; paralyzed, body stiffened and wings curved but may resume breathing after being placed in seawater.

Each ray (including those evidently dead) was kept in these boxes either until its death was evident (no breathing) or it fully recovered and began to try to swim actively. In some rays the rate of spiracle contractions was episodically recorded.

Manuscript submitted 5 June 2003
to the Scientific Editor's Office.

Manuscript approved for publication
30 June 2004 by the Scientific Editor.

Fish. Bull. 102:757–759 (2004).

Table 1

Species composition and survival of sampled rays. DW= disk width.

Species	*n*	TL, cm	DW, cm	Time spent in fish bin (min.)	Survival rate (%)
Bathyraja albomaculata	14	36–61	26–44	20–110 (mean 45)	71.4
B. brachiurops	11	15–67	9–49	31–145 (mean 72)	54.6
B. griseocauda	3	62–83	47–60	30–75 (mean 60)	0.0
B. macloviana	2	36–42	24–29	70–135	0.0
B. magellanica	5	30–44	20–30	50–125 (mean 90)	60.0
Bathyraja sp.	16	24–104	21–74	5–120 (mean 52)	75.0
Psammobatis sp.	15	29–47	18–33	30–200 (mean 98)	60.0

Table 2

Ray survival (S%), mean recovery time (RT, min.), and occurrence of the four "stamina index" categories after different periods of time (T, min.) spent in the fish bin. T=time (minutes). A=alive; I=immobile; D=presumed dead; DD=dead.

				Occurrence of categories (%)			
T	*n*	S	RT	A	I	D	DD
5–30	16	87.5	38.2	18.75	25	18.75	37.5
31–60	20	75.0	55.5	10.0	30.0	40.0	20.0
65–120	24	41.7	102.2	0	20.8	50.0	29.2
125–200	6	16.7	20[1]	0	16.7	83.3	0

[1] Only one individual (*Psammobathis* sp.).

Results

The sampled rays belonged to eight species (Table 1). Of the 66 sampled rays, a total of 21 were dead at sampling, four recovered breathing but then died, and 39 survived. Two rays recorded as category DD in the "stamina index" were released before full recovery after being held for 4 to 9 hours in running water. Even though these individuals were still breathing, both were considered dead because they still had stiffened bodies and curved wings. If they had been in such a state for a long time in their natural habitat, they almost certainly would have been consumed by scavengers or caught again by another trawler. The overall survival rate was 59.1%, female survival rate was 66.7%, and male survival rate was 56.4%.

All five rays assigned to the "stamina index" category A were sampled between 5 and 30 min (mean 20 min) after the catch was poured into the fish bin. All five individuals began immediately to breathe normally and recovered within 5 to 20 minutes.

Of a total of 18 rays assigned to the "stamina index" category I, which were sampled between 15 and 145 min (mean 55.7 min) after haul, 88.9% (n=16) survived. The breathing of these specimens at the time of sampling was usually slow, although occasionally normal. Spiracle contraction rates gradually increased from an initial rate of 5–15 bit/min to 25–28 bit/min for *B.brachiurops* specimens and to 35–38 bit/min for individuals of *B. albomaculata* and *Bathyraja* sp. Upon attaining normal breathing, they remained immobile, but fully recovered between 15 minutes and 3 hours.

The survival rate of 28 rays that were assigned to the "stamina index" category D was 39.3% (n=11). Of the remaining individuals, two rays died after 15 and 45 minutes after being placed in running seawater and 15 rays were dead at the time of sampling. The skates were sampled between 30 and 200 min (mean 84.2 min) after the haul. Those that survived took 5–80 minutes to recover normal breathing and between 15 and 315 minutes to attain full recovery.

A total of 15 rays were assigned the "stamina index" category DD. However seven of them (46.7%) survived. These individuals were sampled between 20 and 115 minutes (mean 63.9 min.) after the haul and fully recovered within 40 to 150 minutes.

Survival rate varied substantially among the eight species sampled (Table 1). In general, ray survival drastically decreased and recovery time increased with the time spent in the fish bin (Table 2). The critical duration in the fish bin appeared to be between one and two hours; only one *Psammobathis* sp. survived more than two hours in the fish bin and exhibited a surprisingly fast recovery.

Discussion

The survival of discarded rays during trawling operations in the Falkland waters is quite important. Although 65.2% of the individuals were initially assigned as dead, the actual mortality was 40.9%, although it took some rays up to six hours to recover. Survival of shallow-water shelf species such as *Psammobatis* sp., in particular, but also *B. brachiurops* and *B. magellanica,* was somewhat higher than relatively deep-water species such as *B. albomaculata*, *B. griseocauda,* and *Bathyraja* sp., which inhabit the shelf edge and upper part of the slope. This survival rate was most likely related to the greater resilience to environmental changes for shallow-water species, whose habitat is more changeable both seasonally and spatially. Male survival was lower, which is in accordance with data for rays and skates obtained in northern Australian waters (Stobutzky et al., 2002).

Recent data from a tropical prawn fishery off northern Australia showed that on average 44% of individuals of a number of ray and shark species survived a trawling event (Stobutzky et al., 2002). The Falkland ray survival rate was higher. This difference may be due either to the higher metabolic rates of tropical ray species (and therefore a higher vulnerability to asphyxia), or to an overestimation of their mortality, which was assessed immediately after individuals where landed on deck (unlike the recovery time allowed in the present study). The latter factor is more probable because in the present study 41.9% of rays initially recorded as dead (D and DD) eventually recovered.

Despite the demonstrated ability of skates to survive after being caught and stored in fish bins, their continued survival is not guaranteed once they are discarded. They may fall prey to the hundreds of albatrosses and other scavenging birds that are associated with trawlers (author's pers. obs.). The consumption of different discarded fish species and squids from trawlers in Falkland waters by seabirds, primarily by black-browed albatrosses, has been studied (Thompson, 1992), but it is not known whether rays are also taken by sea birds and to what extent. Despite the great abundance of seabirds around vessels in the Southwest Atlantic, it is likely that they consume a minor part of discards as found in Australia (Hill and Wassenberg, 2000). Most of the discarded fish probably fall to the sea floor and attract and are consumed by bottom scavengers and bottom dwellers (Laptikhovsky and Fetisov, 1999; Laptikhovsky and Arkhipkin, 2003). Consequently, even after recovering and successfully avoiding the seabirds, the discarded skates may be consumed or mortally injured by these bottom scavengers during the recovery time, which appears to be about 0.5–1.5 hours.

Acknowledgments

I would like to thank the crew of FV *Sil* for their valuable help during sampling procedures and their hospitality onboard; the Director of Fisheries, John Barton, for supporting this work; A. I. Arkhipkin and an anonimous reviewer for valuable comments; and Helen Otley (FIFD) for language editing.

Literature cited

Agnew, D. J., C. P. Nolan, J. R. Beddington, and R. Baranovski.
2000. Approaches to the assessment and management of multispecies skate and ray fisheries using the Falkland Islands fishery as an example. Can. J. Fish. Aquat. Sci. 57:429–440.

Bonfil, R.
1994. Overview of world elasmobranch fisheries. FAO Fish. Tech. Pap. 341, 119 p.

Falkland Islands Government.
2002. Fisheries Department fisheries statistics, 7, 1993–2002. Falkland Islands Government Fisheries Department, Stanley, Falkland Islands.

Hill, B. J., and T. J. Wassenberg.
2000. The probably fate of discards from prawn trawlers fishing near coral reefs. A study in northern Great Barrier Reef, Australia. Fish. Res. 48:277–286.

Laptikhovsky, V., and A. Arkhipkin .
2003. An impact of seasonal squid migrations and fishery on the feeding spectra of subantarctic notothenioids *Patagonotothen ramsayi* and *Cottoperca gobio* around the Falkland Islands. J. Appl. Ichthyol. 19:35–39.

Laptikhovsky, V., and A. Fetisov
1999. Scavenging by fish of discards from the Patagonian squid fishery. Fish. Res. 41:93–97.

Stevens, J. D., R. Bonfil, N. K. Dulvy, and P. A. Walker.
2000. The effects of fishing on sharks, rays and chimaeras (chondrichthyans), and the implication for marine ecosystems. ICES J. Mar. Sci. 57:476–494.

Stobutzki, I. C., M. J. Miller, D. S. Heales, and D. T. Brewer.
2002. Sustainability of elasmobranchs caught as bycatch in a tropical prawn (shrimp) trawl fishery. Fish. Bull. 100:800–821.

Thompson K. R.
1992. Quantitative analysis of the use of discards from squid trawlers by black-browed albatrosses *Diomedea melanophris* in the vicinity of the Falkland Islands. Ibis 134:11–21.

Wakeford, R .C., D. A. J. Middleton, D. J. Agnew, J. H. W. Pompert, and V. V. Laptikhovsky.
In press. Management of the Falkland Islands multispecies ray fishery: addressing sustainability and diversity. Can. J. Fish. Aquat. Sci.

Acknowledgment of reviewers

The editorial staff of *Fishery Bulletin* would like to acknowledge the scientists who reviewed articles published in 2003–2004. Their contributions have helped ensure the publication of quality science.

Dr. G.R. Abbe
Dr. Pere Abello
Mr. Douglas H. Adams
Dr. Vera N. Agostini
Dr. Juergen Alheit
Dr. Robert J. Allman
Mr. Michael D. Arendt
Dr. Alexander I. Arkhipkin
Dr. David A. Armstrong
Dr. Colin Attwood
Ms. Larisa Avens

Mr. M. Scott Baker Jr.
Dr. Donald M. Baltz
Dr. A. Banner
Dr. Jay Barlow
Dr. Steve Berkeley
Dr. Eric P. Bjorkstedt
Dr. James A. Bohnsack
Ms. Genevieve Briand
Dr. Richard W. Brill
Dr. Alejandro M. Brockmann
Dr. Fiona M. Brook
Dr. Elizabeth Brooks
Dr. Nancy Brown-Peterson
Dr. Jay Burnett
Mr. Michael Burton
Dr. Morgan S. Busby

Dr. Michael Canino
Dr. John K. Carlson
Dr. Milani Y. Chaloupka
Dr. David M. Checkley Jr.
Dr. Susan J. Chivers
Dr. Phillip J. Clapham
Dr. William Coles
Mr. L. Alan Collins

Dr. Craig Dahlgren
Dr. Marilyn E. Dahlheim
Dr. Louis B. Daniel III
Dr. Jana L.D. Davis
Dr. Earl G. Dawe
Dr. Edward E. DeMartini
Dr. Heidi Dewar

Dr. Robert W. Elner
Dr. Tomo Eguchi
Dr. Charles E. Epifanio
Dr. Sheryan P. Epperly

Dr. S. Frantini
Dr. Gregory L. Fulling

Ms. Moira Galbraith
Dr. Francisco J. Garcia-Rodriguez
Mr. Bert Geary
Dr. Harry J. Grier
Dr. Churchill B. Grimes
Dr. Donald R. Gunderson

Dr. Chris Habicht
Dr. Lewis J. Haldorson
Dr. J. Mark Hanson
Dr. E. Brian Hartwick
Dr. James T. Harvey
Dr. Jonathan Heifetz
Dr. Kevin T. Hill
Dr. Simeon Hill
Dr. David B. Holts

Dr. J. Jeffrey Isely

Dr. George D. Jackson
Ms. Nadine Johnston
Dr. Lindsay Joll

Dr. Michel J. Kaiser
Mr. Craig R. Kastelle
Dr. Izhar A. Khan
Dr. J. King
Dr. A. Peter Klimley
Dr. Suzanne Kohin

Dr. Thomas E. Laidig
Dr. Richard W. Langton
Ms. Amy Lapolla
Dr. Robert N. Lea
Dr. Christopher M. Legault
Dr. Steven T. Lindley
Dr. Romuald Lipcius
Dr. Kwang Ming Liu
Dr. Kai Lorenzen
Dr. Milton S. Love
Mr. Mark S. Lowry
Dr. Mark Luckenbach

Dr. R. Bruce MacFarlane
Dr. William K. Macy
Dr. Richard McBride
Dr. Susanne McDermott
Ms. Kitty Mecklenburg
Dr. David A. Milton

Dr. T.J. Minello
Mr. Karl W. Mueller
Dr. Ashley Mullen
Dr. Keith D. Mullin
Dr. Michael D. Murphy
Dr. Kate Myers

Dr. Wallace J. Nichols

Dr. Peter F. Olesiuk

Dr. Ernst Peebles
Dr. Karl M. Polivka
Dr. Kenneth H. Pollock
Dr. Allyn B. Powell

Dr. Hans-Joachim Raetz
Dr. Stephen Ralston
Mrs. Tone Rasmussen
Dr. Sherrylynn Rowe
Dr. Peter Rubec
Mr. D.E. Ruzzante

Dr. Yvonne Sadovy
Dr. Bernard Sainte-Marie
Dr. Kurt M. Schaefer
Dr. George R. Sedberry
Dr. Jeffrey Seminoff
Mr. Lawrence Settle
Dr. James B. Shaklee
Dr. Alan Sinclair
Dr. Oscar Sosa-Nishizaki
Dr. Gretchen Steiger
Dr. David L. Stein
Dr. Allan W. Stoner
Dr. D.P. Swain
Dr. Yonat Swimmer

Dr. Yuji Tanaka
Dr. Sven Thatje
Dr. A.M. Tokranov
Dr. M.J. Tremblay
Dr. Marc Trudel

Dr. Fred M. Utter

Dr. Peter Van Tamelen

Dr. Michael Vecchione

Dr. Claire M. Waluda
Mr. William Watson
Dr. George Watters
Dr. Elizabeth L. Wenner
Mr. A.J. Winship
Dr. Sabine Petra Wintner
Dr. Bernd Wursig

Dr. Orio Yamamura
Dr. Richard E. Young

The index and/or table of contents has been removed and photographed separately within this volume year.

For roll film users, this information for the current volume year is at the beginning of the microfilm. For a prior year volume, this information is at the end of the microfilm.

For microfiche users, the index and/or contents is contained on a separate fiche.

Superintendent of Documents **Publications** Order Form

*5178

☐ YES, please send me the following publications:

___ Subscriptions to *Fishery Bulletin*
for $55.00 per year ($68.75 foreign)

The total cost of my order is $ _____ . Prices include regular domestic postage and handling and are subject to change.

_____
(Company or Personal Name) (Please type or print)

_____
(Additional address/attention line)

_____
(Street address)

_____
(City, State, ZIP Code)

_____
(Daytime phone including area code)

_____
(Purchase Order No.)

Charge your order. IT'S EASY!

VISA

MasterCard

Please Choose Method of Payment:

☐ Check Payable to the Superintendent of Documents
☐ GPO Deposit Account ☐☐☐☐☐☐☐–☐
☐ VISA or MasterCard Account
☐☐☐☐☐☐☐☐☐☐☐☐☐☐☐☐
☐☐☐☐ (Credit card expiration date)

To fax your orders (202) 512-2250

_____
(Authorizing Signature)

Mail To: Superintendent of Documents
P.O. Box 371954, Pittsburgh, PA 15250-7954

Thank you for your order!

This statement is required by the Act of August 12, 1970, Section 3685, Title 39, U.S. Code, showing ownership, management, and circulation of the *Fishery Bulletin*, publication number 366-370, and was filed on 02 September, 2004. The *Bulletin* is published quarterly (four issues annually) with an annual subscription price of $55.00 (sold by the Superintendent of Documents, U.S. Government Printing Office, Washington, DC 20402). The complete mailing address of the office of publication is NMFS Scientific Publications Office, NOAA, 7600 Sand Point Way NE, BIN C15700, Seattle, WA 98115. The complete mailing address of the headquarters of the publishing agency is National Marine Fisheries Service, NOAA, Department of Commerce, 1335 East-West Highway, Silver Spring, MD 20910. The name of the publisher is Willis Hobart and the managing editor is Sharyn Matriotti; their mailing address is: NMFS Scientific Publications Office, 7600 Sand Point Way NE, BIN 15700, Seattle, WA 98115. The owner is the U.S. Department of Commerce, 14th St. N.W., Washington, DC 20230; there are no bondholders, mortgages, or other security holders. The purpose, function, and nonprofit status of the organization (agency) and the exempt status for Federal income tax purposes has not changed during the preceding 12 months. The extent and nature of circulation is as follows: total number of copies (A) (average number of copies of each issue during the preceding 12 months) was 1371 and the actual number of copies of the single issue published nearest to the filing dates was 1382. Paid circulation (B) is handled by the U.S. Government Printing Office, Washington, DC 20402, and the total number printed for sales (mail subscriptions and individual sales) was 475 for the average number of copies each issue during the preceding 12 months and 475 the actual number of copies of the single issue published nearest to the filing date (C). Free distribution (D) by mail; samples, complimentary and other free copies (average number of copies each issue during the preceding 12 months) was 792 and the actual number of copies of the single issue published nearest to the filing date was 761. Free distribution outside the mail (E) by carriers or other means was 0 for both average number of copies and actual number of copies. Total free distribution (F) was 0 for both average number of copies and actual number of copies of the single issue published nearest the filing date. The total distribution (G: sum of D and B) (average number of copies each issue during the preceding 12 months) was 1267 and the actual number of copies of the single issue published nearest to the filing date was 1236. There were 65 copies (avg. annual) not distributed (H). The total (I: sum of G and H) is equal to the net press run figures shown in Item A: 1332 and 1301 copies, respectively. I certify that the statements made by me above are correct and complete: (Signed) Willis Hobart, Publisher.

Fishery Bulletin

Guidelines for contributors

Content of papers

Articles

Articles are reports of 10 to 30 pages (double spaced) that describe original research in one or a combination of the following fields of marine science: taxonomy, biology, genetics, mathematics (including modeling), statistics, engineering, economics, and ecology.

Notes

Notes are reports of 5 to 10 pages without an abstract that describe methods and results not supported by a large body of data. Although all contributions are subject to peer review, responsibility for the contents of articles and notes rests upon the authors and not upon the editor or the publisher. It is therefore important that authors consider the contents of their manuscripts carefully. Submission of an article is un-derstood to imply that the article is original and is not being considered for publication elsewhere. Manuscripts must be written in English. Authors whose native language is not English are strongly advised to have their manuscripts checked for fluency by English-speaking colleagues prior to submission.

Preparation of papers

Text

Title page should include authors' full names and mailing addresses (street address required) and the senior author's telephone, fax number, e-mail address, as well as a list of key words to describe the contents of the manuscript. **Abstract** must be less than one typed page (double spaced) and must not contain any citations. It should state the main scope of the research but emphasize the author's conclusions and relevant findings. Because abstracts are circulated by abstracting agencies, it is important that they represent the research clearly and concisely. **General text** must be typed in double-spaced format. A brief introduction should state the broad significance of the paper; the remainder of the paper should be divided into the following sections: Materials and methods, Results, Discussion (or Conclusions), and Acknowledgments. Headings within each section must be short, reflect a logical sequence, and follow the rules of multiple subdivision (i.e. there can be no subdivision without at least two subheadings). The entire text should be intelligible to interdisciplinary readers; therefore, all acronyms and abbreviations should be written out and all lesser-known technical terms should be defined the first time they are mentioned. The scientific names of species must be written out the first time they are mentioned; subsequent mention of scientific names may be abbreviated. Follow *Scientific style and format: CBE manual for authors, editors, and publishers* (6th ed.) for editorial style and the most current issue of the *American Fisheries Society's common and scientific names of fishes from the United States and Canada* for fish nomenclature. Dates should be written as follows: 11 November 1991. Measurements should be expressed in metric units, e.g. metric tons (t). The numeral one (1) should be typed as a one, not as a lower-case el (l).

Footnotes

Use footnotes to add editorial comments regarding claims made in the text and to document unpublished works or works with local circulation. Footnotes should be numbered with Arabic numerals and inserted in 10-point font at the bottom of the first page on which they are cited. Footnotes should be formatted in the same manner as citations. If a manuscript is unpublished, in the process of review, or if the information provided in the footnote has been conveyed verbally, please state this information as "unpubl. data," "manuscript in review," and "personal commun.," respectively. Authors are advised wherever possible to avoid references to nonstandard literature (unpublished literature that is difficult to obtain, such as internal reports, processed reports, administrative reports, ICES council minutes, IWC minutes or working papers, any "research" or "working" documents, laboratory reports, contract reports, and manuscripts in review). If these references are used, please indicate whether they are available from NTIS (National Technical Information Service) or from some other public depository. Footnote format: author (last name, followed by first-name initials); year; title of report or manuscript; type of report and its administrative or serial number; name and address of agency or institution where the report is filed.

Literature cited

The literature cited section comprises works that have been published and those accepted for publication (works in press) in peer-reviewed journals and books. Follow the name and year system for citation format. In the text, write "Smith and Jones (1977) reported" but if the citation takes the form of parenthetical matter, write "(Smith and Jones, 1977)." In the literature cited section, list citations alphabetically by last name of senior author: For example, Alston, 1952; Mannly, 1988; Smith, 1932; Smith, 1947; Stalinsky and Jones, 1985. Abbreviations of journals should conform to the abbreviations given in the *Serial sources for the BIOSIS previews database*. Authors are responsible for the accuracy and completeness of all citations. Literature citation format: author (last name, followed by first-name initials); year; title of report or article; abbreviated title of the journal in which the article was published, volume number, page numbers. For books, please provide publisher, city, and state.

Tables

Tables should not be excessive in size and must be cited in numerical order in the text. Headings in tables should be short but ample enough to allow the table to be intelligible on its own. All unusual symbols must be explained in the table legend. Other incidental comments may be footnoted (use italic arabic numerals for footnote markers). Use asterisks only to indicate probability in statistical data. Place table legends on the same page as the table data. We accept tables saved in most spreadsheet software programs (e.g. Microsoft Excel). Please note the following:

- Use a comma in numbers of five digits or more (e.g. 13,000 but 3000).
- Use zeros before all decimal points for values less than one (e.g. 0.31).

Figures

Figures include line illustrations, computer-generated line graphs, and photographs (or slides). They must be cited in numerical order in the text. Line illustrations are best submitted as original drawings. Computer-generated line graphs should be printed on laser-quality paper. Photographs should be submitted on glossy paper with good contrast. All figures are to be labeled with senior author's name and the number of the figure (e.g. Smith, Fig. 4). Use Helvetica or Arial font to label anatomical parts (line drawings) or variables (graphs) within figures; use Times Roman bold font to label the different sections of a figure (e.g. **A**, **B**, **C**). Figure legends should explain all symbols and abbreviations seen within the figure and should be typed in double-spaced format on a separate page at the end of the manuscript. We advise authors to peruse a recent issue of *Fishery Bulletin* for standard formats. Please note the following:

- Capitalize the first letter of the first word of axis labels.
- Do not use overly large font sizes to label axes or parts within figures.
- Do not use boldface fonts within figures.
- Do not create outline rules around graphs.
- Do not use horizontal lines through graphs.
- Do not use large font sizes to label degrees of longitude and latitude on maps.
- Indicate direction of degrees longitude and latitude on maps (e.g. 170°E).
- Avoid placing labels on a vertical plane (except on *y* axis).
- Avoid odd (nonstandard) patterns to mark sections of bar graphs and pie charts.

Copyright law

Fishery Bulletin, a U.S. government publication, is not subject to copyright law. If an author wishes to reproduce any part of *Fishery Bulletin* in his or her work, he or she is obliged, however, to acknowledge the source of the extracted literature.

Submission of papers

Send four printed copies (one original plus three copies)—clipped, *not stapled*—to the Scientific Editor, at the address shown below. Send photocopies of figures with initial submission of manuscript. Original figures will be requested later when the manuscript has been accepted for publication. Do not send your manuscript on diskette until requested to do so.

Dr. Norman Bartoo
National Marine Fisheries Service, NOAA
8604 La Jolla Shores Drive
La Jolla, CA 92037

Once the manuscript has been accepted for publication, you will be asked to submit a software copy of your manuscript. The software copy should be submitted in WordPerfect or Word format (in Word, save as Rich Text Format). Please note that we do not accept ASCII text files. Color figures must be CMYK files.

Reprints

Copies of published articles and notes are available free of charge to the senior author (50 copies) and to his or her laboratory (50 copies). Additional copies may be purchased in lots of 100 when the author receives page proofs.

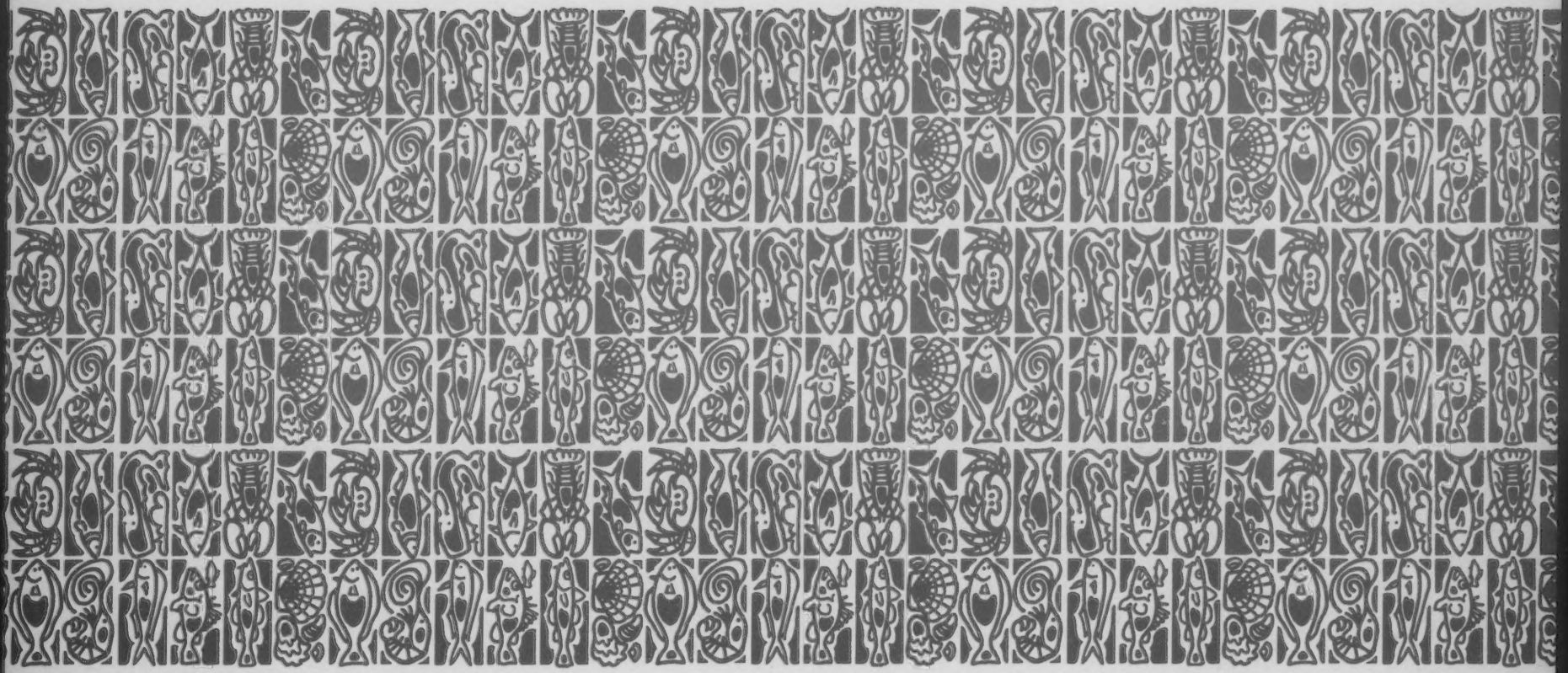

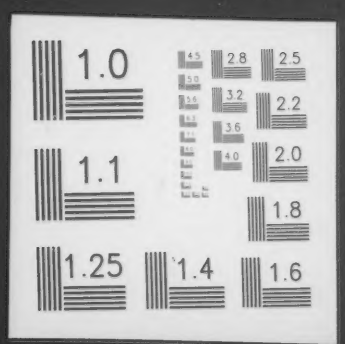
1.0
1.1
1.25
1.4
1.6
1.8
2.0
2.2
2.5
2.8
3.2
3.6
4.0
4.5
5.0
5.6
6.3
7.1
8.0
9.0
10.0